The Feasibility Of Using Infra-Red Radiation In Determining Tooth-Vitality

Paula Elizabeth Lancaster

Submitted in accordance with the requirements for the degree of
Doctor of Philosophy

The University of Leeds
Department of Restorative Dentistry
School of Dentistry

July, 2018

The candidate confirms the work submitted is her own and appropriate credit has been given where reference has been made to the work of others.

This copy has been supplied on the understanding it is copyright material and no quotation from the thesis may be published without proper acknowledgement.

Acknowledgements

Abstract

The aim of this Study was to investigate the feasibility of infra-red radiation determining human tooth-vitality, the basis being that a vital tooth with an internal blood-supply may emit more infra-red radiation and be warmer than a non-vital tooth. The commonest pulp tests are sensibility tests which assess the ability of the nerve fibres within the pulp to respond to a stimulus applied to the tooth, rather than assess the pulp blood-flow.

Development of the vitality test involved cooling the tooth-tissues and capturing the emitted infra-red radiation of re-warming with a thermal camera. Cooling and re-warming of tooth-slices enabled calculation of thermal conductivity and thermal diffusivity of the mineralised tissues - enamel and dentine - and production of a thermal map which characterised these.

Sixteen extracted human molar teeth were tested in a cross-over-study with simulated vitality at four flow-rates: 0.5ml/min, 0.15ml/min, 0.08ml/min and 0.03ml/min under two conditions: pulsed and non-pulsed. The cross-over-design allowed paired testing of the same tooth and independent testing of two dissimilar teeth. The area under the re-warming curve between vital and non-vital teeth was statistically tested. Statistical significance was shown between the paired vital and non-vital teeth at all pulsed flow-rates, and non-pulsed flow-rates of 0.15ml/min and 0.5ml/min. Only the pulsed flow-rate of 0.5ml/min was significant for dissimilar teeth. A thermal map demonstrated re-warming of the vital tooth before the non-vital tooth.

The results suggest infra-red radiation may determine tooth-vitality when the teeth are of the same size and shape, with a blood-flow of 0.03ml/min or above. This could be a realistic blood-flow for the human tooth. Testing teeth of differing size and shape may determine vitality at a blood-flow of 0.5ml/min - higher than realistically expected in the human tooth.

Clinically, the vitality test between a vital and non-vital root-treated tooth points to this model being inverted. This may be due to the insulating nature of the materials used to restore the non-vital tooth. Further clinical investigation is justified to validate the vitality test.

Table of Contents

List of Tables

List of Figures

List of Equations

Chapter 1 Introduction

1.1 General Introduction

This Doctoral Thesis considers: 'The feasibility of using infra-red radiation in determining tooth-vitality'.

Vitality is necessary for life and, in the context of a healthy tooth, vitality infers the presence of a blood-supply (Miller-Keane, 2003). Verifying tooth-vitality and the presence of a blood-supply is a diagnostic challenge encountered by dental professionals, for example following trauma. The clinical outcome of a vitality test can have a profound effect on the patient if a non-diagnosis or misdiagnosis is made, leading to unnecessary treatment, increased cost to the patient, or loss of the tooth if the prescribed root-canal-treatment cannot be endured.

This Study evaluates the feasibility of a diagnostic approach utilising naturally-emitted infra-red radiation from the tooth-tissue to verify tooth-vitality. Simulating and modelling tooth-vitality for evaluation with an imaging technique inevitably involves some exploration of physics, but the primary approach of this work was to consider the problem from a practical clinical perspective.

Evaluation of such a technique requires an understanding of the tooth-tissues and their thermal properties, in particular, enamel and dentine, and how the vascular supply of a vital tooth may provide a detectable temperature-difference compared to a non-vital tooth.

The aim of the following chapters is to extend and enrich current knowledge to enhance the dental clinician's diagnostic armamentarium.

1.2 Background

The dental profession is a relatively new profession falling within the division of medicine and, prior to the eighteenth century, limited dental treatment was available to patients (Hillam, 1990). Academically, the first dental book written in English was claimed by Charles Allen, 'The Operator for the Tooth' (Allen, 1685), within which reference is made to the influence of tooth-loss on the quality of life. It was stated people:

> *'do not chew meat well, loss of teeth renders the pronunciation both troublesome to oneself and unintelligible to others'*

> *'the corruption and want of them is a great a deformity and of as much prejudice to one as anything whatsoever can be'.*

The desire to retain a natural dentition is high but still not achieved by all the population - 94% of adults in England, Wales and Northern Ireland in the 2009 Adult Dental Health Survey were classed dentate, retaining some of their teeth (Steele & O'Sullivan, 2011). Depending on your perspective, this may be regarded as high and positively encouraging, or low and disappointing for the perceived knowledge and ability of the dental profession providing care in the twenty-first century. The loss of teeth still has a detrimental effect on people, not only with loss of function and deformity, but also loss of confidence and self-esteem, which can lead to depressive illness, influencing the overall well-being of a person (Fiske et al., 1998; Trulsson et al., 2002; Nordenram et al., 2013; Rouxel et al., 2016).

Recognition of the presence of a blood-flow through a tooth was described as being 'hot' by Allen:

> *'an artery whose office is to bring directly from the heart, that hot and spirituous blood…..'* (Allen, 1685)

This *'hot and spirituous blood'* will maintain vitality of the tooth's internal soft-tissue (known as the dental pulp) which is encased by the mineralised tooth-tissue. However, a comprehensive tissue-properties-database for thermal assessment of a human at rest (McIntosh & Anderson, 2010) did not recognise the presence of any such blood-flow in a whole tooth. Consideration of Allen's reference, 'hot', may hold an answer to the diagnostic dilemma of determining the presence of a blood-supply giving vitality to the tooth. There is currently no quick, simple and quantifiable vitality test in common clinical use by the practising high-street dentist. The cold test and electric pulp test, which are commonly used, are sensibility-tests. A sensibility test assesses the ability of the nerves fibres within the pulp to respond to a stimulus applied to the tooth, whereas a vitality test assesses the pulp blood-flow. This Study explores the potential to test vitality from a thermal perspective by capturing the naturally-emitted infra-red radiation with a thermal camera.

Dental Professionals are expected to undertake appropriate special investigations and diagnostic procedures to assess, diagnose and manage oral health (GDC, 2015). With the prospect of dental commissioning on the horizon with tiers for treatment provision, some treatments may become the domain of specialists only (NHS England, 2015). However, diagnosing the

clinical problem to ensure the correct referral belongs to all primary care dental professionals and the more valid and reliable they can be the better for the patient, the referring and treating clinician, and the finances of the providers of dental care, e.g., NHS England and/or the patient.

With the technological advancements of recent years, a suitable diagnostic tool using emitted infra-red radiation could be viable to assess vitality. The last literature reporting empirical data on vitality testing using a thermal camera was published in 2000. Hence, it is fitting and timely to re-investigate naturally-emitted infra-red radiation, which is non-ionising, non-invasive and non-destructive, and which could contribute to the retention of the natural dentition and, in the words of our pioneer for dental academia (Allen, 1685):

'I would advise everyone to keep his natural teeth as long as he can'.

1.3 Organisation of the Thesis

This thesis is composed of six chapters presented in a traditional format:

Chapter 1 - which has introduced and provided background of the research topic also presents the layout of the following chapters in the thesis.

Chapter 2 - considers current knowledge of the human tooth with thermal relevance and the influence on the emission of infra-red radiation, the potential causes of tooth-injury, and tests currently available to assess tooth-vitality, which primarily use electromagnetic radiation. The limitations and gaps in current knowledge are outlined which provided justification to investigate tooth-vitality via emitted infra-red radiation.

Chapter 3 - methodologies are informed from the literature, such as the requirements of providing a stable thermal environment and the impact of the emissivity-value of tissue. The advancement of one method led to the production of a thermal map which characterised enamel and dentine, and later assessed tooth-vitality, as well as providing information to model the pulp blood-flow-rate. Accumulation of each method culminated in in-vitro assessment of tooth-vitality which translated clinically.

Chapter 4 - all results are summarised.

Chapter 5 - all findings are discussed.

Chapter 6 - conclusions are presented to answer the research question and areas for further work are suggested. The proposed plan to publish work undertaken within this thesis is also summarised.

Chapter 2 Literature Review

A comprehensive search of the literature which covered the disciplines of dentistry and medical physics was undertaken following the search-strategy described in Appendix A.1.

2.1 Human Dentition

2.1.1 Tooth-Series and Tooth-Types

Most mammals, including the human, possess an upper (maxilla) and lower (mandible) jaw within which teeth are found. The number and type of teeth are variable, e.g., human and mouse (Figure 2-1).
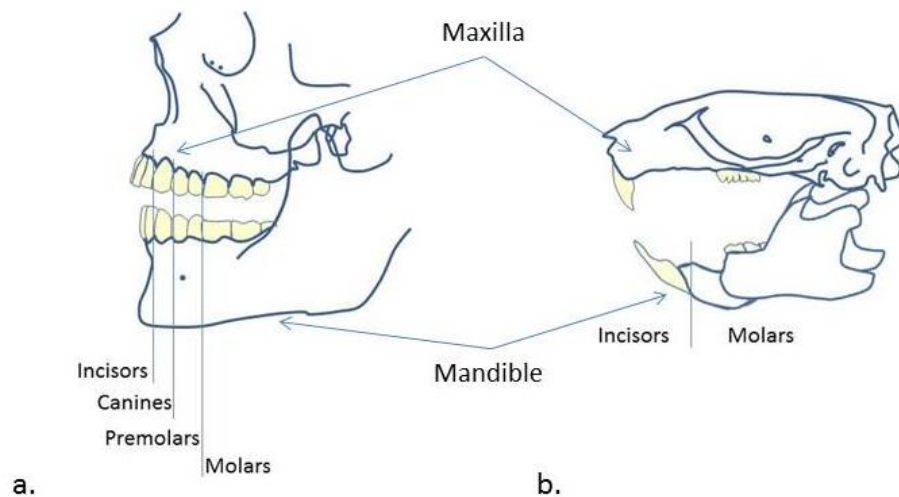
Figure 2-1 Diagram showing two mammalian skulls:
a. human, b. mouse - each with a maxilla and a mandible and respective dentition which differ in tooth-type and number - adapted from http://www.vivo.colostate.edu

The human dentition usually comprises only two sets of teeth - the primary (deciduous or baby) teeth which normally erupt at about 6 months of age, and the secondary (permanent or adult) teeth which normally start to erupt at about 6 years of age (Van Beek, 1983). Unlike other mammals, such as the rat, the human tooth does not continue to grow. If the adult human tooth becomes damaged or diseased there is no natural replacement. Without an appropriate test to confirm or deny the presence of a blood-supply to maintain vitality of the tooth, unnecessary treatment (including tooth-loss) may occur.

There are three types of teeth in the human primary dentition - incisor, canine and molar. Each arch normally has 4 incisors, 2 canines and 4 molars, giving 20 deciduous teeth. There are four types of teeth in the human secondary dentition - incisor, canine, premolar and molar. Each arch normally has 4 incisors, 2 canines, 4 premolars and 6 molars, giving 32 secondary teeth in total (Figure 2-2). Each tooth has a specific location within the dental arch which is indicative of its function.
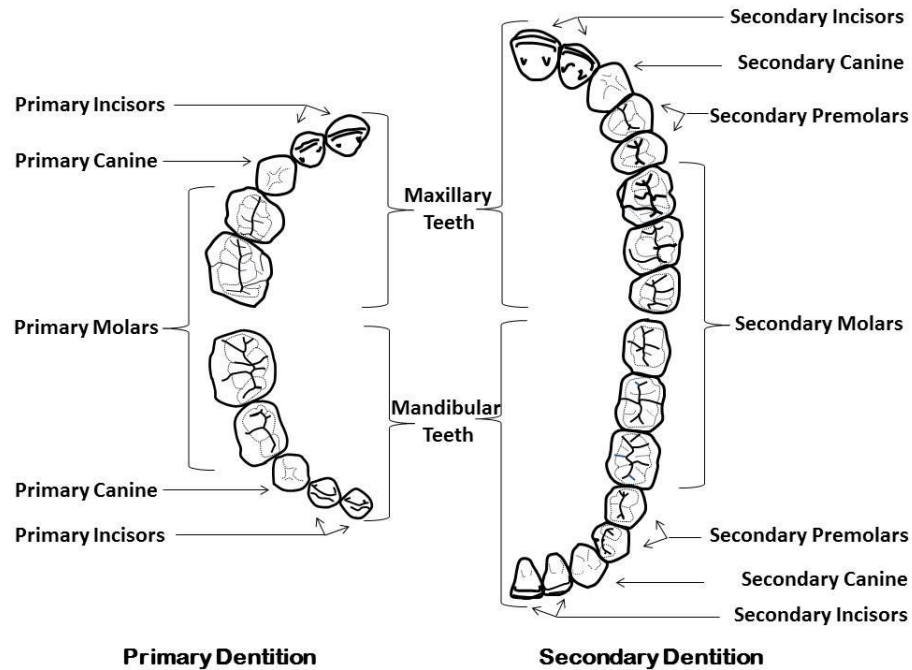
Figure 2-2 Diagram of primary and secondary human dentition showing tooth-number and type – adapted from Van Beek, 1983.

2.1.2 Anatomy of a Human Tooth

The human tooth (Figure 2-3a & b) has a visible portion looking in the mouth - the clinical crown - and an invisible root which is embedded in either jaw-bone (maxilla or mandible) and attached via a ligament - the periodontal ligament. The crown is hard and covered in highly-mineralised tissue - the enamel - which determines the extent of the anatomical crown, and beneath lies a less-mineralised tissue - the dentine. Dentine extends into the root which has a thin mineralised outer layer of cementum. The mineralised tissue protects the soft, innervated, highly-vascularised tissue at the centre of the tooth, called the pulp.

The supporting-bone - alveolar bone - is covered externally with soft tissue, (Figure 2-4) and that closest to the neck of the tooth (but not attached) is the gingival tissue. This extends away from the tooth and over the supporting

bone where, at the mucogingival junction, it becomes alveolar mucosa which is non-keratinised - unlike the gingival tissue. This extends into a sulcus (buccal sulcus) between the cheek and the tooth on each side of the mouth and forms the outer vestibule of the oral cavity. On the inside of the tooth, the mucosa extends to the floor of the mouth and under the tongue. The tongue is located centrally in the lower (mandibular) arch in the oral cavity proper.
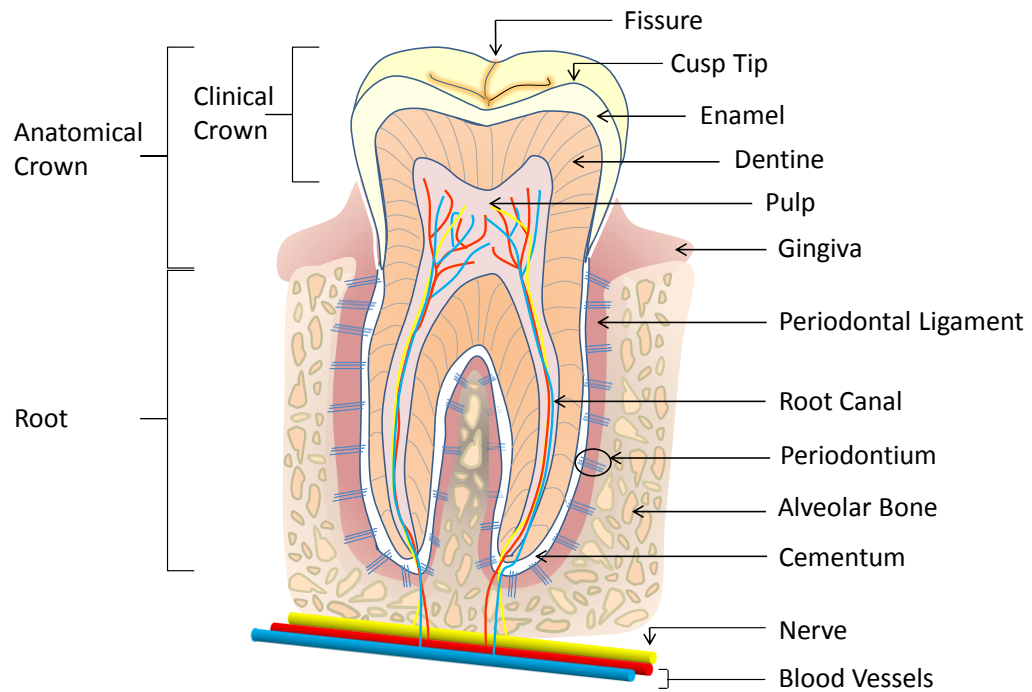
a.
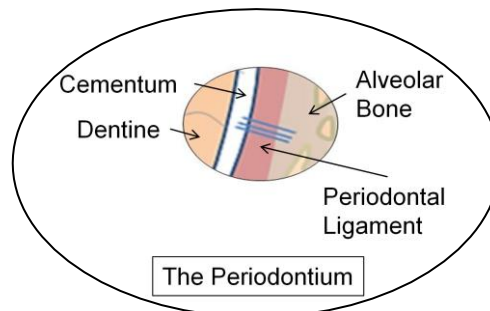
b.

Figure 2-3 Cross-sectional diagram of a human adult molar tooth showing: a. the relationship of the mineralised tooth-tissues of enamel, dentine and cementum with soft pulp-tissue internally and the supporting tooth-tissues of the periodontal ligament and alveolar bone, b. magnified view of the periodontium showing insertion of the periodontal ligament fibres into cementum and the bone - adapted from https://www.britannica.com
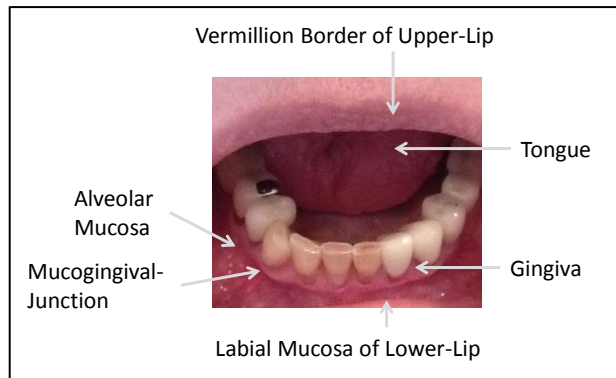
Figure 2-4 Photograph of vascularised soft-tissues surrounding and within the oral cavity.

2.1.3 Importance of Human Teeth

Teeth are important for many reasons and the loss of teeth may be tolerated, or compensated for, with prostheses such as fixed-bridges, implants or removable dentures. Occasionally, some teeth may not develop in a human (hypodontia) and, rarely, no teeth develop (anodontia) (Larmour et al., 2005). Prostheses can have varying degrees of success but none are as ideal as a healthy, natural tooth to satisfy the main functional requirements of mastication, speech, aesthetics and comfort. Dental care professionals need diagnostic aids, such as vitality tests, prior to treatment to enhance preservation of the natural dentition.

2.1.4 Research Models

Current knowledge of the development and some physiological aspects of the tooth, e.g., blood-flow, have been derived from animal investigations rather than humans. This can improve understanding, giving greater insight to the complex, organised processes involved in tooth-development and function. They may be more ethically-accepted and accessible compared to human models. However, the difference between humans and animals should not be forgotten. Figure 2-1 showed a human skull and a mouse skull, where each has a maxilla and mandible, but the number and type of teeth are different. Multiple differences have been identified between human and animal models (Table 2-1).

The impact of such differences are not yet fully understood and inferences from Rodentia, Carnivora or other models to the Primates need to be made cautiously. Recommendation for a more uniform approach between research groups has been made to allow greater comparison of the work undertaken, with knowledge of the strengths and weaknesses of an agreed model (Kirkham et al, 2017). Nonetheless, investigation of the tissues of the actual

species of interest would be far better (Simmer & Fincham, 1995). Within this Study, extracted human teeth were used in-vitro, providing a realisitc model for the size, composition and structure of the tooth-tissues which is important when considering thermal responses, and human volunteers were recruited within the Proof of Concept Study.

Table 2-1 Similarities and differences in jaw pattern, tooth number and development between animal and human (Adams, 1959; Kramer, 1960; Byers, 1984; Linde & Goldberg, 1993; Matthews & Andrew 1995; Thomas, 1995; Legendre, 2002; Bartlett, 2013; Xiong et al., 2013).

Comparatives	Human	Rodentia	Carnivora
Maxilla & Mandible	Yes	Yes	Yes
Growth-Pattern	Determinate (2 sets of teeth)	Indeterminate	Determinate (2 sets of teeth)
Number of Teeth	20 Deciduous (D) 32 Permanent (P)	Mice 16 (P)	Dog 28(D) 42(P)
Tooth-Type	I/C/M(D) I/C/PM/M(P)	Mice I/M	Dog I/C/PM(D) I/C/PM/M(P)
Amelogenesis	Limited	Continuous	Limited
Enamel-Coverage	Encircles Crown	Outer-Face Crown	Encircles Crown
KLK4 Content in Enamel Maturation		Triple Asparagine Compared to Humans	
Dentinogenesis	Limited	Continuous	Limited
Continuity of Hertwig's Epithelial Root-Sheath		Greater Gaps than in Human, Affecting Cementum Deposition	
Pulp Vascular Plexus	Subodontoblastic (SO)	SO & Predentine (PD)	SO, Odontoblastic Deeper Venular
Size & Number of Axons	Normal	Reduced	Normal
D = Deciduous; P = Permanent; I = Incisor; C = Canine; PM = Premolar; M = Molar			

2.1.5 Tooth-Development

The tissues within a tooth may have similar or dissimilar origins, e.g., dentine, cementum and bone are mesenchymal derivatives, whereas enamel is epithelial. The structure of these tissues are quite distinct once formed, irrespective of their origins or underlying mineral which may be similar, e.g., calcium hydroxyapatite, which is found in dentine, cementum and bone, as well as enamel. The tissue-structure also relates to its properties, e.g., density and thermal conductivity, which are of particular interest to this Study, as they influence the transfer of thermal energy. The developmental process gives insight as to how these structural differences may occur.

Human teeth develop from an epithelial dental lamina seen at 6 weeks of embryological development (Nanci, 2012), which thickens and buds, pushing into the underlying tissue of mesenchymal and neural crest (ectomesenchyme) origin. As the bud develops, a dental papilla begins to form (Mina & Kollar, 1987) and it is debated whether the ectomesenchyme permits the epithelial intrusion and reshapes at the same time the bud develops, or if it is solely an epithelial activity (Kim et al, 2017).

Much work on the mouse model has provided knowledge of the epithelial-mesenchymal interactions throughout tooth-development which determine tooth-crown-size and shape (morphogenesis), initiate differentiation of specialised mineral-producing cells (such as odontoblasts) which produce dentine, and ameloblasts which produce enamel (histogenesis), and also provide a population of dental stem-cells in the papilla for growth throughout the tooth's life (Thesleff, 2003; Balic & Thesleff, 2015). Tooth-growth can be defined by three stages: bud, cap and bell (Orban, 1928; Nanci, 2012), in which key structures are consolidated, including the vascular supply (Figure 2-5). Detection of the presence, or absence, of the pulp vascular supply in the tooth is key, without which there is no tooth-vitality.

2.1.5.1 Bud Stage

During the bud stage, nerve-fibres approach the developing dental follicle but entry to the pulp does not occur until dentine formation (dentinogenesis). These are primarily sensory in nature (Nanci, 2012).

2.1.5.2 Cap Stage

The primary enamel knot stimulates epithelial growth downwards, forming cervical loops, which envelop ectomesenchymal tissue internally (Silva & Kailis, 1972), forming a dental papilla which produces dentine-forming odontoblasts and pulp-tissue. Externally, a dental follicle develops. Blood-vessels first enter the dental papilla, and capillaries attach to the outer-enamel epithelium to maintain cellular viability (Nanci, 2012).

2.1.5.3 Bell Stage

Growth continues and the size and shape of the tooth is determined. The enamel knot is thought to control the presence of cusps, their number, height and locations (Jernvall et al, 1994; Miletich & Sharpe, 2004).

2.1.5.4 Late Bell Stage

The ameloblasts differentiate first, followed by odontoblasts which commence dentinogenesis before amelogenesis. The first deposits of

dentine and enamel are thus laid down by odontoblasts and ameloblasts, respectively.
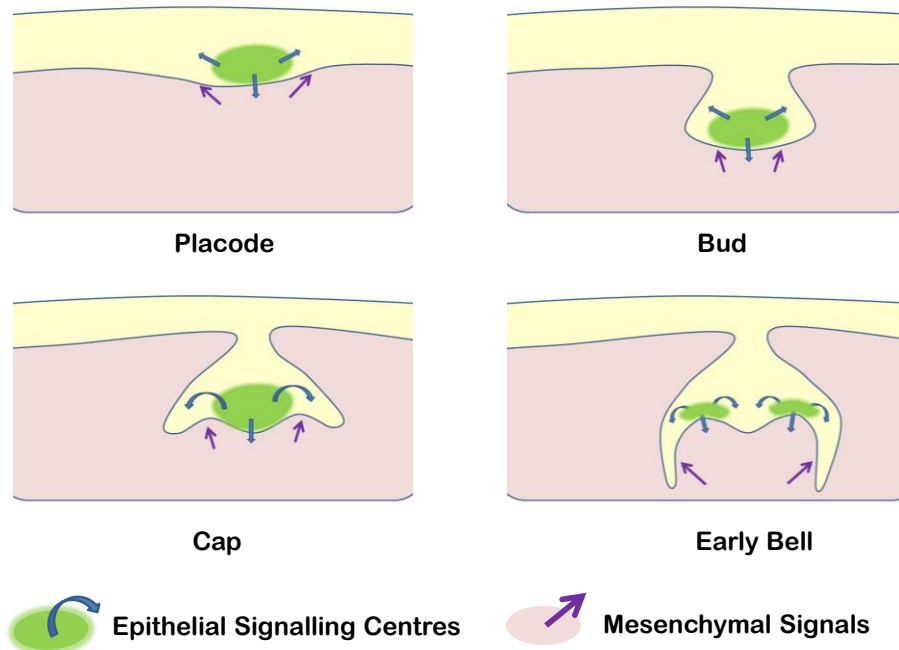
Figure 2-5 Diagram showing the placode, bud, cap and early bell stages of tooth-development, where the epithelium (cream area) penetrates the underlying mesenchymal tissue (pink area).

2.1.5.5 Vascular Supply of the Developing Tooth

Blood-vessels are seen early in the dental papilla, initially in a central position with their nerve-supply and, latterly, more peripherally as smaller vessels. As the dental papilla develops, nutrients and oxygen are required for cellular components, and removal of toxic material is needed to maintain the surrounding tissue. The cap stage was reported as the first phase for blood-vessels to enter the dental papilla (Nanci, 2012) although the early bell stage is also reported as the first sighting of endothelial cells in the mouse embryo (Rothová et al, 2011). A secretory signal, initiated by the odontoblasts, may be directed to the capillary blood-vessels (Yoshida & Ohshima, 1996) at the cap stage, as detection of Vascular Endothelial Growth-Factor (VEGF) has been found. Levels continue to increase during the bell stage (Aida et al, 2005) and may be a stimulating factor for cellular movement.

Blood-vessels may develop from existing blood-vessels (angiogenesis) or differentiate from stem-cells within the dental papilla (vasculogenesis). In-vitro work has not demonstrated development of blood-vessels in tooth-germs but, if peripheral tissues around the tooth-germ with a vascular supply

are included, the dental papilla becomes vascularised (Nait Lechguer et al., 2008). Cellular movement from the surrounding dental follicle of endothelial cells occurred at the late-cap, early-bell stage, which supports the timing of the cap and early-bell stages previously reported. The dental papilla blood-supply appears to form from angiogenesis, rather than vasculogenesis.

2.1.5.6 Root-Dentine

Following crown completion, the inner- and outer-enamel epithelium cells multiply at the cervical loop to produce Hertwig's epithelial root-sheath. This has a double layer of cells (Diekwisch, 2001) enclosing the pulp-tissue which will become the tooth-root. Differentiation of odontoblasts from cells at the edge of the radicular pulp is now initiated from the root-sheath, which may also determine the shape, size and number of roots (Xiong et al., 2013).

2.1.5.7 Periodontium

The periodontium comprises cementum, periodontal ligament and alveolar bone (Figure 2-3b) which develops from complex signalling pathways involving Hertwig's epithelial root-sheath and the dental follicle. These signals lead to the differentiation of three cell-types (Fleischmannova et al., 2010) from the dental follicle, producing:

- cementoblasts which produce dental cementum
- fibroblasts which produce the periodontal ligament
- osteoblasts which produce the alveolar bone.

2.1.6 Mineralised Tooth-Tissue

As described above, there are four mineralized tissues associated with the tooth: enamel, dentine, cementum and alveolar bone. Enamel is usually found surrounding the crown-dentine, whereas cementum is found surrounding the root-dentine and forms part of the periodontium which attaches the tooth to the alveolar bone of the jaw.

The structural and compositional differences in these four mineralised tissues provide an opportunity to distinguish each with a diagnostic test, e.g., radiographs. These tests are clinically valuable in detecting physiological and pathological changes, which may have an effect on the pulp, e.g., dental caries, but they may not detect the vitality-status of the pulp. Development of a non-ionising, clinical diagnostic technique for general practice to assess the vitality-status of the pulp-tissue would be beneficial, as current tests assess the nerve-supply and not the blood-supply. This Study is evaluating the detection of infra-red radiation in determining tooth-vitality and collects

thermal information via the naturally-emitted infra-red radiation. The thermal properties of the tooth relate to the composition and structure of the tissues - both of which affect the naturally-emitted infra-red radiation and the transfer of thermal energy from within or outside the tooth is dependent on the thermal properties (which are considered later).

2.1.6.1 Composition of Mineralised Tooth-Tissue

Mature enamel is highly mineralised compared to dentine, cementum and bone (Table 2-2), although there is general acceptance all four tissues are composed of substituted calcium hydroxyapatite [$Ca_{10}(PO_4)_6(OH)_2$; HA].

Each of the four mineralised tissues also has protein content (Table 2-2) which is mainly Collagen Type I for:

- dentine (Linde, 1985; Linde & Lundgren, 1995; Pashely, 1996),
- cementum (Yamamoto, 2010; Nanci, 2012) and
- bone (Saffar et al., 1997; Fleishmannova et al., 2010; Nanci, 2012)

being of structural importance, with small amounts of non-collagenous proteins, e.g., phosphophoryn, proteoglycans, growth-factors and dentine sialoprotein (Linde, 1985; Linde & Goldberg, 1993; Linde & Lundgren, 1995); whereas enamel proteins are non-collagenous and include the tooth-specific amelogenin, ameloblastin and enamelin which are structural, as well as the proteinases, matrix metalloproteinases-20 (MMP20) and kallikrein-related peptidase-4 (KLK4) (Simmer et al., 2012; Bartlett, 2013; Smith et al., 2017).

Table 2-2 Different composition of enamel, dentine, cementum and bone (Simmer & Fincham, 1995; Nanci, 2012).

	Enamel		Dentine	Cementum	Bone
	Secretory	Mature			Dry-Weight
Mineral	29	95	70	50	67
Protein	66	4	20	50	33
Water	5	1	10	.	.
% wet-weight composition, or % dry-weight for bone					

Enamel matures following initial deposition by the ameloblasts and the mineral content increases with associated reduction in protein and water over time, with a non-homogenous distribution of mineral (Cuy et al., 2002; He et al., 2010; Zheng et al., 2013).

Variation in mineral may also be found according to location in cementum, the inner-layer being less-mineralised than the outer (Nanci, 2012), just as may be found in some dentine (Gradl et al., 2016) and enamel samples (Cardoso et al., 2009). In contrast, Glas 1962, reported very little change in

mineral content across enamel; as did Zuidgeest et al., 1990, for root-dentine. When reviewing different dentine-types (described in greater detail within the structure of mineralised tooth-tissue) differences in mineral can be found between peritubular dentine (dentine surrounding the tubule) which is highly-mineralised like enamel at 95% volume, compared to the less-mineralised intertubular dentine (between the tubules) at 30% volume, (Weiner et al., 1999), showing a heterogenous composition.

2.1.6.2 Structure of Mineralised Tooth-Tissue

Enamel crystals form a prism and inter-prismatic structure (Figure 2-6a & b) following the ameloblast secretions, which mature over time, increasing in size. The crystallites grow during maturation, producing smooth surfaces (Kirkham et al., 2000). They have an ≈ 5µm cross-section diameter (Meckel et al., 1965), arranged in bundles of up to 40,000 crystallites which vary in thickness and width respectively, from 30 x 30nm (Robinson et al., 2003) to 26nm x 68nm diameter (Kerebel et al., 1979). Each prism may extend up to the whole width of enamel, ≈2.5mm (Daculsi et al., 1984). Inter-prismatic enamel is composed of the same mineral as prismatic enamel but has a different spatial orientation. The thickness of enamel varies depending on location – the occlusal surface being thickest, and the cervical area being thinnest where it tapers to end the anatomical crown (Simmer et al., 2010).

Approaching a Cross-Sectional View of Prisms Due To Change of Spatial Orientation

Enamel Crystal Prisms

Inter-Prismatic Crystals

Longitudinal View of Prisms

Deposition Banding

Bending leading to Change in Spatial Orientation
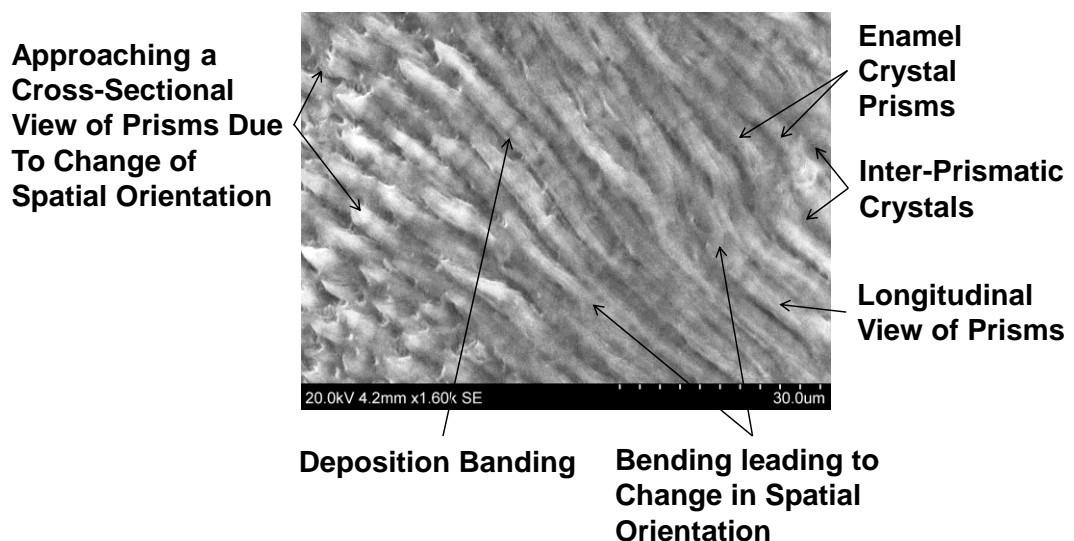
a.
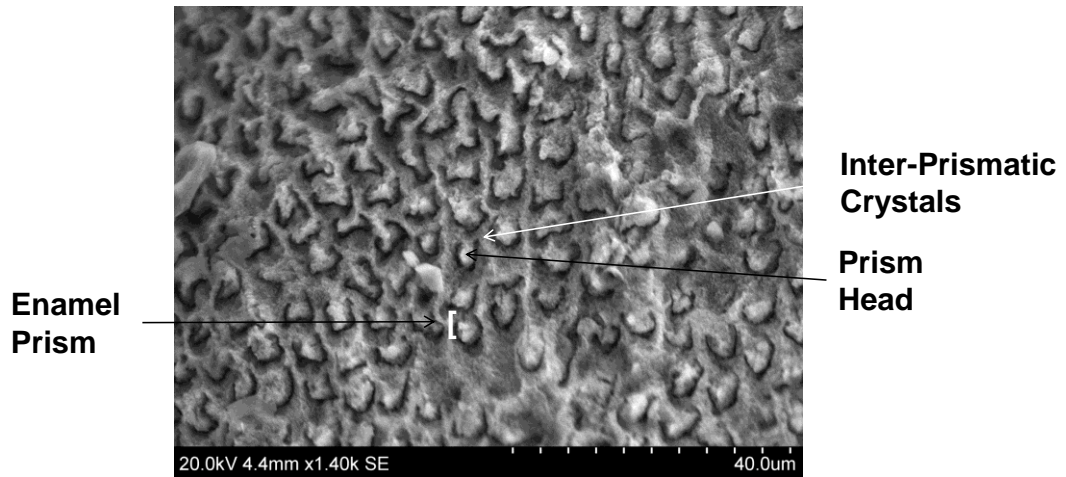
b.

Figure 2-6 Scanning Electron Micrograph of enamel showing:
      a. Longitudinal-section of enamel prisms with changing spatial orientation
      b. Cross-section of enamel prisms and inter-prismatic crystals
      (Medical Illustration - Courtesy of Dr Steve Brookes).

Dentine provides the majority of the mineralised tooth-tissue and, unlike enamel, develops from a collagenous predentine matrix which becomes filled with deposits of intra-fibrillar (Balooch et al., 2008) and extra-fibrillar (Kinney et al., 2001; Kinney et al., 2003) crystals of uniform small plates (Linde, 1985). The intra- and extra-fibrillar ratio of crystals is estimated as 25-30% and 70-75% respectively, similar to bone which also develops from a matrix (Bonar et al., 1985; Pidaparti et al., 1996).

Odontoblasts produce the majority of dentine-types (Table 2-3), secreting both the matrix and mineral. They move inwards, leaving a process extending part-way through the newly-formed dentine, unlike the ameloblast which moves outwards without production of a process. A dentinal tubule is thus formed, (Figure 2-7a & b), housing the odontoblast process giving dentine cellularity, unlike enamel which is acellular. Extension of the odontoblast process may be approximately half-way through the crown-dentine (Garant, 1972; Holland, 1976; Thomas, 1983; Linde & Goldberg, 1993; Pashely, 1996) and, possibly, into the outer-third of root-dentine (Frank & Steuer, 1988; Linde & Goldberg, 1993), with a proposed length between 0.1 and 1mm (Pashley, 1996).
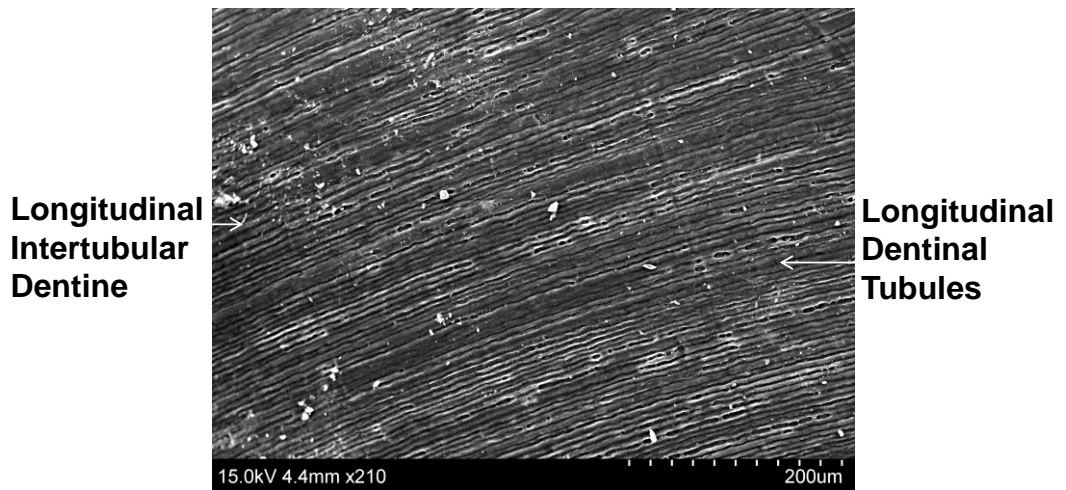
a.
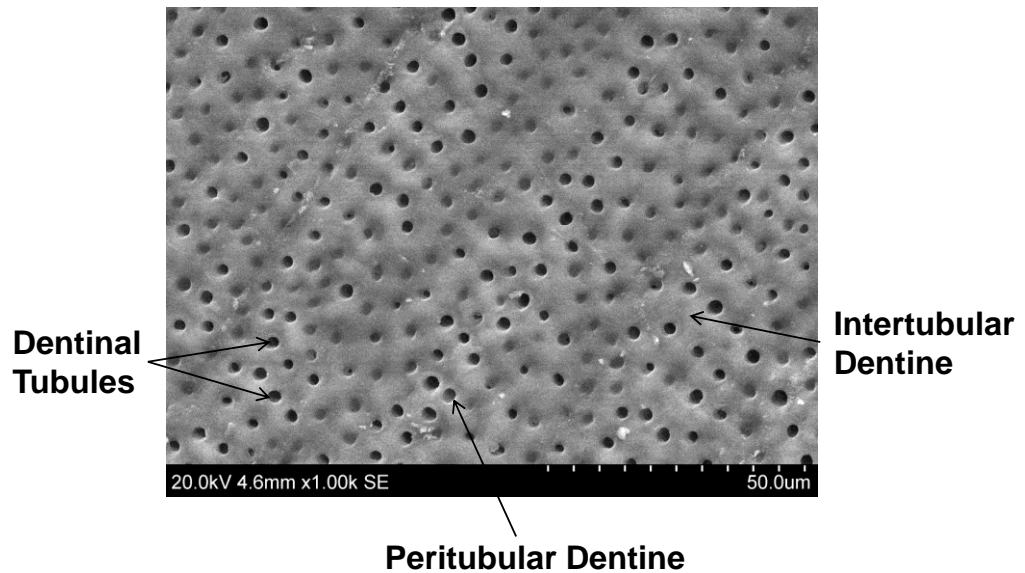
b.

Figure 2-7 Scanning Electron Micrograph of dentine showing:
a. Longitudinal-section of dentinal tubules and intertubular
dentine
b. Cross-section of dentinal tubules with surrounding
peritubular dentine and intertubular dentine
(Medical Illustration - Courtesy of Dr Steve Brookes).

Dentine tubule-diameter varies in size, being smaller at the periphery of dentine (0.6-1.5µm) than the pulp-face (2.5-3.5µm), giving a tapered shape (Fearnhead, 1957; Linde & Goldberg, 1993; Pashely, 1996; Montoya et al., 2015). Approximately 59-76,000 tubules per mm^2 are found at the pulp-surface of young molars (Nanci, 2012) and 15,000 at the amelodentinal junction (Linde & Goldberg, 1993; Pashley, 1996). This approximates to 1% of the surface-area at the amelodentinal junction; and 22% at the pulp-face which is, in effect, 95% water.

Primary dentine forms initially, followed by secondary dentine upon root-completion, which develops at a slower rate. Peritubular dentine forms the periphery of the tubules with a high mineral volume, in contrast to the lower mineral content of intertubular dentine. Dentine may also be deposited within the tubules - intratubular dentine. Tertiary dentine has two forms - firstly, reactionary dentine from the original odontoblast, produced in response to an external stimulus, e.g., caries, which affords some protection to the pulp; secondly, reparative dentine which has a different cellular origin of odontoblast-like cells, following death of the original odontoblast. This results in a structural difference as they have no process and, thus, no tubule (Smith et al., 1995) compared to primary, secondary and tertiary reactionary dentine (Table 2-3). No tubule is present either in the first-formed dentine (mantle dentine), as the odontoblast process develops later.

Table 2-3 Types of dentine with their origin, presence or absence of tubules and type of production (Fearnhead, 1957; Linde & Goldberg, 1993; Smith et al., 1995; Pashely, 1996; Montoya et al., 2015).

Dentine-Type	Origin	Tubules	Production
Mantle[a]	Odontoblast	No	Continuous
Intraglobular[a]	Odontoblast	Yes - lacks Peritubular	Non-continuous
Primary:	Odontoblast	Yes	Continuous
Intertubular[a+b]	.	.	Mineral 30% Vol
Intratubular[c]	.	.	20 Yrs+
Peritubular[a,b+d]	Odontoblast Process?	.	Mineral 95% Vol
Secondary[a]	Odontoblast	Yes	Continuous
Tertiary:		.	
Reactionary[e]	Odontoblast	Yes	Continuous
Reparative[e]	Odontoblast-like Cell	No	Continuous

Several varieties of cementum exist (Table 2-4) and develop prior, or during, function and may be cellular or acellular. It is composed of small uniform plates similar to dentine and bone. A very thin pre-matrix mineralises, and remodelling of cementum may occur due to cementocytes akin to osteoclasts of bone (Diekwisch, 2001; Nanci, 2012).

Table 2-4 Cementum-types with fibre origin, mineralisation, location and function (Yamamoto, et al., 2010; Nanci, 2012).

Cementum-Type	Fibre Origin	Fibre Mineralisation	Location	Function
Acellular	Extrinsic	Variable, Not Central	Cervical ½	Support
Cellular	Intrinsic	Uniform	Apical ½ & Furc	Repair/Adaption
Mixed	Both	Variable	Apical & Furc	Adaption
Acellular Afibrillar	-	-	Patches	Unknown
Furc = furcation				

Bone is structured with an outer compact (cortical) mineral layer and a central medullary cavity with bone marrow and/or trabeculae (cancellous bone). It is layered – lamellae – which may be circumferential (found on inner and outer surfaces), concentric (this is the osteon or Haversian system) or interstitial (fills the spaces between the Haversian canals). Similarities can be seen between bone and dentine, each having a tubule or canal with intertubular or interstitial mineral.

The alveolar bone is traversed by many vessels, e.g., blood and nerve, which is dissimilar to dentine. The socket-side of alveolar bone is bundle bone (100-200µm thick) due the inclusion of the mineralised ends of extrinsic collagen fibres (Sharpey's Fibres) from the periodontal ligament (Saffar et al., 1997). Osteoclasts can be found against the surface of bone occupying Howship's Lacunae, and are responsible for bone-resorption and remodelling, akin to cementocytes in cementum. They are of haematopoietic origin (monocyte/macrophage), not mesenchymal like cementocytes (Fleishmannova et al., 2010; Nanci, 2012).

Attachment of the tooth to the bone is via the periodontium, i.e., cementum-surface infiltrated with mineralised fibres from the periodontal ligament which are attached at the opposite end to bundle bone.

2.1.6.3 Innervation of Mineralised Tooth-Tissue

Enamel is void of innervation, and innervation of cementum is unresolved, as neither light or electron microscopy has demonstrated innervation of cementum, nor has immunohistochemical processing (Maeda et al., 1990).

Sensitivity of dentine is reported and the hydrodynamic theory (Brännström, 1966) provides the accepted explanation. This is due to movement of the dentinal-tubule-fluid being detected, mainly by A-δ-sensory nerve-endings. These may reside within the dentinal tubule (up to 0.4mm) (Fearnhead, 1957) or be within the pulp (Nanci, 2012), in which case it is actually the pulp providing the neural response and not dentine. 40% of dentinal tubules may be innervated in the coronal pulp-horn-area, whereas 0.2-1% may be innervated at the cementoenamel junction (Pashley, 1996).

The Haversian system of bone carries many blood-vessels and autonomic nerves which control the vascular flow and sensory perception. Innervation from the medullary cavity is also present (Nencini & Ivanusic, 2016).

2.1.6.4 Vascularity

Enamel is void of vascularity, whereas cementum is described as being avascular (Diekwisch, 2001; Nanci, 2012) but, when considering the cellular inclusion of cementocytes, a nutritional supply and removal-route for toxins is needed. Whether this is vascular remains uncertain.

Dentine has no blood-vessels but the dentinal tubules are filled with dentinal fluid which has been stated as being a transudate from terminal capillaries, yet permeability barriers to such perfusion from pulp vasculature has also been shown (Bishop, 1992), suggesting the dentinal fluid originates from the odontoblast.

Alveolar bone, like other bone, has many blood-vessels (Saffar et al., 1997).

As seen, there are similarities and differences in the development, composition and structure of the four mineralised tissues which relate to their properties. Thermal energy contributions are also different, as bone with a vascular supply brings a thermal energy source, as may dentine, but enamel does not. Their thermal properties reflect how these tissues enable the transfer of thermal energy. This may be between the tooth-tissues as well as from the tissues of the oral cavity, e.g., tongue, cheek, gingiva; or any contributions to the oral cavity, e.g., food, drink, air – inhaled or exhaled.
The pulp requires protection from any gross variations to avoid irreversible damage and, as will be seen later, the pulp is a vascular tissue providing its own thermal source to the tooth.

The properties of density, thermal conductivity, thermal diffusivity, thermal expansion, specific heat capacity and emissivity are relevant in assessing protection afforded the pulp, and potential to detect the internal thermal energy from the pulp-vasculature. The pulp protection may detract from the ability to detect available internal thermal energy.

2.1.7 Thermal Properties of Mineralised Tooth-Tissue

2.1.7.1 Density

As shown in Table 2-5, enamel has the highest density-range (Manly et al., 1939; Bhussry, 1959; Weatherell et al., 1967; Weidmann et al., 1967; Brown et al., 1970; He et al., 2011; Djomehri et al., 2015; Gradl et al., 2016) of the four mineralised tooth-tissues, followed by dentine, cementum and, finally, bone. Pulp is included for reference.

Table 2-5 Density of enamel, dentine, cementum and bone.

Density of Mineralised Tooth-Tissue and Pulp (g/cm^3)							
Enamel	**Dentine**				**Cementum**	**Bone**	**Pulp**
·	Crown	Root	Hypo-mineralised	Hyper-mineralised	·	·	·
2.01-3.01	1.87-2.4	1.94	0.35 - 1.45	1.82 - 2.74	1.1 - 2.05	0.55-2.00	1.00

Enamel-density may vary with age (He et al., 2011), tooth-type (Weidmann et al., 1967) and location within the tooth, as seen by a decrease in density from the enamel-surface towards the amelodentinal junction (Weatherell et al., 1967; Weidmann et al., 1967; Gradl et al., 2016), although this may not always be the case (Glas, 1962).

Dentine-density can impinge on the range of enamel-densities (Fukase et al., 1992; De Magalhaes et al., 2008; Gradl et al., 2016) and density of crown-dentine may be greater than root-dentine (Black, 1895; Deakens & Manly, 1939; Coklica et al., 1969; Gradl et al., 2016) and these are usually less-dense than enamel of the same tooth (Djomehri et al., 2015; Gradl et al., 2016). Dentine-density may vary across its width and older studies claim is denser near the peripheries (Coklica et al., 1969) – conversely, more recent studies propose it may increase from the pulp to the amelodentinal junction (Gradl et al., 2016). Other studies challenge both of these findings, claiming there is no difference (Zuidgeest et al.,1990). With increasing age, the density generally increases (Miller, 1954; Kinney et al., 2005).

There is limited data available on the density of dental cementum, as reported by Djomehri et al., (2015), who provided a value of 1.24–1.34g/cm^3 for normal cementum, and a value of 1.1–1.22g/cm^3 for affected cementum, following periodontal disease. These values are much lower than previously reported by Manly et al., (1939), of 2.01–2.05g/cm^3. Brekhaus & Armstrong, (1934), made an assumed claim of cementum density to be 2.04g/cm^3. Collection of uncontaminated cementum in sufficient volume to assess its properties is a difficult task and may provide one explanation for the limited data. Additionally, interest in cementum is unlikely to be as prevalent as interest in crown-enamel and dentine which are treated and artificially restored.

Bone-density varies with location, as seen from the structure of cortical and trabecular bone. Trabecular bone-density may range from 0.55-1.18g/cm^3 and cortical bone from 1.85-2.0g/cm^3, with a composite density of 1.18g/cm^3 from the mandible and 0.67g/cm^3 from the maxilla (Seong et al., 2009). This

compares with the ranges of fresh (1-1.7g/cm^3) and dry (0.8-1.4g/cm^3) densities of human femora (Biyikli et al., 1986).

Pulp, which will be discussed later, has been assigned the density of 1g/cm^3 (Lin et al, 2013).

2.1.7.2 Thermal Conductivity

Thermal conductivity is the proportionality constant κ (measured in Watts per meter-Kelvin - Wm·K) for the heat-conduction-rate and is also known as the heat-transport-property, which forecasts the rate at which energy is transferred. Values for metals are high as they are conductors, as seen with copper at 385Wm·K; whereas air with a value of 0.02Wm·K is an insulator (Rickard et al., 1984; Incropera et al., 2007).

Many methods have been used to ascertain the thermal conductivity (Lin et al., 2010c) of enamel and dentine (Table 2-6 & 2-7), such as infra-red thermography (Lin et al., 2010b), thermocouples (Lisanti & Zander, 1950; Phillips et al, 1956; Craig & Peyton, 1961; Braden, 1964) and thermistors (Soyenkoff & Okun, 1958). Values for enamel thermal conductivity ranged from 0.65 to 0.93Wm·K, showing enamel to have low, and, thus, slow conducting properties compared to metals, and is an insulator. This protects the pulp but may prevent energy-transfer from within the tooth for detection. Values vary, which may reflect the different techniques used, the method of calculation, the variation in tissue-samples (e.g., type-of-tooth) with their own structural and compositional differences, as well as the orientation of the enamel prisms when tested. The sample-sizes had a maximum of seven, and data relating to the age of the donor was limited to one study reporting an adult donor. The recording-temperature stated for two studies varied from that approaching human body temperature (26-29°C), to that anticipated at meal-times (Craig & Peyton, 1961) which was 50°C. Experimental conditions appear very different and comparison needs to be made with caution.

No data was found in this search for thermal conductivity of carious enamel.

The mean value from these studies for enamel thermal conductivity (0.8Wm·K) is a third higher than dentine (0.6Wm·K), which ranges from 0.108 to 0.959Wm·K, showing a 10-fold variation in dentine thermal conductivity, compared to a 1.5-fold variation as seen with enamel. This may be due to the dentine structure which may be more variable than enamel, the location on the tooth (which included the crown as well as the root) as cited in one study, the different tooth-samples (which included not only molars and premolars as for enamel, but also incisors), or age-difference of

the samples which were rarely cited. Tubule orientation was given and varied from parallel to perpendicular but did not provide extreme results - on the contrary, they were very similar in studies which provided this information (parallel 0.4-0.6Wm·K and perpendicular 0.4-0.6Wm·K).

Reparative and transparent dentine, as well as dentinogenesis imperfecta dentine, were investigated, all reporting thermal conductivity of a normal range. Carious dentine was not reported in any studies sourced, providing the opportunity for a novel and unique contribution to current knowledge, along with that of enamel.

Enamel has a greater mineral content and density than dentine, and a higher thermal conductivity is consistent with those findings, but it is still an insulator.

The insulating property of enamel and dentine provides protection to the underlying vital pulp-tissue. The overlap in values provides a continuum in the tooth without great risk of thermal damage at the dentine-enamel junction, which may otherwise have caused cracking. This is good for protection but may be an obstacle to detecting any energy-transfer from within the tooth from a vital pulp externally, as the rate-of-change of thermal energy may be too slow to detect and isolate as being from the vitality of the pulp.

Thermal conductivity of cancellous bone from the tibia and femur was found to be 0.404–0.55Wm·K, compared to cortical bone at 0.0742-0.109Wm·K which had respective densities of 0.86-1.38g/ml and 1.7-1.86g/ml (Walker et al., 2017). These densities equate to those of jaw-bone (Seong et al., 2009) and inference may be made that thermal conductivity may be similar to that of jaw-bone, as no such data was recovered in the searches undertaken. Other researchers have shown in-vivo human cancellous bone to have thermal conductivity of 0.36-0.6Wm·K, and for fresh cancellous bone to range from 0.29-0.43Wm·K (Biyikli et al., 1986), which is in-keeping with Walker et al., (2017). Bone is also an insulator and, in contrast to the relationship of enamel which is denser than dentine having increased thermal conductivity, bone appears to have an inverse relationship, as cortical bone is denser than cancellous bone but produces a lower thermal conductivity. There is, however, only one study showing this relationship and further studies are needed to support, or dispute, this finding.

No data was found for the thermal conductivity of cementum (which is present in tiny quantities compared to the availability of the other three

mineralised tissues) making testing difficult. The impact of any heat-transfer to the root-dentine across cementum of the tooth via the periodontal ligament and associated vascular supply is difficult to assess, as there is no knowledge on the rate of heat-transfer in cementum.

Thermal conductivity of the pulp has been taken from water as 0.63Wm·K (Lin et al, 2013).

Table 2-6 Thermal conductivity and thermal diffusivity studies sourced on human enamel between 1958 and 2010.

Author	Year	Sample Size	Tissue Human	Tooth	Age (Years)	Prism Orientation	Recording Method	Recording Temp (^{o}C)	Thermal Conductivity (Wm·K)	Thermal Diffusivity (x10^{-6}m^{2}s)
Soyenkoff & Okun	1958	2	E	Molar	·	Prisms //	Thermistor	26-29	0.649	·
Soyenkoff & Okun	1958	2	E	Molar	·	Prisms L	Thermistor	26-29	0.653	·
Craig & Peyton	1961	7	E	·	·	Prisms //	Thermocouple	50	0.934	·
Braden	1964	·	E	Molar	·	·	Thermocouple	25	·	0.42
Brown, et al.	1970	·	E	Third Molar	·	·	Thermometer	·	·	0.469 **(C)**
Panas, et al.	2003	1 (3smp)	E	Premolar	·	·	Laserflash/ Thermocouple	28	·	0.227-0.409
Matvienko, et al.	2009	·	E	·	·	·	PTR	·	0.91	0.431
Matvienko, et al.	2009	·	E Prismless	·	·	·	PTR	·	0.83	0.455
Lin, et al.	2010b	1	E	Molar	Adult	·	IRT	·	0.81	0.408
3smp = 3 samples from 1 tooth; E = Enamel; // = Parallel; L = Perpendicular; PTR = Photo-thermal radiometry; IRT = Infra-red thermography, (C) = Calculated										

Table 2-7 Thermal conductivity and thermal diffusivity studies sourced on human dentine between 1950 and 2010

Author	Year	Sample Size	Tissue Human	Tooth	Age (Years)	Tubule Orientation	Recording Method	Recording Temp (°C)	Thermal Conductivity (Wm·K)	Thermal Diffusivity (x10^-6 m²s)
Lisanti & Zander	1950	7	De	Molar	·	·	Thermocouple	40-90	0.959	·
Phillips, et al.	1956	4	De	Molar	·	·	Thermocouple	·	0.108	·
Soyenkoff & Okun	1958	2	De	Molar	·	Root //	Thermistor	29	0.402	·
Soyenkoff & Okun	1958	2	De	Molar	·	Crown //	Thermistor	29	0.448	·
Craig & Peyton	1961	8	De	·	·	Tubules //	Thermocouple	50	0.569	·
Craig & Peyton	1961	8	De	·	·	Tubules L	Thermocouple	50	0.582	·
Braden	1964	·	De	Molar	·	·	Thermocouple	25	·	0.26
Brown, et al.	1970	·	De	8's	·	L	Thermometer	·	·	0.187 (C)
Brown, et al.	1970	·	De	8's	·	//	Thermometer	·	·	0.183 (C)
Fanibunda & de Sa	1975	5	De - Normal	·	·	·	Thermistor	<40	0.56 Fresh 0.52 Dehydrat	·
Fanibunda & de Sa	1975	9	De - Repara/trans	·	·	·	Thermistor	<40	0.78 Fresh 0.76 Dehydrat	·
Fanibunda & de Sa	1975	6	De - Dentinogenesis	·	·	·	Thermistor	<40	0.62 Fresh 0.59 Dehydrat	·
Fukase, et al.	1992	·	De	·	·	·	Xenon Flash Bulb	·	0.62	0.258
Minesaki, et al.	1983	·	De	·	·	·	Thermocouple	30 difference	·	0.254
Panas, et al.	2003	1	Whole Tooth	Incisor	·	·	Waterbath/ Thermocouple	-10 to 45	·	0.069-0.349
Panas, et al.	2003	1 (3smp)	De	Premolar	·	·	Laserflash/ Thermocouple	28	·	0.192-0.216
Little, et al.	2005	6	De	·	·	·	Thermocouple	21±1	0.88	·
De Magalhaes, et al.	2008	4	De	8's m&f	18-26	Crown //	Flash Laser	·	0.606 (C)	0.237
De Magalhaes, et al.	2008	1	De	8 m&f	18-26	Crown L	Flash Laser	·	0.363 (C)	0.199
Lin, et al.	2010b	1	De	Molar	Adult	·	IRT	·	0.48	0.201
3smp = 3 samples from 1 tooth; De = Dentine; m&f = Male & Female; // = Parallel; L = Perpendicular; IRT = Infra-red thermography; (C) = calculated										

2.1.7.3 Thermal Diffusivity

Thermal diffusivity describes the capacity to transport thermal energy relative to the capacity to store thermal energy and is a resource of how fast heat travels from warm to cold areas. If the value is high, the material or tissue will be able to react quickly to changes in their thermal environment, as seen with metals such as copper ($111 \times 10^{-6} m^2/s$ at $25^o C$), whereas those with a low thermal diffusivity will be slow to react, taking much longer to reach a new thermal equilibrium, as seen with air ($19 \times 10^{-6} m^2/s$ at $27^o C$) (Incropera et al., 2007; www.engineersedge.com).

The thermal diffusivity of enamel (Lin et al., 2010c) has also been evaluated by many methods (Table 2-6), with values ranging from 0.23 to 0.47 $\times 10^{-6} m^2/s$ which is very low when compared to air, but approximately twice the value of dentine. Enamel is slow to respond to thermal changes, taking time to reach a new equilibrium, which is protective of the internal soft-tissues. Additionally, the next layer of dentine is even slower to respond to thermal change (Table 2-7), with values of 0.18 to $0.26 \times 10^{-6} m^2/s$ providing an extra layer of protection from any extreme temperature-changes in the oral environment. This may further reduce the chance of detecting any energy-change within the mineralised tissues of the tooth-crown from the internal energy-source of the pulp, as the time taken may be too long and any thermal changes may be masked by other contributions, e.g., the periodontal supply, the oral environment - such as inhalation and exhalation of air.

Thermal diffusivity of bone varies with wet femora ranging between 0.1 to $0.14 \times 10^{-6} m^2/s$, and dry femora ranging between 0.1 to $0.23 \times 10^{-6} m^2/s$, which is very similar to dentine (Biyikli et al., 1986) and is unlikely to contribute to any masking of the pulp energy-source.

No values were sourced for cementum. Thermal diffusivity of pulp is taken from water as $0.15 \times 10^{-6} m^2/s$.

2.1.7.4 Thermal Expansion

The linear coefficient of thermal expansion (despite being a ratio is assigned the unit parts per million (ppm) per $^o C$ rise in temperature) is particularly important when considering restoring a tooth, as the restorative material should have similar values otherwise the expansion may lead to cracks in the tooth or a break in the restoration seal leading to leakage and microbial infiltration. This is also the case between enamel and dentine, as excessive discrepancies may lead to cracking of the enamel, or separation of the

enamel from dentine due to thermal stress. In-vitro studies, however, do not compensate for potential heat-sinks which would be seen in the natural tissue via circulating blood of the soft-tissues, or the presence of saliva washing over the teeth, and values need to be viewed carefully. For this Study it is useful to review potential damage from thermal extremes and there appears to be little risk in the range 0-60°C.

Reported values (Table 2-8) for enamel range from 11 to 17x10^{-6}ppm/^{o}C rise, compared to -7 to 12x10^{-6}ppm/^{o}C rise for dentine, with exception of one outlier for dentine. The minus values for dentine indicate a contraction is possible which may be due to water-loss.

Table 2-8 Coefficient of thermal expansion for human enamel and dentine.

Author	Year	Tissue	Coefficient of Thermal Expansion (10^{-6}ppm/^{o}C rise)
Braden	1976	Enamel	11.4
Hengchang, et al.	1989	Enamel	16.96 (±3.83)
Braden	1976	Dentine (De)	5.4 - 8.3
Hengchang, et al.	1989	Dentine (De)	10.59 (±2.38)
		Crown	11.90 (±4.42)
		Root	9.44 (±0.61)
Lloyd, et al.	1978	Dentine (De)	7.5
Lopes, et al.	2012	Dentine (De)	-6.82
Martin-Löf, et al.	1971	Dentine (De)	25 (0-30°C) / 37 (30-60°C)
Roberts	2014	Enamel & De	15.9
		Enamel & De Caries	12.5
		De Mid-crown	10.6
		De Mid-crown Caries	8.9
		Cervical	5.4
		Root-Surface	4.6

2.1.7.5 Specific Heat Capacity

Specific heat capacity is the quantity of heat-energy needed to increase the temperature of 1Kg of a specific material by 1K (unit JKg/K). Water has a specific heat capacity of 4200JKg/K, compared to copper of 385JKg/K (www2.ucdsb.on.ca/tiss/stretton/database/specific_heat_capacity_table.htm)

Table 2-9 shows the studies sourced from 1943 to 2008 reporting the specific heat capacity of tooth-tissue, with whole mineralised tooth-tissue returning a value of 1256JKg/K (Brown, 1970), whereas adult molar-dentine falls between 873-1591JKg/K (De Magalhaes, 2008; Brown, 1970, respectively) and 711-750JKg/K for adult molar-enamel (Brown, 1970). Bone-values range between 1140–2370JKg/K depending on whether it is wet or dry, indicating a greater amount of energy is needed to raise bone-temperature compared to tooth-tissue, and dentine requires more energy

than enamel. This is in agreement with dentine generally being a more efficient insulator than enamel. Specific heat capacity of pulp has been given as 4200Jkg/K, as taken from water (Lin et al, 2013).

Table 2-9 Specific heat capacity of human enamel, dentine and bone

Author	Year	Tooth	Age (Years)	Tissue	Specific Heat Capacity (JKg/K)
Barker, et al.	1972	.	.	Enamel	750
Brown, et al.	1970	Third Molar	.	Enamel	711
Barker, et al.	1972	.	.	Dentine	1170
Brown, et al.	1970	Third Molar	.	Dentine	1591
Fukase, et al.	1992	.	.	Dentine	1283
Henschel	1943	.	.	Dentine	1256
De Magalhaes, et al.	2008	Third Molar	18-26	Dentine (//)	1115
De Magalhaes, et al.	2008	Third Molar	18-26	Dentine (L)	873
Biyikli, et al.	1986	Bone	.	Femora Dry	1140-1640
				Femora Wet	1500-2370
// = Parallel to dentinal tubules; L = Perpendicular to dentinal tubules					

2.1.7.6 Emissivity

Any tissue with a temperature above absolute zero (0Kelvin or -273.15$^\text{o}$C), where molecular motion is predicted to cease, emits some infra-red radiation. Objects, including teeth, will interact differently with the approaching radiation (incident radiation), either reflecting, transmitting or absorbing it (Equation 1 and Figure 2-8).

$$1 = \mathcal{R}(\lambda) + \mathcal{T}(\lambda) + \mathcal{A}(\lambda)$$

$\mathcal{R}(\lambda) = reflected\ radiation\ of\ a\ specific\ wavelength$

$\mathcal{T}(\lambda) = transmitted\ radiation\ of\ a\ specific\ wavelength$

$\mathcal{A}(\lambda) = absorbed\ radiation\ of\ a\ specific\ wavelength$

Equation 1 Unity equals the addition of the reflected, transmitted and absorbed radiation.
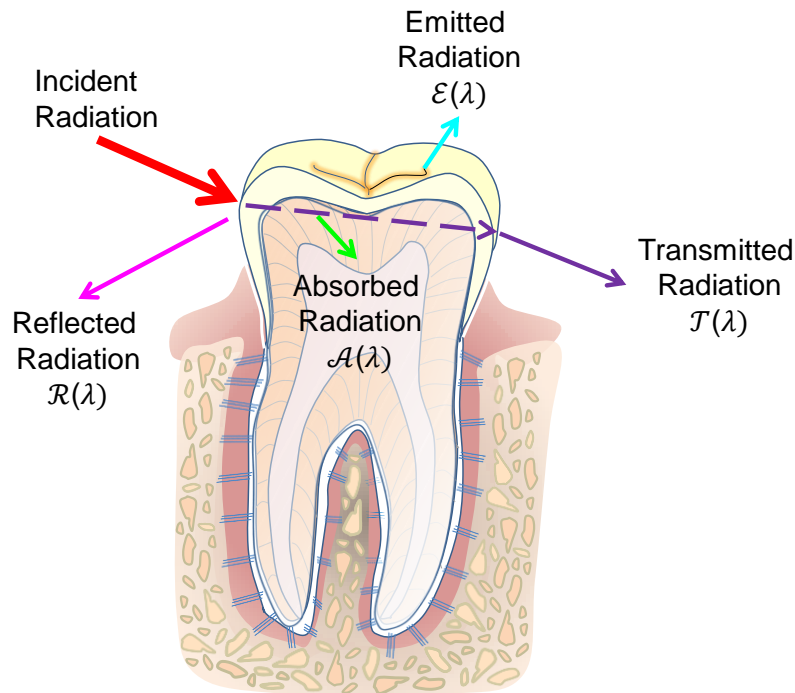
Figure 2-8 Balance of radiant energy adapted to a tooth from Gaussorgues, (1994).

When an object, such as a tooth, is thermally stable within its environment, there is a balance between the radiation entering and the radiation leaving, which depends not only on the incident, reflected, transmitted and absorbed energy (Figure 2-8), but also on the amount of energy released. When energy is absorbed, to balance the equilibrium and prevent an increase in temperature, there must also be a release and this is the emitted radiation ($\mathcal{E}$) or 'emissivity' (Equation 2). Emissivity of a tissue is particularly important when an absolute temperature is needed and the emitted infra-red radiation is collected by a thermal-imaging-device.

$$\mathcal{A}(\lambda) = \mathcal{E}(\lambda)$$

Equation 2 Balance between absorbed and emitted radiation to maintain thermal equilibrium.

The amount of emitted radiation is dependent on temperature, wavelength, material-composition, surface-texture, as well as the viewing angle of the tissue (Gaussorgues, 1994; Vollmer & Möllmann, 2010), although the visible colour is not influential (Hardy, 1934).

An idealistic Blackbody absorbs all incident radiation and can subsequently emit all of it, which provides the maximum potential for emissivity as 1 (Equation 3).

$$\mathcal{E}(\lambda) = 1$$

Equation 3 Maximum emissivity of an ideal Blackbody equals 1.

Reflectance and transmission are thus zero (Equation 4).

$$\mathcal{R}(\lambda) + \mathcal{T}(\lambda) = 0$$

Equation 4 Reflectance and transmission of radiation equals 0
when emissivity equals 1.

Commercially available Blackbodies have reported values of 0.98 or 0.99 rather than 1, and this is the highest empirical value achievable (Vollmer & Möllmann, 2010), which is also that of skin (Hardy, 1934).

To record absolute temperatures of objects for comparison with other infra-red-recording-devices, an emissivity-value is needed. The emissivity-value is the ratio of the emitted radiation from the surface-of-interest, compared to that emitted by a Blackbody at the same temperature and wavelength (Equation 5). The value ranges from 0-1 and has no units.

$$\mathcal{E}(\lambda) = \frac{emission\ of\ surface\ of\ interest}{emission\ of\ Blackbody}$$

Equation 5 The emissivity-value of an object is a ratio
compared to the emissivity of a Blackbody.

When viewing an object which is shiny, and thus reflective, $\mathcal{R}(\lambda)$ is large, with little absorption, resulting in low-emissivity.

For an opaque material, such as a tooth, transmission is virtually zero, $\mathcal{T}(\lambda) = 0$, which leaves reflectance and emissivity to balance the equation (Equation 6):

$$1 = \mathcal{R}(\lambda) + \mathcal{E}(\lambda)$$

Equation 6 Balance of unity derived from reflectance and
emissivity for an opaque material

Normal incidence is the ideal viewing-angle, i.e., 90° perpendicular to the object. When viewing a non-flat surface, such as a tooth, there can be varying emissivity-values and, up to 55° from normal incidence, most objects' emissivity will be approximately the same, but thereafter may be dependent on the viewing angle (Gaussorgues, 1994; Vollmer & Möllmann, 2010). If there are multiple angular surfaces, e.g., fissure of a tooth, radiation

may become locked, resulting in a higher emissivity-value than actually exists.

It is recommended to record thermal images from surfaces with naturally-high emissivity-values or to artificially create them from materials with known values, e.g., black paint or 3M Scotch Super 33+ Black Vinyl Electrical Tape, quoted as $\varepsilon = 0.96$ (British Standards BS ISO 18434-1:2008; FLIR ThermaCAM[TM] Researcher Professional, 2010). This may be acceptable for most objects but, for biological specimens of small size, this may not be feasible, masking some of the detail and may add additional insulation.

The other approach is to calculate an emissivity-value from a known-source, which may be a Blackbody, which is expensive and inaccessible to most, or from other materials with a known-emissivity, such as 3M Scotch Super 33+ Black Vinyl Electrical Tape (approximately £6.00 for 20m).

2.1.7.7 Emissivity of Mineralised Tooth-Tissue

Recognition of the emissivity-value is varied within dental literature. The emissivity-value reviewed in 66 papers which used thermal imaging on the mineralised tooth-tissues, gave values between 0.65 to 0.98 (Table 2-10, review date Oct 2015 – Flow Diagram of Selection of Articles in Appendix A.2).

Publication-dates ranged from 1966 (Crandell & Hill, 1966), for 'Thermography in Dentistry: A Pilot Study' with no report of an emissivity-value, to 2015, reviewing surface-temperature-rise, in absolute value (^{o}C), following thermoplastic obturation (Ulusoy et al., 2015), where emissivity was presented as 0.91 for root-tissue without explanation of its derivation.

Six studies were solely in-vivo (Crandell & Hill, 1966; Hartley et al., 1967; Pogrel et al., 1989; Hussey et al., 1995; Komoriyama et al., 2003; Preoteasa et al., 2010), of which four presented no value for emissivity despite reporting absolute temperatures, and one presented relative values without reference to the emissivity (Crandell & Hill, 1966). The remaining in-vivo study quoted another reference as its source for the human body (Preoteasa et al., 2010), with a value of 0.98. Kells et al., (2000a & 2000b) had both in-vitro and in-vivo components to their study and calculated an emissivity-value of 0.65, which is an outlier to all others.

Nineteen in-vitro studies presented a range of emissivity-values from 0.65-0.98. Gontijo et al., (2008), quoted emissivity of 9µm, which is incorrect as a ratio with no unit, although the study did report absolute values of temperature, which should be interpreted with caution. Consideration was

given to emissivity by four studies (McCullagh et al., 2000; Lipski & Zapałowicz, 2002; Bouillaguet et al., 2005; and Lin et al., 2010b) yet no value was reported. Nevertheless, absolute values were again presented in their outcomes.

Calculation methods varied. Kells et al., (2000a) reported enamel emissivity of a single maxillary incisor following placement in an oven at 70°C for 24 hours. On opening the door, an image was recorded from which a spot-measure was taken. There was no indication where this was on the labial surface of the tooth and it would be very useful to record multiple spot-measures or an area across the surface to provide an average value of the whole enamel surface, rather than a single value. The value was used within a calibration programme of the software from Agema. The returned-value was 0.65 but the exact method by which it was computed is unknown. It is the lowest value found for emissivity of enamel, with all other values being 0.9 and above, and may affect the final temperature values reported within the study, making them slightly higher than others. Lipski reported a root-value of 0.91 in multiple studies (2005a; 2005b; 2010a; 2010b) and makes reference to Kells et al., (2000a), or cites 0.91 without explanation. The value is in-keeping with others, although Kells et al., (2000a), was viewing enamel, not root-tissue.

Without verification, there may be emissivity-differences due to compositional variation between the deciduous and permanent dentitions, leading to different temperature-outcomes. Transfer of emissivity-values, as seen from Da Silva Barbosa et al., (2013) who studied deciduous teeth but used an adult tooth emissivity-value quoted from Ana et al., (2012) - who actually viewed adult third molars in their published paper in 2007 - requires care.

Lin et al., (2010a) provides different values for enamel and dentine, 0.91 and 0.92 respectively, citing the method of calculation as being the manufacturer's instruction; as well as Da Costa Ribeiro et al, (2007) who also calibrated for emissivity at 0.91 for root-tissue. Da Costa Ribeiro, (2007) suggested the calibration should be related to the materials being analysed with reference to McCullagh et al., (2000). McCullagh et al., (2000) does not provide a value for emissivity in the study, which compared temperature-values with thermocouples, which were lower than those from the thermal imager, but they do acknowledge that the accuracy of the thermal-imaging-system is dependent on the emissivity-value of the surface being viewed. Lin

et al., (2010b), within another study, also reports the use of black paint to normalise emissivity but no actual value was provided.

Neev et al., (1993) reported dentine emissivity of 0.8 using black oven-paint which approximated to a Blackbody, and was appropriately made as a reference method (British Standards BS ISO 18434-1:2008; FLIR ThermaCAM^{TM} Researcher Professional, 2010), although the true emissivity-value of the paint was not provided.

A variation in value is to be expected as tooth-tissue is non-homogenous and a uniform approach would be beneficial.

Table 2-10 Emissivity-values in dental literature for mineralised tooth-tissue.

Emissivity (ε)	Author	Year	Tooth	Tissue (E, De, R)	In-vivo (VV) In-vitro (VT)	Sample S or W	Calculation-Method
0.98	Kaneko, et al.	1999	18 Incisors	E Demineralised	VT	W	Assumed
0.98	Preoteasa, et al.	2010	Whole Dentition	E	VV	W	Referenced Voicu et al., 2009
0.97	Meyer & Foth	1996	.	E & De	VT	S	Assumed
0.92	Lin, et al.	2010a	1 Third Molar	De	VT	S	Manufacturer's Guide
0.91	Lipski Lipski, et al. Lipski, et al.	2005a 2010a 2010b	45 Incisors & Canines 36 Incisors 30 Premolars	R	VT	W	Referenced Kells et al., 2000a
0.91	Lipski	2005b	20 Premolars	R	VT	W	.
0.91	Lipski	2006	30 Incisors	R	VT	W	Camera Calibration
0.91	Ana, et al.	2007	9 Third Molars	E & De	VT	S	.
0.91	Da Costa Ribeiro, et al.	2007	24 Incisors	R	VT	W	Referenced McCullagh, 2000
0.91	Da Silva Barbosa, et al.	2013	15 Deciduous Molars	E Deciduous	VT	S	Referenced Ana, 2012, instead of 2007
0.91	Kabbach, et al.	2008	40 Incisors	R-De	VT	W	.
0.91	Lin, et al.	2010a	1 Third Molar	E	VT	S	Manufacturer's Guide
0.91	Kilic, et al.	2013	42 Premolars	R	VT	W	Referenced Lipski 2010 & Kells 2000a
0.91	Ulusoy, , et al.	2015	60 Premolars	R	VT	W	.
0.8	Neev, et al.	1993	24 Molars	De	VT	S	Black paint assumed-emissivity 1
0.65	Kells, et al.	2000a & b	13 Incisors	E	VT/VV	W	Spot-measurement from within hot oven & Software
0.65	Kells, et al.	2000a & b	16 Incisors & Canines	E	VT/VV	W	Spot-measurement from within hot oven & Software

E = Enamel; De = Dentine; R = Root; RDe = Root-Dentine; VV = In-vivo; VT = In-vitro; S = Sectioned flat surface of a slice; W = Whole tooth

2.1.8 Dentally-Related Soft-Tissues

There are multiple soft-tissues associated with the tooth, as seen previously in Figure 2-3 & 2-4. Internally, the pulp-tissue interfaces with the root and crown of the tooth and, externally, the periodontal ligament encompasses the root, and the dentogingival-tissue contacts the tooth-neck. The tongue, cheeks and lips can all touch the clinical crowns of teeth during everyday function; nonetheless, the two soft-tissues of particular importance to this Study are the dental pulp and the periodontal ligament, as both these can contribute to the outcome of data-gathering of diagnostic tests assessing pulp status, providing sensory responses and thermal contribution from the vascular supply essential to maintain tissue-vitality.

2.1.8.1 Composition of Dental Pulp and Periodontal Ligament

The dental pulp has a soft connective tissue, composed primarily of a collagenous matrix (Types I and III) and a water-based ground-substance (Hargreaves et al., 2012). A vascular network is present, as is a neural supply and lymphatic drainage. The cellular components include odontoblasts, fibroblasts, undifferentiated mesenchymal cells, inflammatory cells, macrophages, T-lymphocytes (and also B-lymphocytes although these are rare) as well as leukocytes and associated immunocompetent cells, plus a reservoir of multipotent stem-cells (Nanci, 2012).

The periodontal ligament is one component of the dental periodontium and is also composed of collagen, as an extracellular matrix of collagenous-fibre-bundles (which includes Types I and III, as does the pulp; and also Type XII, which the pulp does not possess) within an amorphous ground-substance of which 70% is water. Elastic fibres are found, e.g., Oxytalan, which may be involved in vascular-regulation, as are non-collagenous proteins, e.g., alkaline phosphatase, proteoglycans and glycoproteins. Cellular components include osteoblasts (which deposit mineralised bone in a similar way as odontoblasts deposit dentine), cementoblasts, osteoclasts, odontoclasts (with potential to resorb tooth-roots), fibroblasts (which are also found within dental pulp), epithelial cell rests of Malassez, monoyctes and macrophages, undifferentiated mesenchymal cells, and pluripotent stem-cells (Nanci, 2012).

2.1.8.2 Structure of Dental Pulp and Periodontal Ligament

The specialised connective-tissue of the periodontal ligament primarily occupies the space between the tooth-root (cementum) and the alveolar bone attaching the tooth to the socket. Thickness can vary between 0.15 and 0.38mm, being thinnest at the mid-root section (Nanci & Bosshardt, 2006). The dental pulp resides within the chamber and canal(s) of a tooth, i.e., the pulp-space, and is virtually surrounded by mineralised tooth-tissue – dentine. The pulp-space is very small, (Table 2-11, Figure 2-9) with an approximate volume of the adult tooth ranging from 6.1mm^3 for the mandibular central incisor, to 68.2mm^3 for the maxillary first molar (Fanibunda, 1986a).

Table 2-11 Mean volume of pulp-space (mm^3) of human adult Teeth (Fanibunda, 1986a).

	Mean Volume of Pulp-Space (mm^3) [Standard Deviation]	
Tooth	**Maxillary**	**Mandibular**
Central Incisor	12.4 [3.3]	6.1 [2.5]
Lateral Incisor	11.4 [4.6]	7.1 [2.1]
Canine	14.7 [4.8]	14.2 [5.4]
First Premolar	18.2 [5.1]	14.9 [5.7]
Second Premolar	16.5 [4.2]	14.9 [6.3]
First Molar	68.2 [21.4]	52.5 [8.5]
Second Molar	44.3 [29.7]	32.9 [8.4]
Third Molar	22.6 [3.3]	31.1 [11.2]
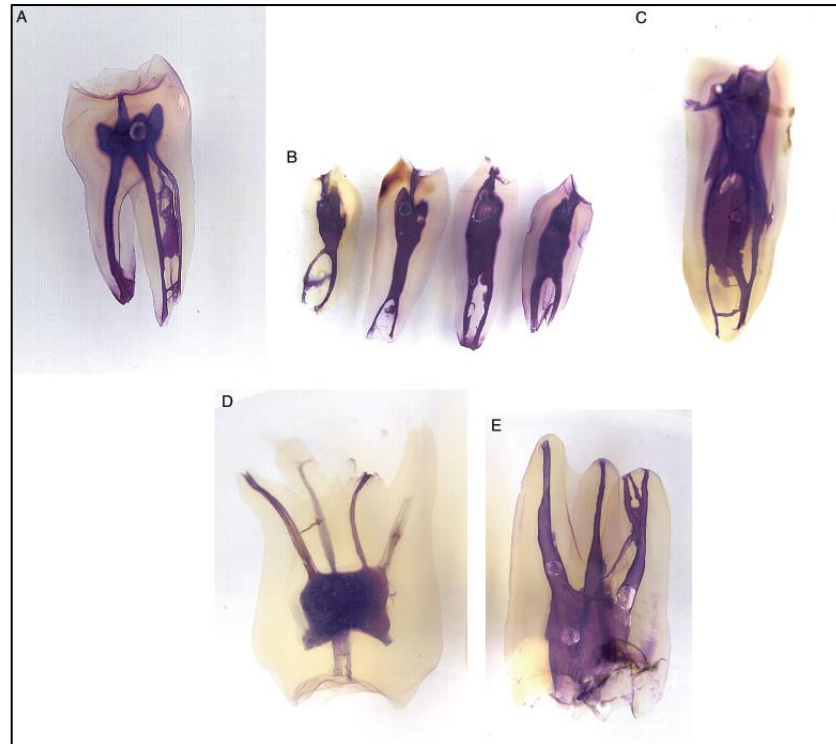
Figure 2-9 Root-canal variation shown with hematoxalin dye in:
      a. mandibular second molar; b. mandibular premolars;
      c. mandibular premolar with three canals;
      d. maxillary second molar; e. maxillary first molar
      Reprinted from Endodontic Topics 10, Vertucci FJ, (2005).
      Root Canal Morphology and its Relationship to Endodontic
      Procedures, 3-29, (2005), Figure 7.
      With permission from John Wiley and Sons 8th May, 2018.
      (Agreement in Appendix A.3.1)

There is a periodontal ligament fibre-system which connects from one tooth to another (transseptal) and also to the gingival tissue. The principle fibres of the ligament form distinct groups (Figure 2.3), e.g., alveolar crest, interradicular, horizontal, oblique and apical which aid tooth-position and function (Cho & Garant, 2000). Sensory-nerve-fibres may also have a role in maintaining the periodontal ligament space and are closely associated with the cells rests of Malassez which, if lost, lead to a reduced periodontal width (Xiong et al., 2013).

The cells and vessels of the pulp can histologically be seen in distinct zones (Figure 2-10), and the pulp is usually composed of non-mineralised tissues. Four layers of tissue are described in the pulp, although there is debate the cell-free zone may be artificially created:

      • odontoblasts line the periphery
      • cell-free zone of Weil seen in the crown-pulp-tissue

• cell-rich zone

• central core of pulp.
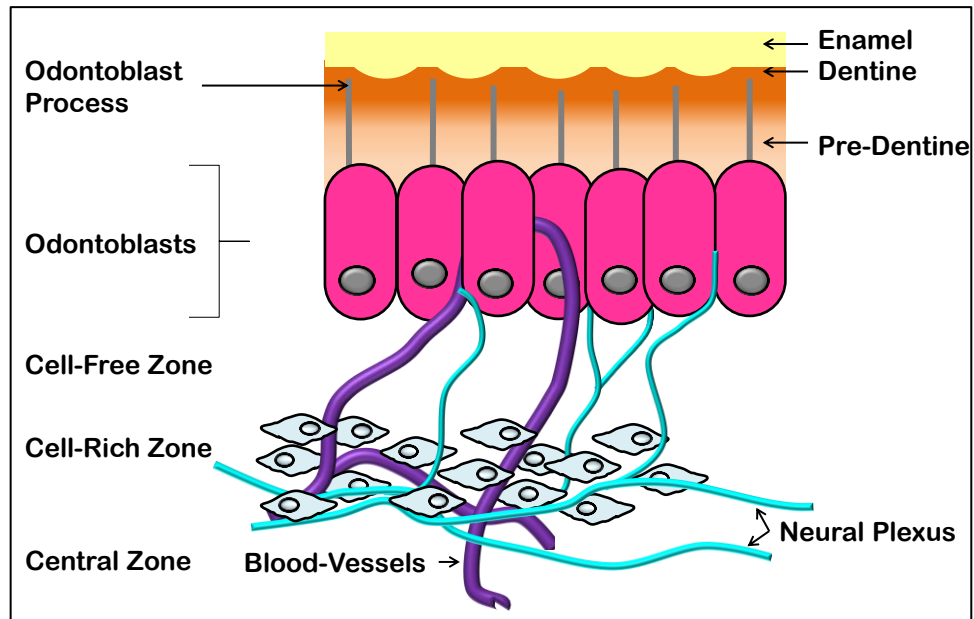
Figure 2-10 Schematic representation of pulp architecture showing enamel, dentine, pre-dentine with odontoblast processes, odontoblasts, cell-free, cell-rich and central zones

2.1.8.3 Innervation

Autonomic innervation (involuntary) of the periodontal ligament is still unknown, with no evidence of a parasympathetic supply, whereas the nerves associated with blood-vessels are thought to be sympathetic and may affect the blood-flow (Nanci, 2012). A rich sensory supply innervates the ligament from the trigeminal nerve (Van Steenberghe, 1979).

Stimulation of sensory receptors from the ligament of individual teeth is not guaranteed, as transfer of the stimulus to multiple teeth via the alveolar bone, tooth contact, liquid movement or the transseptal fibres is possible, which is important when undertaking percussion-tests for diagnostic purposes (Van Steenberghe, 1979; Trulsson, 2006). Directional preferences from stimuli are seen, with anterior teeth being sensitive in a greater number of planes, both vertically and horizontally, than posterior teeth (Trulsson, 2006).

2.1.8.4 Vascularity

The periodontal ligament is profusely vascularised, as seen in Figure 2-11 (Selliseth & Selvig, 1994), receiving blood primarily from the superior and inferior alveolar arteries (Kindlová, 1965; Schroeder & Listgarten, 1997;

Nanci, 2012) and also contributions from gingival blood-vessels from the facial artery (Matsuo & Takahashi, 2002).
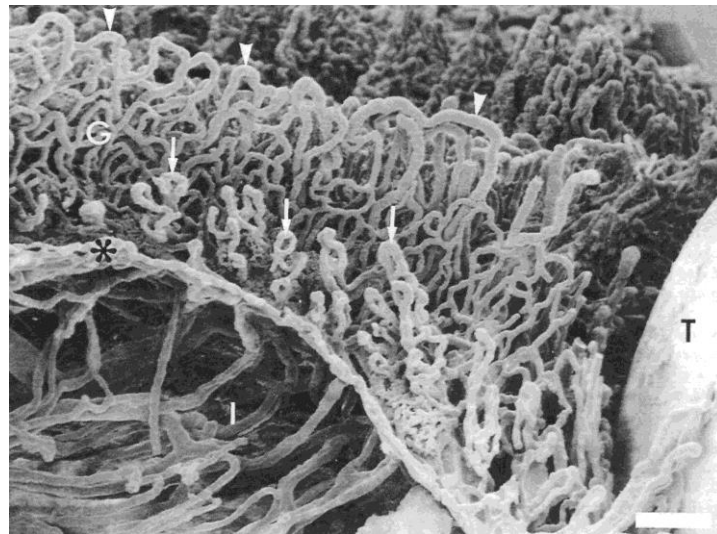
a.
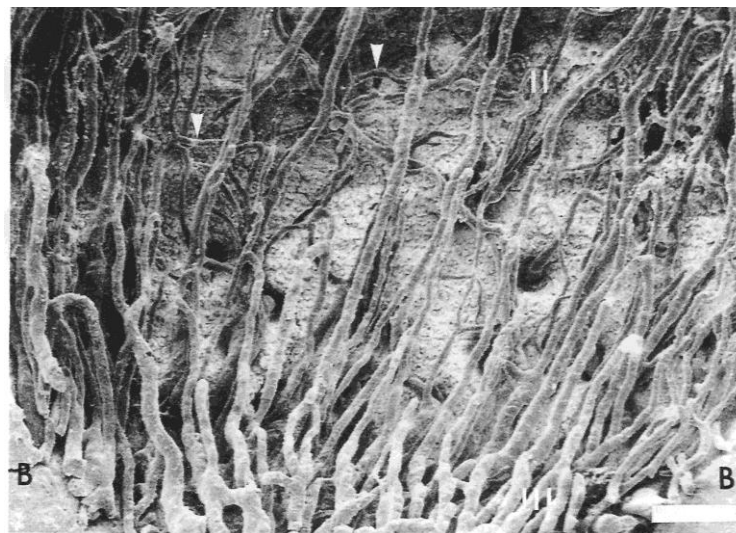
b.

Figure 2-11 Vasculature of the periodontal ligament (PDL).
a. Blood vessels of gingiva (G) and cervical part of PDL (I) following tooth-removal. Capillary loops shown by arrow-heads, and glomeruli-like structures shown by arrows. Second molar tooth (T). White magnification bar = 0.1mm.
b. Middle and apical segments of PDL. Vessel direction occluso-apical but transverse vessels shown by arrow-heads also common. Apically, vessels collect into a venular plexus. Alveolar Bone (B). White magnification bar = 0.1mm.
Reprinted from Journal of Periodontology 65, Selliseth NJ & Selvig KA, 1994. The Vasculature of the Periodontal Ligament: A Scanning Electron Microscopic Study Using Corrosion Casts in the Rat, 1079-1087, 1994. Figure 3 & 5, respectively. With permission from John Wiley and Sons 28th April, 2018. (Agreement in Appendix A.3.2).

The periodontal ligament has a polygonal mesh of vessels supplied by anastomoses with the gingival vascular network cervically, as well as vessels traversing Volkmann Canals, and also the pulp vessels apically (Matsuo & Takahashi, 2002). Each vessel has fine lateral branches which communicate horizontally with neighbouring vessels (Kindlova & Matena, 1962).

Vessels enter via Volkmann Canals of the alveolar bone at a density of 51 ± 8 per mm^2 which travel occluso-apically in the ligament. A two-layered vascular-structure is reported with the arterioles, venuoles and capillaries in the mid-section of the ligament, where the former two are found close to the alveolar-wall and the latter are found near the root-surface (Selliseth & Selvig, 1994).

The afferent capillaries are significantly smaller than the efferent capillaries and arterioles are significantly smaller than venules (Selliseth & Selvig, 1994). These are more abundant in posterior teeth than anterior, and mandibular teeth have a greater supply than maxilla. Single-rooted teeth have a greater supply in the gingival-third than the apical-third, which is greater than the central area (Nanci, 2012).

The presence, or absence, of valves is disputed, with few valves within the venous tissue of the bone being proposed (Matsuo & Takahashi, 2002), compared to no valves being found, allowing multidirectional flow in an equally-pressurised reservoir in the ligament (Selliseth & Selvig, 1994). There is a venous plexus apically, which may provide protection to the occlusal forces and, upon application of occlusal force, there may be an outflow of blood from the ligament vessels via the Volkmann Canals and into the bone-marrow. When reduced, a reverse effect allows inflow back to the periodontal network.

Cervical periodontal structures include the outer-gingiva with a network of vascular loops which have an increased diameter compared to the approaching or exiting capillaries (Selliseth & Selvig, 1994). Sulcus epithelium may have a flat capillary network or a glomeruli-like presentation of vascular vessels (Kindlova, 1970), with curved venous capillary loops which return to the facial vein (Hock & Nuki, 1971; Matsuo & Takahashi, 2002) and depends on gingival health. Good plaque-control presents flat capillaries (Matsuo & Takahashi, 2002), whereas, with poor oral hygiene and gingivitis, the vascular network is a convoluted, intertwined, glomeruli-like system (Egelberg, 1966; Matsuo & Takahashi, 2002).

Junctional epithelium comprises a squamous mesh of vessels with post-capillaries 7-40µm (Egelberg, 1966) which return to the alveolar bone as venules. Many vessels are fenestrated within the junctional epithelium to allow regular and easy exchange of substances across the vascular-wall. The interdental col is supplied from the capillary loops of the periodontal ligament and vessels of the crestal bone (Folke & Stallard, 1967).

The vascular supply to the pulp is also complex (Figure 2-12), with entry via the tooth-apex and accessory foramina and bifurcation-sites.
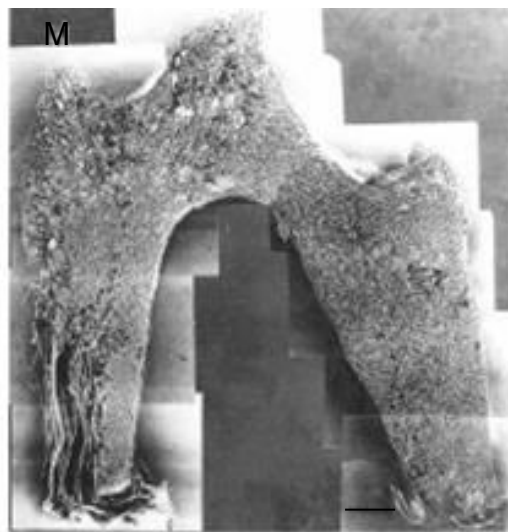
a.
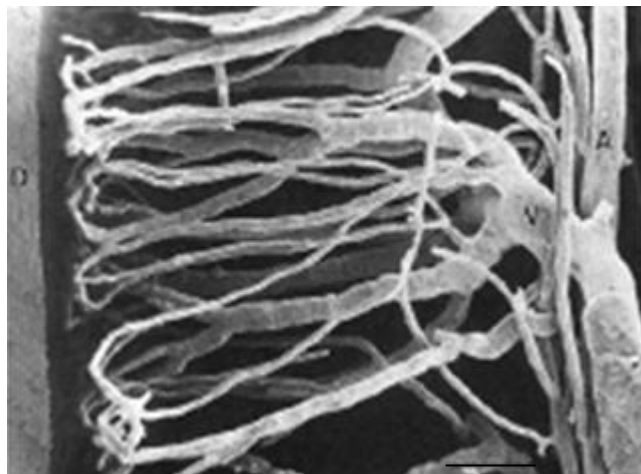
b.

Figure 2-12 Pulp vasculature.
      a. Vascular resin cast of pulp vessels in completed root.
      Black bar = 1mm
      b. Three layers of vascular-network of the pulp. Terminal
      capillary-network left next to the dentine (D). Central
      capillary-network in the middle, and venous network on the
      right. A = arteriole, V = venule, Black bar = 0.1mm
      a & b Reprinted from Journal of Endodontics, 16,

Takahashi K, Changes in the Pulp Vasculature During Inflammation, 92-97, 1990. With permission from Elsevier. (Agreement in Appendix A.3.3).

The main pulp arterial vessels are narrow (largest lumen 50µm), smooth-walled arterioles which travel towards the occlusal-surface centrally, branching to the subodontoblastic area (Matthews & Andrew, 1995). This provides a well-developed and extensive vascular supply of capillary loops on the outer-surface of the pulp close to the dentine, extending only a limited distance down the root. There may only be a plexus on one surface of the root - buccal - with larger vessels on the lingual (Adams 1959; Kramer 1960), which coincides with the presence or absence of odontoblasts. This is beneficial if a thermal signal could be detected buccally from the vascular supply.

Veins can be centrally-positioned (size of 150µm), with irregular walls, and many are found peripherally in the root-canal (Matthews & Andrews, 1995). Venous drainage heads towards the central vein, being apically-directed (Kramer 1960; Scheinin, 1963).

Direct arteriovenous anastomoses are found in the pulp, which is encased within dentine, preventing soft pulp-tissue from swelling. Arteriovenous shunts may aid the direction of flow to avoid potential strangulation and total necrosis of the pulp-tissue (Kramer, 1960). Additionally, venous-venous anastomoses and U-loops of arterioles are present which may act as pressure-regulators (Matthews & Andrews, 1995). Fenestrations of the capillaries have also been seen and reduce in number following completion of dentinogenesis (Matthews & Andrews, 1995). These adaptations may reduce the amount of blood travelling fully through the pulp, restricting the thermal supply.

The pulp vasculature continuously changes to accommodate its status, e.g., immature pulp requires a good vascular supply for growth, an infected pulp requires protection (see inflammation - Section 2.3.5), and an ageing pulp reduces so the vasculature reduces, with loss of the terminal capillary-network (Takahashi, 1990).

As seen, there may be thermal contributions from both the periodontal ligament and pulp due to their vascular supply. Transfer from the periodontal ligament may influence the rate of thermal change in a tooth. However, the energy needs to cross the cementum, traverse root-dentine and reach the crown of the tooth, which may not be the primary source of thermal energy detected.

2.1.8.5 Blood-Volume

Blood-volume ranges from 5-7% for the dog dental-pulp, which equates to the normal blood-volume for the whole human body (Kraintz & Conroy, 1960), although a vascular volume as low as 3% has been cited for the rat (Bletsa et al., 2006). Volumes are seen to be similar from left-to-right within the same animal, complying with bilateral morphological symmetry as seen with tooth-type, but will vary according to tooth-type. Canine mandibular teeth from dogs had the greatest volume at 0.04ml, compared to the lower central incisor of just 0.0004ml, (Kraintz & Conroy, 1960).

2.1.8.6 Pulp-Pressure

Pulp-pressures are cited as ranging from 35mmHg to 40mmHg for the capillary-pressure (Meyer, 1980). Arterioles of 10-70µm provided a pressure of 43mmHg, and venules of diameter 10-80µm provided 19.8mmHg. No difference in pressure was found between the coronal and apical tissues (Matthew & Andrews, 1995). This is dependent on the viscoelastic nature of the vessel-walls. The tissue-fluid-pressure is provided by the circulation in the pulp and a pressure of 15-30mmHg, which is relatively high, is recorded. It is also pulsatile, being in phase with the wave from the arterial pulse (Brown & Beveridge, 1966), the energy of which may also be influenced by the nature of the vessel-wall (Secomb, 2016). In inflammation, the interstitial pressure increases but only in the affected area – nowhere else – giving a pressure-difference of 8-10mmHg. Fluid may be returned to the capillaries in the non-inflamed areas.

2.1.8.7 Blood-Flow-Rate

The relevance of the blood-flow to this Study is its heating potential which is being investigated to determine tooth-vitality. Blood-flow is truly found from the soft-tissue of the pulp internally and the gingival tissue externally, as well as the mineralised tissue of bone, with an interstitial fluid-flow through the dentinal tissue.

The dentinal fluid-flow-rate is 18pl/s per mm^2 when measured from exposed dentine (Matthews & Andrew, 1995), which is so small it may be neglected when considering warming of the tooth.

Blood-flow for the human tooth in absolute units may be unknown (Park et al., 2010), which is consistent with searches undertaken in this Study. On-the-other-hand, no blood-flow in a tooth is cited in the database on Comprehensive Tissue Properties Provided for the Thermal Assessment of a Human at Rest (McIntosh & Anderson, 2010), which is not the case in a

healthy tooth. Confirmation of the presence of a blood-flow within the pulp has previously been explored, e.g., laser doppler and thermal imaging, yet there is still a sparsity of data reporting the actual blood-flow in human teeth, although animal models have provided data shown in Tables 2-12 and 2-13.

A variety of methodologies, (Tables 2-12 & 2-13), have reported the blood-flow-rate in the pulp which range from 2-146ml/min/100g. The pulp blood-flow-rate of the dog was reported to be 22.62ml/min/100g, higher than skeletal muscle and the systemic blood-flow-rate of ≈10 and ≈12ml/min/100g, respectively (Kim et al., 1980). Of the oral tissues, the pulp is claimed to have one of the highest blood-flow-rates (Kim et al., 1980) and, as such, the effect of the vascular supply to the periodontal ligament may be less important.

The first reported pulp blood-flow-rate as a measure of weight of pulp-tissue was presented by Meyer et al., (1964). An average value of 98ml/min/100g from the canine teeth of thirteen dogs was calculated. This measure was virtually five times that of Steiner & Mueller, (1961), who reported a flow of 20ml/min/100g for an assumed complete incisor from seventeen rats. It was not stated whether the mineralised tissue was included in the weight. 33ml/min/100mg was calculated by Meyer et al., (1964) for the complete canine tooth of a dog, still a 50% increase on Steiner & Mueller, (1961). Experimental differences must be acknowledged, i.e., a different tooth, a different species and a different measuring-method.

The blood-flow-rate in the root is half that of the coronal-tip-region of the pulp (Path & Mayer, 1980) and the coronal-tip-region has a flow-rate approximately twice that of the rest of the coronal portion, which is similar to the root and the total combined pulp (Meyer & Path, 1979). This is a positive finding for assessing the thermal transfer in the crown of the tooth, where there is the greatest recorded rate of blood-flow. Further work by Kim et al., (1983 and 1985) reiterated the presence of location-differences. A fast blood-flow-rate at the tip was reported to range from 82ml/min/100g (Kim et al., 1990) to 103ml/min/100g (Path & Meyer, 1980), compared to a slow central rate of 11ml/min/100g (Kim et al., 1985).

Differences between maxillary and mandibular teeth have also been shown, with a 25-50% increase in blood-flow-rate in maxillary teeth compared to mandibular teeth (de Leon et al., 1978; Path & Meyer, 1980) so, theoretically, the maxillary teeth may have greater thermal response. This is important, as trauma to teeth often affects the maxillary teeth more than the mandibular teeth.

Misreporting of Meyer (1993) has occurred by multiple authors who included the citation to represent a pulp blood-flow of 40-50ml/min/100g. However, it was a description relating to blood-flow, not presentation of blood-flow results (Yu & Abbott, 2007; Kodonas et al., 2009 and Braun et al., 2015) and, similarly, Matthews & Andrews (1995) is often quoted giving a blood-flow-rate of 40ml/min/100g. This is, in fact, an average of the work by five others (Tønder & Naess, 1978; Meyer & Path, 1979; Kim et al., 1984; Kim et al., 1986; Kim et al., 1990) rather than work they undertook. These two papers are often cited together.

The blood-flow-rate of the gingival tissue is also cited from similar animal studies and has a range of 41–82ml/min/100g which is within that of the dental pulp, and could influence the thermal findings in the crown of a tooth. The reported blood-flow-rate for alveolar bone is low at 9ml/min/100g (Kaplan et al., 1978) and, with the insulating properties of mineralised bone, this would appear unlikely to override the thermal contribution of the pulp when examining the crown of the tooth, especially as the periodontal ligament and a layer of cementum usually separates the tooth from bone.

The available data presents a blood-flow-rate which is clearly dependent on the pulp-weight, 100g of pulp-tissue being difficult to comprehend as it equates to a 4-ounce steak. Pulp-weight will vary for each tooth-type, as it will between species and, currently, the range of blood-flow-rates for each human tooth appears to be unknown and justifies further investigation.

Table 2-12 Animal studies used to investigate pulp and gingival blood-flow-rate (ml/min/100g tissue).

Author	Year	Animal (sample-size)	Method	Pulp Flow-Rate [SD/SEM] (ml/min/100g tissue)	Gingival Flow-Rate [SD/SEM] (ml/min/100g tissue)
Meyer, et al.	1964	Dog (13)	^{42}K isotope fraction	98 [7] pulp / 33 whole canine	·
Meyer	1970	Dog (7)	Isotope fraction & 25µm spheres	129 [13] max canine	41 [4] maxillary mucosa
Edwall & Kindlova	1971	Dog (39)	^{133}Xe, ^{131}I, ^{125}I tracers	2-14	·
Tönder & Aukland	1975	Dog (15)	H_2 desaturation	17.8 [6.2]	·
de Leon, et al.	1978	Dog (6)	Microsphere ^{85}Sr 15µm	61 [10] max, 43 [9] mand	·
Path & Meyer	1977	Dog (32)	^{86}Rb / 8µm / 15µm	63.4 / 60.8 / 104.6	82 (25µm microspheres)
Meyer & Path	1979	Dog (6) Dog (4)	H_2 / 8µm / 15µm total pulp H_2 / 8µm / 15µm coronal H_2 / 8µm / 15µm coronal tip	22 / 24 / 55 18 / 18 / 60 55 / 67 / 146	·
Path & Meyer	1980	Dog (9)	15µm microsphere coronal tip remaining coronal portion Root	103 max canine 77 mand canine 57 max canine 42 mand canine 52 max canine 39 mand canine	·
Kim, et al.	1980	Dog (14)	15µm radioactive microspheres	22.62 [2.63]	·
Kim, et al.	1983	Dog (21)	^{133}Xe washout	53.12 [3.12] fast / 8.86 [0.53] slow	·
Kim	1985		15µm microspheres/^{133}Xe	55.4 [2.9] peripheral/44.5 [5.8] fast 13.3 [0.6] central / 11.1 [1] slow	·
Kim, et al.	1986	Dog (6)	15µm microspheres ^{57}Co/^{46}Sc	41 [3.8] max & mand canine	·
Park, et al.	2010			33.32	·
Kim, et al.	1990	Dog (4)	^{133}Xe washout	82.4 [6] fast peripheral area	·
Tanaka & Kaneko	2001	Dog (14, 9)	15µm coloured microspheres	16.3 max canine, 16.5 mand canine	·
Liebman & Cosenza	1962	Dog (3)	Electrical impedance	0.06ml/min/canine	·
Steiner & Mueller	1961	Rat (17)	^{86}Rb isotope fraction	20 [8] whole incisor	·
Scheinin	1963	Rat	Corpuscle flow	1000-1500µm/sec arterioles 20-30µm 390-780µm/sec venules 40-80µm	·
Scott, et al.	1972	Rat (11)	Erythrocyte velocity	880µm/sec arterioles 20-40µm	·

Table 2-13 Animal studies used to investigate tissue blood-flow-rate and gingival blood-flow-rate (ml/min/100g tissue).

Author	Year	Animal (sample-size)	Method	Tissue Flow-Rate [SD/SEM] (ml/min/100g tissue)		Gingival Flow-Rate [SD/SEM] (ml/min/100g tissue)
Hock & Nuki	1976	Dog (4)	Erythrocyte velocity	·		1.59 [0.29] mm/sec healthy gingiva 32.1 [2.7] mm/sec healed 46.1 [5.3] mm/sec inflamed
Hock & kim	1987	Dog (4)	^{57}Co 15μm microspheres	·		51.1 [11.4] max healthy gingiva 48.7 [6.7] mand healthy gingiva
Özcan, et al.	1992	Human (9)	^{133}Xe washout	·		55 [13] max inflamed gingiva 54.7 [11.7] mand inflamed gingiva
Kaplan, et al.	1978	Dog (9)	15μm ^{141}Ce microspheres	Mandibular alveolar bone Mandibular basal bone Oral mucosa Gingiva Lip Tongue	9 [2] 4 [1] 20 [3] 49 [7] 16 [2] 15 [1]	

2.1.8.8 Pulp-Weight

Weights of animal pulps will vary depending on species, age, condition and tooth-type examined. In producing the data shown in Tables 2-12 and 2-13, many pulps were weighed but, unfortunately, none of that data was presented, preventing comparison between studies and teeth used (Meyer et al., 1964; Meyer, 1970; Path & Meyer, 1977; de Leon et al.,1978; Kim et al., 1980; Path & Meyer, 1980; Kim et al., 1986).

This makes it difficult to estimate a blood-flow-rate for any tooth-type and also for future research, as current knowledge of pulp-weight is limited, whether human or animal. Three articles were found which recorded weights of pulp-tissue, two of which were human teeth, with a weight of 9.4-269mg which, at most, is a quarter of a gramme (Table 2-14). The mean weight of pulp reported by Méndez & Zarzoza (1999) for third molars (13.1mg) was reported in their abstract as being for premolars. Unfortunately premolars, instead of molars, have been cited within other articles, e.g., Braun et al, (2015), which is misleading.

Table 2-14 Pulp-weight (mg) from dog and human teeth

Author	Year	Species	Age	Tooth (sample-size)	Pulp-Weight (mg)
Tanaka & Kaneko	2001	Dog	7-8m	Max L canine (13) Max R canine (14) Mand L canine (8) Mand R canine (10)	266 269 232 223
Méndez & Zarzoza	1999	Human	18-21yrs	Third molar	13.1 mean (4.33) (SD)
Van Amerongen, et al.	1983	Human	9-15yrs 20-40yrs	Premolar Third molar	9.4-51.2 9.4-51.2
m = Month; yrs = Years; Max = Maxillary; Mand = Mandibular; L = left; R = Right						

2.1.8.9 Factors Affecting Pulp Blood-Flow

Regulation of pulp blood-flow is a complex combination of responses from nerves and blood-vessels, some of which include distant and local factors:

Distant Factors

Both parasympathetic and sympathetic nerves may be involved in blood-flow-regulation. The sympathetic-system is more influential, causing vaso-constriction which can modify the response of sensory nerves, with loss of sensitivity if ischaemic. This may also offer an explanation for loss-of-pain when going to the dentist, as stress may induce vasoconstriction! However, the opposite can also occur, leading to greater pain (Olgart, 1996).

Local Factors

Local control, via intradental sensory nerves, results in vasodilation from C-fibres and A-delta fibres (Aδ fibres) which inhibits sympathetic vasoconstriction when painful stimuli are applied. Inhibition may last for hours following local trauma to the pulp-tissue, as seen from cavity-preparation, or application of heat or cold, which may give false-negative outcomes to vitality tests. Vasoconstriction may also be prevented from local release of vasodilators, e.g., Acetylcholine, Histamine, Bradykinin and Substance P, which are seen in early inflammation. Thus, a rise in blood-flow and pressure within the tooth may lead to toothache, with the characteristic pulsatile-effect if the patient bends over.

Temperature can influence the blood-flow. Applying a cool temperature to tissue can lead to vasoconstriction, with associated reduction in blood-flow to minimise the loss of body-heat (Ernst & Fialka, 1994). This may result from both the autonomic nervous-system and local hormonal effects (Lee et al., 1978). This proposed mechanism is due to increased affinity for noradrenalin by alpha adrenoreceptors and the depressor-effect on the contractile smooth muscle-tissues of the vessel-walls. With further reduction of temperature, the conduction of sympathetic impulses is affected, with slowing of transmission and reversal of the initial vasoconstriction leading to vasodilation. Following localised warming due to increased blood-flow, the nerve impulses recommence leading to the next phase of vasoconstriction (Lewis, 1930, Shepherd et al., 1983). This cycling-effect has been termed the 'hunting reaction'. Empirical evidence supports the reduction of blood-flow (Goodis et al., 2000) to be 62%, and associated with a raised pain-threshold of 46%. This reduction in blood-flow may also influence the potential re-warming of the tooth, even if vital.

2.1.8.10 Simulated Pulp Blood-Flow

There were no studies found reporting measurement of actual pulp blood-flow for the human and many studies have simulated blood-flow for a variety of reasons and there is wide variation in the rates used, as found in the literature, from 0.0042 to 25ml/min (Table 2-15). Calculation of blood-flow-rates presented were not always accurate (as seen by Braun et al, 2015), where a flow-rate of 6mls/min was overestimated:

Mean weight of wet pulp for third molar = 13.1mg Méndez & Zarzoza (1999)
Mean pulp blood-flow ml/min/100g   = 50   Kim (1985)
1g of pulp would have a blood-flow   = 50/100 = 0.5mls/min
13.1mg (0.0131g) pulp blood-flow   = 0.5 x 0.0131
                       = 0.0066ml/min/third molar.

Table 2-15 Simulated blood-flow-rates sourced from the literature

Simulated Blood-Flow-Rates in Human Teeth				
Author	**Year**	**Investigation**	**Tooth**	**Blood-Flow-Rates (ml/min)**
Ramoglu, et al.	2015	Light-curing	Maxillary Central I	0.026
Sari, et al.	2015	Bleaching	Maxillary Central I	0.026
Braun, et al.	2015	Laser-irradiation	Multi-rooted	0/3/6
Park, et al.	2010	Light-curing	Maxillary PM	0.0042/0.028/0.07
Kodonas, et al.	2009	Thermode	Incisor & Canine	0.5/1
Baik, et al.	2001	Bleaching	Maxillary Central I	0.026
Fanibunda	1985	Vitality	Maxillary & Mandibular PM	0.5 – 4
Niklas, et al.	2014	Photoplethysmo-graphy		25
I = Incisor; PM = Premolar				

This can impact on the findings and relevance to the human if the flow-rate is unrealistic. Much work has been undertaken on animal models but, as already presented, the anatomy of the human tooth and associated pulp may be different, with inappropriate comparisons to human pulp blood-flow. Park, et al., (2010) report the human pulp blood-flow as being unknown and used three arbitrary flow-rates of 0.0042, 0.028 and 0.070ml/min for their study, assessing intrapulp-temperature-changes from curing-lights. However, no formal calculation was presented and it was stated these were the flow-rates available on the pump (Park, et al., 2010). Maintenance of such low flow-rates in-vitro has been difficult and higher rates have been used, e.g., 0.5ml/min, which were abandoned in preference for 1ml/min (Kodonas, et al., 2009). The value of 0.026ml/min quoted for a human central incisor by Baik et al., (2001), as being described within the given reference (Kim et al., 1992), was not found within the stated reference. All these values are showing teeth have a low flow-rate of blood, and for this Study the question being asked is whether this low flow-rate is sufficient to provide warming of the tooth which is detectable in a timeline which distinguished it from a tooth without the blood-flow. This is also affected by the insulating properties of the mineralised tissue. It has been suggested this is so low it may not be detectable, or it could be swamped by other sources

of heat such as the gingival blood-flow, which is reported to flow at a similar rate (50ml/min/100g) by Özcan et al., (1992) who studied human gingival-tissue and Kaplan et al., (1978) who studied canine (dog) gingival blood-flow-rate.

2.2 Thermal Status of Teeth

2.2.1 Vascular Influence

From the above description, it can be seen the tooth has two main continuous vascular supplies which contribute to its thermal status when vital, i.e., the pulp and the periodontal ligament. The blood-flow-rate of each overlaps but there is a tendency for the pulp to be greater. The internal root-dentine surface-area will be less for direct pulp-contact compared to externally for the periodontal ligament (Figure 2-13), but it must be recognised the periodontal ligament actually has no direct contact with the external root-dentine as there is an additional, albeit very thin, insulating layer of cement. The gingival tissue sits against the neck of the tooth, rather than being attached to it, with a fluid-filled sulcus lying between the two tissues which may cool, rather than warm, the tooth. There is also additional direct pulp contact to the internal dentine-surface in the pulp-chamber of the crown of the tooth, whereas there is no contact in this region from the periodontal ligament. This may suggest the pulp has a greater tendency to influence the tooth-temperature than the periodontal ligament (Fanibunda, 1985). Conversely, it has been suggested the surrounding periodontal tissues are the major contributors of thermal energy to the tooth, as there was no significant difference in temperature between a vital and non-vital root-treated tooth (Goldberg & Brown, 1965; Brown & Goldberg, 1966). The tooth-temperature was also found to be higher in the same patients when the gingival tissue was inflamed, and lower when not (Shapiro & Ershoff, 1958). These tissues are active and will produce some energy from their normal metabolic activities - however, this is proposed to be a very small contribution to available thermal energy.
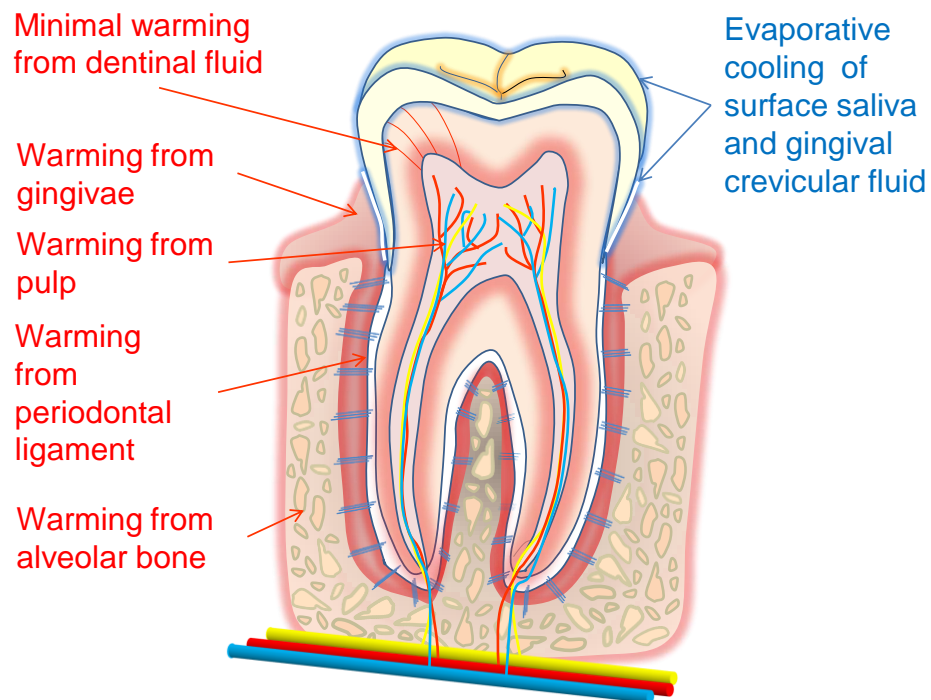
Figure 2-13 Thermal contributions to tooth-temperature.

Consideration also needs to be given to the cooling potential of evaporation of saliva if the mouth is open, and this could affect the whole crown as well as providing cooling of the gingival tissue.

2.2.2 Oral Soft-Tissue Influence

Figure 2-14 shows additional potential contributions to tooth-temperature - such as the surrounding cheeks, lips and tongue – which, primarily, have a warming-effect with an average mouth-temperature of $34^{\circ}C$ (Longman & Pearson, 1987), but cooling via evaporation from these tissues may drop the temperature of the oral environment. During swallowing, tongue movement makes contact with the teeth but this is a temporary change and the moment of contact may be insufficient to change the tooth-temperature for any period of time.
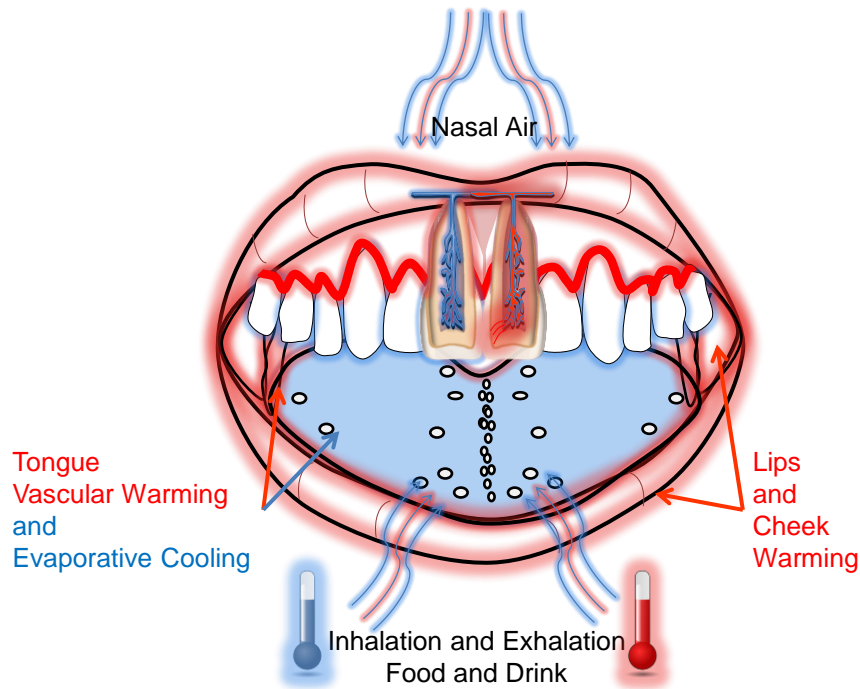
Figure 2-14 Thermal energy contributions to tooth-temperature.

2.2.3 Ingested Food and Drink Influence

Ingestion of hot and cold food instantly changes the temperature of the mouth and impacts on the surfaces of teeth. 74°C was reported as the maximum comfortable drinking-temperature for fluid, although $55\text{-}68^{\circ}$C was more normal (Longman & Pearson, 1987). The vital pulp is protected by the insulating mineralised tissue and the greatest temperature-change from drinking was recorded labially on the central incisors, followed by the palatal of the canines and premolars. A change in tooth-temperature did not go above 20°C when drinking fluid at 52°C in the Longman and Pearson study (1987). A comfortable drinking-temperature as high as 77.4°C (mean 65°C), and as low as 0.4°C (mean 1.62°C), was found from imbibing hot and cold fluid by Barclay et al., (2005), leading to tooth-temperatures as high as 70°C on the palatal surfaces of the upper anterior teeth and buccal surfaces of the lower incisors, and as low as 0°C on the same surfaces. Youngson & Barclay, (2000) found the lingual surfaces of the lower incisors to be the site of maximum temperature (68°C) following drinking coffee, and the palatal surfaces of the upper incisors to record the lowest temperature (15.4°C) when drinking orange-juice at 6°C. The tooth-temperature thus varies considerably depending on the ingested food and drink, but the tooth is able to adapt to such changes.

2.2.4 Inhalation and Exhalation Influence

As living beings, there is a need to breathe - inhaling and exhaling - and this may also have a cooling or warming-effect, depending on the ambient temperature. Mouth-breathing at an ambient temperature of -10°C resulted in a tooth-temperature of 17°C, and at -30°C resulted in 10°C (Beynon, 1973) and hairline-cracks were found in enamel of the anterior teeth. Under these conditions, there was no difference in vital and non-vital tooth-surface-temperature. Despite such low temperatures, the teeth maintained an external surface-temperature above freezing, protecting the pulp.

2.2.5 Tooth-Temperature

The baseline-temperature of the teeth varies with location in the mouth, being hotter posteriorly ($\approx$36^{o}C for molars) and cooler anteriorly with the mouth open ($\approx$29°C for incisors) (Goldberg & Brown, 1965; Brown & Goldberg, 1966; Crandell & Hill, 1966; Fanibunda, 1986b). An average labial tooth-temperature for the six anterior teeth (canine-to-canine) was cited as 30.6^{o}C when the mouth was open, and 37°C when closed, with a 0.4^{o}C increase in temperature palatally, and no difference was seen between vital and non-vital teeth (Brown & Goldberg, 1966). However, Banes & Hammond, (1978), reported the surface-temperature of vital teeth being warmer (29 to 35°C) than their non-vital counterparts (28 to 33°C). Unfortunately, the tooth-type was not recorded in their study.

A temperature differential from the gingival-margin to the incisal-edge was recorded, indicating the gingival region was warmer by 1.28^{o}C (Kells et al., 2000b), and 2.5^{o}C (Pogrel et al., 1989). However, this was an arithmetical error by Pogrel et al., (1989) as the gingival region was 29°C and the incisal-edge was 27.5^{o}C, giving a gradient of 1.5^{o}C, which is much closer to that found by Kells et al., 2000b. The warmest area of the tooth has been reported to be the central gingival region (Shapiro & Ershoff, 1958).

Within the human body there is reported thermal symmetry with variation ranging up to 0.4^{o}C (Vardasca et al., 2012), and this may also be the case for teeth without external contributions.

The oral and dental thermal environment is complex, with multiple factors influencing tooth-temperature. The tooth-structure is also very complex (as previously described) and the vascular contributions associated with maintaining a warm temperature to the tooth relate mainly to the pulp and periodontal ligament - the former being of greatest interest to this Study, and whose contribution to tooth-temperature, if it can be detected, may provide a

vitality test for the tooth. A vitality test may be needed to assess the status of a tooth which may have endured a physiological process, such as tooth-wear; a pathological disease, such as dental caries or periodontal disease; or a traumatic injury, to aid appropriate treatment-planning.

2.3 Tooth and Pulp Injury Leading to Loss-of-Vitality

Tooth and pulp injury may occur in many ways with potential loss-of-vitality.

2.3.1 Mechanical Injury

Normal physiological use of teeth leads to wear and loss of tooth-tissue, which may lead to cracks, fractures, attrition, abrasion and abfraction of the mineralised tissues, making the underlying pulp more vulnerable.

Accidental dental trauma accounts for 5% of all injuries affecting the whole population. Trauma to permanent teeth has been sustained by 25% of school-age children and 33% of adults, often before reaching 19 years (DiAngelis et al., 2012). These injuries are complex to manage, requiring careful diagnosis, planning and follow-up, which includes assessing pulp-vitality. Sensibility tests may not initiate a pulp-response immediately following trauma, often being dependent on a neural response which may initially be impaired (Table 2-16). Every effort should be made to keep pulp-vitality, especially in the immature permanent tooth where root-formation may be incomplete. Apical blood-vessels may be compressed following trauma - temporarily or permanently - resulting in pulp-necrosis unless revascularisation occurs, which is a possibility in immature teeth. Trauma to a young tooth may also lead to compression of the nerve-supply which may be temporarily affected, providing no response to sensibility tests.

Teeth may also be totally displaced (avulsed), a serious injury accounting for 0.5-3% of all dental injuries, with the long-term prognosis being dependent on timing and treatment received, which is often recommended to be replantation of the tooth (Andersson et al., 2012). Stage of root-completion and periodontal ligament status are important considerations. An immature root with an open apex may see revascularisation of the pulp and risk of tooth-resorption must not be forgotten.

Table 2-16 Types of traumatic fractures of permanent teeth and alveolar bone with anticipated outcome pulp testing – adapted from DiAngelis et al., 2012; Andersson et al, 2012.

Traumatic Dental Injury	Clinical Appearance	Pulp Test
Infraction	Crack of enamel, no loss of tissue	Positive if previously vital
Enamel-fracture	Loss of enamel only	Positive if previously vital
Enamel-dentine-fracture	Loss of enamel & dentine	Positive if previously vital
Enamel-dentine-pulp-fracture	Loss of enamel & dentine with pulp-exposure	Positive if previously vital
Crown-root-fracture	Fracture of enamel, dentine, cementum	Usually positive for remaining root-portion
Crown-root-pulp-fracture	Fracture of enamel, dentine, cementum exposing pulp	Usually positive for remaining root-portion
Root-fracture	Mobile crown, with or without displacement	May be negative for 3 months – transient/ permanent neural damage
Alveolar-fracture	Mobility of single or multiple teeth, with possible occlusal changes	Positive or negative findings possible up to 3 months
Concussion	No change visibly, no mobility but tender-to-touch	Probably positive, negative possible up to 3 months, monitor for 1 year
Subluxation	No displacement but mobile and tender-to-touch	Initially negative up to 3 months, potentially followed by positive
Extrusive luxation	Mobile and elongated from extrusion	Probably negative, with false negative potentially for 3 months, monitor
Lateral luxation	Displacement, usually inward or outward, immobile	Negative likely, negative potentially for 3 months, monitor
Intrusive luxation	Displaced into tooth-socket, immobile	Negative likely
Avulsion	Tooth displaced out of socket	Negative but revascularisation may occur

Injury of primary teeth poses a potential risk to the underlying permanent tooth and may result in impaction, malformation or delayed eruption of the permanent tooth. Reimplantation is not recommended for primary teeth to reduce such risks, and there is no agreement on treating the traumatised primary dentition. Reliability of sensibility tests in primary teeth is not good and, depending on the co-operation of the child, tooth-removal may be the best option (Malmgren et al., 2012).

Iatrogenic injury from dental treatment, such as cavity and crown-preparation, generates heat which may cause dehydration and/or inadvertently expose the pulp (Bergenholtz, 1990; Brännström, 1996), and up to 19% of vital teeth showed signs of periapical disease following crown-preparation (Saunders & Saunders, 1998).

2.3.2 Microbial Injury

Tooth and pulp injury may occur from microbial penetration via the crown, following trauma or due to caries, or via the root as periodontal disease. In the absence of microbes, an exposed pulp can heal without abscess-formation and minimal pulp-inflammation (Kakehashi, 1965).

If an irritant is found and removed, such as caries, the acute inflammation of the pulp may be confined and localised (Heyeraas & Kvinnsland, 1992), enabling healing of a reversible pulpitis which may be prior to any short, sharp symptoms from pulp Aδ fibres. Special tests, such as radiographs, may provide additional information to locate the cause if symptoms are reported – however, they give no direct indication of pulp-health.

The pulp may endure multiple phases of irritation, leading to chronic inflammation, irreversible pulpitis and possible necrosis. The symptoms may be a spontaneous, dull, throbbing ache from pulp C-fibres, lasting minutes to hours, rather than seconds. Sometimes, no pain is reported.

2.3.3 Chemical Injury

Bacterial toxins may diffuse through the dentinal tubules and cause pulp irritation prior to bacteria reaching the pulp. Food and drink may be erosive, e.g., fruit-juices and fizzy drinks, leading to the loss of tooth-tissue, reducing pulp protection (Lussi et al., 2004).

Irritation of the pulp from restorative materials was once thought to occur - however, this is not the case (Brännström & Nordenvall, 1978 and Watts, 1979) and it has been shown to be due to microbial-leakage rather than the material itself (Cox, 1987; Bergenholtz, 1990).

2.3.4 Thermal Injury

Normal food-and-liquid-consumption may expose the oral environment, including the teeth, of a human to temperatures between 0°C and 74°C, as previously described (Longman & Pearson, 1987; Youngson & Barclay, 2000), producing a thermal gradient across the tooth (Jacobs et al., 1973). This occurs multiple times every day for most humans, unlike animals who do not actively heat or cool their food. Over time, this leads to thermal-fatigue in enamel which can crack and is unable to repair itself (Brown, et al., 1972). This has been observed at a temperature-difference of 28°C from the normal oral temperature, which is within the temperature-range (0-74°C) of food and drink (Brown, et al.,1970; Jacobs, 1973).

Exposure to seasonal temperature-changes on the anterior teeth can occur from breathing through an open mouth. When this occurs repeatedly in an extreme climate, e.g., in the Antarctic, the number of cracks in teeth increase, which may splinter and fragment. This could be due to freezing of water within the teeth (but at temperatures above zero this is unlikely) and is more likely from dehydration in the cold environment with low relative humidity.

Dental treatment may induce intra-pulp temperature-increases of $33^{o}C$ from hand-pieces (Henschel, 1943), although modern techniques with water-coolant reduce this. Bleaching with light/laser-assistance may reach temperature-increases of $16^{o}C$, and light-curing may lead to temperature-increases of $7.8^{o}C$ (Bouillaguet et al., 2005), whereas the use of lasers can cause temperature-increases of $24.7^{o}C$ intra-pulpally.

Temperature-increases of $5.5^{o}C$ and $11.1^{o}C$ in the pulp of Rhesus Monkeys led to irreversible pulpitis of 15% and 60% respectively, (Zach & Cohen, 1965; Zach, 1972) and $41.5^{o}C$ has been reported as the threshold for initiating pulp-inflammation. Paired human teeth have been exposed to thermal stimuli (Baldissara et al, 1997), both in-vivo and in-vitro, whereby it took between 115–220 seconds to reach a maximum increase in temperature of between $8.9\text{-}14.7^{o}C$ above the baseline-temperature of $34^{o}C$. Pain was reported at an average temperature of $44.6^{o}C$ ($39.5^{o}C$ to $50.4^{o}C$), which is in-keeping with other studies quoting $45^{o}C$ as a pain-threshold. No cellular injury was seen from an increase of $11.2^{o}C$ or tissue-necrosis, nor was there any evidence of protective activity from the odontoblasts, unlike Langeland (1959) and Zach and Cohen, (1965). There was no indication of thermal trauma (Baldissara et al, 1997). The speed of application of the traumatic stimulus may be important for a pain-response, as the tooth does not have time to adapt. Additionally, pulp blood-flow may remove heat before it has chance to damage the tissues (Goodis, et al., 1988; Baldissara et al., 1997). The extent of this buffering-capacity of temperature by blood-flow has been recorded as $1.3^{o}C$ on anaesthetised human teeth, and higher if not anaesthetised as blood-flow may be doubled (Baldissara et al., 1997).

Heat-stimulation may result in two responses - one from the quick-acting Aδ fibres of a sharp pain from a pulp-increase of $0.6^{o}C$, and amelodentinal junction temperature-increase of $11.7^{o}C$; or from the slow-acting C-fibres if heat is applied to increase temperatures beyond this (Närhi et al., 1982).

2.3.5 Pulp-Inflammation

Any of the above injuries could damage the pulp, resulting in symptoms which may be reversible or irreversible. Symptoms may not always be due to an inflammatory response - as seen from sensitivity of exposed dentine caused by dentinal-fluid-movement stimulating the Aδ fibres of the pulp, triggering a short, sharp pain commensurate with the hydrodynamic theory of dentine-sensitivity (Brännström, 1966).

Pulp injury leading to an inflammatory response (Figure 2-15) may be acute, chronic or lead to total necrosis. Inflammation is often protective and usually leads to vasodilation with increased blood-flow (Heyeraas & Kvinnsland, 1992), which, in the pulp, is likely to be transient. Erythrocytes accumulate centrally in the vessel and polymorphonuclear leukocytes undergo margination, leading to stasis. Increased permeability allows fluid-exchange, resulting in oedema and tissue-pressure-changes, which could be detrimental within the mineralised tooth. Strangulation of the apical blood-vessels during the inflammatory process was of concern within the tooth - however, this is not the case (Van Hassel, 1971) and the effect may be localised, avoiding adverse consequence on the whole pulp (Van Hassel, 1971; Tønder & Kvinnsland, 1983). Feedback mechanisms control pressure within the tooth which may be due to absorption and use of the lymph-flow which has been agreed to exist in the tooth (Heyeraas, 1989; Bishop & Malhotra, 1990). Additionally, pulp-arterio-venus-shunts (Kramer, 1960; Meyer & Path 1979; Takahashi, 1985) may reduce coronal-flow due to a fall in perfusion-pressure and the apical tissue may 'steal' the coronal blood-flow. If the pressure exceeds that of the venules they may be compressed, increasing flow-resistance, with stagnation a real possibility. This can damage localised areas, which may ultimately coalesce leading to total necrosis of the pulp-tissue (Kim, 1985; Heyeraas & Kvinnsland, 1992; Yu & Abbott, 2007).

Treatment

Caries

Microbial

Trauma

Chemical

Irritates Pulp → Cell-Damage → Histamine Bradykinin Serotonin

Inflammation

Vasodilation

↑Blood-Flow

Stasis

↑ Permeability

↑ Pressure

Venules Compressed

↓ Blood-Flow

Stagnates

↑ CO_2 + ↓pH

Necrosis
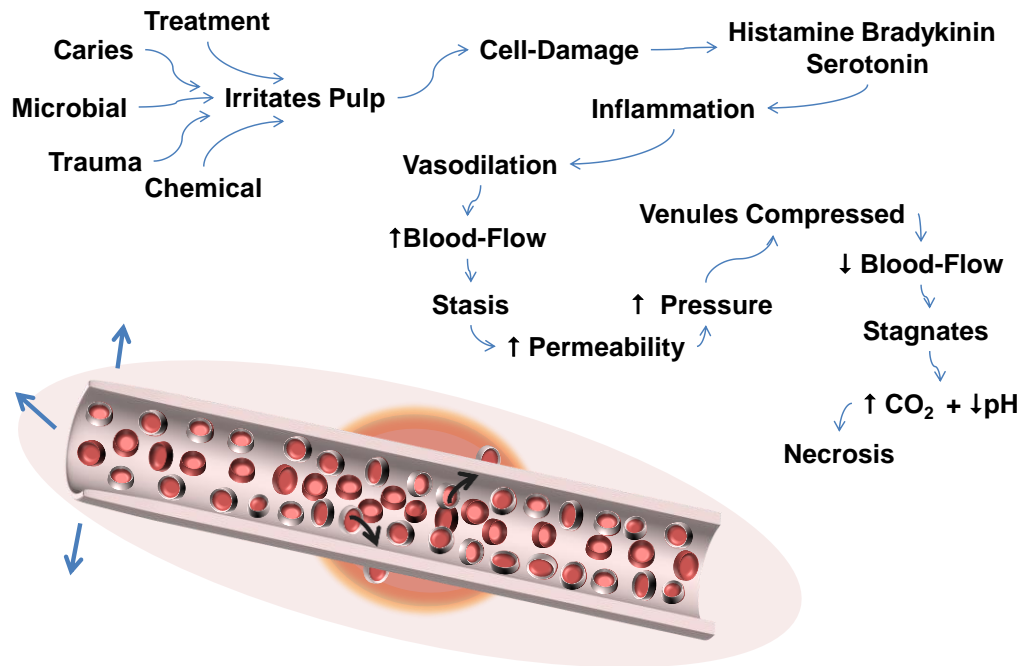
Figure 2-15 Inflammatory-response of pulp.

Reported patient-symptoms do not always relate well to the actual condition of the pulp and makes diagnosis very difficult. A non-vital tooth may be found by chance without symptoms (Baldissara et al., 1997), or a multi-rooted tooth may have one canal with necrotic tissue, whereas the other canals may be healthy. A histological approach confirms its status but this is not clinically feasible and a combined approach to gather as much information as possible aids the clinical decision-making process (Dummer et al., 1980; Rowe & Pitt Ford, 1990).

Data-gathering to establish the health and vitality of a tooth should include a thorough history, a clinical examination and, if the precise location and cause of the problem cannot be identified, special investigations may be needed.

2.4 Special Investigations

Special investigations, such as tooth-images, percussion-tests, photographs, study-models, pulp tests (sensibility tests, test-cavities and vitality tests), aid diagnosis, with variable outcomes (Table 2-17). The commonest pulp tests are sensitivity/sensibility tests, e.g., electrical or thermal (cold and heat-application) (Gopikrishna, et al., 2009). Sometimes test-cavities are undertaken but neither the sensibility tests or the test-cavities provide

information on the vitality of the pulp (Jafarzadeh & Abbot, 2010b) and may not only be painful, but subjective, giving false-positive or negative results.

A sensibility test assesses the ability of the nerve fibres within the pulp to respond to a stimulus applied to the tooth, whereas a vitality test assesses the pulp blood-flow.

Other pulp tests, e.g., Laser Doppler Flowmetry, Pulse Oximetry, Photoplethysmography, Spectrophotometry, Transmitted Laser-Light, Transillumination, Ultraviolet-Light Photography and Surface-Temperature-Measurement, use electromagnetic radiation to determine pulp-vitality.

2.4.1 Electrical Pulp Test

The electrical pulp test applies a low-grade current to the tooth, which is slowly increased for patient comfort (Rowe & Pitt Ford, 1990), directly stimulating low-threshold Aδ fibres. Quantitative values can be recorded, e.g., 0-80, when the patient responds. Comparison between visits is possible but outcomes are unreliable, with sensitivity between 0.21 and 0.94 (Dummer et al.,1980; Georgopoulou et al.,1989, respectively) and accuracy between 75% and 98% (Jespersen et al., 2014; Chen & Abbot et al., 2011, respectively).

Immature-developing-teeth may not have Aδ fibres until 5 years post-eruption (Chen & Abbot, 2009) and thus may not respond in young children prone to traumatic injuries previously described. Review is important and early intervention may result in unnecessary treatment (Assaf et al., 2015). The electrical pulp test is more suited to older teeth, being more favourable than cold tests, as it does not depend on dentinal-fluid-movement which is much-reduced in the mature dentition (Jafarzadeh & Abbott, 2010b). Necrotic pulp-tissue of any age contains electrolytes which can conduct to nerves deeper in the pulp-space, resulting in a false-positive response (Apfel & Gerstein, 1973).

Natural tooth is required for contact, ideally made over the thinnest mineralised tooth-tissue and where the greatest number of nerve-fibres are found, e.g., pulp-horn for the young tooth and cervically for the mature tooth, but this can vary with tooth-type (Rowe & Pitt Ford, 1990; Levin, 2013), e.g., the biting-edge is ideal for incisors, whereas the mesiobuccal-cusp is best for molars (Gopikrishna, et al., 2009). The teeth should be dry, otherwise adjacent teeth may respond, leading to false-positive outcomes.

The requirement of a conducting-medium is debated - Mickel, et al., (2006) prefer it, whereas Martin et al., (1969) claimed it made no difference. Any

relationship to pulp-histology and associated blood-supply to the outcome of an electrical pulp test is inconclusive (Jafarzadeh & Abbott, 2010b). However, a significant relationship is present to necrotic pulp-tissue which fails to respond (Seltzer, 1963).

2.4.2 Thermal Tests

Thermal tests, warm or cold, initiate expansion or contraction of mineralised tissues, causing dentinal-fluid-movement triggering Aδ fibres (Brännström, 1966). As with the electrical-test, no information on vitality is gleaned.

2.4.2.1 Cold Test

A cold test is the commonest, being applied by a variety of coolants, e.g., ice, ethyl chloride, CO_2 snow (Chen & Abbott, 2009). Test sensitivity ranges from 0.35 to 1 with unreliable results similar to the electrical-test, but an accuracy of 83% to 97% can be achieved (Weisleder et al., 2009; Chen & Abbot et al., 2011). It is low-cost compared to the electrical-test, as no expensive equipment is needed and it is easy to undertake. The outcome is subjective, being reported by the patient like the electrical-test but, unlike the electrical-test, it is unquantifiable (Gopikrishna et al., 2009). The length of application and temperature of coolant is variable, making reproducible testing unlikely. Application of $-22^{o}C$ reduced tooth-temperature to $11^{o}C$ without damage, but length of time of application was not reported (Jafarzadeh & Abbott, 2010a). A three minute application at $-80^{o}C$ produced a pulp-temperature between 0 and $-30^{o}C$ but the pulp remained alive. A response within five seconds is normal; or two seconds for dry-ice, which allows more accurate placement, avoiding transfer to adjacent teeth. Cold can be used on crowned-teeth if metal and it is quick and simple. However, in older teeth with increased dentine-thickness, dry-ice may not be as effective.

2.4.2.2 Heat Test

Aδ fibres may be stimulated following expansion of fluid in dentinal tubules or C-fibres may be triggered if the pulp is inflamed or partially necrotic.

Heat-sources include: hot gutta-percha ($120-140^{o}C$), hot-water-baths, warmed instruments or electrical heat-sources (Levin, 2013). Isolation is needed, as is maintenance of the heat-source. Application for two seconds is suggested to be sufficient, and five seconds maximum. Location is important as per the cold test, middle-cervical labial tissue-thickness is the least (Peters et al., 1994; Ruddle 2002). Heat-transfer to the pulp is needed, favouring the large pulp of a young tooth with less mineralised tissue.

Temperature of hot gutta-percha may be variable and it is unreliable – with a reported sensitivity of 0.59 to 1 (Johnson et al., 1970; Dummer, 1980).

Ideally, pulp tests need to be simple, quick, cheap, non-invasive, pain-free, objective, accurate, reproducible and standardised which, currently, they are not. It must be remembered sensibility tests provide no indication of the vitality of the tooth (Jafarzadeh & Abbott, 2010a&b).

2.4.3 Test-Cavity

A cavity is cut into dentine, without local anaesthetic, to initiate a response from the patient (Rowe & Pitt Ford, 1990), which is irreversible and destructive without evidence of its effectiveness (Gopikrishna et al., 2009).

Table 2-17 Pulp Tests: a. sensibility test, b. sensibility and vitality tests with associated sensitivity, specificity, positive predictive value, negative predictive value and accuracy.

a. Sensibility tests

Test	Author	Year	Teeth	Sensitivity	Specificity	PPV	NPV	Accuracy
Electrical Pulp Test	Fuss, et al.	1986	PMs	·	0.90	·	·	·
	Peters, et al.	1994	All	0.60	·	·	·	·
	Petersson, et al.	1999	Various	0.72	0.93	0.88	0.84	0.81
	Evans, et al.	1999	Anterior	0.87	0.96	·	·	·
	Gopikrishna, et al.	2007	80 Anterior	0.71	0.92	0.91	0.74	0.81
	Georgopoulou & Kerani	1989	Various	0.94	0.73	·	·	·
	Seltzer, et al.	1963	166 Various	0.72	0.92	·	·	·
	Johnson, et al.	1970	361 Various	0.57	0.99	·	·	·
	Dummer, et al.	1980	75 Various	0.21	1	·	·	·
	Kamburoğlu & Paksoy	2005	93 Various	0.84	0.96	·	·	·
	Weisleder, et al.	2009	150 Various	0.75	0.92	0.83	0.87	0.81
	Jespersen, et al.	2014	656 Various	0.84	0.74	0.58	0.90	0.75
	Karayilmaz & Kirzioğlu	2011	59 Anterior	0.92	0.88	·	·	·
	Villa-Chávez, et al.	2013	110 Various	0.76	1	1	0.83	0.89
	Chen & Abbot	2011	121 Various	·	·	·	·	0.98
CO$_2$ Snow	Fuss, et al.	1986	PMs	·	0.97	·	·	·
	Peters, et al.	1994	All	0.94	·	·	·	·
CO$_2$	Weisleder, et al.	2009	150 Various	0.89	0.76	0.93	0.74	0.83
	Chen & Abbot	2011	121 Various	·	·	·	·	0.97
Dichlorodifluoromethane	Fuss, et al.	1986	PMs	·	0.99	·	·	·
Ethyl Chloride	Fuss, et al.	1986	PMs	·	0.49	·	·	·
	Petersson, et al.	1999	Various	0.83	0.93	0.89	0.90	0.86
	Evans, et al.	1999	Anterior	0.92	0.89	·	·	·
	Dummer, et al.	1980	75 Adult	0.68	0.70	·	·	·
	Johnson, et al.	1970	361 Various	0.35	0.49	·	·	·

b. Sensibility tests continued, and vitality tests of laser doppler and pulse oximetry

Test	Author	Year	Teeth	Sensitivity	Specificity	PPV	NPV	Accuracy
Tetrafluoroethane Spray	Gopikrishna, et al.	2007	80 Anterior	0.81	0.92	0.92	0.81	0.86
	Weisleder, et al.	2009	150 Various	0.92	0.76	.	.	.
	Jespersen, et al.	2014	656 Various	0.92	0.90	0.86	0.94	0.90
	Villa-Chávez, et al.	2013	110 Various	0.88	1	1	0.90	0.94
Butan-Propan Gas	Kamburoğlu & Paksoy	2005	93 Various	0.93	0.98	.	.	.
	Chen & Abbot	2011	121 Various	.	.	.	.	0.91
Ice-Stick	Fuss, et al.	1986	PMs	.	0.33	.	.	.
Ice	Georgopoulou & Kerani	1989	Various	1	0.62	.	.	.
	Chen & Abbot	2011	121 Various	.	.	.	.	0.85
Hot Gutta-Percha	Petersson, et al.	1999	Various	0.86	0.41	0.48	0.83	0.71
	Dummer, et al.	1980	75 Adult	0.95	0.41	.	.	.
	Georgopoulou & Kerani	1989	Various	1	0.66	.	.	.
	Johnson, et al.	1970	361 Various	0.59	0.39	.	.	.
	Villa-Chávez, et al.	2013	110 Various	0.86	1	1	0.89	0.93
Laser Doppler	Evans, et al.	1999	Anterior	1	1	.	.	.
	Karayilmaz & Kirzioğlu	2011	59 Anterior	1	1	.	.	.
	Chen & Abbot	2011	121 Various	.	.	.	.	0.96
Pulse Oximetry	Gopikrishna, et al.	2007	80 Anterior	1	0.95	0.95	1	.
	Karayilmaz & Kirzioğlu	2011	59 Anterior	0.81	0.95	.	.	.

Sensitivity = Reports how good the test is at correctly detecting a healthy pulp (a/a+c)	Test	Known Outcome	
Specificity = Reports how good the test is at correctly detecting an unhealthy pulp (d/b+d)		+	-	Total
Positive Predictive Value (PPV) = Reports the probability of a healthy pulp being healthy (a/a+b)	+	a	b	a+b
Negative Predictive Value (NPV) = Reports the probability of an unhealthy pulp being unhealthy (d/c+d)	-	c	d	c+d
Accuracy = Reports the proportion of tests which give the correct outcome (a+d)/(a+b+c+d)	Total	a+c	b+d	a+b+c+d

2.4.4 Special Tests From The Electromagnetic Spectrum

One of the most common dental imaging modalities, X-rays, unfortunately contributes little information on the status of the pulp and its vascularity. However, they can show signs of the possible causes or consequences of pulp-disease, such as dental caries or apical radiolucency, and contribute to the larger picture when assimilating information to make a diagnosis. For vitality testing, the range of modalities through the electromagnetic spectrum will be considered.
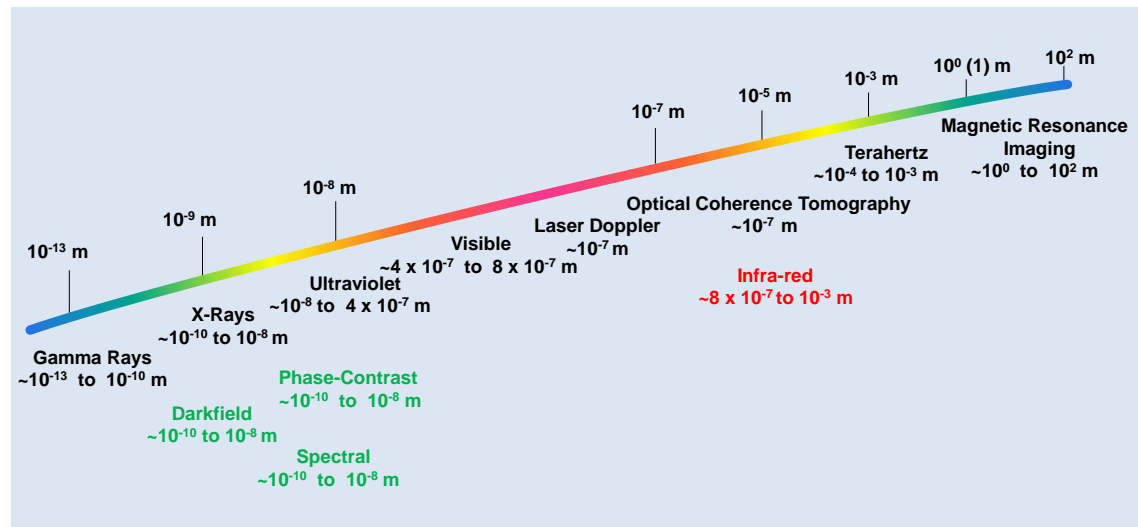
Figure 2-16 Imaging modalities of the electromagnetic spectrum.

Electromagnetic radiation is an energy quantified by the photon, which is portrayed as a particle without mass which carries the electromagnetic force (Close, 2012). It can be characterised by wavelength and frequency. There are many regions of interest for imaging techniques (Figure 2-16). Electromagnetic radiation has the ability to travel through solid, liquid or gaseous matter as well as free-space (where there is no matter), which differentiates it from sound-waves which need matter and are mechanical waves of pressure. Intra-oral ultrasound probes are being developed and there is a possibility that, due to the pulsatile nature of pulp-vascularity, doppler imaging might be an alternative method for imaging vitality (Yoon et al., 2010; Szopinski & Regulski, 2013). No mechanical explanation has ever been presented for the transfer of electromagnetic radiation (Harman, 1982) despite early philosophies by James Clerk Maxwell with reference to particles of the ether, which were later discarded. The nature of electromagnetic radiation has been debated through history - Isaac Newton attempted to disprove Christiaan Huygens Wave Theory in favour of the Particle Theory, despite proposing a Wave Theory himself for colours. Both

approaches were later displaced by a Wave-particle Model and today there is no finite consensus.

2.4.4.1 Principles of Diagnostic Testing

Revisiting the discussion of emissivity and associated interactions of the infra-red electromagnetic radiation, offers an explanation of how diagnostic tests provide outcomes for clinical interpretation.

Radiation (energy) directed towards the tissue-of-interest may be reflected, absorbed, transmitted (scattered) or may produce a secondary-effect, such as fluorescence. Reflection is often at the same angle as the incident radiation and retains the same energy, whereas scattering not only changes its direction, but may also alter its energy. This may be a surface-effect or occur within the tissue, leading to transmission from multiple locations of the tissue which is dependent on the radiation energy (long wavelengths scatter less than short), the structure and composition of the tissue. Another phenomenon may occur if radiation is absorbed by conversion to another type, raising the tissue-energy proportional to that of the radiation - as seen with heat. Absorption may also result in availability of a lower-energy radiation with longer wavelengths, the emission of which is fluorescence (Hall & Girkin, 2004).

Naturally-emitted (such as infra-red radiation), rather than projected radiation, may also be detected. Such interactions provide the opportunity to capture and process the radiation, generating an objective image or value for comparison with a known-control. Clinically, this may be combined with information from the history and examination.

The electromagnetic spectrum provides the radiation source for many special tests used within medicine and dentistry, some in common use (e.g., X-rays) which have new perspectives for their potential from darkfield, spectral and phase-contrast-imaging, whilst others have not yet received development or acceptance within the dental profession, e.g., infra-red radiation.

For the purpose of this Study, the focus and function of the special test is to determine the presence or absence of the pulp blood-flow.

2.4.4.2 Gamma and X-ray Radiation

Gamma radiation requires injection or ingestion of a radioisotope by a patient who becomes the source of the radiation, unlike X rays which are projected through the patient with the image being dependent on the

absorption of the radiation. Both are ionising radiations with associated health-risks, e.g., somatic deterministic and stochastic (Whaites, 2007; White & Pharoah, 2008) which outweigh the possible benefits of assessing the pulp blood-supply.

Future development of X-rays include:

- phase-contrast-images which use the refractive portion of the beam rather than the absorption, provide greater contrast, especially from soft-tissue (Bech et al., 2010 and Sato et al., 2011)
- darkfield images select the scattered radiation from the non-scattered, maximising the angle of scatter. The greater the scattering the better the contrast, especially in mineralised tissue (Egan et al., 2014)
- spectral images use the energy levels of X-rays to provide the required energy of the projected beam, and detectors can report on specified energy-bands of photons. Improved resolution and contrast, compared to conventional X-ray images, are possible (Watt et al., 2003 and Norlin & Fröjdh, 2005).

None of the above developments are yet accessible to the practising dentist and would not provide any information on the presence of a blood-flow.

2.4.4.3 Ultraviolet Radiation

Ultraviolet radiation, when projected onto enamel, can produce fluorescence detected by specialised viewers (Benedict, 1928). It is non-ionising but has potential to damage DNA formation, and care is needed as sensitivity to the Ultraviolet-rays may be found, e.g., systemic lupus erythematous. Ultraviolet-light photography has been reviewed for endodontic diagnosis (Foreman, 1983) as the ability to fluoresce may be lost in pulpless teeth. This may be due to the quenching-action of an increase of iron in the dentine following pulp inflammation/necrosis. It is unreliable and not in use in general dental practice to assess tooth-vitality.

2.4.4.4 Visible Spectrum

This includes techniques such as Digital Fibre Optic Transillumination (DiFOTI), DIAGNOdent and Quantitative Light-induced Fluorescence (QLF). Projected light can provide an image when transmitted and captured with DiFOTI or from QLF-emittance following fluorescence, whereas DIAGNOdent produces a numerical and acoustic signal rather than an image. All are harmless, non-ionising special tests primarily for caries-detection.

Transillumination may demonstrate colour-changes in teeth which originate from pulp-disease leading to the loss of translucency when non-vital. It is not conclusive and may be affected by restorations (Hill,1986).

Photoplethysmography has been used to evaluate blood-flow in teeth and it assesses the optical properties of the tissue which may be influenced by the presence, or absence, of a blood-flow. Compared to Laser Doppler Flowmetry there may be reduced contamination of the signal from the periodontal blood-supply due to the light being transmitted, rather than back-scattered (Gopikrishna et al., 2009). However, when modelled in-vitro, the simulated gingival blood-flow was found to affect the photoplethysmography, and greater affect was seen with infra-red wavelength (9.4×10^{-7}M) than red visible light (6.25×10^{-7}M). Within the model a simulated blood-flow of 25ml/min was applied, which appears unrealistically high compared to previous data (Niklas et al., 2014). Inconclusive results have been reported from a human study (Shoher et al., 1973), whereas another human study reported a difference in young teeth (Miwa et al., 2002). Stability of the probe may be problematic and a support may be advised.

Spectrophotometry has also used dual wavelengths to measure the oxygen-saturation, which has shown promise in initial animal studies (Nissan et al., 1992; Chen & Abbott, 2009).

Pulse Oximetry measures the percentage oxygen-saturation (SaO_2) of arterial blood in tissues calculated from differences in the absorption of transmitted light (red 640nm and infra-red 940nm) by oxygenated and de-oxygenated haemoglobin. Bespoke designs have enabled attachment to the tooth and results indicate promise, with greater reliability than sensibility tests (Levin, 2013). In-vivo studies provide variable outcomes, one being unable to corroborate the presence of healthy pulps (Kahan et al., 1996), whereas Goho, (1999) reported SaO_2 of 93-94% on permanent and deciduous teeth, compared to that of the finger at 97%. Lower saturation-levels (80%) were reported by Munshi et al., (2003). Goho, (1999) and Munshi et al., (2003) both had a control with an endodontically-treated tooth which provided 0% SaO_2. The tooth-structure can scatter the transmitted light which may account for the differences in SaO_2. This is totally objective but a normal blood-flow is needed. When low it may not be detected, and this may occur with vasoconstriction. Additionally, within an older tooth, detection of the blood-flow may be more difficult as calcification continues and false-negative response may be received (Gopikrishna, 2009).

2.4.4.5 Optical Coherence Tomography

Optical coherence tomography projects near infra-red radiation, which is split and recombined upon reflection to produce an image from the interference and back-scattered waves (Colston et al., 1998; Feldchtein et al., 1998; Wilder-smith et al., 2010). There are no health-risks but availability and cost of machines has resulted in little clinical dental use to-date (Wiggin, 2010; Natsume et al., 2011). No indication of pulp blood-flow would be expected within a tooth, as the penetration-depth of only a few millimetres is insufficient.

2.4.4.6 Terahertz

Radiation released from zinc-telluride crystals following exposure to visible or infra-red light and detection of the reflected wave is possible with photoconductive detectors which produce an image (Hall & Girkin, 2004). Clinical use is vague for potential caries-detection. Health-risks are unknown but it is a non-ionising radiation. No device is clinically available for the general dentist (Ferguson et al., 2002 and Crawley et al., 2003) and, due to limited penetration of the mineralised tissue and strong absorption by water, (Wilmink et al., 2011) detection of the pulp blood-flow is unlikely.

2.4.4.7 Magnetic Resonance Imaging

Magnetic resonance imaging (MRI) uses a magnetic field (0.1- 8 Tesla) which initially acts on the hydrogen nuclei of water molecules in the body and aligns them. Additional energy from a radio-wave causes deflection of the magnetic field which, when turned off, returns the magnetic field to normal, emitting a detectable signal. The time taken to return to the normal resting state is used to generate an image. No health-risks are attached but care is needed with metal prostheses, and dental restorations may distort the images (Idiyatullin et al., 2011). A contrast-medium is often used, e.g., Gadolinium, but may not be necessary for detecting pulp-vascularity as first thought (Ploder et al., 2001; Kress et al., 2004; Assaf et al., 2015). Reperfusion, following trauma of anterior teeth in 8-17 year olds, was feasible, as detected with MRI at 6 weeks after the trauma and provided positive findings in nearly twice as many teeth (11 v 6 of 12 teeth) compared to a cold test which, at 6 months post-trauma, reported the same findings as the MRI (Assaf et al., 2015). MRI Machines are large and costly, being impractical for the practising dentist.

2.4.4.8 Laser Doppler Flowmetry

Laser Doppler Flowmetry is a non-ionising technique using visible or infra-red light which is projected towards the tissues (Murray et al., 2004; Jafarzadeh, 2009). This is scattered by moving-tissues, e.g., red blood-cells, which shifts the light-frequency in a similar way as the Doppler-effect shown in Figure 2-17, generating longer and shorter wavelengths which, following back-scattering, are detected on the tooth-surface and processed, along with the static tissue scatter which is not shifted (Gazelius et al., 1986).

Longer wavelength
Low-pitch

Shorter wavelength
High-pitch
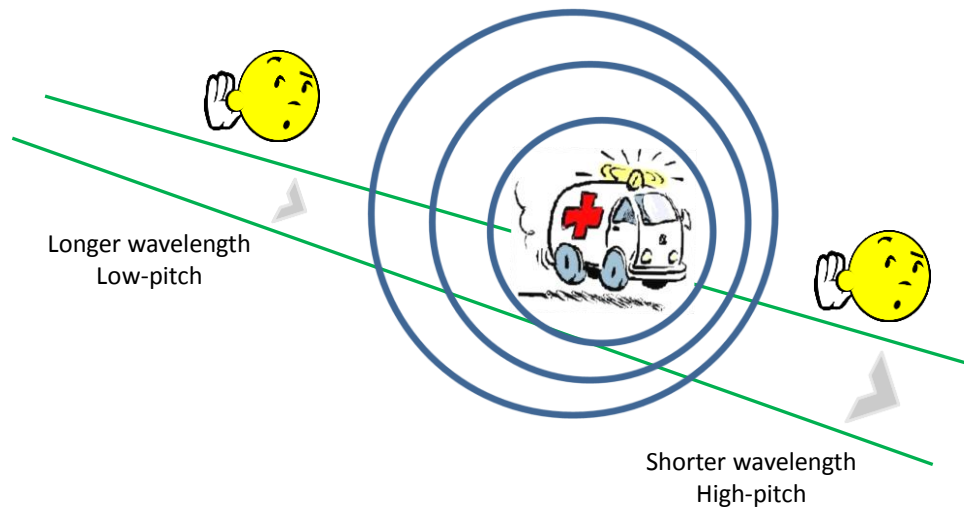
Figure 2-17 Doppler-effect

Comparison with a control is needed and the value provided is related to the number of moving erythrocytes and their mean velocities (Levin, 2013).

Correlation with histological status of the pulp has been suggested where an increase in blood-flow with inflammation has been detected (Wilder-smith, 1988). When compared with other pulp testing methods, such as electrical pulp tests and thermal tests, laser doppler has been shown to correctly identify more vital and non-vital teeth (Karayilmaz & Kirzioglu, 2011). It may reliably detect healthy vital teeth from non-vital teeth but contamination from periodontal blood-flow up to 80% may occur (Soo-ampon et al., 2003).

The location and angulation of the instrument probe on the tooth can affect signal-transmission (Odor et al., 1996), as can the mineralised tooth-tissue and restorations within the tooth (Jafarzadeh, 2009). Keeping the probe stable is difficult, resulting in motion artefact, and often necessitates use of a splint. Measurement is reported in arbitrary units (Perfusion Units) and comparison between visits can be variable (2-14%, Gazelius et al., 1986). An output-signal of approximately 40% less in non-vital teeth compared to vital teeth has been shown in two studies (42.7% Ingólfsson et al., 1994 and

37.3% Roebuck et al., 2000) and may indicate an appropriate value for further investigation if vitality is of concern. It is not in regular use in dental practice.

2.4.4.9 Ultrasound Doppler

Ultrasound does not use electromagnetic radiation but is mentioned for completeness, as the use of Ultrasound Doppler has been reported for detecting dental pulp-spaces (Szopinski & Regulski, 2014), and the pulp blood-flow (Yoon et al., 2010). Ultrasound is non-invasive and non-ionising - however, detecting the pulp blood-flow is difficult but, unlike laser doppler flowmetry, the source of the signals can be identified. It may be a viable method for detecting pulp-vitality but will require training for the operator, equipment may be expensive and it may be more suitable for a hospital dental department than a high-street general dental practitioner.

2.4.4.10 Transmitted Laser-Light

Rather than back-scatter laser-light (as in Laser Doppler Flowmetry), if it is transmitted instead, detection of a blood-flow is possible. However, if the mineralised tissues are thick, as seen on premolar teeth, penetration of tissue is restricted, even at higher energy-levels in a study in 2005. Anterior teeth did allow transmission, and the detection of a blood-flow from the tooth rather than other non-pulp sources was possible (Sasano et al., 2005).

2.4.4.11   Infra-red Radiation

Infra-red radiation may be projected or emitted and is a non-ionising radiation. Enamel is very transparent with projected near-infra-red radiation of 1310nm wavelength compared to visible light, and demineralisation may be detected as dark areas on an image due to an increase in scatter. These may be repeated whenever needed with no risk to the patient but vitality-detection is not reported with projected infra-red radiation.

Detection of a thermal difference of an object is possible from the naturally-emitted infra-red radiation via collection with a thermal camera. In-vivo use of thermography and human mineralised tissue is varied (Table 2-18) and includes assessment of vitality. Confounding oral aspects, such as respiration and the presence of moisture, may make assessment of tooth-temperature difficult and a period of acclimatisation is suggested for the patient prior to assessing the teeth with thermal imaging in a stable thermal environment (Love, 1986). As yet, there is no clinical application for vitality testing within general dental practice despite investigation spanning 34 years - with the last in-vivo study being in 2000.

Table 2-18 In-vivo thermography of human mineralised tooth-tissue.

Author	Year	Assessment
Crandell & Hill	1966	Infection
Hartley, et al.	1967	Vitality
Pogrel, et al.	1989	Vitality
Arrastia, et al.	1994	Tooth-Temp Following Laser-Application
Hussey, et al.	1995	Composite-Curing
Kells, et al.	2000b	Vitality

In-vitro thermography studies collecting the emitted radiation of human teeth are much wider, with assessment of temperature-change from laser-treatment featuring most prominently (Table 2-19) and no in-vitro investigation of vitality was found in the literature using thermography.

Table 2-19 In-vitro thermography of human mineralised tooth-tissue.

Assessment	Author & Year
Curing	Al-Qudah, et al., 2005; Bouillaguet, et al., 2005; Aksakalli, et al., 2014
Lasers	Launay, et al., 1987; Pogrel, et al., 1988; Anić, et al., 1993; Arima & Matsumoto, 1993; Neev, et al., 1993; Arrastia, et al., 1994; Anić & Matsumoto,1995; Arrastia, et al., 1995; Machida, et al., 1995; Wilder-Smith, et al., 1995, Anić, et al., 1996a; Anić, et al., 1996b; Meyer & Foth,1996; Neev, et al., 1996; Whitters & Strang, 2000; Yu, et al., 2000; Yamazaki, et al., 2001; Kishen, et al., 2003; Ishizaki, et al., 2004; Madura, et al., 2004; Wang, et al., 2005; Ana, et al., 2007; Da Costa Ribeiro, et al., 2007; Stock, et al., 2011; Da Silva Barbosa, et al., 2013; Uzunov, et al., 2014
Endodontic Obturation	McCullagh, et al., 1997; McCullagh, et al., 2000; Behnia & McDonald, 2001; Lipski & Zapałowicz, 2002; Lipski & Woźniak, 2003; Lipski, 2004; Lipski, 2005a; Lipski, 2005b; Lipski, 2006; Ulusoy, et al., 2015
Pin-Placement	Biagioni, et al., 1996
Post-Removal	Budd, et al., 2005; Lipski et al., 2010a
Cavity-Preparation	Carson, et al., 1979
De-Bonding of Brackets	Cummings, et al., 1999
Bleaching	Gontijo, et al., 2008, Kabbach, et al., 2008
Irrigation of Root-Canals	Hsieh, et al., 2007
Post-Preparation	Hussey, et al., 1997; Lipski et al., 2010b; Kilic, et al., 2013
Caries	Kaneko, et al., 1999, Zakian, et al., 2010
Emissivity	Kells, et al., 2000a
Ultrasonic-Scaling	Lea, et al., 2004
Thermal Properties & Heat-Transfer	Panas, et al., 2007; Lin, et al., 2010a; Lin, et al., 2010b
Crack-Detection	Matsushita-Tokugawa, et al., 2013

Despite technological advances and greater accessibility to affordable thermal imaging equipment, recent publications have reduced for vitality testing via infra-red thermography. Other devices have also been used in-vivo and in-vitro to assess the temperature-difference of vital and non-vital teeth, e.g., miniature thermometers, thermocouple, thermistors and cholesteric-crystals, showing there is an interest and belief that the vital tooth may have greater thermal energy than a non-vital tooth potentially due

to its vascular-supply which, up to now, has not been translated for clinical use.

From the review of the electromagnetic spectrum, attempts have been made to ascertain the presence or absence of a blood-supply to the tooth rather than test its neural response, as the sensibility tests do. The practicalities of these for dental practitioners are varied. There is no application in dental practice for Gamma and X-rays to detect a blood-flow, with associated health-risks due to their ionising radiation. Optical coherence tomography is unable to penetrate tooth-tissue to the depth required to reach the pulp and its blood-supply. Similarly, with terahertz radiation which, even if the radiation reached the pulp, absorption by water of the radiation would make detection of tooth-vitality unlikely. Ultraviolet radiation has health-risks and the lack of fluorescence is unreliable to predict loss of vitality.

Magnetic resonance imaging may be able to detect the pulp blood-flow but the size and cost of such machines is prohibitive for the high-street dentist. The use of visible-light carries no health-risks but transillumination may be affected by restorations in a tooth and detecting colour-change is not reliable and may change with viewing-conditions and increasing age. Other visible-light techniques, such as pulse oximetry and photoplethysmography, have attempted to detect the blood-flow but contamination from the periodontal ligament has been problematic and the level of blood-flow may be insufficient to permit detection. Laser Doppler may also receive signals from the periodontal ligament but probe location and stability is technically difficult and recordings, despite being promoted as detecting a vital from a non-vital tooth, are measured in arbitrary perfusion-units which make comparison between devices difficult.

Infra-red radiation, especially the naturally-emitted radiation which can be measured by a thermal camera, has been reviewed previously for detecting tooth-vitality, in-vivo but not in-vitro via thermography (Table 2-18, 2-19 & 2-21). Techniques for measuring tooth-temperature have been wide-ranging, with inconclusive results in previously published literature. However, the theory that a vital tooth may have greater thermal energy than a non-vital tooth has potential, especially with recent advances in thermal technology which are being positively embraced, as seen by their use to record tooth-temperature with laser applications. A more detailed consideration of vitality testing via tooth-temperature is needed, which requires consideration of the temperature-measurement technique.

2.4.5 Temperature-Measurement Techniques

Temperature is a means of assessing the hotness or coldness of an object and many devices are capable of measuring temperature, either qualitatively or quantitatively, and may be in contact with the object-of-interest or operate as a contactless-device. Contact-devices measure the heat-transfer from conduction and thus require a medium and include thermometers, thermocouples and thermistors, which provide data but not as an image. Contactless-devices include infra-red thermometers, which record the emitted-infra-red radiation from an object (no transmitting-medium needed) without an image, whereas a thermal camera captures the emitted radiation and provides a 2-D image delivering a spatial reference of the temperature.

2.4.5.1 Thermometers

A thermometer is a contact-device which measures temperature on a scale and includes a thermometric substance, i.e., a substance which physically changes as the temperature changes, e.g., volume of liquid or electrical resistance of a wire (Rickard et al., 1984; Holst, 2000). Determining tooth-temperature with a thermometer is not ideal as it provides a small point-of-contact because of the curved surfaces of a tooth which is not stable without an adhesive and would be difficult to reproduce. Additionally, cross-infection needs to be considered as devices would either need sterilising or be disposable.

2.4.5.2 Thermocouples

A thermocouple has two different metal wires, e.g., nickel chromium and nickel aluminium, which are joined at one end and attached to a reading-device at the other end (e.g., thermometer) via a suitable connector. The two metals naturally generate an electromotive force between themselves which changes when heated and can be measured with a volt-meter which is converted to a temperature via the reading-device. They are very small and may be inserted in a medium, or attached providing point-contact-measurement - which again may not be stable or reproducible. Disposable devices would overcome cross-infection but with added cost (Holst, 2000).

2.4.5.3 Thermistors

A thermistor is a **therm***ally*-sensitive-*res***istor** which may be made from a semi-conductor, rather than a metal. A large change in resistance is seen with a small change in temperature. They provide a fast response, but measure their own temperature. They are accurate ($\pm$ 0.1 – 0.2^{o}C) and

cheap with a limited range of operation (0-100°C), but have similar disadvantages to the previous contact-devices (Holst, 2000).

2.4.5.4 Cholesteric Liquid Crystals

The colour of cholesteric liquid crystals change with temperature and, if applied to the surface of an object, may indicate temperature and temperature-gradients across the surface (Table 2-20). Such a crystal-mixture may include cholesteryl oleyl carbonate, nonanoate and benzoate which has the colour-range between 32°C and 36°C.

Table 2-20 Temperature-colour-change of cholesteric liquid crystals.

Temperature (^{o}C)	Colour
32.0 - 32.9	Red
32.9 - 33	Yellow
33.1 - 34	Green
34.1 - 36	Blue

(Dowden, 1967)

One dental study by Howell, et al., (1970) indicated this type of thermography was a useful adjunct for assessing tooth-vitality. They cannot be re-used due to cross-infection but surface-contact would be good.

2.4.5.5 Infra-red Thermometer

This is a contactless-device which focuses emitted-radiation of certain wavelengths through an optical system on to a sensor, which can convert the radiation to an electrical signal which then provides a numerical value from a known temperature-scale proportional to the amount of emitted-radiation captured. No image is provided. Emissivity-values may be allowed for by some devices, otherwise the temperature may be a qualitative measure which is not comparable between devices (www.omega.com). They are more expensive than some contact-devices but may reach areas contact-devices cannot and there are no concerns about cross-infection. Calibration may be more difficult, as the infra-red thermometer does not have Industry Standards to meet, which thermocouples and thermistors do. The curvature of the surface may affect emissivity and, thus, the recorded-temperature. The device has a field-of-view which needs to be totally capturing radiation from the object-of-interest (not adjacent areas) otherwise the temperature will be contaminated by the surrounding materials.

2.4.5.6 Infra-red Thermography

A thermal camera, like the infra-red thermometer, is a contactless-device capturing naturally-emitted radiation of selected wavelengths but has the

advantage of providing real-time images which can be stored for later analysis, although they are more expensive and require additional software. They can capture data over a larger area than the infra-red thermometer and areas-of-interest can be analysed, rather than points-of-interest as seen with contact-devices. There is no risk of loss of contact.

The thermal camera-lens may be made of Germanium (Ge), which is transparent to infra-red radiation for long-wavelength infra-red (LWIR) devices collecting between 8-14µm. Other options include Zinc Sulphide (ZnS) or Zinc Selenide (ZnSe) which partly transmit visible-light, unlike Ge which is opaque below 2µm. The LWIR is advantageous as it is less-affected by attenuation from ambient humidity, which is important over long-distances and for the oral environment, reducing signal-intensity (Holst, 2000; Vollmer & Möllmann, 2010).

Mid-wavelength infra-red collection (MWIR) falls between 2.5-7.0µm and may have a Silicon (opaque in the visible spectrum), Sapphire, Quartz or Magnesium lens, whereas short-wavelength (SWIR) collection falls between 1.1-2.5µm, and near-infra-red (NIR) lies between 0.7-1.1µm.

Radiation is focused onto a detector such as a bolometer which, when absorbed, changes its resistance, altering the electrical current which is detected and translated in pre-programmed software to provide not only the temperature from a calibrated scale, but also an image in real-time (Holst, 2000). Different specifications include frame-rate-capture and image-quality limitations such as resolution, both spatial and thermal. Allowance needs to be made for parameters such as emissivity, the ambient environmental temperature and the distance between lens and object-of-interest, to provide the most accurate temperature. Some thermal cameras use very little power and are available as hand-held-devices which may be battery-operated rather than mains-operated.

The simplicity of contactless is desirable and, within the dental-setting, contactless avoids risk of cross-infection providing superior metrology, whereas contact-devices need to be disinfected or disposed of, adding to their cost.

2.4.6 Vitality-Assessment via Temperature

A thermal vitality test aims to ascertain the presence or absence of a pulp blood-supply from temperature, rather than test the neural response to a stimulus such as hot or cold. Temperature has previously been investigated using many temperature-recording-devices (Table 2-21). There have been

two in-vitro studies (Fanibunda, 1985; Smith, 2004), neither of which used contactless infra-red thermography to collect data. The flow-rates used to simulate tooth-vitality range from 0.16 to 4ml/min, which may be higher than the in-vivo flow-rate, although the precise flow-rate is unknown. Neither of these studies simulated a pulsed blood-flow which is suggested to exist within the tooth (Brown & Beveridge, 1966). Fanibunda, (1985), used two teeth, a maxillary and mandibular first premolar; whereas Smith, et al., (2004) used only one tooth, an unrestored maxillary first premolar. Both studies cooled the teeth and observed the re-warming sequence and both reported positive outcomes, being able to distinguish a vital tooth from a non-vital tooth due to the thermal response during re-warming.

Of the fourteen in-vivo studies, three used infra-red radiation collection: Hartley et al., (1967); Pogrel et al., (1989); Kells et al.,(2000b). Eight studies did not distinguish a vital tooth from a non-vital tooth via thermal-data, two of which used infra-red radiation (Hartley et al., 1967; Kells et al., 2000b), whereas six did, one of which used infra-red radiation (Pogrel et al., 1989). The positive outcome for Pogrel et al., (1989) was dependent on the treatment status of the teeth, i.e., root treated without a metal post, as more rapid re-warming was found in a non-vital tooth with a metal post than a vital tooth and variable outcomes were found from transplanted or teeth involved in osteotomy without root treatment.

The results are inconclusive, with approximately half the total studies found being favourable and half not - however, it is approximately eighteen years since the last study using infra-red radiation collected by a thermal camera and that was on one volunteer. More than a decade prior to that, Pogrel et al., (1989), reported positive findings for assessing tooth-vitality via thermal-data. Nevertheless, there is no clinical system available in practice with which to assess vitality via temperature collected by a thermal camera.

With reduction in cost and size, making accessibility of such devices (which are non-invasive, non-contact and non-ionising) far easier, further investigation is justified.

Table 2-21 In-vitro and in-vivo studies assessing vitality from tooth-temperature.

Author	Year	Study-Type	Vitality Simulation	Flow-Rate ml/min	Temperature Collection	Active Disruption of Equilibrium	Vitality-Difference
Goldberg & Brown	1965	VV	.	.	Thermocouple	No	No
Brown & Goldberg	1966	VV	.	.	Thermocouple	No	No
Crandell & Hill	1966	VV	.	.	Infra-red Thermometer	No	No
Hartley, et al.	1967	VV	.	.	Infra-red Thermography	No	No
Howell, et al.	1970	VV	.	.	Cholesteric Crystals	No	Yes
Beyon	1973	VV	.	.	Thermocouple	Yes - cold and warm	No
Stoops & Scott	1976	VV	.	.	Thermistor	Yes - 10^oC water	Yes - tooth-surface
Banes & Hammond	1978	VV	.	.	Thermistor	No	Yes - tooth-surface
		VV	.	.	Thermistor	No (FVC)	No
Fanibunda	1985	VT	Saline/ Non-pulsed	0, 0.5, 1.0, 2.0, 4.0	Thermistor	Yes - cryo-spray	Yes
Fanibunda	1986a	VV	.	.	Thermistor	No	Yes - time/temp
Fanibunda	1986b	VV	.	.	Thermistor	Yes - polishing	Yes - critical period
Pogrel, et al.	1989	VV	.	.	Hughes Probeye Thermal Video	Yes - air-cooling to 22^oC	Yes - re-warming-rate subject to type of endodontic treatment
Kells, et al.	2000b	VV	.	.	Infra-red Thermography	Yes - cooling	No
Smith, et al.	2004	VT	Water/ Non-pulsed	0, 0.16, 0.33, 0.5, 0.66, 0.83, 0.99, 1.16, 1.32, 1.5	Thermometer	Yes - iced-water	Yes - re-warming-rate & surface-temperature
		VV	.	.	Thermometer	Yes - water & air	No
VV = In-vivo; VT = In-vitro; FVC = Full Veneer Crown							

2.5 Summary

The human tooth is a complex and intricate arrangement of both avascular and vascular tissues. The knowledge already available within the literature on the tooth, whether human or animal, is extensive, as is information on different sensibility tests seeking to imply the presence, or absence, of a blood-supply to the tooth from a neural response, which have sensitivity-values ranging from 0.21 to 1 and specificity-values ranging from 0.33 to 1. Vitality testing is important and current methods, such as laser doppler, are not in common use even though they are reported to have a sensitivity and specificity of 1. Nevertheless, it is not yet as comprehensive as it could be and a true vitality test which is simple, non-invasive, non-destructive and reliable would be more informative for the clinician in making diagnostic decisions to restore or remove a tooth. Infra-red imaging is advancing with technological developments making it more affordable and accessible. It may provide superior metrology with no cross-infection-risk due to contactless data-collection, with good thermal resolution providing an image of the whole area-of-interest of the teeth. Additionally, the thermal camera can record digital-data in real-time which can be stored.

Infra-red radiation justifies further investigation and may be a potential candidate for a vitality test and, currently, there is limited data available on how the test may best be undertaken. There has been no in-vitro investigation which could improve understanding of the test requirements and only three in-vivo studies. Two applied a thermal disruption - one reported a thermal difference between the vital and non-vital teeth (Pogrel et al., 1989) and one did not (Kells et al., 2000b). The third, without thermal disruption, reported no thermal difference between vital and non-vital teeth (Hartley et al., 1967).

It is intended this Study will add to current knowledge on the feasibility of using infra-red radiation in determining tooth-vitality.

2.6 Aim

The aim of the Study is to assess the feasibility of using infra-red radiation in determining tooth-vitality. The null hypothesis being that:

> $H_0 =$ *there is no difference in the amount of infra-red radiation collected with a thermal camera from the surface of a vital and non-vital tooth.*

Whereas the alternative hypothesis being:

> $H_1 =$ *there is a difference in the amount of infra-red radiation collected with a thermal camera from the surface of a vital and non-vital tooth.*

In order to achieve the Study aim multiple steps are needed prior to analysis of infra-red radiation to determine tooth-vitality. These objectives include:

i. development of a suitable environment in which to undertake in-vitro empirical work which is thermally stable

ii. determination of the emissivity of human mineralised tooth-tissues in-vitro against a known reference-point for use as a thermal camera parameter

iii. calculation and evaluation of the thermal properties of human enamel and dentine against known values using infra-red radiation

iv. creation of thermal maps from the calculated thermal properties of the mineralised tooth-tissues to characterise enamel and dentine using infra-red radiation

v. development of a model to evaluate the human pulp blood-flow for each adult tooth from knowledge available in the literature

vi. an in-vitro simulation of a pair of teeth within an alveolar bone whereby vitality may be applied to the periodontal ligament and one tooth with and without a pulse

vii. development of an in-vitro cooling-unit to cool the teeth

viii. analysis and evaluation of collected infra-red radiation during a re-warming sequence using a thermal camera to determine vitality of a pair of teeth in the in-vitro simulation within a stable thermal environment

ix. development of an in-vivo cooling-unit to cool the teeth

x. analysis and evaluation of collected infra-red radiation during a re-warming sequence using a thermal camera to determine vitality of a pair of teeth in-vivo, one of which was vital and one root-treated.

These objectives will enable the feasibility of infra-red radiation determining tooth-vitality to be assessed.

Chapter 3 Method

3.1 Development of a Stable In-Vitro Thermal Environment

In the literature, thermal stability of the environment was reported by Love (1986) and Kells et al., (2000b) to be important for thermal imaging. Stabilisation of patients prior to taking thermal images was recommended (Love, 1986); and Kells et al., (2000b) reported confounding from air-conditioning used to macro-control the environmental temperature. For this Study several methods of thermal environment were developed for in-vitro investigations and are discussed in Chapter 5 Section 5.1 and the final design, authored here, was bespoke and original and addresses the first objective to develop a suitable environment in which to undertake in-vitro empirical work which is thermally stable.

3.1.1 Method

3.1.1.1 Equipment-Preparation

A room (Height 2.34m x Width 3.66m x Depth 3.05m) with a wall-mounted air-conditioning-unit (Daikin Inverter, Japan), in which no natural light entered, was used. The room had matt-black walls, artificial lighting and a stable, level work-surface.

Macro-control of the room-temperature was via the air-conditioning, which had range-settings from 18-30°C. This generated warm or cool air which circulated around the room.

A solid-framed, aluminium-cube (Height 32cm x Width 47cm x Depth 47cm) was constructed from six aluminium-sheets of 0.15cm-thickness and twelve matching-lengths of aluminium-angles (Forward Metals Online - forwardmetals.co.uk). Two full-length hinges (32cm) were attached to two of the sheets and the frame, producing a front and rear door. The doors were fastened for ease, with four knurled-thumb-screws, two per door (Accugroup.co.uk). Nine rubber-feet raised the base off the work-surface (Polyurethane Rubber Self-Adhesive Bumper-Feet – Hill Croft Northwest Ltd). From hereon, this aluminium-box is referred to as the Cube (Figure 3-1). The side-sheets of aluminium were removable, allowing specific access-holes to be placed within the doors for cable-entry and exit, transfer of specimens, application of cooling-units, as well as visual observation internally, as needed. A circular hole was cut in the top-surface,

where an aluminium-mount was developed and attached to hold the thermal camera.

Attached to the two non-door-sides of the Cube were internal (Height 6cm x Width 15cm x Depth 2.5cm) and external (Height 16cm x Width 16cm x Depth 5cm) aluminium-heat-sinks. Between the external heat-sink and the Cube-wall, thermoelectric peltier units (ActiveCool AC4G TE) were cemented, with the cool side of the peltier facing the Cube-wall. An electric-cooling-fan (Height 12cm x Width 12cm x Depth 2.5cm, 12Volts, 0.3Amps) was attached to each external heat-sink powered from the mains electricity supply by 12Volts 6Amps 72Watts transformers (www.LightingX.co.uk) with jack-plug connections protected by project-boxes. The peltier units were also powered by transformers from the mains electricity supply via a temperature-controller (TD100 Temperature-Controller Auber Instruments, auberins.com).
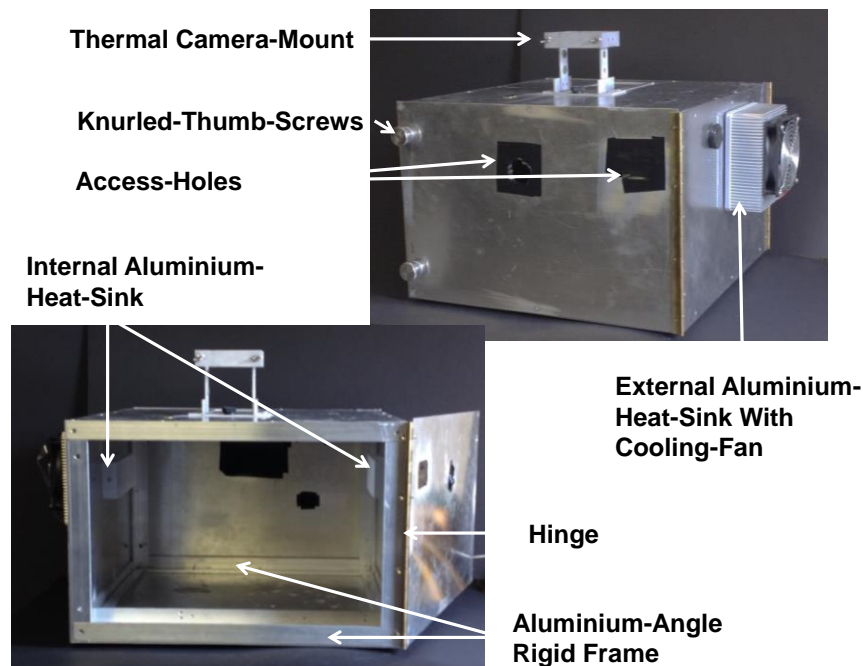
Figure 3-1 The Cube - A stable thermal environment was created by the aluminium Cube, which comprised 6 aluminium-sheets attached to an aluminium-angle frame. Two hinges, the full height of the Cube, attached two of the side-sheets to the frame creating doors, which were secured by knurled-thumb-screws. Access-holes were cut into the doors to provide access for cables, wires and tubing as needed. Aluminium-heat-sinks were attached internally and externally with a thermoelectric peltier cooling-unit cemented in between. An electrically-powered cooling-fan was attached to the external heat-sink. A camera-mount was placed above the circular hole in the top-surface of the Cube to enable viewing of the samples.

A sensor from the temperature-controller of 0.1^{o}C sensitivity allowed micro-control of the internal temperature. Activation of the sensor enabled:

i. addition of heat from an internally-positioned heating-pad (25cm x 35cm, 2 amp, 15watts, Warmeplatte, Biogreen, Germany) when the temperature dropped 0.1^{o}C below the required temperature

ii. cooling by the two thermoelectric peltier units when the temperature rose 0.1^{o}C above the required temperature.

Accessories were added and fixed within the Cube as needed for each stage, e.g., rigid-stands to support equipment, such as Hotplate Bibby Techne DB-2TC.

3.1.1.2 Data-Capture

The stability of the thermal environment was assessed over 3 x 60-minute-sequences for the following thermal control:

1. room air-conditioning only

2. thermoelectric-cooling only

3. both room air-conditioning and thermoelectric-cooling.

Data was recorded from the sensor of the temperature-controller at minute-intervals for a required environmental temperature of 22°C.

3.1.1.3 Data-Processing

Data was processed and analysed in Microsoft Excel 2010 (Microsoft®).

The results for the development of a stable in-vitro thermal environment are in Chapter 4 Section 4.1 and associated discussion in Chapter 5 Section 5.1.

3.2 Emissivity-Determination of Mineralised Human Tooth-Tissue

Determination of the emissivity-value of mineralised human tooth-tissue in the literature was reported to range between 0.65 (Kells et al., 2000a) and 0.98 (Kaneko et al., 1999; Preoteasa et al., 2010). Empirical calculation was undertaken by Kells et al., (2000a) but not Kaneko et al., (1999) or Preoteasa et al., (2010). A simple and recognised method of emissivity-assessment was planned to provide emissivity-values for the teeth-slices and enamel-surface of the whole teeth used in this Study within the stable thermal environment of the Cube. This addresses the second objective - to determine the emissivity of human mineralised tooth-tissues in-vitro against a known-reference-point for use as a thermal camera parameter.

3.2.1 Method

3.2.1.1 Equipment-Preparation

The thermal camera (FLIR SC305 with x4 lens, provided 100μm spatial resolution), was mounted in its stand attached to the Cube. The thermal camera parameters of reflected-apparent-temperature (assessed with a thermal image of crumpled aluminium-foil) were recorded to be 27.2^{o}C and humidity of 50% (from the temperature and humidity-sensor - Prime Capsule Data-Logger – www.perfect-prime.com) when assessing the tooth-slices with a Cube temperature of 22°C, and 34.6^{o}C and 29% when assessing the whole teeth with a Cube temperature of 30°C.

A rigid aluminium-stand with a Bibby Hotplate Techne DB-2TC (www.bibby-scientific.com) with two wells for removable aluminium-blocks was used for a stable heat-source. This was fixed to the Cube at a focal distance of 8cm from the hotplate for viewing with the thermal camera.

A hand-carrier with a copper-baseplate (0.5mm x 50mm x 50mm) and attached thermal tape (6Wm·K; www.thegamebooth.co.uk) was developed, with attached thermocouple (Type-K SA1XL-KI-SRTC – www.omega.co.uk) linked to a Fluke 52 II Thermometer, which was calibrated annually. 3M Scotch Super 33+ Black Vinyl Electrical Tape was used for the known emissivity-reference-point 0.96 ($\varepsilon = 0.96$) which was placed on the carrier or the tooth.

3.2.1.2 Sample-Preparation

Ethical approval was gained from Leeds Dental Institute Research Tissue-Bank (151111/PL/77 Appendix A.4.1 & A.4.2) for the teeth. Slices were

prepared bucco-lingually from one tooth at 1mm intervals with an Accutom-5 (Struers, Copenhagen, Denmark) and polished with an 800-grit abrasive-sheet, whilst being cleansed with distilled water as necessary. Photographs and radiographs (60kV, 0.125seconds) were taken of each slice. The slices were immersed in distilled water and stored flat in boxes, which were refrigerated until needed.

Slices of teeth were paper-dried, following removal from distilled water, and positioned on the copper-based hand-carrier with a compressible thermal tape. 3M Scotch Super 33+ Black Vinyl Electrical Tape of known emissivity ($\varepsilon = 0.96$) was applied to the surface of the thermal tape. The carrier with tooth-slices was placed on the hotplate set at 30°C within the Cube (at a viewing-distance of 8cm) which had been stabilized to a thermal environment of 22°C $\pm0.1^{o}$C by micro- and macro-regulation.

Whole teeth (n=14) sourced and prepared for the in-vitro vitality-study (described in section 3.5) were assessed for enamel-surface emissivity in a thermal environment of 30°C. Small rectangular pieces of 3M Scotch Super 33+ Black Vinyl Electrical Tape were attached to each tooth. The emissivity-reference-point of 3M Scotch Super 33+ Black Vinyl Electrical Tape black was within the same field-of-view as the tooth-slices, or attached to the tooth-surface.

3.2.1.3 Data-Capture

The tooth-slices were viewed with the thermal camera (Figure 3-2a & b) until thermal equilibrium was reached, as were the whole teeth. Three consecutive sequences were made of two slices, which were repeated on two occasions, and twelve whole teeth were viewed once, with two being viewed on three separate occasions.
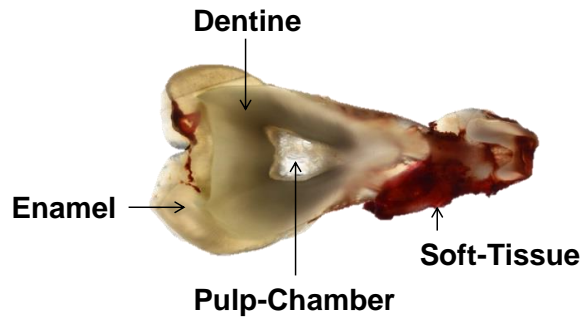
a.
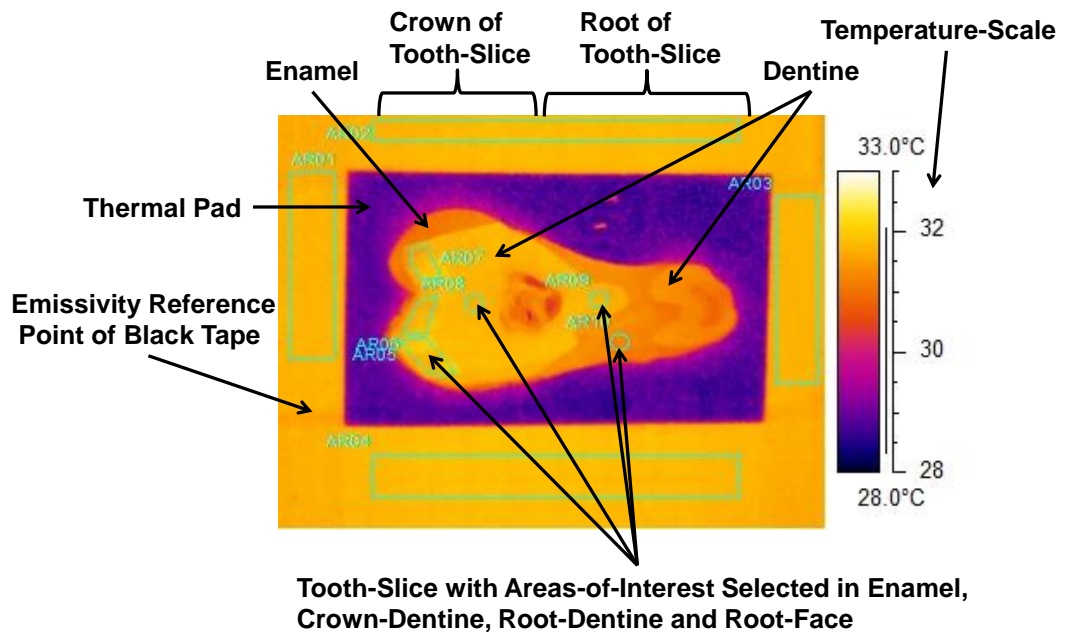
b.

Figure 3-2 a. A slice of prepared tooth used for emissivity-evaluation, showing enamel, dentine, pulp-chamber and soft-tissue
b. Thermograph with areas-of-interest selected in enamel, crown-dentine, root-dentine and root-face.

3.2.1.4 Data-Processing

Calculation of the emissivity of enamel, crown-dentine, root-dentine and root-face from the tooth-slices, and enamel of the buccal-surface of the whole teeth, was undertaken from the thermographs in thermal equilibrium using a laptop and ThermaCAM Researcher Professional 2.10 Software against the temperature of the known emissivity-reference-point of the black tape shown in Figure 3-2b. Microsoft Excel 2010 was used to process the results.

The results for determining the emissivity of mineralised human tooth-tissue are in Chapter 4 Section 4.2 and associated discussion in Chapter 5 Section 5.2.

3.3 Characterisation of the Thermal Properties of Enamel and Dentine

The thermal properties of the mineralised tooth-tissue influence the rate of thermal exchange from the warm blood-supply of the tooth to the cooler external surface of the tooth-crown. The range of values attached to the properties of thermal conductivity and thermal diffusivity vary widely in the literature. Infra-red radiation has been used to assess these properties and this is repeated to compare values against known outcomes and to advance the current technique to characterise enamel from dentine by their thermal properties. This addresses the third objective to calculate and evaluate the thermal properties of human enamel and dentine against known values using infra-red radiation, and the fourth objective to create a thermal map from the thermal properties of the mineralised tooth-tissues which characterise enamel and dentine using infra-red radiation.

3.3.1 Method

3.3.1.1 Equipment-Preparation

A period of 35 minutes for stabilisation was allowed for the Cube to reach the required $22^{o}C$, prior to viewing the slices of teeth in a stable thermal environment.

The thermal camera was placed in the camera-mount and switched on at the same time as the thermal stabilisation commenced, to allow warming. The reflective apparent temperature of $27.2^{o}C$, emissivity 0.96 and humidity of 50% was applied to the software parameters. A recording-rate of 9-frames-per-second was prescribed and data collected with ThermaCAM Researcher Professional 2.10 Software, via a laptop, and stored.

The hotplate with aluminium-block was positioned within a fixed aluminium-stand in the Cube (Figure 3-3) and provided optimum focal distance of 8cm from the thermal camera to the sample-surface. One well of the hotplate held an ice-block with no heat application, and the other held an aluminium heating-block which was set at $30^{o}C$ (Figure 3-4) and allowed to stabilise.
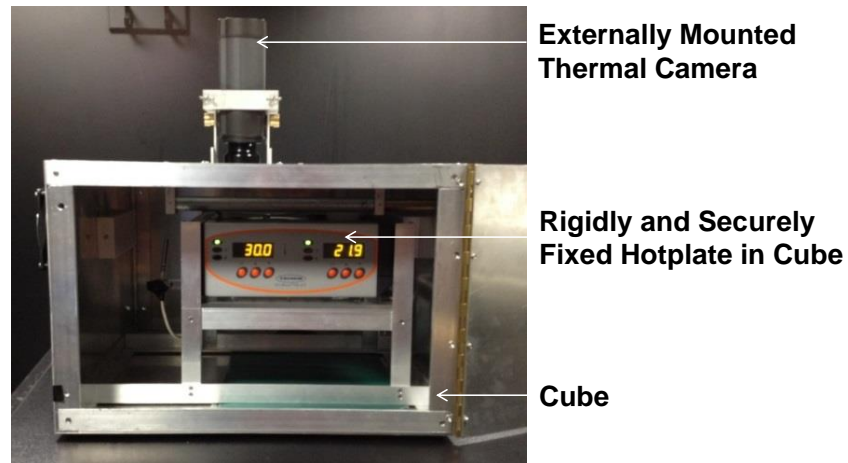
Figure 3-3 The Cube provides a stable environment for in-vitro investigations, with securely-mounted-camera externally and a hotplate in a rigid, fixed-stand internally.
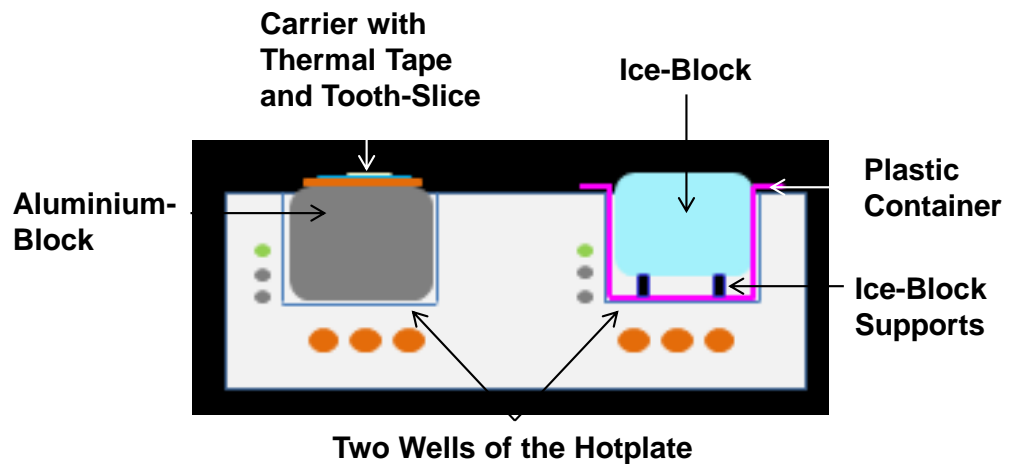
Figure 3-4 Hotplate with cross-section of two wells with an aluminium-heating-block and an ice-block.

Front and rear access to the Cube was via hinged-doors with small access-holes for the necessary cables for the hotplate, heating-pad, thermocouple and temperature-regulator-sensor and a letter-box opening for the carrier.

3.3.1.2 Sample-Preparation

Two lower-third molars were approved for use by Leeds Dental Institute Research Tissue-Bank (151111/PL/77 Appendix A.4.1 & A.4.2), one of which was used previously for emissivity-evaluation. The second tooth was also cut bucco-lingually into 1mm-thick slices, polished by the same method, and stored flat in a box in distilled water in a refrigerator.

Photographs and radiographs were taken of the tooth-slices. The radiographic images were taken of each tooth-slice at 60kV 0.125seconds,

using a Focus 50420 radiographic unit (Instrumentarium Dental, TUUSULA, Finland). The thickness of each tooth-slice was measured with a digimatic micrometer (IP65 Quantumike Mitutoyo, Hampshire, UK).

The slices of teeth were dried with paper and positioned on the thermal tape of the hand-carrier, which was, in-turn, placed on the ice-block via the letter-box opening (Figure 3-5) until a temperature of 2^oC was achieved on the thermometer and then transferred to the hotplate.
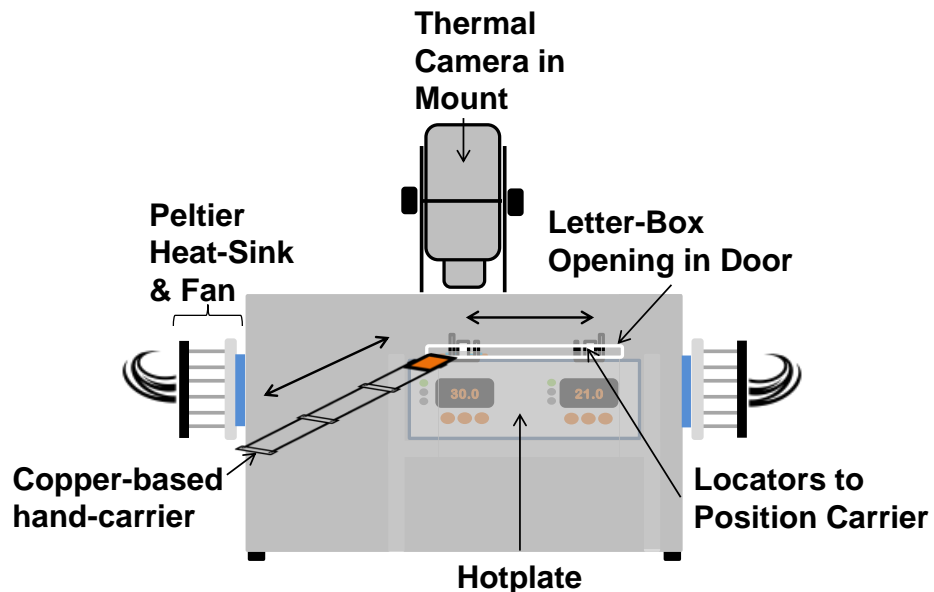
Figure 3-5 The Cube with letter-box-opening for the hand-carrier in the front door for manual transfer between the cold well with an ice-block and the hotplate.

3.3.1.3 Data-Capture

Recording and data-capture commenced prior to transfer of the tooth-slices to the hotplate. Each sequence was recorded for 10 minutes to allow re-warming to thermal equilibrium. Once the sequence was completed, the tooth-slices were replaced to their compartment of the box in distilled water.

3.3.1.4 Data-Processing

Data-processing of the recorded sequences of heat-transfer of the internal surfaces of enamel and dentine was through selected areas-of-interest, similar to those in Figure 3-6 of the tooth-tissue and also of the thermal tape, which provide the average temperature for the area selected. ThermaCAM Researcher Professional 2.10 Software was embedded into a Macro-enabled Microsoft Excel File (Microsoft®) which automated the task of collecting each temperature for each area-of-interest for each frame within the sequence (Figure 3-7) via Visual Basic for Applications (syntax for area-

of-interest Appendix A.5.1). This was run to provide the re-warming-data, allowing time-temperature-curves per frame-rate to be produced.
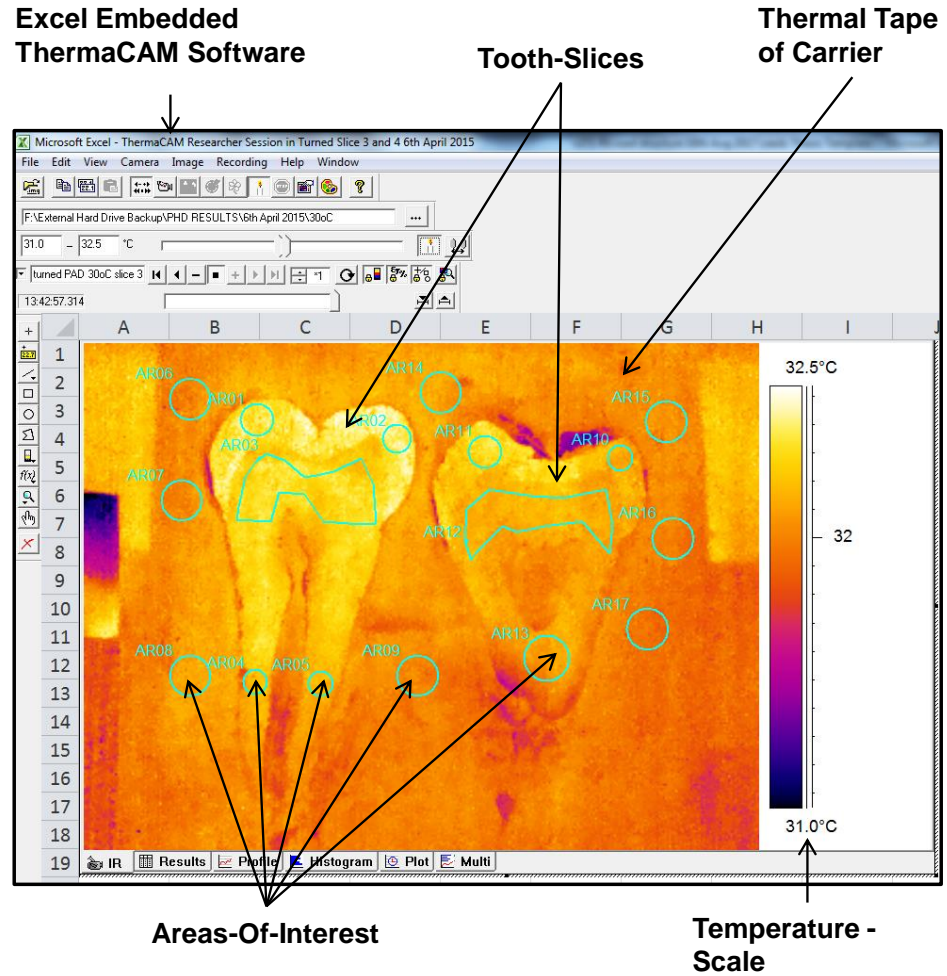
Figure 3-6 Screen-shot of excel sheet with embedded ThermaCAM software showing two slices of teeth and a selection of areas-of-interest to calculate temperature-over-time-data.
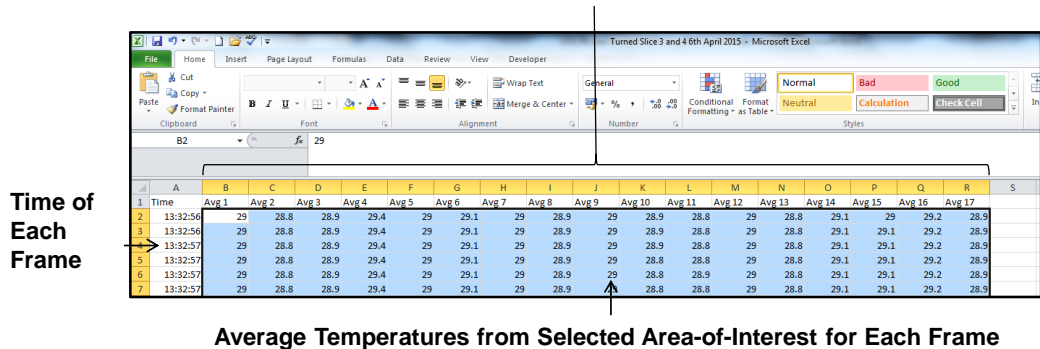
Figure 3-7 Screen-shot of temperature-data-output of selected areas-of-interest produced in macro-enabled excel sheet.

Data-per-second was selected with Macro-enabled Microsoft Excel File (Microsoft®) (Visual Basic for Applications 9th Row Appendix A.5.2) for further analysis (Figure 3-8).

9th Row of Data Selected to Provide Temperature/Second

Figure 3-8 Selection of Every Ninth Frame of Data in a Macro-Enabled Excel Sheet to Provide Data-Per-Second.

The first 70% of re-warming-data was discarded and the remaining 30% was analysed (Lin et al., 2010b). The time-temperature-data was assessed in Matlab (MathWorks®) using bespoke software (Appendix A.5.3) in the curve-fitting-application, using the exponential equation:

$$f(x) = C0 * \exp\left(-1 * {}^{x}/_{\tau_c}\right) + C1$$

Equation 7 Exponential equation for curve-fitting

Curve-fitting to this exponential equation enabled calculation of the characteristic-time-to-relaxation (τ_c). This was calculated for each area-of-interest of the mineralised tissue, i.e., enamel, dentine and demineralised tissue, as was an area-of-interest on the thermal tape. The value of characteristic-time-to-relaxation of thermal tape was subtracted from that of the area-of-interest of mineralised tissue, to give the raw-value for difference of characteristic-time-to-relaxation.

Using the formula below, the difference between the characteristic-time-to relaxation of the thermal tape and the area-of-interest of the tooth enabled the thermal diffusivity to be calculated:

$$\alpha = \frac{4H^2}{\pi^2 \tau_c Diff}$$

Where:

$$\alpha = thermal\ diffusivity (10^{-7} m^2/\text{Sec})$$

$$H = Half\ the\ thickness\ of\ the\ selected\ tissue\ (m)$$

$$\tau_c Diff\ =\ \tau_c tissue - \tau_c thermal\ tape\ (seconds)$$

Equation 8 Thermal Diffusivity

Having ascertained the value of thermal diffusivity for a tissue, the thermal conductivity could be produced from this equation, using known values of density and specific heat capacity from previous research (Lin et al., 2010b):

$$\kappa = \alpha * \sigma * c_p$$

Where:

$$\kappa = Thermal\ Conductivity\ (W \cdot mK)$$

$$\alpha = Thermal\ Diffusivity\ (10^{-7} m^2/\text{Sec})$$

$$\sigma = Density\ (Kg/m^3)$$

$$2800\ for\ enamel\ and\ 2248\ for\ dentine\ (Lin\ et\ al., 2010b)$$

$$c_p = Specific\ Heat\ Capacity\ (J/Kg\ K)$$

$$710\ for\ enamel\ and\ 1066.4\ for\ dentine\ (Lin\ et\ al., 2010b)$$

Equation 9 Thermal Conductivity

The same thermal sequences were processed in ThermaCAM Researcher Professional 2.10 Software to produce greyscale bitmaps (Figure 3-9) once the hand-carrier was stationary on the hotplate. The complete sequence of bitmaps was numbered from 001 with RenameMaster v3.11. Additional bespoke software used the bitmaps of each frame of heat-transfer-data to produce a re-warming curve for each pixel of the bitmap after the temperature-range and number of frames were specified. The characteristic-time-to-relaxation and the integral of the curve (area-under-the-curve) were calculated within Matlab (MathWorks®) (Appendix A.5.4). These values were then converted to a greyscale (0-255) to produce respective thermal maps, which included enamel and dentine within each image.
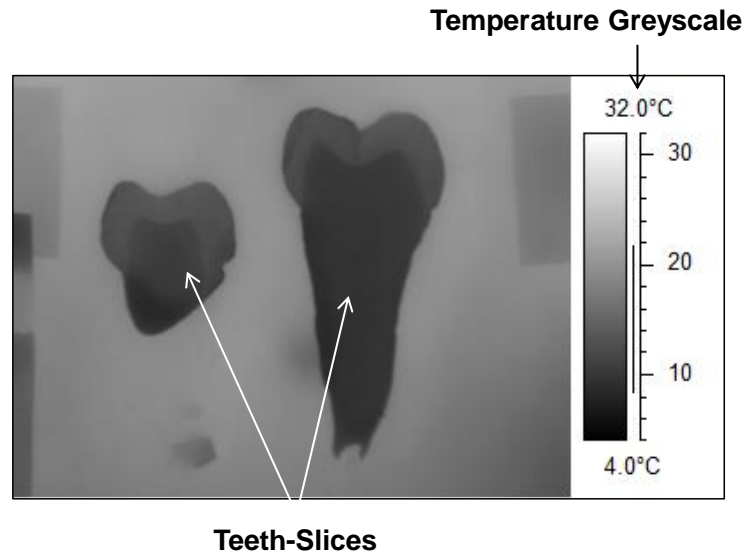
Figure 3-9 Greyscale bitmap from thermal sequence with a 4°C to 32°C range used in the production of both types of thermal maps - characteristic time-to-relaxation and area-under-the-curve.

The results from characterising the thermal properties of enamel and dentine are in Chapter 4 Section 4.3 and associated discussion is in Chapter 5 Section 5.3.

3.4 Pulp Blood-Flow-Rate Model

The literature searches found no specific blood-flow-rates per human tooth-type and a model is presented which estimates such values. The literature provided two sources of pulp-weight (Van Amerongen et al., 1983; Mendez & Zarzoza, 1999) and knowledge of the average volume of the adult tooth by Fanibunda, 1986a. Development of a model using this data based on the reported density of the pulp being the same as water (Lin et al., 2013) enables a theoretical range of blood-flow-rates to be modelled for the whole human adult dentition and addresses the fifth objective to develop a model to evaluate the human pulp blood-flow for each adult tooth.

3.4.1 Data from Literature

The mean mass of pulp (Mendez & Zarzoza, 1999) for third molars was reported as 13.1mg. The range of the pulp-mass for premolars and third molars was reported as 9-51mg (Van Amerongen et al., 1983).

The average volume of the pulp was reported as 25mm^3 (Stock et al., 2004). The mean volumes of pulp-space (mm^3) per tooth are presented in Table 2-11 (Fanibunda, 1986a).

The density of pulp was reported as being the same as water at 1g/cm^3, where 1cm^3 = 1ml = 1g and 1cm^3 = 1000mm^3 (Lin et al., 2013).

The mean pulp blood-flow-rate for 100g was reported as 50ml/min (Kim et al.,1985).

3.4.2 Method

With an assumption that water was to fill the pulp volume, a mass for each tooth can be estimated:

An average volume for the pulp has been given as 25mm^3 (Stock et al., 2004) and would give a weight of 0.025g.

The average volume of pulp (25mm^3) provides a water weight of 0.025g (25/1000)

The flow-rate may lie at 50ml/min/100g which equates to 0.5ml/min/g.

Flow-rate of 50ml/min/100g = a flow-rate of 50/100 = 0.5ml/min/g

The average pulp would have a blood-flow-rate estimated at 0.0125ml/min/g.

0.5*0.025=0.0125ml/min/g

The mean weight of pulp reported for third molars was 13.1mg (Mendez & Zarzoza, 1999). Taking the mean weight of 13.1mg and using the general statement of pulp blood-flow being 50ml/min/100g, a value of 0.0066ml/min/third molar can be estimated:

Mean weight of wet pulp for third molar   *= 13.1mg*
Mean pulp blood-flow ml/min/100g   *= 50*
1g of pulp would have a blood-flow   *= 50/100 = 0.5ml/min*
13.1mg (0.0131g) of pulp has a blood-flow   *= 0.5 x 0.0131*
                                                    = 0.0066ml/min/third molar.

When compared to the value from the volume model, a water constant (ω) can be applied from actual weight-to-volume. This can be applied to all the average volumes of teeth (Fanibunda, 1986a), to estimate a blood-flow ml/min for the full adult human dentition.

When the range of 9-51mg for the pulp-weight is taken (Van Amerongen et al., 1983), a range of blood-flow-rates can be estimated per tooth-type.

The results from modelling the pulp blood-flow-rate are in Chapter 4 Section 4.4 and associated discussion in Chapter 5 Section 5.4.

3.5 In-Vitro Feasibility of Using Infra-Red Radiation In Determining Tooth-Vitality

The feasibility of using infra-red radiation to determine tooth-vitality has not been attempted in-vitro and requires a model which simulates vitality. The models previously used within the literature do not simulate the supporting alveolar bone or provide a vessel simulation for the blood-flow (Fanibunda, 1985; Smith et al., 2004) and this required development prior to assessing tooth-vitality. The human blood-flow is generated by the heart which produces a detectable pulse and the effect of a pulse has not been reported within the literature for any in-vitro assessment of vitality in the two studies by Fanibunda (1985) and Smith et al., (2004). The thermal effect when simulating vitality in the tooth, as detected by capturing the infra-red radiation with or without a pulse, was unreported. The method of assessing the presence or absence of vitality may necessitate a thermal disruption prior to the test, and the level of disruption is again unknown and will be assessed following application of a controlled thermal disruption via development of a cooling-unit. This addresses the sixth objective to develop an in-vitro simulation of a pair of teeth within an alveolar bone whereby vitality may be applied to the periodontal ligament and one tooth with and without a pulse; the seventh objective to develop an in-vitro cooling-unit to cool the teeth; and the eighth objective of this Study to analyse and evaluate the collected infra-red radiation during a re-warming sequence using a thermal camera to determine vitality of a pair of teeth in the in-vitro simulation within a stable thermal environment.

3.5.1 Method

3.5.1.1 Equipment-Preparation

A cooling-unit was developed, comprising a thermoelectric peltier (TEC1 – 12706) powered from the mains electricity supply through a transformer (12Volts 6Amps 72Watts www.LightingX.co.uk) with an adjustable voltage-regulator, and a copper-plate waterblock (EK-Supreme LTX AMD CSQ) connected by G¼ Threaded Barbed Adapters (EK-HFB Fitting) to a pump with built-in reservoir (EK-DBAY DCP-2.2 12Volts DC - www.ekwb.com) via tubing (Clear Translucent Silicone-Soft-Rubber-Tubing - various diameters www.advancedfluidsolutions.co.uk) which held and circulated Thermal Coolant (ThermalTake UV Coolant - www.scan.co.uk). The thermoelectric peltier's heating-face was attached to the copper-plate waterblock via a 1mm-thick thermal conducting-tape (6Wm·K; www.thegamebooth.co.uk). The copper-plate waterblock, with coolant circulated via a pump and through

silicone-tubing, removed heat from the face of the peltier (Figure 3-10 a. b. & c.). The cold, outer-facing-surface of the peltier had a 2mm-thick thermal conducting-tape (6Wm·K; www.thegamebooth.co.uk), and a thermocouple (SA1XL-KI-SRTC – Omega.co.uk) was positioned between the peltier and the thermal tape. The required temperature prior to application of the teeth was -8°C. A length of cooling-circuit silicone-tubing was submerged in cold water, in a polystyrene box (internal dimensions Height 17cm x Width 26cm x Depth 35cm) and right-angled-connectors for soft-rubber-tubing (www.autosiliconehoses.com) prevented kinking of the tubing on entry and exit of the polystyrene box. The copper-plate waterblock with peltier was mounted in an aluminium-frame in the Cube with guides which allowed forward and reverse-movement by manual operation external to the Cube to enable tooth-contact (Figure 3-11). The Cube provided a stable thermal environment, as previously described.

Copper-Plate Waterblock with Peltier and Thermal Tape
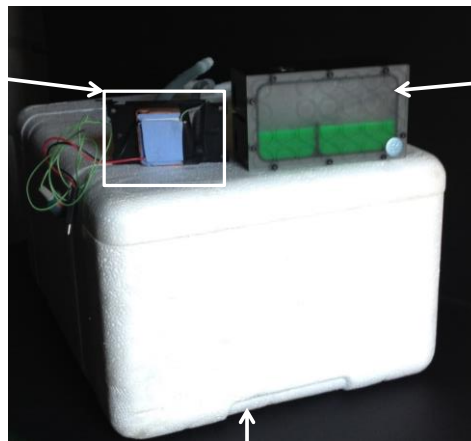
Pump with Coolant-Reservoir

Polystyrene Box with Water

a.

Thermal Tape
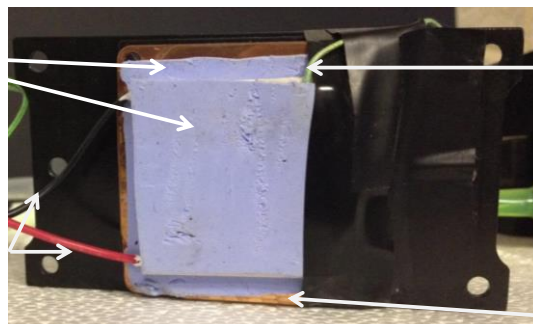
Thermocouple between Thermal Tape and Thermoelectric Peltier

Thermoelectric Peltier Wires

Copper-Plate Waterblock

b.

Coolant Inlet and Outlet

Copper-Plate Waterblock

Thermal Tape on Both Surfaces of Thermoelectric Peltier
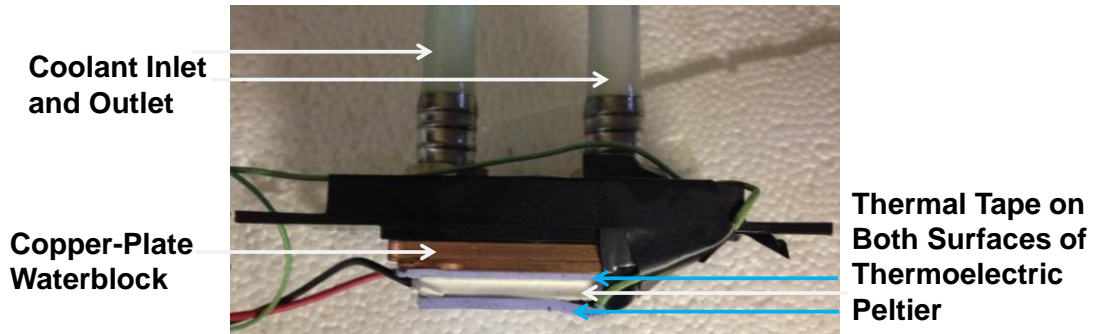
c.

Figure 3-10 Thermoelectric peltier cooling-unit with copper-plate waterblock and pump
  a. Pump with reservoir for thermal coolant
  b. Enlarged view of copper-plate (white square in a.) thermal tape and copper-plate waterblock with thermocouple
  c. Bird's-eye-view of copper-plate waterblock, with coolant inlet and outlet and peltier (white arrows) between thermal tape (blue arrows).

Teeth in Thermal Equilibrium Prior to Cooling

Even-Contact to the Occlusal-Surface of Teeth

Compressible Thermal Tape on Peltier Surface

Temperature-Scale
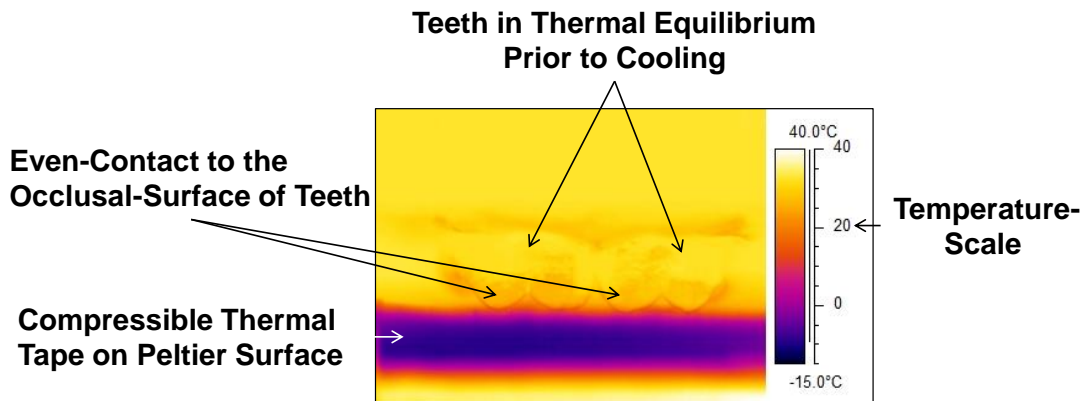
Figure 3-11 Thermograph of application of thermoelectric peltier cooling-unit to teeth.

A two-channel pump (Figure 3-12) with PVC manifold-tubing (Watson-Marlow Sci Q 400 403U/VM2 50RPM - with PVC Manifold-Tubing black-black internal diameter 0.76mm, orange-blue internal diameter 0.25mm, Watson-Marlow Ltd, www.watsonmarlow.com) circulated distilled water as the simulated blood-flow. The manifold-tubing was sheathed to a larger-diameter silicone-tubing (2mm internal-diameter with 1mm-wall-thickness) which fed into a water-bath (Grant Instruments, Cambridge) at 37°C, controlled by a temperature-controller (TD100 Temperature-Controller Auber Instruments, auberins.com).
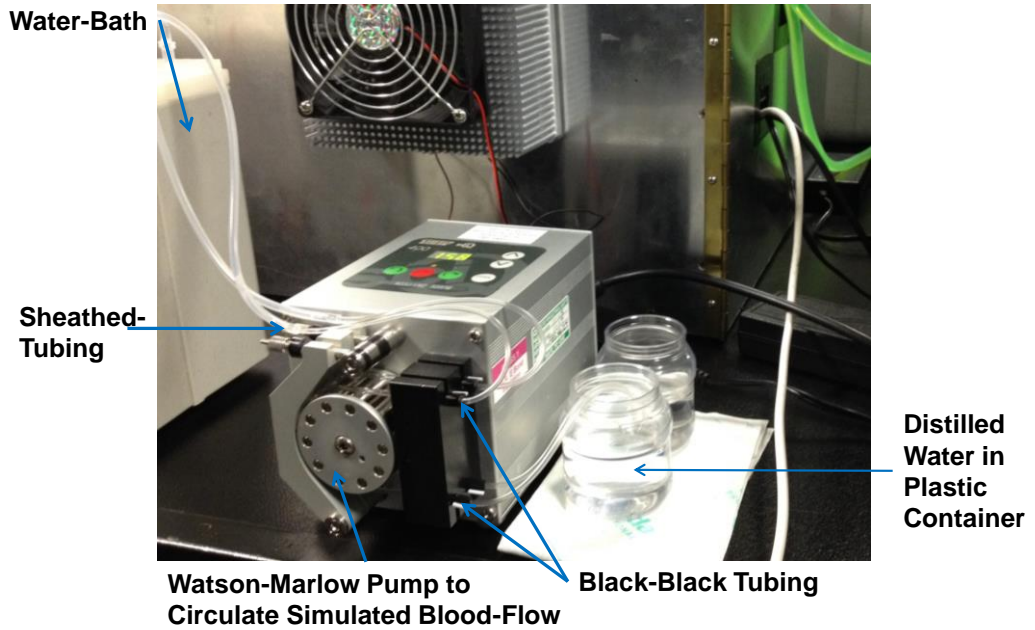
Figure 3-12 Watson-Marlow pump provided desired flow-rate.

On leaving the water-bath, tubing was guided through an acrylic holder (Acrylic Block and Solid Perspex Rods www.wholesalepos.com), where two plastic cams (www.ebay.co.uk) attached to a motor with an output speed of 60rpm (Philips, 12Volts, DC, 60RPM Motor, RS Components – 440-082 https://uk.rs-online.com) provided a simulated pulse when required, by compressing the tubing within a recessed acrylic-block (Figure 3-13).
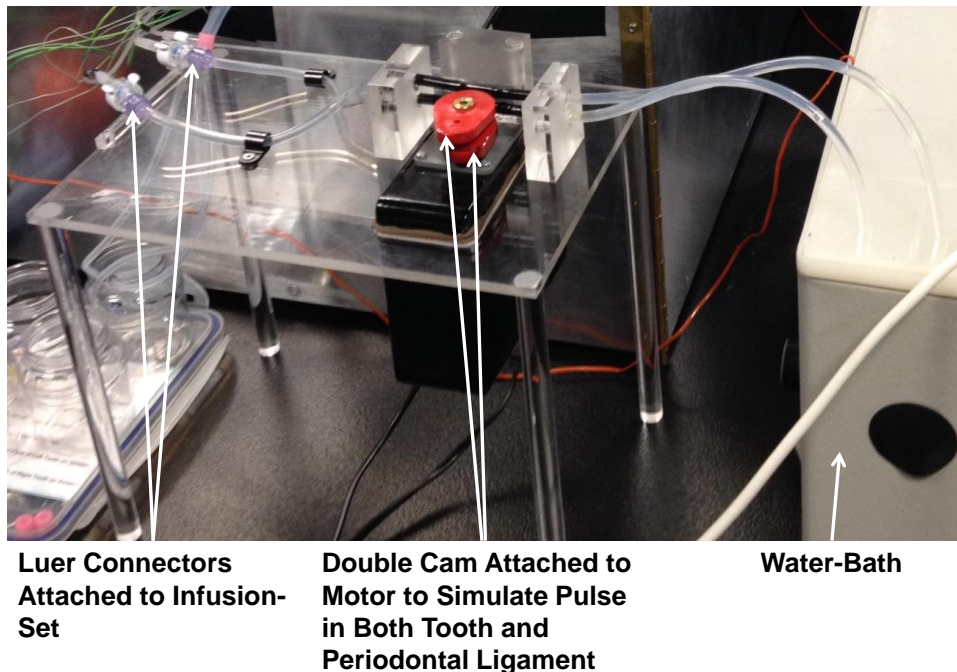
Figure 3-13 Equipment to simulate pulse from compression of tubing via two circulating cams (red) powered by a 60rpm electric-motor housed within the black project-box suspended in the acrylic-sheet. Both the tooth and periodontal ligament blood-flow were pulsed simultaneously by the two cams.

Luer connectors (Luer Lock-Plug Cole-Palmer - www.colepalmer.co.uk).
secured into clips attached to the acrylic mount enabled the luer connector
from the 23-gauge infusion-set (Terumo® Surflo® Winged-Infusion-Set (23-
Gauge, External Diam. 0.6mm) www.medisupplies.com) to securely engage
with the tubing. This provided an inflow of water at the desired flow-rates of
≈0.5ml/min from the black-black tubing and 0.15ml/min, 0.08ml/min and
0.03ml/min from the orange-blue tubing. Water was collected, via the tube
attached to the root of each tooth, into a plastic pot which was weighed
before and after each sequence on a high-precision digital weighing-scale
(Digital Miligram Jewelry Scale - GEM50 Smart Weigh). Each sequence was
timed via an iPhone for the collection of water and the flow-rate was
calculated from:

$$FlowRate\ (ml/\min) = \frac{(weight\ of\ pot+water\ (g)) - (weight\ of\ pot\ (g))}{time\ (mins)}$$

$$where\ 1g\ of\ water = 1ml$$

Equation 10 Flow-rate-calculation.

The above application was used with a Cube temperature of 30°C, reflected
apparent temperature of 34.6^{o}C and humidity of 29%, to provide a flow-rate
of 0.5ml/min, 0.15ml/min, 0.08ml/min and 0.03ml/min and application of the
cooling-unit was to the occlusal-surface of the teeth. Figure 3-14 shows the
full experimental set-up.
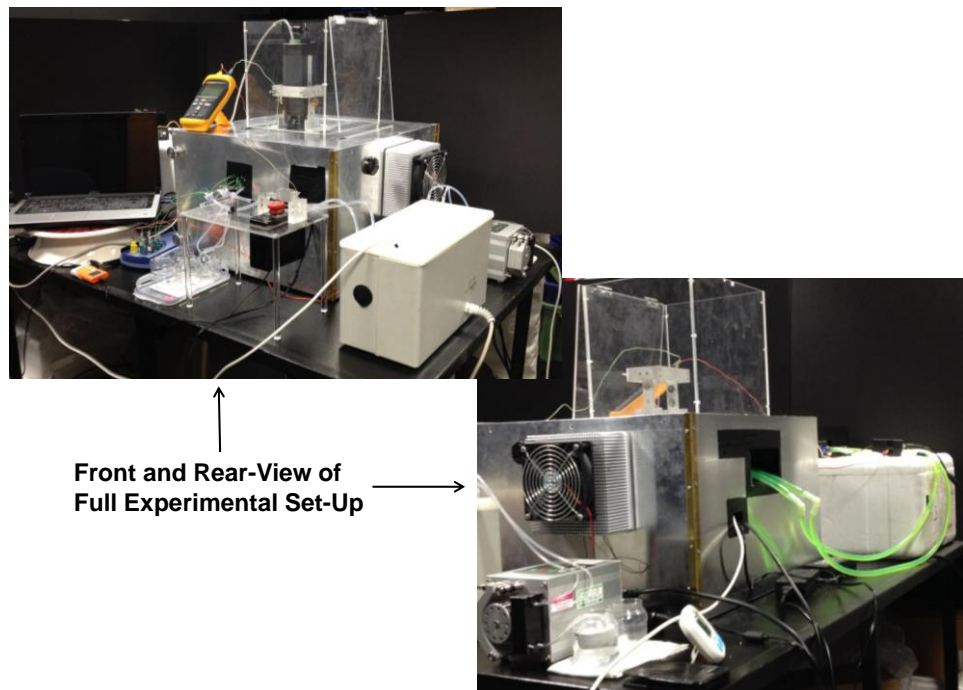
Figure 3-14 Full experimental set-up.

3.5.1.2 Sample-Preparation

The sixteen human molar teeth collected from Leeds Dental Institute Research Tissue-Bank (151111/PL/77 Appendix A.4.1 & A.4.2) were accessed via the apical foramen of each root-canal and prepared with hand-endodontic K-files from Size 8 – 35 (www.henryschein.co.uk). Irrigation of the canals was with sodium hypochlorite (2% Milton) dispensed via an endodontic-syringe after each use of the files. This continued until patency of the tooth was confirmed with the flow of liquid through the tooth, i.e., fluid applied through one root which flowed through the tooth and exited the tooth via another root.

The teeth were paired to match, as closely as possible, by tooth-size. Each pair of teeth were held within a purpose-built unit, numbered 1 to 8, for ease of placement and removal from a fixed, rigid aluminium-frame attached to the Cube at a focal distance of 8cm from the thermal camera. The frame had two supports to hold the paired-units which were secured with wing-nuts for tightening and removal (Figure 3-15a & b).

Paired-Teeth in Holding-Unit and Secured with Wing-Nuts
Camera-Mount
Jack-Plug in Protected Box for Transformer and Mains Supply
Access-Hole
Internal Heat-Sink
Thermal Sensor
Door-Hinge
External Heat-Sink with Cooling-Fan
Holes for Knurled-Thumb-Screws
Heating-Pad
Rigid and Fixed Aluminium-Stand with Two Supports for Teeth-Pairs

a.

**Wing-Nuts to Secure
Paired-Teeth Holding-Unit 4**

**Thermal
Sensor**

Rigid-Stand

**Inlet and Outlet
Tubing and
Thermocouples**

**Support With Screw-Locators
for Paired-Teeth Holding-Units**

b.

Figure 3-15 The Cube:
a. With rigid-stand to support the paired-teeth holding-unit
b. Close-up view of the support-unit securely attached with wing-nuts - as highlighted by white box of image a.

The pairs of teeth were embedded within a simulated alveolar bone of the jaw of Aluwax (www.Aluwaxdental.com) and secured with Green Stick Compound (www.kerrdental.com). Within the Aluwax, each tooth-root was wrapped with a 300mm-length of tubing from the 23-gauge winged-infusion-set. Aluwax was carried to the cementoenamel-junction.

Between the tooth-root and the tubing, a thermocouple was placed on the lingual-aspect (SA1XL-KI-SRTC – www.omega.co.uk). A thermocouple was also placed into the pulp-chamber via a root-canal (5SRTC-TT-KI-40-1M – www.omega.co.uk), until resistance was felt. A 23-gauge cannula was placed into a root-canal from the infusion-set. These were secured with Loctite Superglue and sealed with Aluwax. One root was used as the outlet for the simulated blood-flow, with a silicone-tube attached as a sheath to the root. A radiograph was taken (70kV, 7mA, 0.16s) of each pairing to review placement of the thermocouples (Pair 1 - Figure 3-16, Pair 2-8 Appendix A.6).

Whole teeth were prepared for simulated vitality, as described above, and stored in damp tissue within a sealed plastic bag in a rigid-box under refrigeration, until needed.
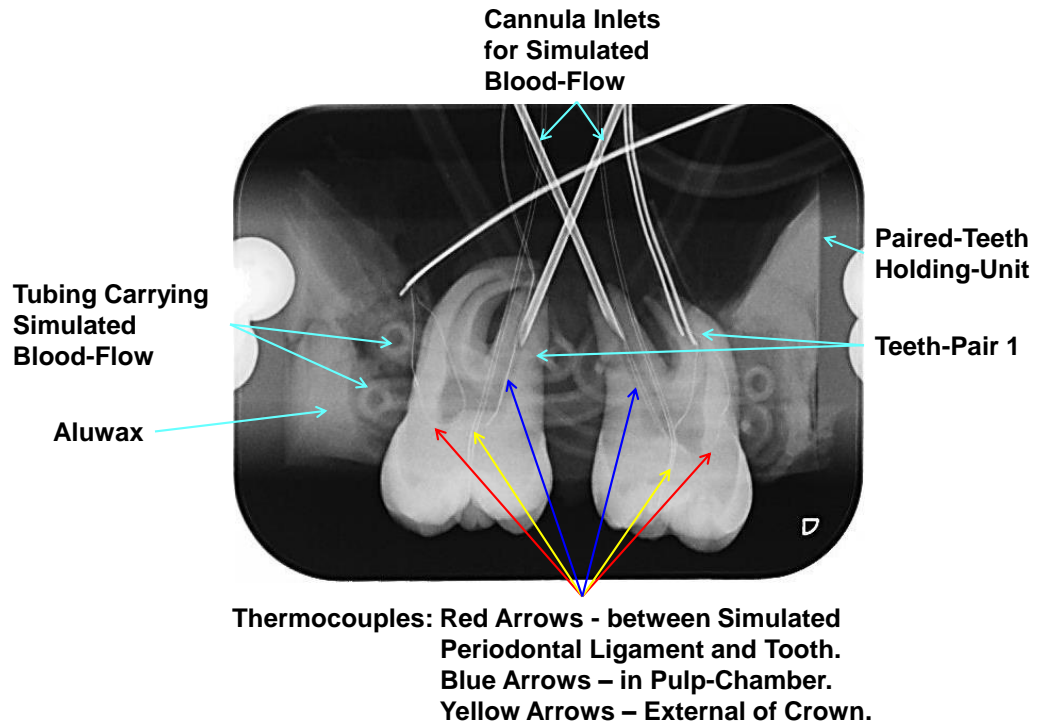
Figure 3-16 Radiograph of Teeth-Pair 1. A cannula inlet-flow to each of the teeth and tubing carrying blood-flow within the simulated jaw. Thermocouples positioned between the tooth and simulated periodontal ligament (red arrows), within the pulp-chamber (blue arrows), and on the external surface of the tooth crown (yellow arrows).

3.5.1.3 Data-Capture

Application of the cooling-unit to the occlusal-surface of the teeth of Pair 4 was made whilst the thermal camera was recording until the internal temperature of the thermocouple in the tooth on the right-side of the screen reduced by, $0^{o}C$, $2^{o}C$, $4^{o}C$, $6^{o}C$, $8^{o}C$ and $10^{o}C$. The simulated blood-flow was applied to provide the following vitalities in a cross-over-design:

a. Nothing (Nil)

b. Right-tooth on screen (RTS)

c. Left-tooth on screen (LTS)

d. Periodontal ligament (PDL)

e. Right-tooth on screen with periodontal ligament (RTS PDL)

f. Left-tooth on screen with periodontal ligament (LTS PDL)

g. Pulsed right-tooth on screen with periodontal ligament (RTS PDLP)

h. Pulsed left-tooth on screen with periodontal ligament (LTS PDLP).

This provided a simulation of:

a. two non-vital teeth, without periodontal blood-flow (NIL)

b. one vital tooth on the right-side of the screen and one non-vital tooth on the left (RTS)

c. one vital tooth on the left-side of the screen and one non-vital tooth on the right (LTS)

d. two non-vital teeth, both with periodontal blood-flow (PDL)

e. one vital tooth on the right-side of the screen and one non-vital tooth on the left, both with periodontal blood-flow (RTS PDL)

f. one vital tooth on the left-side of the screen and one non-vital tooth on the right, both with periodontal blood-flow (LTS PDL)

g. one vital tooth on the right-side of the screen with simulated pulse and one non-vital tooth on the left, both with pulsed periodontal blood-flow (RTS PDLP)

h. one vital tooth on the left-side of the screen with simulated pulse and one non-vital tooth on the right, both with pulsed periodontal blood-flow (LTS PDLP).

All thermocouples were connected to the Data-logger (Pico Thermocouple Data-Logger TC-08 – www.omega.co.uk) which saved the recorded temperatures every second.

3.5.1.4 Data-Processing

Analysis was from production of the time-series of re-warming, collected by the thermal camera which was running throughout the sequence of cooling and re-warming. The area-of-interest was the buccal-surface of the two teeth in each pair. This allowed the area-under-the-curve to be calculated from the sum of temperatures across the set timeline of re-warming. The re-warming temperatures were aligned to commence at the same temperature. This was prepared in Microsoft Excel using the embedded ThermaCAM Researcher Professional 2.10 Software, as previously described.

The difference in area-under-the-curve (AUC) was calculated by subtracting the value of left-tooth from the right-tooth, irrespective of simulated vitality:

$$Difference\ in\ AUC = AUC\ Right\ Tooth - \ AUC\ Left\ Tooth$$

Equation 11 Calculation of difference in area-under-the-curve.

The maximum temperature-difference of the aligned re-warming sequences was also calculated for each sequence in the same way, i.e., right-tooth minus left-tooth.

The final difference to be calculated between the two teeth of each pair was the characteristic-time-to-relaxation difference. Subtraction was the same, i.e., right-tooth minus left-tooth.

Thermal maps were produced from the area-under-the-curve via the bespoke Matlab software described in Chapter 3, Section 3.3.

This allowed the most suitable drop-in-temperature to be estimated to detect a difference between a vital and non-vital tooth by three different methods and each was reviewed for the most appropriate. The ideal time to cool the teeth was then also calculated.

Once the timeline was established, all 8 Pairs were treated as above, with cooling for the newly-acquired time which was recorded by a digital-timer (www.muddler.co.uk) and data was collected by the thermal camera for processing.
Descriptive data was prepared following analysis in Microsoft Excel.

Each molar tooth was placed with a dissimilar molar tooth, and these two teeth can be statistically analysed as independent-samples and subject to the assumptions of the statistical test which includes normality testing of the data, a parametric Independent-samples t-test could be performed if the data is normally distributed. If it is not, a non-parametric test may be used, e.g., Mann-Whitney U test, with consideration of the test assumptions (Laerd Statistics, 2015).

Each molar tooth was exposed to being a vital tooth and non-vital tooth, allowing statistical analysis with a parametric paired-samples t-test if the data was normally distributed, and assumptions met. If not, a non-parametric test may be needed, e.g., Wilcoxon signed-rank test or sign test, subject to satisfying the assumptions of that test (Laerd Statistics, 2015).

Statistical Tests were undertaken in IBM SPSS Statistics Version 21.

The results from assessing the in-vitro feasibility of using infra-red radiation in determining tooth-vitality are in Chapter 4, Section 4.5 and associated discussion in Chapter 5, Section 5.5.

3.6 Proof of Concept In-Vivo Volunteer-Study

The aim of this Study was to assess the feasibility of using infra-red radiation in determining tooth-vitality and, following the in-vitro work, translation of the methods to an in-vivo volunteer-study was commenced as proof of concept.

This required an appropriate cooling-method for the thermal disruption of the teeth which needed to be acceptable to the volunteer, unlike the application of a cold ice-stick (Kells et al., 2000b). The relationship of the human pulse to the heat-exchange in the vital tooth could also be assessed. This addressed the ninth objective to develop an in-vivo cooling-unit to cool the teeth, and tenth objective to analyse and evaluate the collected infra-red radiation during a re-warming sequence using a thermal camera to determine vitality of a pair of teeth in-vivo, one of which was vital and one root–treated.

3.6.1 Method

3.6.1.1 Ethical Approval and Recruitment

Ethical approval of the Study-design was sought from the Dental Research Ethics Committee (240315/PL/159 - Appendix A.4.3). The Study aims to recruit twelve healthy volunteers in total, of which two have been recruited and reported.

Volunteer Information was circulated and expressions of interest received. An Information-Sheet was issued (Appendix A.4.4) and an appointment then arranged on the Dental Translational Clinical Research Unit (DenTCRU) for discussion, answer any questions and assess suitability to take part. Written informed consent was gained following a minimum period of 24 hours from receipt of the Information-Sheet and booking an appointment.

Each volunteer was allocated a number on a Case-Report-Sheet for the clinical session. Volunteer information was collected which included: age, gender, ethnic-origin and medical history. Discussion and inspection of the Volunteer's anterior-teeth using a plastic disposable dental-mirror was undertaken to ascertain the presence of a natural vital and non-vital tooth. These teeth were to have no facings or crowns.

Inclusion criteria stipulated Volunteers were to:

- be age 18 years and over, healthy, willing and able to provide full and informed consent

- have a natural root-treated (dead) and non-root-treated (live) tooth within the anterior-teeth.

Exclusion criteria stipulated:

- no students or members of staff under management of the Principal Investigator could participate

- anterior-teeth with artificial coverings, such as crowns or veneers on teeth under investigation, were unacceptable

- no increased mobility of anterior-teeth was to be evident

- if the volunteer was undergoing dental treatment of anterior-teeth they could not be included

- no volunteer was to have an allergy to plastic

- teeth hypersensitive to cold water would exclude the Volunteer from the Study.

3.6.1.2 Equipment-Preparation

A vertically adjustable work-station with chin-and-headrest, and a thermal camera-stand with gimbal to set a focal distance of 8cm was developed (in conjunction with Kirkstall Precision Engineers, Leeds – www.kirkstallprecision.co.uk). The thermal camera was switched on at the start of the appointment and mounted on the gimbal attached to the work-station. Sundries e.g., cheek-retractors, cotton-wool-rolls, gauze, Vaseline, plastic cups, plastic disposable intra-oral dental-mirror, were prepared on the work-station (Figure 3-17 & 3-18). Personal protective equipment: eye-protection, plastic bib, gloves and clinical gowns for the operator and assistant were also available.
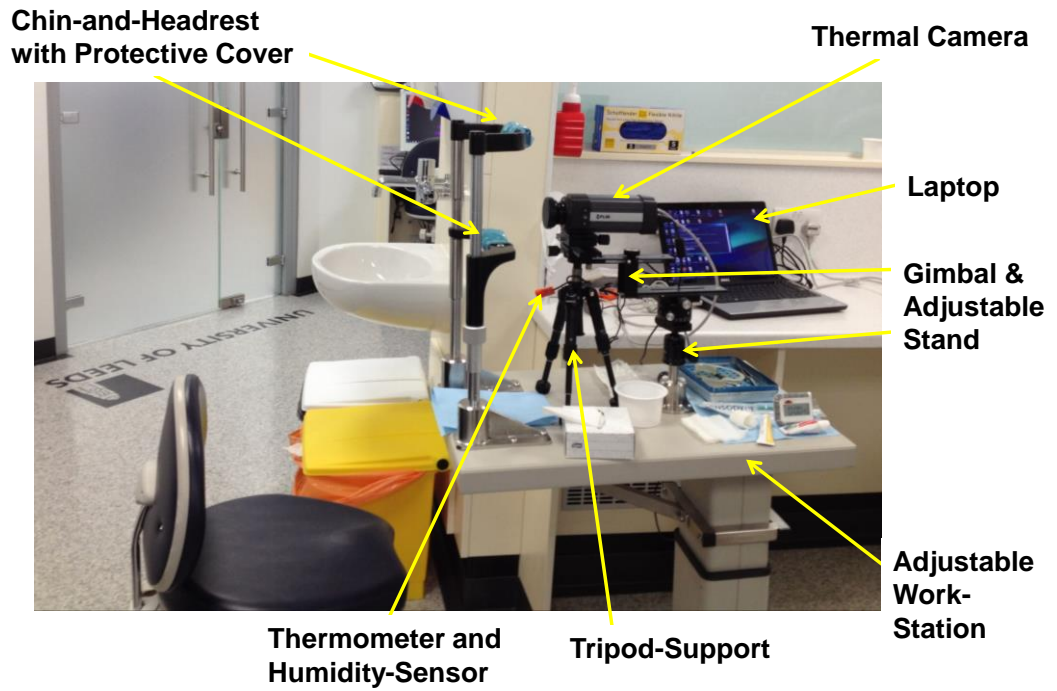
Figure 3-17 Clinical preparation of work-station.
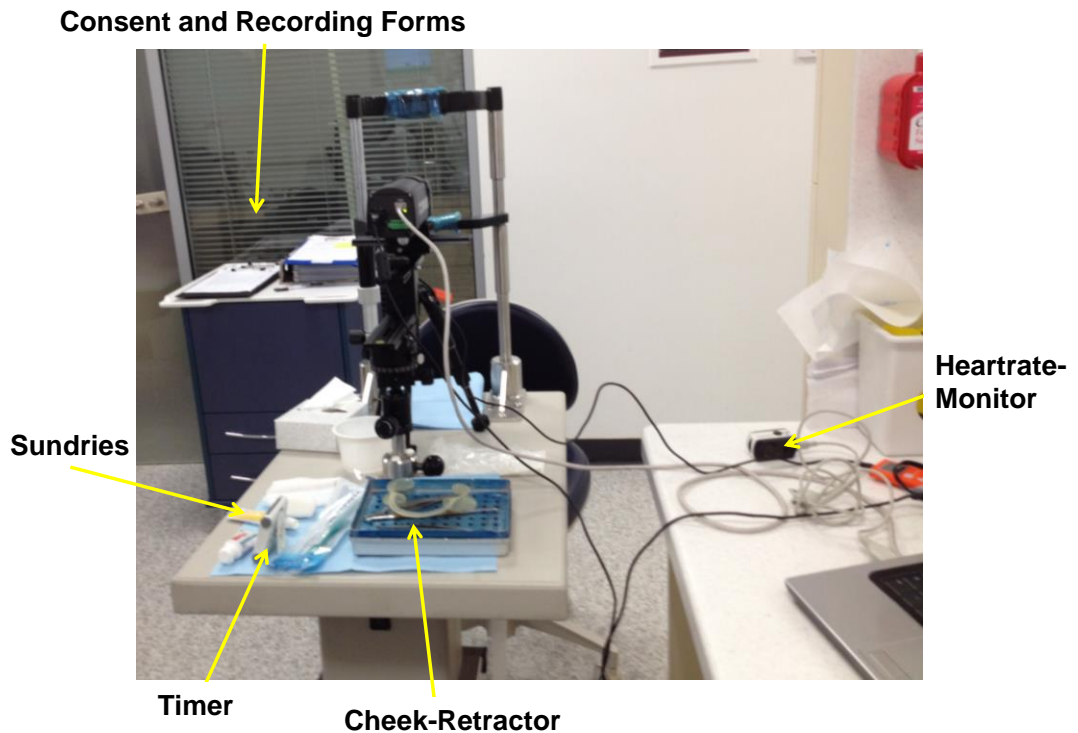
Figure 3-18 Clinical and administration work-areas.

The digital recording of all aspects – heartwave, thermal imaging, room-humidity and temperature - was prepared from a single laptop to record the same timeline. A heartrate-monitor (CMS 50E Pulse Oximeter, Contec Medical Systems Co., Ltd, China www.contecmed.com) used the

manufacturer's software, and bespoke software (Medical Physics Leeds Teaching Hospital Trust) was developed for the time of the peak wave. The temperature and humidity-sensor - Prime Capsule Data-Logger – (www.perfect-prime.com) used the manufacturer's software and the thermal imaging from the FLIR SC305 Thermal Camera was collected via ThermaCAM Researcher Professional 2.10.

A bespoke ice-filled-wax occlusal-bite-block (Figure 3-19) produced from a 3D printed mould (Courtesy of Professor David Brettle, Medical Physics, Leeds Teaching Hospital Trust) was stored in a domestic freezer ready for use.
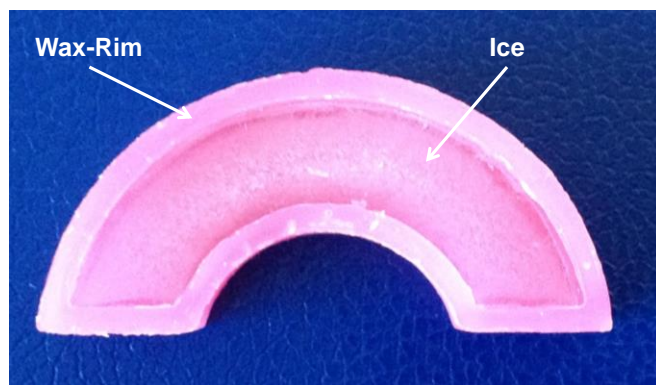
Figure 3-19 Bespoke ice-filled-wax occlusal-bite-block to cool teeth.

3.6.1.3 Volunteer-Preparation

Once suitability was ascertained and consent gained to continue with the Study, a digital photograph of the anterior-teeth was taken with a digital camera. This time allowed a period of stabilisation of approximately 15-20 minutes for the Volunteer in the clinical environment.

The Volunteer cleaned their teeth with the toothbrush (Sensodyne 3.5) and toothpaste (Oral-B Pro-Expert 15ml Tube) provided, then rinsed. The volunteer was seated adjacent to the work-station with chin-and-headrest (Figure 3-20).
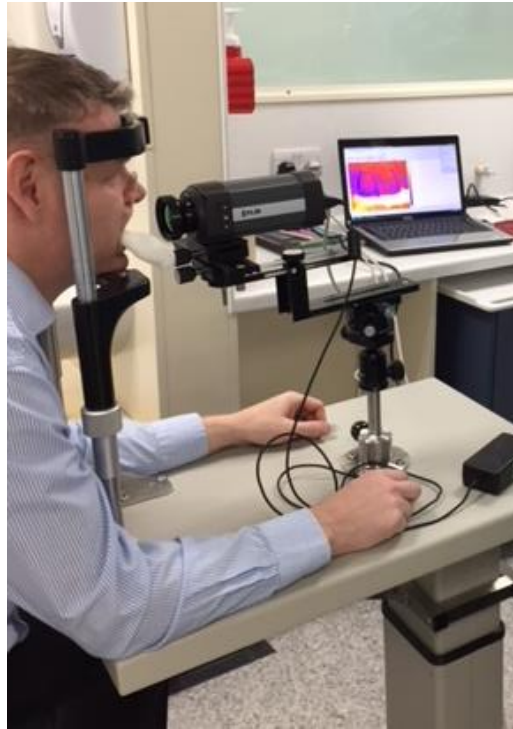
Figure 3-20 Demonstration of work-station with chin-and-headrest and thermal camera in position.

A pulse-oximeter with heartrate-monitor (Figure 3-21) was attached to the Volunteer's finger to collect the time of the peak of the PQRST Wave, i.e., R, with bespoke software.

Figure 3-21 Photograph of pulse-oximeter with heartrate-monitor.

Vaseline was applied to the Volunteer's lips prior to placement of the cheek-retractor, following which the anterior-teeth were dried with cotton-wool.

An ice-filled-wax occlusal-bite-block was removed from a domestic freezer and allowed to warm until a thin film of melted ice was visible, and the temperature measured with an infra-red thermometer (GM700-EN-01 Shenzhen Jumaoyuan Science and Technology Co. Ltd, China).

The ice-filled-wax occlusal-bite-block was positioned in the mouth and the Volunteer closed onto the block with their teeth, applying a cold thermal disruption to these teeth from the incisal-edges. This was retained for 45 seconds, then removed.

Following the recording, the cheek-retractor was removed and paper-tissues offered to remove any debris. All waste materials were disposed of via clinical waste, or sent for sterilization, e.g., cheek-retractor. The Clinical Unit was disinfected by the Research Team, as per normal clinical process.

The Volunteer was asked whether the process was acceptable and to make any comments on the procedure. A £10.00 Love2Shop Voucher was given as an appreciation-gift, and receipted.

3.6.1.4 Data-Capture

Paper data-sheets were completed for each Volunteer prior to recording any digital-data.

The digital recording of all aspects – heartwave, thermal imaging, room-humidity and temperature - commenced from a single laptop with associated software, recording the same timeline for all devices prior to placing the ice-filled-wax occlusal-bite-block. The thermal sequence of the anterior-teeth was recorded for 5 minutes and timed by a digital-timer (Muddler.co.uk).

The volunteers comments on the process were recorded on paper data-sheets.

3.6.1.5 Data-Processing

The recorded-data was processed and analysed with ThermaCAM Researcher Professional 2.10 and converted from the devices software to a format for use in Microsoft Excel. Volunteer information from paper data-sheets were processed by hand.

The Proof of Concept In-Vivo Volunteer-Study results are in Chapter 4 Section 4.6 and associated discussion in Chapter 5 Section 5.6.

Chapter 4 Results

The stability of the thermal environment generated by development of the Cube, as described in Chapter 3, Section 3.1, is shown in Figure 4-1 to 4-3.

4.1 Development of a Stable In-Vitro Thermal Environment
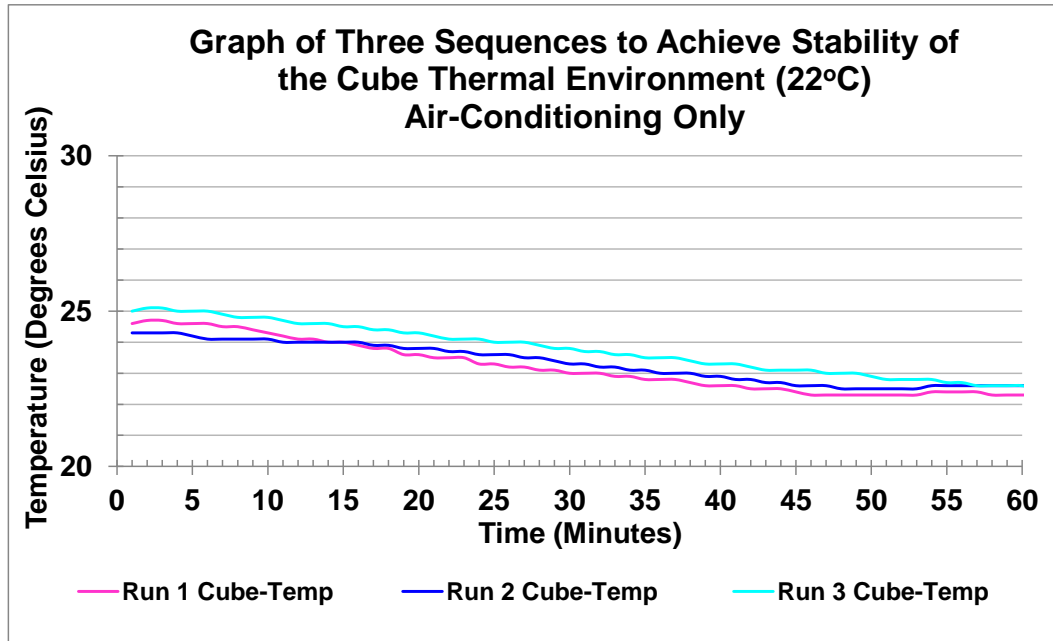
Figure 4-1 Line graph of three stabilisation sequences using air-conditioning only which did not achieve thermal stability of the cube at 22°C within 60 minutes.
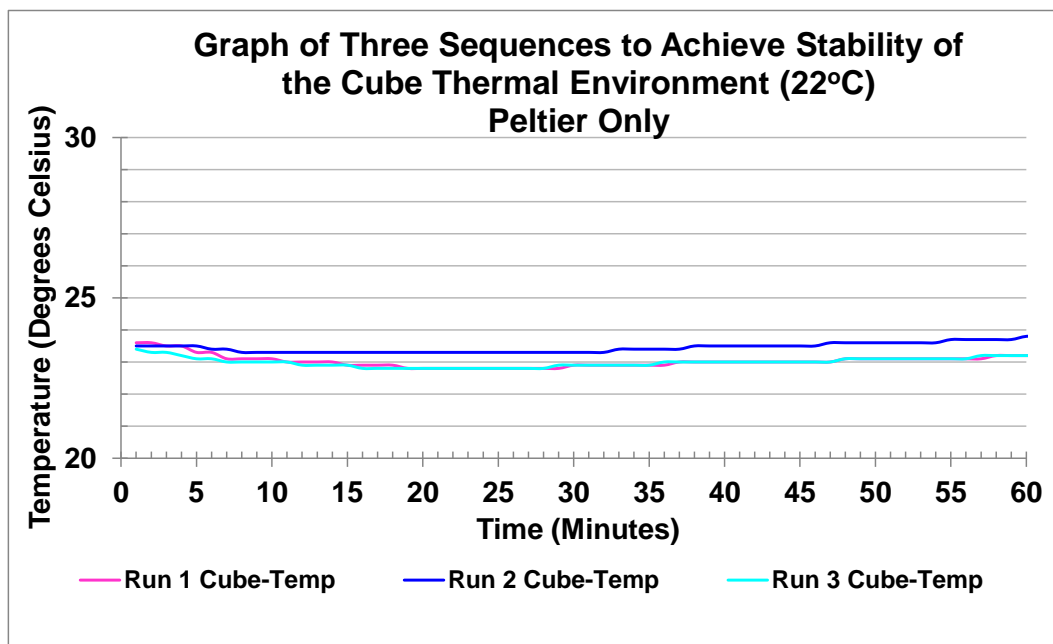
Figure 4-2 Line graph of three stabilisation sequences using thermoelectric peltier cooling only which did not achieve thermal stability of the cube at 22°C within 60 minutes.
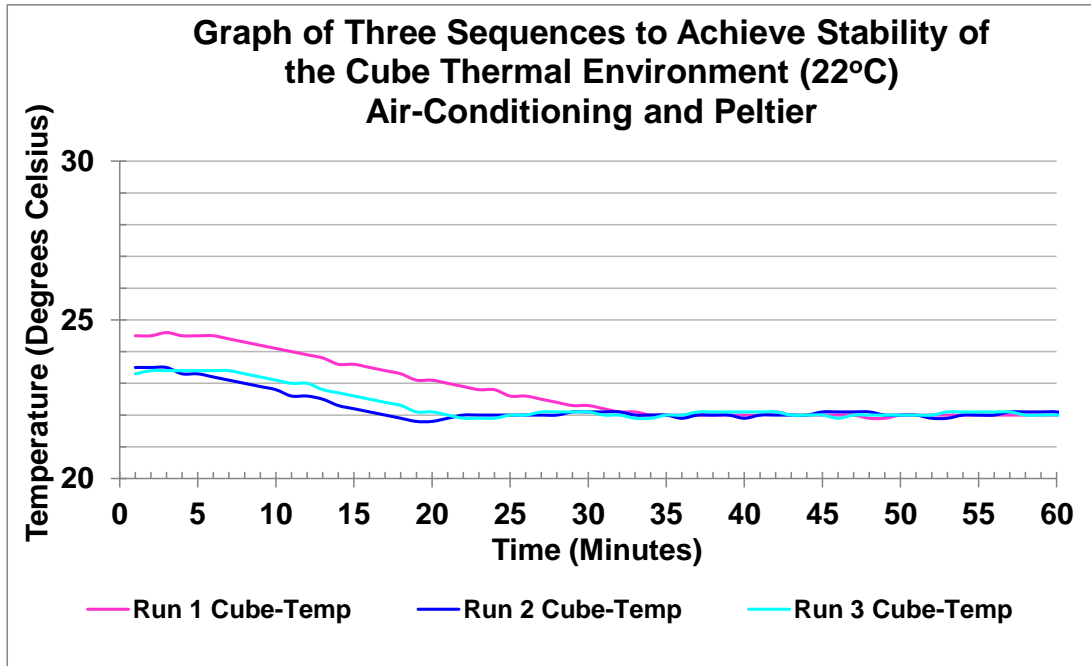
Figure 4-3 Line graph of three stabilisation sequences using air-conditioning and thermoelectric peltier cooling which achieved thermal stability of the cube at 22°C within 60 minutes.

Figure 4-1 shows the thermal environment of the Cube does not achieve the desired temperature of 22°C over the 60 minute-sequence with only macro-control from the room air-conditioning in any of the three runs. Similarly, Figure 4-2 demonstrates the micro-control of the thermoelectric peltier cooling does not achieve the desired temperature of 22°C over the 60 minute-sequence in any of the three runs. Figure 4-3 shows the desired thermal environment of 22°C is achieved with both macro-control from the air-conditioning and micro-control from the thermoelectric peltier cooling in all three runs.

It took 34 minutes in run-one to achieve 22°C, 17 minutes in run-two and 21 minutes in run-three, providing a mean time of 24 minutes. A minimum stabilization period of 35 minutes was needed to achieve the required environmental temperature of the Cube.

The thermal environment of the Cube remained stable for the rest of the 60 minute-sequence ±0.1^{o}C for all three runs.

The discussion from developing a stable in-vitro thermal environment is in Chapter 5 Section 5.1.

4.2 Emissivity-Determination of Mineralised Human Tooth-Tissue

The Cube provided a stable thermal environment within which the other in-vitro investigations were conducted. The first of these was to determine the emissivity value of the tooth-tissue, as described in Chapter 3, Section 3.2. The results are shown in Figure 4-4 to 4-7 and Table 4-1 to 4-9.

4.2.1 Tooth-Data

The samples used were whole teeth and tooth-slices.
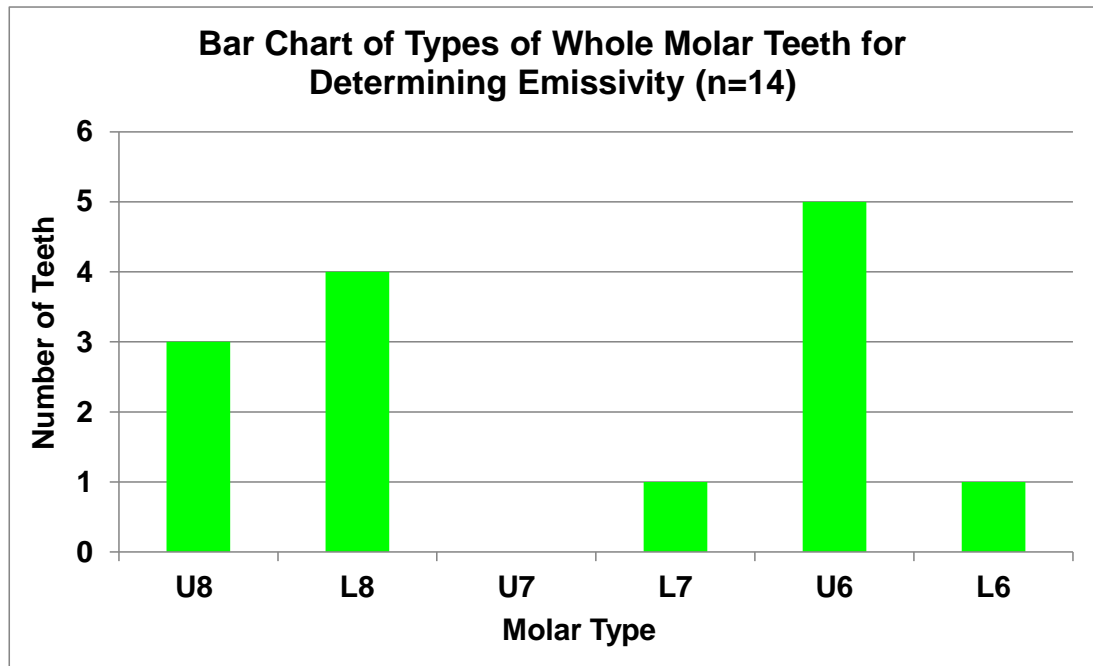
Figure 4-4 Bar chart of molar teeth collected for determining emissivity - commonest being the upper-first molar (U6) where U = upper and L = lower.

The 14 whole teeth evaluated for emissivity of surface-enamel were all molar teeth (Figure 4-4): 3 upper-third molars (U8), 4 lower-third molars (L8), 1 lower-second molar (L7), 5 upper-first molars (U6) – the commonest, 1 lower-first molar (L6).
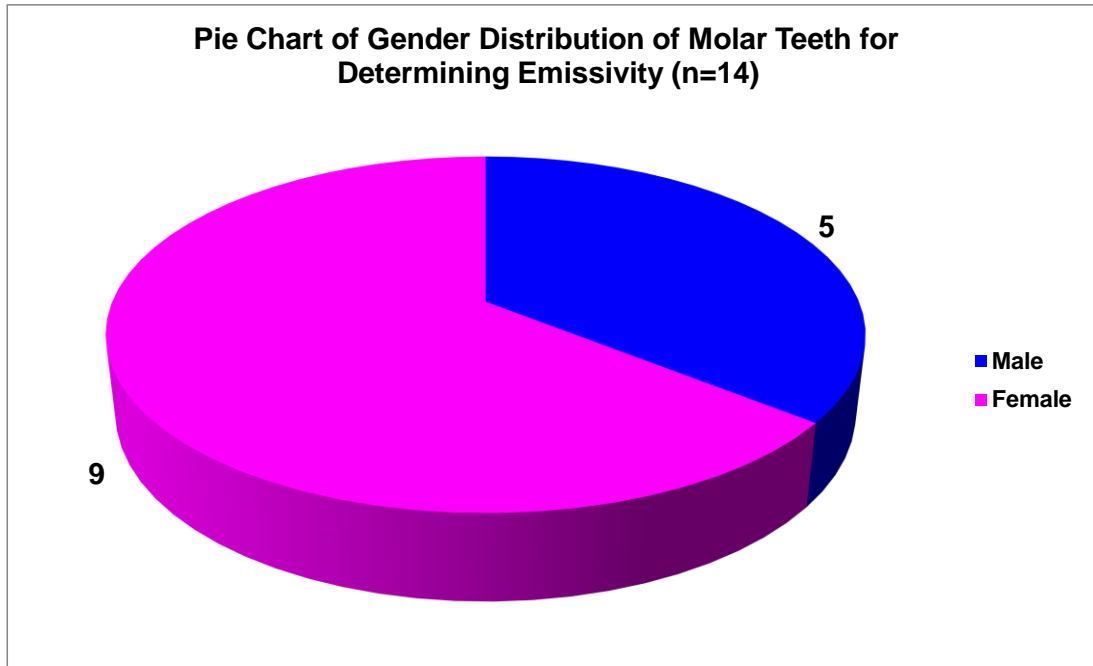
Figure 4-5 Pie chart of 5 male and 9 female donors of teeth for emissivity-determination.

The molar teeth were donated by 5 males and 9 females (Figure 4-5).
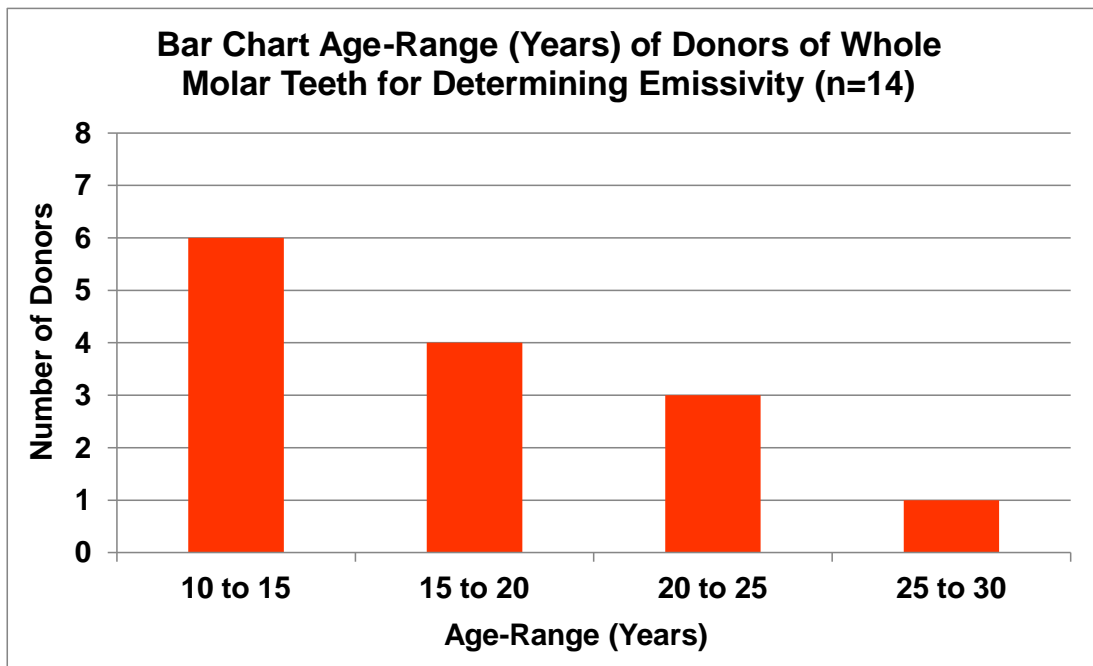
Figure 4-6 Bar chart age-range (years) of donors of whole molar teeth used for determining emissivity – most collected from the youngest age-range of 10 to 15 years.

The mean age of the donors of the whole teeth was 16 years and 11 months, ranging from 10 years to 28 years. 6 fall in the age-band 10-15

years – the most from any, 4 in the age-band 15-20 years, 3 in the age-band 20-25 years and 1 in the age-band 25-30 years (Figure 4-6).

12 donors were of white ethnic origin and the remaining 2 were unknown.

The two tooth-slices examined were samples from a lower-third molar of a female donor, aged 18 years, of unknown ethnic origin.

4.2.2 Enamel Emissivity-Values

The emissivity-values for the area-of-interest, as calculated against the temperature of the 3M Scotch Super 33+ Black Vinyl Electrical Tape with known emissivity of 0.96 ($\varepsilon = 0.96$), are shown below.

Table 4-1 Sample 1 enamel-temperatures and emissivity-values of two areas-of-interest over three runs repeated – highest emissivity-value 0.996 lowest value 0.956.

Sample	Tissue	Series	Run	AOI	Temp (^{o}C)	Mean Tape-Temp (^{o}C)	Emissivity (ε)
1	Enamel	1	A	5	31.800	31.775	0.964
Sliced		1	B	5	31.800	31.825	0.957
		1	C	5	31.700	31.725	0.956
	Mean				31.767		0.959
		2	D	5	31.800	31.750	0.971
		2	E	5	31.900	31.950	0.959
		2	F	5	31.800	31.750	0.961
	Mean				31.833		0.964
		1	A	6	31.900	31.775	0.978
		1	B	6	31.900	31.825	0.986
		1	C	6	31.800	31.725	0.978
	Mean				31.867		0.981
		2	D	6	31.900	31.750	0.996
		2	E	6	32.100	31.950	0.982
		2	F	6	31.900	31.750	0.983
	Mean				31.967		0.987
AOI = Area-of-Interest			**Highest Value**			**Lowest Value**	

Table 4-2 Sample 2 enamel-temperatures and emissivity-values of three areas-of-interest over three runs repeated – highest emissivity-value 0.975 lowest value 0.935.

Sample	Tissue	Series	Run	AOI	Temp (°C)	Mean Tape-Temp (°C)	Emissivity (ε)
2	Enamel	1	G	5	31.900	31.875	0.967
Sliced		1	H	5	31.800	31.750	0.975
		1	I	5	31.800	31.750	0.972
	Mean				31.833		0.971
		2	J	5	31.700	31.725	0.962
		2	K	5	31.700	31.675	0.965
		2	L	5	31.800	31.750	0.966
	Mean				31.733		0.964
		1	G	6	31.800	31.875	0.943
		1	H	6	31.700	31.750	0.956
		1	I	6	31.700	31.750	0.956
	Mean				31.733		0.952
		2	J	6	31.600	31.725	0.935
		2	K	6	31.600	31.675	0.940
		2	L	6	31.700	31.750	0.957
	Mean				31.633		0.944
		1	G	7	31.900	31.875	0.956
		1	H	7	31.800	31.750	0.966
		1	I	7	31.800	31.750	0.965
	Mean				31.833		0.962
		2	J	7	31.700	31.725	0.946
		2	K	7	31.600	31.675	0.947
		2	L	7	31.700	31.750	0.955
	Mean				31.667		0.949
AOI = Area-of-Interest			Highest Value			Lowest Value	

Table 4-1 and 4-2 show the emissivity-values for three consecutive sequences which were repeated, of the internal surfaces of sliced enamel, which range from 0.956 and 0.935 to 0.996 and 0.975 for sample 1 and 2, respectively.

Table 4-3 Mean emissivity-values of enamel from Sample 1 and 2 with an overall mean value of 0.965.

Sample	AOI	Mean Emissivity of Enamel [SD]		Total Mean [SD]
		Series 1	Series 2	
1	5	0.959	0.964	0.962
	6	0.981	0.987	0.984
	Mean	0.97 [0.013]	0.976 [0.014]	0.973 [0.013]
2	5	0.971	0.964	0.968
	6	0.952	0.944	0.948
	7	0.962	0.949	0.956
	Mean	0.962 [0.01]	0.952 [0.011]	0.957 [0.011]
Overall Mean		0.966 [0.011]	0.964 [0.016]	0.965 [0.013]
AOI = Area-of-Interest; SD = Standard Deviation				

Table 4-3 shows the mean emissivity-values of the internal surfaces of enamel from five areas-of-interest in two slices of the same tooth, giving an overall-value of 0.965.

Table 4-4 Whole teeth emissivity-values of surface-enamel for 14, teeth, 0.97 being the highest and 0.94 being the lowest.

Tooth	Tape-Temperature (^{o}C)	Tooth-Temperature (^{o}C)	Emissivity of Enamel-Surface (ε)
1	31.4	31.3	0.955
2	31.4	31.5	0.965
3	31.6	31.7	0.970
4	31.7	31.8	0.970
5	31.6	31.6	0.959
6	31.6	31.7	0.966
7	31.4	31.4	0.961
8	31.4	31.5	0.967
9	31.8	31.8	0.963
10	31.8	31.8	0.959
11	31.1	31.2	0.958
12	31.2	31.3	0.954
13	31.8	31.8	0.940
14	31.7	31.6	0.948
Mean			0.960
SD			0.009
SD = Standard Deviation	Highest Value		Lowest Value

The emissivity-value of the surface of enamel from 14 whole teeth (Table 4-4) range from a low of 0.94 to a high of 0.97, with a mean value of 0.96 [SD 0.009].

Table 4-5 Repeat whole teeth emissivity-values of surface-enamel for two teeth giving a mean value of 0.95 for each.

Tooth	Tape-Temperature (^{o}C)	Tooth-Temperature (^{o}C)	Emissivity of Enamel-Surface (ε)
13	32	31.8	0.940
13	31.8	31.8	0.958
13	31.9	31.8	0.951
Mean			0.950
SD			0.009
14	31.8	31.7	0.948
14	31.7	31.6	0.954
14	31.9	31.7	0.947
Mean			0.950
SD			0.004

Table 4-5 shows emissivity-values for two whole teeth which were repeated, and both teeth delivered a mean value of emissivity at 0.95. The reliability statistics for three repeat measures of emissivity on the enamel-surface for Tooth 13 and 14 was good at 0.67 (Table 4-6).

Table 4-6 Reliability statistics (Cronbach's Alpha) for emissivity for two whole teeth was good at 0.67.

Reliability Statistics	
Cronbach's Alpha	Number of Items
0.67	2

4.2.3 Dentine Emissivity-Values

Table 4-7 Sample 1 dentine-temperatures and emissivity-values of two areas-of-interest over three runs repeated – highest emissivity-value crown-dentine 0.957, lowest value root-dentine 0.913.

Sample	Tissue	Series	Run	AOI	Temp (^{o}C)	Mean Tape-Temp (^{o}C)	Emissivity (ε)
1	Dentine	1	A	7	31.700	31.775	0.952
Sliced	Crown	1	B	7	31.700	31.825	0.941
		1	C	7	31.700	31.725	0.945
	Mean				31.700		0.946
		2	D	7	31.700	31.750	0.955
		2	E	7	31.900	31.950	0.957
		2	F	7	31.700	31.750	0.946
	Mean				31.767		0.953
	Root	1	A	8	31.600	31.775	0.919
		1	B	8	31.500	31.825	0.913
		1	C	8	31.600	31.725	0.916
	Mean				31.567		0.916
		2	D	8	31.600	31.750	0.938
		2	E	8	31.700	31.950	0.917
		2	F	8	31.600	31.750	0.919
	Mean				31.633		0.925
AOI = Area-of-Interest			Highest Value			Lowest Value	

Table 4-8 Sample 2 dentine-temperatures and emissivity-values of three areas-of-interest (crown, root and root-face dentine) over three runs repeated - highest emissivity-value in crown-dentine 0.954 lowest value on root-face 0.817.

Sample	Tissue	Series	Run	AOI	Temp (°C)	Mean Tape-Temp (°C)	Emissivity (ε)
2	Dentine	1	G	8	31.700	31.875	0.926
Sliced	Crown	1	H	8	31.700	31.750	0.946
		1	I	8	31.700	31.750	0.954
	Mean				31.700		0.942
		2	J	8	31.600	31.725	0.943
		2	K	8	31.600	31.675	0.947
		2	L	8	31.600	31.750	0.938
	Mean				31.600		0.943
	Root	1	G	9	31.700	31.875	0.923
		1	H	9	31.700	31.750	0.944
		1	I	9	31.700	31.750	0.952
	Mean				31.700		0.940
		2	J	9	31.600	31.725	0.932
		2	K	9	31.600	31.675	0.947
		2	L	9	31.700	31.750	0.941
	Mean				31.633		0.940
Face	Root	1	G	10	31.300	31.875	0.830
		1	H	10	31.200	31.750	0.844
		1	I	10	31.200	31.750	0.844
	Mean				31.233		0.839
		2	J	10	31.100	31.725	0.817
		2	K	10	31.100	31.675	0.843
		2	L	10	31.200	31.750	0.847
	Mean				31.133		0.836
AOI = Area-of-Interest			**Highest Value**			**Lowest Value**	

Table 4-7 and 4-8 show the emissivity-values for three consecutive sequences of the internal surfaces of sliced dentine, which range from 0.913 (pink cell Table 4-7) for root-dentine to 0.957 (green cell Table 4-7) for crown-dentine in sample 1, and from 0.923 for root-dentine to 0.954 (green cell Table 4-8) for crown-dentine in sample 2. The root-face-dentine of sample 2 has a lower value than both internal dentine-surfaces at a minimum value of 0.817 (pink cell Table 4-8) and a maximum value of 0.847.

Table 4-9 Mean emissivity-values of dentine from Sample 1 and 2 with a mean value of 0.946 for internal surface of crown-dentine, 0.931 for internal surface of root-dentine and 0.838 for the external root-face.

Sample	AOI	Mean Emissivity of Dentine [SD]						Total Mean [SD]
		Series 1			Series 2			
		Sliced Crown	Sliced Root	Root-Face	Sliced Crown	Sliced Root	Root-Face	
1	7	0.946	.	.	0.953	.	.	0.950 [0.006]
	8	.	0.916	.	.	0.925	.	0.921 [0.009]
2	8	0.942	.	.	0.943	.	.	0.943 [0.01]
	9	.	0.940	.	.	0.940	.	0.940 [0.011]
	10	.	.	0.839	.	.	0.836	0.838 [0.012]
Overall Mean		0.944 [0.01]	0.928 [0.016]	0.839 [0.008]	0.948 [0.007]	0.933 [0.012]	0.836 [0.016]	0.905 [0.043]
AOI = Area-of-Interest; SD = Standard Deviation								

Table 4-9 shows the mean emissivity-values of the internal surfaces of dentine from five areas-of-interest in two slices of the same tooth, two from crown-dentine with a mean value of 0.944 and 0.948 giving an overall-value of 0.946, and two from root-dentine of 0.928 and 0.933 giving an overall mean of 0.931. The root-face of dentine was only available on sample 2 and gave an overall mean value of emissivity of 0.838 from two repeated sequences.

The lowest overall mean emissivity was found from the root-face of dentine (0.838 Table 4-9), and the highest value was found from enamel (0.965 Table 4-3).

4.2.4 Summary of Mean Emissivity-Values
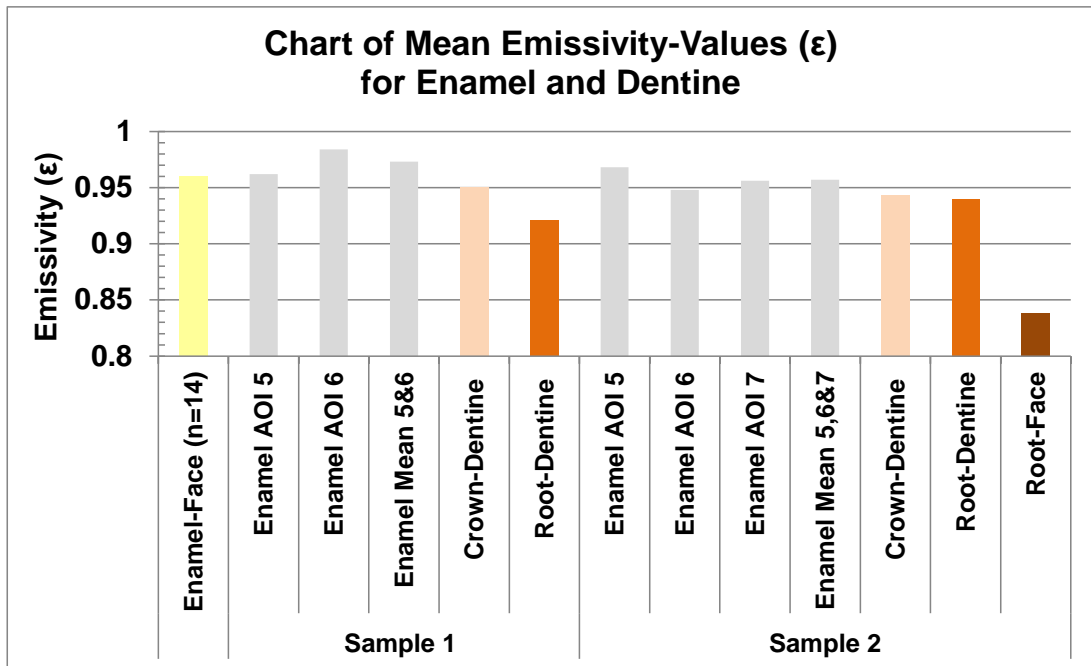
Figure 4-7 Chart of mean emissivity-values - enamel and dentine. Enamel has the highest value, root-face dentine has the lowest with crown-dentine and root-dentine in between.

The overall mean emissivity-values of enamel were found to be similar, at 0.965 (Table 4-3) for the internal surface and 0.96 (Table 4-4) for the external surface, and were overall the highest mean values of the mineralised tooth-tissues. Crown-dentine tended to have a higher emissivity than root-dentine (Figure 4-7). The root-face had the lowest emissivity-value of all mineralised tooth-tissue (0.838 Table 4-9). Enamel-values overlap dentine-values, although there is a tendency for enamel to have a higher emissivity than dentine, and crown-dentine tends to have a higher emissivity than root-dentine.

The discussion of calculating emissivity-values is in Chapter 5 Section 5.2.

4.3 Characterisation of the Thermal Properties of Enamel and Dentine

The emissivity-value of both human enamel and dentine were previously calculated. The next step was to determine the thermal properties of enamel and dentine from the characteristic-time-to-relaxation, which was calculated from curve-fitting the data collected by the thermal camera during a re-warming sequence, as described in Chapter 3, Section 3.3. The results are shown in Figure 4-8 to 4-30 and Table 4-10 to 4-12.

4.3.1 Tooth-Data

Both teeth sliced were third molars - one lower molar from an 18 year old female (as previously described) and referred to as Tooth 1 (3006141b), and one upper molar from a 28 year old female also of unknown ethnic origin, referred to as Tooth 2 (2107141a). Tooth 2 had a carious lesion.

4.3.2 Recording-Conditions

4.3.2.1 Copper-Baseplate, Aluminium Hotplate and Cube Temperature During Data-Capture

Three Graphs are presented in Figure 4-8, 4-9 & 4-10, for two slices from Tooth 1 which demonstrate the relationship between the temperatures of the copper-baseplate of the hand-carrier, the aluminium hotplate and the Cube.
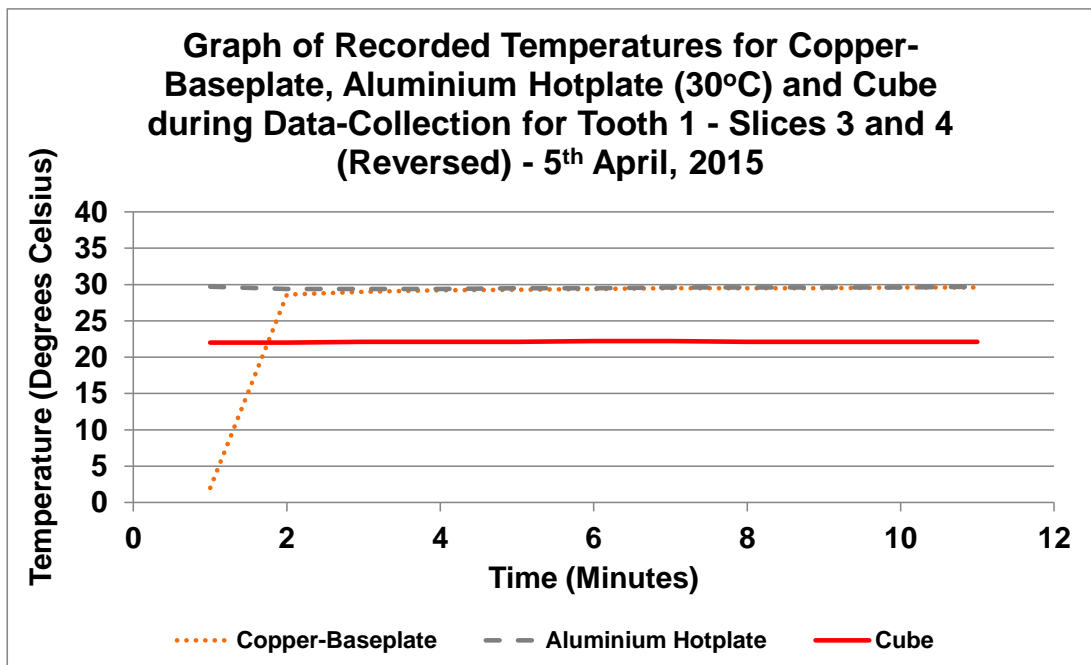
Figure 4-8 Graph showing re-warming temperatures of copper-baseplate achieving ≈30°C following cooling to 2°C, thermal stability of the cube (22°C) and aluminium hotplate (≈30°C) during data-collection for Tooth 1 Slices 3 and 4 (reversed) – 5th April, 2015.
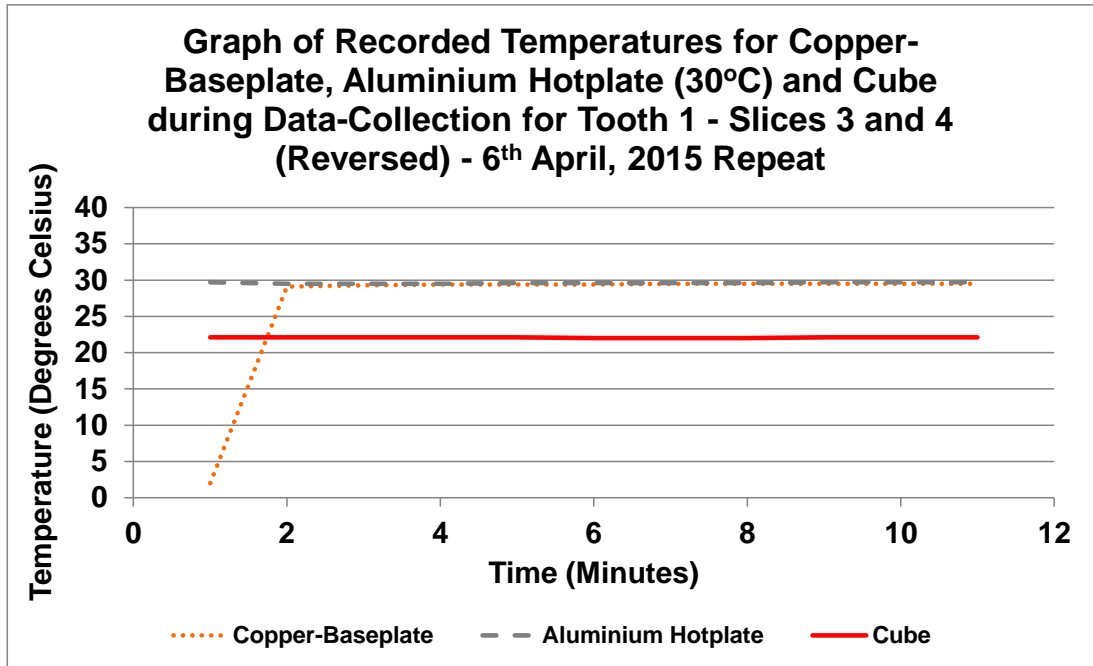
Figure 4-9 Graph showing re-warming temperatures of copper-baseplate achieving ≈30°C following cooling to 2°C, thermal stability of the cube (22°C) and aluminium hotplate (≈30°C) during the repeat data-collection for Tooth 1 Slices 3 and 4 (reversed) – 6th April, 2015 showing similarity to the first data-collection.
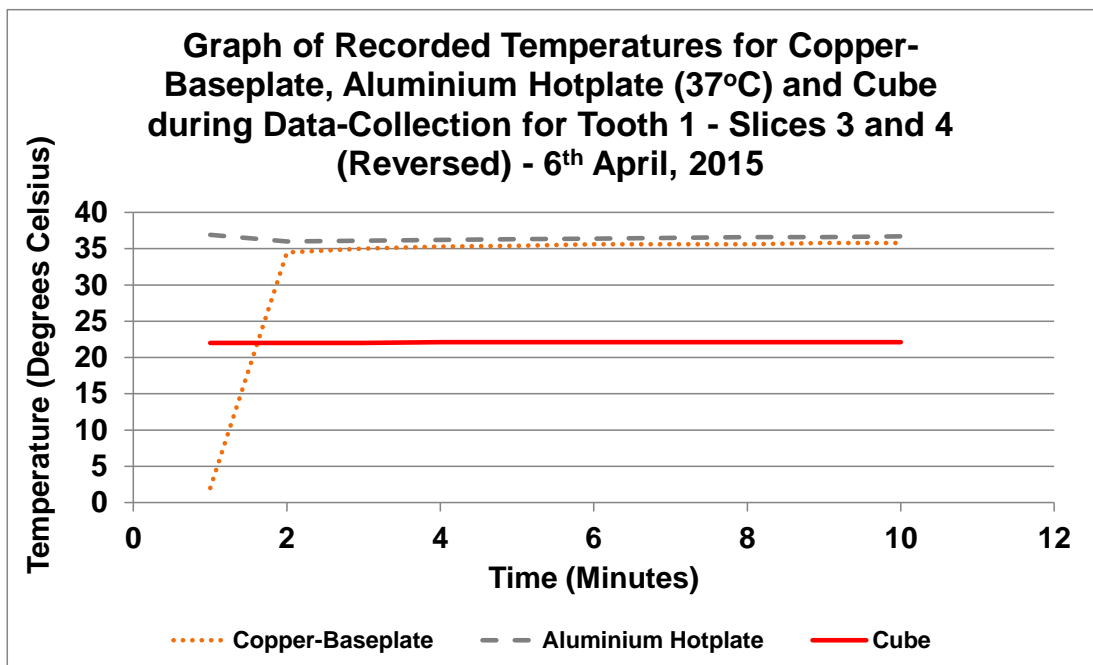
Figure 4-10 Graph showing re-warming temperatures of copper-baseplate achieving ≈37°C following cooling to 2°C, thermal stability of the cube (22°C) and aluminium hotplate (≈37°C) during data-collection for Tooth 1 Slices 3 and 4 (reversed) 37°C – 6th April, 2015.

Figure 4-8, 4-9 and 4-10 demonstrate a stable hotplate (grey broken-line) ≈30°C, or ≈37°C with a linear rise in temperature from 2°C for the copper-baseplate of the hand-carrier (orange dotted-line) following cooling on the ice-block, which reached thermal stability of either ≈30°C, or ≈37°C in approximately 1 minute. The Cube environment (red solid-line) remained stable (22°C) at both aluminium hotplate temperatures.

4.3.2.2 Cube-Temperature

The thermal environment of all sequences was very stable. The temperature of the Cube ranged from a low of 21.8°C to a high of 22.3°C for Tooth 1 (3006141b), which gave a maximum variation of 0.5°C and falls within ±0.3°C of the required 22°C. The highest temperature of 22.3°C was recorded only once when the hotplate was set at 30°C. Similarly, the lowest temperature of 21.8°C was recorded only once when the hotplate was also set at 30°C.

The range for Tooth 2 (2107141a) was a low of 21.9°C and a high of 22.2°C, giving a maximum variation of 0.3°C and falls within the ±0.3°C recorded for Tooth 1.

4.3.2.3 Copper-Baseplate Temperatures
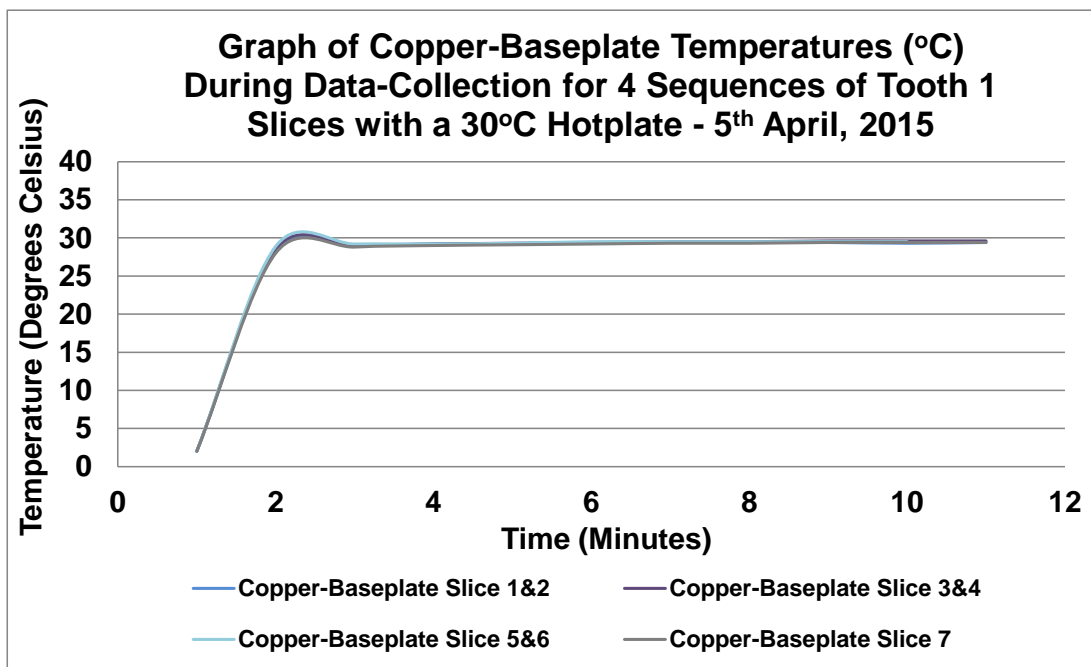
Figure 4-11 Line graph of copper-baseplate temperatures of 4 sequences (7 Slices) of Tooth 1 over 11 minutes, showing the consistency of re-warming to thermal equilibrium at ≈30°C following cooling on ice to 2°C - 5th April, 2015.
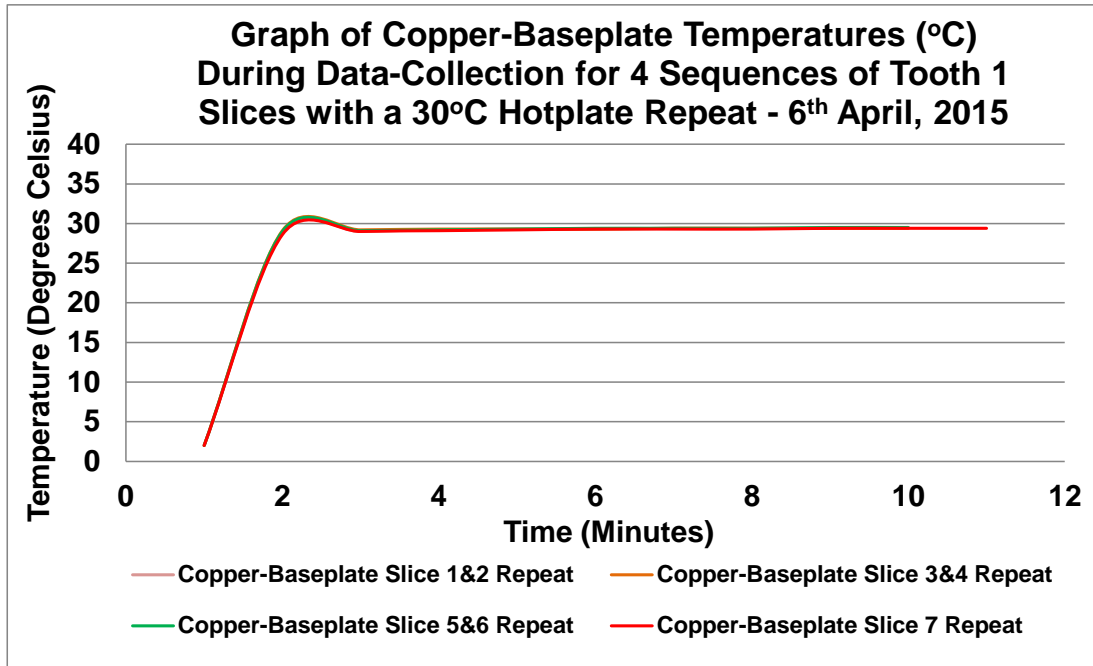
Figure 4-12 Line graph repeat of copper-baseplate temperatures of 4 sequences (7 Slices) of Tooth 1 over 11 minutes, showing the consistency of re-warming to thermal equilibrium at ≈30°C following cooling on ice to 2°C - 6th April, 2015.
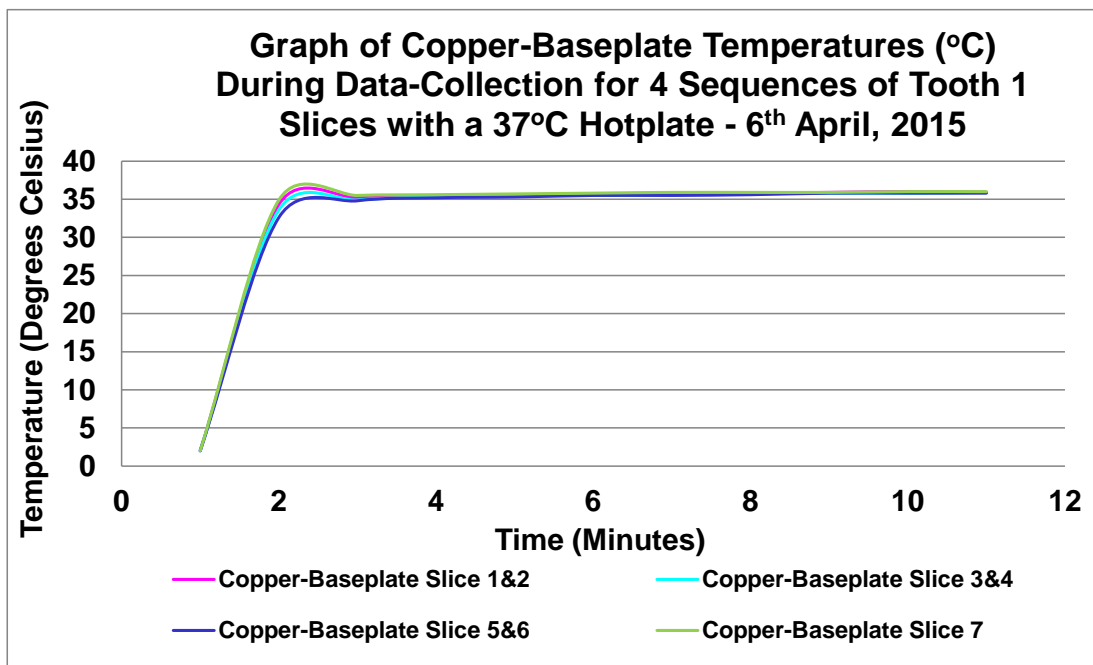
Figure 4-13 Line graph of copper-baseplate temperatures of 4 sequences (7 Slices) of Tooth 1 over 11 minutes, showing the consistency of re-warming to thermal equilibrium at ≈37°C following cooling on ice to 2°C - 6th April, 2015.
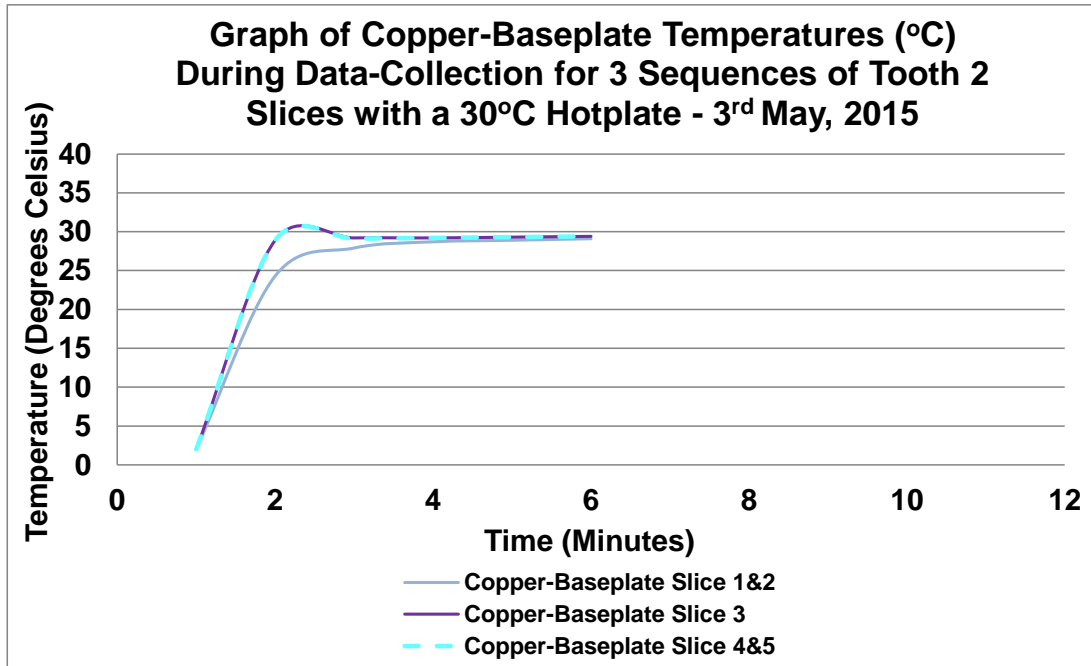
Figure 4-14 Line graph of copper-baseplate temperatures of 3 sequences (5 Slices) of Tooth 2 over 6 minutes, showing the slowest re-warming to thermal equilibrium at ≈30°C following cooling on ice to 2°C – 3rd May, 2015.

All samples on the copper-baseplate were cooled on ice to 2°C prior to transfer. No recording on the copper-baseplate stabilised in excess of the set 30°C or 37°C and only one reached the set value of 37°C - Slices 1 and 2 reversed for Tooth 2.

In the first minute of re-warming, the copper-baseplate provided a rapid linear increase in temperature (Figure 4-11, 4-12, 4-13), with the exception of one recording from Tooth 2 (2107141a Slice 1 and 2) at 30°C (Figure 4-14), where it took approximately two minutes to plateau.

Following the initial heat-transfer, there was a much-reduced energy-exchange as the temperature plateaued. For a hotplate temperature of 30°C, the copper-baseplate plateaued at a maximum temperature of 29.6°C for Tooth 1 (Slice 3 and 4), and 29.4°C for Tooth 2 (Slice 3,4 and 5).

The range of difference in maximum temperature for Tooth 1 at 30°C was 0.5°C (29.1°C to 29.6°C) and 0.1°C for the repeated sequences (29.4°C to 29.5°C). For Tooth 2, the range of maximum difference in temperature was 0.3°C (29.1°C to 29.4°C). All were within a temperature-range of 0.5°C.

For the hotplate temperature of 37°C, the copper-baseplate maximum plateau was at 36°C for Tooth 1 (Slice 1, 2, 7 and reversed 7); and at 37°C for Tooth 2 (Slice 1 and 2 reversed). The range of difference in maximum

temperature for the 37°C sequences for Tooth 1 was 0.4^{o}C   (35.6^{o}C to 36°C) and Tooth 2 was 0.1^{o}C (36.9^{o}C to 37°C).

4.3.2.4 Hotplate-Temperatures During Data-Capture

Tooth 1

For the required temperature of 30°C for the hotplate, the lowest temperature recorded was 29°C and the highest was 29.8^{o}C during Tooth 1 sequences, giving less than 1°C variation.

Repeat sequence temperatures of the hotplate for Tooth 1 ranged from a minimum temperature of 29.2^{o}C to a maximum of 29.8^{o}C, again giving less than 1°C variation.

For the required temperature of 37°C for the hotplate, the lowest temperature recorded was 36°C and the highest was 37°C during Tooth 1 sequences, giving a 1°C variation.

Tooth 2

For the required temperature of 30°C for the hotplate, the lowest temperature recorded was 29.3^{o}C and the highest was 29.9^{o}C during Tooth 2 sequences, giving less than 1°C variation.

For the required temperature of 37°C for the hotplate, the lowest temperature recorded was 36.8^{o}C and the highest was 37.6^{o}C during Tooth 2 sequences, giving less than 1°C variation.

Throughout all sequences there was no variation in the hotplate greater than 1°C.

4.3.3 Slice-Dimensions

Tooth 1

Tooth 1 was cut into 8 Slices (Table 4-10a) and Slice 3 was the thickest, with central enamel and central crown-dentine at 1.116mm and root-dentine at 1.062mm. The first Slice was the thinnest, with a sliver of enamel at 0.38mm. The left enamel-region for Slice 4 was fractured during handling.

Tooth 2

Tooth 2 was cut into 6 Slices (Table 4-10b) and Slice 1 was the thickest, with enamel at 1.937mm and root-dentine at 1.232mm. The thinnest Slice was destroyed during polishing. Slice 2 was the next thinnest, with enamel at 0.789mm, crown-dentine at 0.799mm and root-dentine at 0.791mm.

The greatest difference of thickness within the slices was 0.066mm in both Tooth 1 and 2.

Table 4-10 Tooth-slice-thickness (mm) a. Tooth 1 (3006141b) sound b. Tooth 2 (2107141a) carious.

Slice	Left Enamel	Centre Enamel	Right Enamel	Left Crown-Dentine	Centre Crown-Dentine	Right Crown-Dentine	Left Root-Dentine	Centre Root-Dentine	Right Root-Dentine
	Tooth 1 (3006141b) Thickness (mm)								
1	.	0.387	.	.	.	.	.	.	.
2	0.689	0.692	0.690	0.690	0.692	0.692	0.676	0.678	0.676
3	1.106	1.116	1.110	1.115	1.116	1.110	1.057	0.996	1.062
4	Fractured	0.676	0.675	0.688	0.676	0.676	0.664	0.642	0.664
5	0.697	.	0.695	0.698	0.702	0.697	0.691	0.694	0.694
6	0.698	.	0.698	0.712	0.700	0.700	.	0.694	.
7	0.776	0.780	0.778	0.784	0.782	0.781	0.784	0.782	0.785
8	0.709	0.710	0.712	0.714	0.712	0.714	.	.	.

a.

Slice	Left Enamel	Centre Enamel	Right Enamel	Left Crown-Dentine	Centre Crown-Dentine	Right Crown-Dentine	Left Root-Dentine	Centre Root-Dentine	Right Root-Dentine
	Tooth 2 (2107141a) Thickness (mm)								
1	.	1.937	.	.	.	.	.	1.232	.
	.	1.705	.	.	.	.	.	.	.
2	0.814	0.810	0.789	0.806	.	0.799	0.794	0.799	0.791
3	1.174	1.227	1.161	1.169	1.223	1.166	1.166	1.157	1.164
4	0.811	0.852	0.806	0.811	.	0.807	0.810	.	0.811
5	0.888	0.889	0.887	0.889	0.891	0.889	0.888	0.886	0.885
6	Destroyed in Polishing								

b.

4.3.4 Photographic and Radiographic Images of Tissues
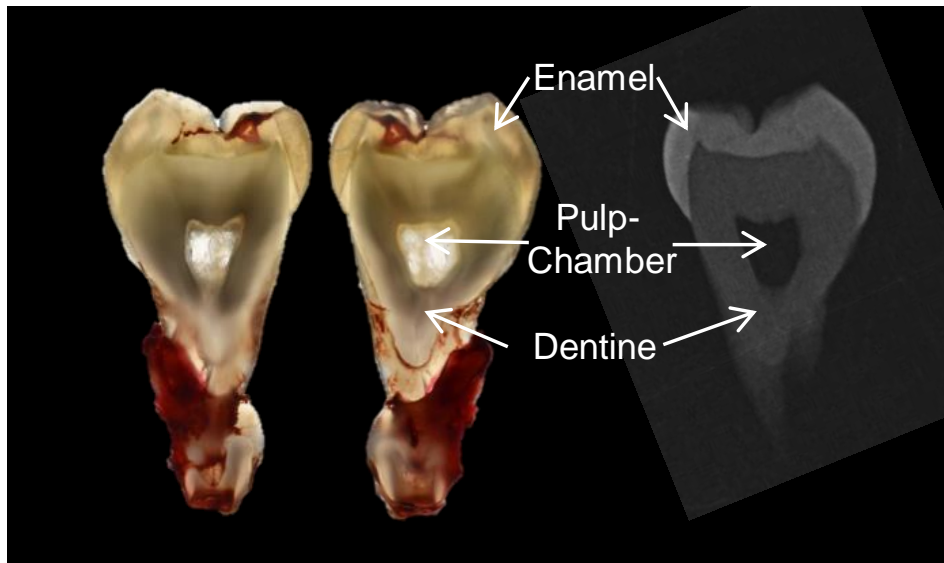
Figure 4-15 Tooth 1 tissue-slice 6, photographed both sides (front and back) and corresponding radiograph taken at 60kV 7mA 0.125s showing highly-mineralised enamel as light grey, less-mineralised dentine as darker grey and the location of the pulp-chamber as virtually black in the centre of the tooth.
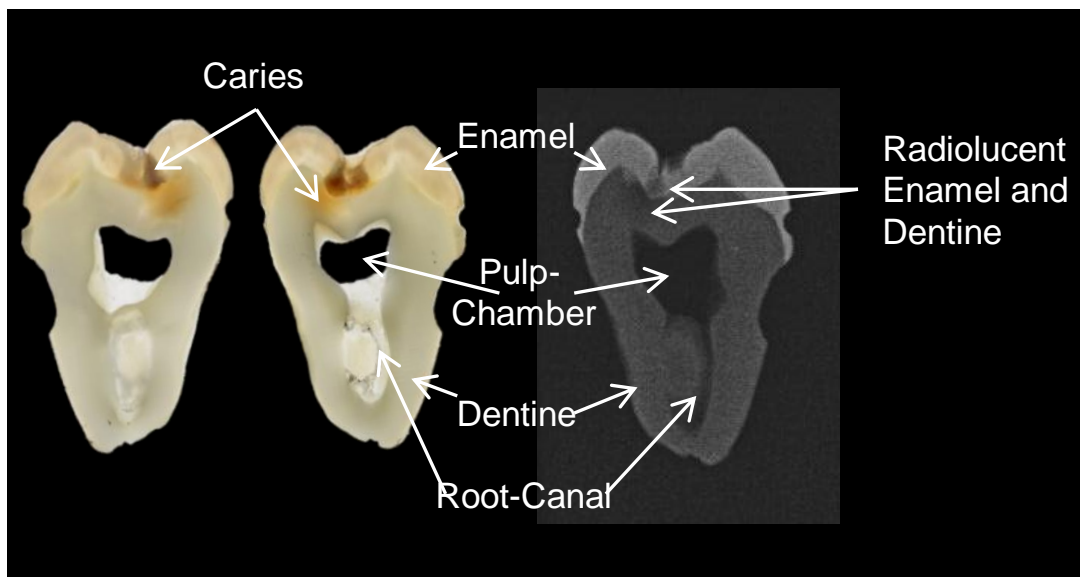
Figure 4-16 Tooth 2 tissue-slice 4, photographed both sides (front and back) and corresponding radiograph taken at 60kV 7mA 0.125s showing enamel, pulp-chamber, dentine, root-canal and demineralised carious tooth-tissue in both enamel and crown-dentine which is radiographically more radiolucent than the respective normal tissue.

Photographs shown in Figure 4-15 and 4-16 depict the enamel and dentine on both sides of both Slices, as well as the carious demineralised-region in

enamel and dentine of Tooth 2 Slice 4. The radiograph of each Slice was taken from one side only, which is also shown in each figure. Reduced mineral content in the pulp-chamber and root-canals, as well as the carious demineralised areas in both enamel and dentine are seen as radiolucent areas on the radiograph. Radiographically, clear contrast of the enamel and dentine are seen at the enamel-dentine junction.

4.3.5 Time-Temperature Curves
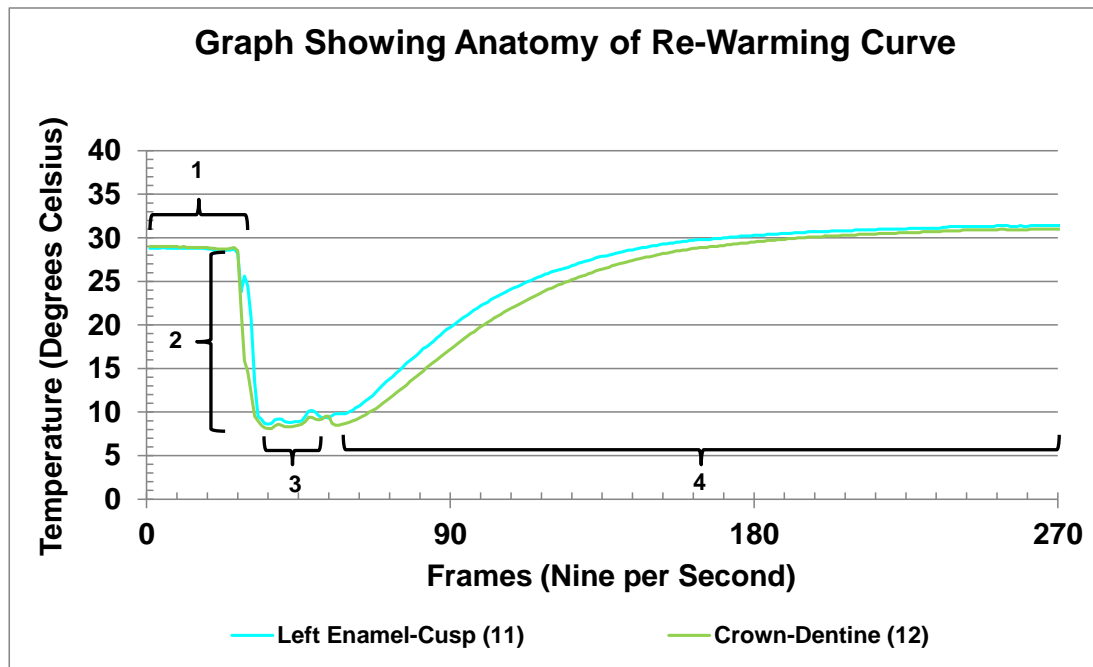
Figure 4-17 Line graph showing anatomy of re-warming curve. **Phase 1 shows the temperature recorded by the thermal camera of the hotplate from two areas-of-interest prior to arrival of tooth-tissue-sample. Phase 2 shows the temperature of these two areas on arrival of the cooled copper-baseplate carrying tooth-tissue-samples. Phase 3 is the temperature of the two areas during stabilisation of the copper-baseplate on the hotplate. Phase 4 is the temperature of the two areas-of-interest of tooth-tissue (Left Enamel-Cusp (11) and Crown-Dentine (12)) during re-warming over a period of ≈23 seconds, after which thermal equilibrium is reached. The numbers (11) and (12) indicate the tooth-tissue-sample areas-of-interest selected within the Software.**

Figure 4-17 shows the sequence of temperature exchange during the re-warming sequence and shows an example of two areas-of-interest, Left Enamel-Cusp (11) and Crown-Dentine (12), selected from Tooth 1 Slice 6.
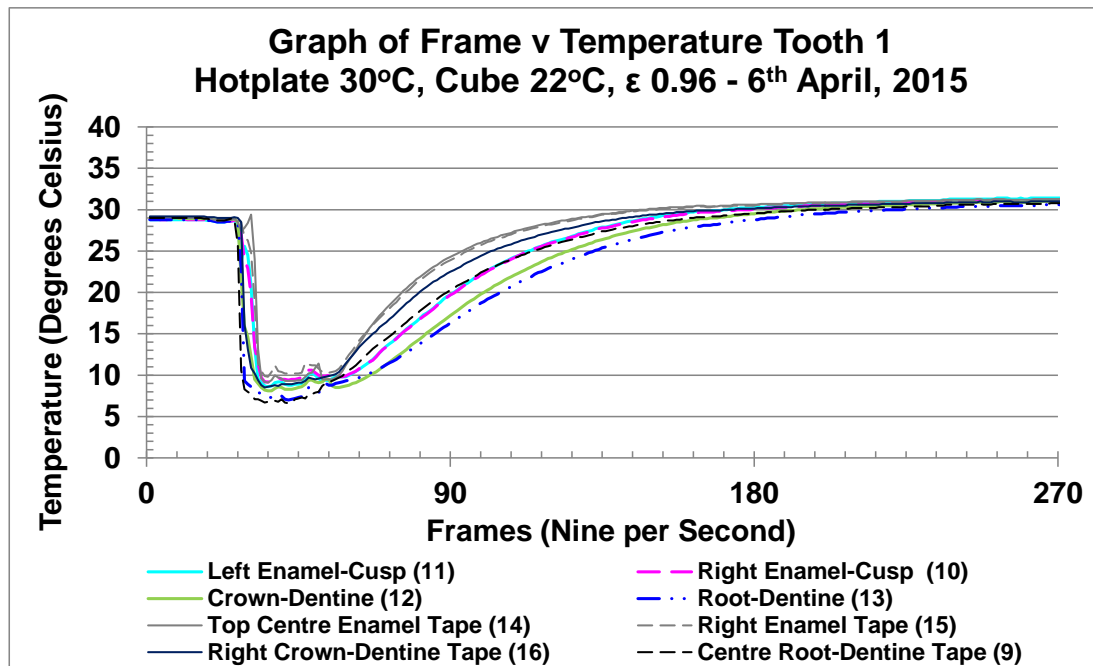
Figure 4-18 Line graph of re-warming temperature per frame of tooth-tissue-sample Tooth 1, Slice 6 following cooling. Hotplate temperature 30°C, Cube temperature 22°C and emissivity (ε) 0.96. Eight areas-of-interest shown: Left enamel-cusp (11), Right enamel-cusp (10), Crown-dentine (12), Root-dentine (13), Top centre enamel tape (14), Right enamel tape (15), Right crown-dentine tape (16), Centre root-dentine tape (9). The three tape areas-of-interest (14, 15, 16), with a steeper curve gradient, re-warm faster than any of the tooth-tissues. Centre root-dentine tape (9) re-warms at a similar rate as enamel but is faster than the crown-dentine (12) and root-dentine (13). Both areas of enamel (10, 11) have equivalent re-warming rates which are faster than crown- and root-dentine. Crown-dentine re-warms faster than root-dentine. After 270 frames (30 seconds), all areas-of-interest reach a plateau which remained stable for the rest of the re-warming sequence.

The re-warming curve of Tooth 1 Slice 6 (Figure 4-18) demonstrates the temperature changes during the re-warming sequence on a hotplate at 30°C. The initial temperature shows the temperature of the hotplate with the eight areas-of-interest marked as described within the legend. Following cooling on ice the sample was transferred to the hotplate above which the thermal camera recorded the re-warming sequence of each sample.
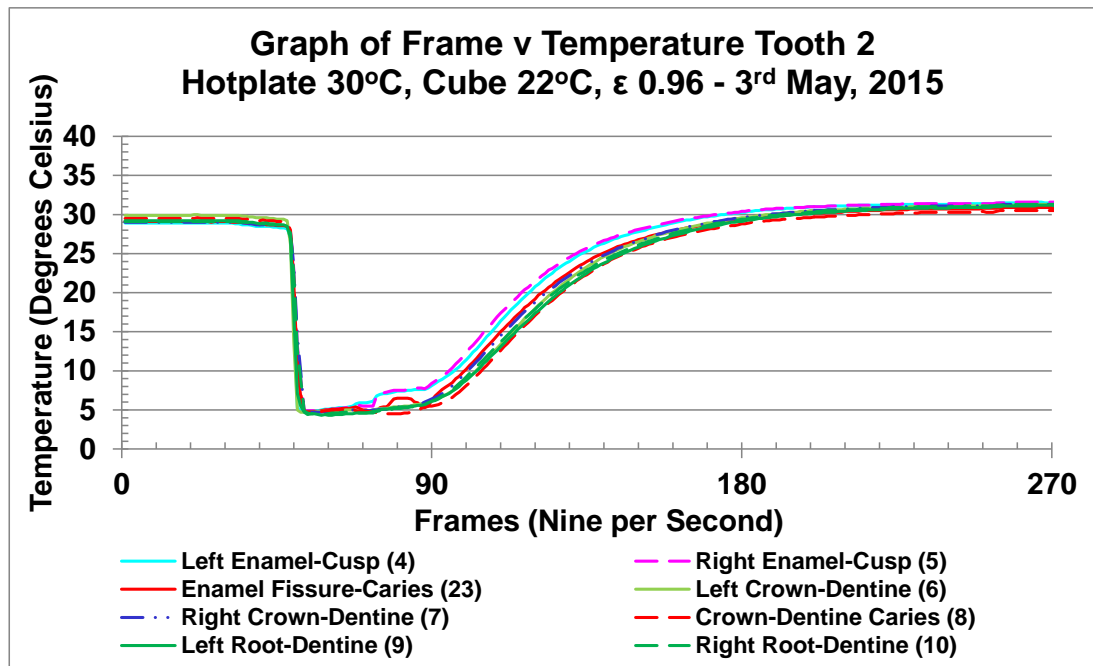
Figure 4-19 Line graph of re-warming temperature per frame of tooth-tissue-sample Tooth 2, Slice 4 following cooling. Hotplate temperature 30°C, Cube temperature 22°C and emissivity (ε) 0.96. Eight areas-of-interest shown: Left enamel-cusp (4), Right enamel-cusp (5), Enamel fissure-caries (23) Left crown-dentine (6), Right crown-dentine (7), Crown-dentine caries (8), Left root-dentine (9), Right root-dentine (10). Enamel (4, 5) re-warms faster than enamel fissure-caries (23). Enamel fissure-caries re-warms at a similar rate to the right crown-dentine (7). Crown-dentine caries (8) is slowest to re-warm. After 270 frames (30 seconds), all areas-of-interest reach a plateau which remained stable for the rest of the re-warming sequence.

A similar process occurs within Figure 4-19, for Tooth 2 Slice 4 which had demineralised areas of enamel and dentine. Both demineralised tissues re-warmed slower than their respective sound tissues.
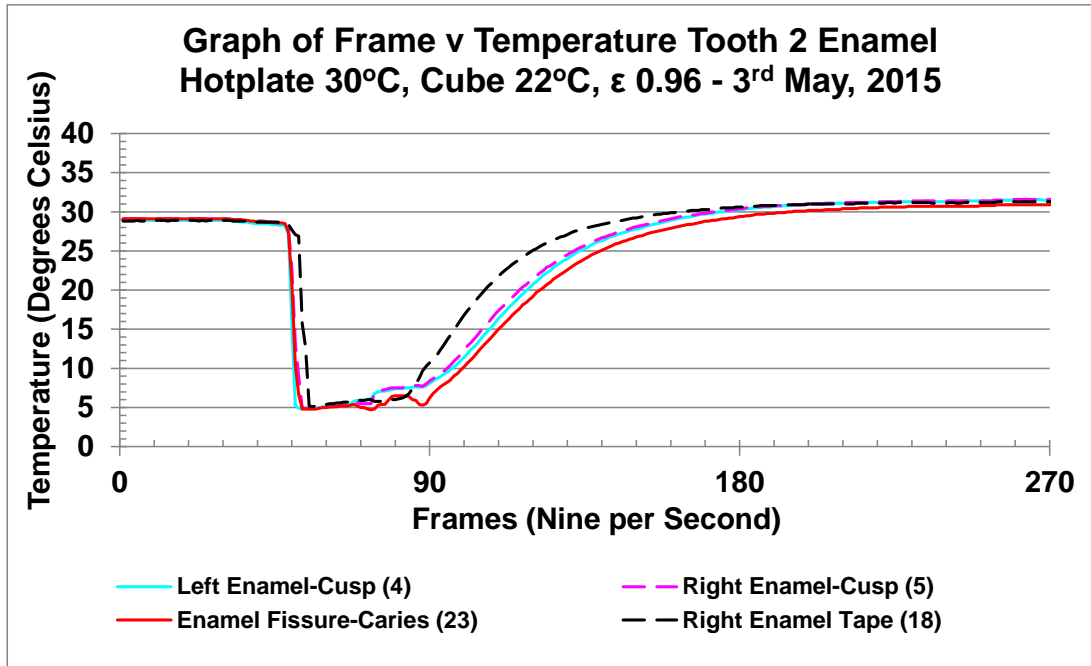
Figure 4-20 Line graph of re-warming temperature per frame of tooth-tissue-sample Tooth 2, Slice 4 enamel areas-of-interest, following cooling. Hotplate temperature 30°C, Cube temperature 22°C and emissivity (ε) 0.96. Four areas-of-interest shown: Left enamel-cusp (4), Right enamel-cusp (5), Enamel fissure-caries (23), Right enamel tape (18). The right enamel tape (18) re-warms faster than enamel (4, 5). Enamel fissure-caries (23) is slowest to re-warm. After 270 frames (30 seconds), all areas-of-interest reach a plateau which remained stable for the rest of the re-warming sequence.

After cooling, re-warming occurs at the quickest rate in the tape (18) than any of the enamel-tissue (Figure 4-20). Both areas of sound enamel (4, 5) warm at very similar rates which were quicker than the demineralized enamel fissure (23).
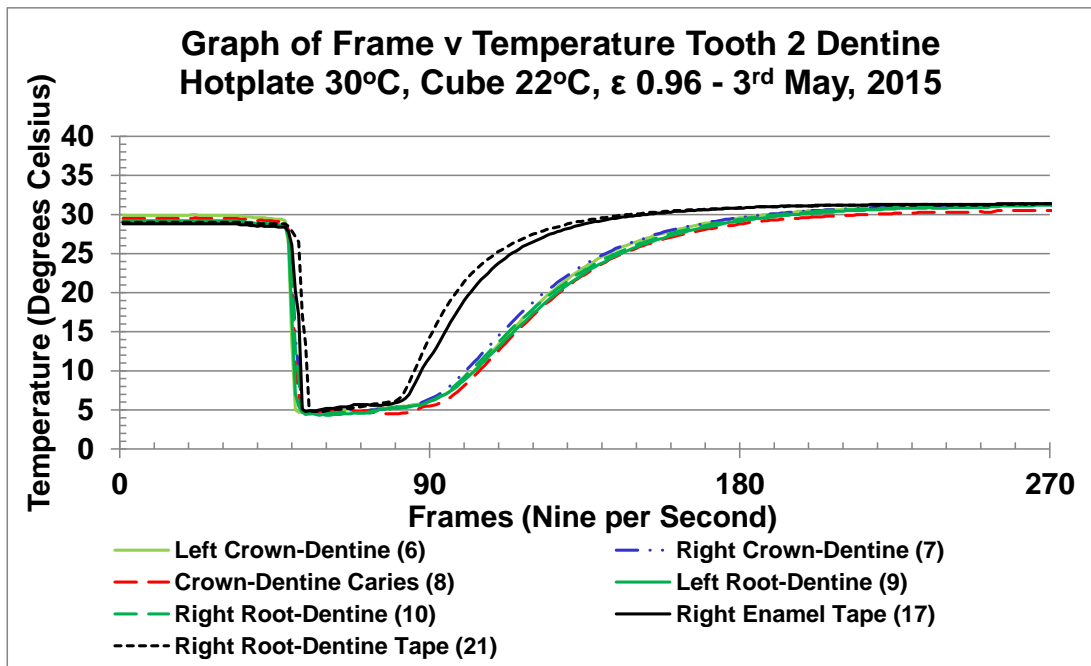
Figure 4-21 Line graph of re-warming temperature per frame of tooth-tissue-sample Tooth 2, Slice 4 Dentine areas-of-interest, following cooling. Hotplate temperature 30°C, Cube temperature 22°C and emissivity (ε) 0.96. Seven areas-of-interest shown: Left crown-dentine (6), Right crown-dentine (7), Crown-dentine caries (8), Left root-dentine (9), Right root-dentine (10), Right enamel tape (17), Right root-dentine tape (21). The tapes (17, 21) re-warm faster than all dentine tooth-tissue. Right crown-dentine re-warms slightly faster than other dentine tissues. Carious crown-dentine is slowest to re-warm (8). After 270 frames (30 seconds), all areas-of-interest reach a plateau which remained stable for the rest of the re-warming sequence.

Similarly for dentine (Figure 4-21), the two tapes (17, 21) re-warm faster than any of the dentine-tissues. Crown-dentine (6, 7) re-warms faster than the root-dentine (9, 10) and the crown-dentine caries (8) is slightly slower to commence the warming process. The final temperature reached by crown-dentine caries (8) is slightly lower than the other mineralised tissues.

4.3.6 Curve-Fitting-Data

The stable data of the final 30% of collection was used for curve-fitting to the exponential curve with a timeline of seconds, as the three graphs below demonstrate (Figure 4-22 to 4-24) for Tooth 1 Slice 6 and Tooth 2 Slice 4.
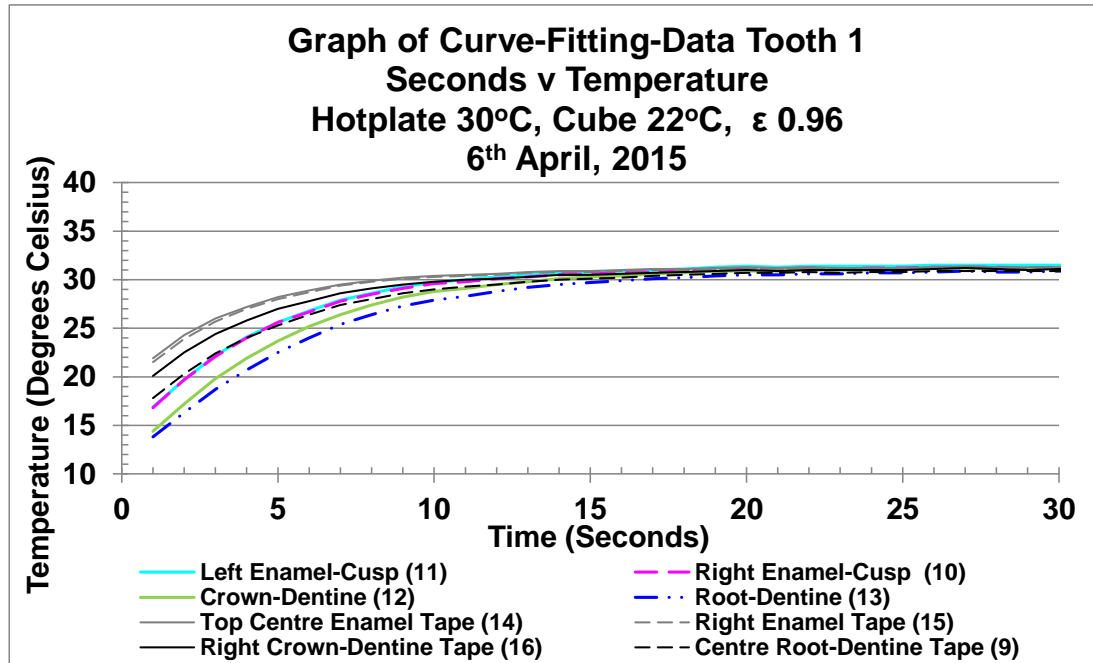
Figure 4-22 Line graph of recorded temperatures per second from the last stable 30% of re-warming for Tooth 1 Slice 6, used for calculating the Characteristic-time-to-relaxation (Ṫc) with an exponential equation. Three tapes re-warm faster than the tooth-tissue, taking less time to reach thermal equilibrium. Root-dentine tape is the slowest of the four tapes to achieve equilibrium, but faster than dentine. Enamel is the fastest tooth-tissue, followed by crown-dentine and, finally, root-dentine to achieve thermal equilibrium.

In Tooth 1 Slice 4 the last 30% of selected data from each of the re-warming sequences was used for curve-fitting following conversion to a timescale of seconds rather than frames. Different rates of re-warming are seen between the selected areas-of-interest, with the enamel tapes (14, 15) being the quickest and root-dentine (13) the slowest for Tooth 1 Slice 6 (Figure 4-22).
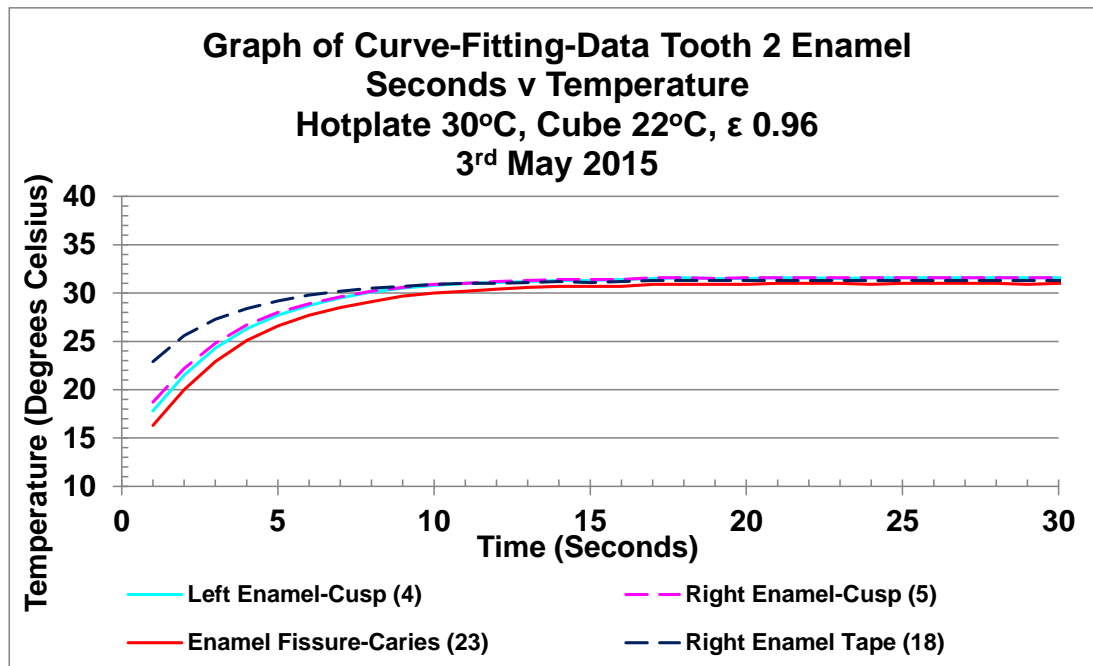
Figure 4-23 Line graph of recorded temperatures per second from the last stable 30% of re-warming for Tooth 2 Slice 4, used for calculating the Characteristic-time-to-relaxation (Tc) with an exponential equation. The tape (18) re-warms faster than the tooth-tissue, taking less time to reach thermal equilibrium. Enamel fissure-caries (23) is the slowest to achieve equilibrium and remains slightly cooler (31.6^{o}C). The two areas of sound enamel are equally fast to achieve thermal equilibrium.
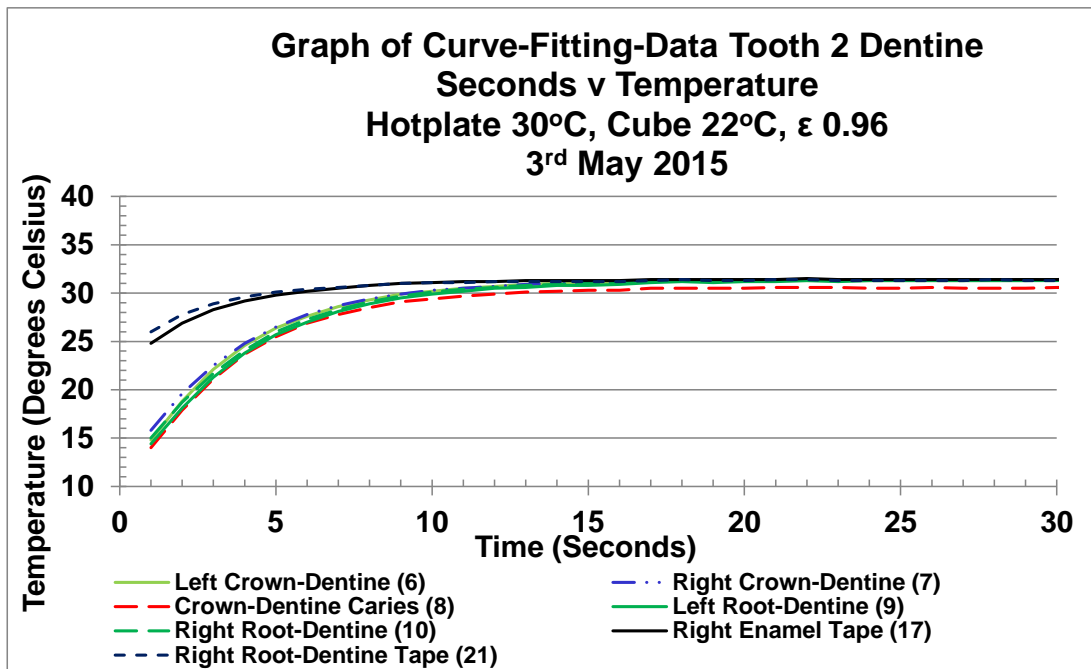
Figure 4-24 Line graph of recorded temperatures per second from the last stable 30% of re-warming for Tooth 2 Slice 4, used for calculating the Characteristic-time-to-relaxation (Tc) with an exponential equation. The two tapes (17, 21) re-warm faster than the tooth-tissue, taking less time to reach thermal equilibrium. Crown-dentine caries (8) is the slowest to achieve equilibrium and remains slightly cooler (31.6°C). The two areas of sound crown-dentine are slightly quicker to achieve thermal equilibrium than root-dentine.

In Tooth 2 Slice 4, enamel tape (18) is faster than any enamel tissue, and demineralised enamel fissure is the slowest to achieve thermal equilibrium (Figure 4-23). In Figure 4-24, it can be seen the tape (17, 21) is reaching thermal equilibrium before the tooth-tissues and the demineralised crown-dentine is the slowest to reach thermal equilibrium. Both the demineralised areas of enamel and dentine were of a lower temperature (31.6°C) than the other mineralized tissues at their equilibrium (Figure 4-23 & 4-24).

4.3.7 Characteristic-Times-to-Relaxation

The characteristic-time-to-relaxation values (τ_c) represent the time to achieve thermal equilibrium for each area-of-interest (Lin et al., 2010b) and calculations were undertaken in bespoke software.
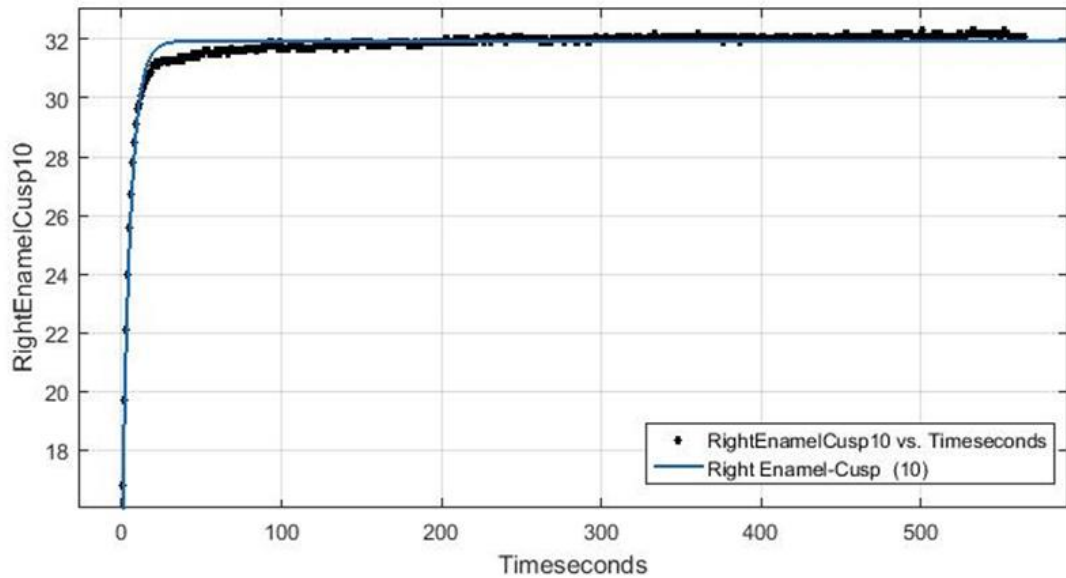
Figure 4-25 Curve-fitting graph produced in Matlab for enamel area-of-interest (10) on Tooth 1 Slice 6, re-warming from 16°C to 32°C over time (seconds). A good fit of the re-warming-data (black line) is seen to the exponential equation (blue line).
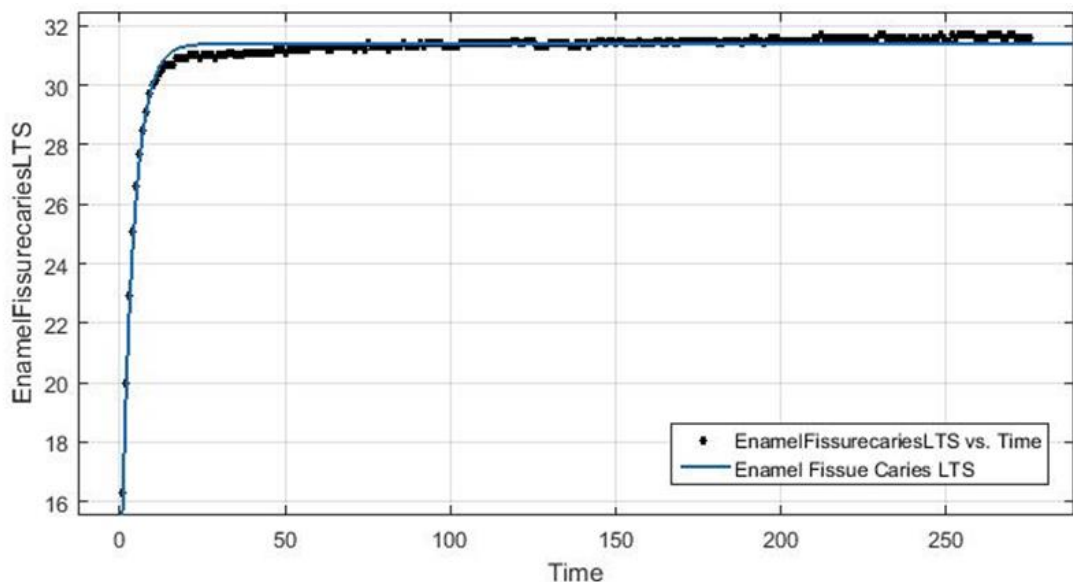
Figure 4-26 Curve-fitting graph produced in Matlab for enamel fissure-caries area-of-interest (23) on Tooth 2 Slice 4, re-warming from 16°C to 31.6°C over time (seconds). A good fit of the re-warming-data (black line) is seen to the exponential equation (blue line).

The two graphs shown in Figure 4-25 and 4-26 from curve-fitting within the bespoke programme for Matlab both show good fits with the exponential equation used. Table 4-11 shows the characteristic-time-to-relaxation (seconds) achieved from all the areas-of-interest in Tooth 1 and Tooth 2.

The characteristic-time-to-relaxation values (τ_c) represent the time to achieve thermal equilibrium for each area-of-interest. The enamel areas-of-interest for the tape (Table 4-11, Tooth 1 – (14) at 4.94 seconds and (15) at 4.96 seconds, and Tooth 2 – (17) at 3.39 seconds and (18) at 3.31 seconds) demonstrate a shorter characteristic-time-to-relaxation reaching thermal equilibrium before the enamel in both (Tooth 1 Slice 6 – (10) at 5.17 seconds and (11) at 5.13 seconds, and Tooth 2 Slice 4 – (4) at 3.49 seconds and (5) at 3.51 seconds).

The characteristic-time-to-relaxation for root-dentine tape (Tooth 2 Slice 4 – (21) at 3.53 seconds) is shorter than all dentine-tissues (6, 7, 8, 9, 10). Only the root-dentine (13 at 6.47 seconds) for Tooth 1 Slice 6 has a longer characteristic-time-to-relaxation than the dentine tape of (9 at 6.23 seconds and 16 at 5.51 seconds).

The two enamel-tissues (11 and 10) of Tooth 1 Slice 6 have characteristic-time-to-relaxation values (5.13 and 5.17 seconds, respectively). The crown-dentine (12) is longer than the enamel (5.63 seconds) and the root-dentine (13) longer again (6.47 seconds).

In the demineralised Slice, the two areas of sound enamel (4 and 5) have characteristic-time-to-relaxation values (3.49 and 3.51 seconds, respectively) - the shortest times of any tooth-tissue in Slice 4. The enamel fissure-caries (23) is slightly longer (3.71 seconds), which is shorter than root-dentine (10 - 3.89 seconds and 9 - 3.99 seconds) and crown-dentine caries (8 - 3.85 seconds) and falls between the two values of crown-dentine (6 - 3.64 seconds and 7 - 3.74 seconds).

There is no overlap of any tissue-type confidence interval, which gives a plausible range of values for the characteristic-time-to-relaxation from Tooth 1 Slice 6, nor of the tape from enamel to crown-dentine to root-dentine. The R-square is 0.92 or above for all areas-of-interest, indicating the variance of the data and the ordinary least square regression-line prediction of the model is precise.

Tooth 2 Slice 4 shows there is overlap of the confidence intervals for sound enamel (4 at 3.49 seconds and 5 at 3.51 seconds) and enamel fissure-caries (23), and the caries lesion has the longest characteristic-time-to-relaxation (3.71 seconds). The confidence intervals for one area-of-interest of crown-dentine (6 at 3.64 seconds) overlap with both areas of sound enamel (4 and 5), and the caries areas-of-interest for both enamel (23) and crown-dentine (8) overlap. There is no overlap in confidence intervals between root-dentine (9 and 10) and sound enamel (4 and 5), but there is for carious enamel (23). There is one area-of-interest of overlap for crown-dentine (7) and root-dentine (10) but the other crown-dentine (6) does not, and carious crown-dentine (8) overlaps with both root-dentine (9 and 10) confidence intervals. The R-square is 0.91 or above for all areas-of-interest, indicating variance of the data and the ordinary least square regression-line prediction of the model is precise.

Table 4-11 Characteristic-time-to-relaxation values (seconds) for Tooth 1 Slice 6 and Tooth 2 Slice 4 recorded at 30°C with confidence interval and R-square values.

Tooth 1 Slice 6 30°C 6th April, 2015			
	Characteristic-Time-To-Relaxation (T$_c$) Seconds	95% Confidence Interval for (T$_c$) Seconds	R-square
Centre Root-Dentine Tape(9)	6.23	5.991 to 6.468	0.95
Right Enamel-Cusp (10)	5.17	4.996 to 5.337	0.96
Left Enamel-Cusp (11)	5.13	4.970 to 5.286	0.97
Crown-Dentine (12)	5.63	5.463 to 5.789	0.97
Root-Dentine (13)	6.47	6.281 to 6.665	0.97
Top Centre Enamel Tape(14)	4.94	4.691 to 5.193	0.92
Right Enamel Tape (15)	4.96	4.716 to 5.208	0.92
Right Crown-Dentine Tape (16)	5.51	5.261 to 5.749	0.93
Tooth 2 Slice 4 30°C 3rd May, 2015			
	Characteristic-Time- To-Relaxation (T$_c$) Seconds	95% Confidence Interval for (T$_c$) Seconds	R-square
Left Enamel-Cusp (4)	3.49	3.382 to 3.603	0.98
Right Enamel-Cusp (5)	3.51	3.389 to 3.631	0.98
Left Crown-Dentine (6)	3.64	3.545 to 3.743	0.99
Right Crown-Dentine (7)	3.74	3.632 to 3.840	0.99
Crown-Dentine Caries (8)	3.85	3.686 to 4.015	0.97
Left Root-Dentine (9)	3.99	3.880 to 4.104	0.99
Right Root-Dentine (10)	3.89	3.793 to 3.992	0.99
Right Enamel Tape (17)	3.39	3.195 to 3.590	0.95
Right Enamel Tape (18)	3.31	3.149 to 3.462	0.96
Right Root-Dentine Tape (21)	3.53	3.266 to 3.792	0.91
Enamel Fissure-Caries (23)	3.71	3.590 to 3.836	0.98

4.3.8 Thermal Diffusivity and Thermal Conductivity

The characteristic-time-to-relaxation values from Table 4-11 were used to compute thermal diffusivity and thermal conductivity as shown in Table 4-12.

Tooth 1 Slice 6 has values of thermal diffusivity and conductivity which fall within known-ranges for enamel and root-dentine, as highlighted in the green cells. Crown-dentine delivers a value twice that of the prior known-values. Tooth 2 Slice 4 has values of thermal diffusivity and conductivity which fall within know-ranges (or just outside the known-ranges for the areas of enamel) (green cells). The demineralised area of enamel has the lowest value of thermal diffusivity and conductivity, which falls below the known-ranges. For dentine, the values fall in close proximity to known-values for thermal conductivity and diffusivity, and the demineralised area-of-interest gives the lowest value.

Table 4-12 Calculation of thermal diffusivity and thermal conductivity from the characteristic-times-to-relaxation as per equations – thermal diffusivity ($4H^2/\pi^2 Tc\ Diff$) and thermal conductivity ($\alpha*\sigma*c_p$) – enamel and dentine-values within known-ranges highlighted within green cells, and lowest values from demineralised carious tissue within the pink cells.

		H = 0.5 Thickness (m)	Tc (Sec)	Tc Thermal Pad (Sec)		Tc Difference (Sec)		Thermal Diffusivity ($10^{-7}m^2$/Sec) ($4H^2/\pi^2 Tc\ Diff$) α		Density (Kg/m^3) σ	Specific Heat-Capacity (J/Kg K) c_p	Thermal Conductivity (Wm·K) ($\alpha*\sigma*c_p$) k	
Tooth-Slice	Tooth 1			Left	Right	Left	Right	Left	Right			Left	Right
	Lin Value Enamel	·	·	·	·	·	·	4.08		·	·	0.81	
	Panas Value Enamel	·	·	·	·	·	·	2.27		·	·	0.45	
	Left Enamel-Cusp	0.000349	5.13	4.942	·	0.19	·	2.65	·	2800	710	0.53	·
	Right Enamel-Cusp	0.000349	5.17	·	4.962	·	0.21	·	2.41	2800	710	·	0.48
	Lin Value Dentine	·	·	·	·	·	·	2.01		·	·	0.48	
	Panas Value Dentine	·	·	·	·	·	·	1.92		·	·	0.46	
	Crown-Dentine	0.000352	5.63	5.51		0.12		4.15		2248	1066	0.99	
	Root-Dentine	0.000347	6.47	6.23		0.24		2.00		2248	1066	0.48	
Tooth-Slice	Tooth 2			Left	Right	Left	Right	Left	Right			Left	Right
	Lin Value Enamel	·	·	·	·	·	·	4.08		·	·	0.81	
	Panas Value Enamel	·	·	·	·	·	·	2.27		·	·	0.45	
	Left Enamel-Cusp	0.000455	3.492	3.31	·	0.18	·	4.61	·	2800	710	0.92	·
	Centre Enamel Caries	0.000426	3.713	3.31		0.4		1.83	·	2800	710	0.36	
	Right Enamel-Cusp	0.000403	3.51	·	3.31	·	0.2	·	3.29	2800	710	·	0.65
	Lin Value Dentine	·	·	·	·	·	·	2.01		·	·	0.48	
	Panas Value Dentine	·	·	·	·	·	·	1.92		·	·	0.46	
	Left Crown-Dentine	0.000455	3.64	3.31	·	0.34	·	2.48	·	2248	1066	0.6	
	Right Crown-Dentine Caries	0.000404	3.85	·	3.31	·	0.55	·	1.21	2248	1066	·	0.29
	Right Crown-Dentine	0.000404	3.74	·	3.39	·	0.34	·	1.92	2248	1066	·	0.46
	Right Root-Dentine	0.000455	3.89	·	3.53	·	0.36	·	2.31	2248	1066	·	0.55
	Left Root-Dentine	0.000455	3.99	3.53	·	0.46	·	1.81	·	2248	1066	0.43	·
	Tc = Characteristic-Times-To-Relaxation; Panas et al., 2003; Lin et al., 2010b			Within Quoted Range				Carious Tissue					

4.3.9 Thermal Maps

The re-warming response and spatial relationship of the tooth-tissues are seen within thermal maps, the first to be produced, are in Figure 4-27.
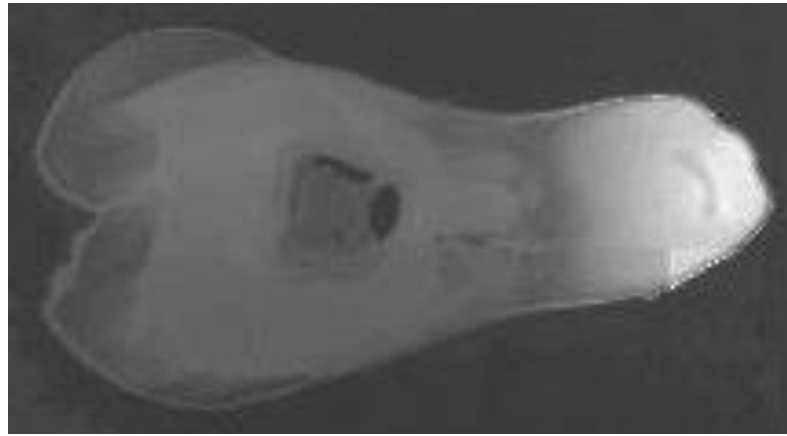
a.
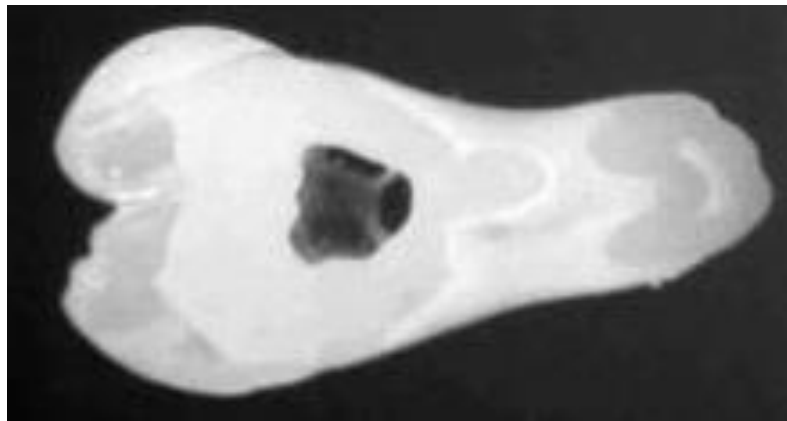
b.
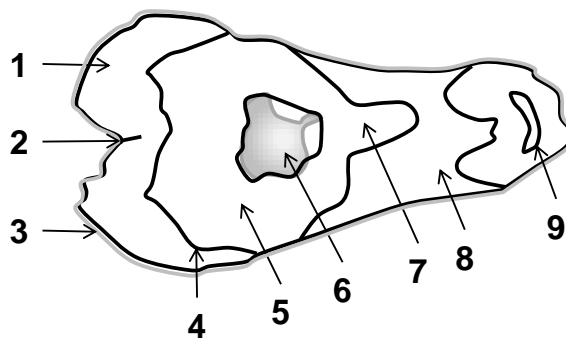
1 = Enamel
2 = Fissure
3 = Surface Layer of Enamel
4 = AmeIodentinal Junction
5 = Crown-Dentine

6 = Pulp-Chamber
7 = Root-Dentine
8 = Curvature of Root-Face
9 = Root-Canal

c.

Figure 4-27 First Thermal Maps of Tooth 1 Slice 4:

a. **Characteristic-Time-To-Relaxation – contrast between enamel and dentine at the amelodentinal junction is seen, with contrast of a thin surface-layer of enamel with occlusal-surface fissure. Homogenous areas of grey are seen in both enamel and dentine. The pulp-chamber-wall is seen in detail, with contrast from presence or absence of mineralised tissue. The curvature of the root-face merges with the cut-face. Contrasting greyscale indicates presence of a root-canal in the apical area. Root-tip contrasts with enamel and crown-dentine.**
b. **Area-Under-The-Curve – shows the features of the characteristic-time-to-relaxation map (a) in a different greyscale, without the sharp contrast of the surface-enamel-layer. Contrast and sharpness of the root-surface and the pulp-chamber is greater.**
c. **Schematic Diagram Of Anatomical Structures.**

The thermal maps can be compared to two other images produced from electromagnetic radiation - the photograph and the X-ray (Figure 4-28).
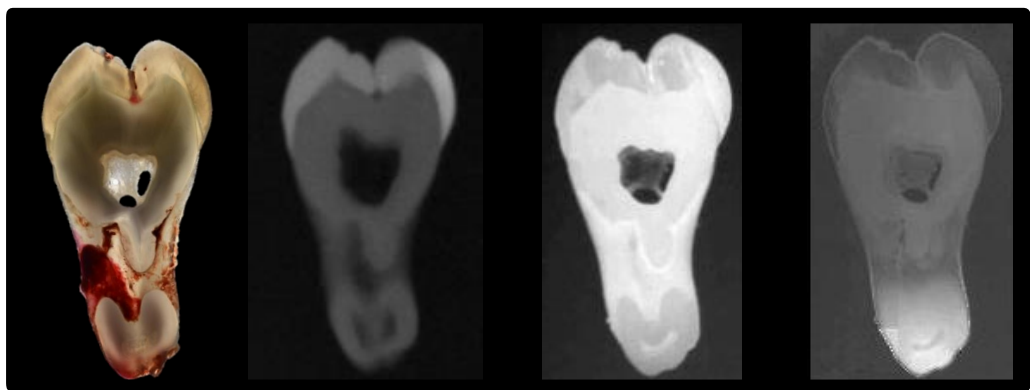
| Photograph | X-ray | Area-Under-The-Curve | Characteristic-Time-To-Relaxation |

Figure 4-28 Four electromagnetic radiation images
Tooth 1 Slice 4:
Photograph – sharp image of enamel and dentine demarcated by the amelodentinal junction, with a vertical fissure visible in enamel. A thin wall of mineral is seen at the base of the pulp-chamber in this section of tooth-slice, which is perforated in areas. Curvature of uncut root-face seen with attached soft-tissue debris.
X-ray – Blurred contrast between enamel and dentine, with enamel occlusal-fissure visible as a fine contrasting-line within enamel. Black contrasting centre of pulp-chamber, with no detail of pulp-wall. Apical root-canals contrast with root-dentine, as does the root-surface.
Area-under-the-curve – sharp image with contrasting greys of enamel and dentine at the amelodentinal junction. Pulp-chamber-wall with contrast from presence or absence

**of mineralised tissue. Curvature of root-face is
sharply defined between cut-surface. Contrasting greyscale
of root-canal in the apical area.**
**Characteristic-Time-To-Relaxation – contrast between
enamel and dentine at the amelodentinal junction with
sharp contrasting surface-layer of enamel with
occlusal-fissure. Contrast in pulp-chamber-wall.**
**The curvature of the root-face is diffuse, and contrasting
greyscale apically indicates presence of a root-canal.**

The same process produced similar results for other Slices (Figure 4-29) which also highlighted the demineralised areas from caries due to the different thermal properties (Figure 4-30).

| Photograph | X-ray | Area-Under-The-Curve | Characteristic-Time-To-Relaxation |
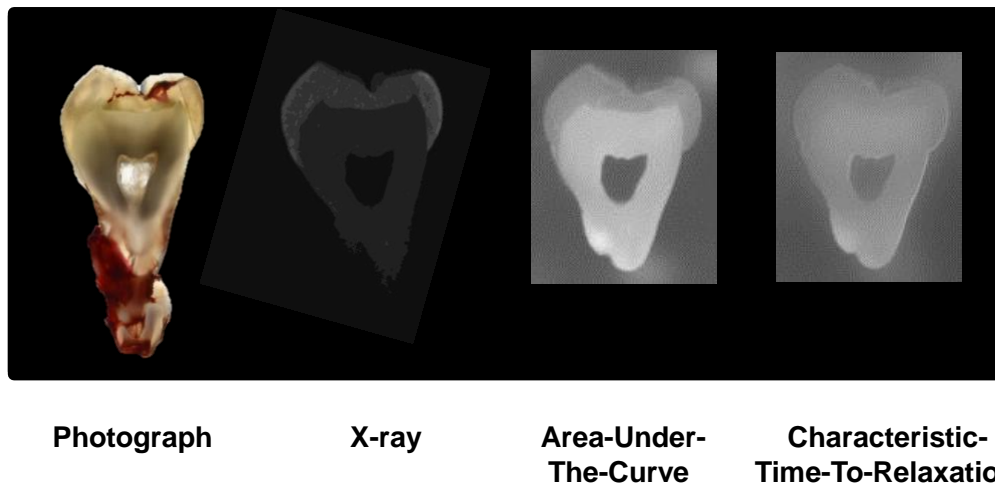
Figure 4-29 Tooth 1 Slice 6
**A temperature-scale of 4°C to 32°C and data from 9 frames
for the area-under-the curve and 135 frames for the
characteristic-time-to-relaxation at 30°C.**
**Photograph - enamel and dentine with sharp
demarcation of the amelodentinal junction with some
colour-contrast between enamel and dentine. A lighter
pulp-chamber area is visible with mineralised tissue at the
base in this tooth-slice. Retained soft-tissue on external
root-surface. The external boundary of the tooth-slice-
crown and root are defined.**
**X-ray - enamel as light-grey contrasts with the darker grey
of dentine beneath, at the amelodentinal junction. The
external boundary of the crown is defined quite sharply
and the root-boundary is seen but more diffusely than the
crown. A nearly-black area is seen centrally where the
pulp-chamber is positioned.**
**Area-under-the-curve - sharply defines the external
border of the tooth-slice. Enamel and dentine are dark and
light-grey respectively, with sharp separation at the
amelodentinal junction. Central pulp-chamber is virtually
black with sharp contrast between the grey dentine. An
area of white on the left-side of the apical-root-periphery is**

seen.
Characteristic-time-to-relaxation – the tooth-slice is clearly
defined, as are enamel and dentine. The amelodentinal
junction is diffuse. The pulp-chamber contrasts with
dentine with a thin, lighter rim facing the pulp. Light-grey
is seen in the apical-root-area to the left and there is some
heterogeneity of the greyscale from the crown-dentine to
the root-dentine.

| Photograph | X-ray | Area-Under-The-Curve | Characteristic-Time-To-Relaxation |
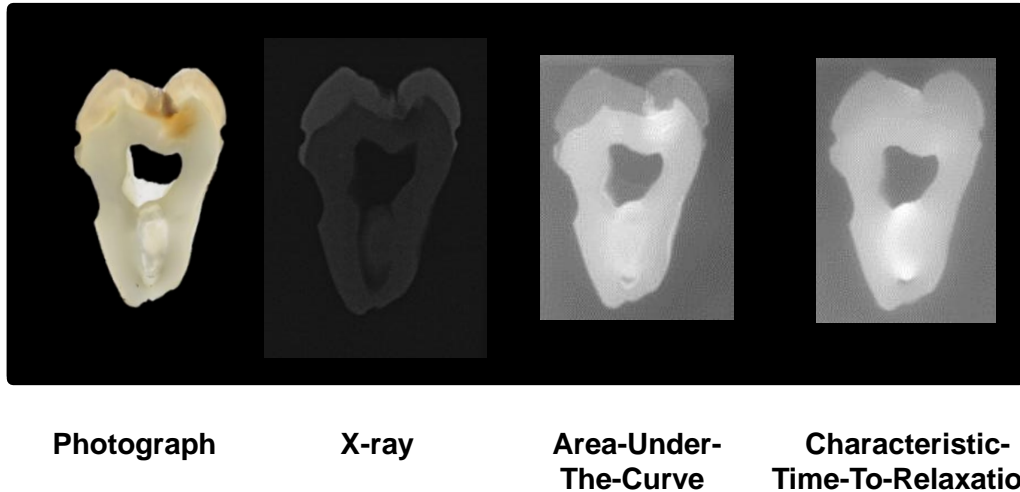
Figure 4-30 Tooth 2 Slice 4

A temperature-scale of 4°C to 32°C and data from 9 frames
for the area-under-the curve and 135 frames for the
characteristic-time-to-relaxation at 30°C.
Photograph - sharp external boundary of the tooth-crown
and root, with two notches within the cervical enamel on
each side, and a larger notch into dentine on the left root-
face. A colour-change occurs from enamel to dentine at
the amelodentinal junction. Additionally, a rhomboid area
of colour-change in enamel can be seen at the base of the
cuspal-inclines, which extends beyond the amelodentinal
junction and into dentine under the right-cusp on the
image. The central pulp-chamber can be seen with a black
background and surrounding thin layer of virtually white
tissue towards the root and the left-side of the pulp-
chamber. In the root centrally, colour-changes can be
seen, with areas which are light and dark creamy-grey
where the root-canal traverses from the root-apex to the
pulp-chamber.
X-ray - tooth-slice-outline with lighter grey area of enamel
sharply defined at the amelodentinal junction from darker
grey dentine. A darker area is seen in enamel from the
radiolucency of the demineralised lesion at the base of the
cuspal-inclines, which extends into the dentine. All
notches are clearly shown and the pulp-chamber is
sharply defined from the dentine with a darker area
showing the presence of reduced mineral from the root-
canal.

Area-under-the-curve shows a sharp outline to the tooth-slice, with three notches. The dark-grey of the enamel sharply contrasts with the light-grey of dentine. A lighter, virtually white area, is seen where the demineralised tissue is present in enamel and dentine, which have diffuse boundaries. The pulp-chamber is sharply demarcated towards the occlusal-surface and there is the presence of a change in greyscale where the thin mineralised tissue is seen. Laterally, on the left wall of the pulp-chamber, a thin, lighter line is seen before the dark-grey of the bulk of dentine. Similarly, a light-grey line is seen on the right root-surface externally. Centrally, an area of light-grey coloration can be seen in the location of the root-canal with a dark region apically.

Characteristic-time-to-relaxation shows a clearly-defined tooth-slice, with three notches. Enamel and dentine have some contrast and the amelodentinal junction is detected. No contrast is seen in the area of demineralisation coronally and the pulp-chamber is defined with a dark-grey background. A lighter, virtually white region, is seen where the root-canal traverses from the floor of the pulp-chamber to a darker area near the apex.

The discussion of characterisation of the thermal properties of enamel and dentine is in Chapter 5 Section 5.3.

4.4 Model to Calculate Pulp Blood-Flow-Rate

Prior to simulating vitality in the in-vitro model, a theoretical model of fluid-exchange within each adult tooth was developed, as described in Chapter 3, Section 3.4. The results are shown in Figure 4-31 to 4-32 and Table 4-13 to 4-18.

4.4.1 Estimated Range of Pulp-Mass by Water-Volume

Table 4-13 Estimated mass of water per maxillary tooth-volume.

Tooth	Maxillary Tooth-Volume (mm^3)	Mass of Water (g/cm^3)	Mass of Water (g/mm^3)	Mass of Water Per Tooth-Volume (g/mm^3)
Central Incisor	12.4	1	0.001	0.0124
Lateral Incisor	11.4	1	0.001	0.0114
Canine	14.7	1	0.001	0.0147
First Premolar	18.2	1	0.001	0.0182
Second Premolar	16.5	1	0.001	0.0165
First Molar	68.2	1	0.001	0.0682
Second Molar	44.3	1	0.001	0.0443
Third Molar	22.6	1	0.001	0.0226
Average	25	1	0.001	0.0250

Using data from literature on tooth-volumes and knowledge of the mass of water when the volume of each tooth is occupied by water, a mass per tooth-volume can be calculated (g/mm^3) (Table 4-13) and used to estimate the tooth blood-flow from data on blood-flow-by-weight from the literature (Table 4-14).

Table 4-14 Estimated blood-flow per volume of maxillary tooth.

Tooth	Maxillary Mass of Water/Tooth-Volume (g/mm^3)	Blood-Flow-Volume (ml/min/100g)	Blood-Flow-Volume (ml/min/g)	Tooth Blood-Flow (ml/min)
Central Incisor	0.0124	50	0.5	0.0062
Lateral Incisor	0.0114	50	0.5	0.0057
Canine	0.0147	50	0.5	0.0074
First Premolar	0.0182	50	0.5	0.0091
Second Premolar	0.0165	50	0.5	0.0083
First Molar	0.0682	50	0.5	0.0341
Second Molar	0.0443	50	0.5	0.0222
Third Molar	0.0226	50	0.5	0.0113
Average	0.0250	50	0.5	0.0125

This process can be repeated for the mandibular teeth.

Table 4-15 Estimated blood-flow per volume of mandibular tooth.

Tooth	Mandibular Mass of Water/Tooth-Volume (g/mm³)	Blood-Flow-Volume (ml/min/100g)	Blood-Flow-Volume (ml/min/g)	Tooth Blood-Flow (ml/min)
Central Incisor	0.0071	50	0.5	0.0036
Lateral Incisor	0.0081	50	0.5	0.0041
Canine	0.0152	50	0.5	0.0076
First Premolar	0.0159	50	0.5	0.0080
Second Premolar	0.0159	50	0.5	0.0080
First Molar	0.0535	50	0.5	0.0268
Second Molar	0.0339	50	0.5	0.0170
Third Molar	0.0321	50	0.5	0.0161

Having calculated the mass of water per tooth and using the literature-data of 50ml/min/100g, the blood-flow per tooth can be estimated for each adult human tooth (Table 4-14 & 4-15).

Taking the mean mass of pulp from a third molar 13.1mg and using the general statement of pulp blood-flow being 50ml/min/100g, a value can be calculated for the third molar:

Mean mass of wet pulp for third molar = 13.1mg Mendez & Zarzoza, 1999

Mean pulp blood-flow ml/min/100g   = 50   Kim 1985

1g of pulp would have a blood-flow   = 50/100 = 0.5ml/min

13.1mg (0.0131g) pulp blood-flow   = 0.5 x 0.0131

*   = 0.0066ml/min/third molar.*

This can be used to estimate a water constant (ω) (Table 4-16 & 4-17) which can be applied to all other teeth, the constant being derived from the knowledge of actual pulp weight of the third molar and the estimated blood-flow (Kim 1985), as emboldened.

Table 4-16 Estimated blood-flow-rate per maxillary tooth-type, ranging from 0.0033ml/min for the central incisor, to 0.0198ml/min for the first molar.

Maxillary Tooth	(a) Tooth Blood-Flow (ml/min/g)	(b) Tooth Blood-Flow (ml/min/third) Molar via Mendez 1999 Kim 1985	(c) Water Constant (b/a) (ω)	Estimated Maxillary Teeth Blood-Flow-Rate (a*c) (ml/min/per Tooth-Type)
Central Incisor	0.0062	.	0.58	0.0036
Lateral Incisor	0.0057	.	0.58	0.0033
Canine	0.0074	.	0.58	0.0043
First Premolar	0.0091	.	0.58	0.0053
Second Premolar	0.0083	.	0.58	0.0048
First Molar	0.0341	.	0.58	0.0198
Second Molar	0.0222	.	0.58	0.0128
Third Molar	0.0113	**0.0066**	**0.58**	**0.0066**
Average	0.0125	.	0.58	0.0073

Table 4-17 Estimated blood-flow-rate per mandibular tooth-type, ranging from 0.0015ml/min for the central incisor, to 0.011ml/min for the first molar.

Mandibular Tooth	(a) Tooth Blood-Flow (ml/min/g)	(b) Tooth Blood-Flow (ml/min/third) Molar via Mendez 1999 Kim 1985	(c) Water Constant (b/a) (ω)	Estimated Mandibular Teeth Blood-Flow-Rate (a*c) (ml/min/per Tooth-Type)
Central Incisor	0.0036	.	0.41	0.0015
Lateral Incisor	0.0041	.	0.41	0.0017
Canine	0.0076	.	0.41	0.0031
First Premolar	0.0080	.	0.41	0.0033
Second Premolar	0.0080	.	0.41	0.0033
First Molar	0.0268	.	0.41	0.0110
Second Molar	0.0170	.	0.41	0.0070
Third Molar	0.0161	**0.0066**	**0.41**	**0.0066**

Applying a water constant (ω) calculated at 0.58 and 0.41 for maxillary and mandibular teeth respectively, to each of the maxillary and mandibular teeth provides an estimated blood-flow-rate per tooth-type (Table 4-16, 4-17 & Figure 4-31).
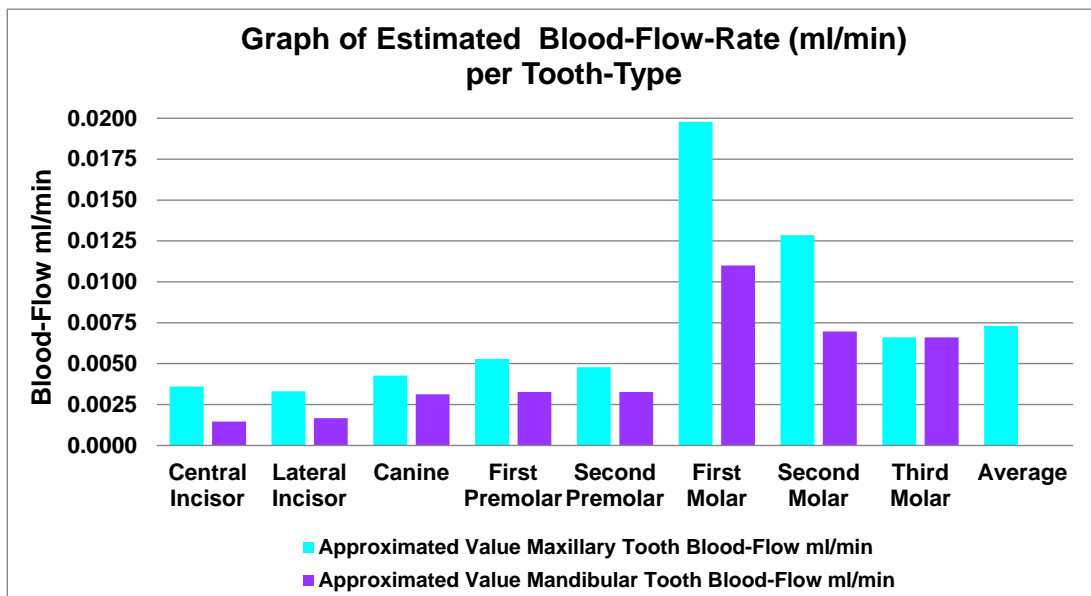
Figure 4-31 Graph of estimated blood-flow-rate per tooth-type – which range from 0.0033ml/min for the maxillary lateral incisor up to 0.0198ml/min for the first maxillary molar and from 0.0015ml/min for the mandibular central incisor up to 0.011ml/min for the first mandibular molar.

Estimated blood-flow-rates in human mandibular teeth are, overall, lower than maxillary teeth.

Table 4-18 Estimated range of blood-flow from pulp mass of premolar and third molars - as reported by Van Amerongen, et al., 1983 and blood-flow per 100g by Kim 1985 which provides a minimum value of 0.0045ml/min and a maximum value of 0.0255ml/min.

	Mass (mg)	Converted (g)	Blood-Flow-Volume Kim 1985 (ml/min/g)	Blood-Flow-Rate per Tooth (ml/min)
Minimum	9	0.009	0.5	0.0045
Maximum	51	0.051	0.5	0.0255

Application of a published blood-flow per mass of tissue (Kim, 1985) to the reported mass of pulp for premolar or third molar teeth (Van Amerongen et al., 1983), enabled a prediction of pulp blood-flow of a minimum of 0.0045ml/min to a maximum of 0.0255ml/min (Table 4-18 & Figure 4-32), and the mean mass for third molars from Mendez & Zarzoza, (1999) falls between these two values at 0.0066ml/min.
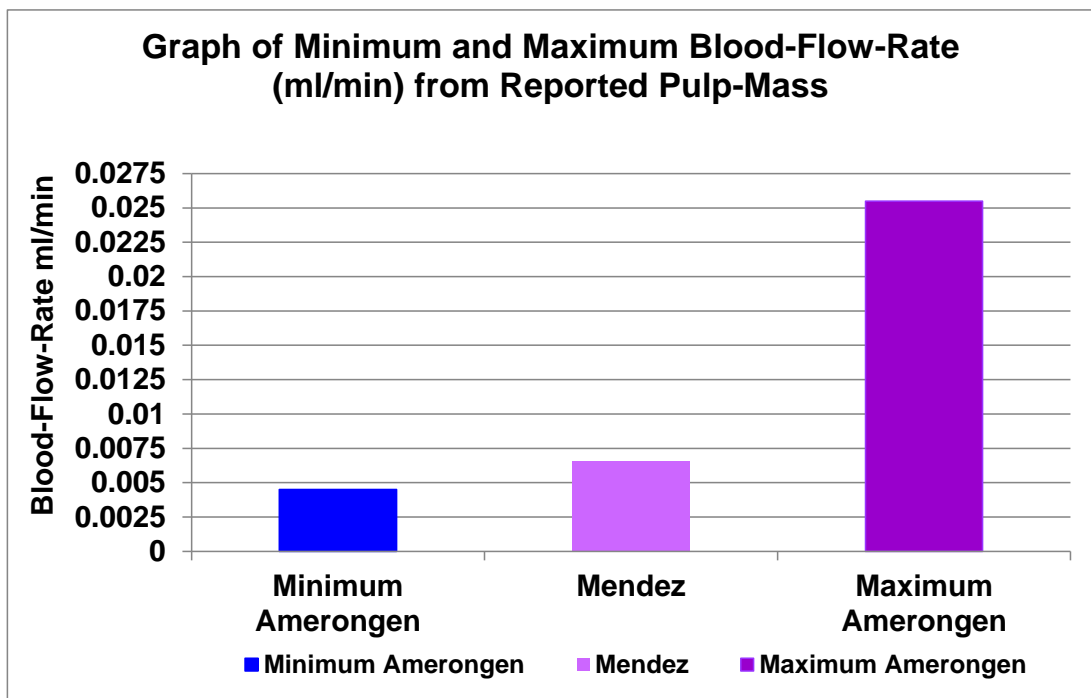
Figure 4-32 Graph of estimated range of blood-flow from pulp-mass reported by Van Amerongen et al, 1983 which has a minimum value of 0.0045ml/min and a maximum value of 0.0255ml/min and Mendez et al., 1999, which has a value of 0.0066ml/min using a blood-flow 50ml/min/100g Kim 1985.

The discussion of modelling the blood-flow is in Chapter 5 Section 5.4.

4.5 In-Vitro Feasibility of Using Infra-Red Radiation In Determining Tooth-Vitality

Having established a stable thermal environment within the Cube and the parameter of emissivity for human enamel and a theoretical fluid-exchange to simulate vitality in a tooth; the next step was to determine the feasibility of detecting a temperature-difference due to the presence of a simulated blood-flow in the vital tooth compared to a non-vital tooth, using the emitted infra-red radiation collected by a thermal camera. This was described in Chapter 3, Section 3.5 and the results are presented in Figure 4-33 to 4-83 and Table 4-19 to 4-68.

4.5.1 Tooth-Data
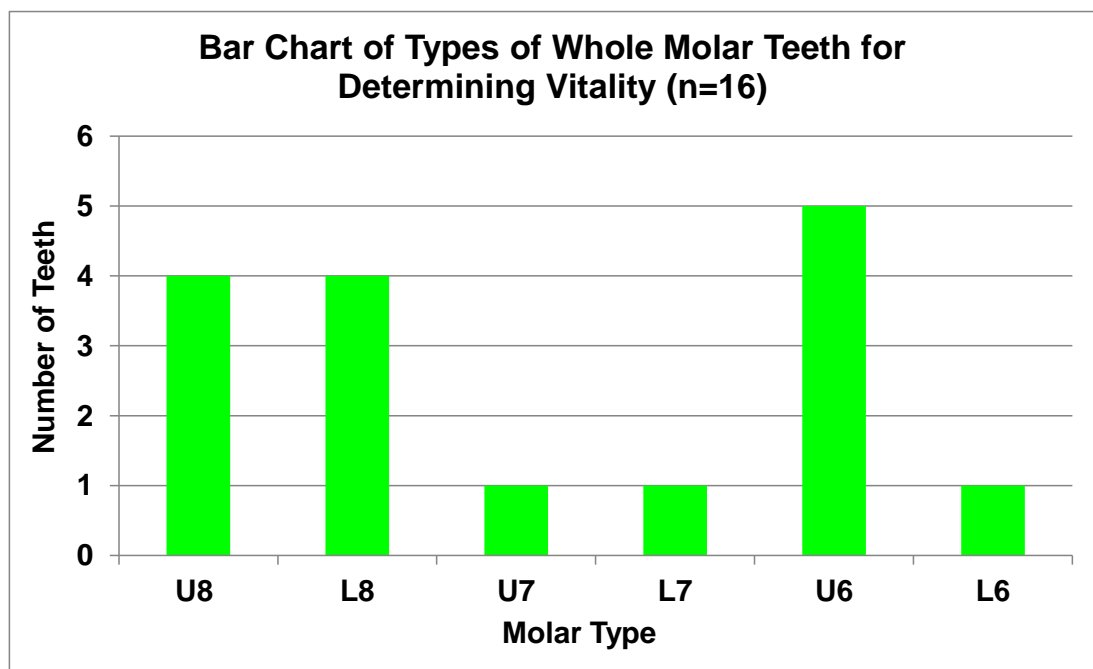
Figure 4-33 Bar chart of molar teeth for determining tooth-vitality - commonest being the upper-first molar (U6).

The 16 whole teeth for in-vitro simulated vitality were all molar teeth, the commonest being the upper-first molar – Figure 4-33. The molar teeth were donated by 6 males and 10 females.
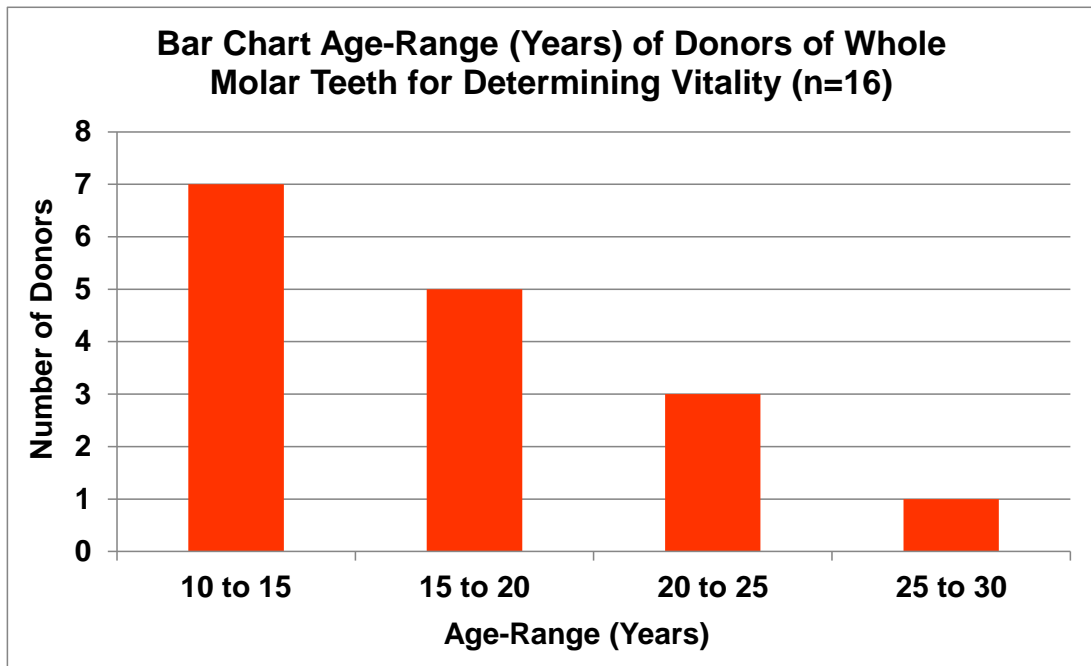
Figure 4-34 Bar chart age-range (years) of donors of molar teeth used for determining vitality – most collected from the youngest age-range 10 to 15 years.

The mean age of the donors was 16 years and 7 months, ranging from 10 to 28 years. 14 donors were of white ethnic origin and the remaining 2 unknown.

4.5.2 Determination of Ideal Temperature-Reduction and Assessment Variable for Vitality Testing

Multiple sequences were run to determine the most suitable temperature-reduction to see if a difference in the infra-red radiation could be detected between a simulated vital and non-vital tooth. The surface temperatures of the teeth were aligned for analysis (Figure 4-35 and 4-36). The periodontal ligament, internal and external temperatures of the tooth pair were recorded with thermocouples as shown in Figure 4-37 to 4-40. Three variables were used to assess the difference between a vital and non-vital tooth from the re-warming curve: area-under-the-curve, maximum temperature-difference and the characteristic-time-to-relaxation. The results are presented below.

4.5.2.1 Thermal Sequence and Alignment for Analysis of Vitality

**Graph of Surface-Temperatures of Teeth - Pair 4
Internal Temperature Reduction 8°C with Vitality of
Periodontal Ligament & Left Tooth (PDL LTS)
0.08ml/min**
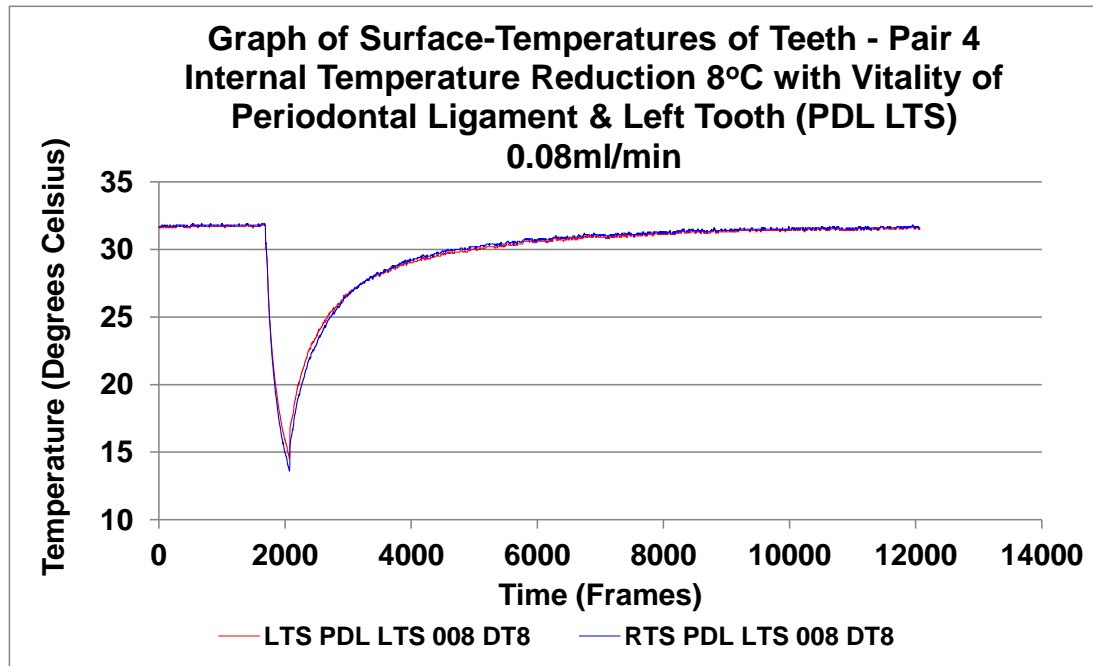
Figure 4-35 Line Graph – Thermal sequence for Pair 4 flow-rate 0.08ml/min (008) and internal temperature-reduction of 8°C (DT8) with simulated blood-flow in both the periodontal ligament and left-tooth on screen (PDL LTS) over time. Both teeth of Pair 4 (right-tooth on screen (RTS) and left-tooth on screen (LTS) were initially in thermal equilibrium (frames 0-1687) where the LTS had simulated vitality – red line – 31.6^{o}C and RTS was non-vital – blue line – 31.7^{o}C. Both teeth were cooled by the cooling-unit applied to the occlusal-surfaces. A drop in temperature of the area-of-interest covering the buccal-surfaces of both teeth was seen (frames 1687-2071). Upon removal of the cooling-unit, the re-warming phase commenced until thermal equilibrium was re-established. The temperature of the vital tooth (LTS – red line) does not fall as low as the non-vital tooth (RTS – blue line), 14.6^{o}C compared to 13.6^{o}C, and the red line of the vital tooth is visible above the blue line of the non-vital tooth. The red line remains above the blue during re-warming until approximately 2800 frames where there is a 0.1^{o}C difference, following which thermal equilibrium is re-established (±0.1^{o}C).
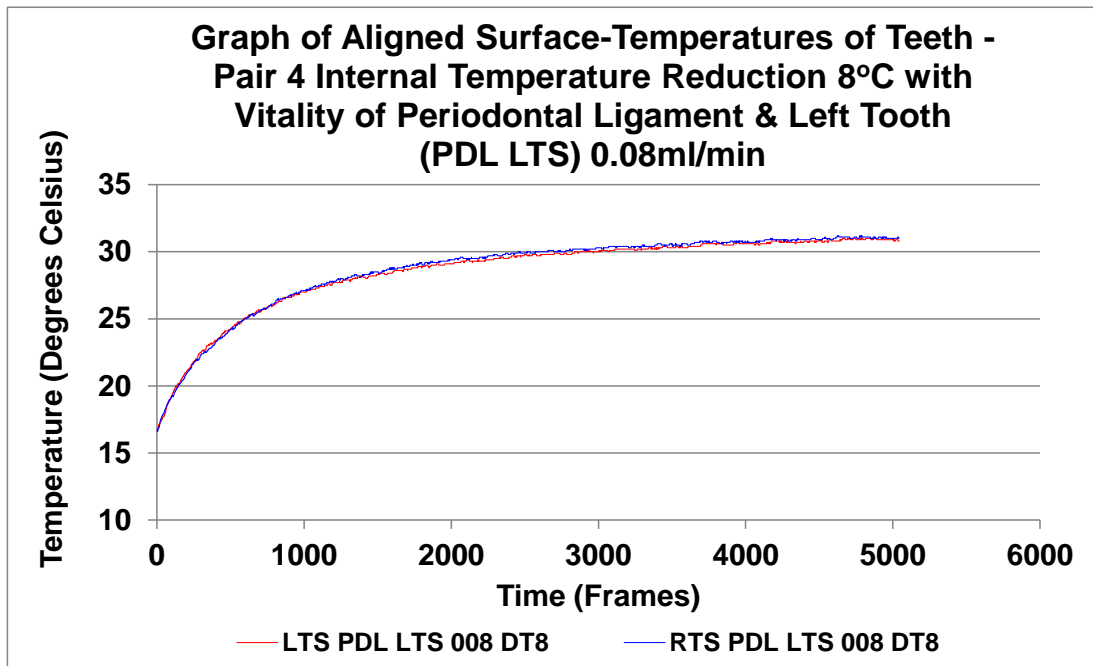
Figure 4-36 Line Graph – Aligned re-warming temperatures Pair 4 used for analysis. Both teeth commenced re-warming sequence from the same thermal position and the temperatures of each area-of-interest from the two teeth in the paired-unit were aligned. The area-under-the-curve, the maximum temperature-difference and characteristic-time-to-relaxation was calculated for each tooth over a timeline of 5045 frames.

4.5.2.2 Thermocouple Data – Internal, External and Periodontal Ligament Temperatures

Graph of Thermocouple Recordings of Periodontal Ligament Temperatures Pair 4 Simulated Vitality PDL LTS Flow-Rate 0.08ml/min Temperature-Reduction 0ºC, 10ºC, 8ºC, 6ºC, 4ºC, 2ºC 2ºC Pulsed

Peltier °C   Left Tooth PDL °C   Right Tooth PDL °C
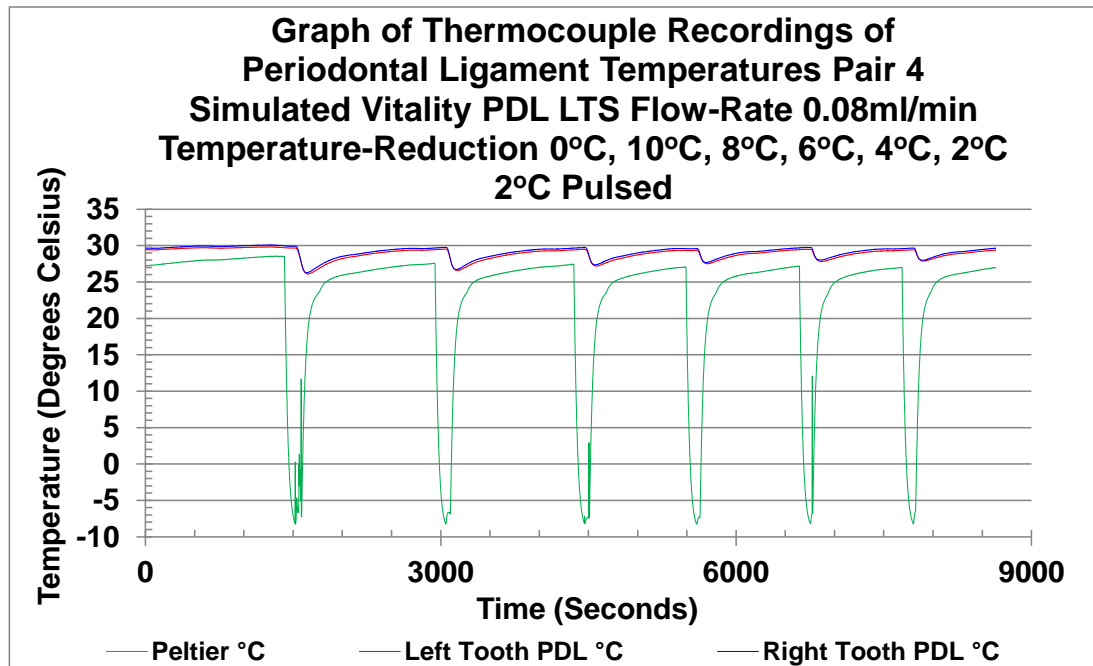
Figure 4-37 Line Graph – Thermocouple recorded temperatures from the peltier cooling-unit and the region of the simulated periodontal ligament attachment of the root of both teeth for Pair 4, flow-rate 0.08ml/min with simulated blood-flow in both the periodontal ligament and left-tooth on screen (PDL LTS). The cooling-unit achieved a surface-temperature of -8°C prior to application to the occlusal-surfaces of the teeth for each cooling-sequence (green line). The temperature of the root-surface periodontal ligament did not vary greatly prior to application of a cold thermal disruption, as seen in the first stage of the sequence (up to ≈ 1500 seconds) and represents a 0°C change. Separate sequences achieved an internal temperature-reduction of 10°C (≈1600 seconds), 8°C (≈3200 seconds), 6°C (≈4500 seconds), 4°C (≈5500 seconds), 2°C (≈6800 seconds) and a 2°C reduction with a pulsed simulated blood-flow (≈7800 seconds) measured by the internal thermocouple of the right-tooth of the pair. The level of cooling seen in the periodontal ligament was greatest with the greatest internal cooling, with a maximum reduction of 3.4°C (29.7 to 26.3°C) at 10°C internal drop in temperature in the right-tooth and 3.4°C (29.5 to 26.1°C) in the left. A minimum reduction of 1.6°C and 1.7°C on the left and right-surfaces respectively, occurred with the pulsed simulation and a 2°C internal temperature-reduction. Both teeth have similar temperature-reductions in the periodontal ligament on cooling.
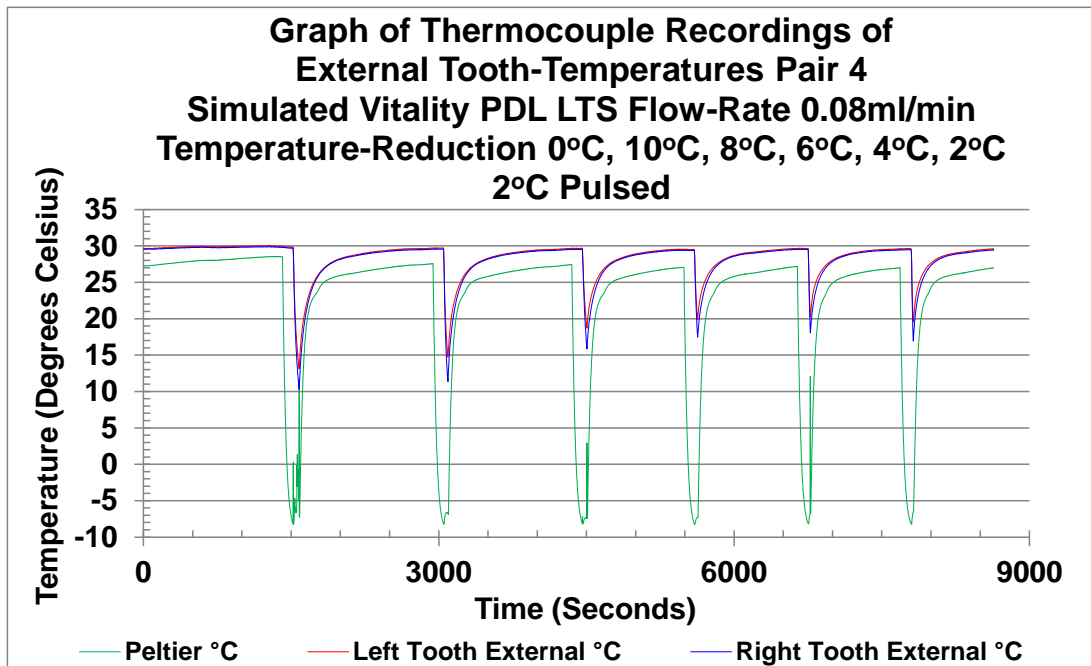
Figure 4-38 Line Graph – Thermocouple recorded temperatures from the peltier cooling-unit and external surfaces of the crown of both teeth for Pair 4 flow-rate 0.08ml/min with simulated blood-flow in both the periodontal ligament and left-tooth on screen (PDL LTS) during internal temperature-reductions of 0°C, 10°C, 8°C, 6°C, 4°C, 2°C and a 2°C reduction with simulated pulse. The external temperatures of the teeth without thermal disruption show little thermal variation (up to ≈ 1500 seconds). The maximum external tooth-surface temperature-reduction is seen with the greatest internal temperature-reduction for the right-tooth at 19.2°C. The greatest reduction of 16.6°C for the left-tooth is also with the internal temperature drop of 10°C (≈1600 seconds). The least external temperature-reduction is with a 2°C internal temperature-reduction for both right and left teeth (11.5°C and 9.4°C respectively at ≈6800 seconds). The right-tooth has a greater reduction than the left.
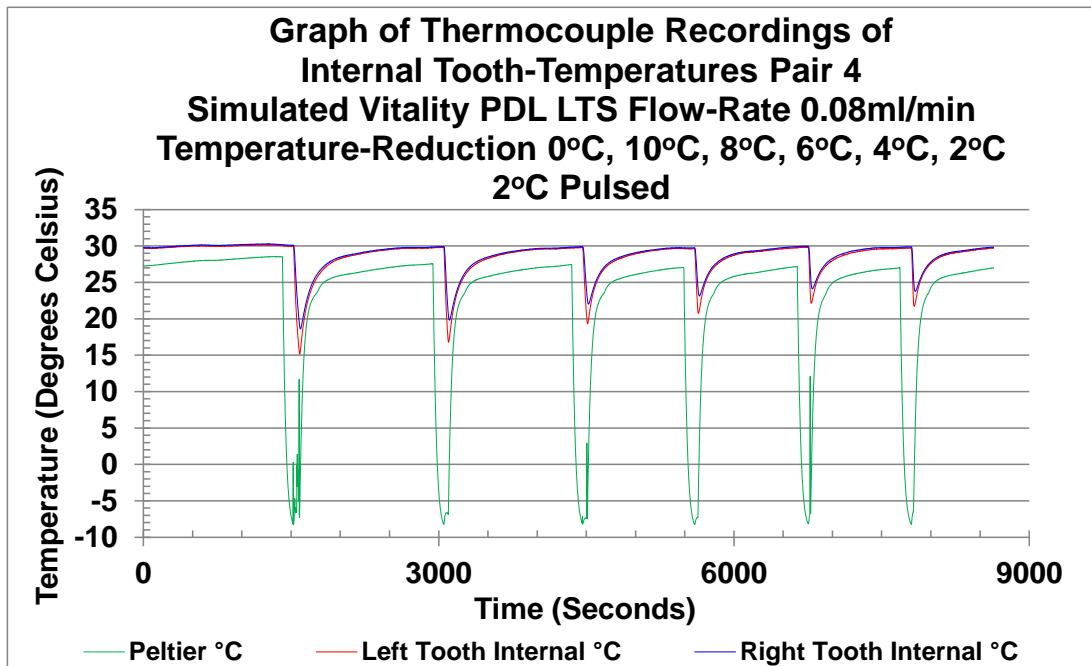
Figure 4-39 Line Graph – Thermocouple recorded temperatures from the peltier cooling-unit and internal pulp-chamber of both teeth for Pair 4 flow-rate 0.08ml/min with simulated blood-flow in both the periodontal ligament and left-tooth on screen (PDL LTS) during internal temperature-reductions of $0^{o}C$, $10^{o}C$, $8^{o}C$, $6^{o}C$, $2^{o}C$ and a $2^{o}C$ reduction with simulated pulse. Without thermal disruption there is little thermal variation in the temperature of the internal tooth (up to ≈ 1500 seconds). The maximum internal tooth temperature-reduction is seen from the left-tooth at $14.5^{o}C$, with the greatest internal temperature-reduction for the right-tooth at $11.2^{o}C$. The least internal temperature-reduction is with a $2^{o}C$ internal temperature-reduction for both right and left teeth ($7.6^{o}C$ and $5.7^{o}C$, respectively). The left-tooth has the greatest reduction. Internal temperature continues to drop following removal of the cooling-unit once the required temperature-reduction had been achieved.
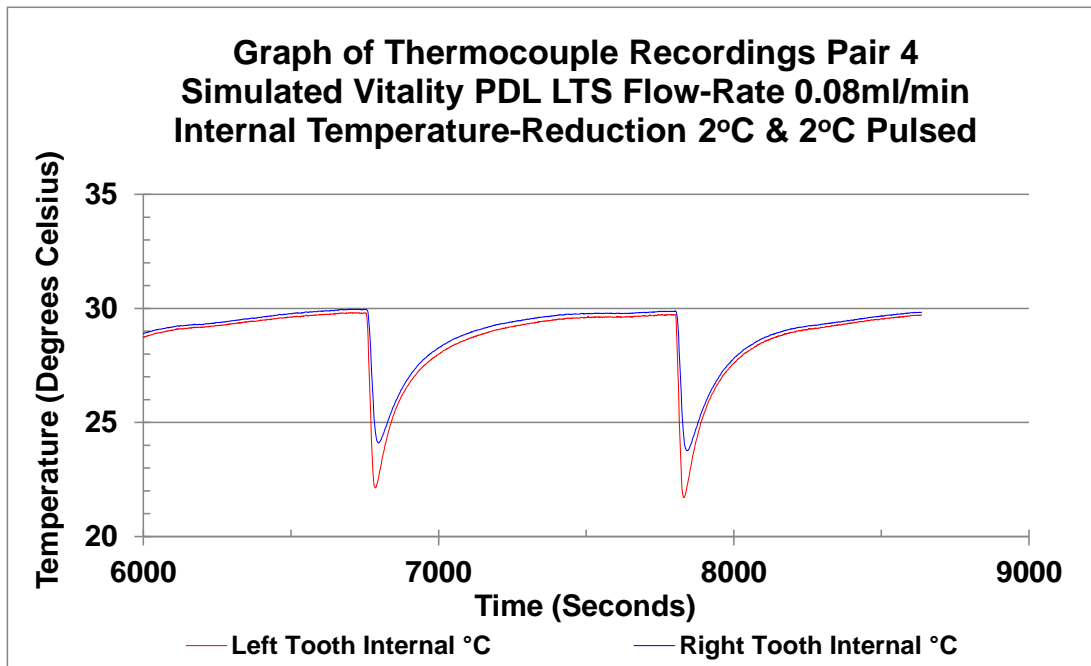
Figure 4-40 Temperatures recorded with thermocouples from the the internal pulp-chamber for 2°C (≈6800 seconds) and pulsed 2°C drop (≈7800 seconds). The pulsed sequence had a slightly greater temperature-reduction than the non-pulsed of ≈0.4^{o}C for both teeth.

4.5.2.3 Difference in Area-Under-The-Curve of Vital and Non-Vital Teeth

The difference in area-under-the-curve for each aligned re-warming sequence was calculated in the same direction, irrespective of simulated vitality. Each sequence had a simulated vital periodontal ligament, and a simulated vital and non-vital tooth which were switched in a cross-over-design (PDL LTS = simulated vitality in periodontal ligament and the left-tooth on screen, or PDL RTS = simulated vitality in periodontal ligament and the right-tooth on screen). The value from the left-tooth was always subtracted from the right-tooth. This may be anticipated to produce a positive value when the right-tooth was vital, and a negative value when the left-tooth was vital. The overall raw-data for the difference in area-under-the-curve is shown in Table 4-19, with graph presentation in Figure 4-41 to 4-44 by flow-rate.

Table 4-19 Difference in area-under-the-curve for aligned re-warming in Pair 4 with simulated vitality of periodontal ligament and one tooth at four flow-rates (0.5ml/min, 0.15ml/min, 0.08ml/min, 0.03ml/min) and seven variables of temperature-reduction ($0^{o}C$, $2^{o}C$, $2^{o}C$ Pulsed, $4^{o}C$, $6^{o}C$, $8^{o}C$, $10^{o}C$) where the area-under-the-curve was calculated by subtracting the left-tooth-value from the right-tooth-value.

Difference in Area-Under-The-Curve (^{o}C/Time) of Right-Tooth Minus Left-Tooth Pair 4							
Vitality (Flow-Rate ml/min)	Internal Temperature-Reduction Measured with Thermocouples ^{o}C						
	0	2	2 Pulsed	4	6	8	10
PDL LTS (0.5)	192.2	-1225.1	-1230.2	-1584.4	-1837.8	-2167.5	-2633.5
PDL RTS (0.5)	-10.4	912.3	2571.4	1411.0	2455.2	3987.9	4235.7
PDL LTS (0.15)	66.1	-225.8	35.7	-269.6	-74.3	126.3	-50.2
PDL RTS (0.15)	-177.0	260.1	0.3	1195.0	2077.2	2545.1	4429.9
PDL LTS (0.08)	277.0	452.2	324.6	499.8	496.1	706.4	880.7
PDL RTS (0.08)	-50.9	932.2	1261.6	1147.2	2014.0	2019.8	1974.3
PDL LTS (0.03)	282.7	576.8	437.5	597.7	767.5	931.5	772.6
PDL RTS (0.03)	-577.4	705.8	1453.9	785.4	1007.4	834.9	759.8
PDL LTS = Simulated Blood-Flow in Periodontal Ligament and Left-Tooth on Screen PDL RTS = Simulated Blood-Flow in Periodontal Ligament and Right-Tooth on Screen ^{o}C = Degrees Celsius							
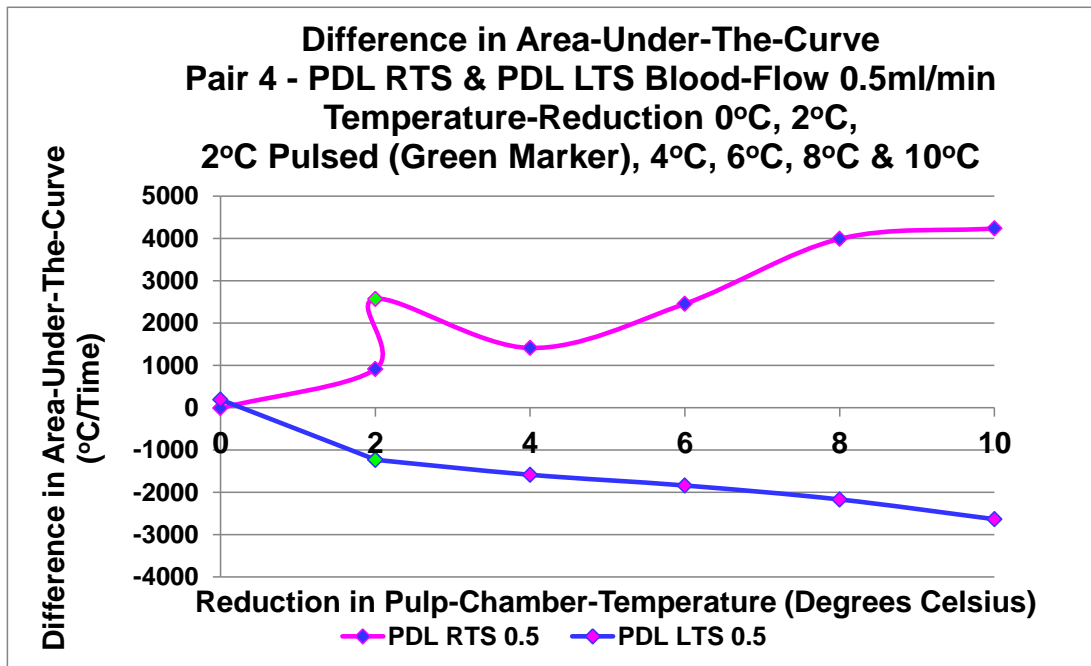
Figure 4-41 Line graph of difference in area-under-the-curve Pair 4 at 0.5ml/min flow-rate following seven variables of temperature-reduction (0°C, 2°C, 2°C Pulsed, 4°C, 6°C, 8°C, 10°C), where the greatest difference in area-under-the-curve for simulations of vitality in the right-tooth (PDL RTS - pink line) and left-tooth (PDL LTS – blue line) were found, with the greatest temperature-reduction 10°C. An 8°C temperature-reduction produces a clear difference in area-under-the-curve for both right and left simulations. There is a decreasing difference from 8°C temperature-reduction to 0°C, where there is a very small difference, being closest to zero of all sequences. The exception to this trend is when a simulated pulse is applied with a 2°C reduction (green marker). For the PDL RTS this increases the difference to a level similar to that of a 6°C temperature-reduction. This does not occur in the PDL LTS pulsed simulation (green marker), which follows the gradual trend of decreasing area-under-the-curve with reducing temperature-reduction. The PDL RTS has a tendency to have a greater difference than the PDL LTS from a temperature-reduction of 6°C and above.
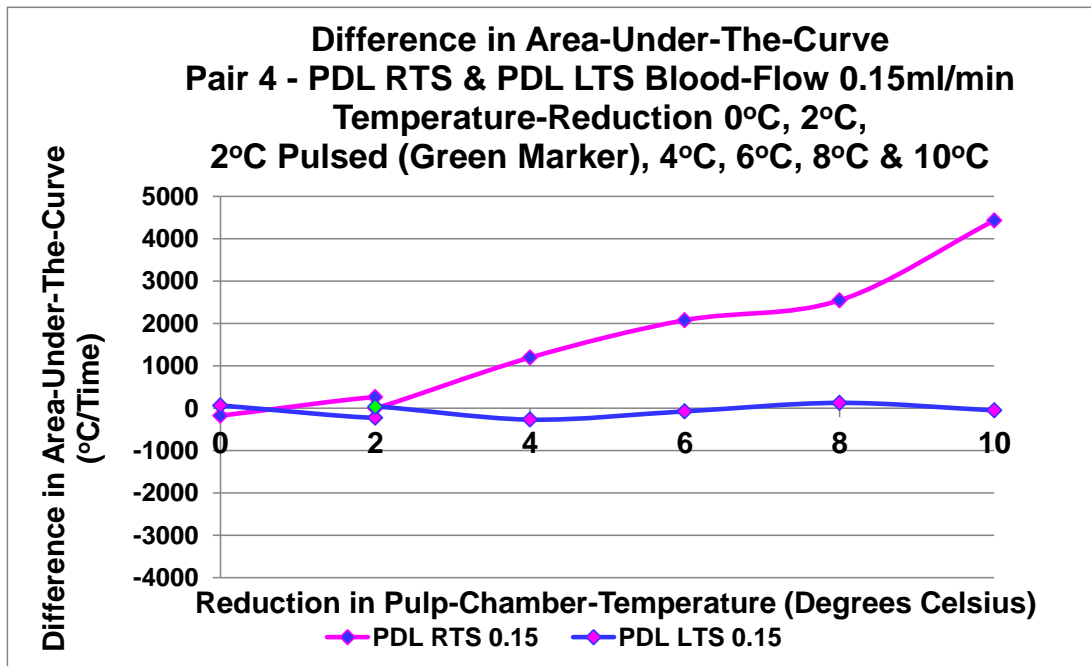
Figure 4-42 Line graph of difference in area-under-the-curve Pair 4 at 0.15ml/min flow-rate following seven variables of temperature-reduction (0°C, 2°C, 2°C Pulsed, 4°C, 6°C, 8°C, 10°C), where the greatest difference in area-under-the-curve for simulations of vitality in the right-tooth (PDL RTS - pink line) were found with the greatest temperature-reduction 10°C, and for the left-tooth (PDL LTS – blue line) at 4°C temperature-reduction. A 4°C temperature-reduction produces a clear difference in area-under-the-curve for the right simulation. The left simulation fluctuates across the X-axis, with a range of difference from -269 to 126°C/Time. There is a decreasing difference from 10°C to 0°C for the right simulation, and the difference from the 2°C pulsed reduction (green marker) is less than the non-pulsed. The PDL RTS has a tendency to have a greater difference than the PDL LTS from a temperature-reduction of 4°C and above.
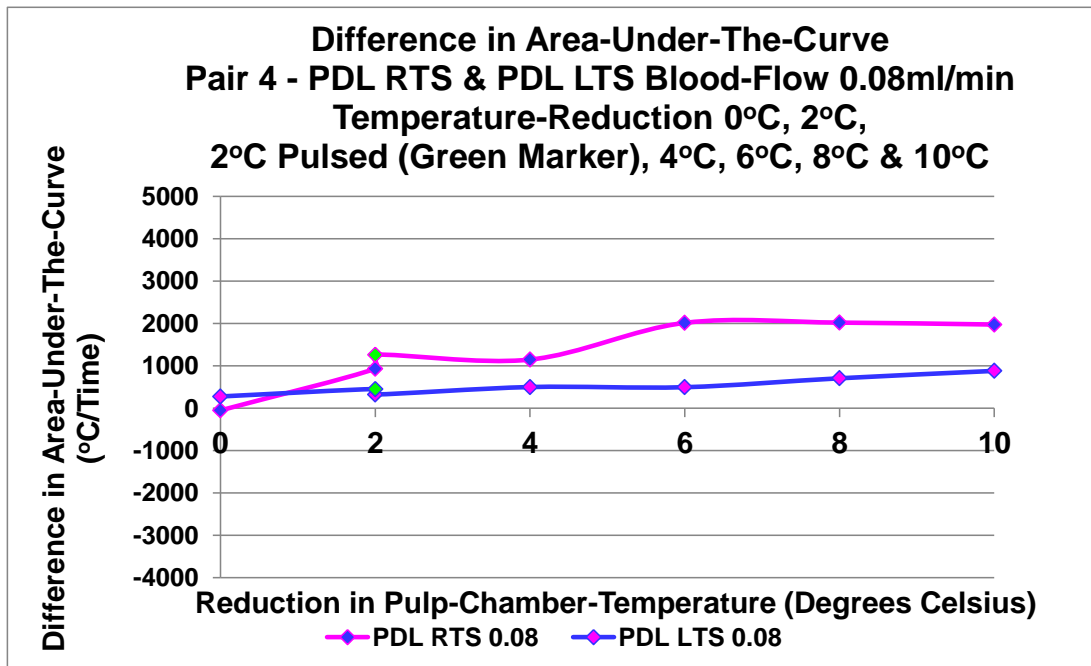
Figure 4-43 Line graph of difference in area-under-the-curve Pair 4 at 0.08ml/min flow-rate following seven variables of temperature-reduction (0°C, 2°C, 2°C Pulsed, 4°C, 6°C, 8°C, 10°C) where the greatest difference in area-under-the-curve for simulations of vitality in the right-tooth (PDL RTS - pink line) were found, with the temperature-reduction of 6°C, with reduced discrimination from 6°C and above. An increase in difference from zero temperature-reduction to 2°C, and from 4°C to 6°C is seen. The left-tooth (PDL LTS – blue line) has a very gradual increase in difference, including that seen from a simulated pulse (green marker) at 2°C temperature-reduction and all differences lie above zero.
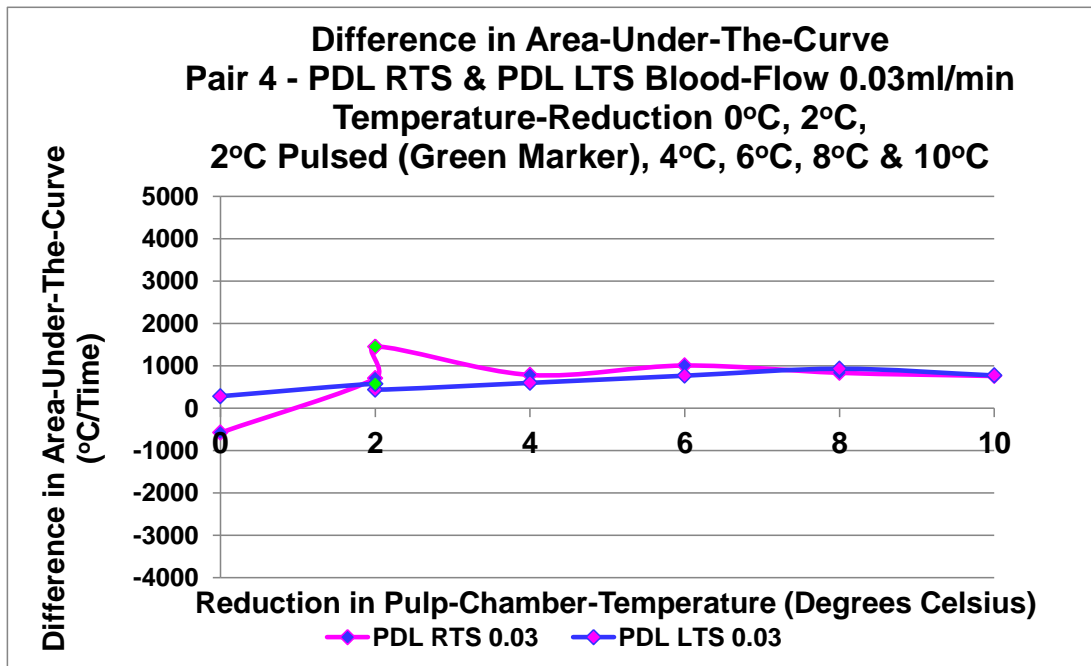
Figure 4-44 Line graph of difference in area-under-the-curve Pair 4 at 0.03ml/min flow-rate following seven variables of temperature-reduction (0°C, 2°C, 2°C Pulsed, 4°C, 6°C, 8°C, 10°C) where the greatest difference in area-under-the-curve for simulations of vitality in the right-tooth (PDL RTS - pink line) were found with the temperature-reduction of 2°C with simulated pulse (green marker). There is no clear difference in area-under-the-curve for simulation of PDL RTS and PDL LTS at a temperature-reduction of 4°C to 10°C. The simulated vitality in the left-tooth (PDL LTS – blue line) has positive values for the difference at all temperature-reductions.

The highest flow-rate (0.5ml/min) and greatest temperature-reduction (10°C) provided the greatest difference in area-under-the-curve. At lower flow-rates, the greatest temperature-reduction (10°C) provided similar differences in area-under-the-curve to an 8°C temperature-reduction.

4.5.2.4 Maximum Temperature-Difference Between Vital and Non-Vital Teeth

The maximum temperature-difference between the simulated vital and non-vital teeth during the re-warming sequence was evaluated. The subtraction was in one direction. The left-tooth-temperature was subtracted from the right, where positive values would be anticipated when the right-tooth was vital, and negative values when the left-tooth was vital. The overall raw-data

for the maximum temperature-difference is shown in Table 4-20, with graph presentation in Figure 4-45 to 4-48 by flow-rate.

Table 4-20 Maximum temperature-difference Pair 4 during aligned re-warming with simulated vitality of periodontal ligament and one tooth at four flow-rates (0.5ml/min, 0.15ml/min, 0.08ml/min, 0.03ml/min) and seven variables of temperature-reduction ($0^{o}C$, $2^{o}C$, $2^{o}C$ pulsed, $4^{o}C$, $6^{o}C$, $8^{o}C$, $10^{o}C$), calculated by subtracting the temperature of the left-tooth from the right-tooth. PDL LTS 0.5ml/min had a greater maximum temperature-difference with greater cooling and remained in sequence with the addition of a pulse at $2^{o}C$ temperature-reduction.

Maximum Temperature-Difference (^{o}C) Between Right-Tooth Minus Left-Tooth Pair 4							
Vitality (Flow-Rate ml/min)	Internal Temperature-Reduction Measured with Thermocouples ^{o}C						
	0	2	2 Pulsed	4	6	8	10
PDL LTS (0.5)	-0.1	-0.8	-0.9	-1.0	-1.2	-1.3	-1.5
PDL RTS (0.5)	0.1	0.5	1.1	0.6	0.9	1.5	1.6
PDL LTS (0.15)	-0.1	-0.5	-0.4	-0.6	-0.5	-0.5	-0.7
PDL RTS (0.15)	0.0	0.3	0.3	0.6	0.8	1.0	1.6
PDL LTS (0.08)	0.0	-0.4	-0.4	-0.4	-0.4	-0.5	-0.3
PDL RTS (0.08)	0.1	0.5	0.5	0.7	0.8	0.8	0.8
PDL LTS (0.03)	0.0	-0.3	-0.4	-0.5	-0.3	-0.3	-0.5
PDL RTS (0.03)	0.0	0.4	0.6	0.5	0.5	0.5	0.5
PDL LTS = Simulated Blood-Flow in Periodontal Ligament and Left-Tooth on Screen PDL RTS = Simulated Blood-Flow in Periodontal Ligament and Right-Tooth on Screen ^{o}C = Degrees Celsius							
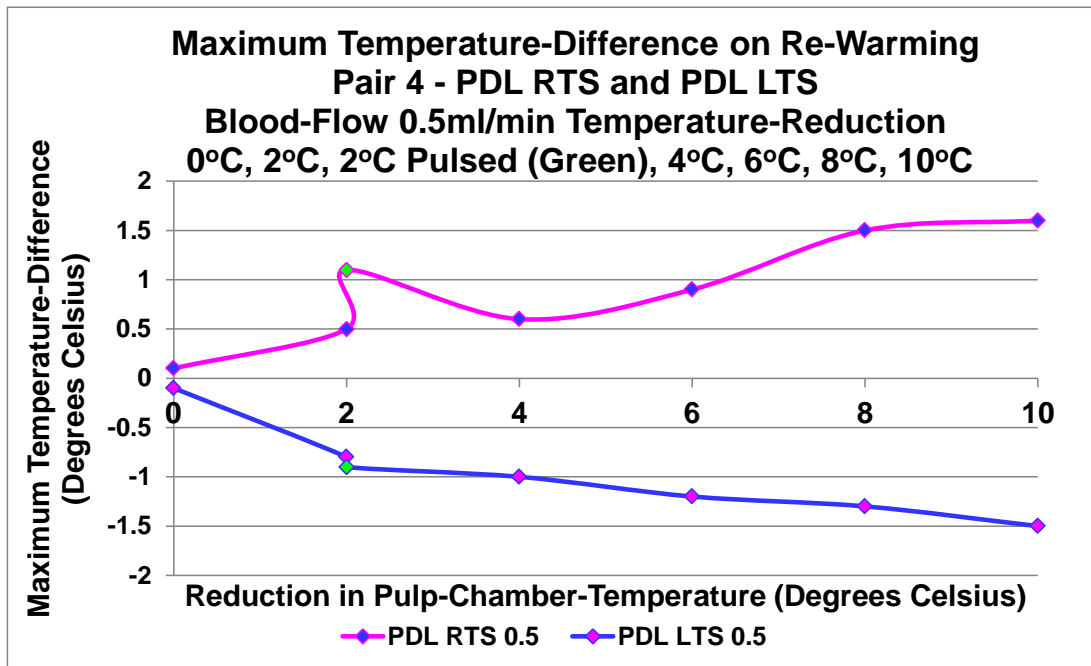
Figure 4-45 Line graph of maximum temperature-difference Pair 4 at 0.5ml/min flow-rate following seven variables of temperature-reduction (0°C, 2°C, 2°C Pulsed, 4°C, 6°C, 8°C, 10°C). There is an increase in maximum temperature-difference between right and left teeth, with increased temperature-reduction for both simulations, i.e., PDL RTS and PDL LTS. Both achieved a maximum temperature-difference of 1.5^{o}C or above at the maximum temperature-reduction. The effect was slightly reduced for an 8°C temperature-reduction, and the simulated pulse (green marker) increased the temperature-difference above the 6°C temperature-reduction for the PDL RTS, and increased slightly for the PDL LTS. The least difference in maximum temperature was clearly seen with no temperature-reduction, and the greatest was shown with the greatest temperature-reduction of 10°C.
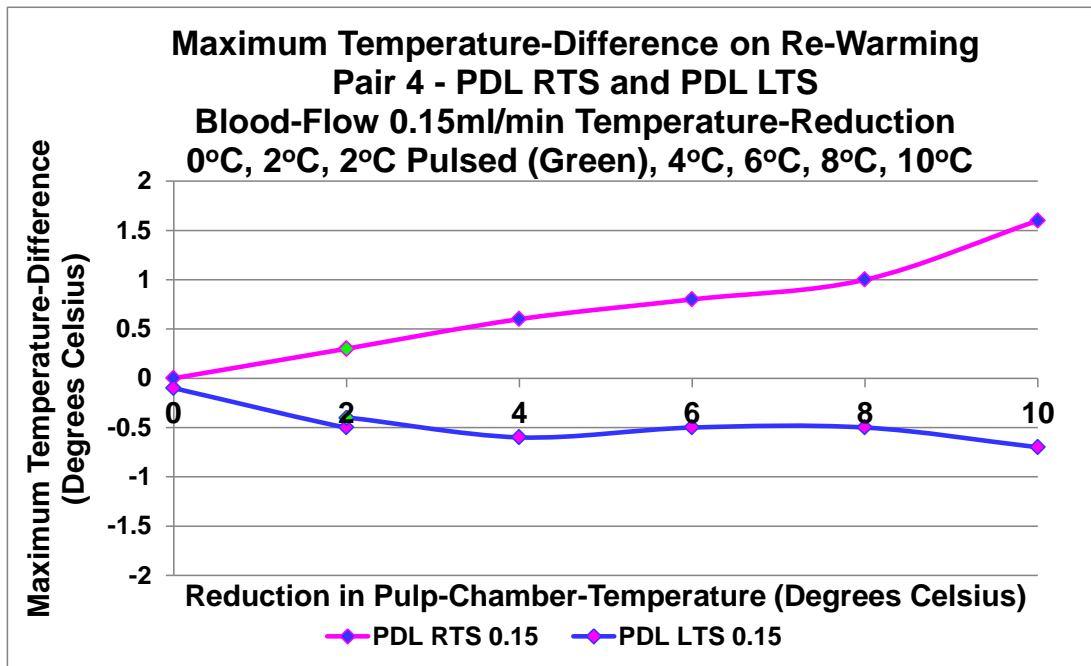
Figure 4-46 Line graph of maximum temperature-difference Pair 4 at 0.15ml/min flow-rate following seven variables of temperature-reduction (0^oC, 2^oC, 2^oC Pulsed, 4^oC, 6^oC, 8^oC, 10^oC). There was an increased maximum temperature-difference between right and left teeth, with increased temperature-reduction for the PDL RTS simulation, reaching in excess of 1.5^oC with a temperature-reduction of 10^oC. There was no additional increase for the pulsed simulation (green marker) at 2^oC temperature-reduction. The PDL LTS fluctuated from 2^oC to 10^oC, the maximum being slightly in excess of 0.5^oC, again seen with maximum temperature-reduction. A reduced maximum temperature-difference is seen when a simulated pulse (green marker) was applied for PDL LTS, compared to no change in the PDL RTS. There was a difference in temperature when a temperature-reduction was applied, and the greatest difference was seen with the greatest temperature-reduction.
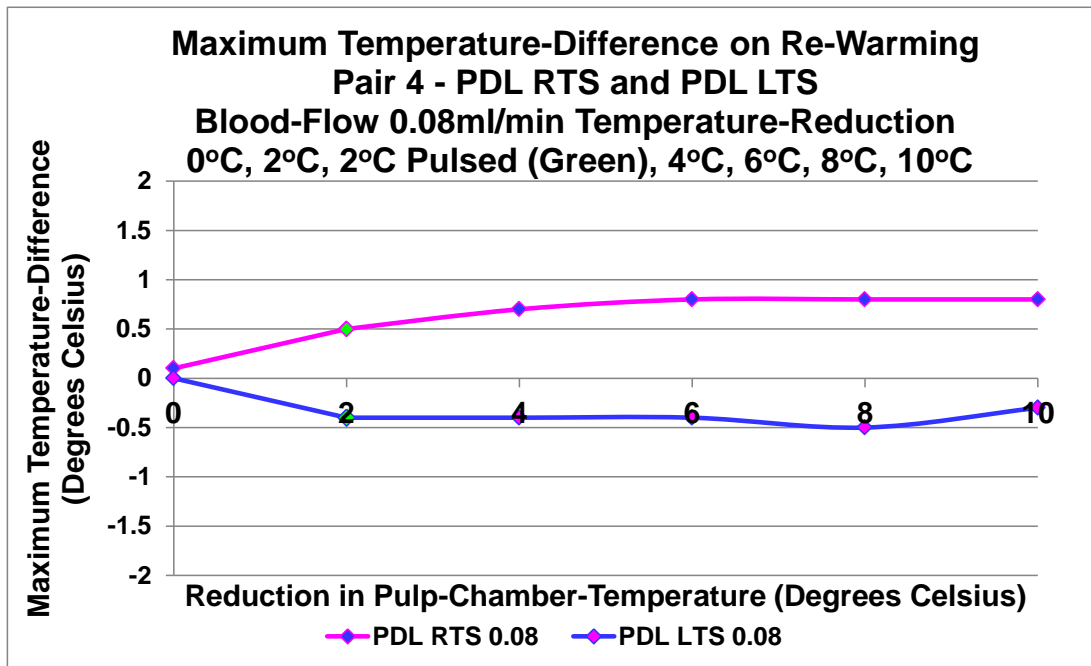
Figure 4-47 Line graph of maximum temperature-difference Pair 4 at 0.08ml/min flow-rate following seven variables of temperature-reduction (0°C, 2°C, 2°C Pulsed, 4°C, 6°C, 8°C, 10°C). There was an increase in maximum temperature-difference between right and left teeth, with increased temperature-reduction for the PDL RTS simulation, particularly from 0°C to 2°C temperature-reduction, but there was no increased effect with the simulation of a pulse (green marker). The PDL LTS had a minimal increase in temperature-difference from 2°C to 10°C, the greatest effect being seen from 0°C to 2°C temperature-reduction and there was no increased effect with a simulated pulse (green marker). The effect exceeds 0.5°C from 2°C to 10°C for the PDL RTS, and fell slightly below 0.5°C for 2°C, 4°C, 6°C and 10°C temperature-reduction, reaching 0.5°C for only 8°C for PDL LTS.
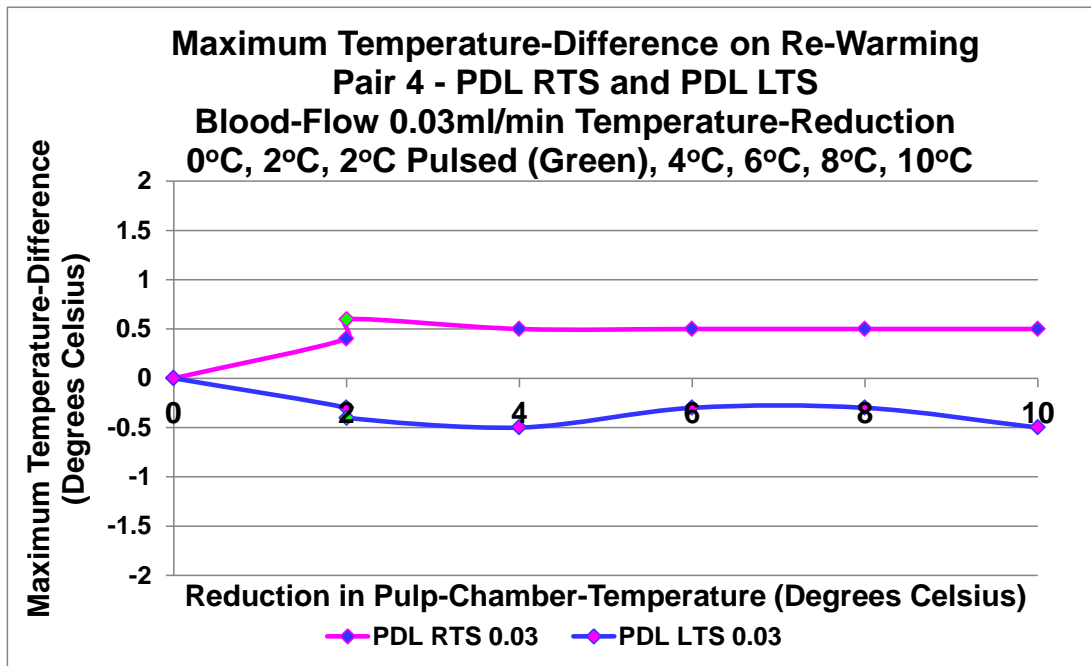
Figure 4-48 Line graph of maximum temperature-difference Pair 4 at 0.03ml/min flow-rate following seven variables of temperature-reduction ($0^{o}C$, $2^{o}C$, $2^{o}C$ Pulsed, $4^{o}C$, $6^{o}C$, $8^{o}C$, $10^{o}C$). There was an increased maximum temperature-difference between right and left teeth, with increased temperature-reduction for both PDL RTS and PDL LTS simulation, particularly from $0^{o}C$ to $2^{o}C$ temperature-reduction and there was an increased effect with the simulation of a pulse (green marker). The PDL RTS had a minimal increase in temperature-difference from $2^{o}C$ to $4^{o}C$, and this levels from $4^{o}C$ to $10^{o}C$, achieving a maximum $0.5^{o}C$ difference. The PDL LTS fluctuated from $2^{o}C$ to $10^{o}C$ and did not reach a difference in excess of $0.5^{o}C$.

The highest flow-rate (0.5ml/min) and greatest temperature-reduction ($10^{o}C$) provided the greatest difference in maximum temperature. At lower flow-rates, the greatest temperature-reduction ($10^{o}C$) provided no additional benefit compared to a $4^{o}C$ temperature-reduction.

4.5.2.5 Characteristic-Time-To-Relaxation Difference
Between Vital and Non-Vital Teeth

The difference in characteristic-time-to-relaxation between the simulated vital and non-vital teeth during the re-warming sequence was evaluated. The subtraction was in one direction. The left-tooth was subtracted from the right, where positive values would be anticipated when the left-tooth was vital, and negative values when the right-tooth was vital - the opposite to the area-under-the-curve differences and the maximum temperature-differences. This is due to the expectation that the vital tooth would have a shorter time to reach thermal relaxation than the non-vital tooth. The overall raw-data for the difference in characteristic-time-to-relaxation is shown in Table 4-21, with graph presentation in Figure 4-49 to 4-52 by flow-rate.

Table 4-21 Difference in Characteristic-Time-To-Relaxation Pair 4 during aligned re-warming with simulated vitality of periodontal ligament and one tooth at four flow-rates (0.5ml/min, 0.15ml/min, 0.08ml/min, 0.03ml/min) and seven variables of temperature-reduction (0^oC, 2^oC, 2^oC pulsed, 4^oC, 6^oC, 8^oC, 10^oC) calculated by subtracting the time of the left-tooth from the right-tooth. The greatest time difference is seen with the greatest temperature-reduction at 0.15ml/min for the simulation in the right-tooth.

Characteristic-Time-To-Relaxation Difference (Seconds) Between Right-Tooth Minus Left-Tooth Pair 4						
Vitality (Flow-Rate ml/min)	Internal Temperature-Reduction Measured with Thermocouples ^oC					
	2	2 Pulsed	4	6	8	10
PDL LTS (0.5)	20.29	22.70	22.27	20.06	22.15	23.28
PDL RTS (0.5)	-6.88	-20.54	-11.15	-18.87	-24.15	-27.63
PDL LTS (0.15)	7.72	6.56	6.39	2.82	2.29	1.18
PDL RTS (0.15)	-12.94	-8.43	-23.84	-30.50	-28.44	-32.20
PDL LTS (0.08)	1.53	3.09	1.57	0.12	-0.97	-3.26
PDL RTS (0.08)	-0.68	-3.71	-3.85	-20.00	-13.82	-8.33
PDL LTS (0.03)	2.60	2.75	3.70	0.87	-0.07	0.12
PDL RTS (0.03)	0.98	-3.23	2.14	0.46	0.45	-1.98
PDL LTS = Simulated Blood-Flow in Periodontal Ligament and Left-Tooth on Screen PDL RTS = Simulated Blood-Flow in Periodontal Ligament and Right-Tooth on Screen ^oC = Degrees Celsius						

Difference In Charactersitic-Time-To-Relaxation (Seconds) on Re-Warming Pair 4 - PDL RTS & PDL LTS Blood-Flow 0.5ml/min Temperature-Reduction 2°C, 2°C Pulsed (Green), 4°C, 6°C, 8°C, 10°C
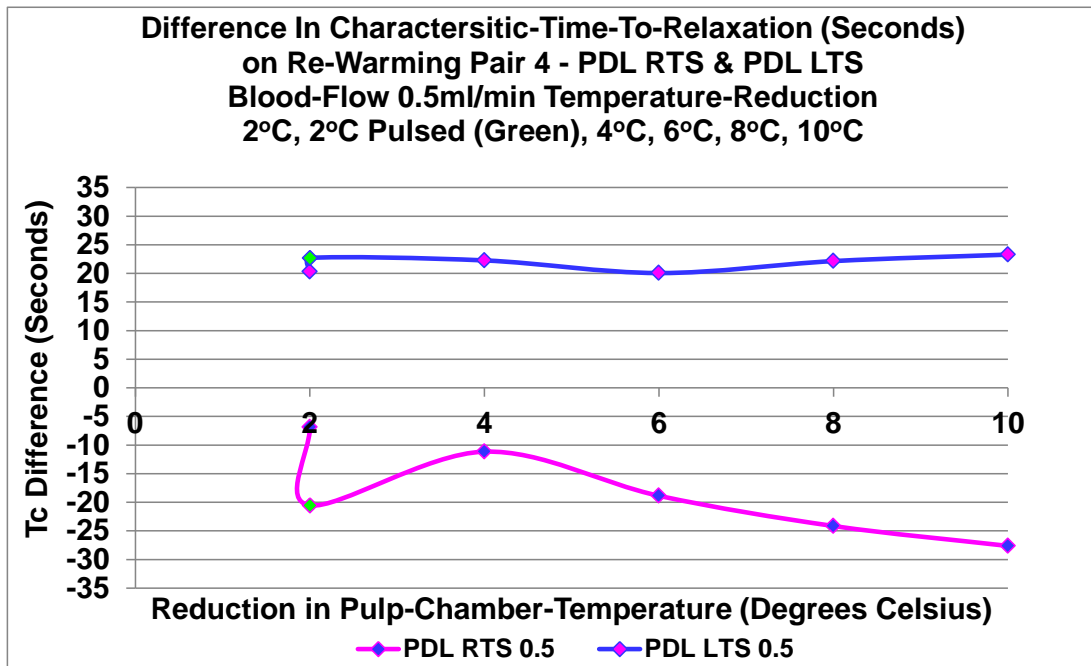
Figure 4-49 Line graph of difference in Characteristic-Time-To-Relaxation Pair 4 at 0.5ml/min flow-rate following six variables of temperature-reduction (2°C, 2°C Pulsed, 4°C, 6°C, 8°C, 10°C). The difference in characteristic-time-to-relaxation between the right and left teeth of each simulation provided a similar outcome for all temperature-reduction for the PDL LTS 0.5ml/min, ranging from 20.06 to 23.28 seconds, showing there is a difference. The least difference was found from a temperature-reduction of 6°C and the maximum difference was seen from a temperature-reduction of 10°C. The simulated pulse (green marker) had an increased difference in characteristic-time-to-relaxation than the non-pulsed 2°C temperature-reduction. The PDL RTS demonstrated an increased difference from a 2°C temperature-reduction to 10°C. The pulsed simulation (green marker) peaks at a level above that of a 6°C temperature-reduction. The maximum difference was seen with the maximum temperature-reduction (-27.63 seconds) and the minimum difference was seen with the non-pulsed simulation at a minimum temperature-reduction (-6.88 seconds).
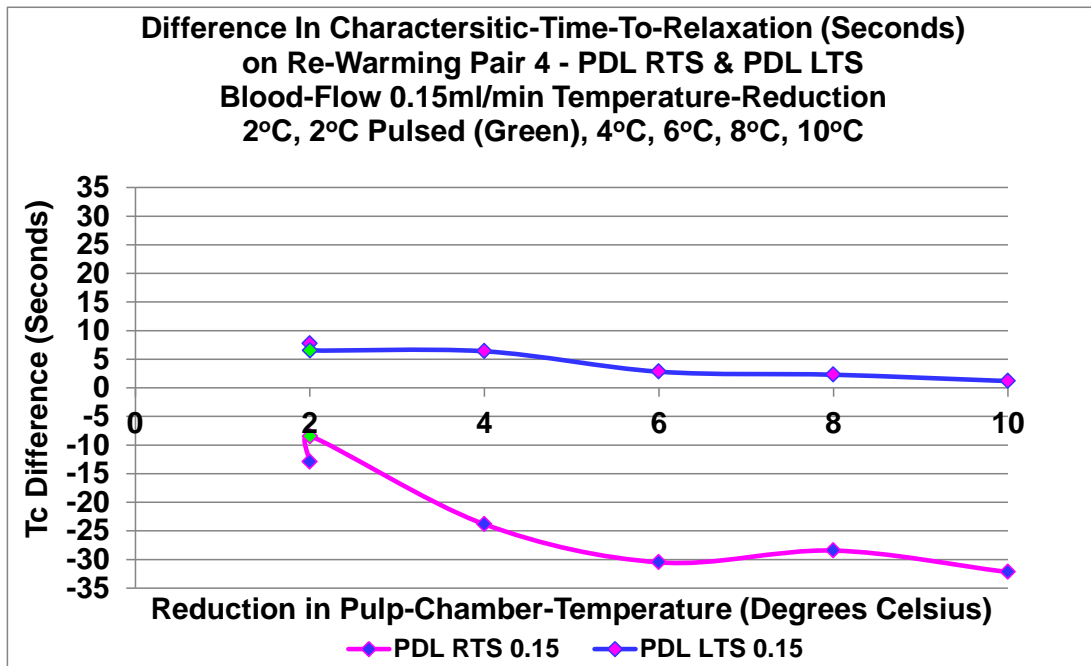
Figure 4-50 Line graph of difference in Characteristic-Time-To-Relaxation Pair 4 at 0.15ml/min flow-rate following six variables of temperature-reduction (2°C, 2°C Pulsed, 4°C, 6°C, 8°C, 10°C). The difference in characteristic-time-to-relaxation between the right and left teeth of each simulation provided a gradual reduction in value, with increasing temperature-reduction for the PDL LTS ranging from 7.72 to 1.18 seconds, showing there was a small difference. The simulated pulse (green marker) had a decreased difference in characteristic-time-to-relaxation than the non-pulsed 2°C temperature-reduction. The PDL RTS demonstrated an increased characteristic-time-to-relaxation difference from a 2°C temperature-reduction to 10°C, with pulsed simulation (green marker) being least (-8.43 seconds), and the 8°C temperature-reduction being slightly less than the 6°C temperature-reduction, and a temperature-reduction of 10°C provided the greatest difference in characteristic-time-to-relaxation (-32.2 seconds).

Difference In Charactersitic-Time-To-Relaxation (Seconds) on Re-Warming Pair 4 - PDL RTS & PDL LTS Blood-Flow 0.08ml/min Temperature-Reduction 2ºC, 2ºC Pulsed (Green), 4ºC, 6ºC, 8ºC, 10ºC
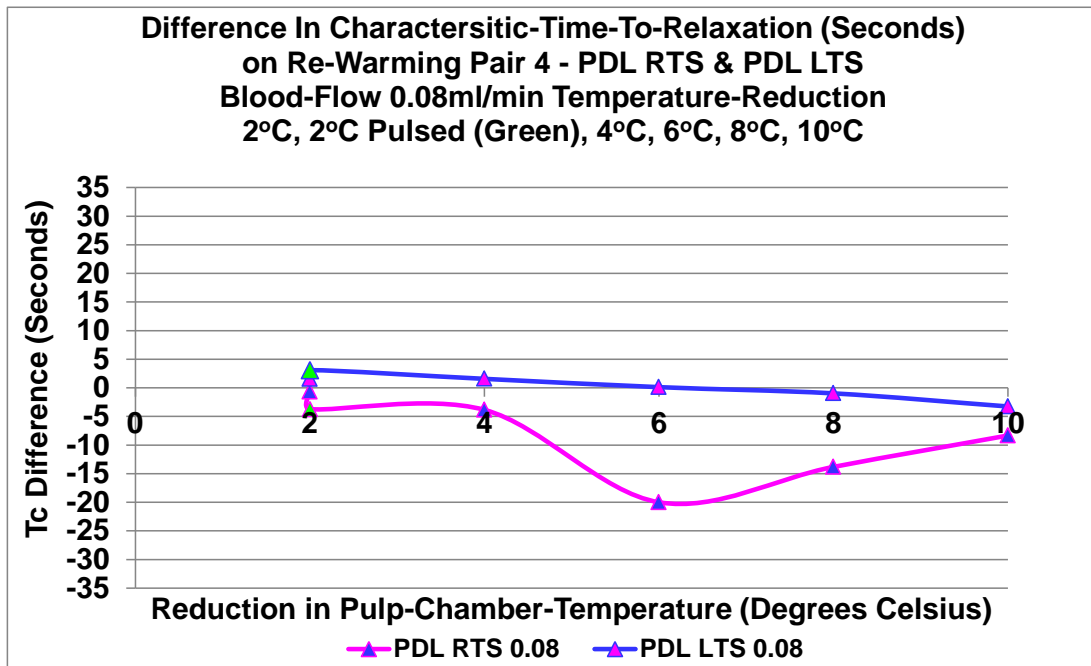
Figure 4-51 Line graph of difference in Characteristic-Time-To-Relaxation Pair 4 at 0.08ml/min flow-rate following six variables of temperature-reduction ($2^{o}C$, $2^{o}C$ Pulsed, $4^{o}C$, $6^{o}C$, $8^{o}C$, $10^{o}C$). The difference in characteristic-time-to-relaxation between the right and left teeth of each simulation provided a gradual reduction in value with increasing temperature-reduction for the PDL LTS, crossing the X-axis between $6^{o}C$ and $8^{o}C$ of temperature-reduction. The simulated pulse (green marker) had an increased difference in characteristic-time-to-relaxation than the non-pulsed $2^{o}C$ temperature-reduction. The PDL RTS demonstrated an increased characteristic-time-to-relaxation difference from a $4^{o}C$ temperature-reduction to $6^{o}C$, with the pulsed simulation (green marker) having a greater difference than the non-pulsed $2^{o}C$ temperature-reduction. A reduced difference is seen from $8^{o}C$ and $10^{o}C$.

**Difference In Charactersitic-Time-To-Relaxation (Seconds)
on Re-Warming Pair 4 - PDL RTS & PDL LTS
Blood-Flow 0.03ml/min Temperature-Reduction
2ºC, 2ºC Pulsed (Green), 4ºC, 6ºC, 8ºC, 10ºC**
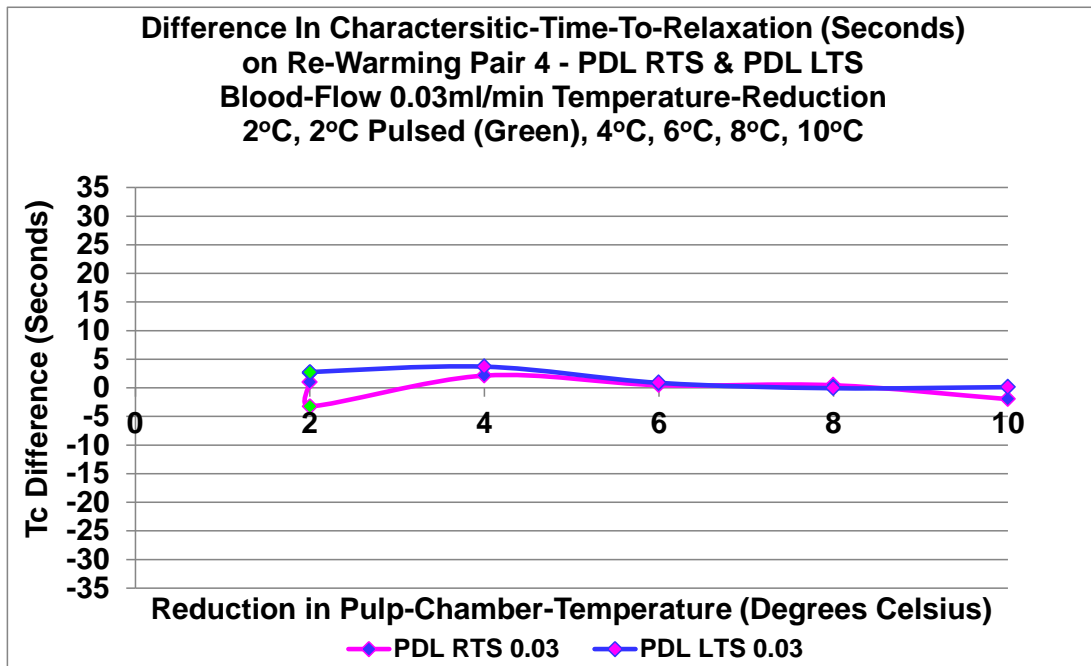
Figure 4-52 Line graph of difference in Characteristic-Time-To-Relaxation Pair 4 at 0.03ml/min flow-rate following six variables of temperature-reduction (2^oC, 2^oC Pulsed, 4^oC, 6^oC, 8^oC, 10^oC). The difference in characteristic-time-to-relaxation between the right and left teeth of each simulation was very small and the two simulations overlapped between a 6^oC and 8^oC temperature-reduction. The greatest difference between the two simulations was seen with a temperature-reduction of 2^oC with a simulated pulse (green marker).

The clearest method to see a difference between the left and right simulations was the area-under-the-curve, at the highest flow-rate and with a temperature-reduction of between 6^oC and 8^oC.

4.5.3 Simulated Vitality Heat-Exchange Maps

The re-warming sequences were visualised as heat-exchange maps, as described in Figure 4-53, using the area-under-the-curve over a timeline of one minute for a flow-rate of 0.5ml/min and a temperature-reduction of 10^oC. The temperature-range used was 20^oC to 32^oC. Greyscale and colour images are presented (Figure 4-54 and 4-55).
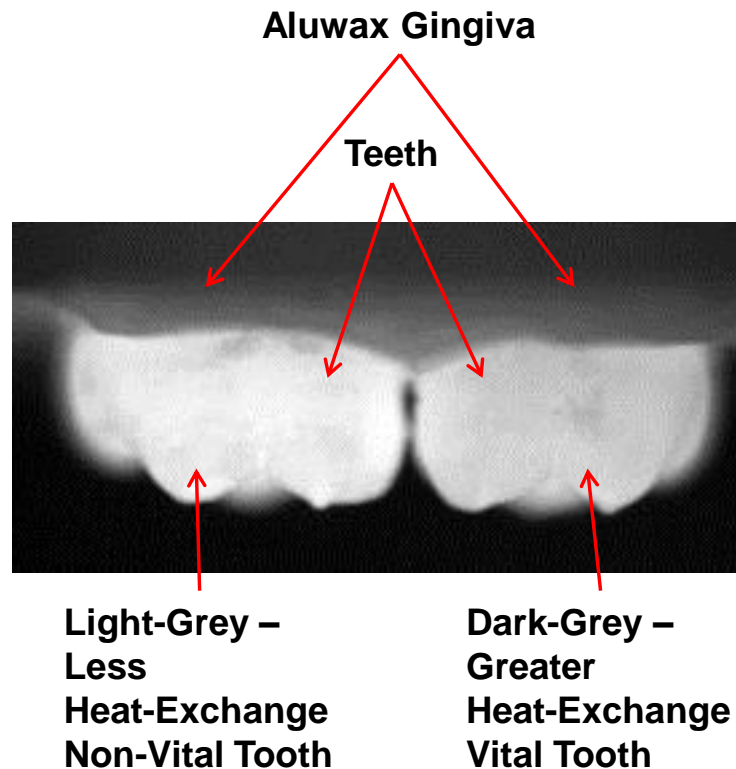
Figure 4-53 Description of area-under-the-curve heat-exchange map Pair 4 at 0.5ml/min with 10°C temperature-reduction. The greyscale image shows a pair of molar teeth held within Aluwax and the tooth-holding-unit. The light-grey areas of the image are cool areas, following the temperature-reduction from application of the cooling-unit to the occlusal-surfaces of the teeth. After removal of the cooling-unit, the heat-exchange in the tooth from simulated vitality is seen as changes in greyscale, producing a darker grey in the crown-area with warming.

A sequence of six re-warming images at 10-second-intervals over one minute are shown in Figure 4-54, which demonstrate the gradual re-warming of Pair 4 with simulated vitality at 0.5ml/min in PDL LTS and PDL RTS, with an internal temperature-reduction of 10°C. Two images are shown, one with simulated vitality in the left-tooth on screen, and one with the right-tooth on screen. The only change in the two pairs is the simulation of vitality, which has been crossed-over. A colour sequence is also presented following preparation in Image J (Figure 4-55). It is clearly visible in these innovative images that the respective vital tooth is re-warming before the non-vital tooth in each sequence, by the change in greyscale or lightening of the blue colour.

Simulated Vitality Left-Tooth   Simulated Vitality Right-Tooth
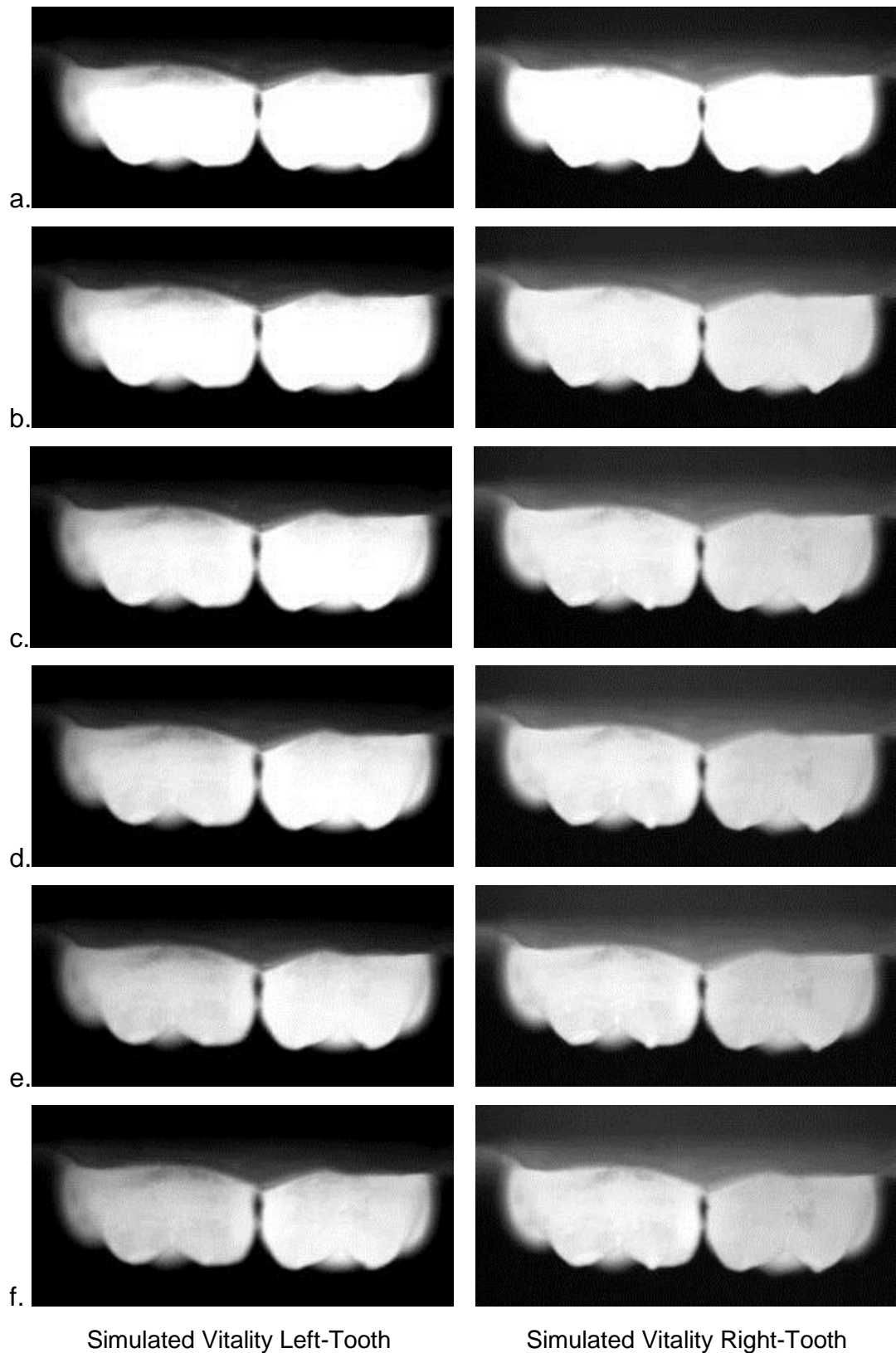
Figure 4-54 Heat-Exchange Maps Pair 4
10 (a), 20 (b), 30 (c), 40 (d), 50 (e), 60 (f) seconds of re-warming to demonstrate simulated vitality seen by the increasing greyscale of the simulated vital left-tooth and simulated vital right-tooth, in respective sequences.

Simulated Vitality Left-Tooth   Simulated Vitality Right-Tooth
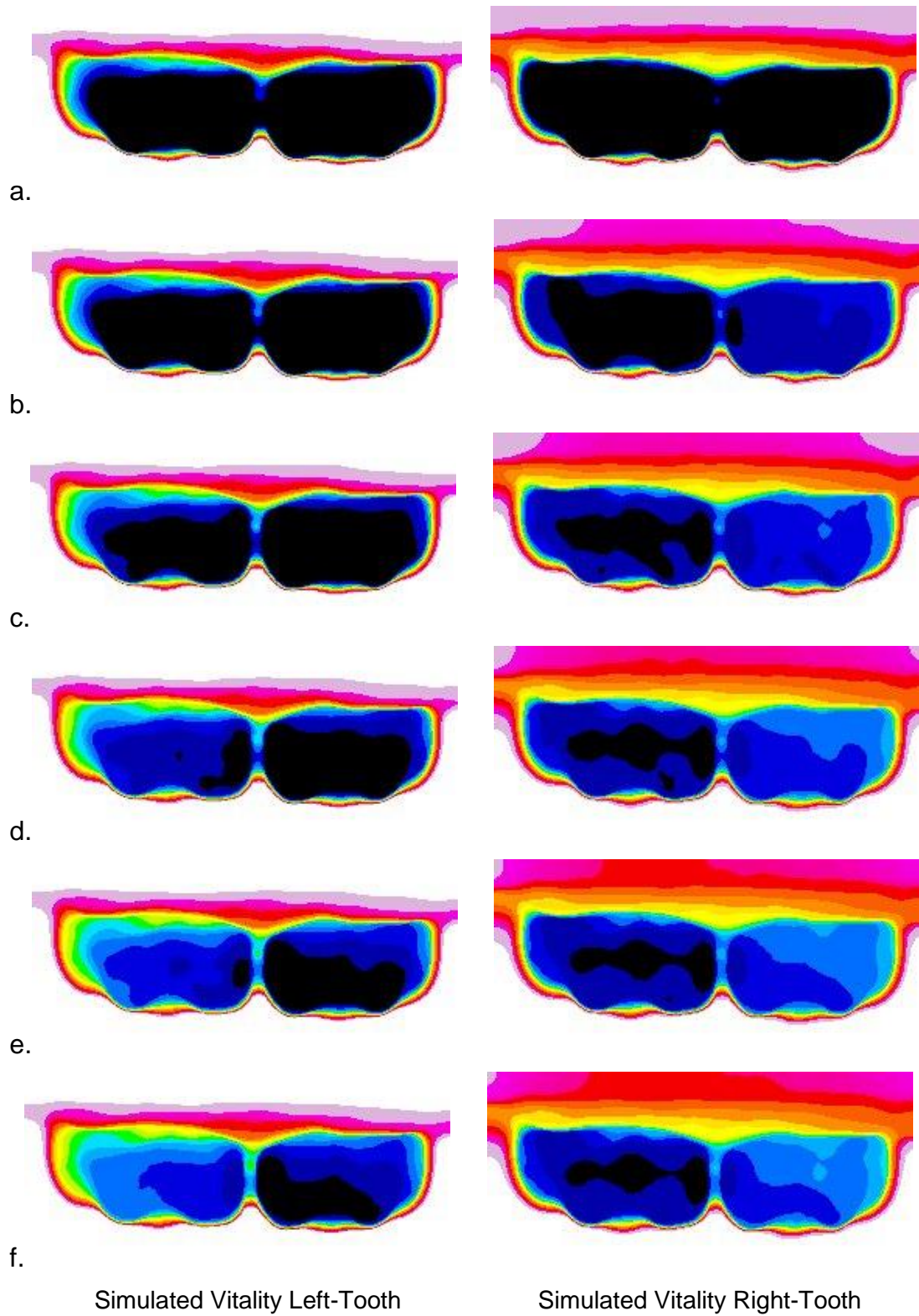
Figure 4-55 Colour Heat-Exchange Maps Pair 4
     10 (a), 20 (b), 30 (c), 40 (d), 50 (e), 60 (f) seconds of re-warming to demonstrate simulated vitality seen by the increasing light blue of the simulated vital left-tooth and simulated vital right-tooth, in respective sequences.

4.5.4 Surface-Temperatures and Cooling-Times

Table 4-22 Surface-Temperatures of Pair 4 at Four Flow-Rates (0.5ml/min, 0.15ml/min, 0.08ml/min, 0.03ml/min): Pre- and Post-Cooling-Unit-Application and Associated Timelines, and Lowest Temperature Achieved

Pair	Condition	Flow-Rate ml/min	ΔT ^{0}C	Start Temp of Tooth ^{0}C		Frame No.	Temp of Tooth at Removal of Peltier ^{0}C		Frame No.	Cooling Time		Lowest Temp ^{0}C	
				LTS	RTS		LTS	RTS		Frames	Seconds	LTS	RTS
P4	PDL LTS	0.5	10	31.4	31.5	1597	14.8	13.0	2100	503	56	14.6	12.8
			8	31.6	31.6	1533	15.8	14.4	1925	392	44	15.7	14.2
			6	31.6	31.7	1451	17.2	16.0	1757	306	34	17.1	15.9
			4	31.5	31.5	1389	18.9	17.5	1625	236	26	18.9	17.5
			2	31.6	31.7	1564	20.8	20.0	1742	178	20	20.8	20.0
			2P	31.6	31.6	1562	21.4	20.3	1729	167	19	21.3	20.2
P4	PDL RTS	0.5	10	31.5	31.5	1988	13.2	13.2	4241	2253	250	13.2	13.2
			8	31.4	31.4	2169	13.1	12.9	2965	796	88	13.1	12.9
			6	31.4	31.4	2006	16.6	16.6	2671	665	74	16.5	16.6
			4	31.4	31.4	2237	18.3	18.0	2591	354	39	18.1	17.8
			2	31.5	31.5	2175	21.4	21.0	2390	215	24	20.7	20.3
			2P	31.4	31.4	2215	17.1	16.7	2611	396	44	16.9	16.6
P4	PDL LTS	0.15	10	31.6	31.6	2583	14.3	12.8	3139	556	62	14.1	12.6
			8	31.5	31.5	2332	15.4	14.3	2768	436	48	15.3	14.2
			6	31.4	31.4	2494	16.9	15.8	2820	326	36	16.9	15.8
			4	31.5	31.5	2345	18.8	17.5	2590	245	27	18.7	17.4
			2	31.4	31.4	2457	20.6	19.4	2626	169	19	20.5	19.3
			2P	31.5	31.5	2858	20.4	19.4	3024	166	18	20.2	19.2
P4	PDL RTS	0.15	10	31.5	31.5	1742	12.6	13.6	4412	2670	297	12.6	13.6
			8	31.2	31.1	2309	16.4	17.7	4118	1809	201	16.3	17.7
			6	31.1	31.0	1944	19.6	20.8	3710	1766	196	19.5	20.8
			4	31.1	31.1	1882	22.5	23.3	2865	983	109	22.3	23.2
			2	31.3	31.2	1810	24.2	24.9	2208	398	44	24.1	24.8
			2P	31.4	31.2	2104	24.1	24.7	2451	347	39	23.8	24.4

P4 = Pair 4; PDL LTS = Simulated Blood-Flow in Periodontal Ligament and Left-Tooth on Screen; PDL RTS = Simulated Blood-Flow in Periodontal Ligament and Right-Tooth on Screen; LTS = Left-Tooth on Screen; RTS = Right-Tooth on Screen; P = Pulsed; ml/min = millilitres per minute; ΔT = Difference in Internal Tooth-Temperature; ^{0}C = Degrees Celsius

Lowest Starting-Temperature of the Pairing	Highest Starting-Temperature of the Pairing at Peltier Removal	Lowest Temperature of the Pairing at Peltier Removal	PDL LTS 8°C Reduction-Time	Lowest Temperature of the Pairing

Pair	Condition	Flow-Rate ml/min	ΔT °C	Start Temp of Tooth °C		Frame No.	Temp of Tooth at Removal of Peltier °C		Frame No.	Cooling Time		Lowest Temp °C	
				LTS	RTS		LTS	RTS		Frames	Secs	LTS	RTS
P4	PDL LTS	0.08	10	31.8	31.8	1600	13.3	12.6	2108	508	56	13.1	12.4
			8	31.8	31.8	1685	14.8	13.8	2060	375	42	14.5	13.6
			6	31.6	31.6	1517	17.5	16.9	1900	383	43	17.3	16.7
			4	31.5	31.5	1636	18.8	18.2	1913	277	31	18.4	17.9
			2	31.7	31.7	1728	20.2	19.6	1891	163	18	19.7	19.0
			2P	31.5	31.5	1880	19.3	18.5	2045	165	18	18.8	18.0
P4	PDL RTS	0.08	10	31.3	31.3	2215	13.5	12.5	2791	576	64	13.4	12.4
			8	31.2	31.2	2293	16.8	16.9	3121	828	92	16.7	16.8
			6	31.2	31.2	2248	19.9	20.7	3275	1027	114	19.8	20.6
			4	31.2	31.2	1698	19.4	19.7	2090	392	44	19.3	19.7
			2	31.2	31.2	1742	21.1	21.0	1941	199	22	20.7	20.6
			2P	31.3	31.3	1597	20.6	20.4	1822	225	25	20.3	20.2
P4	PDL LTS	0.03	10	31.8	31.8	1629	13.3	12.4	2147	518	58	13.2	12.3
			8	31.7	31.7	1758	14.3	13.5	2154	396	44	14.3	13.5
			6	31.7	31.7	1520	16.1	15.4	1855	335	37	16.0	15.4
			4	31.9	31.9	1592	17.6	16.7	1823	231	26	17.5	16.6
			2	31.5	31.5	1372	19	18.4	1549	177	20	19.0	18.4
			2P	31.3	31.3	1425	18.9	18.4	1604	179	20	18.4	17.9
P4	PDL RTS	0.03	10	31.4	31.3	1877	12.5	11.5	2469	592	66	12.5	11.5
			8	31.1	31.1	1774	13.7	13.0	2241	467	52	13.7	13.0
			6	31.2	31.2	1716	14.7	14.1	2052	336	37	14.7	14.1
			4	31.3	31.3	1900	16.6	16.1	2168	268	30	16.6	16.1
			2	31.3	31.3	1525	19.5	19.4	1735	210	23	19.3	19.2
			2P	31.3	31.3	1537	17.5	17.1	1780	243	27	17.5	17.1

P4 = Pair 4; PDL LTS = Simulated Blood-Flow in Periodontal Ligament and Left-Tooth on Screen; PDL RTS = Simulated Blood-Flow in Periodontal Ligament and Right-Tooth on Screen; LTS = Left-Tooth on Screen; RTS = Right-Tooth on Screen; P = Pulsed; ml/min = millilitres per minute; ΔT = Difference in Internal Tooth-Temperature; °C = Degrees Celsius

| Lowest Starting-Temperature of the Pairing | Highest Starting-Temperature of the Pairing at Peltier Removal | Lowest Temperature of the Pairing at Peltier Removal | PDL LTS 8°C Reduction-Time | Lowest Temperature of the Pairing |

Table 4-22 provides the tooth-surface temperatures of Pair 4 captured with the thermal camera during each temperature-reduction from 2^oC to 10^oC and the timeline for cooling. The baseline start-temperatures of the tooth-surfaces range from 31^oC to 31.9^oC. The lowest temperature of the tooth surfaces at the point of removal of the cooling-unit was 11.5^oC for the right-tooth of the PDL RTS sequence with a flow-rate of 0.03ml/min, giving a maximum external reduction of nearly 20^oC. There was a further drop in the surface-temperature of some teeth - up to 0.7^oC - following removal of the cooling-unit.

The timeline for an 8^oC temperature-reduction was taken from the left-tooth. The thermocouple used for the temperature-reduction was within the right-tooth and, thus, there was no flow-effect on the thermocouple, providing a stable measuring point. This provided a mean timeline of 45 seconds cooling (green highlighted squares of (44+48+42+44)/4=44.5 seconds).

4.5.5 Flow-Rates of Simulated Vitality Pairs 1–8

The flow-rates of each simulation for all eight Pairs of teeth are presented in Table 4-23, with repeated sequences for Pair 7.

Table 4-23 Simulated Vitality Flow-Rates - Pairs 1-8, Repeated in Pair 7. The highest value of each desired flow-rate is shaded red and the lowest blue. Mean and standard deviation calculated for all 8 teeth. The greatest range in flow-rate is seen at 0.5ml/min (0.19ml/min) and the least range is seen at 0.03ml/min (0.03ml/min).

Flow-Rate (ml/min)	Teeth Pair	RTS	LTS	PDL	PDL LTS TOOTH	PDL LTS PDL	PDL RTS TOOTH	PDL RTS PDL	PDL LTSP TOOTH	PDL LTSP PDL	PDL RTSP TOOTH	PDL RTSP PDL
0.5	1	0.45	0.45	0.44	0.45	0.45	0.45	0.44	0.45	0.45	0.45	0.44
	2	0.42	0.46	0.50	0.44	0.44	0.47	0.45	0.46	0.45	0.47	0.46
	3	0.46	0.46	0.48	0.44	0.48	0.47	0.47	0.45	0.45	0.48	0.46
	4	0.46	0.46	0.46	0.46	0.46	0.47	0.46	0.46	0.41	0.46	0.46
	5	0.47	0.45	0.45	0.45	0.37	0.45	0.36	0.45	0.38	0.46	0.37
	6	0.47	0.49	0.42	0.47	0.46	0.43	0.42	0.47	0.46	0.46	0.41
	Total Mean 7	0.47	0.47	0.47	0.47	0.46	0.47	0.46	0.46	0.46	0.47	0.46
	8	0.50	0.40	0.46	0.41	0.55	0.46	0.43	0.42	0.47	0.47	0.44
	Mean	0.46	0.46	0.46	0.45	0.46	0.46	0.44	0.45	0.44	0.46	0.44
	Stand. Dev.	0.02	0.03	0.02	0.02	0.05	0.01	0.03	0.02	0.03	0.01	0.03
Repeats	7	.	.	.	.	.	.	.	.	.	.	.
	1	.	.	0.46	0.47	0.46	0.47	0.46	0.46	0.46	0.46	0.45
	2	.	.	0.46	0.47	0.46	0.47	0.46	0.47	0.46	0.47	0.46
	3	.	.	0.46	0.47	0.46	0.47	0.46	0.47	0.46	0.47	0.46
	Mean	.	.	0.46	0.47	0.46	0.47	0.46	0.47	0.46	0.47	0.46
	1	.	.	0.47	0.47	0.45	0.46	0.45	0.46	0.45	0.47	0.46
	2	.	.	0.47	0.47	0.45	0.46	0.45	0.46	0.45	0.46	0.45
	3	.	.	0.47	0.47	0.45	0.46	0.45	0.46	0.45	0.46	0.45
	Mean	.	.	0.47	0.47	0.45	0.46	0.45	0.46	0.45	0.46	0.45
	Total Mean 7	.	.	0.47	0.47	0.46	0.47	0.46	0.46	0.46	0.47	0.46
0.15	1	.	.	0.14	0.14	0.14	0.15	0.15	0.15	0.15	0.15	0.15
	2	.	.	0.15	0.15	0.15	0.17	0.16	0.15	0.15	0.17	0.16
	3	.	.	0.18	0.18	0.18	0.18	0.18	0.18	0.18	0.18	0.18
	4	.	.	0.14	0.17	0.17	0.17	0.16	0.18	0.17	0.17	0.17
	5	.	.	0.15	0.14	0.11	0.16	0.12	0.15	0.11	0.16	0.13
	6	.	.	0.15	0.13	0.14	0.14	0.14	0.14	0.14	0.15	0.14
	7	.	.	0.14	0.14	0.14	0.14	0.14	0.14	0.14	0.14	0.14
	8	.	.	0.18	0.13	0.14	0.14	0.13	0.14	0.16	0.15	0.15
	Mean	.	.	0.15	0.15	0.15	0.16	0.15	0.15	0.15	0.16	0.15
	Stand. Dev.	.	.	0.02	0.02	0.02	0.02	0.02	0.02	0.02	0.01	0.02
0.08	1	.	.	0.08	0.08	0.08	0.09	0.09	0.09	0.08	0.09	0.09
	2	.	.	0.08	0.08	0.09	0.10	0.09	0.09	0.09	0.10	0.09
	3	.	.	0.08	0.08	0.08	0.08	0.07	0.08	0.08	0.08	0.07
	4	.	.	0.08	0.08	0.08	0.08	0.08	0.08	0.08	0.08	0.08
	5	.	.	0.09	0.08	0.06	0.09	0.08	0.08	0.06	0.09	0.08
	6	.	.	0.08	0.07	0.08	0.09	0.09	0.07	0.08	0.09	0.09
	7	.	.	0.07	0.08	0.07	0.09	0.07	0.09	0.07	0.08	0.07
	8	.	.	0.11	0.09	0.09	0.10	0.09	0.10	0.09	0.10	0.09
	Mean	.	.	0.08	0.08	0.08	0.09	0.08	0.09	0.08	0.09	0.08
	Stand. Dev.	.	.	0.01	0.01	0.01	0.01	0.01	0.01	0.01	0.01	0.01
0.03	1	.	.	-	0.02	0.02	0.03	0.03	0.03	0.03	0.03	0.03
	2	.	.	0.03	0.04	0.04	0.05	0.04	0.04	0.04	0.05	0.04
	3	.	.	0.03	0.03	0.03	0.03	0.03	0.03	0.03	0.03	0.03
	4	.	.	0.03	0.03	0.03	0.03	0.03	0.03	0.03	0.03	0.03
	5	.	.	0.03	0.04	0.03	0.03	0.02	0.04	0.03	0.03	0.02
	6	.	.	0.03	0.02	0.03	0.03	0.03	0.03	0.03	0.03	0.03
	7	.	.	0.02	0.02	0.02	0.02	0.02	0.02	0.02	0.02	0.02
	8	.	.	0.03	0.02	0.02	0.02	0.02	0.02	0.02	0.02	0.02
	Mean	.	.	0.03	0.03	0.03	0.03	0.03	0.03	0.03	0.03	0.03
	Stand. Dev.	.	.	0.00	0.01	0.01	0.01	0.01	0.01	0.01	0.01	0.01

SIMULATED VITALITY
RTS = Right-Tooth on Screen; LTS = Left-Tooth on Screen; PDL = Periodontal Ligament;
PDL LTS = Periodontal Ligament and Left-Tooth on Screen;
PDL RTS = Periodontal Ligament and Right-Tooth on Screen;
PDL LTSP = Periodontal Ligament and Left-Tooth on Screen Pulsed;
PDL RTSP = Periodontal Ligament and Right-Tooth on Screen Pulsed.

Highest Value of the Desired Flow-Rate		Lowest Value of the Desired Flow-Rate	
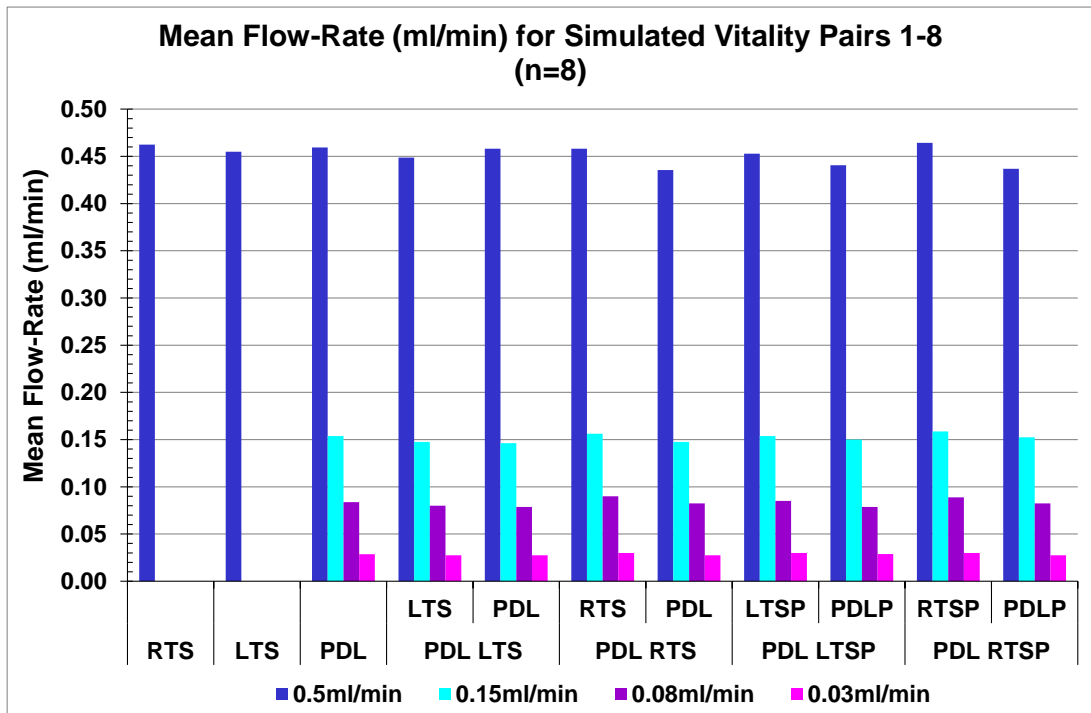
Figure 4-56 Graph of mean flow-rate (ml/min) – simulated vitality;
Right Tooth on Screen (RTS), Left Tooth on Screen (LTS),
Periodontal Ligament (PDL), Periodontal Ligament and
Left Tooth on Screen (PDL LTS), Periodontal Ligament and
Right Tooth on Screen (PDL RTS), Periodontal Ligament
with simulated pulse (PDLP) and Left Tooth on Screen with
simulated pulse (LTSP) combined gives PDL LTSP, and
Periodontal Ligament with simulated pulse and Right
Tooth on Screen with simulated pulse (RTSP) combined
gives PDL RTSP at 0.5ml/min, 0.15ml/min, 0.08ml/min,
0.03ml/min in Pairs 1–8 (n=8).
0.5ml/min has the greatest mean range of 0.02ml/min.
0.03ml/min has no range, achieving 0.03ml/min in all
sequences.

The mean flow-rate for 0.5ml/min ranged from 0.44–0.46ml/min, with two outliers within the group - the lowest flow-rate being 0.36ml/min (PDL of PDL RTS P5) and the highest 0.55ml/min (PDL of PDL LTS P8).

The mean flow-rate for 0.15ml/min ranged from 0.15–0.16ml/min, with P3 being consistently higher at 0.18ml/min, with two other values of 0.18ml/min from P4 (LTS from PDL LTSP) and P8 (PDL only). The lowest flow-rate of 0.11ml/min was found in P5 for the periodontal ligament in PDL LTS and PDL LTSP.

The mean flow-rate for 0.08ml/min ranged from 0.08-0.09ml/min. The highest flow-rate of 0.11ml/min was in P8 for the periodontal ligament simulation (PDL) and the lowest rate was in P5 for the periodontal ligament simulation of PDL LTS and PDL LTSP.

The simulation for 0.03ml/min achieved the desired mean flow-rate across all variations. A high of 0.05ml/min was seen in P2 for the RTS in both the non-pulsed and pulsed variable of PDL RTS. A low of 0.02ml/min was found across the whole range of P7, all variations except the PDL for P8, P1 for both the LTS and the periodontal ligament for PDL LTS, the PDL in P5 for both the pulsed and non-pulsed variation of PDL RTS, and for P6 only the LTS for the variation of PDL LTS.

The three repeat-sequences for P7 0.5ml/min, which were undertaken twice, show a range of 0.01ml/min and 0.02ml/min respectively, and an overall experimental error of 6-8% from 0.5ml/min.

4.5.6 Thermal Environment During Data-Collection

The stability of the Cube was controlled and provided an experimental error of 0.33-1% from the required 30°C.

Table 4-24 Temperature-range (^{o}C) of the Cube during in-vitro data-collection from Pairs 1-8 with simulated vitality of the periodontal ligament, periodontal ligament and a tooth at four flow-rates (0.5ml/min, 0.15ml/min, 0.08ml/min, 0.03ml/min). The warmest temperature of the Cube was 30.1^{o}C (pink cells) and the coolest temperature was 29.7^{o}C (blue cell).

Teeth Pair	Flow-Rate (F-R) (ml/min)	Low	High	F-R	Low	High	F-R	Low	High	F-R	Low	High
Temperature-Range of Thermal Environment (Cube) During Data-Collection Sequences P1-P8 (Degrees Celsius)
1	0.5	29.80	30.10	0.15	29.90	30.00	0.08	29.80	30.00	0.03	29.90	30.00
2		29.90	30.00		29.80	30.00		29.80	30.10		29.80	30.00
3		29.80	30.00		29.80	30.00		29.80	30.00		29.80	30.00
4		29.80	30.00		29.80	30.00		29.80	30.10		29.80	30.00
5		29.80	30.00		29.80	30.10		29.80	30.00		29.80	30.10
6		29.80	30.00		29.80	30.00		29.80	30.00		29.80	30.10
7		29.70	30.10		29.80	30.10		29.80	30.10		29.80	30.00
8		29.90	30.00		29.80	30.00		29.80	30.00		29.80	30.00
		29.7	30.1		29.8	30.1		29.8	30.1		29.8	30.1
RANGE		\multicolumn{2}{c}{0.40}		\multicolumn{2}{c}{0.30}		\multicolumn{2}{c}{0.30}		\multicolumn{2}{c}{0.30}
		\multicolumn{2}{c}{Coolest}					\multicolumn{2}{c}{Warmest}			
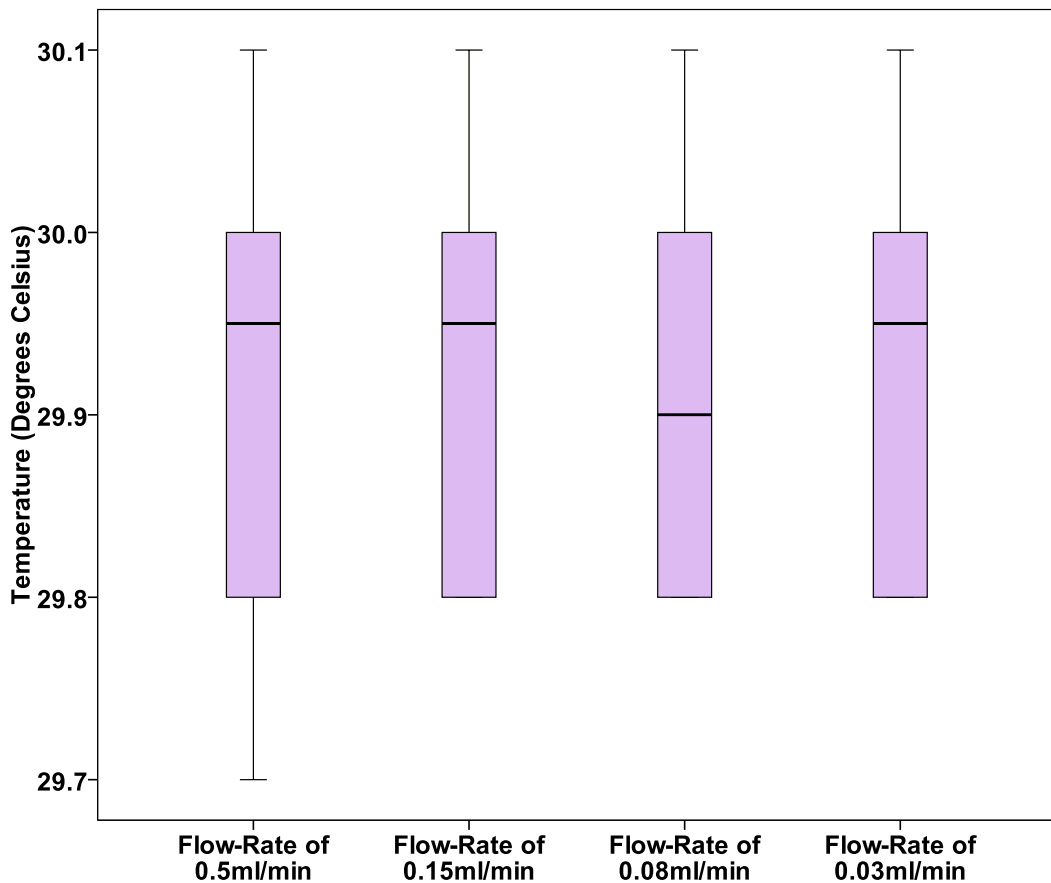
Figure 4-57 Boxplot of temperature-range of the Cube (Degrees Celsius) during data-collection of simulated vitality at four flow-rates (0.5ml/min, 0.15ml/min, 0.08ml/min, 0.03ml/min) in Pairs 1-8. Median value of each flow-rate was 29.95°C, 29.95°C, 29.9°C and 29.95°C, respectively.

4.5.7 Temperature of Thermoelectric Cooling-Unit

Table 4-25 Temperature-range (°C) of cooling-unit during in-vitro data-collection from Pairs 1-8 with simulated vitality of the periodontal ligament, periodontal ligament and a tooth at four flow-rates (0.5ml/min, 0.15ml/min, 0.08ml/min, 0.03ml/min). Warmest temperature was -7.14°C (pink cells) and coolest temperature was -8.3°C (blue cell), with a maximum range of 1.16°C across all four flow-rates.

Cooling-Unit Temperatures During Data-Collection-Sequences P1-P8 (Degrees Celsius)											
Teeth Pair	Flow-rate F-R (ml/min)	Low	High	F-R	Low	High	F-R	Low	High	F-R	Low	High
1	**0.5**	-8.11	-8.00	**0.15**	-8.05	-8.00	**0.08**	-8.03	-8.00	**0.03**	-8.11	-8.00
2		-8.30	-8.00		-8.11	-7.92		-8.07	-8.00		-8.20	-8.04
3		-8.13	-8.00		-8.08	-8.00		-8.22	-8.02		-8.04	-8.02
4		-8.00	-8.00		-8.13	-8.03		-8.16	-8.00		-8.13	-8.00
5		-8.00	-7.92		-8.07	-8.00		-8.07	-7.14		-8.03	-7.70
6		-8.09	-7.90		-8.08	-8.00		-8.04	-8.00		-8.02	-8.00
7		-8.08	-8.00		-8.11	-8.00		-8.11	-8.00		-8.03	-8.00
8		-8.01	-7.90		-8.16	-8.00		-8.06	-7.97		-8.04	-7.90
		-8.30	-7.9		-8.16	-7.92		-8.22	-7.14		-8.20	-7.70
RANGE		0.40			0.24			1.08			0.5	
		Coolest						Warmest				
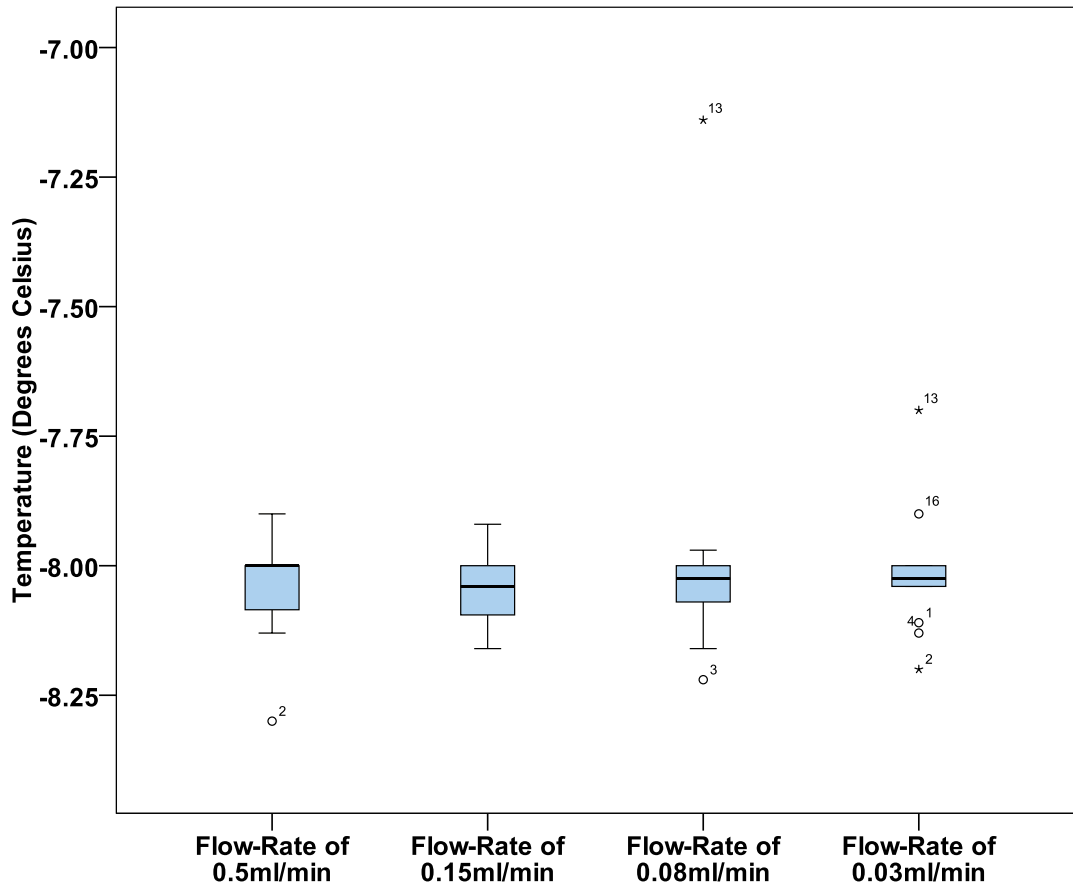
Figure 4-58 Boxplot of temperature-range of cooling-unit (Degrees Celsius) during data-collection of simulated vitality at four flow-rates (0.5ml/min, 0.15ml/min, 0.08ml/min, 0.03ml/min) in Pairs 1-8. Median value of each was -8°C, -8.04^{o}C, -8.03^{o}C and -8.03^{o}C, respectively.

4.5.8 Tooth-Surface-Temperatures

The temperatures of all eight Pairs of teeth and the mean surface-temperatures of the teeth, with all variables of simulated vitality, are shown below prior to cooling and after cooling, enabling the difference to be assessed. Repeat sequences were made for Pair 7 at flow-rate 0.5ml/min.

4.5.8.1 Tooth-Surface-Temperatures Prior to Cooling

Table 4-26 Tooth-surface-temperatures prior to cooling P1-P8 for simulated vitality of the periodontal ligament (PDL), left-tooth on screen (LTS), right-tooth on screen (RTS) and no simulated vitality (Nil). The coolest pre-cooling temperature was for the PDL at 30.3°C at both 0.5ml/min and 0.15ml/min (blue cells) and the warmest pre-cooling temperature was 32.1°C at 0.5ml/min (pink cells) for both the LTS and RTS.

Tooth-Surface-Temperatures Prior to Cooling (Degrees Celsius)									
Flow-Rate	Pair	PDL		LTS		RTS		NIL	
		LTS	RTS	LTS	RTS	LTS	RTS	LTS	RTS
0.5ml/min	1	31.3	31.5	31.2	31.4	31.4	31.9	31.1	31.4
	2	31.6	31.4	31.6	31.4	31.2	31.3	31.4	31.2
	3	30.3	30.7	30.4	30.5	30.8	31.1	31.3	31.7
	4	31.7	31.7	31.5	31.5	31.8	31.9	31.6	31.6
	5	31.4	31.5	31.1	31.2	31.3	31.7	31.1	31.2
	6	31.4	31.5	31.8	31.7	31.7	31.8	31.3	31.3
	7	31.5	31.6	31.6	31.4	32.1	32.1	31.5	31.6
	8	31.5	31.3	32.1	31.8	31.6	31.4	31.1	30.8
0.15ml/min	1	31.4	31.6	.	.	.	.	.	.
	2	31.6	31.4	.	.	.	.	.	.
	3	30.3	30.4	.	.	.	.	.	.
	4	31.3	31.4	.	.	.	.	.	.
	5	31.1	31.3	.	.	.	.	.	.
	6	31.4	31.5	.	.	.	.	.	.
	7	32.0	32.0	.	.	.	.	.	.
	8	31.5	31.2	.	.	.	.	.	.
0.08ml/min	1	31.5	31.7	.	.	.	.	.	.
	2	31.6	31.4	.	.	.	.	.	.
	3	31.3	31.4	.	.	.	.	.	.
	4	31.2	31.3	.	.	.	.	.	.
	5	30.9	31.1	.	.	.	.	.	.
	6	31.3	31.4	.	.	.	.	.	.
	7	31.5	31.5	.	.	.	.	.	.
	8	31.3	31.0	.	.	.	.	.	.
0.03ml/min	1	31.4	31.6	.	.	.	.	.	.
	2	31.4	31.2	.	.	.	.	.	.
	3	31.2	31.4	.	.	.	.	.	.
	4	31.4	31.4	.	.	.	.	.	.
	5	30.7	30.9	.	.	.	.	.	.
	6	31.4	31.5	.	.	.	.	.	.
	7	31.6	31.6	.	.	.	.	.	.
	8	31.1	30.8	.	.	.	.	.	.
SIMULATED VITALITY									
RTS = Right-Tooth on Screen; LTS = Left-Tooth on Screen; PDL = Periodontal Ligament; NIL = No Simulated Vitality									
Coolest					Warmest				

Table 4-27 Tooth-surface-temperatures prior to cooling P1-P8 for simulated vitality of the periodontal ligament and left-tooth on screen (PDL LTS), periodontal ligament and right-tooth on screen (PDL RTS), with and without simulation of a pulse. The coolest pre-cooling temperature was 29.8°C at 0.08ml/min (blue cell) and the warmest pre-cooling temperature was 32.3°C at 0.15ml/min (pink cell).

Tooth-Surface-Temperatures Prior to Cooling (Degrees Celsius)								
Flow-Rate	Pair	PDL LTS		PDL RTS		PDL LTSP		PDL RTSP	
		LTS	RTS	LTS	RTS	LTS	RTS	LTS	RTS
0.5ml/min	1	31.9	31.7	31.4	31.7	31.3	31.4	31.1	31.3
	2	31.6	31.4	31.6	31.5	31.5	31.2	31.4	31.3
	3	30.8	31.1	30.9	31.2	31.2	31.5	30.8	31.2
	4	31.4	31.4	31.5	31.5	31.7	31.7	31.5	31.5
	5	31.2	31.4	31.0	31.3	31.0	31.1	31.2	31.5
	6	31.9	31.8	31.3	31.6	31.6	31.6	31.7	31.7
	7	31.6	31.6	31.6	31.7	31.6	31.6	31.4	31.7
	8	31.6	31.5	31.5	31.3	31.6	31.4	31.3	31.1
0.15ml/min	1	31.6	31.8	31.6	31.8	31.6	31.7	31.4	31.7
	2	30.8	30.6	31.4	31.3	31.2	31.0	31.7	31.6
	3	30.4	30.5	30.6	30.7	30.5	30.5	30.2	30.3
	4	31.5	31.4	30.7	30.7	31.2	31.1	31.2	31.2
	5	31.3	31.3	31.1	31.3	31.4	31.5	31.1	31.4
	6	31.8	31.8	31.2	31.4	31.5	31.5	31.5	31.7
	7	32.0	32.0	32.2	32.3	31.9	31.9	31.9	32.0
	8	31.7	31.4	31.5	31.3	31.9	31.7	31.4	31.2
0.08ml/min	1	31.1	31.4	30.8	31.1	31.4	31.6	31.2	31.5
	2	31.3	31.2	31.6	31.7	30.9	30.8	31.6	31.5
	3	30.5	30.5	29.8	29.9	30.7	30.8	29.9	30.0
	4	31.8	31.9	31.6	31.6	31.1	31.2	31.4	31.4
	5	31.4	31.4	30.6	30.9	31.4	31.5	30.5	30.7
	6	31.7	31.7	31.5	31.7	31.4	31.4	31.6	31.8
	7	31.5	31.4	31.7	31.7	31.5	31.4	31.5	31.6
	8	31.9	31.7	31.6	31.3	31.8	31.5	31.5	31.2
0.03ml/min	1	31.3	31.5	31.1	31.3	31.2	31.4	30.9	31.1
	2	30.9	30.8	31.4	31.3	30.8	30.7	31.3	31.2
	3	31.2	31.4	30.1	30.2	31.4	31.6	29.9	30.0
	4	31.5	31.5	31.6	31.6	31.2	31.3	31.2	31.3
	5	31.7	31.8	30.4	30.6	31.2	31.3	30.6	30.8
	6	31.4	31.4	31.3	31.4	31.3	31.3	31.4	31.4
	7	32.0	31.9	31.9	31.8	31.4	31.3	31.6	31.6
	8	31.8	31.6	31.6	31.2	31.6	31.4	31.4	31.0
SIMULATED VITALITY								
RTS = Right-Tooth on Screen; LTS = Left-Tooth on Screen; PDL LTS = Periodontal Ligament and Left-Tooth on Screen; PDL RTS = Periodontal Ligament and Right-Tooth on Screen; PDL LTSP = Periodontal Ligament and Left-Tooth on Screen Pulsed; PDL RTSP = Periodontal Ligament and Right-Tooth on Screen Pulsed								
Coolest				Warmest				

4.5.8.2 Repeat Pre-Cooling Tooth-Surface-Temperatures

Table 4-28 Repeat pre-cooling surface-temperature for Pair 7 with simulated vitality of periodontal ligament and one vital tooth (either right or left) over three consecutive sequences, repeated, at a flow-rate of 0.5ml/min. Coolest temperature 30.8°C (blue cell) and warmest temperature 32°C (pink cells). The mean pre-cooling temperature ranges from 31.3°C [Standard Deviation (SD) 0.1°C] (blue-bordered cell) the non-vital tooth of the pair, to 31.8°C [SD 0.2°C] (red-bordered cells) the vital tooth of the pair.

P7 Repeats 0.5ml/min	Tooth-Surface-Temperatures Pre-Cooling (Degrees Celsius)							
	PDL LTS		PDL RTS		PDL LTSP		PDL RTSP	
	LTS	RTS	LTS	RTS	LTS	RTS	LTS	RTS
1	32.0	31.8	31.9	31.9	31.6	31.6	31.3	31.6
2	31.7	31.6	31.6	31.7	31.6	31.5	31.3	31.5
3	31.7	31.6	31.5	31.5	31.7	31.5	31.2	31.7
Mean	31.8	31.7	31.7	31.7	31.6	31.5	31.3	31.6
SD	0.2	0.1	0.2	0.2	0.1	0.1	0.1	0.1
1	30.9	30.8	31.9	32.0	31.7	31.6	31.6	31.7
2	31.8	31.9	31.5	31.7	31.7	31.7	31.7	32.0
3	31.6	31.6	31.4	31.5	31.4	31.4	31.4	31.6
Mean	31.4	31.4	31.6	31.7	31.6	31.6	31.6	31.8
SD	0.5	0.6	0.3	0.3	0.2	0.2	0.2	0.2
Total Mean	31.6	31.6	31.6	31.7	31.6	31.6	31.4	31.7
SD of Means	0.21	0.32	0.04	0.04	0.08	0.07	0.07	0.08

Table 4-29 Repeat pre-cooling surface-temperatures for Pair 7 with periodontal simulation only over three consecutive sequences at a flow-rate of 0.5ml/min. Coolest temperature 31.3°C (blue cell) and warmest temperature 31.9°C (pink cells). The mean pre-cooling temperature ranges from 31.4°C [Standard Deviation (SD) 0.1°C] (blue-bordered cell) the right-tooth of the pair, to 31.7°C [SD 0.2°C] (red-bordered cell) also the right-tooth of the pair.

P7 Repeats 0.5ml/min	Tooth-Surface-Temperatures Pre-Cooling (Degrees Celsius)	
	PDL	
	LTS	RTS
1	31.4	31.3
2	31.6	31.6
3	31.4	31.4
Mean	31.5	31.4
SD	0.1	0.2
1	31.9	31.9
2	31.4	31.5
3	31.5	31.6
Mean	31.6	31.7
SD	0.3	0.2
Total Mean	31.5	31.6
SD of Means	0.09	0.16

4.5.8.3 Mean Values of Tooth-Surface-Temperature Pre-Cooling for Each Variable of Eight Pairs

No Simulated Vitality (Nil)

Table 4-30 Mean tooth-surface-temperature of left and right-tooth (n=8) of Pair 1-8 with no simulation of vitality (nil) pre-cooling, the mean difference being 0.05^{o}C, with a minimum value of 30.8^{o}C and a maximum value of 31.7^{o}C.

Mean Tooth-Surface-Temperature Pre-Cooling (Degrees Celsius) n=8									
Flow-Rate (ml/min)	Nil Left					Nil Right			
	Mean	SD	Min	Max	Range	Mean	SD	Min	Max	Range
0	31.30	0.19	31.10	31.60	0.50	31.35	0.29	30.80	31.70	0.90
SD = Standard Deviation; Min = Minimum; Max = Maximum									

The mean difference between left and right-tooth-surface-temperature pre-cooling with no simulated vitality was 0.05^{o}C in favour of the right-tooth, which also had the coolest (30.8^{o}C) and warmest (31.7^{o}C) values, giving the greatest range of pre-cooling temperatures of 0.9^{o}C.

Simulated Vitality in a Tooth Only at 0.5ml/min (LTS or RTS)

Table 4-31 Mean tooth-surface-temperature of both the left and right-tooth (n=16) with or without simulation of vitality at 0.5ml/min, in Pairs 1-8 (LTS or RTS) pre-cooling, the mean difference being 0.1^{o}C, with a minimum value of 30.4^{o}C (vital simulation) and a maximum value of 32.1^{o}C (both vital and non-vital simulation).

Mean Tooth-Surface-Temperature Pre-Cooling (Degrees Celsius) n=16									
Flow-Rate (ml/min)	Vital Tooth Only					Non-Vital Tooth Only			
	Mean	SD	Min	Max	Range	Mean	SD	Min	Max	Range
0.5	31.53	0.44	30.40	32.10	1.70	31.43	0.39	30.50	32.10	1.60
SD = Standard Deviation; Min = Minimum; Max = Maximum									

The mean difference between vital and non-vital tooth-surface-temperature pre-cooling with simulated vitality in one of the teeth was 0.1^{o}C in favour of the vital tooth, which also recorded the coolest value (30.4^{o}C). The warmest value (32.1^{o}C) was recorded from both vital and non-vital simulation and the greatest range of pre-cooling temperatures was 1.7^{o}C.

Simulated Vitality in Periodontal Ligament for Four Flow-Rates (PDL)

Figure 4-59 Graph of mean tooth-surface-temperature of the left and right-tooth (n=8) with simulated periodontal vitality (PDL) pre-cooling for four flow-rates (0.5ml/min, 0.15ml/min, 0.08ml/min, 0.03ml/min), showing an overall reduction in tooth-surface-temperature for both the right and left-tooth from 0.5ml/min to 0.03ml/min. The same tooth-surface-temperature was found for 0.15ml/min and 0.08ml/min according to side and a warmer temperature was found on the right-tooth.

Table 4-32 Mean tooth-surface-temperature with simulated periodontal vitality (n=8) at four flow-rates (0.5ml/min, 0.15ml/min, 0.08ml/min, 0.03ml/min) in Pairs 1-8 (PDL) pre-cooling. The mean difference between the left and right-tooth was 0.06°C at 0.5ml/min, 0.02°C at 0.15ml/min, 0.08ml/min and 0.03ml/min. Coolest mean temperature was 31.28°C [SD 0.28°C] (blue cell) and warmest mean temperature was 31.4°C [SD 0.31°C] (pink cell), a difference of 0.12°C.

Mean Tooth-Surface-Temperature Pre-Cooling (Degrees Celsius) n=8									
Flow-Rate (ml/min)	Periodontal Ligament Flow – Left-Tooth					Periodontal Ligament Flow – Right-Tooth			
	Mean	SD	Min	Max	Range	Mean	SD	Min	Max	Range
0.5	31.34	0.44	30.30	31.70	1.40	31.40	0.31	30.70	31.70	1.00
0.15	31.33	0.49	30.30	32.00	1.70	31.35	0.45	30.40	32.00	1.60
0.08	31.33	0.22	30.90	31.60	0.70	31.35	0.22	31.00	31.70	0.70
0.03	31.28	0.28	30.70	31.60	0.90	31.30	0.31	30.80	31.60	0.80
SD = Standard Deviation; Min = Minimum; Max = Maximum									

The mean difference between left and right-tooth-surface-temperature pre-cooling with simulated vitality in the periodontal ligament had a maximum of 0.12^{o}C across all four flow-rates, the warmest being at the highest flow-rate from the right-tooth (pink cell) and the coolest at the lowest flow-rate from the left-tooth (blue cell).

Simulated Vitality in Periodontal Ligament and One Tooth, With and Without a Pulse for Four Flow-Rates

Graph of Mean Tooth-Surface-Temperature Pre-Cooling (Degrees Celsius) for Simulated Tooth and Periodontal Vitality, With and Without Pulsatile-Effect at Four Flow-Rates (n=16).
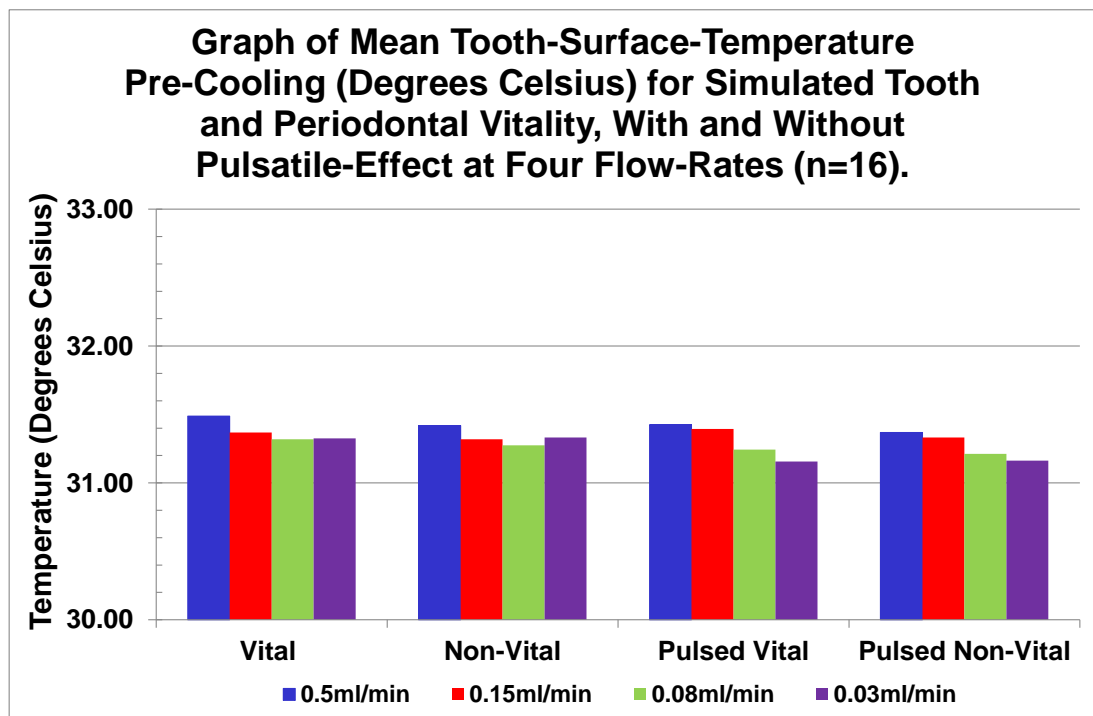
Figure 4-60 Graph of mean tooth-surface-temperature of the left and right-tooth (n=16) with and without pulsed simulated vitality of a tooth and periodontal ligament (PDL LTS or PDL RTS, PDL LTSP or PDL RTSP) pre-cooling for four flow-rates (0.5ml/min, 0.15ml/min, 0.08ml/min, 0.03ml/min). An overall reduction in tooth-surface-temperature from 0.5ml/min to 0.03ml/min was seen in the pulsed simulation. A similar trend was found without a pulsed simulation, apart from the lowest flow-rate of 0.03ml/min which had a slight increase in temperature compared to the 0.08ml/min. The highest pre-cooling tooth-surface-temperature was found in the vital non-pulsed simulation at the highest flow-rate and the coolest tooth-surface-temperature was found in the lowest flow-rate of the pulsed simulation of both vital and non-vital teeth.

Table 4-33 Mean tooth-surface-temperature with simulated periodontal vitality and one tooth (n=16) at four flow-rates (0.5ml/min, 0.15ml/min, 0.08ml/min, 0.03ml/min) in Pairs 1-8 (PDL LTS or PDL RTS) pre-cooling.
The mean difference between the left and right-tooth was 0.07°C at 0.5ml/min, 0.05°C at 0.15ml/min, 0.04°C at 0.08ml/min and no difference at 0.03ml/min. The coolest mean temperature was 31.28°C [SD 0.57°C] (blue cell) and warmest mean temperature 31.49°C [SD 0.28°C] (pink cell), a difference of 0.16°C.

Mean Tooth-Surface-Temperature Pre-Cooling (Degrees Celsius) n=16									
Flow-Rate (ml/min)	Vital Tooth with Periodontal Vitality					Non-Vital Tooth with Periodontal Vitality			
	Mean	SD	Min	Max	Range	Mean	SD	Min	Max	Range
0.5	31.49	0.28	30.80	31.90	1.10	31.42	0.25	30.90	31.80	0.90
0.15	31.37	0.52	30.40	32.30	1.90	31.32	0.52	30.50	30.20	1.70
0.08	31.32	0.53	29.90	31.90	2.00	31.28	0.57	29.80	31.90	2.10
0.03	31.33	0.46	30.20	32.00	1.80	31.33	0.51	30.10	31.90	1.80
SD = Standard Deviation; Min = Minimum; Max = Maximum									

Table 4-34 Mean tooth-surface-temperature with pulsed simulated periodontal vitality and one tooth (n=16) at four flow-rates (0.5ml/min, 0.15ml/min, 0.08ml/min, 0.03ml/min) in Pairs 1-8 (PDL LTSP or PDL RTSP) pre-cooling.
The mean difference between the left and right-tooth was 0.06°C at 0.5ml/min and 0.15ml/min, 0.03°C at 0.08ml/min and no difference at 0.03ml/min. The coolest mean temperature was 31.16°C [SD 0.39°C Vital and 0.44°C Non-vital] (blue cells) and warmest mean temperature 31.43°C [SD 0.23°C] (pink cell), a difference of 0.27°C.

Mean Tooth-Surface-Temperature of Teeth Pre-Cooling (Degrees Celsius) n=16									
Flow-Rate (ml/min)	Pulsed Vital Tooth with Periodontal Vitality					Pulsed Non-Vital Tooth with Periodontal Vitality			
	Mean	SD	Min	Max	Range	Mean	SD	Min	Max	Range
0.5	31.43	0.23	31.00	31.70	0.70	31.37	0.24	30.80	31.70	0.90
0.15	31.39	0.47	30.30	32.00	1.70	31.33	0.47	30.20	31.90	1.70
0.08	31.24	0.47	30.00	31.80	1.80	31.21	0.48	29.90	31.60	1.70
0.03	31.16	0.39	30.00	31.60	1.60	31.16	0.44	29.90	31.60	1.70
SD = Standard Deviation; Min = Minimum; Max = Maximum									

The mean values of the surface-temperatures of the 16 teeth with four different flow-rates pre-cooling were all within half a degree Celsius, ranging from 31.16°C to 31.49°C (a difference of 0.33°C).

The flow-rate of 0.5ml/min provided the highest mean tooth-surface-temperature in all four simulations (PDL LTS, PDL RTS, PDL LTSP, PDL RTSP) at 31.49°C for the vital tooth. The pulsed-simulations followed a trend of higher tooth-surface-temperatures with higher flow-rates. The non-pulsed simulation varied at the lowest flow-rate (0.03ml/min at 31.33°C) with a higher tooth-surface-temperature than the 0.08ml/min simulation. The overall trend was that the higher the flow-rate the higher the tooth-surface-

temperature, and the vital teeth, whether pulsed or not, have fractionally higher temperatures than the non-vital teeth. The numerical value of such a difference is very small (vital and non-vital differ by 0.07^{o}C, 0.05^{o}C, 0.04^{o}C and 0.00^{o}C with decreasing flow-rate, and pulsed vital and non-vital differ by 0.06^{o}C, 0.06^{o}C, 0.03^{o}C and 0.00^{o}C with decreasing flow-rate) and were within thermal equilibrium limits. Additionally, the difference between vital pulsed and non-pulsed, and non-vital pulsed and non-pulsed shows a maximum difference of 0.17^{o}C for the lowest flow-rate, in favour of the non-pulsed model.

4.5.8.4 Lowest Tooth-Surface-Temperature Post-Cooling

Table 4-35 Lowest tooth-surface-temperature post-cooling Pair 1-8 for simulated vitality of the periodontal ligament (PDL), left-tooth on screen (LTS), right-tooth on screen (RTS), and no simulated vitality (Nil). The coolest post-cooling tooth-surface-temperature was 9.1^{o}C at Nil simulation (blue cell) and the warmest was 26.4^{o}C at 0.5ml/min in the right-tooth of LTS (pink cell).

Flow-Rate	Pair	PDL		LTS		RTS		NIL	
		LTS	RTS	LTS	RTS	LTS	RTS	LTS	RTS
0.5ml/min	1	17.5	16.9	16.1	14	15.9	14.7	20.9	19.7
	2	13.3	15.5	10	13.1	11.3	14.4	9.1	12.3
	3	14.6	21.4	13.8	19.9	12.5	19	15.6	22
	4	16.3	14.6	16.6	14.9	16.4	14.8	16.8	15.5
	5	21.4	25.4	23	26.4	17	22.5	21.3	25.5
	6	13.5	11.8	13.9	12.2	13.6	12.7	10.1	9.3
	7	18.3	18.3	17.3	16.9	19.0	19.1	20.4	21.7
	8	20.9	21.9	17.7	20.2	22.6	22.9	16.2	18.4
0.15ml/min	1	16.2	15	·	·	·	·	·	·
	2	11.2	13.8	·	·	·	·	·	·
	3	13.1	17.8	·	·	·	·	·	·
	4	18.4	15.7	·	·	·	·	·	·
	5	20	24.4	·	·	·	·	·	·
	6	11.3	9.6	·	·	·	·	·	·
	7	18.6	18.1	·	·	·	·	·	·
	8	19	20.5	·	·	·	·	·	·
0.08ml/min	1	15.6	14.3	·	·	·	·	·	·
	2	10.7	13.5	·	·	·	·	·	·
	3	15	20.2	·	·	·	·	·	·
	4	17	14.2	·	·	·	·	·	·
	5	19.7	23.8	·	·	·	·	·	·
	6	10.5	9.4	·	·	·	·	·	·
	7	18.1	18.7	·	·	·	·	·	·
	8	18.7	20.3	·	·	·	·	·	·
0.03ml/min	1	15.4	14.8	·	·	·	·	·	·
	2	10.5	13.6	·	·	·	·	·	·
	3	14.7	19.4	·	·	·	·	·	·
	4	17.6	14.8	·	·	·	·	·	·
	5	18.9	22.9	·	·	·	·	·	·
	6	12.1	10.4	·	·	·	·	·	·
	7	19.9	21.3	·	·	·	·	·	·
	8	16.4	18.6	·	·	·	·	·	·
SIMULATED VITALITY RTS = Right-Tooth on Screen; LTS = Left-Tooth on Screen; PDL = Periodontal Ligament; NIL = No Simulated Vitality									
Coolest					Warmest				

Lowest Tooth-Surface-Temperatures Post-Cooling (Degrees Celsius)

Table 4-36 Lowest tooth-surface-temperature post-cooling Pair 1-8 for simulated vitality, with and without simulation of a pulse of the periodontal ligament and left-tooth on screen (PDL LTS or PDL LTSP), periodontal ligament and right-tooth on screen (PDL RTS or PDL RTSP). The coolest post-cooling tooth-surface-temperature was 9.2°C at 0.15ml/min and 0.08ml/min (blue cells) both with simulated pulse, and the warmest was 27.2°C at 0.15ml/min (pink cell) without simulated pulse.

Lowest Tooth-Surface-Temperatures Post-Cooling (Degrees Celsius)								
Flow-Rate	Pair	PDL LTS		PDL RTS		PDL LTSP		PDL RTSP	
		LTS	RTS	LTS	RTS	LTS	RTS	LTS	RTS
0.5ml/min	1	16.8	15.3	15.4	14.2	16.4	15.8	15	14.1
	2	9.8	12.3	11.7	14.1	9.9	12.2	15.9	17.7
	3	14.8	22.6	13.5	20.2	14.2	21.2	14.4	21.4
	4	16.9	15.4	16.2	15	16.5	14.9	16.5	15.4
	5	21.7	25.1	17.4	22.8	16.6	21.2	19.5	24.3
	6	11.9	9.8	13.6	12.8	12.6	10.6	12	10.9
	7	20.3	20.1	19.3	19.7	20.2	20.5	19.7	20.6
	8	18.1	20.7	22.7	23.1	18	20.3	21.3	22.2
0.15ml/min	1	14.5	13.3	16.9	15.2	15.7	14.3	16.1	14.4
	2	10.9	13.3	11.3	13.8	9.2	11.7	10.5	13.1
	3	13.4	18.3	13.8	18.5	12.9	17.6	13.1	18
	4	15.9	14.5	15.7	14.2	15.4	14.1	15.3	13.6
	5	25.4	27.2	18	23.2	19.6	23.9	17.6	23
	6	11.3	9.8	11.2	10.5	11.8	10.2	11.8	11.1
	7	19.2	18.9	19.8	19.5	21.5	22.7	17.9	17
	8	18.7	21.1	21.2	21.9	19.8	22.8	18.9	20.4
0.08ml/min	1	16.2	15.3	15.3	13.9	15	13.7	20.2	19.1
	2	10.4	12.7	9.5	12.2	10.1	12.4	10.2	13
	3	14.3	19.2	13.8	16.9	15.5	20.2	14.8	20
	4	17.1	14.3	17.6	14.5	16.8	13.8	19	16
	5	21.3	24.9	17.2	22.3	18.1	22.3	24.4	26.9
	6	11.1	9.8	10.9	9.8	12.6	11.5	9.8	9.2
	7	20.9	22.5	19.7	21	21.1	22	19.7	20
	8	19.4	19.4	24.9	24.6	18.2	20	18.2	19.8
0.03ml/min	1	14.5	13.5	14.8	13.5	16.3	15.1	16.2	14.9
	2	9.8	12.5	13.4	15.9	9.5	12.2	9.5	12.3
	3	14.5	19.5	14.3	19.3	15.1	20	12.7	17.6
	4	17	13.8	16.7	13.7	17.4	14.3	16.6	13.7
	5	19.9	23.5	16.5	21.8	17.9	22.2	19.9	24.1
	6	11.9	10.8	10.9	9.8	12.1	10.8	10.9	9.7
	7	18.2	16.7	23.9	25	18.1	17.3	19.5	19.9
	8	18.7	18.6	19	19.5	18.7	18.8	20.1	20.7
SIMULATED VITALITY								
RTS = Right-Tooth on Screen; LTS = Left-Tooth on Screen;								
PDL LTS = Periodontal Ligament and Left-Tooth on Screen;								
PDL RTS = Periodontal Ligament and Right-Tooth on Screen;								
PDL LTSP = Periodontal Ligament and Left-Tooth on Screen Pulsed;								
PDL RTSP = Periodontal Ligament and Right-Tooth on Screen Pulsed								
Coolest Value					Warmest Value			

4.5.8.5 Repeat Tooth-Surface-Temperature Post-Cooling

Table 4-37 Repeat lowest post-cooling tooth-surface-temperature for Pair 7 with simulated vitality of periodontal ligament and one vital tooth (either right or left) over three consecutive sequences repeated at a flow-rate of 0.5ml/min. Coolest tooth-surface-temperature 16.9°C (blue cell) and warmest tooth-surface-temperature 25.7°C (pink cell). The mean lowest post-cooling tooth-surface-temperature ranges from 18.2°C [Standard Deviation (SD) 1°C] (blue bordered-cells), to 22.4°C [SD 3.4°C] (red-bordered cell).

Lowest Tooth-Surface-Temperature Post-Cooling (Degrees Celsius)								
P7 Repeats	PDL LTS		PDL RTS		PDL LTSP		PDL RTSP	
0.5ml/min	LTS	RTS	LTS	RTS	LTS	RTS	LTS	RTS
1	17.3	16.9	21.3	22.7	18.5	18.3	19.9	22.0
2	18.0	17.9	18.7	18.8	20.7	21.8	19.5	21.5
3	19.3	19.8	18.4	19.4	20.6	21.8	19.0	19.7
Mean	18.2	18.2	19.5	20.3	19.9	20.6	19.5	21.1
SD	1.0	1.5	1.6	2.1	1.2	2.0	0.5	1.2
1	22.6	23.2	19.3	18.9	21.6	22.5	18.1	17.6
2	25.7	25.4	19.4	19.9	20.3	20.2	18.5	18.2
3	19.0	17.6	18.9	18.4	19.2	18.6	23.3	24.3
Mean	22.4	22.1	19.2	19.1	20.4	20.4	20.0	20.0
SD	3.4	4.0	0.3	0.8	1.2	2.0	2.9	3.7
Total Mean	20.3	20.1	19.3	19.7	20.2	20.5	19.7	20.6
SD of Means	3.0	2.7	0.2	0.9	0.3	0.1	0.4	0.7

Table 4-38 Repeat tooth-surface-temperature for Pair 7 with periodontal simulation over three consecutive sequences at a flow-rate of 0.5ml/min. Coolest post-cooling temperature 16.9°C (blue cell) and warmest temperature 19.3°C (pink cells). The mean post-cooling temperature ranges from 18.0°C [Standard Deviation (SD) 1.7°C] (blue-bordered cell) the right-tooth of the pair to 18.6°C [SD 0.7°C] (red-bordered cell) also the right-tooth of the pair.

Lowest Tooth-Surface-Temperature Post-Cooling (Degrees Celsius)		
P7 Repeats 0.5ml/min	PDL	
	LTS	RTS
1	17.7	17.1
2	19.3	20.0
3	17.3	16.9
Mean	18.1	18.0
SD	1.1	1.7
1	18.4	18.4
2	19.0	19.3
3	18.2	18.0
Mean	18.5	18.6
SD	0.4	0.7
Total Mean	18.3	18.3
SD of Total Means	0.45	0.76

4.5.8.6 Mean Values of Tooth-Surface-Temperature
Post-Cooling for Each Variable of Eight Pairs

No Simulated Vitality (Nil)

**Table 4-39 Mean tooth-surface-temperature of left and right
tooth (n=8) of Pair 1-8 with no simulation of vitality (nil)
post-cooling, the mean difference being 1.75^{o}C, with a
minimum value of 16.3^{o}C and a maximum value of 18.05^{o}C.**

Mean Lowest Tooth-Surface-Temperature Post-Cooling (Degrees Celsius) n=8									
Flow-Rate (ml/min)	Nil Left					Nil Right			
	Mean	SD	Min	Max	Range	Mean	SD	Min	Max	Range
0	16.30	4.69	9.10	21.30	12.20	18.05	5.39	9.30	25.50	16.20
SD = Standard Deviation; Min = Minimum; Max = Maximum									

The mean difference between left and right-tooth-surface-temperature post-cooling with no simulated vitality was 1.75^{o}C in favour of the right-tooth, which also had the warmest value (25.5^{o}C), whereas the left-tooth had the coolest value (9.1^{o}C), giving the greatest range of post-cooling temperature to be 16.4^{o}C.

Simulated Vitality in a Tooth Only at 0.5ml/min (LTS or RTS)

**Table 4-40 Mean tooth-surface-temperature of both the left and
right teeth (n=16) with or without simulation of vitality at
0.5ml/min, without periodontal simulation in Pairs 1-8 (LTS
or RTS) post-cooling, the mean difference being 0.16^{o}C,
with a minimum value of 10.0^{o}C (vital simulation) and a
maximum value of 26.4^{o}C (non-vital simulation).**

Mean Lowest Tooth-Surface-Temperature Post-Cooling (Degrees Celsius) n=16									
Flow-Rate (ml/min)	Vital Tooth Only					Non-Vital Tooth Only			
	Mean	SD	Min	Max	Range	Mean	SD	Min	Max	Range
0.5	16.78	3.78	10.00	23.00	13.00	16.62	4.14	11.30	26.40	15.10
SD = Standard Deviation; Min = Minimum; Max = Maximum									

The mean difference between vital and non-vital tooth-surface-temperature post-cooling with simulated vitality in one of the teeth was 0.16^{o}C in favour of the vital tooth, which also recorded the coolest value (10.0^{o}C). The warmest value (26.4^{o}C) was recorded from the non-vital simulation and the greatest range of post-cooling temperatures was 16.4^{o}C.

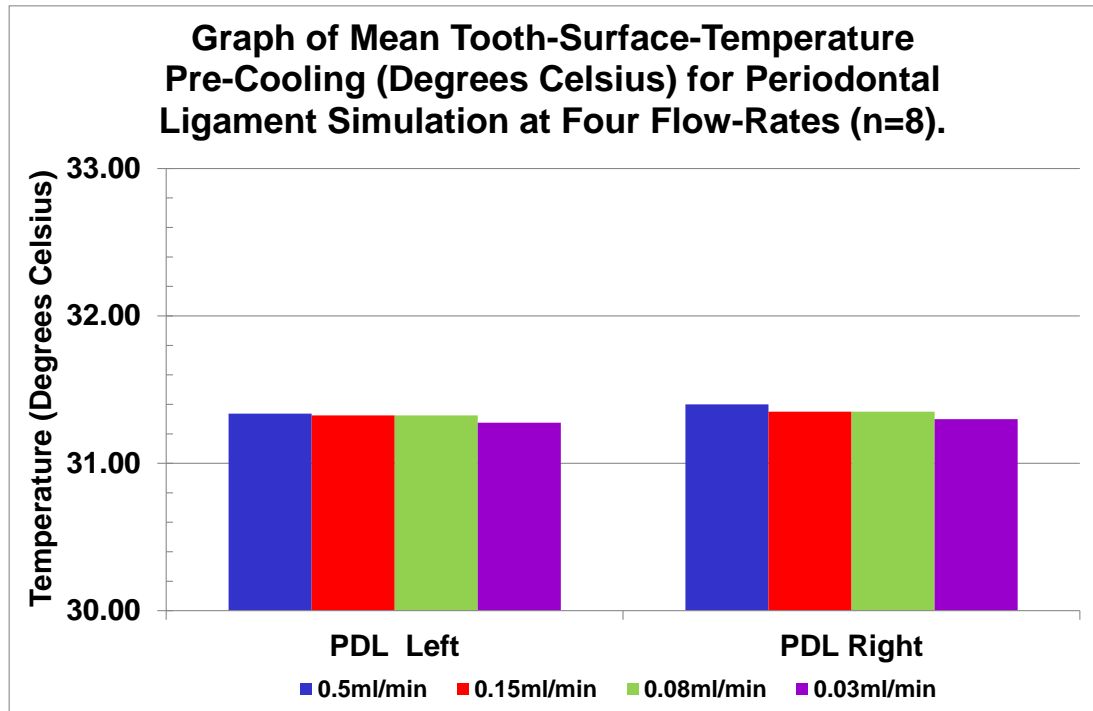**Simulated Vitality in Periodontal Ligament for Four Flow-Rates (PDL)**
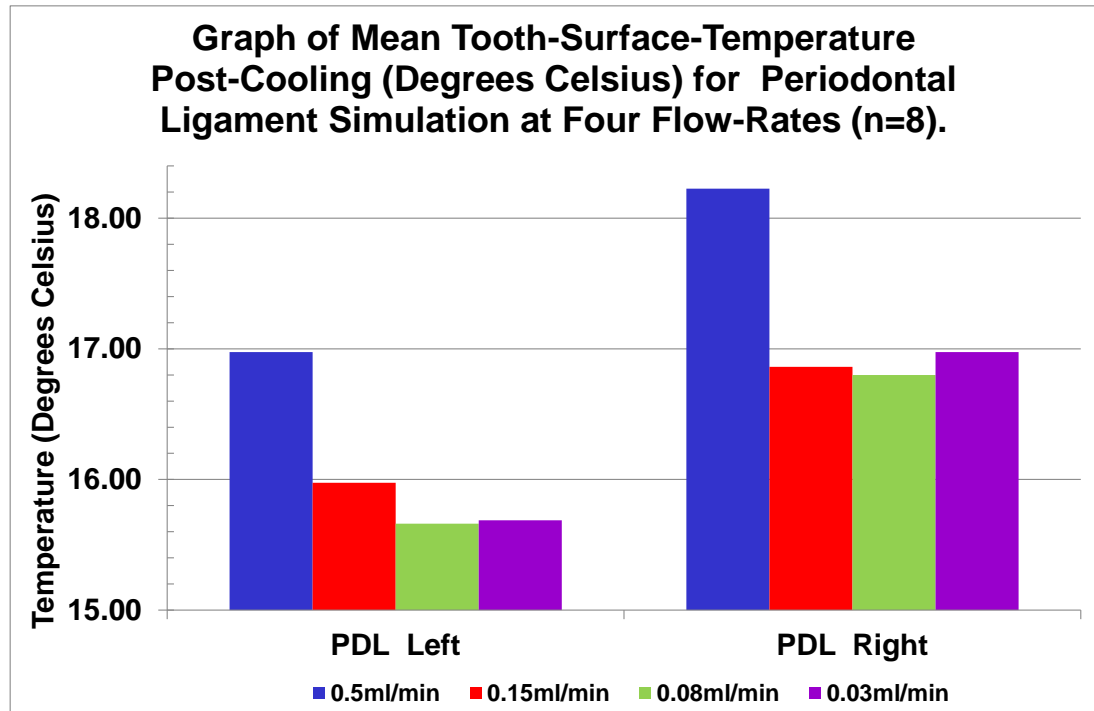
Figure 4-61 Graph of mean tooth-surface-temperature of the left and right-tooth (n=8) with simulated periodontal ligament vitality (PDL) post-cooling for four flow-rates (0.5ml/min, 0.15ml/min, 0.08ml/min, 0.03ml/min) showing an overall reduction in tooth-surface-temperature for both the left and right-tooth from 0.5ml/min to 0.08ml/min. 0.03ml/min is slightly warmer than 0.08ml/min in the left-tooth and is warmer than both 0.08ml/min and 0.15ml/min in the right-tooth. Less cooling and warmer temperatures were found at all flow-rates on the right-tooth.

Table 4-41 Mean tooth-surface-temperature with simulated periodontal ligament vitality (n=8) at four flow-rates (0.5ml/min, 0.15ml/min, 0.08ml/min, 0.03ml/min) in Pairs 1-8 (PDL) post-cooling. The mean difference between the left and right-tooth was 1.25°C at 0.5ml/min, 0.88°C at 0.15ml/min, 1.14°C at 0.08ml/min and 1.29°C at 0.03ml/min. The coolest mean temperature was 15.66°C [SD 3.48°C] (blue cell) and the warmest mean temperature 18.23°C [SD 4.45°C] (pink cell) a difference of 2.57°C.

Mean Lowest Tooth-Surface-Temperature Post-Cooling (Degrees Celsius) n=8									
Flow-Rate (ml/min)	Periodontal Ligament Flow – Left-Tooth					Periodontal Ligament Flow – Right-Tooth			
	Mean	SD	Min	Max	Range	Mean	SD	Min	Max	Range
0.5	16.98	3.13	13.30	21.40	8.10	18.23	4.45	11.80	25.40	13.60
0.15	15.98	3.61	11.20	20.00	8.80	16.86	4.46	9.60	24.40	14.80
0.08	15.66	3.48	10.50	19.70	9.20	16.80	4.71	9.40	23.80	14.40
0.03	15.69	3.23	10.50	19.90	9.40	16.98	4.25	10.40	22.90	12.50
SD = Standard Deviation; Min = Minimum; Max = Maximum									

The mean difference between the left and right-tooth-surface-temperature post-cooling with simulated vitality in the periodontal ligament had a maximum of 2.57^{o}C across all four flow-rates, the warmest being at the highest flow-rate from the right-tooth (pink cell) and the coolest at 0.08ml/min flow-rate from the left-tooth (blue cell).

<u>Simulated Vitality in Periodontal Ligament and One Tooth, With and Without a Pulse for Four Flow-Rates</u>
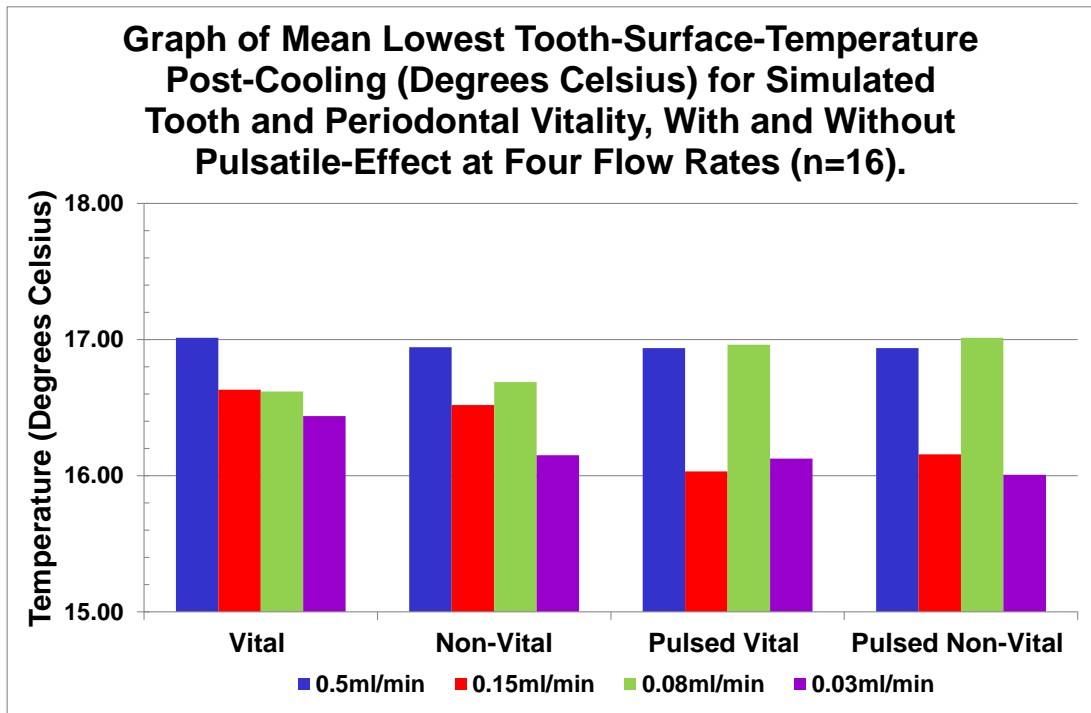
Figure 4-62 Graph of mean tooth-surface-temperature of the left and right-tooth (n=16) with simulated periodontal ligament and one tooth-vitality, with and without a pulse (PDL LTS or PDL LTSP, PDL RTS or PDL RTSP) post-cooling for four flow-rates (0.5ml/min, 0.15ml/min, 0.08ml/min, 0.03ml/min). An overall reduction in tooth-surface-temperature for vital teeth at 0.5ml/min to 0.03ml/min was seen in the non-pulsed simulation. 0.08ml/min interrupts the trend for the non-pulsed, non-vital teeth. This trend was also found for non-vital teeth with a simulated pulse, with the exception of 0.08ml/min. The pulsed vital simulation had two flow-rates (0.5ml/min and 0.08ml/min) which cooled less and 0.15ml/min cooled the most. The highest post-cooling tooth-surface-temperature was found in two sequences – vital non-pulsed simulation 0.5ml/min and non-vital pulsed 0.08ml/min and the coolest tooth-surface-temperature was found in the lowest flow-rate (0.03ml/min) of the pulsed simulation of the non-vital teeth.

Table 4-42 Mean tooth-surface-temperature with simulated periodontal vitality and one of the teeth (n=16) at four flow-rates (0.5ml/min, 0.15ml/min, 0.08ml/min, 0.03ml/min) in Pairs 1-8 (PDL LTS or PDL RTS) post-cooling.
The mean difference between the left and right-tooth was 0.07^{o}C at 0.5ml/min, 0.11^{o}C at 0.15ml/min, 0.07^{o}C at 0.08ml/min and 0.29^{o}C at 0.03ml/min. The coolest mean temperature was 16.15^{o}C [SD 3.96^{o}C] (blue cell) and warmest mean temperature 17.01^{o}C [SD 4.03^{o}C] (pink cell), a difference of 0.86^{o}C.

Mean Lowest Tooth-Surface-Temperature Post-Cooling (Degrees Celsius) n=16									
Flow-Rate (ml/min)	Vital Tooth with Periodontal Vitality					Non-Vital Tooth with Periodontal Vitality			
	Mean	SD	Min	Max	Range	Mean	SD	Min	Max	Range
0.5	17.01	4.03	9.80	23.10	13.30	16.94	4.42	9.80	25.10	15.30
0.15	16.63	4.48	10.50	25.40	14.90	16.52	4.56	9.80	27.20	17.40
0.08	16.62	4.59	9.80	24.60	14.80	16.69	4.89	9.50	24.90	15.40
0.03	16.44	4.26	9.80	25.00	15.20	16.15	3.96	10.80	23.90	13.10
SD = Standard Deviation; Min = Minimum; Max = Maximum									

Table 4-43 Mean tooth-surface-temperature with pulsed simulated periodontal vitality and one of the teeth (n=16) at four flow-rates (0.5ml/min, 0.15ml/min, 0.08ml/min, 0.03ml/min) in Pairs 1-8 (PDL LTSP or PDL RTSP) post-cooling.
The mean difference between the left and right-tooth was 0.00^{o}C at 0.5ml/min, 0.13^{o}C at 0.15ml/min, 0.05^{o}C at 0.08ml/min and 0.12^{o}C at 0.03ml/min. The coolest mean temperature was 16.01^{o}C [SD 3.94^{o}C Non-vital 0.03ml/min] (blue cell) and warmest mean temperature 17.01^{o}C [SD 4.66^{o}C] (pink cell), a difference of 1°C.

Mean Lowest Tooth-Surface-Temperature Post-Cooling (Degrees Celsius) n=16									
Flow-Rate (ml/min)	Pulsed Vital Tooth with Periodontal Vitality					Pulsed Non-Vital Tooth with Periodontal Vitality			
	Mean	SD	Min	Max	Range	Mean	SD	Min	Max	Range
0.5	16.94	4.09	9.90	24.30	14.40	16.94	3.63	10.60	21.30	10.70
0.15	16.03	4.05	9.20	23.00	13.80	16.16	4.36	10.20	23.90	13.70
0.08	16.96	4.46	9.20	26.90	17.70	17.01	4.66	9.80	24.40	14.60
0.03	16.13	4.01	9.50	24.10	14.60	16.01	3.94	9.50	22.20	12.70
SD = Standard Deviation; Min = Minimum; Max = Maximum									

The mean value of the lowest tooth-surface-temperature of the 16 teeth with four different flow-rates after cooling ranged from 16.01^{o}C to 17.01^{o}C (a difference of 1°C).

The simulated flow-rate of 0.03ml/min for the non-vital pulsed variant provided the lowest mean tooth-surface-temperature overall at 16.01^{o}C, closely followed by the 0.15ml/min vital pulsed variant at 16.03^{o}C. Three of the four vitality simulations recorded their lowest tooth-surface-temperature with the lowest flow-rate, two of which were non-vital simulations (vital 16.44^{o}C, non-vital 16.15^{o}C and non-vital pulsed 16.01^{o}C) but the vital pulsed variant does not follow this trend, with 0.15ml/min flow-rate having the lowest

tooth-surface-temperature at 16.03^{o}C, compared to the 0.03ml/min flow-rate at 16.13^{o}C, a small difference of 0.1^{o}C.

The warmest mean lowest tooth-surface-temperature (17.01^{o}C) following cooling was seen in two simulated variants - 0.5ml/min vital and 0.08ml/min pulsed non-vital.

The greatest range of temperature-reduction within the simulated flow-rates was 17.7^{o}C, for the 0.08ml/min pulsed vital teeth; and between the whole of the four flow-rates, a maximum temperature range of 18°C was seen between 9.2^{o}C for the pulsed vital teeth with flow-rate of 0.15ml/min and 0.08ml/min and 27.2^{o}C for the non-vital tooth with flow-rate 0.15ml/min.

Pair 5 shows persistently warmer tooth-surface-temperatures following cooling, especially for the RTS through all the flow-rates and variants used.

4.5.8.7 Difference in Tooth-Surface-Temperature Between Pre- and Post-Cooling

Table 4-44 Difference in tooth-surface-temperature between pre- and post-cooling Pair 1-8 for simulated vitality of the periodontal ligament (PDL), left-tooth on screen (LTS), right-tooth on screen (RTS) and no simulated vitality (Nil). The greatest temperature-difference was 22.3^{o}C at Nil simulation (pink cell) and the least was 4.8^{o}C at 0.5ml/min simulation LTS (blue cell).

Difference in Tooth-Surface-Temperatures Between Pre- and Post-Cooling (Degrees Celsius)									
Flow-Rate	Pair	PDL		LTS		RTS		NIL	
		LTS	RTS	LTS	RTS	LTS	RTS	LTS	RTS
0.5ml/min	1	13.8	14.6	15.1	17.4	15.5	17.2	10.2	11.7
	2	18.3	15.9	21.6	18.3	19.9	16.9	22.3	18.9
	3	15.7	9.3	16.6	10.6	18.3	12.1	15.7	9.7
	4	15.4	17.1	14.9	16.6	15.4	17.1	14.8	16.1
	5	10	6.1	8.1	4.8	14.3	9.2	9.8	5.7
	6	17.9	19.7	17.9	19.5	18.1	19.1	21.2	22
	7	13.2	13.3	14.3	14.5	13.1	13.0	11.1	9.9
	8	10.6	9.4	14.4	11.6	9	8.5	14.9	12.4
0.15ml/min	1	15.2	16.6	.	.	.	.	.	.
	2	20.4	17.6	.	.	.	.	.	.
	3	17.2	12.6	.	.	.	.	.	.
	4	12.9	15.7	.	.	.	.	.	.
	5	11.1	6.9	.	.	.	.	.	.
	6	20.1	21.9	.	.	.	.	.	.
	7	13.4	13.9	.	.	.	.	.	.
	8	12.5	10.7	.	.	.	.	.	.
0.08ml/min	1	15.9	17.4	.	.	.	.	.	.
	2	20.9	17.9	.	.	.	.	.	.
	3	16.3	11.2	.	.	.	.	.	.
	4	14.2	17.1	.	.	.	.	.	.
	5	11.2	7.3	.	.	.	.	.	.
	6	20.8	22	.	.	.	.	.	.
	7	13.4	12.8	.	.	.	.	.	.
	8	12.6	10.7	.	.	.	.	.	.
0.03ml/min	1	16	16.8	.	.	.	.	.	.
	2	20.9	17.6	.	.	.	.	.	.
	3	16.5	12	.	.	.	.	.	.
	4	13.8	16.6	.	.	.	.	.	.
	5	11.8	8	.	.	.	.	.	.
	6	19.3	21.1	.	.	.	.	.	.
	7	11.7	10.3	.	.	.	.	.	.
	8	14.7	12.2	.	.	.	.	.	.
SIMULATED VITALITY RTS = Right-Tooth on Screen; LTS = Left-Tooth on Screen; PDL = Periodontal Ligament; NIL = No Simulated Vitality									
Least Difference				Greatest Difference					

Table 4-45 Difference in tooth-surface-temperatures between pre- and post-cooling Pair 1-8 for simulated vitality, with and without simulated pulse, of the periodontal ligament and left-tooth on screen, periodontal ligament and right-tooth on screen (PDL LTS, PDL LTSP, PDL RTS, PDL RTSP). The greatest difference in tooth-surface-temperature was 22.6^{o}C at 0.08ml/min (pink cell) with simulated pulse (RTS of PDL RTSP), and the least was 3.8^{o}C at 0.08ml/min (blue cell) with simulated pulse (RTS of PDL RTSP).

Difference in Tooth-Surface-Temperatures Between Pre- and Post-Cooling (Degrees Celsius)									
Flow-Rate	Pair	PDL LTS		PDL RTS		PDL LTSP		PDL RTSP	
		LTS	RTS	LTS	RTS	LTS	RTS	LTS	RTS
0.5ml/min	1	15.1	16.4	14.9	15.6	16	17.5	16.1	17.2
	2	21.8	19.1	21.6	19	19.9	17.4	15.5	13.6
	3	16	8.5	17	10.3	17.4	11	16.4	9.8
	4	14.5	16	15.2	16.8	15.3	16.5	15	16.1
	5	9.5	6.3	14.4	9.9	13.6	8.5	11.7	7.2
	6	20	22	19	21	17.7	18.8	19.7	20.8
	7	11.3	11.5	11.4	11.1	12.3	12.0	11.7	11.1
	8	13.5	10.8	13.6	11.1	8.8	8.2	10	8.9
0.15ml/min	1	17.1	18.5	14.7	16.6	15.9	17.4	15.3	17.3
	2	19.9	17.3	20.1	17.5	22	19.3	21.2	18.5
	3	17	12.2	16.8	12.2	17.6	12.9	17.1	12.3
	4	15.6	16.9	15	16.5	15.8	17	15.9	17.6
	5	5.9	4.1	13.1	8.1	11.8	7.6	13.5	8.4
	6	20.5	22	20	20.9	19.7	21.3	19.7	20.6
	7	12.8	13.1	12.4	12.8	10.4	9.2	14	15
	8	13	10.3	10.3	9.4	12.1	8.9	12.5	10.8
0.08ml/min	1	14.9	16.1	15.5	17.2	16.4	17.9	11	12.4
	2	20.9	18.5	22.1	19.5	20.8	18.4	21.4	18.5
	3	16.2	11.3	16	13	15.2	10.6	15.1	10
	4	14.7	17.6	14	17.1	14.3	17.4	12.4	15.4
	5	10.1	6.5	13.4	8.6	13.3	9.2	6.1	3.8
	6	20.6	21.9	20.6	21.9	18.8	19.9	21.8	22.6
	7	10.6	8.9	12	10.7	10.4	9.4	11.8	11.6
	8	12.5	12.3	6.7	6.7	13.6	11.5	13.3	11.4
0.03ml/min	1	16.8	18	16.3	17.8	14.9	16.3	14.7	16.2
	2	21.1	18.3	18	15.4	21.3	18.5	21.8	18.9
	3	16.7	11.9	15.8	10.9	16.3	11.6	17.2	12.4
	4	14.5	17.7	14.9	17.9	13.8	17	14.6	17.6
	5	11.8	8.3	13.9	8.8	13.3	9.1	10.7	6.7
	6	19.5	20.6	20.4	21.6	19.2	20.5	20.5	21.7
	7	13.8	15.2	8	6.8	13.3	14	12.1	11.7
	8	13.1	13	12.6	11.7	12.9	12.6	11.3	10.3
SIMULATED VITALITY									
RTS = Right-Tooth on Screen; LTS = Left-Tooth on Screen; PDLLTS = Periodontal Ligament and Left-Tooth on Screen; PDLRTS = Periodontal Ligament and Right-Tooth on Screen; PDLLTSP = Periodontal Ligament and Left-Tooth on Screen Pulsed; PDLRTSP = Periodontal Ligament and Right-Tooth on Screen Pulsed									
Least Difference					Greatest Difference				

4.5.8.8 Mean Values of Difference in Tooth-Surface-Temperature Between Pre- and Post-Cooling for Each Variable of Eight Pairs

No Simulated Vitality (Nil)

Table 4-46 Mean difference in tooth-surface-temperature between pre- and post-cooling of the left and right-tooth (n=8) of Pair 1-8 with no simulation of vitality (Nil), was 1.7^{o}C.

Mean Difference in Tooth-Surface-Temperature Between Pre- and Post-Cooling (Degrees Celsius) n=8									
Flow-Rate (ml/min)	Nil Left					Nil Right			
	Mean	SD	Min	Max	Range	Mean	SD	Min	Max	Range
0	15.00	4.74	9.80	22.30	12.50	13.30	5.35	5.70	22.00	16.30
SD = Standard Deviation; Min = Minimum; Max = Maximum									

The mean difference between left and right-tooth-surface-temperatures following cooling with no simulated vitality was 1.7^{o}C, with the right-tooth being warmer, with less mean temperature-reduction, than the left. The greatest range of temperature-difference was 16.30^{o}C from the right.

Simulated Vitality in a Tooth Only at 0.5ml/min (LTS or RTS)

Table 4-47 Mean difference in tooth-surface-temperature between pre- and post-cooling of the left and right-tooth (n=16) with or without simulation of vitality at 0.5ml/min Pairs 1-8 (LTS or RTS). The mean difference between tooth-surface-temperature of the vital and non-vital tooth was 0.06^{o}C.

Mean Difference in Tooth-Surface-Temperature Between Pre- and Post-Cooling (Degrees Celsius) n=16									
Flow-Rate (ml/min)	Vital Tooth Only					Non-Vital Tooth Only			
	Mean	SD	Min	Max	Range	Mean	SD	Min	Max	Range
0.5	14.75	3.83	8.10	21.60	13.50	14.81	4.16	4.80	19.90	15.10
SD = Standard Deviation; Min = Minimum; Max = Maximum									

The mean difference in tooth-surface-temperature between pre- and post-cooling of the vital and non-vital tooth was 0.06^{o}C in favour of the non-vital tooth, which also recorded the least temperature-difference (4.80^{o}C). The greatest temperature-difference (21.6^{o}C) was recorded from the vital simulation, and the greatest range of temperature-difference was 15.1^{o}C for the non-vital tooth.

Simulated Vitality in Periodontal Ligament for Four Flow-Rates (PDL)
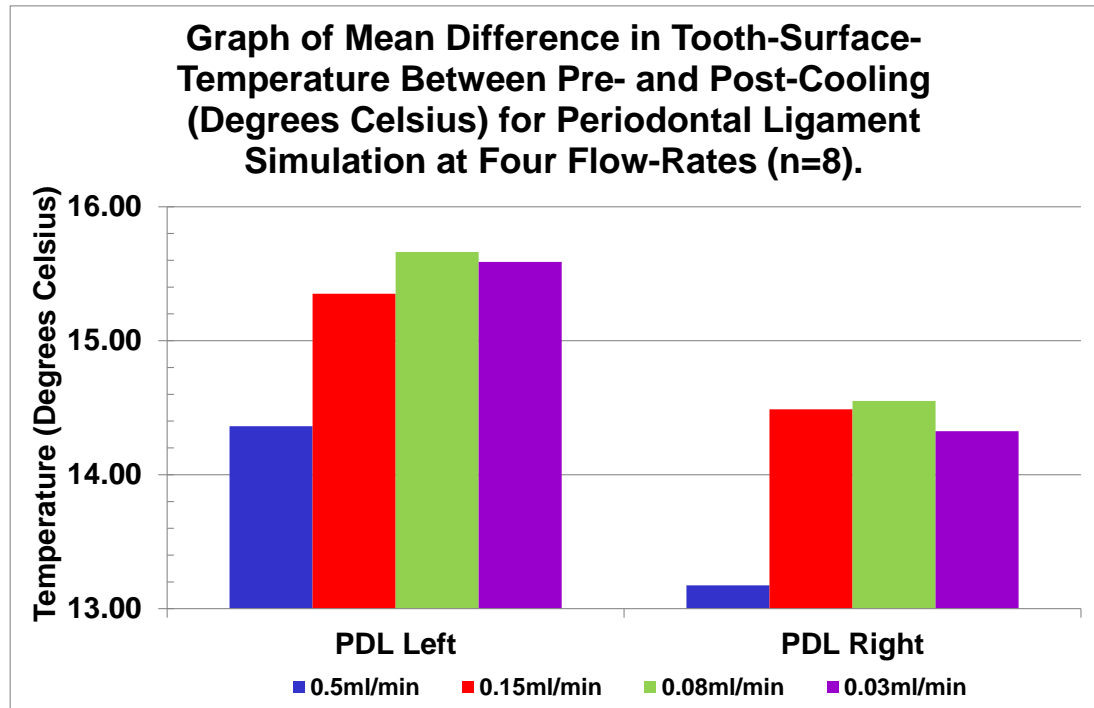
Figure 4-63 Graph of mean difference in tooth-surface-temperature between pre- and post-cooling of the left and right-tooth (n=8) with simulated periodontal ligament vitality (PDL) for four flow-rates (0.5ml/min, 0.15ml/min, 0.08ml/min, 0.03ml/min). 0.08ml/min had the greatest difference in tooth-surface-temperature for both left and right simulations. 0.5ml/min had the least difference. The left simulation had greater tooth-surface-temperature-difference than the right at all flow-rates.

Table 4-48 Mean difference in tooth-surface-temperature between pre- and post-cooling with simulated periodontal ligament vitality (n=8) at four flow-rates (0.5ml/min, 0.15ml/min, 0.08ml/min, 0.03ml/min) in Pairs 1-8 (PDL). The mean difference in tooth-surface-temperature between left and right simulations was 1.18^{o}C at 0.5ml/min, 0.86^{o}C at 0.15ml/min, 1.11^{o}C at 0.08ml/min and 1.26^{o}C at 0.03ml/min. The maximum mean temperature-difference was 22.00^{o}C (pink cell) and minimum mean temperature-difference was 6.10^{o}C (blue cell).

Mean Difference in Tooth-Surface-Temperature Between Pre- and Post-Cooling (Degrees Celsius) n=8										
Flow-Rate (ml/min)	Periodontal Ligament Flow – Left-Tooth					Periodontal Ligament Flow – Right-Tooth				
	Mean	SD	Min	Max	Range	Mean	SD	Min	Max	Range
0.5	14.36	3.06	10.00	18.30	8.30	13.18	4.58	6.10	19.70	13.60
0.15	15.35	3.54	11.10	20.40	9.30	14.49	4.57	6.90	21.90	15.00
0.08	15.66	3.60	11.20	20.90	9.70	14.55	4.83	7.30	22.00	14.70
0.03	15.59	3.30	11.70	20.90	9.20	14.33	4.38	8.00	21.10	13.10
SD = Standard Deviation; Min = Minimum; Max = Maximum										

The mean difference between left and right-tooth-surface-temperature following cooling with simulated vitality in the periodontal ligament had a maximum of 1.26^{o}C across all four flow-rates, the least at 0.86^{o}C at 0.15ml/min and the greatest being 1.26^{o}C at 0.03ml/min.

Simulated Vitality in Periodontal Ligament and One Tooth, With and Without a Pulse for Four Flow-Rates
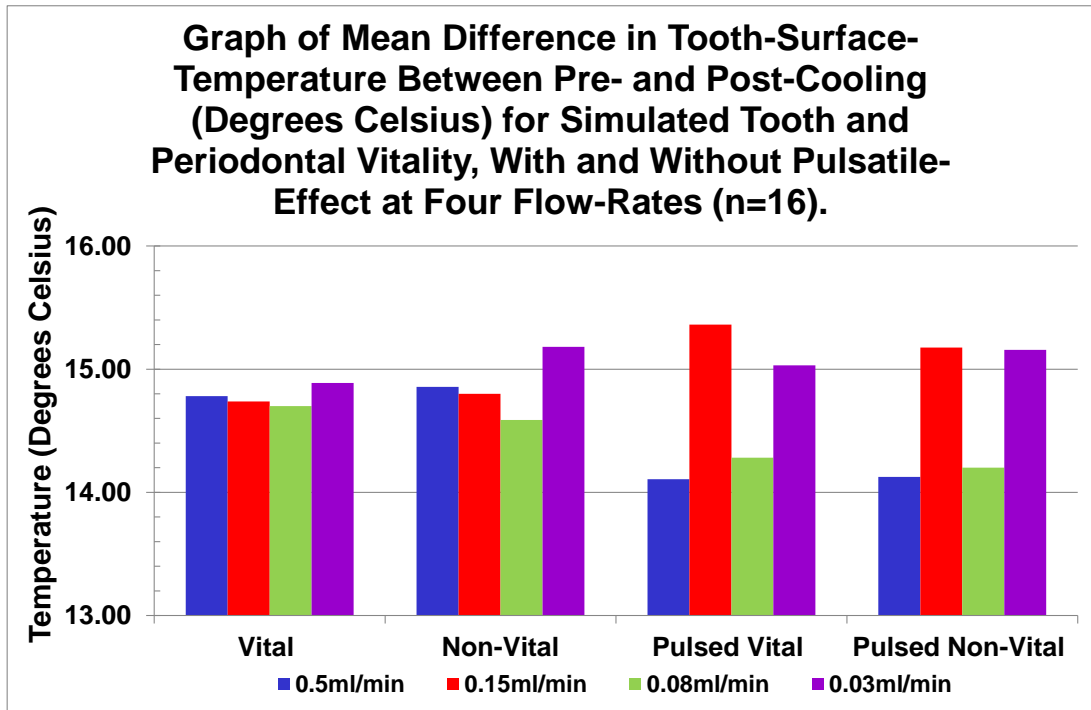
Figure 4-64 Graph of mean difference of tooth-surface-temperature between pre- and post-cooling of the left and right-tooth (n=16) with simulated periodontal ligament and one tooth-vitality, with and without simulated pulse (PDL LTS or PDL LTSP, PDL RTS or PDL RTSP) for four flow-rates (0.5ml/min, 0.15ml/min, 0.08ml/min, 0.03ml/min). The greatest mean difference in tooth-surface-temperature was in the pulsed vital simulation at 0.15ml/min. The greatest mean difference for both non-pulsed simulations was at 0.03ml/min. The least mean difference for both non-pulsed simulations was at 0.08ml/min, and for both the pulsed simulations at 0.5ml/min.

Table 4-49 Mean difference of tooth-surface-temperature between pre- and post-cooling temperature with simulated periodontal vitality and one of the teeth (n=16) at four flow-rates (0.5ml/min, 0.15ml/min, 0.08ml/min, 0.03ml/min) in Pairs 1-8 (PDL LTS or PDL RTS). The mean difference between the left and right-tooth was 0.08^{o}C at 0.5ml/min, 0.06^{o}C at 0.15ml/min, 0.11^{o}C at 0.08ml/min and 0.29^{o}C at 0.03ml/min. The least temperature-difference was 4.1^{o}C (blue cell) and greatest temperature-difference was temperature 22.10^{o}C (pink cell).

Mean Difference in Tooth-Surface-Temperature Between Pre- and Post-Cooling (Degrees Celsius) n=16										
Flow-Rate (ml/min)	Vital Tooth with Periodontal Vitality					Non-Vital Tooth with Periodontal Vitality				
	Mean	SD	Min	Max	Range	Mean	SD	Min	Max	Range
0.5	14.78	4.10	9.50	21.80	12.30	14.86	4.44	6.30	22.00	15.70
0.15	14.74	4.41	5.90	20.90	15.00	14.80	4.54	4.10	22.00	17.90
0.08	14.70	4.66	6.70	21.90	15.20	14.59	4.90	6.50	22.10	15.60
0.03	14.89	4.26	6.80	21.60	14.80	15.18	3.77	8.00	20.60	12.60
SD = Standard Deviation; Min = Minimum; Max = Maximum										

Table 4-50 Mean difference of tooth-surface-temperature between pre- and post-cooling with pulsed simulated periodontal vitality and one of the teeth (n=16) at four flow-rates (0.5ml/min, 0.15ml/min, 0.08ml/min, 0.03ml/min) in Pairs 1-8 (PDL LTSP or PDL RTSP). The mean difference between left and right teeth was 0.02^{o}C at 0.5ml/min, 0.18^{o}C at 0.15ml/min, 0.08^{o}C at 0.08ml/min and 0.13^{o}C at 0.03ml/min. The least temperature-difference was 3.8^{o}C (blue cell) and greatest temperature-difference was 22.60^{o}C (pink cell).

Mean Difference in Tooth-Surface-Temperature Between Pre- and Post-Cooling (Degrees Celsius) n=16										
Flow-Rate (ml/min)	Pulsed Vital Tooth with Periodontal Vitality					Pulsed Non-Vital Tooth with Periodontal Vitality				
	Mean	SD	Min	Max	Range	Mean	SD	Min	Max	Range
0.5	14.11	4.12	7.20	20.80	13.60	14.13	3.67	8.20	19.70	11.50
0.15	15.36	4.01	8.40	22.00	13.60	15.18	4.26	7.60	21.30	13.70
0.08	14.28	4.62	3.80	22.60	18.80	14.20	4.75	6.10	21.80	15.70
0.03	15.03	4.06	6.70	21.70	15.00	15.16	3.86	9.10	21.80	12.70
SD = Standard Deviation; Min = Minimum; Max = Maximum										

The mean values of the difference in tooth-surface-temperatures between pre- and post-cooling of the 16 teeth with four different flow-rates following cooling provided a minimum and maximum mean difference in tooth-surface-temperature, i.e., mean cooling of 14.11^{o}C and 15.36^{o}C, respectively (a difference of 1.25^{o}C). These two values were both from the pulsed vital variant at flow-rates of 0.5ml/min for the minimum cooling, and 0.15ml/min for the maximum cooling.

Maximum mean cooling for both the non-pulsed variants was seen with the lowest flow-rate of 0.03ml/min - the non-vital sequence having greater mean cooling of 15.18^{o}C compared to 14.89^{o}C for the vital sequence. Both pulsed variants, vital and non-vital, showed maximum cooling from the flow-rate

0.15ml/min (15.36^{o}C and 15.18^{o}C, respectively) but the lowest flow-rate of 0.03ml/min was close (mean difference in temperature 15.03^{o}C and 15.16^{o}C for the vital and non-vital sequences, respectively). The least cooling occurred with both pulsed variants, vital and non-vital, from the highest flow-rate, 0.5ml/min (14.11^{o}C and 14.13^{o}C, respectively).

Within the vital and non-vital non-pulsed variant, the least cooling occurred from a flow-rate of 0.08ml/min, with the non-vital cooling less than the vital.

The greatest range of mean cooling was 18.8^{o}C from the 0.08ml/min flow-rate in the pulsed vital group. The least range of mean cooling was 11.5^{o}C for the pulsed non-vital sequence at 0.5ml/min.

4.5.9 Thermal Sequence and Alignment for Analysis of In-vitro Vitality from the Difference in Area-Under-the-Curve

Each variable was aligned to commence re-warming from the same temperature, as previously shown in Section 4.5.2.1, and the difference in the area-under-the-curve was calculated. The tables of raw-data for each of the eight Pairs of teeth are shown in Appendix A.7. Figure 4-65 to 4-69 show the difference in area-under-the-curve for Pair 7.
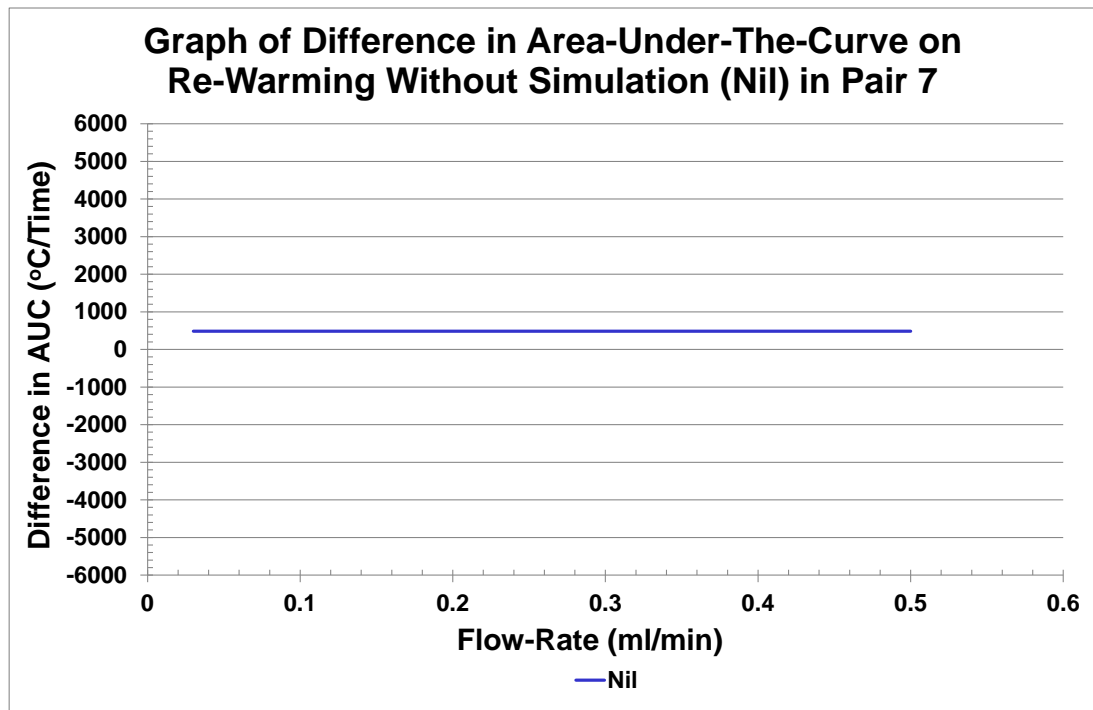
Figure 4-65 Graph of difference in area-under-the-curve according to flow-rate with no simulated vitality (Nil – blue line) which resulted in a positive difference in area-under-the-curve of 485°C/Time for Pair 7 following subtraction of the left-tooth from the right-tooth.
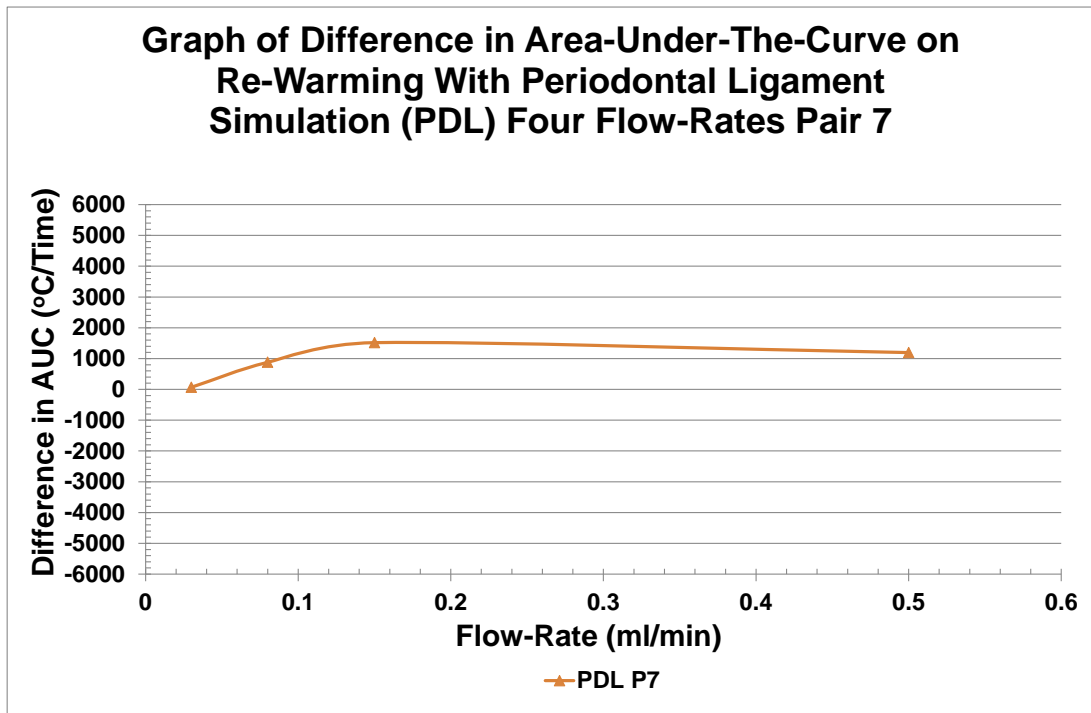
Figure 4-66 Graph of difference in area-under-the-curve according to flow-rate with simulated vitality of the periodontal ligament (PDL – brown line) resulted in a positive area-under-the-curve of 68°C/Time, 878°C/Time, 1517°C/Time and 1194°C/Time at flow-rates of 0.03ml/min, 0.08ml/min, 0.15ml/min and 0.5ml/min respectively, for Pair 7 following subtraction of the left-tooth from the right-tooth.

Graph of Difference in Area-Under-The-Curve on Re-Warming With Periodontal Ligament & Left or Right Tooth Simulation (PDL LTS & PDL RTS) Four Flow-Rates Pair 7
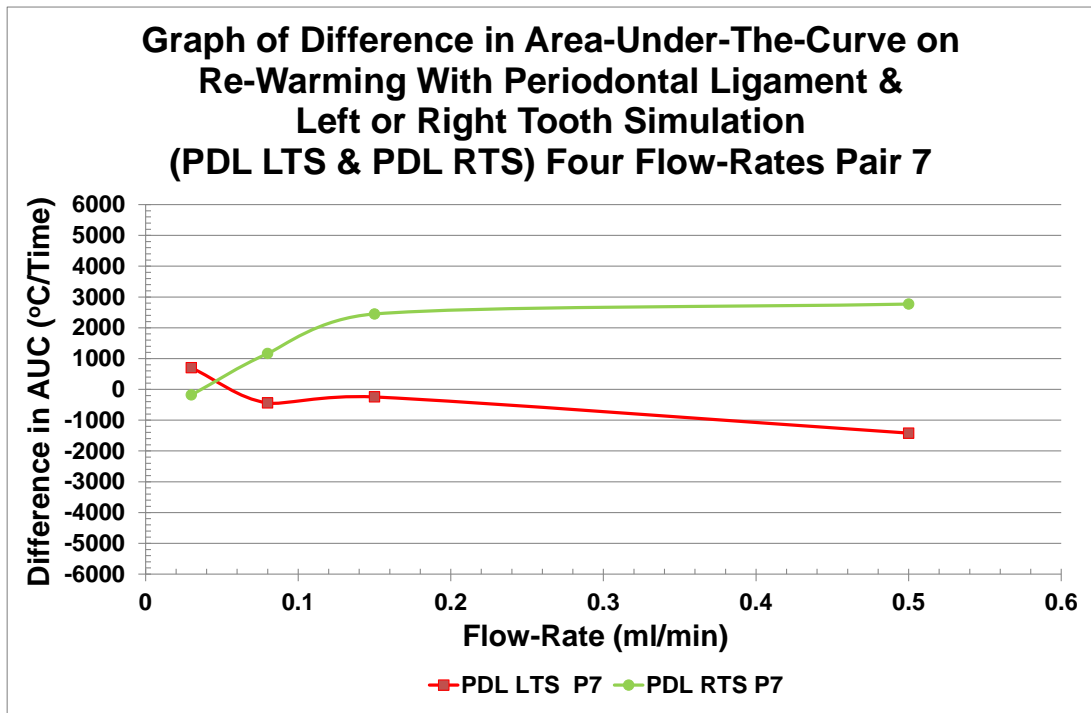
Figure 4-67 Graph of difference in area-under-the-curve according to flow-rate with simulated vitality of the periodontal ligament and either the right or left-tooth (PDL LTS – red line or PDL RTS – light-green line) resulted in:
PDL RTS - a positive area-under-the-curve of 1162°C/Time, 2448°C/Time, 2770°C/Time and a negative value of -182°C/Time at flow-rates of 0.08ml/min, 0.15ml/min, 0.5ml/min and 0.03ml/min respectively, for Pair 7 following subtraction of the left-tooth from the right-tooth.
PDL LTS - a negative area-under-the-curve of -444°C/Time, -247°C/Time, -1421°C/Time and a positive value of 699°C/Time at flow-rates of 0.08ml/min, 0.15ml/min, 0.5ml/min and 0.03ml/min respectively, for Pair 7 following subtraction of the left-tooth from the right-tooth.
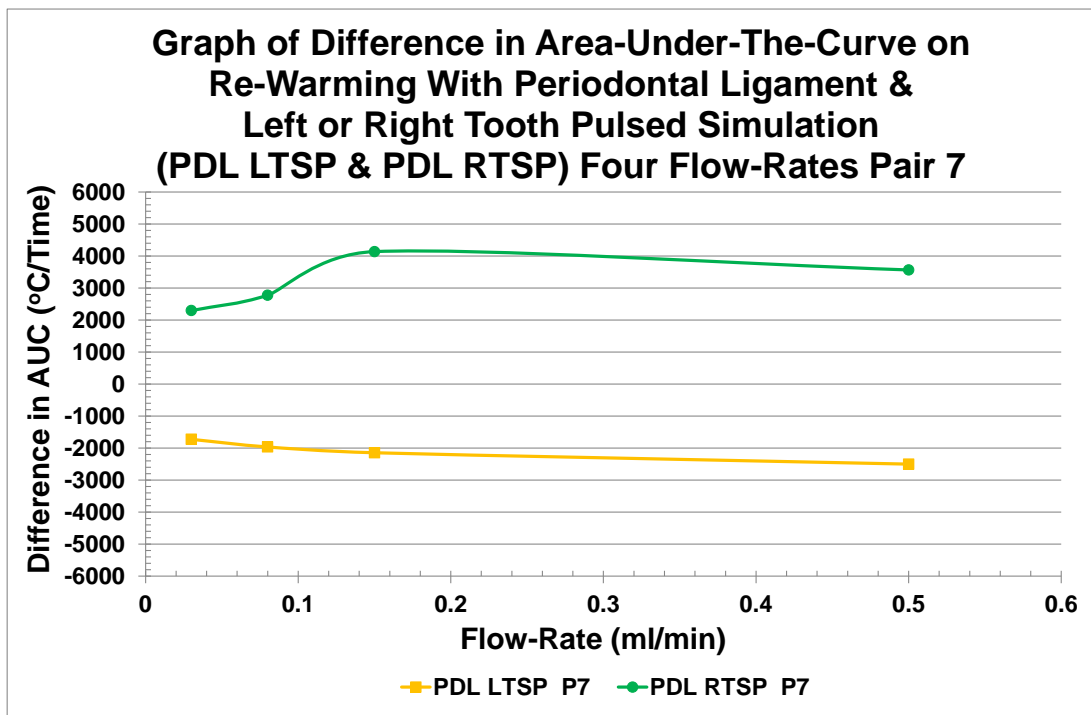
Figure 4-68 Graph of difference in area-under-the-curve according to flow-rate with pulsed simulated vitality of the periodontal ligament and either the right or left-tooth (PDL LTSP – yellow line or PDL RTSP – dark-green line) resulted in:

PDL RTSP a positive area-under-the-curve for all flow-rates of 2297°C/Time, 2777°C/Time, 4140°C/Time and 3566°C/Time at 0.03ml/min, 0.08ml/min, 0.15ml/min and 0.5ml/min respectively, for Pair 7 following subtraction of the left-tooth from the right-tooth.

PDL LTSP a negative area-under-the-curve for all flow-rates of -1726°C/Time, -1964°C/Time, -2145°C/Time and -2500°C/Time at flow-rates of 0.03ml/min, 0.08ml/min, 0.15ml/min and 0.5ml/min respectively, for Pair 7 following subtraction of the left-tooth from the right-tooth.
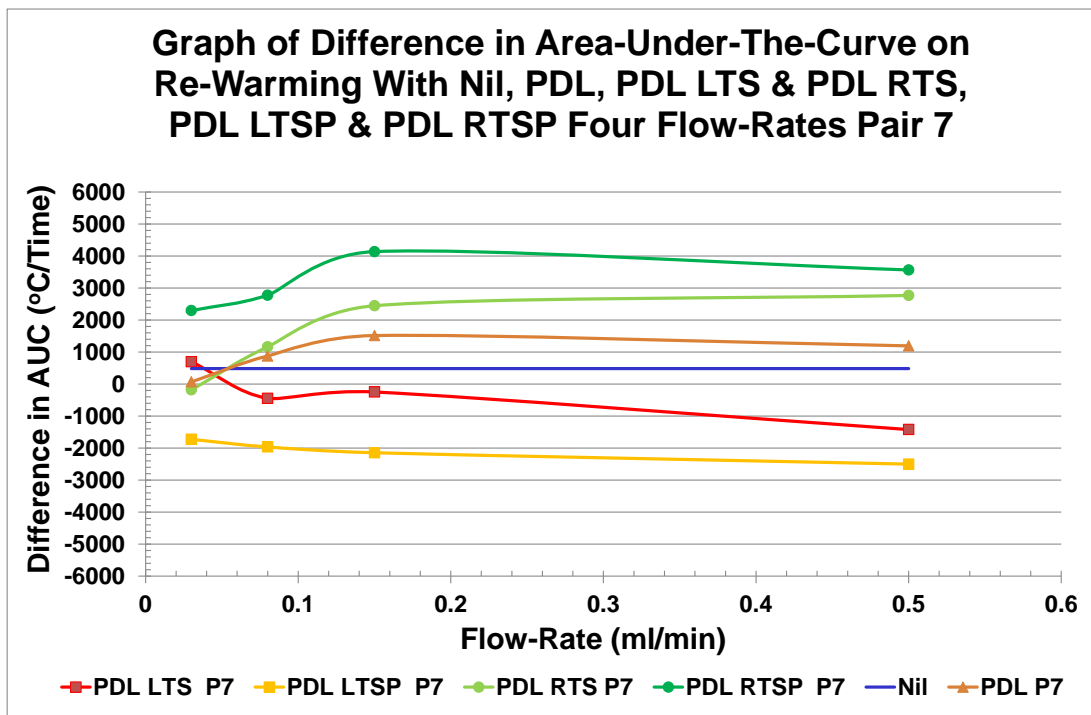
Figure 4-69 Summary Graph of all differences in area-under-the-curve for Pair 7 by flow-rate, where there is a positive trend in favour of the right-tooth without simulated vitality (blue line - positive value). Simulated vitality of the periodontal ligament increased this difference from 0.08ml/min to 0.5ml/min (brown line). Addition of simulated tooth-vitality increased the difference further than the periodontal ligament at 0.08ml/min to 0.5ml/min for the right-tooth and there was a clear negative value for left- tooth-vitality from 0.08ml/min to 0.5ml/min. A trend for increased values in the difference in area-under-the-curve with increased flow-rate from 0.03ml/min to 0.15ml/min for the pulsed simulations on both right and left was seen, and this always had a greater difference in area-under-the-curve than non-pulsed simulations.

The difference in the area-under-the-curve values of each of the eight pairs of dissimilar teeth were used to calculate the mean values of each of the variables (Table 4-51). This data was used to produce graphs of the mean difference in area-under-the-curve for simulation of the periodontal ligament with a vital tooth, either left or right, each with and without a simulated pulse (Figure 4-70 to 4-72).

Table 4-51 The mean values of difference in area-under-the-curve for independent dissimilar teeth from eight pairs of Molar Teeth (Pair 1 to 8) at four flow-rates – 0.03ml/min, 0.08ml/min, 0.15ml/min and 0.5ml/min where the model has a greater mean area-under-the-curve for the right-tooth than the left, giving a positive value for no simulation. This trend followed with simulated vitality in the periodontal ligament only, with a slight increase in positive value. A further increase was seen in the mean difference in area-under-the-curve with the addition of simulated vitality to the right-tooth which increased with increasing flow-rate. Pulsed vitality simulation for the right-tooth increased the mean difference in area-under-the-curve even more, and this followed the trend of increasing with increasing flow-rate to 0.15ml/min, with a slight reduction at 0.5ml/min. The left-tooth mean values were negative from 0.08ml/min and increased in negativity with increasing flow-rate, the 0.03ml/min flow-rate was positive but less than with the periodontal only flow-rate. The addition of a simulated pulse to the left-tooth-vitality resulted in an increase in mean difference in area-under-the-curve with increasing flow-rate for all flow-rates.

Mean Difference in Area-Under-The-Curve (^{o}C/Time) for Independent Dissimilar Teeth P1-8 At Four Flow-Rates (ml/min)						
Flow-Rate	PDL LTS	PDL LTSP	PDL RTS	PDL RTSP	Nil	PDL
0.5	-1069	-1637	2626	2860	589	765
0.15	-470	-1001	2404	2911	589	932
0.08	-64	-741	1600	2304	589	883
0.03	596	-702	745	1927	589	697
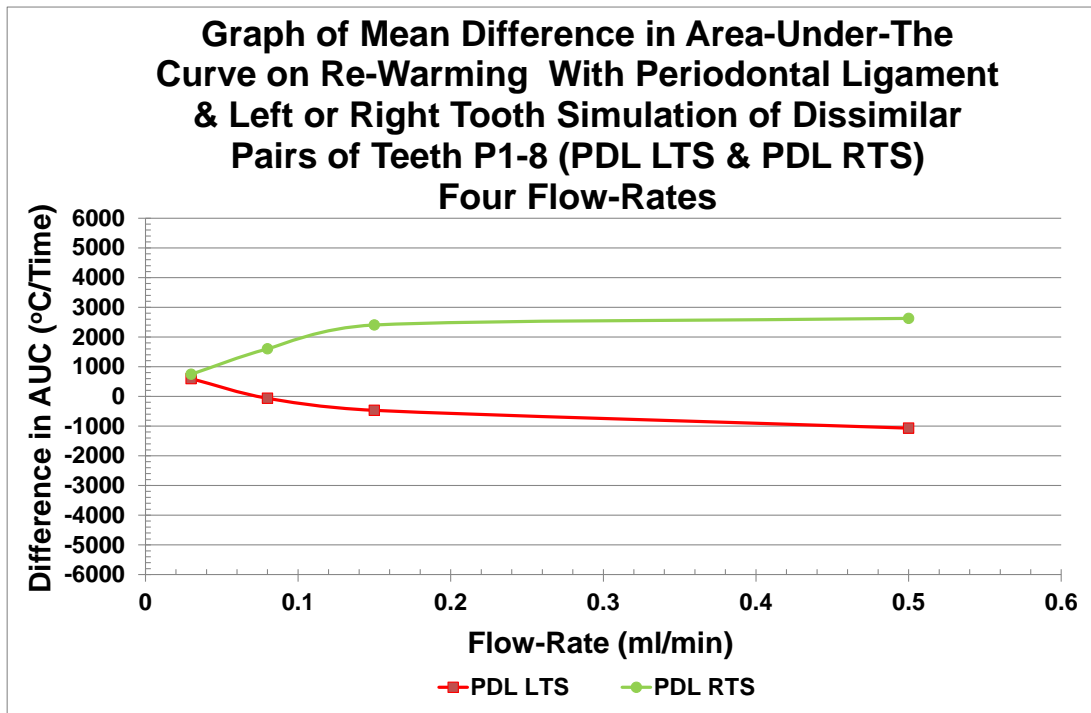
Figure 4-70 Graph shows the mean difference in area-under-the-curve for independent dissimilar teeth from eight pairs of molar teeth (Pair 1 to 8) at four simulated flow-rates – 0.03ml/min, 0.08ml/min, 0.15ml/min and 0.5ml/min following subtraction of the left-tooth from the right-tooth, and at the lowest flow-rate of 0.03ml/min the mean difference for both is positive at 596°C/Time and 745°C/Time for the left and right-tooth-vitality, respectively. An increase in difference in area-under-the-curve is seen for both simulations and the left-tooth mean difference becomes negative at 0.08ml/min, and both right and left simulated vitality mean differences increase at 0.15ml/min and 0.5ml/min.
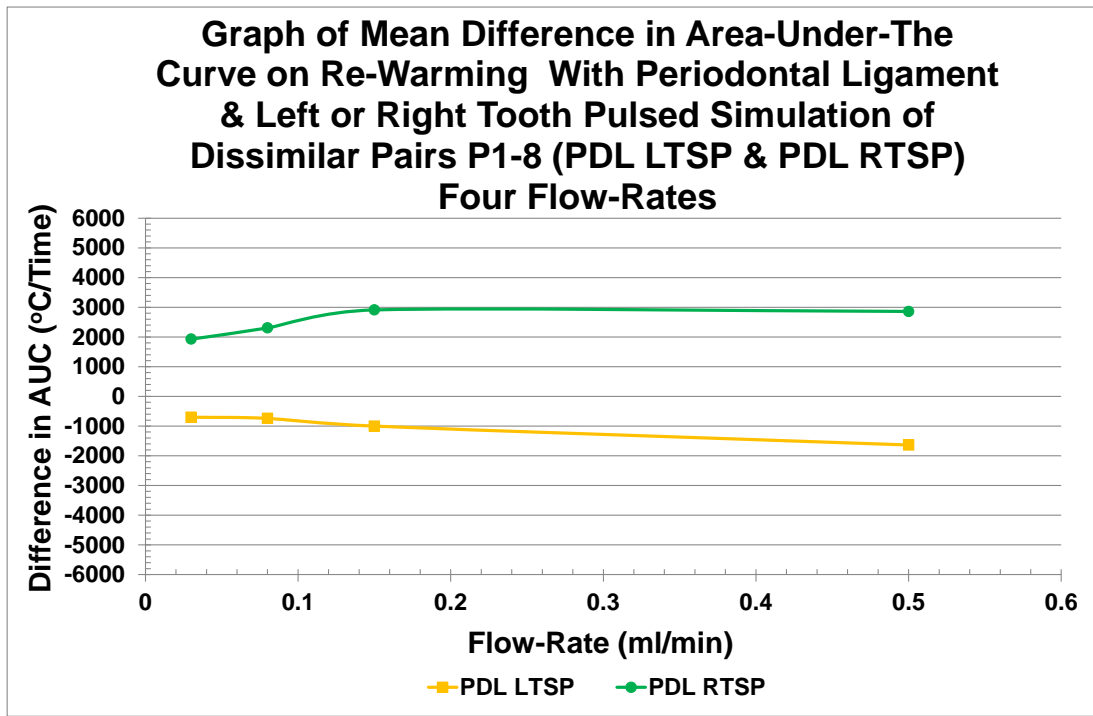
Figure 4-71 Graph shows the mean difference in area-under-the-curve for independent dissimilar teeth from eight pairs of molar teeth (Pair 1 to 8) at four simulated pulsed flow-rates – 0.03ml/min, 0.08ml/min, 0.15ml/min and 0.5ml/min following subtraction of the left-tooth from the right-tooth. At the lowest flow-rate of 0.03ml/min the mean difference for both are -702°C/Time and 1927°C/Time for the left and right pulsed tooth-vitality, respectively. An increase in difference in area-under-the-curve is seen for both simulations from 0.03ml/min to 0.15ml/min.
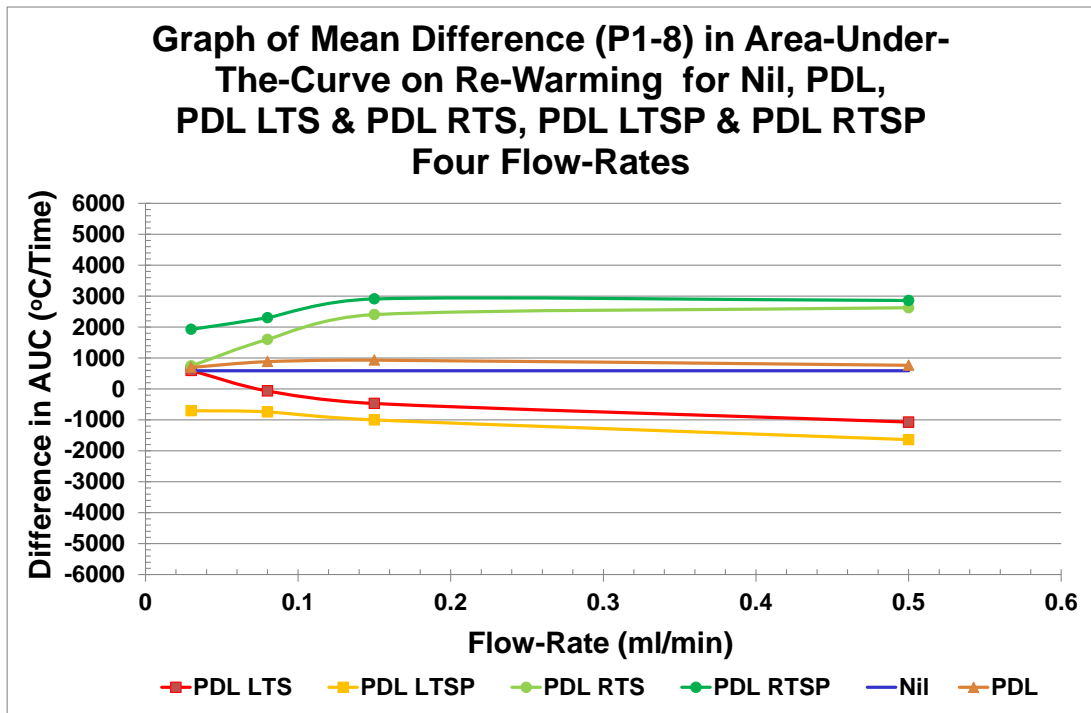
Figure 4-72 Summary Graph of all mean differences of area-under-the-curve for independent dissimilar teeth from eight pairs of Molar Teeth (Pair 1 to 8) at four pulsed flow-rates – 0.03ml/min, 0.08ml/min, 0.15ml/min and 0.5ml/min following subtraction of the left-tooth from the right-tooth. There is a positive trend in favour of the right-tooth without simulated vitality (blue line - positive value). The simulated vitality of the periodontal ligament increased this difference from 0.08ml/min to 0.5ml/min (brown line). The addition of tooth-vitality increased the difference further than the periodontal ligament at 0.03ml/min to 0.5ml/min for the right-tooth, and there was a negative value for left-tooth-vitality from 0.08ml/min to 0.5ml/min. A trend for increased values in the mean difference in area-under-the-curve with increased flow-rate from 0.03ml/min to 0.15ml/min for the pulsed simulations on both right and left was seen, and this always had a greater difference in area-under-the-curve than non-pulsed simulations.

The difference in area-under-the-curve values of each of the eight pairs of same matching teeth were also used to calculate the mean values of each of the variables (Table 4-52). This data was used to produce a summary graph of the mean difference in area-under-the-curve for the simulation of the periodontal ligament with a vital tooth, either right or left, each with and without a simulated pulse (Figure 4-73).

Table 4-52 The mean values of the difference in area-under-the-curve for the same teeth in a cross-over-design as vital and non-vital from eight pairs of Molar Teeth (Pair 1 to 8) at four flow-rates – 0.03ml/min, 0.08ml/min, 0.15ml/min and 0.5ml/min. An increase in mean difference in area-under-the-curve from a negative starting value of -613°C/Time of the right-tooth was seen which increased to a maximum positive value at 0.15ml/min. The left-tooth was initially negative and remained so, with increasing negativity as the flow-rate increased. Pulsed vitality simulation for the right-tooth increased the mean difference in area-under-the-curve even more and this followed the trend of increasing with increasing flow-rate, with the exception of 0.15ml/min which was lower than 0.08ml/min but still positive. The left-tooth mean pulsed values were negative from 0.03ml/min but decreased at 0.08ml/min and then increased in negativity with increasing flow-rate.

Mean Difference in Area-Under-The-Curve (^{o}C/Time) for P1-8 Four Flow-Rates Same Pair (ml/min)				
Flow-Rate	PDL LTS	PDL LTSP	PDL RTS	PDL RTSP
0.5	-1799	-2479	1766	1990
0.15	-1199	-2166	1843	1608
0.08	-1030	-1364.5	543	1706
0.03	-862	-2116	-613	520
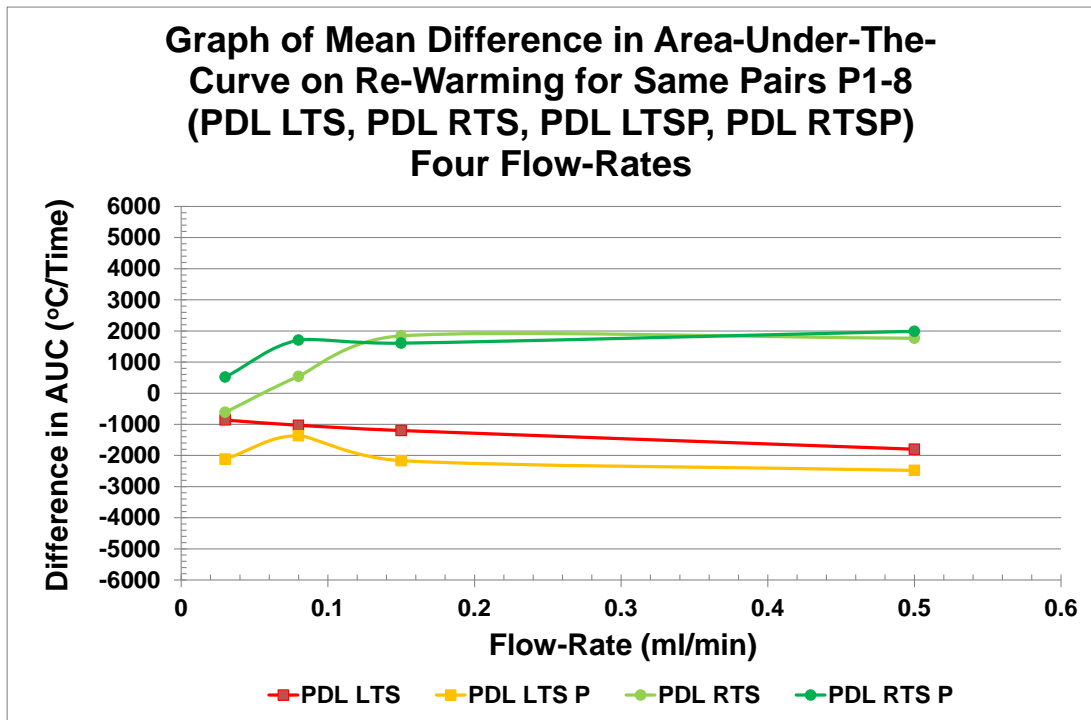
Figure 4-73 Summary Graph of all mean differences of area-under-the-curve for matching similar teeth from eight pairs of molar teeth (Pair 1 to 8) at four pulsed flow-rates – 0.03ml/min, 0.08ml/min, 0.15ml/min and 0.5ml/min following subtraction of the left-tooth from the right-tooth. At the lower two flow-rates, the pulsed simulation gives a greater difference in area-under-the-curve than non-pulsed, and was positive for right-side-vitality and negative for left-side-vitality. The left-tooth continues this trend across all flow-rates and the right-tooth breaks the trend at 0.15ml/min. The non-pulsed simulations at 0.03ml/min both resulted in a negative value, and from 0.08ml/min to 0.5ml/min the values were positive from right-side-vitality, and negative from left-side-vitality.

4.5.10 Area-Under-The-Curve Thermal Maps Pair 7
0.03ml/min

a.

b.

c.

d.

e.

f.

Simulated Vitality Left-Tooth   Simulated Vitality Right-Tooth
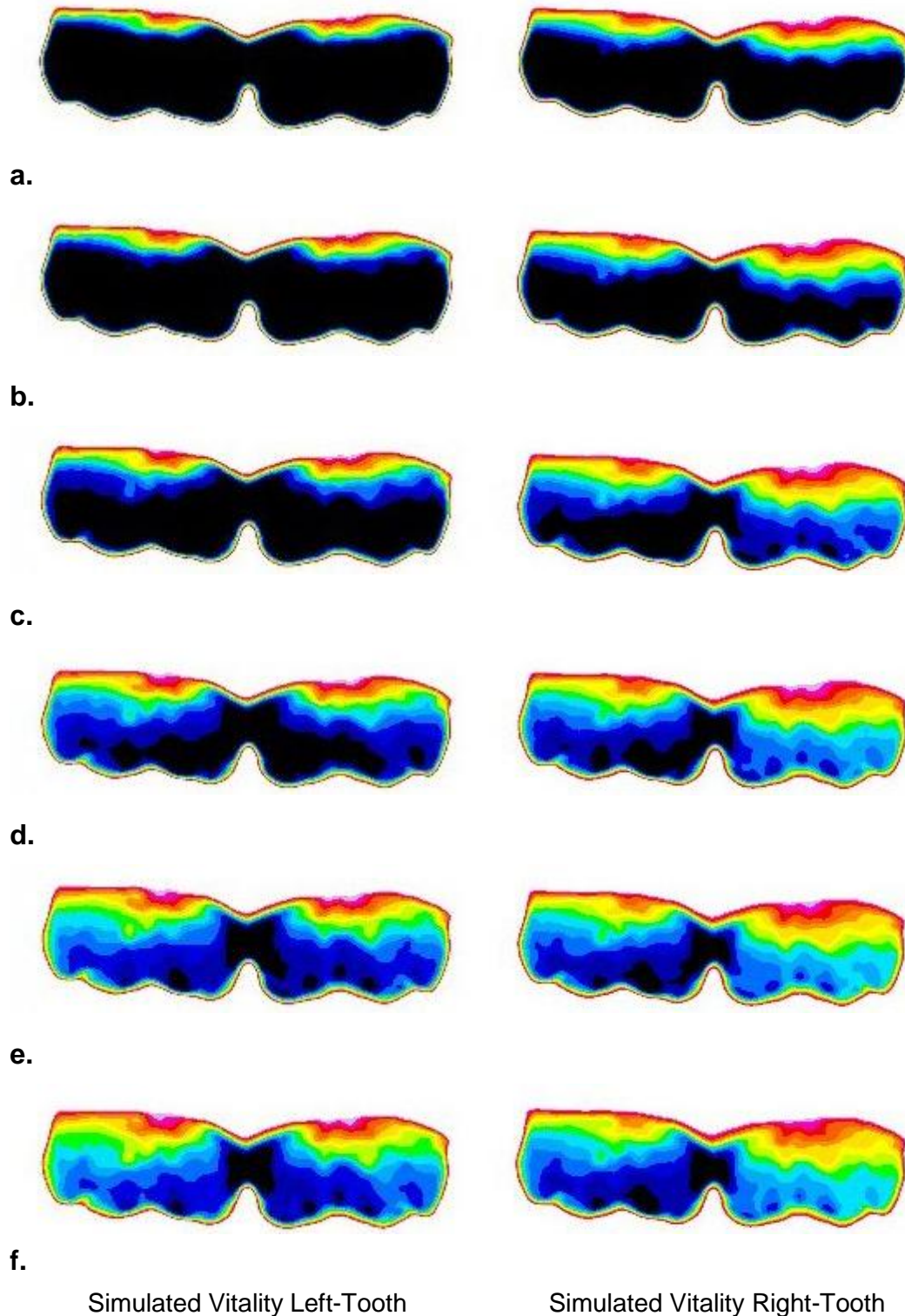
Figure 4-74 Colour Heat-Exchange Maps Pair 7 0.03ml/min flow-rate after cooling for 45 seconds where a. is 10, b. is 20, c. is 30, d. is 40, e. is 50 and f. is 60 seconds of re-warming to demonstrate simulated vitality seen by the increasing light-blue of the simulated vitality of the left-tooth and simulated vitality of the right-tooth, in respective sequences.

4.5.11 Statistical Tests

The opportunity to review data collected from the molar teeth under two simulated conditions – vital and non-vital – enabled analysis as 'Dissimilar Independent Molar Pairs' and 'Same Matched Molar Pairs'. The area-under-the-curve (^{o}C/Time) are presented below for each of the dissimilar independent molar pairs at four flow-rates, with and without pulse-effect. The differences are derived from subtracting the non-vital-data from the vital.

Table 4-53 Area-under-the-curve (^{o}C/Time) for dissimilar
independent molar teeth pairs when vital and non-vital,
with and without pulse-effect and the difference found at
a. 0.03ml/min flow-rate, b. 0.08ml/min flow-rate,
c. 0.15ml/min flow-rate, d. 0.5ml/min flow-rate.
L = left-tooth vital sequence, R = right-tooth vital sequence,
Diff = Difference.

a.

Area-Under-The-Curve (^{o}C/Time) Differences Independent Pairs 0.03ml/min						
	Difference in Vital and Non-vital Teeth			Difference in Pulsed Vital and Non-vital Teeth		
Pair	Vital	Non-vital	Diff	Vital	Non-vital	Diff
1a L	142426	144584	-2158	145231	145978	-747
2a	140556	141226	-671	141334	141477	-143
3a	144339	144452	-113	147186	146017	1169
4a	142636	143372	-736	144075	143726	349
5a	148336	148996	-660	146189	146264	-75
6a	142276	143020	-743	143429	143246	183
7a	142474	143174	-699	144600	142874	1726
8a	144560	143551	1010	147662	144508	3154
1b R	143438	141336	2102	146297	142885	3412
2b	146899	146083	816	143034	141829	1205
3b	140425	140016	409	140816	138490	2326
4b	143203	142368	835	143364	141636	1728
5b	142849	141527	1322	147872	146305	1568
6b	142658	140832	1827	144229	141206	3023
7b	150753	150935	-182	148722	146425	2297
8b	144656	145821	-1165	146978	147123	-145

b.

Area-Under-The-Curve (°C/Time) Differences Independent Pairs 0.08ml/min						
	Difference in Vital and Non-vital Teeth			Difference in Pulsed Vital and Non-vital Teeth		
Pair	Vital	Non-vital	Diff	Vital	Non-vital	Diff
1a L	143923	145397	-1474	144640	145511	-871
2a	141845	141371	475	141786	141109	677
3a	141561	140868	693	146406	145730	677
4a	144811	145156	-346	142413	142291	122
5a	148926	149593	-667	146383	146907	-524
6a	143214	143903	-689	144700	144563	137
7a	149049	148605	444	150259	148295	1964
8a	148320	146246	2074	150761	147014	3747
1b R	145716	142196	3520	151787	148476	3311
2b	147324	145622	1703	144704	142571	2133
3b	139159	138322	837	143767	141796	1971
4b	144989	143996	993	147831	146219	1612
5b	145725	143750	1975	151542	149853	1689
6b	144999	141447	3553	146827	141337	5490
7b	147141	145979	1162	149167	146390	2777
8b	152130	153069	-939	147149	147698	-549

c.

Area-Under-The-Curve (°C/Time) Differences Independent Pairs 0.15ml/min						
	Difference in Vital and Non-vital Teeth			Difference in Pulsed Vital and Non-vital Teeth		
Pair	Vital	Non-vital	Diff	Vital	Non-vital	Diff
1a L	146212	146827	-615	146552	147409	-857
2a	143647	142631	1016	143602	141877	1725
3a	142833	142843	-9	144655	143520	1135
4a	143065	143208	-143	142297	142515	-217
5a	152875	153217	-343	148795	149556	-760
6a	146431	145553	878	146492	144939	1553
7a	146383	146136	247	152349	150204	2145
8a	150048	147321	2727	153150	149861	3289
1b R	150411	146646	3764	148915	144479	4435
2b	147199	145668	1531	146429	144800	1629
3b	144778	143610	1167	144983	143109	1874
4b	143223	139910	3313	144547	141009	3538
5b	148468	146214	2254	148717	146239	2478
6b	147990	142699	5291	148825	143438	5387
7b	149730	147281	2448	149169	145030	4140
8b	149798	150336	-538	148215	148407	-191

d.

Area-Under-The-Curve (°C/Time) Differences Independent Pairs 0.5ml/min						
	Difference in Vital and Non-vital Teeth			Difference in Pulsed Vital and Non-vital Teeth		
Pair	Vital	Non-vital	Diff	Vital	Non-vital	Diff
1a L	150558	149966	592	148514	148580	-66
2a	146406	143900	2507	148203	145037	3166
3a	149924	149561	364	151328	150291	1037
4a	146009	146210	-201	147250	146125	1124
5a	151741	151590	151	147607	147432	175
6a	148759	147670	1088	149330	147374	1956
7a	150484	149063	1421	151791	149291	2500
8a	151318	148685	2633	151763	148557	3206
1b R	135357	130375	4982	125160	119670	5490
2b	148990	147953	1037	151580	151251	330
3b	148574	147070	1504	150350	148173	2176
4b	149150	145648	3502	149035	145147	3888
5b	149911	147566	2345	151478	149252	2226
6b	151827	146788	5038	150627	145638	4990
7b	149951	147181	2770	150994	147428	3566
8b	151309	151480	-171	150929	150712	217

4.5.11.1 Group Statistics - Non-Pulsed Dissimilar Independent Pairs

Table 4-54 Group Statistics - The mean area-under-the-curve (°C/Time) was greater for vital teeth in all flow-rates (0.03ml/min 143905 ± 2731, 0.08ml/min 145552 ± 3267, 0.15ml/min 147068 ± 3038, 0.5ml/min 148767 ± 3955°C/Time) compared to non-vital teeth (0.03ml/min 143831 ± 2972, 0.08ml/min 144720 ± 3653, 0.15ml/min 145631 ± 3229, 0.5ml/min 146919 ± 4856°C/Time), indicating a greater overall temperature during re-warming time for vital teeth.

Group Statistics

	Vitality Status	N	Mean	Std. Deviation	Std. Error Mean
AUC Independent Teeth 0.03ml/min	Vital	16	143905.2500	2731.06481	682.76620
	Non-vital	16	143830.8125	2972.25847	743.06462
AUC Independent Teeth 0.08ml/min	Vital	16	145552.0000	3266.99297	816.74824
	Non-vital	16	144720.0000	3652.62207	913.15552
AUC Independent Teeth 0.15ml/min	Vital	16	147068.1875	3038.00391	759.50098
	Non-vital	16	145631.2500	3228.83681	807.20920
AUC Independent Teeth 0.5ml/min	Vital	16	148766.7500	3954.95779	988.73945
	Non-vital	16	146919.1250	4855.90786	1213.97697

4.5.11.2 Satisfying the Test Assumptions - Non-Pulsed Dissimilar Independent Pairs

The dependent variable of time was a continuous scale and the independent variable (temperature) had two categorical dissimilar pair measurements of 'vital' and 'non-vital'. The data was assessed for outliers via Boxplots (Figure 4-75) and normality by the Shapiro-Wilk Test (Table 4-55) for each flow-rate.
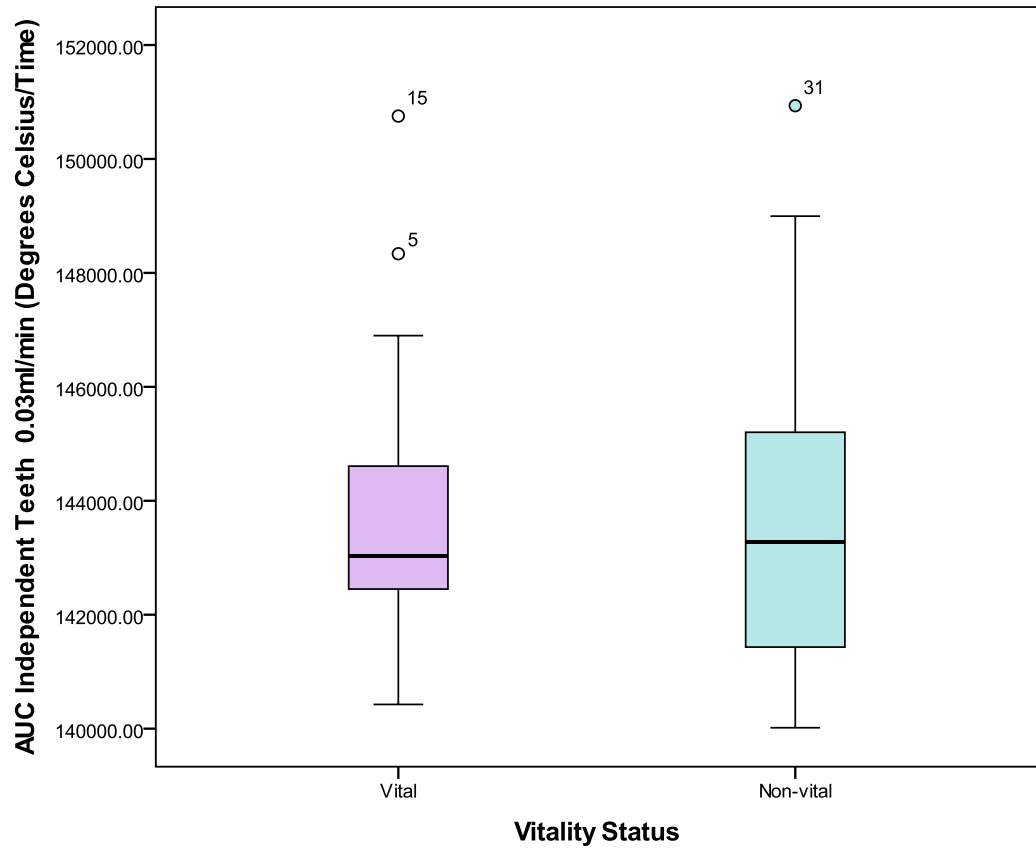
a.
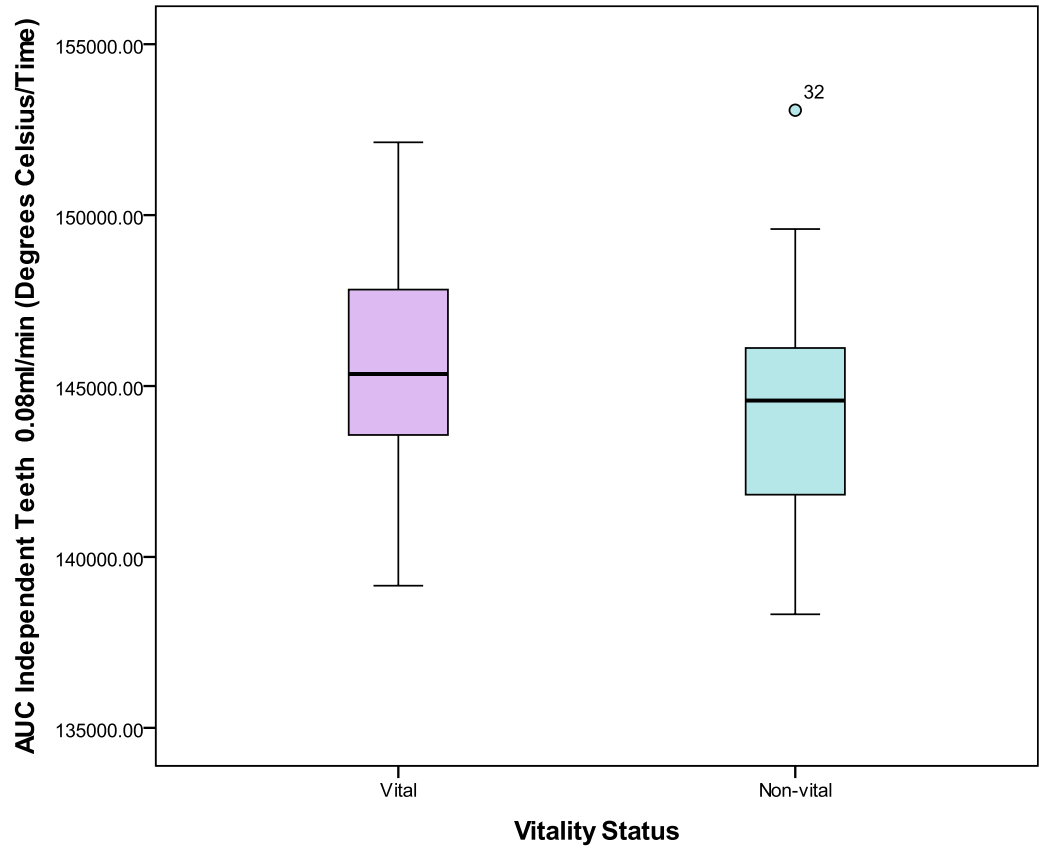
b.
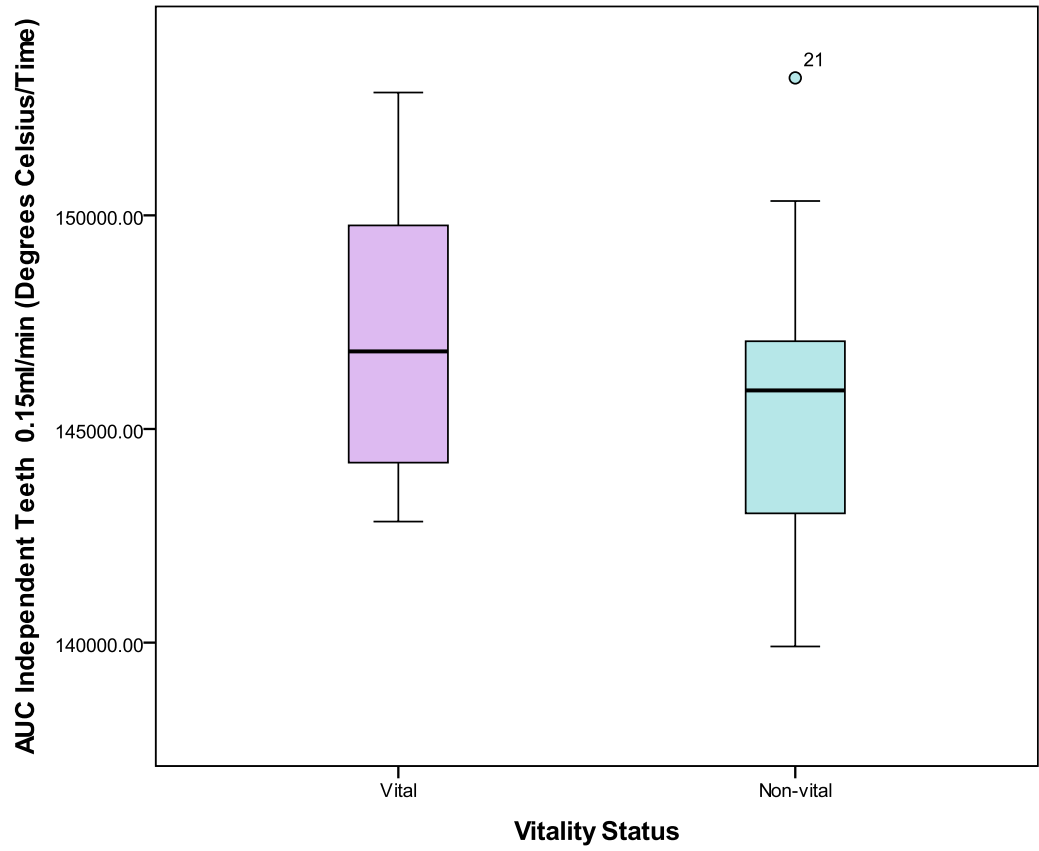
c.
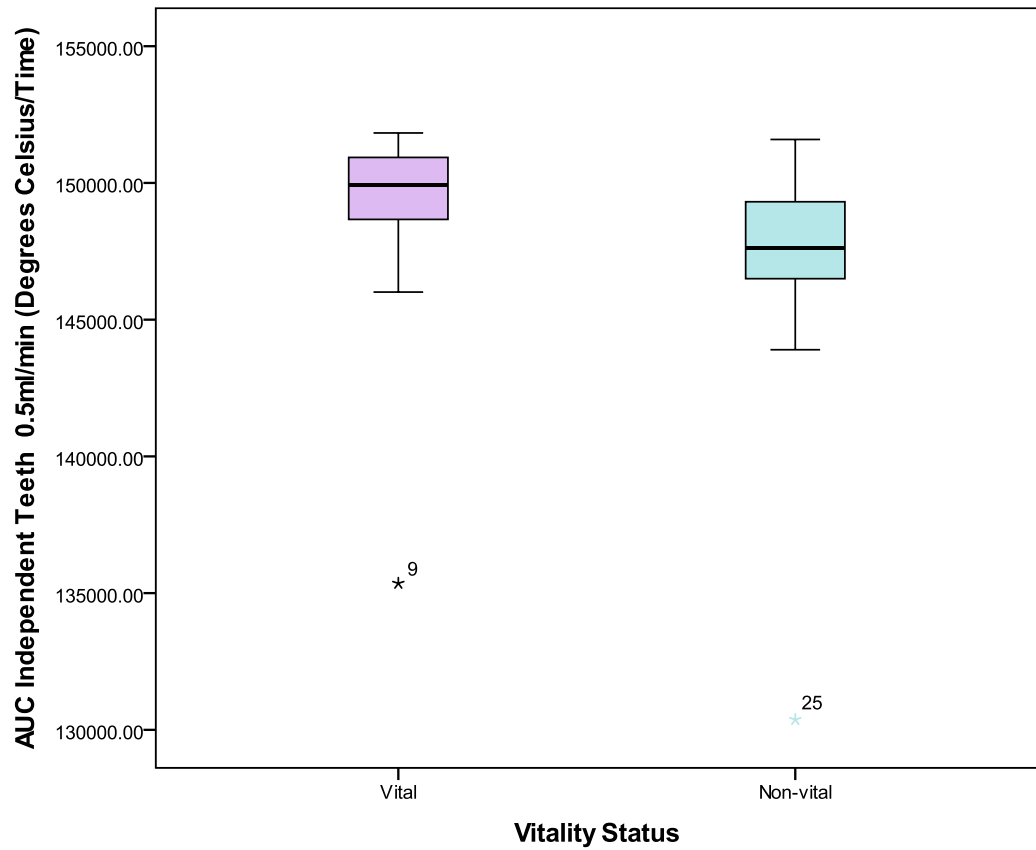
d.

Figure 4-75 Boxplots showing the distribution of area-under-the-curve (AUC) for independent dissimilar molar pairs when vital and non-vital (n=16), without a pulse, across four flow-rates a. 0.03ml/min, b. 0.08ml/min, c. 0.15ml/min, d. 0.5ml/min. Boxplots shows outliers in all flow-rates, which are extreme for flow-rate 0.5ml/min only, falling more than 3 box-lengths from the edge. As these are extreme outliers they could influence the statistical outcome for that flow-rate.

Table 4-55 Shapiro-Wilk Test for Normality for non-pulsed dissimilar independent pair-data all four flow-rates. The vital and non-vital area-under-the-curve was normally distributed except for the highest flow-rate of 0.5ml/min in both vital and non-vital simulations, and the vital simulation of 0.03ml/min as assessed by Shapiro-Wilk Test Sig. being less than 0.05. The 0.035 value was accepted.

Tests of Normality

	Vitality Status	Kolmogorov-Smirnov[a]			Shapiro-Wilk		
		Statistic	df	Sig.	Statistic	df	Sig.
AUC Independent Teeth 0.03ml/min	Vital	.204	16	.073	.877	16	.035
	Non-vital	.163	16	.200[*]	.911	16	.122
AUC Independent Teeth 0.08ml/min	Vital	.104	16	.200[*]	.989	16	.998
	Non-vital	.151	16	.200[*]	.969	16	.827
AUC Independent Teeth 0.15ml/min	Vital	.122	16	.200[*]	.949	16	.471
	Non-vital	.175	16	.200[*]	.947	16	.439
AUC Independent Teeth 0.5ml/min	Vital	.293	16	.001	.660	16	.000
	Non-vital	.272	16	.003	.679	16	.000

*. This is a lower bound of the true significance.

a. Lilliefors Significance Correction

The Independent-samples t-test was suitable to test statistical significance for three flow-rates, but not 0.5ml/min, which had extreme outliers and a Shapiro-Wilk value below 0.05. Thus, the Shapiro-Wilk null hypothesis was rejected ($p < .05$) indicating the data-distribution was not distributed normally. A non-parametric test was assessed for appropriateness for the flow-rate of 0.5ml/min, e.g., Mann-Whitney U test.

The data for the 0.5ml/min flow-rate satisfied the assumptions for the Mann-Whitney U test (a dependent variable on a continuous scale, with one independent variable with two categorical groupings – vital and non-vital – with independent observations, and the data was viewed as having the same shape – Independent Samples Mann-Whitney U test Population Pyramid Appendix A.8.1). The test was undertaken to determine differences in area-under-the-curve (^{o}C/Time) between vital and non-vital teeth.

4.5.11.3 Independent–Samples T-Test for Non-pulsed Dissimilar Independent Pairs

Table 4-56 Independent-Samples T-Test: There was homogeneity of variances for mean area-under-the-curve for vital and non-vital teeth, as assessed by Levene's Test for Equality of Variances for the three flow-rates tested (0.03ml/min p = 0.733, 0.08ml/min p = 0.748 and 0.15ml/min p = 0.850). The mean area-under-the-curve (AUC -^{o}C/Time) for vital teeth was higher in the three flow-rates than the non-vital teeth by 74 (95% CI, -1987 to 2135) for flow-rate 0.03ml/min, 832 (95% CI, -1670 to 3334) for flow-rate 0.08ml/min and 1437 (95% CI, -827 to 3701) for flow-rate 0.15ml/min. No statistically significant difference in mean area-under-the-curve was found between vital and non-vital teeth: flow-rate 0.03ml/min p = 0.942, flow-rate 0.08ml/min p = 0.502 and flow-rate 0.15ml/min p = 0.205.

Independent Samples Test

		Levene's Test for Equality of Variances		t-test for Equality of Means						95% Confidence Interval of the Difference	
		F	Sig.	t	df	Sig. (2-tailed)	Mean Difference	Std. Error Difference		Lower	Upper
AUC Independent Teeth 0.03ml/min	Equal variances assumed	.119	.733	.074	30	.942	74.43750	1009.11581		-1986.45192	2135.32692
	Equal variances not assumed			.074	29.788	.942	74.43750	1009.11581		-1987.06813	2135.94313
AUC Independent Teeth 0.08ml/min	Equal variances assumed	.105	.748	.679	30	.502	832.00000	1225.12477		-1670.03856	3334.03856
	Equal variances not assumed			.679	29.634	.502	832.00000	1225.12477		-1671.33459	3335.33459
AUC Independent Teeth 0.15ml/min	Equal variances assumed	.036	.850	1.296	30	.205	1436.93750	1108.34491		-826.60477	3700.47977
	Equal variances not assumed			1.296	29.889	.205	1436.93750	1108.34491		-826.95624	3700.83124
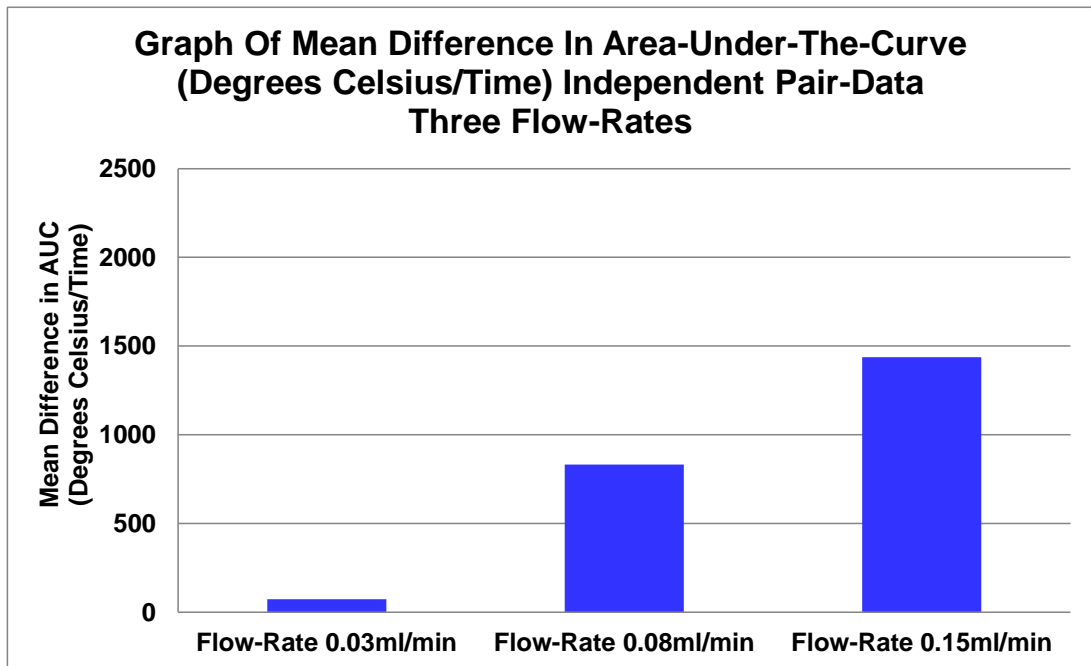
Figure 4-76 Graph of mean differences of area-under-the-curve (AUC) for three flow-rates (0.03ml/min, 0.08ml/min and 0.15ml/min) showing a greater mean difference with increasing flow-rate.

For the independent, dissimilar paired molar teeth with simulated vitality, this Study rejects the alternative hypothesis and fails to reject the null hypothesis for three flow-rates of 0.03ml/min, 0.08ml/min and 0.15ml/min.

4.5.11.4 Mann-Whitney U Test for Non-Pulsed Dissimilar Independent Pairs

Table 4-57 Mann-Whitney U Test: Area-under-the-curve for vital and non-vital teeth was not statistically significantly different where p = 0.056 using an exact sampling distribution for U.

Hypothesis Test Summary

	Null Hypothesis	Test	Sig.	Decision
1	The distribution of AUC Independent Teeth 0.5ml/min is the same across categories of Vitality Status.	Independent-Samples Mann-Whitney U Test	.056[1]	Retain the null hypothesis.

Asymptotic significances are displayed. The significance level is .05.

[1] Exact significance is displayed for this test.

For the independent, dissimilar paired molar teeth with simulated vitality, this Study rejects the alternative hypothesis and fails to reject the null hypothesis for flow-rate of 0.5ml/min.

4.5.11.5 Summary of Statistical Tests for Non-Pulsed Dissimilar Independent Molar Pairs

For the independent, dissimilar paired molar teeth with simulated vitality, this Study rejects the alternative hypothesis and fails to reject the null hypothesis for all four flow-rates.

4.5.11.6 Group Statistics - Pulsed Dissimilar Independent Pairs

A similar analysis was undertaken for simulation with a pulse.

Table 4-58 Group Statistics - The mean area-under-the-curve (AUC) was greater for vital teeth in all flow-rates (0.03ml/min 145064 ± 2346, 0.08ml/min 146883 ± 3153, 0.15ml/min 147356 ± 2987, 0.5ml/min 148496 ± 6409°C/Time), compared to non-vital teeth (0.03ml/min 143749 ± 2467, 0.08ml/min 145360 ± 2779, 0.15ml/min 145400 ± 2924, 0.5ml/min 146247 ± 7338°C/Time), indicating a greater overall temperature during re-warming time for vital teeth.

Group Statistics

	Vitality Status	N	Mean	Std. Deviation	Std. Error Mean
AUC Pulse Independent Teeth 0.03ml/min	Vital	16	145063.6250	2345.61554	586.40388
	Non-vital	16	143749.3125	2467.04005	616.76001
AUC Pulsed Independent Teeth 0.08ml/min	Vital	16	146882.6250	3152.48981	788.12245
	Non-vital	16	145360.0000	2779.14253	694.78563
AUC Pulsed Independent Teeth 0.15ml/min	Vital	16	147355.7500	2986.54836	746.63709
	Non-vital	16	145399.5000	2923.91452	730.97863
AUC Pulse Independent Teeth 0.5ml/min	Vital	16	148496.1875	6408.72255	1602.18064
	Non-vital	16	146247.3750	7337.48599	1834.37150

4.5.11.7 Satisfying the Test Assumptions - Pulsed Dissimilar Independent Pairs

The dependent variable of time was a continuous scale and the independent variable (temperature) had two categorical dissimilar pair measurements of 'vital' and 'non-vital'. The data was assessed for outliers via Boxplots (Figure 4-77) and normality by the Shapiro-Wilk Test (Table 4-59) for each flow-rate.
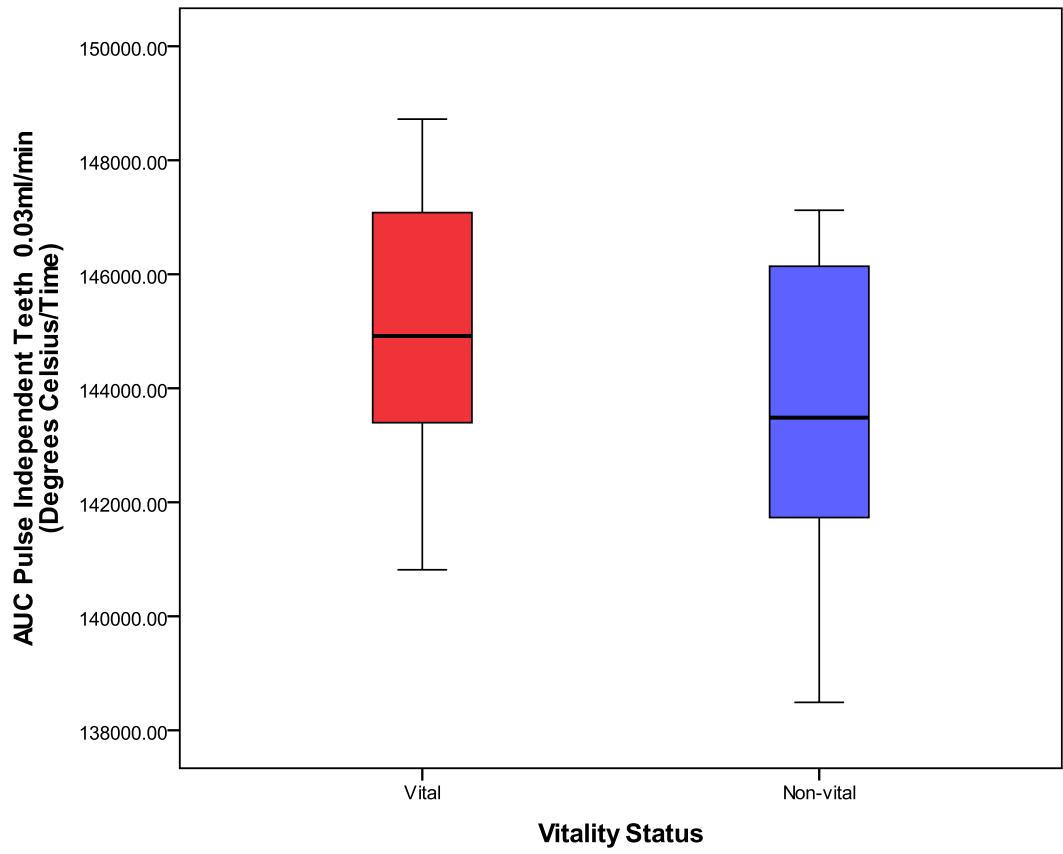
a.
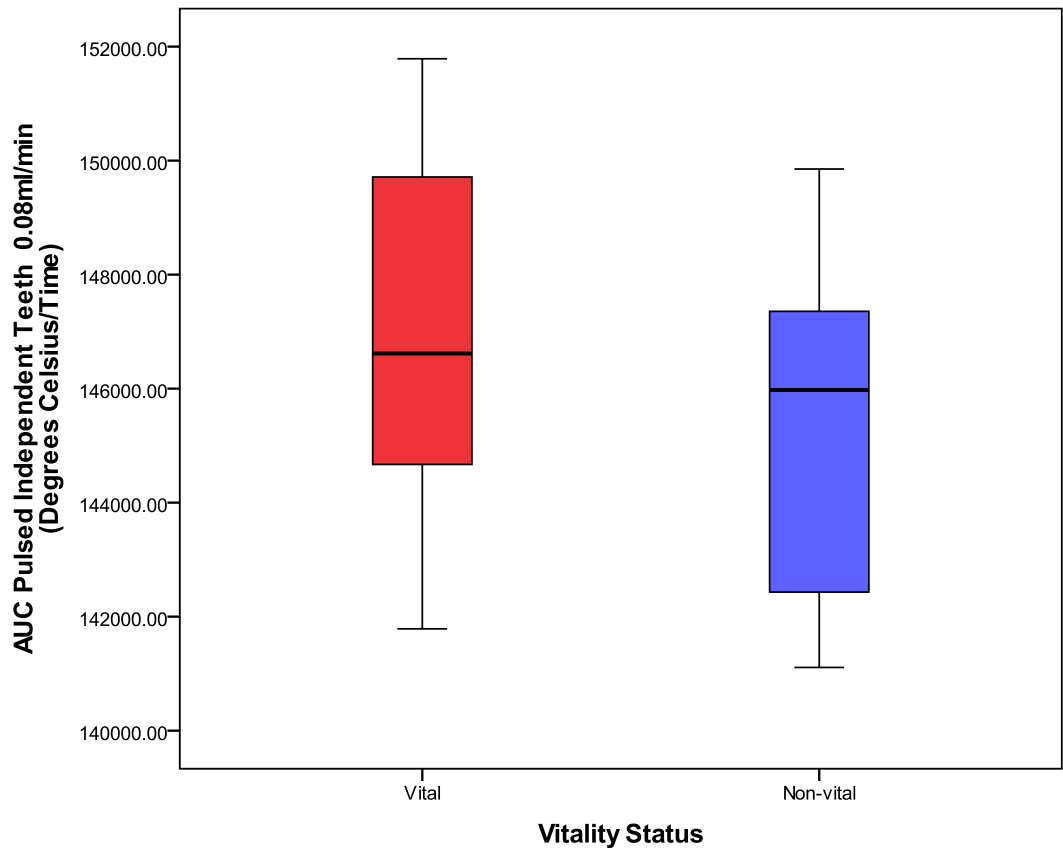
b.
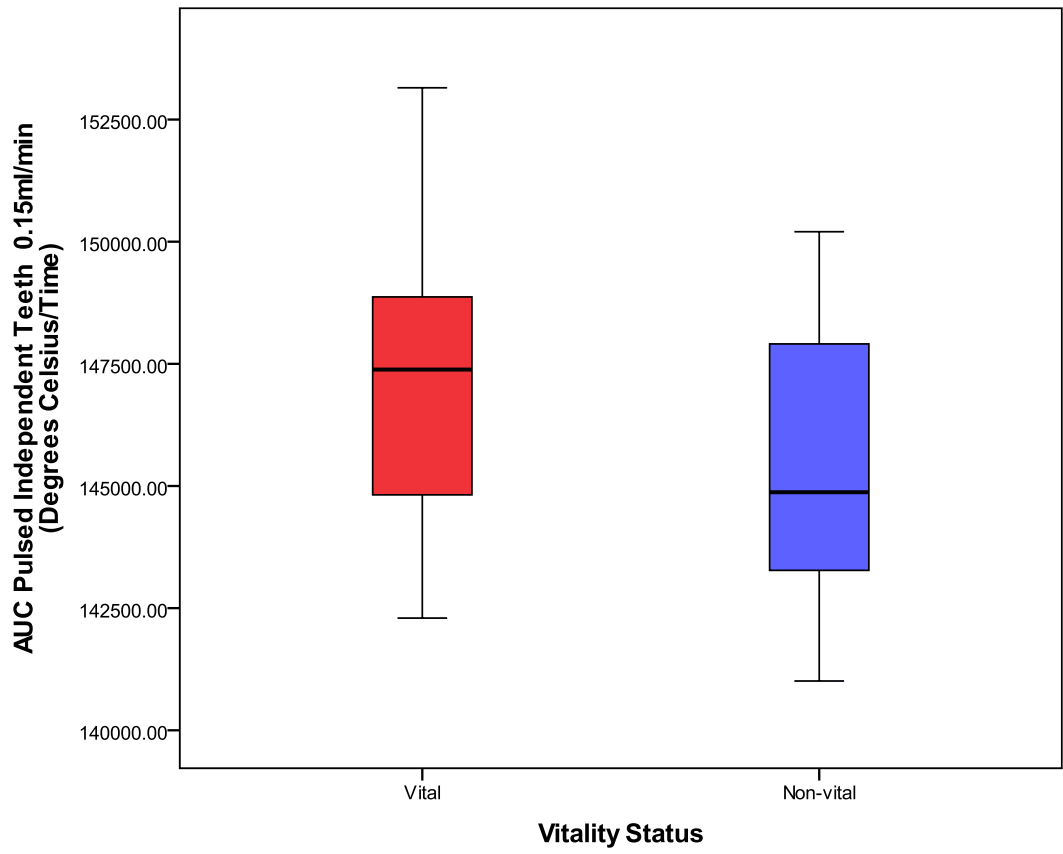
c.
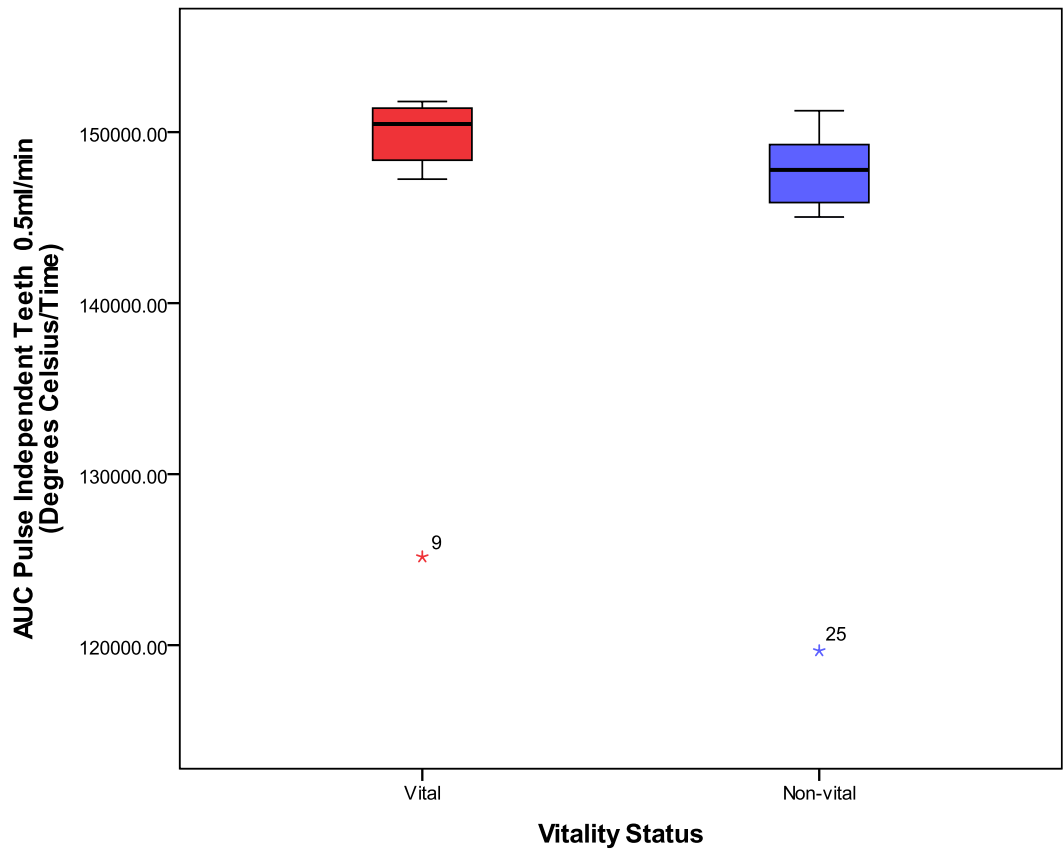
d.

Figure 4-77 Boxplots showing distribution of area-under-the-curve for independent dissimilar molar pairs when vital and non-vital (n=16), with a pulse, across four flow-rates (0.03ml/min, 0.08ml/min, 0.15ml/min and 0.5ml/min). Boxplot shows two extreme outliers for flow-rate 0.5ml/min, falling more than 3 box-lengths from the edge and they could influence the outcome for that flow-rate.

Table 4-59 Shapiro-Wilk Test for Normality for pulsed dissimilar independent pair data all four flow-rates. The vital and non-vital area-under-the-curve was normally distributed except for the highest flow-rate of 0.5ml/min in both vital and non-vital simulations which had Shapiro-Wilk Sig. both less than 0.05

Tests of Normality

		Kolmogorov-Smirnov[a]			Shapiro-Wilk		
	Vitality Status	Statistic	df	Sig.	Statistic	df	Sig.
AUC Pulse Independent Teeth 0.03ml/min	Vital	.122	16	.200*	.965	16	.746
	Non-vital	.192	16	.118	.931	16	.255
AUC Pulsed Independent Teeth 0.08ml/min	Vital	.130	16	.200*	.954	16	.561
	Non-vital	.155	16	.200*	.933	16	.272
AUC Pulsed Independent Teeth 0.15ml/min	Vital	.147	16	.200*	.957	16	.611
	Non-vital	.175	16	.200*	.937	16	.313
AUC Pulse Independent Teeth 0.5ml/min	Vital	.360	16	.000	.485	16	.000
	Non-vital	.372	16	.000	.520	16	.000

*. This is a lower bound of the true significance.

a. Lilliefors Significance Correction

The Independent-samples t-test was suitable to test statistical significance for three flow-rates. Flow-rate 0.5ml/min, which had extreme outliers and a Shapiro-Wilk value below 0.05 and the Shapiro-Wilk null hypothesis was rejected ($p < .05$) indicating the data-distribution was not distributed normally. A non-parametric test was appropriate for the flow-rate of 0.5ml/min, e.g., Mann-Whitney U test.

The data for flow-rate 0.5ml/min with simulated pulse satisfied the assumptions for the Mann-Whitney U test (a dependent variable on a continuous scale, with one independent variable with two categorical groupings – vital and non-vital – with independent observations, and the data was viewed as having the same shape – Population Pyramid appendix A.8.2). The test was undertaken to determine differences in area-under-the-curve (^{o}C/Time) between the vital and non-vital teeth with a simulated pulse.

4.5.11.8 Independent–Samples T-Test for Pulsed Dissimilar Independent Pairs

Table 4-60 Independent-Samples T-Test: There was homogeneity of variances for the mean area-under-the-curve for vital and non-vital teeth with a simulated pulse, as assessed by Levene's Test for Equality of Variances for three flow-rates tested (0.03ml/min p = 0.832, 0.08ml/min p = 0.689 and 0.15ml/min p = 0.998). The mean area-under-the - curve (^{o}C/Time) for vital teeth was higher in the three flow-rates than the non-vital teeth by 1314 (95% CI, -424 to 3052) for flow-rate 0.03ml/min, 1523 (95% CI, -623 to 3668) for flow-rate 0.08ml/min and 1956 (95% CI, -178 to 4090) for flow-rate 0.15ml/min. No statistically significant difference in mean area-under-the-curve was found between vital and non-vital teeth with a simulated pulse: flow-rate 0.03ml/min p = 0.133, flow-rate 0.08ml/min p = 0.158 and flow-rate 0.15ml/min p = 0.071.

Independent Samples Test

		Levene's Test for Equality of Variances		t-test for Equality of Means						
									95% Confidence Interval of the Difference	
		F	Sig.	t	df	Sig. (2-tailed)	Mean Difference	Std. Error Difference	Lower	Upper
AUC Pulse Independent Teeth 0.03ml/min	Equal variances assumed	.046	.832	1.544	30	.133	1314.31250	851.03609	-423.73507	3052.36007
	Equal variances not assumed			1.544	29.924	.133	1314.31250	851.03609	-423.92043	3052.54543
AUC Pulsed Independent Teeth 0.08ml/min	Equal variances assumed	.164	.689	1.449	30	.158	1522.62500	1050.64936	-623.08725	3668.33725
	Equal variances not assumed			1.449	29.536	.158	1522.62500	1050.64936	-624.50275	3669.75275
AUC Pulsed Independent Teeth 0.15ml/min	Equal variances assumed	.000	.998	1.872	30	.071	1956.25000	1044.89076	-177.70162	4090.20162
	Equal variances not assumed			1.872	29.987	.071	1956.25000	1044.89076	-177.74181	4090.24181
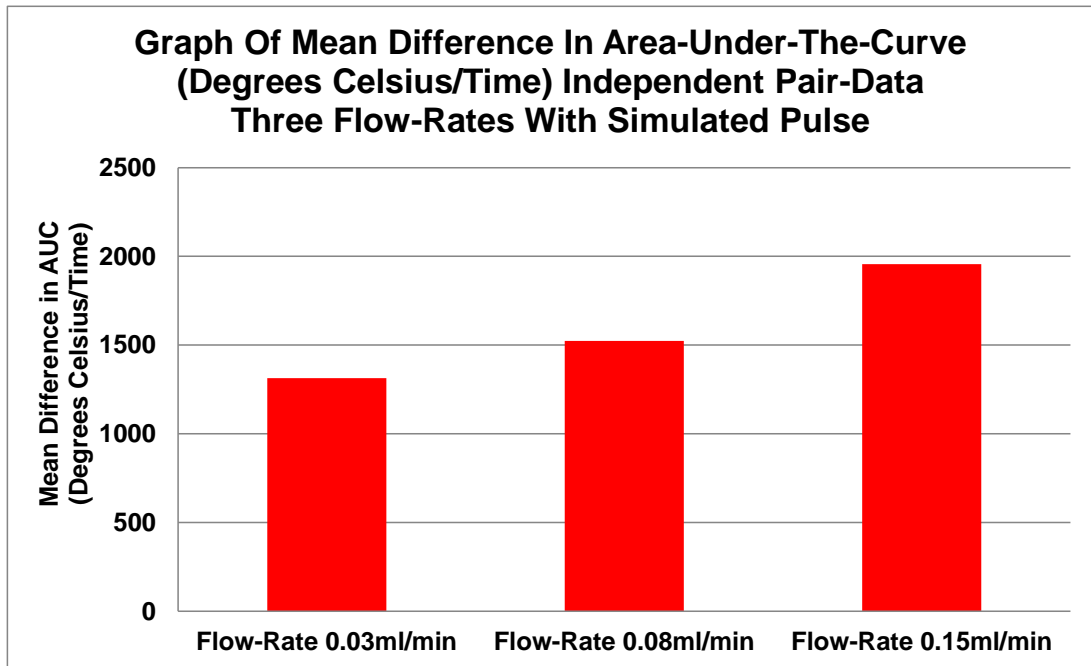
Figure 4-78 Graph of mean difference of area-under-the-curve (AUC) for three flow-rates (0.03ml/min, 0.08ml/min and 0.15ml/min) showing a greater mean difference with increasing flow-rate.

For the independent, dissimilar paired molar teeth with pulsed simulated vitality, this Study rejects the alternative hypothesis and fails to reject the null hypothesis for three flow-rates of 0.03ml/min, 0.08ml/min and 0.15ml/min.

4.5.11.9 Mann-Whitney U Test for Pulsed Dissimilar Independent Pairs

Table 4-61 Mann-Whitney U Test: Area-under-the-curve for vital and non-vital teeth was statistically significantly different where p = 0.012 using an exact sampling distribution for U.

Hypothesis Test Summary

	Null Hypothesis	Test	Sig.	Decision
1	The distribution of AUC Pulse Independent Teeth 0.5ml/min is the same across categories of Vitality Status.	Independent-Samples Mann-Whitney U Test	.012[1]	Reject the null hypothesis.

Asymptotic significances are displayed. The significance level is .05.

[1] Exact significance is displayed for this test.

For the independent, dissimilar paired molar teeth with pulsed simulated vitality, this Study rejects the null hypothesis for flow-rate of 0.5ml/min.

4.5.11.10 Summary of Statistical Tests for Pulsed
Dissimilar Independent Molar Pairs

For the independent, dissimilar paired molar teeth with pulsed simulated vitality, this Study rejects the alternative hypothesis and fails to reject the null hypothesis for three flow-rates 0.03ml/min, 0.08ml/min and 0.15ml/min and rejects the null hypothesis for 0.5ml/min.

4.5.11.11 Same Matched Molar Pairs of Teeth with Vital
and Non-Vital-Data

The opportunity to review data collected from the molar teeth under two conditions – vital and non-vital – enabled analysis as 'Dissimilar Independent Molar Pairs' as just described, and 'Same Matched Molar Pairs' which will be described next. The area-under-the-curve (^{o}C/Time) is presented below for each of the 'Same Matched Molar Pairs' at four flow-rates, with and without pulse-effect. The difference is derived from subtracting the non-vital-data from the vital. Statistical testing was performed as same paired, rather than independent as per the dissimilar teeth.

Table 4-62 Area-under-the-curve for same matched pairs of molar teeth when vital and non-vital, with and without pulse-effect and the difference found at a. 0.03ml/min flow-rate, b. 0.08ml/min flow-rate, c. 0.15ml/min flow-rate, d. 0.5ml/min flow-rate. L = left-tooth vital sequence, R = right-tooth vital sequence, Diff = Difference.

a.

Area-Under-The-Curve Difference Same Pairs 0.03ml/min					
	Difference in Vital and Non-vital Teeth			Difference in Pulsed Vital and Non-vital Teeth		
Pair	Vital	Non-vital	Diff	Vital	Non-vital	Diff
1a L	142476	141336	1140	145231	143028	2203
2a	142235	146083	-3849	141414	141829	-414
3a	144339	140016	4323	147186	139949	7236
4a	142636	142588	48	144075	142229	1846
5a	148336	142253	6083	147996	146305	1691
6a	142276	141296	980	143429	141673	1756
7a	148486	150935	-2449	146187	146425	-239
8a	146443	145821	623	149972	147123	2849
1b R	143438	144728	-1289	146412	145978	434
2b	146899	142571	4328	143034	141596	1437
3b	140425	144452	-4027	142309	146017	-3708
4b	143401	143372	29	143668	143726	-58
5b	143470	148996	-5526	147872	147764	108
6b	142954	143020	-66	144578	143246	1332
7b	150753	148367	2386	148722	144011	4711
8b	144656	145400	-744	146978	147068	-90

b.

Area-Under-The-Curve Difference Same Pairs 0.08ml/min						
	Difference in Vital and Non-vital Teeth			Difference in Pulsed Vital and Non-vital Teeth		
Pair	Vital	Non-vital	Diff	Vital	Non-vital	Diff
1a L	143923	142700	1223	147463	148476	-1013
2a	141845	145806	-3960	142122	142571	-449
3a	141561	139671	1890	146488	141796	4692
4a	145077	143996	1081	143855	146219	-2364
5a	148926	145281	3645	151004	149853	1151
6a	143214	141543	1671	144700	142578	2122
7a	149049	146960	2090	150259	147741	2518
8a	153670	153069	600	151956	147698	4258
1b R	146133	145397	735	151787	148342	3445
2b	147536	141371	6165	144704	141438	3265
3b	140581	140868	-286	143767	145739	-1972
4b	144989	145437	-448	147831	143625	4207
5b	146915	149593	-2678	151542	150947	595
6b	145032	143903	1128	147701	144563	3138
7b	148168	148605	-437	150477	148295	2182
8b	152130	151964	166	147149	148352	-1203

c.

Area-Under-The-Curve Difference Same Pairs 0.15ml/min						
	Difference in Vital and Non-vital Teeth			Difference in Pulsed Vital and Non-vital Teeth		
Pair	Vital	Non-vital	Diff	Vital	Non-vital	Diff
1a L	147306	146646	659	146761	144479	2282
2a	143783	145668	-1885	144233	144800	-568
3a	142922	143610	-688	144962	143109	1854
4a	143065	140306	2758	142297	141294	1003
5a	152875	149353	3522	148795	146557	2238
6a	146431	142875	3556	146492	143438	3053
7a	147116	147281	-166	152349	149115	3234
8a	152180	150336	1844	153150	148911	4239
1b R	150411	147816	2595	148915	147521	1393
2b	147199	142910	4289	146429	142561	3869
3b	144778	142860	1917	144983	143699	1284
4b	143419	143208	211	144677	142515	2163
5b	150951	153217	-2266	148921	149556	-635
6b	148089	145553	2536	148825	144939	3886
7b	149730	146737	2993	152207	150204	2002
8b	149798	147321	2477	148764	149861	-1097

d.

Area-Under-The-Curve Difference Same Pairs 0.5ml/min					
Pair	Difference in Vital and Non-vital Teeth			Difference in Pulsed Vital and Non-vital Teeth		
Pair	Vital	Non-vital	Diff	Vital	Non-vital	Diff
1a L	134077	131055	3023	121750	119931	1819
2a	147226	147953	-728	150973	151251	-277
3a	149924	148343	1582	151444	148173	3271
4a	146009	146131	-123	147250	145147	2103
5a	151741	148797	2944	150446	149252	1194
6a	149424	146788	2636	149330	145992	3338
7a	150274	147828	2446	151935	147015	4920
8a	154101	151480	2620	145319	141850	3469
1b R	134380	132073	2308	124110	120643	3467
2b	148990	144741	4249	151580	147703	3878
3b	150125	149561	564	150350	150478	-129
4b	149334	146210	3123	149035	146125	2909
5b	150868	151590	-723	151478	149823	1654
6b	151827	148253	3573	150912	147374	3538
7b	150072	148546	1526	150389	149230	1159
8b	151309	151797	-488	144938	145489	-552

4.5.11.12 Group Statistics – Non-Pulsed Same Matched Pairs

Analysis was undertaken for non-pulsed same matching molar pairs.

Table 4-63 Group Statistics - The mean area-under-the-curve was greater for vital teeth in all flow-rates (0.03ml/min 144576 ± 2819, 0.08ml/min 146172 ± 3678, 0.15ml/min 147503 ± 3283, 0.5ml/min 148211 ± 5771°C/Time), compared to non-vital teeth (0.03ml/min 144452 ± 3032, 0.08ml/min 145385 ± 3902, 0.15ml/min 145981 ± 3318, 0.5ml/min 146430 ± 6140°C/Time), indicating a greater overall temperature during re-warming time for vital teeth.

Paired Samples Statistics

		Mean	N	Std. Deviation	Std. Error Mean
Pair 1	AUC Vital Same Pair 0.03ml/min	144576.4375	16	2819.33898	704.83474
	AUC Non-vital Same Pair 0.03ml/min	144452.1250	16	3032.34587	758.08647
Pair 2	AUC Vital Same Pair 0.08ml/min	146171.8125	16	3678.10553	919.52638
	AUC Non-vital Same Pair 0.08ml/min	145385.2500	16	3901.58434	975.39608
Pair 3	AUC Vital Same Pair 0.15ml/min	147503.3125	16	3283.31635	820.82909
	AUC Non-vital Same Pair 0.15ml/min	145981.0625	16	3318.42891	829.60723
Pair 4	AUC Vital Same Pair 0.5 ml/min	148211.2500	16	5770.80431	1442.70108
	AUC Non-vital Same Pair 0.5ml/min	146430.0000	16	6140.26373	1535.06593

### 4.5.11.13 Satisfying the Test Assumptions Non-Pulsed Same Matched Pairs

The dependent variable of time is a continuous scale and the independent variable (temperature) has two categorical 'same' pairs, measurements were made as 'vital' and 'non-vital', which enables the area-under-the-curve (^{o}C/Time) to be calculated.

The difference of each same pair for all four flow-rates, without a pulse, (vital minus non-vital) were assessed for outliers via Boxplots (Figure 4-79) and normality by the Shapiro-Wilk Test (Table 4-64) for each flow-rate.
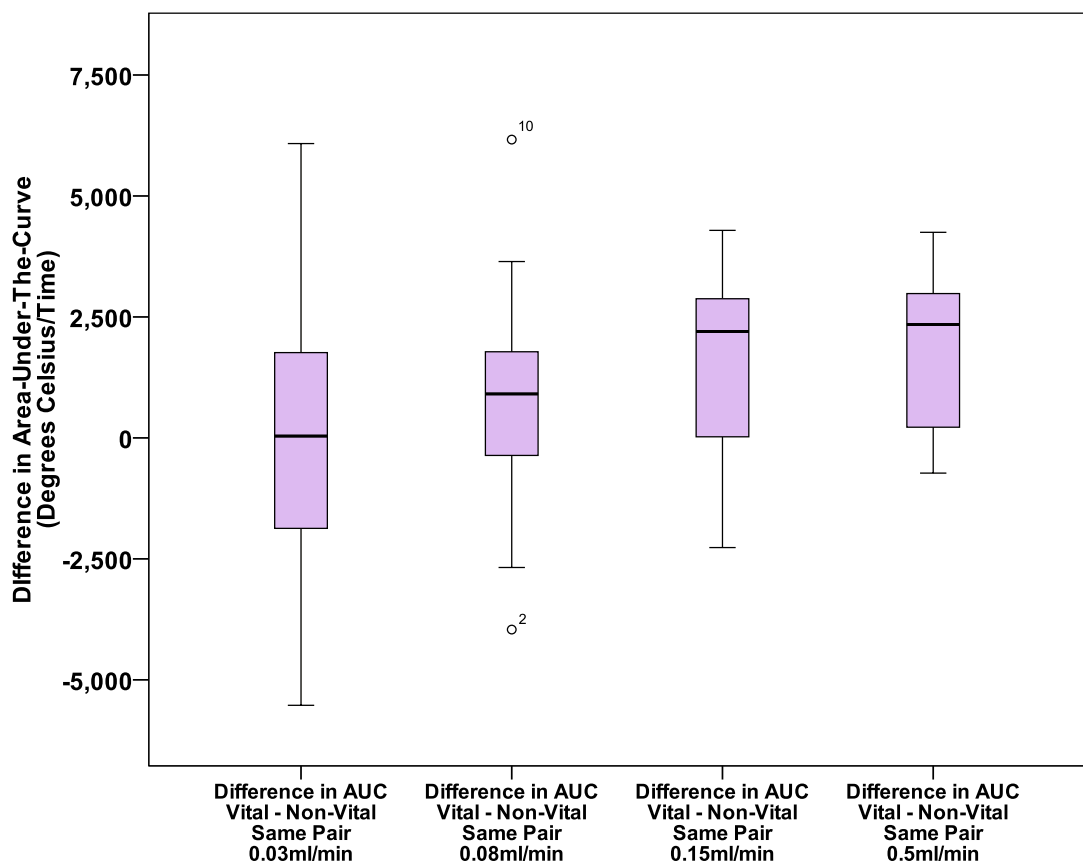
Figure 4-79 Boxplot of distribution of difference in area-under-the-curve for same pair vital and non-vital testing, without a pulse, across four flow-rates (0.03ml/min, 0.08ml/min, 0.15ml/min and 0.5ml/min). Boxplot shows two outliers for flow-rate 0.08ml/min, both from Pair 2 (2 = 2a and 10 = 2b). The outliers fall more than 1.5 box-lengths from the edge and this pairing had the restored tooth, unlike all other pairs. These are not extreme outliers to unduly influence the outcome and it was decided to retain the values as true for this analysis, in the knowledge the pairing is different due to the restoration.

Table 4-64 Shapiro-Wilk Test for Normality for non-pulsed same matched pairs for all four flow-rates. The difference between vital and non-vital teeth was normally distributed, as assessed by Shapiro-Wilk Test Sig. column which provided the following values all above 0.05: flow-rate 0.03ml/min p = 0.901, flow-rate 0.08ml/min p = 0.438, flow-rate 0.15ml/min p = 0.216, flow-rate 0.5ml/min p = 0.131.

Tests of Normality

	Kolmogorov-Smirnov[a]			Shapiro-Wilk		
	Statistic	df	Sig.	Statistic	df	Sig.
Difference in AUC Vital - Non-vital Same Pair 0.03 ml/min	.125	16	.200[*]	.974	16	.901
Difference in AUC Vital - Non-vital Same Pair 0.08 ml/min	.172	16	.200[*]	.947	16	.438
Difference in AUC Vital - Non-vital Same Pair 0.15 ml/min	.189	16	.128	.927	16	.216
Difference in AUC Vital - Non-vital Same Pair 0.5 ml/min	.190	16	.124	.913	16	.131

*. This is a lower bound of the true significance.

a. Lilliefors Significance Correction

The Paired-samples t-test was suitable to test statistical significance for all flow-rates.

Table 4-65 Paired T-Test - Statistical significance of mean difference between the overall temperature of vital and non-vital teeth was determined with the paired-samples t-test using the area-under-the-curve (^{o}C/Time) during the re-warming time selected. A non-statistically significant increase of 124 (95% CI, -1574 to 1822), p = 0.878, and 787 (95% CI, -447 to 2020), p = 0.194, was shown for flow-rates 0.03ml/min and 0.08ml/min, respectively. A statistically significant increase of 1522 (95% CI, 466 to 2579), p = 0.008, and 1781 (95% CI, 922 to 2640), p = 0.0005, was shown for flow-rates 0.15ml/min and 0.5ml/min, respectively.

Paired Samples Test

		Paired Differences							
					95% Confidence Interval of the Difference				
		Mean	Std. Deviation	Std. Error Mean	Lower	Upper	t	df	Sig. (2-tailed)
Pair 1	AUC Vital Same Pair 0.03ml/min - AUC Non-vital Same Pair 0.03 ml/min	124.31250	3186.41566	796.60392	-1573.60855	1822.23355	.156	15	.878
Pair 2	AUC Vital Same Pair 0.08ml/min - AUC Non-vital Same Pair 0.08 ml/min	786.56250	2314.11976	578.52994	-446.54488	2019.66988	1.360	15	.194
Pair 3	AUC Vital Same Pair 0.15ml/min - AUC Non-vital Same Pair 0.15 ml/min	1522.25000	1983.06045	495.76511	465.55168	2578.94832	3.071	15	.008
Pair 4	AUC Vital Same Pair 0.5 ml/min - AUC Non-vital Same Pair 0.5ml/min	1781.25000	1611.83914	402.95978	922.36155	2640.13845	4.420	15	.000
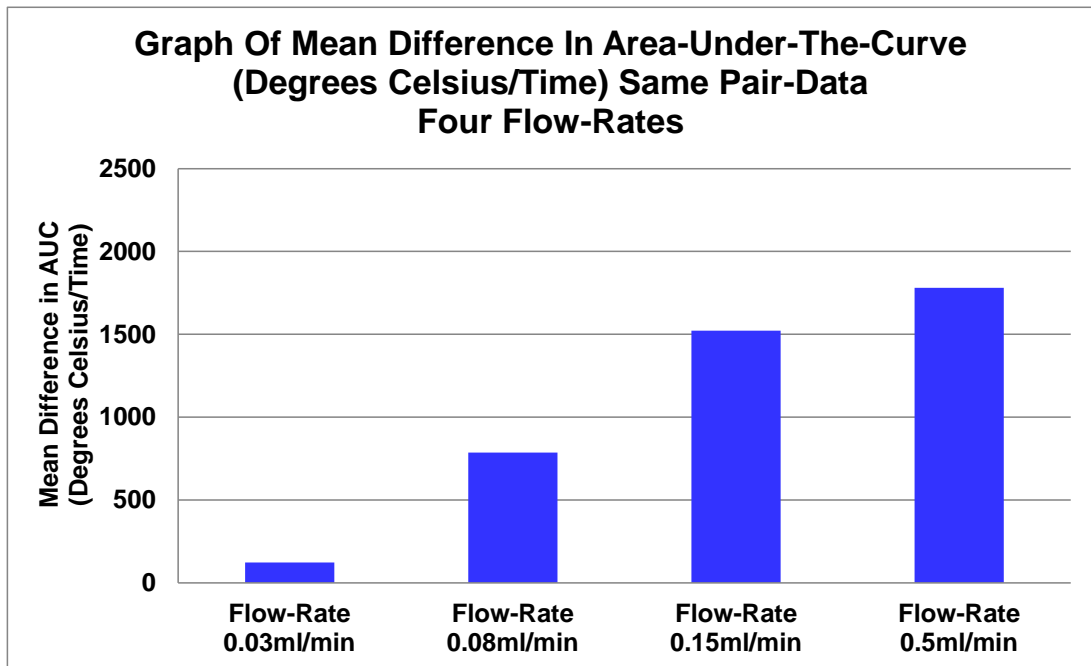
Figure 4-80 Graph of mean difference of area-under-the-curve for four flow-rates which increases with increasing flow-rate.

The mean difference was statistically significantly different from zero for flow-rates 0.15ml/min and 0.5ml/min and, therefore, the null hypothesis can be rejected and the alternative hypothesis accepted. This was not the case for flow-rates 0.08ml/min and 0.03ml/min and this Study fails to reject the null hypothesis and rejects the alternative hypothesis.

4.5.11.14 Summary of Statistical Tests for Non-Pulsed Same Matched Molar Pairs

The null hypothesis can be rejected in favour of the alternative hypothesis for flow-rates 0.15ml/min and 0.5ml/min.

4.5.11.15 Group Statistics – Pulsed Same Matched Pairs

Table 4-66 Group Statistics - the mean area-under-the-curve (^oC/Time) was greater for vital teeth in all flow-rates (0.03ml/min 145566 ± 2477, 0.08ml/min 147675 ± 3224, 0.15ml/min 147673 ± 3134, 0.5ml/min 146417 ± 9436), compared to non-vital teeth (0.03ml/min 144248 ± 2430, 0.08ml/min 146140 ± 3023, 0.15ml/min 145785 ± 3017, 0.5ml/min 144205 ± 9631), indicating a greater overall temperature during re-warming time for vital teeth.

Paired Samples Statistics

		Mean	N	Std. Deviation	Std. Error Mean
Pair 1	AUC Pulsed Vital Same Pair 0.03ml/min	145566.4375	16	2477.28354	619.32088
	AUC Pulsed Non-vital Same Pair 0.03ml/min	144247.9375	16	2429.91398	607.47849
Pair 2	AUC Pulsed Vital Same Pair 0.08ml/min	147675.3125	16	3224.21498	806.05374
	AUC Pulsed Non-vital Same Pair 0.08ml/min	146139.5625	16	3023.36226	755.84056
Pair 3	AUC Pulsed Vital Same Pair 0.15ml/min	147672.5000	16	3134.39678	783.59920
	AUC Pulsed Non-vital Same Pair 0.15ml/min	145784.9375	16	3016.62890	754.15723
Pair 4	AUC Pulsed Vital Same Pair 0.5ml/min	146416.6250	16	9436.40759	2359.10190
	AUC Pulsed Non-vital Same Pair 0.5ml/min	144204.6875	16	9630.91546	2407.72887

4.5.11.16 Satisfying the Test Assumptions – Pulsed Same Matched Pairs

The dependent variable of time is a continuous scale and the independent variable (temperature) has two categorical 'same' pairs, measurements were made as 'vital' and 'non-vital', which enables the area-under-the-curve (^oC/Time) to be calculated.

The difference of each same pair for all four flow-rates, with a pulse, (vital minus non-vital) was assessed for outliers via Boxplots (Figure 4-81) and normality by the Shapiro-Wilk Test (Table 4-67) for each flow-rate.
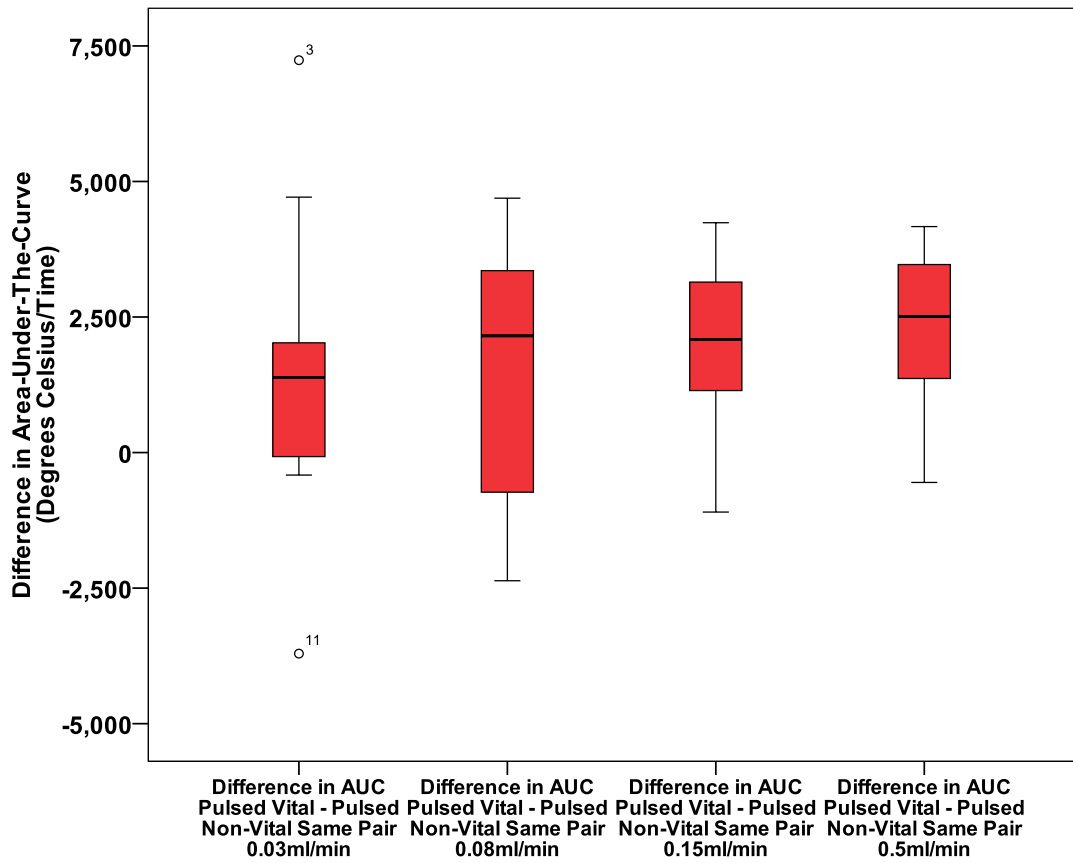
Figure 4-81 Boxplot of distribution of difference in area-under-the-curve for same matched pair vital and non-vital testing, with a pulse, across four flow-rates (0.03ml/min, 0.08ml/min, 0.15ml/min and 0.5ml/min). Boxplot shows two outliers for flow-rate 0.03ml/min, both from Pair 3 (3 = 3a and 11 = 3b). The outliers fall more than 1.5 box-lengths from the edge. These are not extreme outliers to unduly influence the outcome and it was decided to retain the values.

Table 4-67 Shapiro-Wilk Test for Normality for non-pulsed same matched pairs for all four flow-rates. The difference between the vital and non-vital teeth was normally distributed as assessed by Shapiro-Wilk Test which provided the following values all above 0.05: flow-rate 0.03ml/min p = 0.182, flow-rate 0.08ml/min p = 0.230, flow-rate 0.15ml/min p = 0.349, flow-rate 0.5ml/min p = 0.083.

Tests of Normality

	Kolmogorov-Smirnov[a]			Shapiro-Wilk		
	Statistic	df	Sig.	Statistic	df	Sig.
Difference in AUC Pulsed Vital - Pulsed Non-vital Same Pair 0.03ml/min	.173	16	.200[*]	.922	16	.182
Difference in AUC Pulsed Vital - Pulsed Non-vital Same Pair 0.08ml/min	.162	16	.200[*]	.928	16	.230
Difference in AUC Pulsed Vital - Pulsed Non-vital Same Pair 0.15ml/min	.122	16	.200[*]	.940	16	.349
Difference in AUC Pulsed Vital - Pulsed Non-vital Same Pair 0.5ml/min	.191	16	.120	.901	16	.083

*. This is a lower bound of the true significance.

a. Lilliefors Significance Correction

The Paired-T Test was suitable to test statistical significance for all flow-rates.

Table 4-68 Paired T-Test - Statistical significance of mean difference between the overall temperature of vital and non-vital teeth was determined with the paired-samples t-test using the area-under-the-curve (^{o}C/Time) during the re-warming time selected. A statistically significant increase of 1319 (95% CI, 34 to 2603), p = 0.045, and 1536 (95% CI, 291 to 2781), p = 0.019, was shown for flow-rates 0.03ml/min and 0.08ml/min, respectively. A statistically significant increase of 1888 (95% CI, 1021 to 2754), p < 0.0005, and 2212 (95% CI, 1390 to 3034), p < 0.0005, was also shown for flow-rates 0.15ml/min and 0.5ml/min, respectively.

Paired Samples Test

		Paired Differences							
		Mean	Std. Deviation	Std. Error Mean	95% Confidence Interval of the Difference		t	df	Sig. (2-tailed)
					Lower	Upper			
Pair 1	AUC Pulsed Vital Same Pair 0.03ml/min - AUC Pulsed Non-vital Same Pair 0.03ml/min	1318.50000	2409.77235	602.44309	34.42295	2602.57705	2.189	15	.045
Pair 2	AUC Pulsed Vital Same Pair 0.08ml/min - AUC Pulsed Non-vital Same Pair 0.08ml/min	1535.75000	2336.90189	584.22547	290.50288	2780.99712	2.629	15	.019
Pair 3	AUC Pulsed Vital Same Pair 0.15ml/min - AUC Pulsed Non-vital Same Pair 0.15ml/min	1887.56250	1626.30444	406.57611	1020.96604	2754.15896	4.643	15	.000
Pair 4	AUC Pulsed Vital Same Pair 0.5ml/min - AUC Pulsed Non-vital Same Pair 0.5ml/min	2211.93750	1541.94191	385.48548	1390.29465	3033.58035	5.738	15	.000
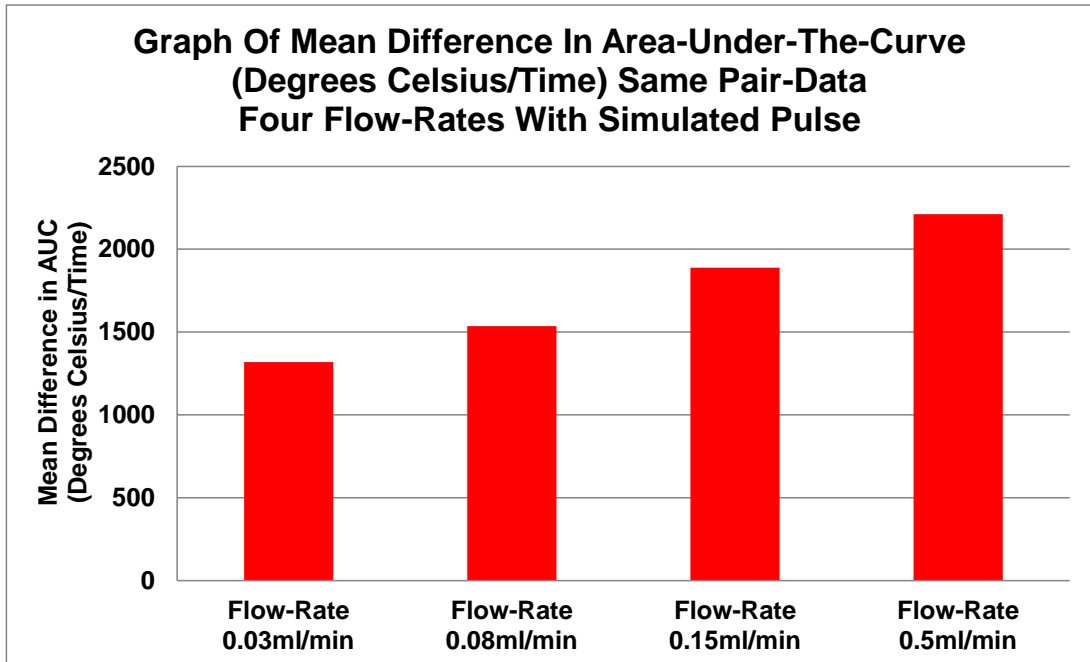
Figure 4-82 Graph of mean difference in area-under-the-curve for four flow-rates which increases with increasing flow-rate.

The mean difference was statistically significantly different from zero for all four flow-rates and, therefore, the null hypothesis can be rejected and the alternative hypothesis accepted.

4.5.11.17 Summary of Statistical Tests for Non-Pulsed Same Matched Molar Pairs

The null hypothesis can be rejected in favour of the alternative hypothesis for all four flow-rates.

4.5.11.18 Overall Statistical Significance

All the statistical significances are presented in Figure 4-82, where the presence of a simulated pulse increases statistical significance at decreasing flow-rates for the same matching molar teeth to the point of being statistically significant at the lowest flow-rate of 0.03ml/min. A projected flow-rate of 0.02ml/min is suggested to provide the statistical significance of 0.05 for detection of vitality between a vital and non-vital same matching molar tooth with simulated pulse (black line).

The discussion of the in-vitro feasibility of using infra-red radiation in determining tooth-vitality is in Chapter 5 Section 5.5.
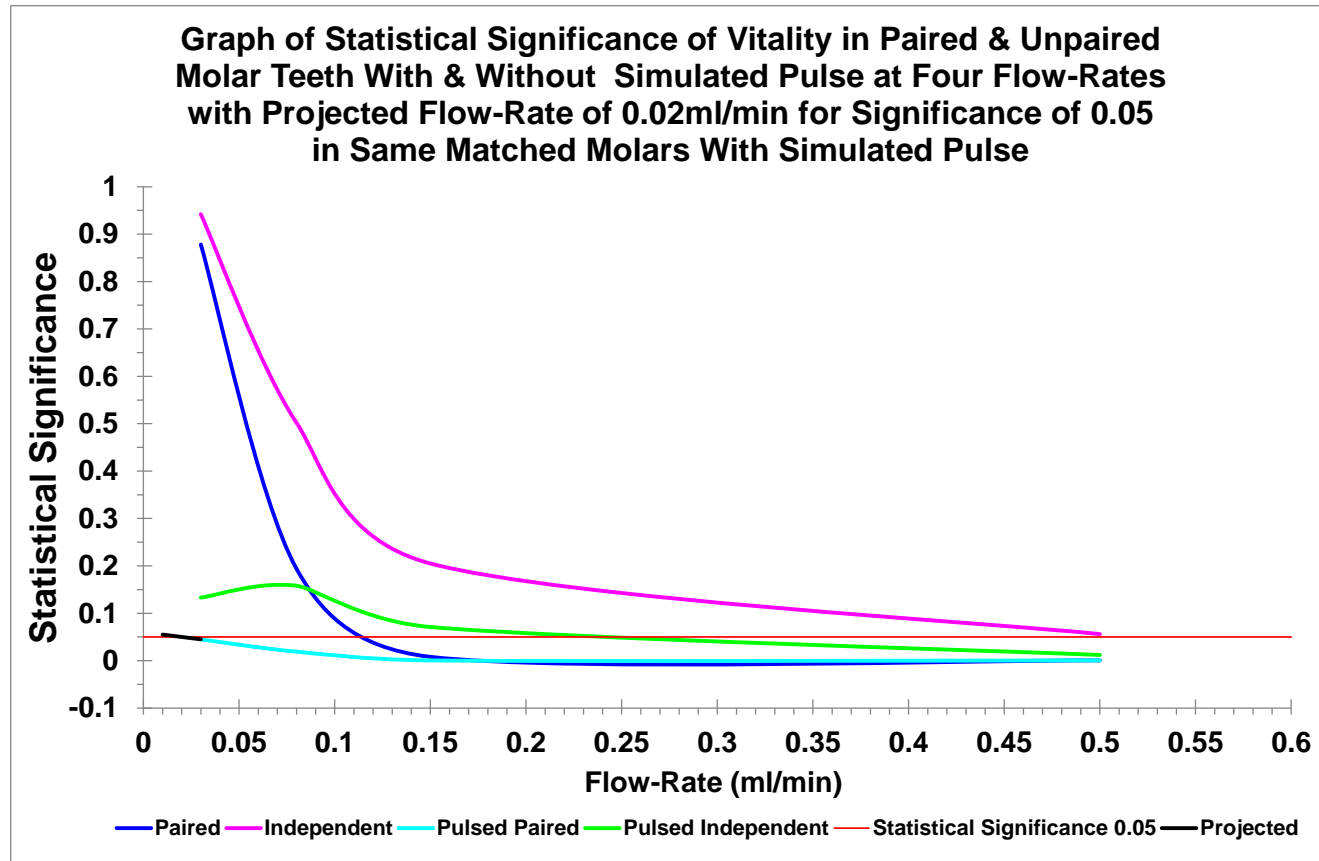
Figure 4-83 Graph of statistical significance from four flow-rates (0.03ml/min, 0.08ml/min, 0.15ml/min and 0.05ml/min) in same matched molar teeth (blue line) and independent molar teeth (pink line) without simulated pulse, and turquoise and green line respectively, with simulated pulse. A projection to ascertain the flow-rate of 0.02ml/min for 0.05 statistical significance for the same matched molar teeth with a simulated pulse is shown by a black extension of the turquoise line.

4.6 Proof of Concept In-Vivo Volunteer-Study

This Volunteer-Study provided the opportunity for proof of concept to assess vitality in-vivo, as described in Chapter 3, Section 3.6, having ascertained there was a detectable thermal difference between a simulated vital and non-vital tooth in-vitro following cooling. A bespoke cooling-unit was developed for in-vivo use and the results are shown in Figure 4-48 to 4-95 and Table 4-69 to 4-71.

4.6.1 Volunteer-Data

Table 4-69 Volunteer Descriptive-Data.
Two female Volunteers of white ethnic origin were recruited, age-range 34 to 51 years.

Volunteer	Gender	Age (Years)	Ethnic Origin	Medical History
1	Female	51	White	High Blood Pressure
2	Female	34	White	NAD

Darker Non-Vital Maxillary Canine

a.
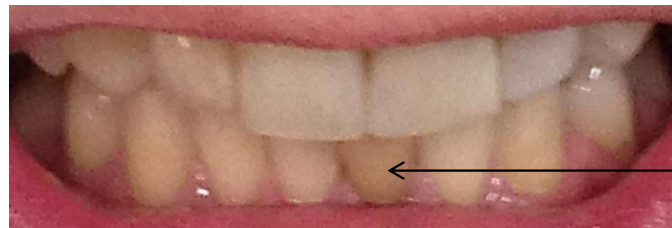
Darker Non-Vital Mandibular Central Incisor

b.

Figure 4-84 Photographs of anterior teeth of two Volunteers:
a. Volunteer 1, b. Volunteer 2. The photographs show a darker maxillary left canine tooth which is non-vital for Volunteer 1, and a darker mandibular left central incisor which was non-vital for Volunteer 2. Both teeth were reported to be root-treated.

4.6.2 Baseline Pre-Cooling Thermographs

The baseline-temperatures of the teeth were taken from thermographs set with a scale of 8-38°C (Figure 4-85). All show a warmer intra-oral environment compared to the more exposed teeth which are cooler. The

posterior teeth are warmer than the anterior teeth. The numerical temperature-data from the baseline thermographs are shown in Table 4-70.
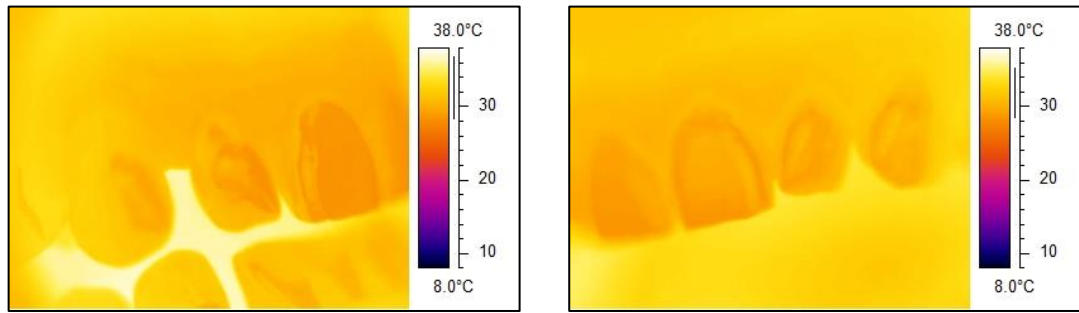
a.

b.
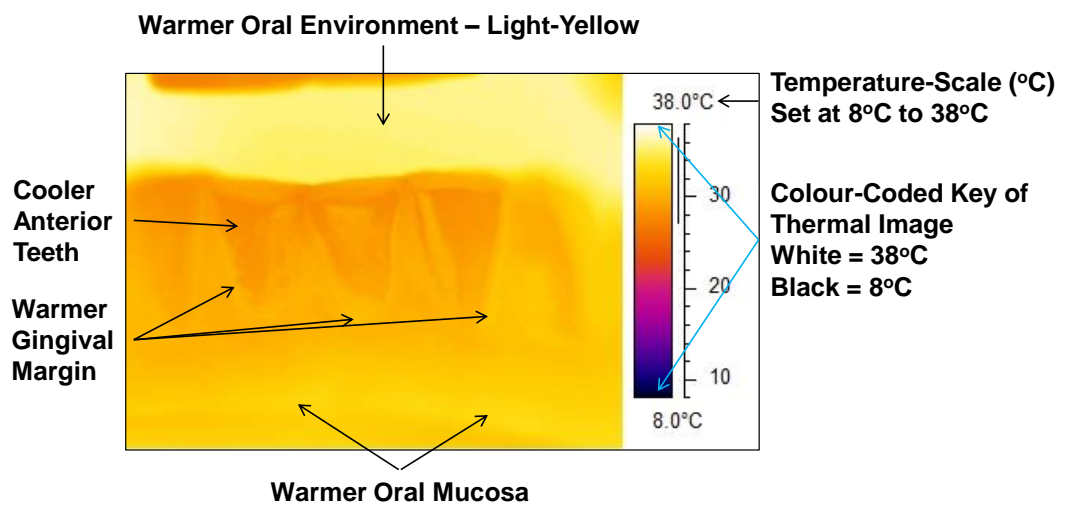
c.

Figure 4-85 Baseline Thermographs - Volunteer 1 a. right-image of maxillary incisors and canine, b. left-image of maxillary incisors and canine. Volunteer 2 c. mandibular anterior incisors. The temperature-scale of each image was 8°C to 38°C, as shown by the scale on the right of each image, with a colour-coded key for the temperature of structures in the thermograph, ranging from black at 8°C to white at 38°C. All images show a warmer intra-oral environment by the lighter-yellow colour, compared to the more exposed anterior teeth which are cooler with a darker yellow-orange colour. The posterior teeth are warmer with a lighter-yellow colour than the anterior teeth. The surface contour of the teeth provide different temperatures, shown by the varying yellow-orange scale, with the gingival contour being warmer shown by the lighter-yellow as is the oral mucosa.

4.6.3 Baseline-Temperatures From Thermograph

Table 4-70 Baseline-tissue-temperature, Volunteer 1, prior to vitality testing: a. vital maxillary right canine region b. non-vital maxillary left canine region. Volunteer 2, prior to vitality testing: c. mandibular anterior incisors. Gingival temperature increases posteriorly with distance into the oral environment in both the maxilla and mandible - left and right maxillary canine gingiva have a temperature of 31.73^{o}C and 31.81^{o}C respectively, and left and right mandibular lateral incisors 31.4^{o}C and 31°C respectively, (pink cells - Table a, b, c). Whole tooth-temperature increases posteriorly in the maxilla from 29.36^{o}C to 30.24^{o}C on the left, and 28.39^{o}C to 31.18^{o}C on the right, and the mandibular whole tooth temperature remains relatively constant with only 0.1^{o}C difference between the mandibular central and lateral incisor on the right, and no difference on the left (orange cells – Table a, b, c). A temperature gradient from the cooler incisal-surface to the warmer gingival-surface of the tooth exists, with a minimum line-difference of 0.8^{o}C for the maxillary right canine and central incisors (blue cells - Table a), and a maximum line-difference of 2.6^{o}C for the mandibular central incisors (red cells - Table c). A gradient also exists across the tooth-surface from mesial to distal, with a minimum line-difference of 1.2^{o}C for the mandibular central incisors and mandibular right lateral incisor (purple cells - Table c), to a maximum line-difference of 3°C for the maxillary right canine (green cell - Table a).

a.

Volunteer 1 Starting Temperatures - Vital UR3 (^{o}C)								
	UR3 Gingiva 31.81			UR2 Gingiva 30.12			UR1 Gingiva 30.2	
	Distal	Mid	Mesial	Distal	Mid	Mesial	Distal	Mid	Mesial
Cervical Area	31.99	31.25	30.11	30.50	29.43	29.13	28.47	28.46	28.49
Mid Area	31.95	31.27	30.08	29.54	29.46	28.96	28.37	28.36	28.36
Incisal Area	32.06	31.57	30.48	30.51	30.02	28.96	28.19	28.29	28.46
Cervical–Incisal Line-Difference	·	0.8	·	·	1.9	·	·	0.8	·
Mesio–Distal Line-Difference	·	3	·	·	2.3	·	·	1.6	·
Gingival-Half Area	31.19			29.71			28.47		
Incisal-Half Area	31.04			29.39			28.29		
Distal-Half Area	31.94			29.69			28.42		
Mesial-Half Area	30.58			29.07			28.39		
Whole Tooth Area	31.18			29.54			28.39		
UR = Upper Right								

b.

Volunteer 1 Starting Temperatures - Non-Vital UL3 (°C)								
	UL1 Gingiva 30.93			UL2 Gingiva 31.05			UL3 Gingiva 31.73		
	Mesial	**Mid**	**Distal**	**Mesial**	**Mid**	**Distal**	**Mesial**	**Mid**	**Distal**
Cervical Area	29.56	29.32	29.27	29.46	29.35	29.84	30.62	30.69	30.46
Mid Area	29.43	29.51	29.79	30.00	29.33	29.69	30.17	30.49	30.59
Incisal Area	28.77	28.89	29.09	29.53	29.07	29.72	30.44	29.96	30.28
Cervical–Incisal Line-Difference	·	1.3	·	·	1.2	·	·	1.8	·
Mesio–Distal Line-Difference	·	1.8	·	·	1.9	·	·	2.0	·
Gingival-Half Area	29.47			29.58			30.30		
Incisal-Half Area	29.21			29.45			30.17		
Distal-Half Area	29.39			29.35			30.23		
Mesial-Half Area	29.32			29.58			30.24		
Whole Tooth Area	29.36			29.48			30.24		
UL = Upper Left								

c.

Volunteer 2 Starting Temperatures Non-Vital LL1 (°C)								
	LR2 Gingiva 31		LR1 Gingiva 30.9		LL1 Gingiva 31.2		LL2 Gingiva 31.4	
	Distal	**Mesial**	**Distal**	**Mesial**	**Mesial**	**Distal**	**Mesial**	**Distal**
Cervical Area	29.7	29.5	29.4	29.8	30.3	29.9	30	29.9
Mid Area	29.4	29.1	28.5	29.1	29.1	29.2	29.5	29.3
Incisal Area	28.8	28.3	28.1	28.5	29.4	28.3	28.4	28.7
Cervical-Incisal Line-Diff	2.1		2.6		2.6		2.1	
Mesio-Distal Line-Diff	1.2		1.2		1.2		1.4	
Gingival-Half Area	29.4		29.1		29.3		29.6	
Incisal-Half Area	28.6		28.3		29.2		28.6	
Distal-Half Area	29.2		28.6		29.1		29.2	
Mesial Half Area	28.9		29.1		29.4		29.1	
Whole Area	29.0		28.9		29.2		29.2	
LR = Lower Right; LL = Lower Left; Diff = Difference								

4.6.4 Recording-Conditions

The recording-conditions in the clinical environment were very stable throughout the recording-sequence (Figure 4-86).
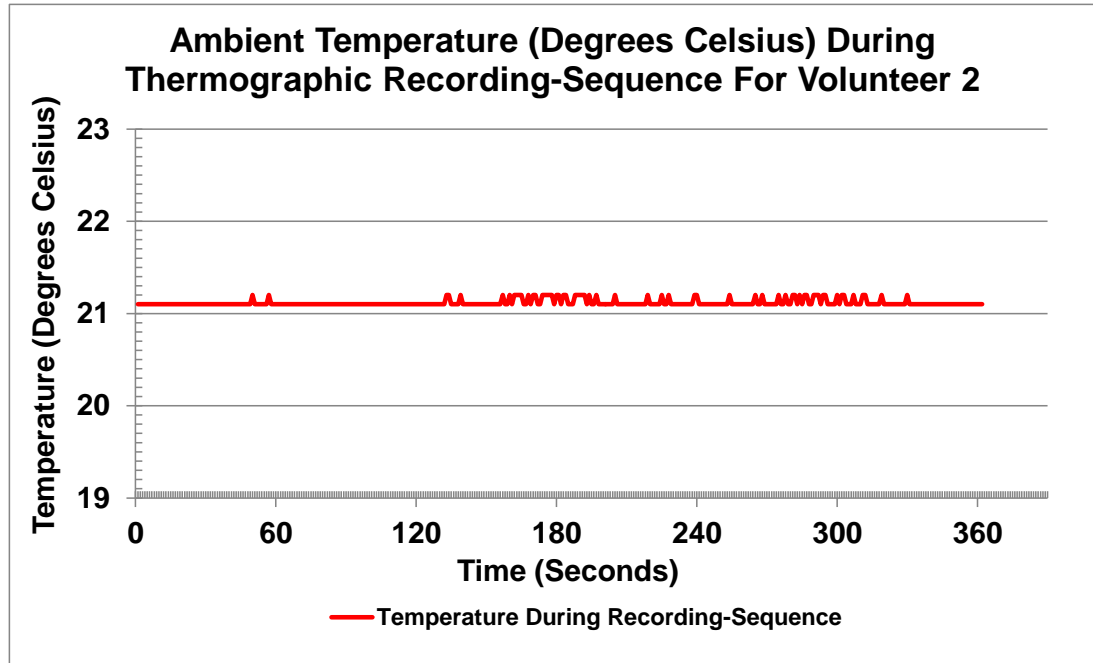
Figure 4-86 Graph of ambient temperature (Degrees Celsius) at 21.1°C with a variation of 0.1°C during recording for Volunteer 2.

4.6.5 Post-Cooling Thermographs

Following disruption of the thermal steady-state of the teeth with the application of the bespoke ice-filled-wax occlusal-bite-block, the re-warming sequence was observed (Figure 4-87) on reported non-vital teeth which had previously been root-treated (maxillary left canine for Volunteer 1, mandibular left central incisor for Volunteer 2), and adjacent vital teeth and the contralateral teeth which are all purported to be vital, having had no treatment. Two thermal sequences were needed for Volunteer 1 to capture data for the contralateral teeth, whilst only one sequence was needed for Volunteer 2.
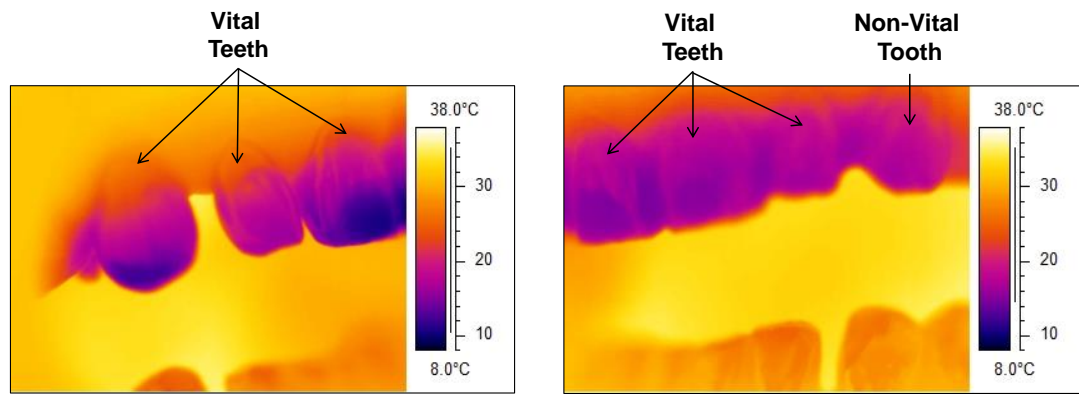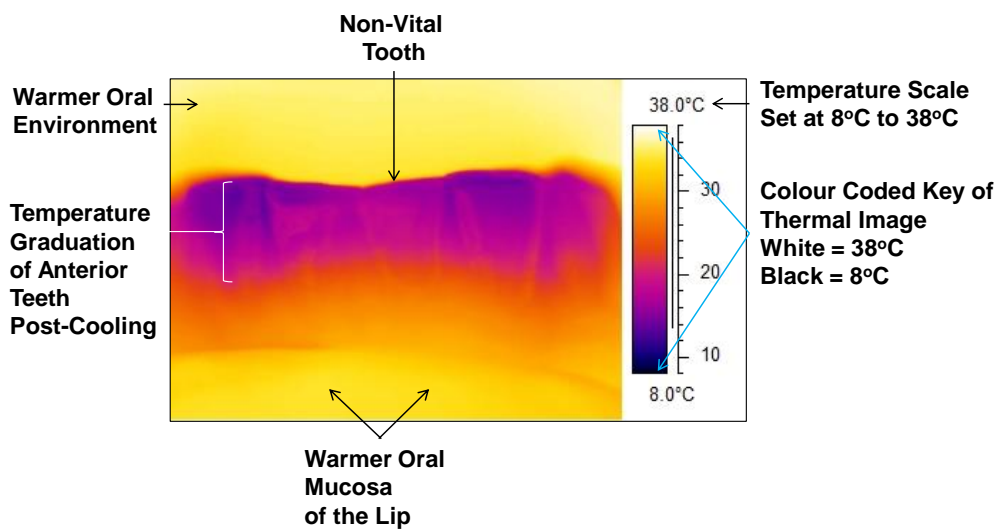
Figure 4-87 Post-cooling thermographs: Volunteer 1 a. right-image of vital maxillary incisors and vital maxillary canine, b. left-image of vital maxillary incisors and non-vital maxillary canine. Volunteer 2 c. lower vital anterior incisors (lower right lateral and central incisor and lower left lateral incisor) and non-vital lower left central incisor. The temperature-scale of each image was 8°C to 38°C, as shown by the scale on the right of each image, with a colour coded key for the temperature of structures in the thermograph, ranging from black at 8°C, to white at 38°C. All images show a warmer intra-oral environment by the lighter-yellow colour. The anterior teeth are cooler, with a graduation of temperature post-cooling from the coolest purple of the incisal-edge to the orange colour of the cervical-neck.

Table 4-71 Baseline, coolest and difference in tooth-temperature prior to re-warming: a. Volunteer 1, b. Volunteer 2.

a. The lowest whole-tooth-temperature recorded for Volunteer 1 was 16.2°C for the maxillary right central incisor (blue cell), and the highest temperature, following cooling, was 20.1°C for the maxillary right lateral incisor (pink cell). The greatest temperature-reduction was 12.66°C for the maxillary left central incisor (green cell), and the least was 9.44°C for the maxillary right lateral incisor (orange cell).

b. The lowest whole-tooth-temperature recorded for Volunteer 2 was 16.1°C for the mandibular right lateral incisor (blue cell), which also provided the greatest temperature-reduction of 12.9°C (green cell). The highest temperature recorded, following cooling, was 18.3°C on the mandibular left central incisor (pink cell), which gave the least temperature-difference of 10.9°C for the non-vital lower left central incisor (orange cell).

a.

Volunteer 1 Cooled-Surface-Temperatures of Teeth (°C)						
Whole Tooth	UR3	UR2	UR1	UL1	UL2	UL3
Baseline	31.18	29.54	28.39	29.36	29.48	30.24
Coolest	19.6	20.1	16.2	16.7	17.7	18.7
Difference	11.58	9.44	12.19	12.66	11.78	11.54
Re-warming Phase Commenced	20.1	20.5	16.4	17.2	18.9	20.3
Difference from Baseline	11.08	9.04	11.99	12.16	10.58	9.94
UR = Upper Right; UL = Upper Left						

b.

Volunteer 2 Cooled-Surface-Temperatures of Teeth (°C)				
Whole Tooth	LR2	LR1	LL1	LL2
Baseline	29	28.9	29.2	29.2
Coolest	16.1	17.4	18.3	16.4
Difference	12.9	11.5	10.9	12.8
Re-warming Phase Commenced	16.1	17.4	18.3	16.4
Difference from Baseline	12.9	11.5	10.9	12.8
LR = Lower Right; LL = Lower Left				

4.6.6 Re-Warming Sequence of Teeth-of-Interest
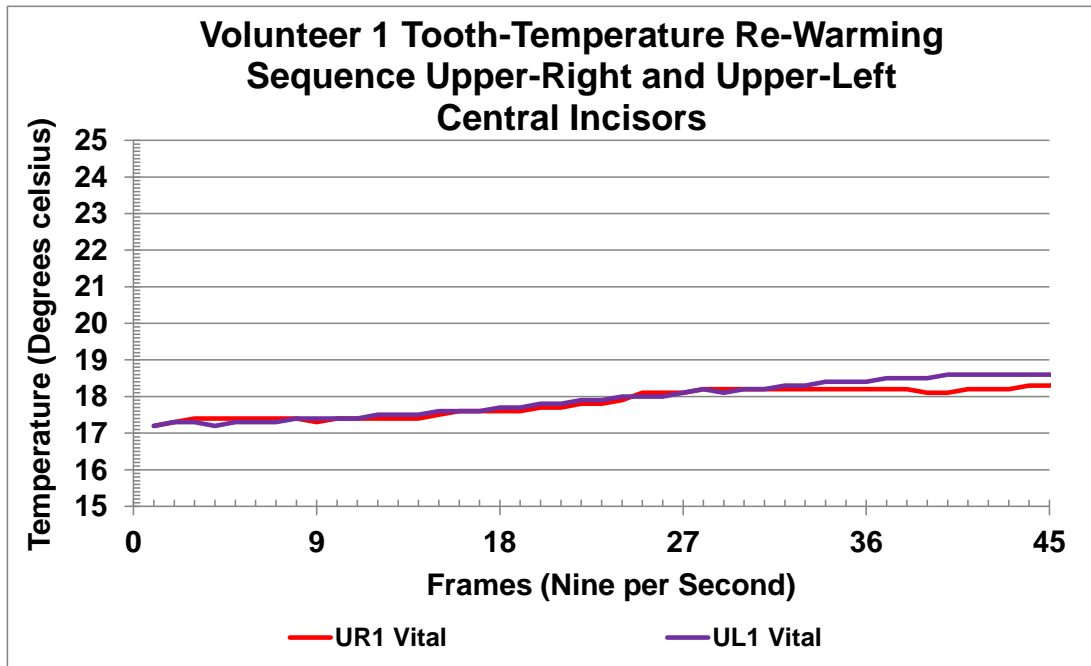
Figure 4-88 Graph of re-warming sequence of vital upper (maxillary) central incisors in Volunteer 1, where the right and left central incisors are virtually in equilibrium until frame 31, when the left central incisor warms more rapidly, with a maximum temperature-difference of 0.5°C.
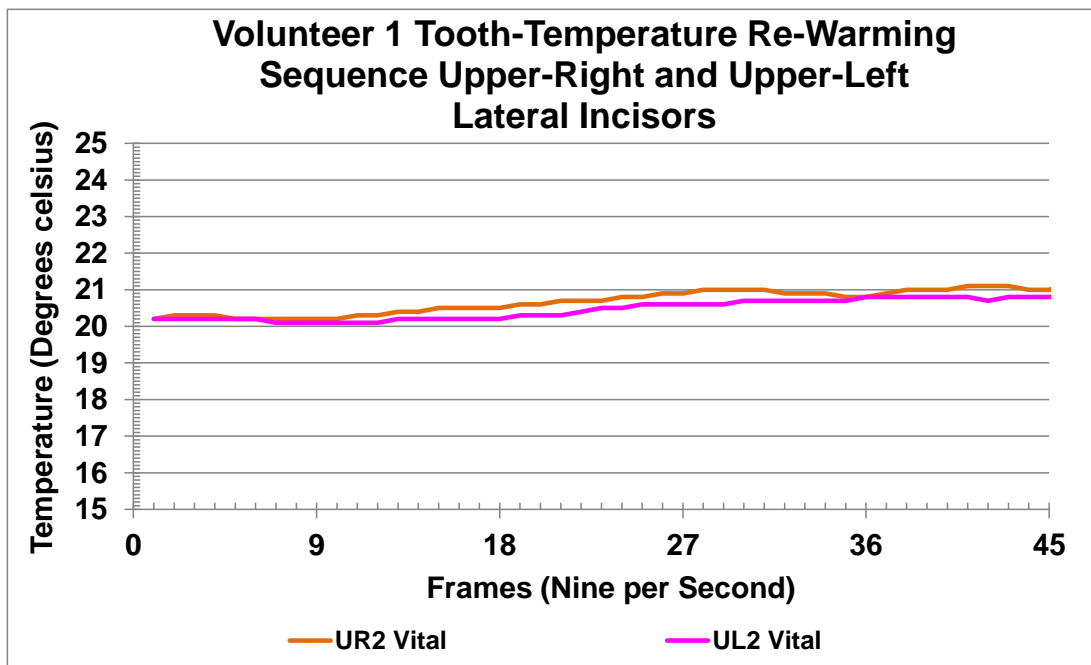
Figure 4-89 Graph of re-warming sequence of vital upper (maxillary) lateral incisors in Volunteer 1, which have a maximum temperature-difference of 0.4°C, where the right lateral incisor is slightly warmer than the left.
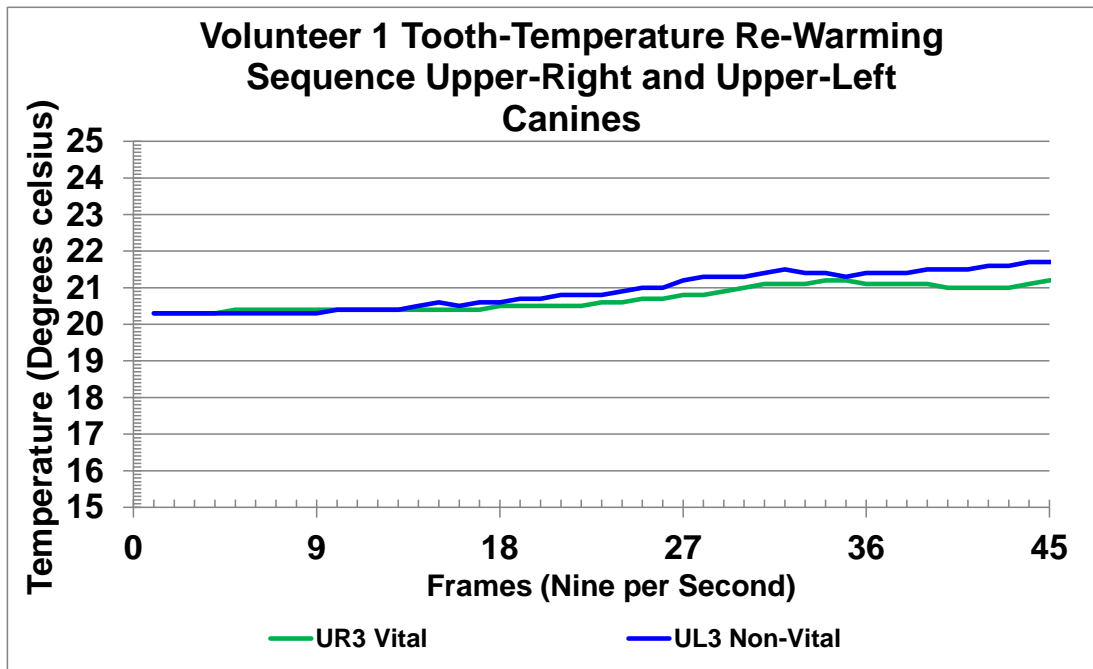
Figure 4-90 Graph of re-warming sequence of vital upper (maxillary) right canine and non-vital upper-left canine in Volunteer 1, where, initially, the non-vital upper-left canine (blue line) has a marginally lower temperature than the vital upper-right canine (green line). The temperatures equalise and the non-vital canine re-warms at a quicker rate than the vital canine, with a maximum temperature-difference of 0.6°C.
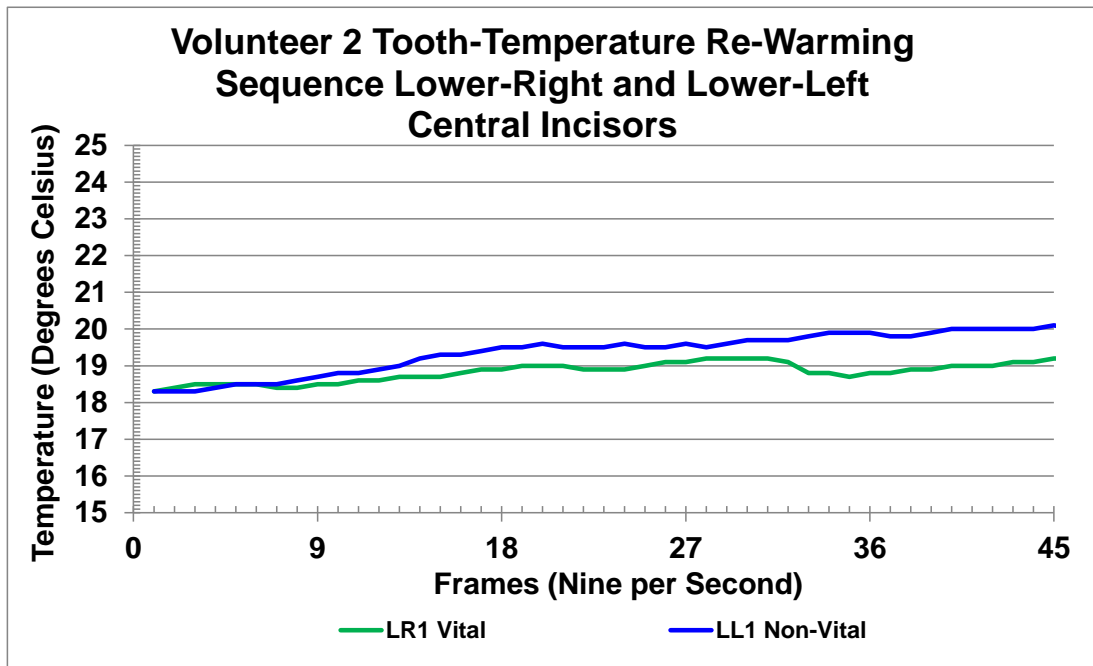
Figure 4-91 Graph of re-warming sequence of lower (mandibular) central incisors in Volunteer 2, where, initially, the non-vital lower-left central incisor (blue line) is cooler than the vital lower-right central incisor (green line). The temperatures equalise, following which the non-vital lower-left incisor re-warms faster than the vital tooth, with a maximum temperature-difference of 1.2°C.
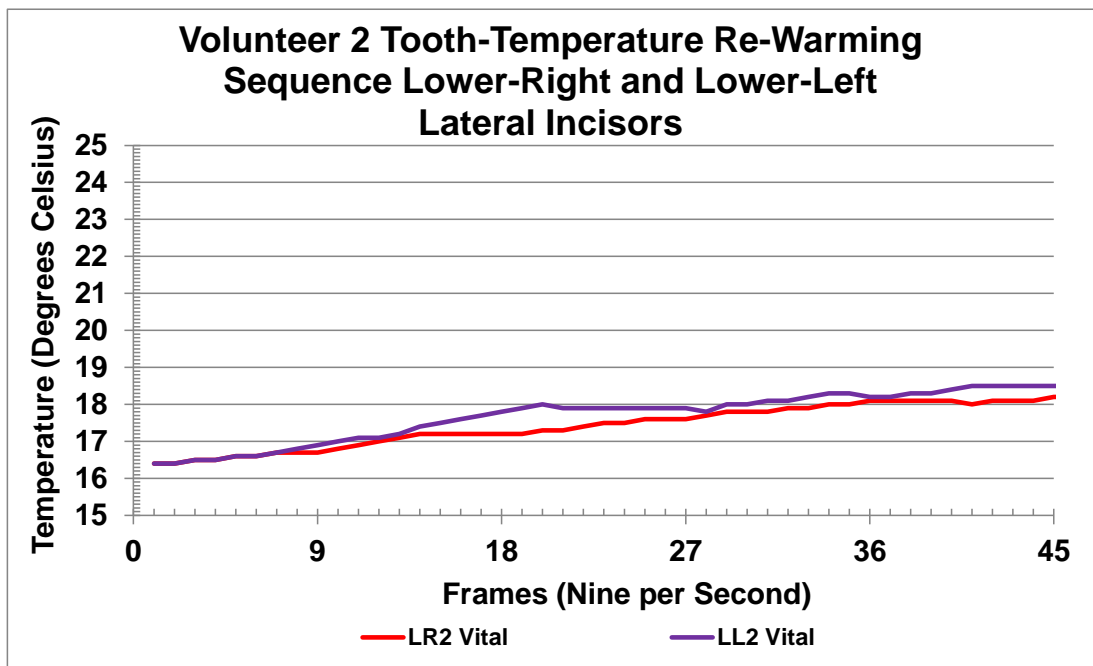
Figure 4-92 Graph of re-warming sequence of lower (mandibular) lateral incisors in Volunteer 2, where, initially, both have the same temperature and the lower-left lateral incisor (purple line) re-warms quicker than the lower-right lateral incisor (red line), with a maximum temperature-difference of 0.7°C

4.6.7 Area-Under-The-Curve of Re-Warming Sequence

**Volunteer 1 Area-Under-The-Curve
Initial 5 Seconds Re-Warming**
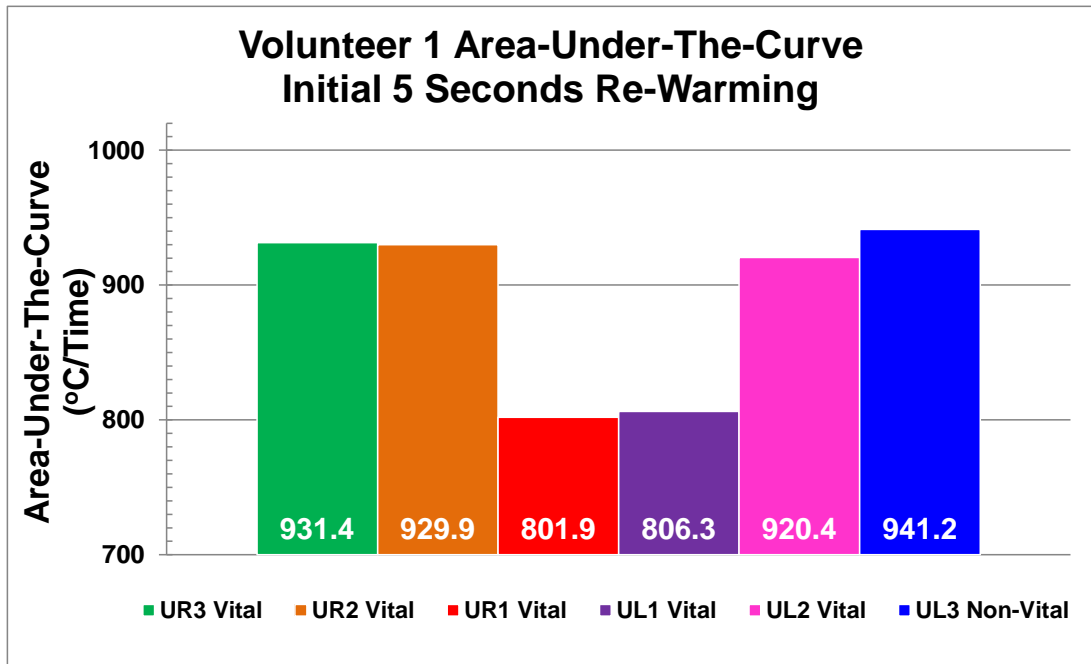
Figure 4-93 Graph of area-under-the-curve of re-warming sequence for 6 anterior teeth for Volunteer 1, where the greatest value was from the non-vital upper (maxillary) left canine (941.2°C/Time). The maximum difference of 9.8°C/Time was seen between the vital and non-vital canine teeth. The upper right central incisor had the least area-under-the-curve (801.9°C/Time). The minimum difference of 4.4°C/Time was seen between the two central incisors - less than half that of the canine teeth. The lateral incisors had the reverse re-warming sequence, whereby the right lateral warmed at a quicker rate than the left, hence a negative difference of -9.5°C.
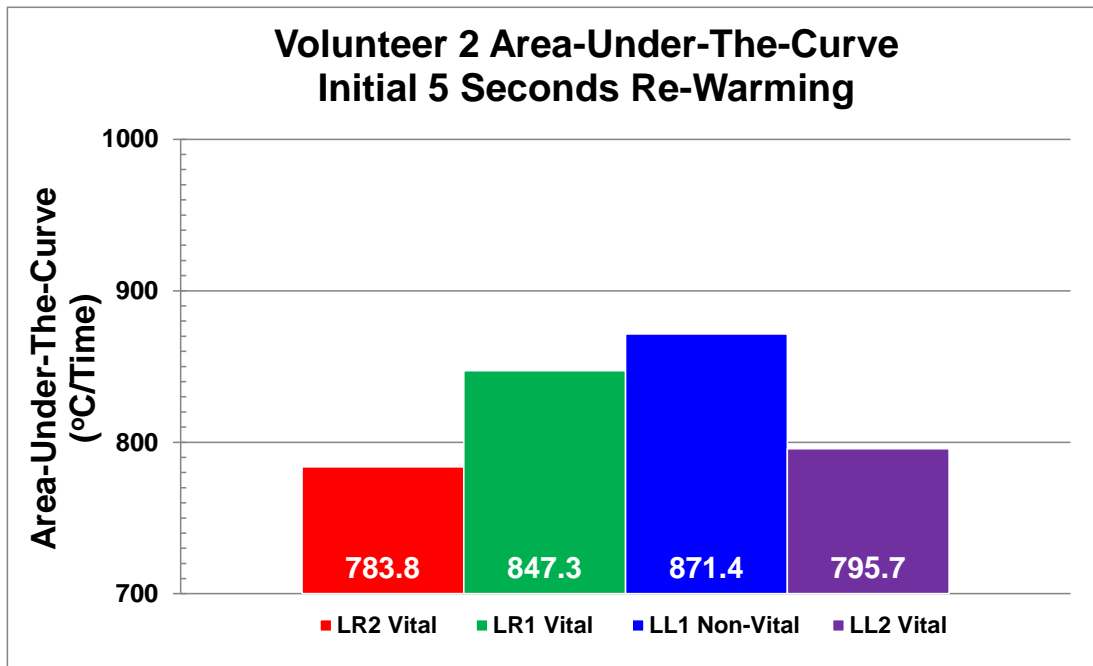
Figure 4-94 Graph of area-under-the-curve of re-warming sequence
for 4 anterior teeth for Volunteer 2, where the greatest value
was from the non-vital lower (mandibular) left central
incisor (871.4^{o}C). The difference between the two central
incisors was 24.1^{o}C/Time. The difference between the vital
lateral incisors was 11.9^{o}C/Time, less than half that of the
central incisors.

4.6.8 Pulse Relationship to Re-Warming Tooth-Temperature
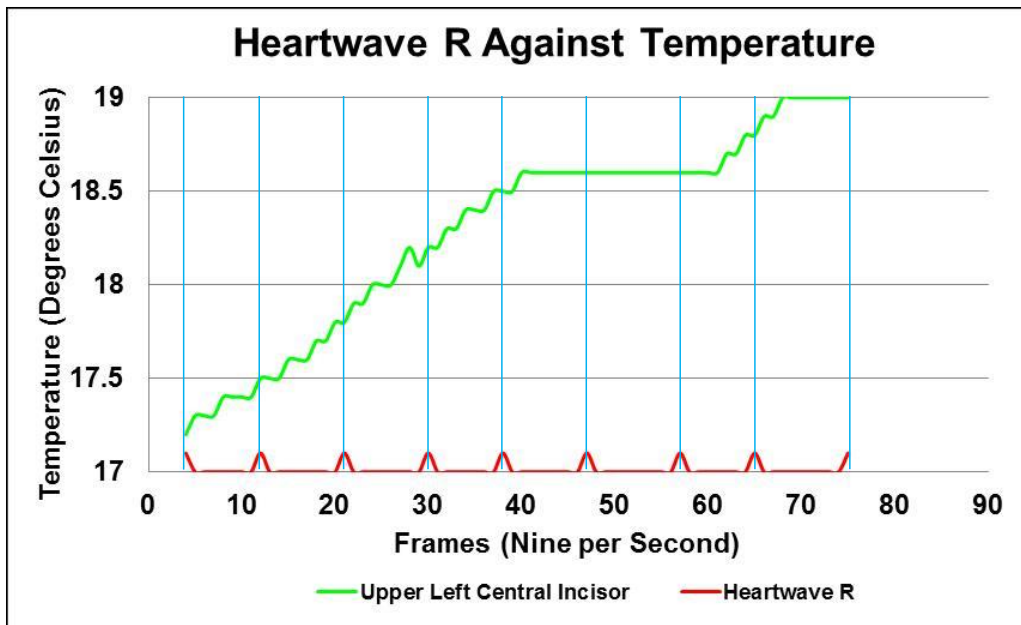
Figure 4-95 Graph of relationship between heart-wave point R
(red line) and rise in temperature of the tooth-surface
(green line), where no relationship was found.

4.6.9 Volunteer Acceptability of the Process

Both Volunteers found the process acceptable and, following an adjustment to the wax of the ice-filled-wax occlusal-bite-block, this was more comfortable and stable in-situ. Neither Volunteer commented that the cooling-process was sensitive.

The discussion of the Proof of Concept In-Vivo Volunteer-Study is in Chapter 5 Section 5.6.

Chapter 5 Discussion

The aim of this work was to investigate the feasibility of using infra-red radiation in determining tooth-vitality. Multiple phases were identified, the first of which was the development of a stable thermal environment in which to undertake thermal imaging in-vitro and led to the development of the Cube (Chapter 3 Section 3.1), the results of which were presented in Chapter 4 Section 4.1.

5.1 Development of a Stable In-Vitro Thermal Environment

5.1.1 Prototypes

A series of protective outer-shells (Figure 5-1) were piloted during development of the thermal environment, using both insulating and conducting materials to provide an enclosure within which to operate, such as:

a. Polystyrene box (H33 x W40 x D56cm) with a removable-lid and a viewing-window to allow data-collection from the thermal camera

b. Perspex box (H31 x W28 x D38.5cm) constructed with a screw-secured-lid and a sliding-shield across a viewing-window, which was raised and lowered as needed for undertaking data-collection

c. Meccano prototype frame (H32 x W47 x D47cm) constructed with detachable aluminium-sheets, with a camera-mounting attached on the upper-facing-surface to keep the camera perpendicular (normal) to the samples. A circular viewing-window was cut into the upper-face, above which the camera was positioned. Removal of a side-sheet enabled access.

These prototypes were all unsuitable. With Polystyrene, internal visibility was difficult whilst maintaining an internal thermally-stable environment. Access was time-consuming with the screw-lid of Perspex and both this, and polystyrene, had insulating properties which proved very slow to influence a change in internal temperature. The Meccano version with aluminium-sheets was conducting, allowing the macro-temperature control to have a quicker influence, but required micro-cooling internally when the temperature rose, and this was managed by the temperature-controller. Access by removal of a side-sheet was initially slow and affected the thermal environment, so further development led to a fixed-frame with hinged-doors, locked with knurled-thumb-screws which were quick and simple to use. Small access-areas could be cut into the aluminium as needed, and changed for different

investigations. This gave great flexibility of the unit and visibility without loss of thermal stability, as seen from the various investigations undertaken within the Cube in this Study.

1. Polystyrene box with viewing-platform for thermal camera

2. Perspex box with viewing-platform for thermal camera

3. Meccano frame and screw-attached aluminium sides with thermal camera-mounting

Fixed-mount for thermal camera

Entry and exit for cables, etc.

Peltier unit

Knurled thumb-screw fastenings

Cooling-fan

Heat-sink

4. Solid-framed aluminium cube with thermoelectric peltier units, heat-sinks, cooling-fans and access via a hinged-door, fastened with knurled thumb-screws and thermal camera in fixed-mounting

Figure 5-1 Three Prototypes and Final Development of the Thermal Environment a.k.a the Cube

5.1.2 Basis for a Stable Thermal Environment

Development of the Cube reduced external environmental temperature-confounders, such as air-conditioning-currents which have a cyclic-effect and, in the room used in this Study, was found to range over 4°C. The air-conditioning-unit should be capable of removing the heat generated within

the room, e.g., by any occupants, or equipment (Love, 1986; Ring & Ammer, 2000), and was required, along with the micro-climate control, to achieve thermal stability (Chapter 4, Figure 4-3). Air-conditioning is not a uniform controller of the ambient temperature, and fluctuations within the surroundings would be unhelpful, affecting the temperature of the object-of-interest, as described by Love (1986) and Kells et al, (2000b). It is not just the overall temperature which is of interest but also the air-flow which should also be constant (Love, 1986). Additionally, thermal contributions may be detected from any operator in close proximity to the recording-area (Vollmer & Möllman, 2010) and, by shielding the samples, these were reduced, if not totally eliminated, during data-capture in-vitro.

Within the laboratory investigations, every effort was made to reduce these variations to fully appreciate the capabilities of the thermographic technique - hence development of an isolated thermal environment, such as the Cube. No other study investigating tooth-vitality in-vitro with infra-red thermography was found within the published literature - this may be the first and as such is a unique contribution to knowledge. Two in-vitro studies had used either a thermistor (Fanibunda, 1985) or a thermometer (Smith et al., 2004). Fanibunda (1985) suggested only the relative changes in tooth-temperature were recorded and an incubator at $30^{\circ}C$ was used to simulate an oral temperature with the door open, which raises a question about the thermal stability of the recording environment which was not reported. Smith et al., (2004) provided protection by 'boxing with polystyrene' and stated an ambient temperature of $21^{\circ}C$ was maintained, although again no data was presented for this.

The report by Love (1986) on the need to stabilise the environment for human volunteers emphasised the importance of such stability, especially if quantitative data was being collected. This did relate to skin-temperature-measurement but the same philosophy would be required when looking at any tissue with a thermal image. The influence of variations in ambient temperature on heat-transfer should not be underestimated, with thermal cameras having the capability of recording very small temperature-differences ($0.05^{\circ}C$ in this Study) and there is an awareness of possible diagnostic errors from environmental fluctuations in temperatures when at this level. Development of the Cube reduced such external environmental temperature-confounders in-vitro.

5.1.3 Ideal Environmental Temperature for Human Studies

To be able to translate the results of this study in-vitro to an in-vivo study required a clinically realistic operating-temperature and this was reported as $22^{o}C$, to avoid any shivering or sweating (Love, 1986). These two situations may affect the vascular-supply, either by causing vasodilation or vasoconstriction, both of which should be avoided when looking at thermal information and that was the initial desired target-temperature for the Cube. This was raised to $30^{o}C$ for the in-vitro simulation to test tooth-vitality based on the temperatures of the anterior teeth with the mouth open (Goldberg & Brown, 1965; Brown & Goldberg, 1966; Crandell & Hill, 1966; Banes & Hammond, 1978; Fanibunda, 1986b), as the molar teeth used had no surrounding soft-tissue such as lips, cheeks or tongue in the simulation.

The final design of the Cube enabled the macro- and micro-controlled environment to reach the required temperature of $22^{o}C$ to remain stable over a period of 28 minutes, with minimum fluctuation ($\pm0.1^{o}C$). This was only achieved with both macro- and micro-control. The longest time taken to achieve the required temperature was 34 minutes, which provided a minimum stabilization time of 35 minutes. One thermal sensor was used to record the temperature in a set position close to the recording field-of-view and it is accepted there may be thermal variation within the boundaries of the Cube - however, this is likely to be small and especially small within the defined field-of-view used in this Study. The in-vitro vitality testing on eight pairs of molar teeth (P1-P8) over the four flow-rates required a Cube temperature of $30^{o}C$ which had a range of $0.4^{o}C$, with a high of $30.1^{o}C$ and a low of $29.7^{o}C$ (Chapter 4 Section 4.5).

Previous in-vitro studies by Panas et al, (2007) and Lin et al, (2010b) who investigated thermal properties of tooth-tissues did not provide such a protected, stable environment, but did use air-conditioning within the room, which could have affected their reported outcomes.

5.1.4 Summary

The Cube provided a very stable environment within which to conduct the in-vitro work, eliminating environmental temperature-confounders with macro- and micro-thermal control following 35 minutes of stabilisation for an ambient Cube temperature of $22^{o}C$. This was adapted for a higher ambient temperature of $30^{o}C$ where good stability was also achieved.

5.2 Emissivity-Determination of Mineralised Human Tooth-Tissue

From the literature there was variability in emissivity-values for the mineralised tissues of the teeth which was not evaluated per study. Instead, other studies' values were often presented (Lipski, 2005a; da Costa Ribeiro et al., 2007; da Silva Barbosa et al., 2013; Lipski et al., 2010a; Lipski et al., 2010b; Preoteasa et al., 2010; Killic et al., 2013), or it was not considered at all (Crandell & Hill, 1966; Hartley et al., 1967; Pogrel et al., 1989; Hussey et al., 1995; Hussey et al., 1997; Komoriyama et al., 2003) and, when it was considered, a value was not always given (McCullagh et al., 2000; Lipski & Zapałowicz, 2002; Bouillaguet et al., 2005; Lin et al., 2010b). Additionally, there was some misunderstanding of emissivity (Gontijo et al., 2008), and a method (Chapter 3, Section 3.2) to determine the emissivity of the mineralised tooth-tissue was needed for this Study. The results, which will now be discussed, were presented in Chapter 4, Section 4.2.

5.2.1 Emissivity-Evaluation

Referencing others' values, as seen from the literature, or taking a standard-value, may introduce discrepancies when reporting absolute temperatures, and comparison of such values needs to be treated with awareness of the method of calculation. Therefore, a method to evaluate emissivity at the beginning of this Study would allow greater consistency of reporting absolute values for comparison between studies, and is to be recommended.

The British Standards, and Manufacturer's Infra-red Thermography Handbook provided a simple but recognised method by using a reference-point of known-emissivity and such a method was used in-vitro for this Study. This may not be acceptable in-vivo for a human subject, as the tape may leave a residue on the tooth-surface, a nasty taste from the tape-adhesive, or stain from the black paint. If relative values are reported, or when differences are calculated between the same tissue-temperatures, the actual emissivity becomes less of a concern than when reviewing the absolute temperature, so long as the same emissivity-value is used throughout the investigation.

Kells et al., (2000a) assessed emissivity following a long period of thermal stabilisation for one tooth, which would dehydrate the tooth. $70^{o}C$ is an unrealistic value for long-term thermal stability of a tooth in a human, although temperatures as high as $77.4^{o}C$ have been recorded for ingested hot liquids (Barclay, et al., 2005). This temperature will have affected the composition of the layers of mineralised tissues – dentine ≈10% water,

enamel ≈5% water (Simmer & Fincham, 1995; Nanci, 2012) - which can affect the emissivity-value calculated (Gaussorgues, 1994; Vollmer & Möllmann, 2010). Kells et al., 2000a, used a spot-measurement on the tooth, rather than an area-of-interest as used within this Study. Within a spot-measure any anomalies, e.g., demineralisation, surface-texture-change from enamel deposition, or placement of forceps when removing the tooth, may skew the value (Gaussorgues, 1994; Vollmer & Möllmann, 2010). An area-of-interest-measurement provided an average value of the area selected, averaging any local anomalies. When a curved-surface is being evaluated (rather than a flat-surface) as seen for the spot-measurement, this again may influence the value, as normal incidence is the ideal viewing-angle (Gaussorgues, 1994; Vollmer & Möllmann, 2010). Both curved and flat-surfaces were used in this Study to assess emissivity-values.

5.2.2 Enamel-Surface-Emissivity

This Study has evaluated an area-of-interest for emissivity against a known-emissivity-reference-point of 3M Scotch Super 33+ Black Vinyl Electrical Tape (ε=0.96) using the thermal camera software and reports these findings for an area-of-interest for the first time from multiple teeth (14 whole molar teeth) rather than 1 incisor tooth (Kells et al., 2000a). The age-range was 10 to 28 years (mean 16 years 11 months) for the donors and the enamel-surface emissivity-value ranged from 0.94 to 0.97, with a mean value of 0.96 [SD=0.009] (Chapter 4, Table 4-4) at a tissue-sample-temperature between 31°C and 32°C.

Two previous studies reported were calculating the emissivity at sample-temperatures of 70°C (Kells et al., 2000a) and 50°C (Lin et al., 2010a), both higher than that of the in-vivo tissue, whereas this Study reports the values recorded at a realistic oral temperature, as it is known that, with increasing temperature, the emissivity-value may also increase (Gaussorgues, 1994; Vollmer & Möllmann, 2010).

The length of time the teeth used in this Study had been in the oral environment after eruption was unknown and, thus, the degree of maturity of enamel was also unknown, which may affect the mineral content, as enamel increases in mineral composition following eruption.

The internal emissivity-value of the enamel and dentine was assessed at a similar temperature (31°C to 32°C) for two slices of a third molar from an 18 year-old female. Two areas-of-interest were selected on Slice 1 and three on Slice 2 which were assessed three times each, consecutively, and then

repeated on a separate occasion. The value of the internal surface of enamel ranged from 0.935 to 0.975 for the two slices, with an overall mean for both slices of 0.965 [SD=0.013] (Chapter 4, Table 4-3).

The sliced internal surface of enamel and the external surface of enamel are very similar at 0.965 and 0.96 respectively, and fall within the previously reported values in the literature. Temperatures of recording were similar in this Study, but dissimilar compared with other studies. Mineral composition is high in enamel, with natural surface-irregularities from deposition by the ameloblasts, internally forming both enamel prisms and inter-prismatic crystals (Chapter 2, Section 2.1.6.1 & 2.1.6.2), and on the surface as perikymata. These surface-textures appear to emit infra-red radiation in a similar way, despite one being an internal surface and one an external surface. Assessment of an area-of-tissue may also account for this, as a local change may be compensated for within the area-calculation, compared to a spot-measurement.

5.2.3 Dentine-Surface-Emissivity

Dentine was evaluated from the internal surface of the slices of teeth in the same way as enamel, and values were calculated for crown-dentine, root-dentine and root-face-dentine when accessible. Values vary (Chapter 4, Table 4-9), with crown-dentine returning the highest emissivity (mean of two slices 0.946), followed by root-dentine (mean 0.931), then root-face-dentine (mean 0.838). Overlap is seen between enamel and dentine and this may relate to the density of the tissues which also overlap (Chapter 2, Table 2-5). The root-face returns the lowest value of all mineralised tooth-tissue assessed, and not only has a greater curvature than the flat-surface of the cut crown-dentine and root-dentine, but may also contain remnants of cementum which has a reduced mineral content at 50% (Chapter 2, Table 2-2) and density at $1.1\text{-}2.05 g/cm^3$, compared to the rest of dentine at 70% and $1.94\text{-}2.4 g/cm^3$, respectively. There may be soft-tissue-traces from the periodontal ligament as well, which influence the activity of the radiant energy.

Root-dentine may be less dense than crown-dentine, which are both less-dense than enamel of the same tooth (Djomehri et al., 2015; Gradl et al., 2016) and this is mirrored by the emissivity-values calculated in this Study. Enamel is recorded with the highest emissivity (it has the greatest mineralisation and density), followed by crown-dentine, then root-dentine and, finally, the root-surface - be that of cementum, dentine and/or soft-tissue-remains. The crown-dentine and root-dentine values are slightly

higher than the published values of 0.8, produced from comparison with a black paint assumed to have an emissivity of 1 (Neev et al., 1993). This is very improbable as a perfect blackbody is empirically unlikely and, if the reference-emissivity was reduced, the sample-emissivity would increase. The temperature of assessment was also unknown. The previously highest reported value calculated was 0.92 (Lin et al., 2010a) at a calculation-temperature of ≈50°C. All tissue-samples are non-homogenous and will vary in mineral-composition, structure and density, all of which can affect the emissivity-values and may account for some of the variation.

5.2.4 Acceptance of Methodology

The method used was simple, with a cheap, removable emissivity-reference-point and would be recommended for providing actual emissivity-values for any in-vitro study. This would allow consistency of methodology between research groups, providing comparable absolute temperatures. In this Study the tape was placed on the whole-tooth-sample and by the side of the slices. This may be criticised as the tape was not physically on the slices - however, a 1mm-slice will reach thermal equilibrium very quickly once the hand-carrier reaches the hotplate.

The colour of teeth can often change and darken when non-vital, which does not affect the emissivity-value, as this is a visible spectrum phenomenon enabling humans to see colour and does not affect the amount of absorbed, or emitted, infra-red radiation (Hardy, 1934).

5.2.5 Summary

From the literature sourced, no other Study has reported emissivity-evaluation of enamel and dentine on multiple samples, whether whole or sliced, against a reference-point of known-emissivity, at an oral temperature matching that of the human and this makes a unique contribution to our knowledge. Enamel had a high emissivity, which was similar whether from the internal flat-surface of sliced enamel or the external curved-enamel-surface of a whole tooth. Dentine also had a high emissivity (but not as high as enamel), which varied with location, crown-dentine being the highest, compared to root-dentine. The root-face had the lowest emissivity-value but was still a good emitter of infra-red radiation.

The method of calculation was cheap, simple and practical and would improve comparison of absolute temperatures between in-vitro studies. These values were used for the thermal recordings in-vitro and in-vivo as no in-vivo reference-point was available.

5.3 Characterisation of the Thermal Properties of Enamel and Dentine

Assessment of the thermal properties of human enamel and dentine was undertaken by a method adapted from that described by Lin et al.,(2010b) and Panas et al., (2007) (Chapter 3, Section 3.3) and the results were presented in Chapter 4, Section 4.3. Progression of the method previously described began with the use of a thermally stable environment – the Cube – in which to view the tissues. Multiple slices from multiple samples were examined, rather than slices from one sample as previously done (Lin et al., 2010b and Panas et al., 2007), and the use of a demineralised, naturally-occurring carious lesion had not been described in the literature sourced, providing a unique opportunity for original research in this Study. Emissivity-values from the prior investigation in this Study were used (Chapter 4, Section 4.2). Finally, the data collected was further processed within bespoke software to produce a thermal map for each tooth-slice, based on the tissues' thermal properties which successfully characterised enamel and dentine in one image, via two different methods – the area-under-the-curve during re-warming, and characteristic-time-to-relaxation for the whole-tooth-slice.

5.3.1 System-Development

5.3.1.1 Stable Environment

Provision of a quantifiably stable thermal environment had not been used prior to this Study which used the Cube. This removed a potential confounder of an unstable thermal environment, allowing the thermal imaging technique to be assessed for its capability without such interferences.

5.3.1.2 Hand-Carrier

Development of the laboratory technique needed a carrier-system to transport the samples from the cold thermal disruption provided by ice, to the warmth of the hotplate and, initially, an internal device was rotated to lift the carrier off the ice and then slide to the hotplate. This was cumbersome to operate and proved very difficult to change samples, requiring opening of the doors which affected the stability of the thermal environment. A totally independent hand-carrier was developed which could be inserted via a narrow, letter-box-style window in the door. This method allowed easy removal of the carrier to exchange samples for the next sequence and thermal stability was unaffected (Figure 5-2).

A   B
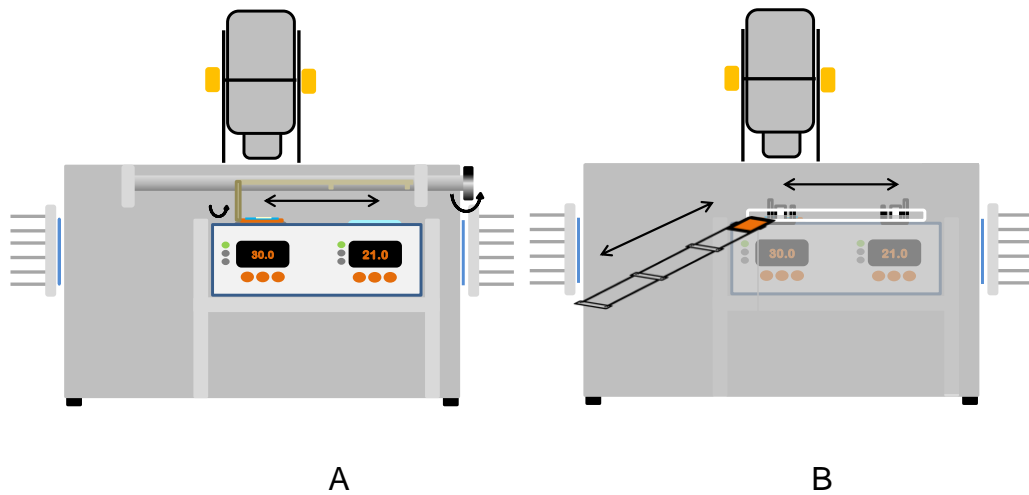
Figure 5-2 A: Initial Carrier – rotate and slide B: Final Hand-Carrier

A variety of materials were explored to provide the carrier-baseplate, e.g., aluminium or copper, and also a conducting-medium on which to place the samples, e.g., conducting-paste (≈1.8Wm·K Halnziye Hy610 Gold), conducting-tapes (Farnells 3M Thermal Conductivity Tape - 0.4Wm·K and the Gamebooth – 6 Wm·K). A conducting-tape was used which was soft and compressible, allowing the tooth-samples to nestle into it, giving the best reversible, surface-contact for heat-transfer. This was used for all samples. Permanent fixing of the samples was not desirable, as this would require numerous baseplates introducing inconsistency and, additionally, would necessitate the changing of each baseplate. Previous studies with a maximum of two slices had mounted them in either an acrylic-resin-plate (Lin et al, 2010b) or on to a copper-plate with a dental-filling-material (Panas et al., 2007). The thermal tape was very versatile, providing thermal conductivity, rather than insulation as would occur from the filling-material. It caused no damage or known contamination of the samples, enabling repeat use, unlike a paste or bond which would have been difficult to remove, risking damage to the samples. Great care was taken to avoid introducing any air-bubbles under the tape during placement on the copper-baseplate as this could have affected the heat-transfer.

5.3.1.3 Thermal Disruption

The hotplate, with two wells, enabled heat to be applied at the selected temperature. The second well would not cool, maintaining only ambient temperature. A block-of-ice was removed from a container in which two supports were placed and the ice-block replaced, resulting in the ice sitting-proud of the container-periphery. This was supported by the sides of the well (Chapter 3, Figure 3-4), allowing the baseplate to contact the ice without

excessive pooling of water as the ice melted, as this dripped into the space provided underneath. The ice-block had to be changed after a maximum of five sequences, which caused some disruption to the stability of the Cube which was then allowed to stabilise. The cooling-mechanism required further development (as seen in Chapter 3, Section 3.5, for the in-vitro vitality test of whole teeth where a cooling-unit was used). A Cube temperature of 30°C rather than 22°C would have melted the ice far quicker. When a clinical application is required, the cooling-mechanism may involve cryogenic sprays which are available for use in dentistry, or ice which is cheap and easy to produce.

5.3.1.4 Thermal Consistency of Environment, Hand-Carrier and Hotplate

The thermal environment of the Cube delivered an excellent setting for the investigations, with a maximum variation of 0.5^{o}C throughout all the recordings (Chapter 4, Section 4.3.2.2). This reduced the influence of any external confounders from air-conditioning, air-currents, operator-emissions or sunlight, which may affect the warming-sequence of the specimens.

Variation in temperatures throughout the data-collection of the hotplate was expected as the cold copper-baseplate at 2°C made contact with the warm hotplate. Initially, this led to a drop in temperature of the hotplate. The required temperatures were set at 30°C or 37°C. During both of these conditions stability remained within 1°C (Chapter 4, Section 4.3.2.4). The thermocouple of the copper-baseplate had a limited area-of-contact compared to the total area of the hand-carrier but there was an indication of even-heat-exchange with steady-warming. The copper-baseplate was consistently taken to a baseline-temperature of 2°C before warming, and the maximum temperature reached within the 30°C samples were all within 0.5^{o}C (Chapter 4, Section 4.3.2.3). Within each sequence there was very small variation in temperature, with 0.4^{o}C for the sound tissue and 0.1^{o}C for the demineralised tissue. These values provide assurance that the effects seen within the sequences, and between the sequences, are due to the thermal properties of the tissues, rather than variation in the thermal environment and equipment.

Only one slice did not warm as rapidly and this may be due to operator-error in not placing the hand-carrier correctly, or excessive moisture on the base delaying re-warming.

5.3.2 Tooth-Slices

This Study reviewed multiple slices of tooth-tissue from two teeth rather than a single-sample or two samples from one tooth, although it is acknowledged this is still not a large sample-size. A demineralised, naturally-occurring carious lesion was also present in the teeth-slices, providing a unique opportunity to evaluate the thermal properties of the lesion.

The slice-thickness influences the rate of heat-transfer, and the thicker it is the slower the transfer and the greater the 3-dimensional heat-transfer, compared to thinner sections. This is considered within the calculations of thermal diffusivity and conductivity where the sample-thickness is used (Chapter 4, Table 4-12). Relatively, this is unimportant in producing either thermal map, as the enamel and dentine are exposed to the same conditions irrespective of the thickness, and the characterisation between enamel and dentine should be unaffected, but heat-transfer will not be as rapid, thus affecting the characteristic-time-to-relaxation.

The previous studies (Lin et al., 2010b; Panas et al., 2007) had slice-thickness of 2.2mm - 3.15mm, whereas the range for the samples presented in this Study (i.e., Tooth 1 Slice 6 and Tooth 2 Slice 4 - 0.7mm to 0.9mm Chapter 4, Table 4-10) were virtually a third thinner than those previously used, and heat-transfer to thermal equilibrium would be respectively quicker with less 3-dimensional-effects.

5.3.3 Application of Heat

This Study used slices of teeth which were laid flat on the hotplate at a constant 30°C – the approximate temperature of the anterior teeth in an open mouth (Brown & Goldberg, 1966; Fanibunda, 1986b) – allowing heat-transfer vertically to all areas at the same time; whereas Lin et al., (2010b), applied heat to the occlusal-surface of the tooth via a flow of contained hot-water (60°C) and heat-transfer was longitudinal across the crown and down the root, but it is unlikely to have simultaneously contacted all the occlusal-surface. Panas et al., (2007), also used hot-water (38°C) to heat the copper-baseplate which contacted the flat-surface of the tooth-slices in a similar way as the hotplate in this Study. The water may have lost some of its thermal energy in transit from its source where the temperature was measured, whereas the hotplate retained a stable temperature providing a continuous energy-source. A layer of thermal insulation was present in both the other studies - between the tooth-tissue and the copper-plate for Panas et al., (2007), and an additional layer of black paint added to the surface by Lin et

al., (2010b). This may result in a small difference in values of time-to-relaxation and neither study compensated for this possibility in the final calculation of thermal diffusivity, whereas in this Study the value applies totally to the tooth-tissue.

5.3.4 Thermal Sequence

The data collected was processed in a number of ways and the first was to display the overall heat-exchange process as a graph (Chapter 4, Section 4.3.5). Two samples have been presented in their entirety, and for each there are a number of areas-of-interest selected. An area is more representative of the sample temperature (than a single point or a single line of data as used by Panas et al., 2007 and Lin et al., 2010a & 2010b) and takes the mean value of temperature from an area incorporating any extremes (which a point cannot), thus providing a better reflection of the overall tissue.

The literature indicates there will be some difference in the thermal properties across the dental tissues due to the non-homogenous chemical-composition and the structure, (Chapter 2, Section 2.1.6.1 & 2.1.6.2). Enamel has a higher mineral-content than dentine and it would be anticipated the thermal properties would lead to a quicker exchange of heat via enamel (rather than dentine) which is predicted from previously reported values (Chapter 2, Table 2-6 & 2-7). This is demonstrated within the graphs, and enamel areas-of-interest on opposing sides of the sample behave similarly, having a quicker re-warming-rate than dentine - seen by the steeper gradient of each curve. Crown-dentine presents with a marginally-quicker re-warming-rate than root-dentine, but slower than enamel (Chapter 4, Section 4.3.5 – Figure 4-18 to 4-19). For the demineralised tissue, the chemical-composition, and later in the pathological process the tissue-structure, will change and this results in a slower rate of re-warming in both the carious enamel and dentine.

5.3.5 Curve-Fitting

Curve-fitting of the latter-third of re-warming-data with a seconds-timeline (rather than a frames-timeline) used the exponential equation described by Lin et al., (2010b) and produced the characteristic-time-to-relaxation for each area-of-interest, i.e., the time to reach thermal equilibrium.

The curve-fitting achieved was strong, as indicated by the R-Square values which all have a value above 0.9 (Chapter 4, Table 4-11). R-Square (coefficient of determination) is calculated iteratively within the curve-fitting-

process as a statistical measure of how strongly the data fits a regression-line (best fit-line for the data) and can lie between 0 and 1 (0% to 100%), the nearer 1, the stronger the model can account for the outcomes around the mean.

The characteristic-time-to-relaxation-values were used to calculate the thermal diffusivity and conductivity and were also used in producing one of the thermal maps.

5.3.6 Thermal Diffusivity and Thermal Conductivity

Recorded values of thermal diffusivity and thermal conductivity are wide-ranging and this is expected, as the tissues are unlikely to be totally homogenous within a tooth or between teeth. Any expectation of the thermal diffusivity and conductivity to be consistent in such a diverse biological composite is unrealistic. There are previously reported values for enamel and dentine which provide a range for thermal diffusivity and conductivity (Chapter 2, Table 2-6 & 2-7) but no value was found in the literature for demineralised tooth-tissues of enamel or dentine due to caries, which provided an opening to make an original contribution to current knowledge.

The findings of this Study recorded the demineralised areas of enamel and dentine to have a lower thermal conductivity and diffusivity than normal tissue within the same tooth (Chapter 4, Table 4-12). Following exposure to the thermal disruption of cooling and re-warming, enamel from Tooth 1 produces a value within the known-range of thermal diffusivity and conductivity (2.41-2.65x10^{-7}m^2/sec and 0.48-0.53Wm·K, respectively) and values are slightly higher from Tooth 2 (3.29-4.61x10^{-7}m^2/sec and 0.65-0.92Wm·K, respectively). The areas-of-interest selected with caries in Tooth 2 produces values of 1.83x10^{-7}m^2/sec and 0.36Wm·K for thermal diffusivity and conductivity, respectively. These are lower than the normal tissues of the same tooth and a different tooth.

Loss-of-mineral in the pathological process of dental caries may explain the lower rate of heat-exchange in the enamel-fissure caries-area, but care is needed as this area also encompasses a fissure which may influence the heat-exchange. The value is less than half the mean of the two other enamel values in Tooth 2 for both thermal diffusivity (1.83 v 3.95x10^{-7}m^2/sec) and conductivity (0.36 v 0.79Wm·K). It is also lower than the ranges provided by Panas et al., (2003) and Lin et al., (2010b) at 2.27–4.08x10^{-7}m^2/sec for thermal conductivity and 0.45–0.81Wm·K for thermal diffusivity.

The area of caries within the dentine also had a slower heat-exchange. The area-of-interest of the carious dentine was in the crown-dentine and it was less than any other crown-dentine thermal diffusivity (Tooth 1 & Tooth 2 of 4.15 and $1.92\text{-}2.48\text{x}10^{-7}\text{m}^2$/sec, respectively) or conductivity (Tooth 1 & Tooth 2 of 0.99 and 0.46-0.6Wm·K, respectively) by ≈ a third at $1.21\text{x}10^{-7}\text{m}^2$/sec and 0.29Wm·K, respectively.

These two properties, thermal diffusivity and conductivity, for root-dentine were also greater than the carious crown-dentine area by ≈ a third (Tooth 1 & Tooth 2 root-dentine thermal diffusivity of 2.00 and $1.81\text{-}2.31\text{x}10^{-7}\text{m}^2$/sec, respectively) and conductivity (Tooth 1 & Tooth 2 of 0.48 and 0.43-0.55Wm·K, respectively).

No comparison could be made with other findings for demineralised tissue and this data can be added to further our knowledge of the thermal properties of tooth-tissue, making a unique contribution. They are specific to this tooth, and other lesions in different teeth may be different depending on the degree of mineral-loss.

The conclusion of Panas et al., (2003) may provide a more realistic understanding of the tissue-behaviour, which was that enamel tends to have a quicker thermal conductivity than dentine; which is also demonstrated in this Study. Additionally, it may be said demineralised tissue from the pathological process of caries tends to have reduced thermal conductivity depending on the stage of disease, compared to healthy tissues of the same sample. Inter-sample variations may not always follow the above findings, due to the varied nature of the mineralised tissues, the orientation of dentinal tubules and enamel prisms, the age of the tooth and its history, as well as the stage of disease.

5.3.7 Characterisation of Enamel and Dentine by Thermal Mapping

Two methods were used to characterise enamel and dentine thermal properties by calculating the characteristic-time-to-relaxation, and the area-under-the-curve for each point in the tooth, and mapping to a 2D image file. This had not been undertaken in previous studies and allowed thermal information to be compared with, and added to, other image-data-sets (such as photographs or X-rays) in an original and novel way (Chapter 4, Figure 4-27 to 4-30).

When the whole area of the tooth-slice was selected, the thermal relationship of enamel, crown-dentine and root-dentine can be seen in one

image and differentiates enamel from dentine. This may be from their thermal properties (as per the calculations previously described) or it could be from cooling via evaporation of water from each of the tissues. Evaporation was the basis of caries-detection with thermal imaging, described by Kaneko, et al., (1999), and Zakian, et al., (2010), neither of whom considered the thermal properties in their studies. Both caries-studies reported positive outcomes and thermography may be a useful adjunct for the diagnostic armamentarium. Comparison is made across the optical image of a photograph, an X-ray and the two thermal maps, all of which use electromagnetic radiation to produce their respective images.

The first image produced from the characteristic-time-to-relaxation data does distinguish enamel from dentine and clearly has an outer-layer surrounding the enamel, which is thermally different from the bulk of enamel on the characteristic-time-to-relaxation map and this may be due to the deposition method of enamel where the final outer-layer of enamel is void of the prismatic structure. The demarcation between enamel and dentine is seen on both thermal maps with a change in greyscale, the darker greyscale indicating the enamel with a more rapid exchange of heat. The fissure is also seen within enamel. The top/right-cusp in the image (Figure 4-27/28) shows a line tracking from the cervical region to the occlusal, and which later cracked. There are areas of homogenous thermal exchange with uniform greyscale in the enamel.

Dentine has uniform grey areas as well, but there are changing areas of grey visible. These are particularly found where the pulp-chamber is present and the thin tissue of the pulp-wall is detected by the thermal exchange. The photograph also shows this region but it is not detected by the radiograph as the tissue does not sufficiently attenuate X-rays.

The curvature of the root is visible within the photograph and it can also be seen on both the thermal maps, but is more defined from the area-under-the-curve map. The radiograph shows this region as a darker-grey, as there is less mineralised tissue present. The root-face has been sliced and there is a root-canal visible on the two thermal images and evidence of a change in mineral-density radiographically, but the photograph is not clearly showing the canal.

The root-tip on the characteristic-time-to-relaxation is light-grey and may not have achieved good thermal contact due to its curvature and shows a reduced thermal-exchange-rate. The carious lesion (Chapter 4, Figure 4-30)

also demonstrates a slower rate of heat-exchange – light-greyscale - the same as the root-canal-region with reduced mineralised tissue.

5.3.8 Summary

The Cube provided a very stable environment for examining the thermal properties of mineralised tooth-tissue with infra-red thermography. Thermal diffusivity and conductivity fell within the known-range and the lower values for demineralised tissues were reported for the first time, making a unique contribution to knowledge.

A thermal map of the tooth-slices characterised enamel and dentine and the presence of demineralised tissue could be detected. This had not previously been reported. The heat-exchange detected by the thermal maps may offer a technique to detect heat-exchange between a vital and non-vital tooth and justifies further investigation on a whole-tooth, not a slice.

5.4 Model Calculation of Pulp Blood-Flow-Rate

In this Study, the heating–potential of the blood-flow within teeth is being explored to determine tooth-vitality using infra-red radiation. However, the precise blood-flow to each of the adult human teeth is unknown. Animal models (Chapter 2, Tables 2-12 & 2-13) have been used to provide information about the pulp-tissue, which is proposed to have one of the highest blood-flow-rates of all the oral tissues (Kim et al., 1980). The range of blood-flow-rates found in the literature is very wide at 2-146ml/min/100g. Such a range may not be unexpected, as biological tissues will vary within subject and between subjects of the same species, as well as between different species. The methodologies of data-collection were based on two main species – dog and rat – which requires careful interpretation when making inference to man.

It is a promising finding for the vitality test being investigated within this Study, that the coronal pulp has a greater blood-flow than the root, (Meyer & Path, 1979; Path & Meyer, 1980) as this is the anatomical location available for examination for the vitality test. If the crown is exposed to a cold thermal disruption, the higher flow-rate will re-warm this area more rapidly, allowing an opportunity to detect a thermal difference. The maxillary teeth often have a greater aesthetic impact than the lowers which are shielded by soft-tissue, and may be more vulnerable to trauma when the mouth is open. There is a reported increase in blood-flow-rate of up to 50% in the maxillary teeth compared to the mandibular (de Leon et al., 1978; Path & Meyer, 1980) which, again, is advantageous, providing a greater heating-potential for a vitality test such as this based on thermal exchange.

5.4.1 Blood-Flow and Pulp-Weight

In the literature, a method of determining pulp blood-flow-rate measured pulp-weight, and two studies provided the weight of human pulp-tissue which ranged from 9.4mg - 51mg and these were used in modelling the blood-flow-rate.

5.4.2 Assumptions

There are multiple assumptions with the model presented in Chapter 3 Section 3.4 and the results in Chapter 4, Section 4.4; the application of the properties of water to the pulp, using average values for the volume of the pulp, as well as using the weight of pulp-tissue from only two studies and only two teeth-types. From these, a water constant was made and applied to all teeth, which was different in the maxilla to the mandible. These values of

pulp-weight and pulp-volume will vary from human-to-human and be dependent on patient-age, time of pulp-removal following extraction of the tooth, disease-status and past history. Future work to ascertain an average value of human pulp-weight-per-tooth would be useful to improve the above calculation, as reliability and validity must be viewed with some caution.

5.4.3 Rationale for Applied Flow-Rates

Based on the available literature and the modelling described, a flow-rate as high as 0.5ml/min was applied for the simulated vitality, which is comparable to other studies assessing simulated vitality. Fanibunda, (1985), used 0, 0.5, 1.0, 2.0 and 4.0ml/min. Smith et al., (2004), also used a 0.5ml/min flow-rate for one of 10 flow-rates, as well as two lower rates of 0.33ml/min and 0.16ml/min, which appear more compatible with the modelled in-vivo blood-flow-rates which appear to be low.

Park et al., (2010), report the human pulp blood-flow as being unknown and used three arbitrary flow-rates of 0.0042, 0.028 and 0.070ml/min for their study, assessing intra-pulp-temperature-changes from curing-lights. The two lower values fall within the ranges calculated from human pulp-weight for premolars and third molars from Van Amerongen, et al., (1983), as well as the volume-model with water constant (ω). However, no formal calculation was presented and it was stated these were the flow-rates available on the pump. Maintenance of such low flow-rates in-vitro has been difficult to maintain and higher rates have been used due to that, e.g., 0.5ml/min (which was abandoned) and 1ml/min used (Kodonas et al, 2009).

All these values show teeth have a low blood-flow-rate and, for this Study, the question being asked is whether this low flow-rate is sufficient to provide warming of the tooth detectable in a timeline to distinguish it from a tooth without a blood-flow. It has been suggested this is so low that it may not be detectable, or swamped by other sources of heat, such as the gingival blood-flow. However, the gingival flow-rate may have a similar value - 50ml/min/100g is presented by Ozcan et al., (1992) who studied human gingival tissue, and Kaplan et al., (1978) who studied canine (dog) gingival blood-flow-rate. Thermal contribution may also be received from the bone, primarily alveolar bone, which has a rate one-fifth of the average pulp-rate at 9ml/min/100g in the dog.

Four rates were selected for this Study: 0.03ml/min, 0.08ml/min, 0.15ml/min and 0.5ml/min. This provided comparison with others' work and reached a level comparable to the molar-model whilst maintaining an empirically

achievable flow-rate. This provided potential for inference to the human tooth.

5.4.4 Summary

A new model has been presented and although there are limitations as described, it provides a basis for all future in-vitro applications where a simulated blood-flow-rate can be applied to the type of tooth collected. This may provide a more consistent approach between research groups, enabling better comparison of their findings.

5.5 In-Vitro Feasibility of Using Infra-Red Radiation In Determining Tooth-Vitality

The principle of assessing tooth-vitality from the thermal energy supplied by the blood-flow has been known for many years. The first use of infra-red radiation and thermography was an in-vivo study by Hartley et al., (1967) which found no thermal difference between the vital and non-vital teeth of the subjects. Fourteen studies (Table 2-23) found in published literature have investigated temperature as a plausible method to assess vitality since 1965, using a variety of temperature-measurement-methods, both contact (thermocouple and thermistor) and contactless (thermography). Two were in-vitro (Fanibunda, 1985; Smith et al., 2004) and neither used thermography but both applied a cold thermal disruption, unlike Hartley et al., (1967). This Study, assessing the in-vitro feasibility of using infra-red radiation in determining tooth-vitality, is thought to be the first, and also applies a cold thermal disruption.

In this Study, previous work developing the Cube provided a stable thermal environment and the emissivity-values previously calculated were also used for enamel of whole teeth. The blood-flow-rates were varied, ranging from 0.03ml/min which approximates those of the model for the first maxillary molar to 0.5ml/min, as used in other studies. Knowledge of the production of thermal maps presented a novel opportunity to assess vitality.

5.5.1 Molar-Model

The previous two studies both used premolar teeth: Fanibunda, (1985) had a maxillary and mandibular premolar, and Smith et al., (2004) had a single maxillary premolar. From the practical aspect of tooth-availability, as well as the need to have an inlet and outlet via separate roots, a molar-model was developed. To provide an inlet and outlet in anterior teeth of incisors and canines with a single root would be more difficult and, as seen in the two other studies, a multi-rooted tooth was selected. This is the first assessment of simulated vitality with a molar-model.

5.5.2 Tooth-Data

A collection of 16 molar teeth was ethically approved (Appendix A.4.1 & A.4.2) and these teeth included at least 1 tooth from each category of molar, i.e., a maxillary or mandibular first, second or third molar. The commonest tooth available was the maxillary first molar (U6, with 5 of these), and the mandibular first molar and both second molars were the least commonly available. More teeth were available from females (10) than males (6), and

the age ranged from 10 years to 28 years, with a mean distribution of 16 years and 7 months.

The younger the tooth, the larger the pulp-chamber and root-canals which provide a greater volume for the simulated blood-flow to occupy and, in turn, implies a reduced-thickness of surrounding mineralised tissue through which the thermal transfer occurs before detection is possible. This is advantageous to the Study, although this would need to be considered for the clinical application of older teeth which may have increased deposition of secondary and tertiary dentine (Chapter 2, Section 2.1.6.2 and Table 2-3). One tooth had a restoration (Pair 2 – left-tooth on screen). Caries was present in some teeth to varying degrees which may have affected the rate of heat-transfer, as seen from the results of the thermal conductivity and diffusivity-values for the demineralised carious tissue which was reduced, compared to reported sound tissue (Chapter 4, Table 4-12). This may have influenced the cooling-effect – however, data-collection was from the buccal-surface of the teeth which were unrestored and caries-free. These samples provide a true representation of teeth which would be tested for vitality, compared to a perfectly sound tooth used by Smith et al., (2004). The status of the two premolars used by Fanibunda, (1985) was not reported as sound, carious or restored.

5.5.3 Experimental Design

5.5.3.1 Configuration of Pairs for Simulated Tooth-Vitality

The teeth were paired according to size, and only one pair was a true anatomical pair from the same donor (Pair 7). Within nature, there is a bilateral morphological symmetry and teeth occupy equivalent locations within each jaw on the right and left, and an attempt was made to duplicate this by size-matching. Thermal symmetry is also found within healthy tissues - ±0.4^{o}C (Vardasca et al., 2012), and measuring the temperature of dissimilar tissues increases the normal variation and was to be avoided if possible but, inevitably, teeth from different donors, even of the same type, will not carry the same level of symmetry.

The simulation in this Study provided support to the paired teeth via an artificial alveolus produced by Aluwax containing aluminium-particles, which aided heat-transfer to the teeth. The precise comparison of thermal exchange of the Aluwax and bone was unknown, as the available data on Aluwax did not include thermal conductivity or diffusivity. Stability within the holder was excellent once an addition of greenstick compound had been

made. Prior to this, on application of the cooling-unit to the occlusal-surface, some movement was seen from the pairs within the holder which affected the visibility of the buccal-aspect of the teeth-surfaces.

Neither of the other studies had used this method – Fanibunda, (1985) developed a water-tight acrylic-pouch around each tooth, following a wax-up to simulate the alveolus; and Smith et al., (2004) did not refer to any support-mechanism used for the single tooth.

5.5.3.2 Simulated Periodontal Blood-Flow

Replication of the natural periodontal vasculature is unrealistic, and an attempt to provide a similar thermal contribution was made via the tubing wrapped around each root to carry the warm water in a vessel simulating the blood-vessels. This method does have a single route for the entry and exit of the warmed blood-flow, unlike the natural tissue with multi-directional flow of the heat carrying blood in many vessels. This may have led to a reduction in temperature as the water flows through the tubing, and a system of encircling the teeth alternately, reduced this effect. Temperatures recorded with thermocouples indicate a small difference of $0.2^{o}C$ between the left and right periodontal ligament prior to cooling (Chapter 4, Figure 4-37), which is within the natural limits of symmetry ($0.4^{o}C$). Cooling was within $0.1^{o}C$ on each side, providing a maximum of $3.4^{o}C$ and a minimum of $1.6^{o}C$ reduction. These temperatures were measured from a small area, and are dependent on the location of the thermocouples which were measured to be equidistant from the simulated gingival-margin. The temperatures recorded suggest each tooth is receiving a similar source of thermal energy and the cooling of each tooth is within acceptable limits, as recorded from the periodontal ligament.

In the study by Fanibunda, (1985), water flowed through the pouch at a constant, unreported temperature from a water-bath, whereas Smith et al., (2004) immersed the tooth-root in a water-bath of $37^{o}C$. Both these methods provided direct water-contact over the entire root-surface, one flowing and one static, whereas this Study provided a simulated flow through a vessel. The thermal stability of the two water-sources is unknown, whereas this Study provided a steady temperature of ≈$30^{o}C$ to the periodontal ligament for both teeth within each pairing – Pair 1 to Pair 8.

5.5.3.3 Simulated Pulp Blood-Flow

A similar situation occurs when attempting to simulate the blood-flow to the pulp, which has a similarly-complex vascular-network to that of the

periodontal ligament, and the aim was to provide a thermal source which replicates that of the natural vascularity. Preparation of the tooth allowed insertion of a cannula with uniform dimensions which could be applied to all sixteen teeth. These were placed within a root-canal, with the knowledge there was a patent passage through the tooth for water to flow. There was no expectation that all pulp-tissue had been removed and this would add a more natural situation to the flow through the tooth, where the blood would be contained within vessels rather than having direct contact with the internal face of the mineralised dentine, which may increase the opportunity for thermal exchange. Entry and exit was via a different tooth-root and there had to be a flow through the tooth for this to happen. This is artificial as, in the natural tooth, there would be both entry and exit of the blood in each root-canal. The simulated flow may have led to areas of stagnation within the tooth where the water did not exchange. Fanibunda, (1985) used tubing in both canals for entry and exit of the water, whereas Smith et al., (2004) did not describe the precise details of how the water entered or exited the tooth. The insertion of a cannula in the exit-root was initially used in this Study - however, it was immediately apparent this would not be successful. Water did not exit the small diameter of the cannula so, instead, a tube was attached around the root which offered no resistance to the outward-flow of water.

Securing a water-tight seal was not simple. Many materials were explored, from wax (sticky, Aluwax and greenstick), to dentine-bond and waterproof-adhesives, but the most successful was Loctite Superglue.

The water-temperature flowing through the teeth was measured by an internal thermocouple, inserted via a root (the same as the cannula) or a third root, if present. The presence of a simulated blood-flow was not expected to demonstrate vitality when at rest, as a thermal equilibrium with the surroundings was anticipated. In this state, the same temperature should be achieved in a vital and non-vital tooth, as shown in the early studies by Goldberg & Brown, (1965); Brown & Goldberg, (1966); Crandell & Hill, (1966) and Hartley et al., (1967), where the external temperature of vital and non-vital teeth was measured and found to be the same. The external tooth-temperature was also measured by a thermocouple on the opposite side to where the thermal recording was made.

Figure 4-38 & 4-39 show the stability of these measures without thermal disruption, and both were within acceptable natural limits for flow-rates up to

and including 0.5ml/min. No internal tooth-temperatures were recorded in the other two studies.

5.5.3.4 Provision of Simulated Blood-Flow-Rates

The experimental design aimed to provide four different flow-rates and this was provided by a pump with associated tubing of varying diameters. The flow-rates were measured for simulations of the eight pairs (Chapter 4, Figure 4-56), and the mean values for the variables applied show a 0.02ml/min-range was found for the highest flow-rate (0.44-0.46ml/min). For both flow-rates of 0.15ml/min and 0.08ml/min, a mean difference of 0.01ml/min was found (0.15-0.16ml/min and 0.08-0.09ml/min, respectively) and for 0.03ml/min the mean value was achieved.

There will be some experimental variation in all investigations and repeat measures were taken within Pair 7 at 0.5ml/min (Table 4-23). Three consecutive sequences were run twice, on separate occasions, and mean experimental error from 0.5ml/min was of the order of 6-8% and 2% from an achieved flow-rate of 0.46ml/min. This was higher than Fanibunda, (1985) at 1.8%. Smith et al., (2004) did not comment on experimental variation. The flow-delivery to the teeth by Fanibunda, (1985) was gravitational, from a set-height, which produced less experimental error than the pump used in this Study. An infusion-pump was used by Smith et al., (2004).

The heart provides the pumping mechanism to the naturally-circulating blood, resulting in a pulse-effect. The flow applied by gravity and the infusion-pump were smooth and continuous, as was the flow provided by the pump in this Study. A pulse-effect, to simulate the naturally-occurring pulse, had not previously been applied when assessing tooth-vitality in-vitro from a thermal perspective and provided an opportunity for a unique contribution. This was included in the design of this Study and applied at a rate of 60rpm, which approximates the average heartbeat. The flow-rate was unaffected. The simulated pulsatile-effect was not correlated to the heat-exchange in-vitro and could be used to maximise the sensitivity of the thermal mapping and is an area of further work.

Each of the studies included 0.5ml/min as one of the flow-rates as well as no simulation. Water was used by Smith et al., (2004), and, in this Study, distilled water was used, whereas Fanibunda, (1985) used saline. Other solutions may be used which increase the fluid-viscosity but risk blocking the system.

5.5.3.5 Thermal Environment

The Cube provided a stable thermal environment as previously discussed.

5.5.4 Measurement of Thermal Differences

Measurement techniques of tooth-temperature vary between the in-vitro studies - a thermistor and a thermometer were used by Fanibunda, (1985) and Smith et al., (2004), respectively - whereas this Study used a thermal camera to collect the infra-red radiation emitted to assess the thermal status between vital and non-vital teeth. The thermal camera was contactless and avoided cross-infection risk or interference with the surface of the teeth and, as identified in the literature, offered superior metrology compared to the other two studies which required direct contact with the tooth. Additionally, the thermal camera records a real-time-sequence which can be analysed at a later date, with a frame-rate-collection of 9-per-second for this camera. A permanent record of data collected was made from the thermistor as a graph on paper in 1985. Smith et al., (2004) logged data in intervals of a second, from the thermometer to a computer. Technological advances provide some benefits in data-collection, which is now easy to duplicate and can be analysed without loss of the original data, using different computer software. The thermistor and thermometer measure a point-of-contact on the tooth, whereas the thermal image enables multiple areas-of-interest or varying size and location to be assessed, providing an average value of the area.

Interpretation and analysis of the collected data also varies between the studies. The thermistor graph enabled calculation of the area-under-the-re-warming sequence and was measured in cm/seconds, whereas the thermometer presented the surface-temperature of the tooth against time with different simulations of flow-rate. This allows potential comparison between studies using temperature, but not cm/seconds. However, different teeth were used under different conditions, and caution would be advised.

Within this Study, the whole thermal sequence was captured and data was processed for each pair of teeth from the same temperature-point of the re-warming sequence, producing a time-temperature-series for both teeth of the pair. Additional analysis allowed the same tooth to be aligned as a vital and non-vital tooth as per the cross-over-design, which reduced potential confounders/errors and allowed validation of the positive effect. This cross-over-effect was seen for both the independent dissimilar pairing of teeth in their 1-8 Pairs and also for the matched same tooth Pairs. This data could be used in a similar way as the data for evaluating the thermal properties

(Section 4.3), and the area-under-the-curve could be calculated, or the characteristic-time-to-relaxation. Additionally, temperature-differences between the vital and non-vital tooth simulation under the same conditions could be assessed. Smith et al., (2004) had one tooth, which was used repeatedly at different flow-rates, as were the teeth by Fanibunda, (1985), and within this Study. Only this Study had a vital and non-vital tooth available within the same sequence of data-capture and under the same environmental conditions, which reduced confounders.

All three methods of data-processing were applied for phase one of the simulated vitality test which established the most informative method, which was the area-under-the-curve. The production of a thermal map during the re-warming sequence was also undertaken.

5.5.5 Thermal Disruption

The rationale for applying a cold thermal disruption is based on the principle that, with vitality, a tooth will re-warm quicker, having greater thermal energy than a non-vital tooth. This is subject to the other tissues supporting the tooth with a blood-supply not overriding the thermal energy available from the blood-flow of the pulp.

Within this Study, a cooling-unit was developed using a thermoelectric peltier which provided a wide range of controllable, sustainable cooling temperatures, unlike ice which melted and required regular replacement for the earlier in-vitro investigations. The temperature of the cooling-unit ranged from -7.14 to -8.3^{o}C when used for the sequences on the eight pairs (Table 4-25). The ideal tooth-temperature-reduction to show the best difference in thermal exchange on re-warming between a vital and non-vital tooth was initially unknown, if one existed.

Phase one of the simulated vitality testing investigates this by applying the cooling-unit to the occlusal-surfaces of the teeth until the internal temperature of the right-tooth of Pair 4 on screen reduced by 0, 2, 4, 6, 8 and 10°C. This was applied for four simulated flow-rates – 0.5ml/min, 0.15ml/min, 0.08ml/min and 0.03ml/min. The simulation of the teeth-pairs included vitality to the periodontal ligament and to each tooth separately, so the simulations had the left and right-tooth as vital and non-vital with a periodontal blood-flow (PDL LTS and PDL RTS). The pulsed simulation was applied to all four flow-rates at the level of a 2°C internal drop-in-temperature. This process had not been reported by any other study in-vitro to assess the ideal cooling and was a novel investigation.

The data was reviewed as the difference in:

- area-under-the-curve
- temperature
- characteristic-time-to-relaxation.

5.5.5.1 Area-Under-The-Curve

The area-under-the-curve provides information on the re-warming sequence following alignment of the temperatures of both vital and non-vital teeth. The expectation of the difference in the area-under-the-curve if there is a greater thermal exchange due to vitality, would be a positive-value when the right-tooth was vital and a negative-value when the left-tooth was vital. This may increase with increased cooling, as there is a greater temperature-differential which may reduce more rapidly due to the thermal energy available in a vital tooth. If the temperature-reduction is insufficient, the presence of the thermal energy due to vitality may not be detected in the time taken to reach thermal equilibrium in the stable thermal environment of 30°C, as the environment also provides thermal energy to each tooth. The mineralised tissues are insulating and the thermal-effect from vitality will take time to travel through the tissues and be detected from the surface of the tooth. If the cooling is superficial the impact from vitality may be less, whereas if cooling is deeper, the potential to detect thermal changes from an internal source are more likely.

At the highest simulated flow-rate (Chapter 4, Figure 4-41) there was a clear difference between the vital and non-vital teeth, with positive and negative-values of the difference in the area-under-the-curve as expected, but the effect was less for left-side vitality – with one exception. This exception was the control with no thermal disruption and the teeth were virtually in thermal equilibrium, producing a positive outcome. This is accepted, as a perfectly-balanced-model producing a difference of zero would be unlikely. This was a feature of the Pair 4 model for all four flow-rates in equilibrium. This may be due to the different teeth used within the pairs - in Pair 4, the left-tooth was larger than the right - or it may be due to a marginal cooling-effect of the tooth with simulated vitality which increases with reducing flow-rate. The simulated periodontal supply remains constant with either the left or right side of simulated tooth-vitality, but may provide more warming to one side, thus reducing the overall effect, and this may offer an explanation of reduced values for left-side vitality.

The reduced-effect for the left-side vitality may also be due to the measurement of the temperature-reduction always being recorded from the thermocouple in the right-tooth. This is in a consistent location, but the conditions change with the changing sides of vitality. When the right-tooth is vital, there is a continuous warming-sequence from the simulated vitality. The reduction-in-temperature of the tooth to achieve the necessary internal temperature, as detected by the internal thermocouple, may be greater than when the left-tooth is vital. This results in greater cooling of the teeth with the right-side vitality simulation at the higher flow-rates and may show a greater difference in the area-under-the-curve.

The difference in area-under-the-curve between a temperature-reduction of $8^{o}C$ and $10^{o}C$ is small and, with an $8^{o}C$ reduction, the re-warming sequence shows a clear difference in the detected thermal energy of a vital and non-vital tooth. This is applicable to both vitality simulations, where the source of thermal energy is the pulp blood-flow and the periodontal ligament. However, all thermal disruptions show a difference for the time taken to achieve a $10^{o}C$ reduction and, for future clinical use, the least thermal disruption with the clearest difference was seen with an $8^{o}C$ reduction at a flow-rate of 0.5ml/min.

The overall values reduce with a reducing simulated flow-rate, but the trend for a greater difference with increasing temperature-reduction remains to a flow-rate of 0.08ml/min. The effect is seen more clearly from the right-side vitality, which remains a positive-value with a thermal disruption throughout all flow-rates and at the lowest flow-rate the effect of the pulse increases the difference in the area-under-the-curve, whereas the left-side vitality switches between both negative and positive-values at 0.15ml/min and becomes totally positive at 0.08ml/min and 0.03ml/min. This is indicating the thermal energy from the left-side is less than the right-side, even though it has vitality.

An internal reduction of $8^{o}C$ provides the best outcome at the highest flow-rate ($16^{o}C$-$18.5^{o}C$ tooth-surface temperature-reduction), with a gradual reduction in difference in area-under-the-curve with reducing flow-rate and temperature. At a flow-rate of 0.15ml/min the tooth-surface temperature-reduction ranges across $13.5^{o}C$-$17^{o}C$; at 0.08ml/min a temperature-reduction of $14.5^{o}C$-$18^{o}C$ was seen and at 0.03ml/min a temperature-reduction of $17.5^{o}C$-$18^{o}C$ was seen. With no real knowledge of the human blood-flow-rate, if a vitality-difference can be detected, the best chance may

be with an internal temperature-reduction of 8°C with the natural pulse, and this would be more clinically acceptable than a 10°C reduction.

5.5.5.2 Temperature

There is a similar trend for the difference in area-under-the-curve with the maximum difference in temperature. At the higher flow-rates and a greater temperature-reduction, there is a greater maximum temperature-difference (Chapter 4, Figure 4-45). The model also shows a slight positive maximum temperature-difference for right-side vitality at equilibrium and a slight negative maximum temperature-difference for left-side vitality. This is seen with reducing flow-rates, until no difference is detected at the lowest flow-rate.

At the lowest flow-rate, the temperature-difference levels at approximately 0.5°C, which is very close to the accepted 0.4°C for normal thermal symmetry. This would not reliably distinguish vitality. Additionally, temperatures cross in some sequences and, with the knowledge of simulated vitality, the maximum temperature-difference may appear quite convincing for a vitality test. However, without that knowledge, maximum temperature-differences also occur in the other direction. The maximum temperature-difference is a point-measurement and is not felt suitable to test vitality.

5.5.5.3 Characteristic-Time-To-Relaxation

These values were produced from the same data and, at the highest flow-rate, the greatest cooling provides the greatest difference in characteristic-time-to-relaxation (Chapter 4, Figure 4-49), following the same trend as the area-under-the-curve and temperature. The graphs are reversed due to the time to reach equilibrium being quicker in the simulated vital than non-vital tooth, so with right-side vitality it would have a shorter time than the non-vital left-side, leading to a negative-value for right-side vitality. The trend changes at 0.08ml/min and the greatest difference is seen from a 6°C temperature-reduction, and at the lowest flow-rate there is very little difference seen between the vital and non-vital simulations. This requires bespoke software and is more time-consuming to produce. This has not been reported in the literature as a potential method for assessing vitality and is deemed less suitable than the area-under-the-curve.

The most promising method to detect a difference in thermal energy between a vital and non-vital tooth is the difference in the area-under-the-curve which uses all the data collected, does not require any bespoke

software and is simple to calculate. Temperature-difference is from a single point of the re-warming sequence and the characteristic-time-to-relaxation is a timeline to thermal equilibrium, whereas the area-under-the-curve uses all information of the re-warming sequence and could have greater sensitivity. The ideal temperature-reduction was proposed to be $8^{o}C$.

5.5.6 Cooling-Time

The timeline to achieve an $8^{o}C$ internal temperature-reduction was estimated from the left-side simulated vitality sequences over all four flow-rates (Table 4-22). This avoided any flow-influence on the thermocouple and provided a timeline of 45 seconds cooling with a thermoelectric peltier cooling-unit at $\approx -8^{o}C$. This is very much shorter than the 10 minutes cooling by Smith et al., (2004) and is more clinically acceptable. Drinking cold fluid at $0.4^{o}C$ can produce a surface-temperature of $0^{o}C$ (Barclay et al., 2005), and the lowest-recorded surface-temperature of the tooth during cooling to a $10^{o}C$ internal-reduction with a flow-rate of 0.03ml/min, was $11.5^{o}C$ following application of the cooling-unit (Table 4-22, blue cell). $12.9^{o}C$ was the lowest tooth-temperature recorded, with an $8^{o}C$ internal-reduction, which is much higher than that recorded from ingestion of cold fluid. The cold fluid, however, was a momentary-contact, whereas the cooling-unit was sustained. Mouth-breathing at ambient temperatures of $-10^{o}C$ resulted in a tooth-temperature of $17^{o}C$; and at $-30^{o}C$ a tooth-temperature of $10^{o}C$, and these temperatures caused no damage to the pulp (Beynon, 1973). The required drop-in-temperature was achievable and appears safe for clinical use.

This timeline of 45 seconds cooling was used within phase two of the simulated vitality test.

5.5.7 Vitality-Assessment Thermal Maps

The area-under-the-curve was one method used to produce the thermal maps which characterised enamel and dentine. The same process was applied to the re-warming sequence of the simulated pairs of teeth to assess vitality, which may be visible from the heat-exchange. The sequence shown in greyscale (Chapter 4, Figure 4-54) has Pair 4 with simulated vitality first in the left-tooth on the left of the page - and then the right-tooth on the right of the page. Over the course of sixty seconds, the change in greyscale of the left-tooth and the right-tooth in the respective sequences clearly shows a greater heat-exchange in the simulated vital tooth in both sequences. The simulated vital tooth darkens in greyscale with the greater heat-exchange. By changing the simulated vitality from left-to-right within the same model,

this is the only variable which has changed and this produced the change in greyscale for both simulated vital teeth. The colour maps (Figure 4-55) show the same sequence, where warming of the tooth is shown by lightening of the blue colour. This outcome was also seen for the lowest flow-rate 0.03ml/min following 45 seconds cooling for Pair 7 (Figure 4-74). This has not been seen within published literature and makes a novel and unique contribution towards vitality testing.

5.5.8 Vitality Test of Eight Pairs of Teeth

The eight pairs of teeth previously described were subjected to a vitality test which required 45 seconds cooling and observation of the thermal sequence to collect the emitted infra-red radiation with a thermal camera. The assumption was that a vital tooth would emit more infra-red radiation than a non-vital tooth, due to having greater thermal energy from the pulp-vitality.

The model prepared for each pair allowed multiple variables to be altered, some of which could not occur naturally, such as having two vital teeth without a periodontal blood-flow. Due to having only two tubes on the pump one natural variation was not possible, which was two vital teeth with a periodontal blood-flow. However, the aim was to assess vitality by comparing a vital and non-vital tooth so this combination was not needed.

For all eight pairs, the surface-temperatures were measured throughout the thermal sequence, providing a wealth of data, not only on the vitality test but also on the new model.

5.5.8.1 Tooth-Surface-Temperatures During Thermal Sequence

The temperature of the tooth-surface was recorded by the thermal camera throughout the vitality test. The temperatures pre- and post-cooling recorded by the thermal camera were of particular interest, giving the temperature-reduction. For the simulated options (some of which would never occur in nature) the temperature of the teeth prior to the test were viewed for thermal equilibrium ($\pm0.4^{o}$C) (Vardasca et al., 2012) and level of cooling following application of the cooling-unit.

The control, where there was no simulated flow in either tooth or the periodontal ligament (Nil), the mean tooth-surface-temperatures prior to cooling (Chapter 4, Table 4-30) were within 0.05^{o}C of one another (left = 31.3^{o}C [SD 0.19] and right = 31.35^{o}C [SD 0.29]). This was within the natural variation of thermal symmetry and also within the reported temperatures of the teeth in-vivo (29°C to 35°C) which depends on their anatomical location (Brown & Goldberg, 1966; Goldberg & Brown, 1966; Crandell & Hill, 1966;

Fanibunda, 1986b). This was provided by the thermal environment and shows stability between the eight pairs viewed. The left-tooth cooled more than the right, with a mean reduction of 15°C and 13.3°C (left and right, respectively, Table 4-46). This may have been due to uneven-contact by the cooling-unit (despite attempting to make even-contact) or uneven-cooling of the peltier surface. The cooling-unit had one thermocouple attached to record its surface-temperature on one side, rather than one either side, which would have confirmed the presence of absence of even-cooling between the two sides.

This difference was considered prior to analysis and the surface-temperatures within each pairing, both independent dissimilar pair and the same pair were aligned to the same baseline-temperature.

The temperature-variations with one vital tooth only were of a similar order, with mean pre-cooling-temperatures ≈31.5°C (Table 4-31) and a mean reduction of ≈14.8°C (Table 4-47). These results pooled the left-and-right values of vitality and non-vitality at one simulated flow-rate 0.5ml/min, preventing side-anomalies being identified but did provide a larger sample size (n=16 rather than 8). There was a 0.1°C difference in favour of the vital tooth pre-cooling. This was the expected direction of increase due to the increased thermal energy supply – however, it was small. All these were measured at the highest flow-rate, and a reduction in flow-rate would reduce the applied thermal energy and move the vital model nearer to the control of Nil previously reported.

With the introduction of a periodontal simulation and two non-vital teeth, which may occur in nature, the mean start-temperatures for all four flow-rates were within 0.06°C for the left teeth, and 0.1°C for the right and, between right-and-left, the maximum variation was 0.12°C (Table 4-32). The simulation was providing an acceptable baseline-temperature with simulated vitality for the periodontal ligament and there was an initial slight bias in heating the right-side more than the left (maximum 0.06°C), which was within the normal limits of thermal symmetry. Following cooling with only the periodontal simulation the left-side teeth cooled the most, with a maximum difference between left-and-right of 1.26°C (Table 4-48). The mean temperature-reduction ranged from a maximum of 15.66°C on the left with a flow-rate of 0.08ml/min, to a minimum of 13.18°C on the right with a flow-rate of 0.5ml/min. This provided good cooling. The minimum reduction may be expected from the highest flow-rate which would provide greater thermal

energy to the model, and the maximum reduction may be expected from the lowest flow-rate - in this case 0.08ml/min, rather than 0.03ml/min.

The simulations with a periodontal ligament and a tooth were conducted with, and without, a simulated pulse. The mean temperatures of all these simulations were within 0.4°C (highest 31.49°C for vital teeth with flow-rate 0.5ml/min(Table 4-33) and lowest 31.16°C for the pulsed simulation at 0.03ml/min for both vital and non-vital teeth (Table 4-34), giving an equilibrium reported within nature. The mean temperature-reductions were between 14°C and 15.5°C, the greatest being 15.36°C (pulsed vital teeth 0.15ml/min Table 4-50), and the least being 14.11°C (pulsed vital teeth 0.5ml/min Table 4-50). The gradual change in temperature-reduction expected to increase with reduced application of thermal energy was not seen; instead, for the non-pulsed sequences, the temperature-reduction reduced with the reducing flow-rate, with the exception of the lowest flow-rate which provided, as expected, the greatest reduction in both the vital and non-vital simulations at 0.03ml/min. For the pulsed simulation, one exception interrupted the increase in temperature-reduction with reduction of the flow-rate, and that was 0.15ml/min in both the vital and non-vital simulations giving the greatest temperature-reduction.

The level of cooling achieved for all variables was within 2.5°C for all sequences, achieving a maximum mean reduction of 15.66°C (PDL Only Left 0.08ml/min) and a minimum mean reduction of 13.18°C (PDL Only Right 0.5ml/min), both within Table 4-48.

The reductions seen, (13.18°C-15.66°C) as recorded with the thermal camera following 45 seconds cooling, were in the range to that produced from the thermocouples at the lowest achieved temperature (14.4-18.2°C Table 4-22) when calculating the timeline for application of the cooling-unit. It was determined that 45 seconds was an appropriate cooling-time. The greatest temperature-reduction was found in a simulation with a low thermal contribution at 0.08ml/min, which reduced the tooth-temperature from 31.33°C to 15.66°C, with a reduction of 15.66°C. This is an acceptable clinical temperature-reduction, as temperatures as low as this have been reported (15.4°C) following ingestion of orange-juice at 6°C (Youngson & Barclay, 2000), although this would have been a momentary-recording of the low temperature rather than a sustained application of a cooling-unit for 45 seconds, and 0°C was recorded following ingestion of cold fluid at 0.4°C (Barclay et al., 2005). The cooling-unit was also only applied to the occlusal-surfaces (not enveloping the whole tooth) and there would be a gradual

reduction in temperature down the tooth-surface. The thermal camera allows an area-of-interest on the buccal-surface of the tooth to be selected which would have a temperature-graduation, which is averaged, unlike the thermocouple which makes a spot-measurement. The thermocouple temperature would be dependent on its location on the tooth - the closer to the occlusal-surface, the colder the temperature recorded - and the 2.5^{o}C difference between the two measuring-techniques is accepted.

The gradual cooling-effect from the occlusal-surface may make the cooling-technique more clinically acceptable, as reports are recorded that cooling the teeth with ice-sticks can be uncomfortable, especially when placed centrally on the labial-surface of incisors, and were deemed unsuitable (Kells et al., 2000b). The temperature-reduction achieved locally with this method in-vitro was 10.41^{o}C [SD=0.18] with a 10-second-application. This was two-thirds the temperature-reduction of this in-vitro Study with less than a quarter of the contact-time, but the area-of-interest was very localised which may overestimate the temperature-reduction of the entire buccal-surface. The starting-tooth-temperatures for Kells et al., (2000b) were also low at 20°C, which was the ambient room-temperature.

Smith et al., (2004) cooled their tooth in-vitro for 10 minutes with iced-water without simulated blood-flow, but no report of the lowest temperature achieved was made and a 10-minute cooling-period would be clinically unacceptable. A rise of ≈7°C was demonstrated over 4 minutes following cooling, but the starting and finishing temperatures were omitted. Fanibunda, 1985, applied the thermal disruption consistently but reported the area-under-the-curve as mm^2, and no comparison can be made with the level of cooling achieved with the cryo-spray.

5.5.8.2 Difference In The Area-Under-The-Curve

Use of the area-under-the-curve was discussed above and the difference in the values between vital and non-vital teeth are produced in the same way. The baseline-temperatures were aligned for both the independent pairs of molar teeth within each holder, and then a second pairing was made between two sequences to align the temperatures of the same tooth with and without simulated vitality.

This gave two situations which may occur clinically:

Firstly, if the contralateral tooth is present it may provide an opportunity for comparison with the tooth under investigation, usually being of the same size, shape and mirror-image location within the mouth. This would simulate

the in-vitro paired-data on the same tooth which was subjected to being a vital and non-vital tooth across two sequences, which in-vivo may be recorded in one sequence.

Secondly, if the contralateral tooth is missing or restored, a comparison may not be possible and a dissimilar tooth may be used for comparison. Within this molar-model, all teeth are molars but with one exception - they are not matched-pairs and provide an independent, dissimilar-pair for comparison.

The production of the difference in the area-under-the-curve was always in the same direction, right-tooth minus left-tooth, and this would be expected to give a positive-value when the right-tooth was vital, and a negative-value when the left-tooth was vital. On the graph, the vital right-tooth would be above the zero line and the vital left-tooth would be below the zero line.

The graphs are shown in the results for Pair 7 (Figure 4-65 to 4-69). When there was no simulation (Nil) there was slight bias towards the right-tooth having a greater area-under-the-curve, as seen by the blue line sitting above zero.

When the simulation involved only the periodontal ligament, again there was a bias towards the right, at a slightly greater level than with no simulation. There is thermal energy entering the model and this will raise the temperature of the teeth and, if this was identical in each tooth (which is unlikely even in-vivo, as shown by acceptance of $0.4^{o}C$ difference from left-to-right), the difference in the area-under-the-curve would remain around the Nil-level. There is an increase in the difference in the area-under-the-curve, from the flow-rate of 0.03ml/min to 0.15ml/min, which increases further at 0.5ml/min. At 0.03ml/min the difference in the area-under-the-curve is $68^{o}C$/Time, indicating a slightly greater value in the right-tooth than the left. The positive bias towards the right-tooth needs to be considered when comparing the overall findings. All sequences which represent an in-vivo situation have a periodontal contribution and this may lift the findings towards the positive side.

Of particular interest are the simulations with a periodontal flow and a vital tooth, and simulation options to the right or left teeth could be changed without affecting the periodontal contribution. Additionally, a simulated pulse could be applied to all blood-flows. An in-vitro study with a simulated pulse had not been reported in the literature and provided opportunity for a unique contribution in developing a novel model to ascertain if the reported pulse-

effect within the pulp (Brown & Beveridge, 1966) could influence the thermal exchange of a vital tooth compared to a non-pulsed model.

The difference in area-under-the-curve for non-pulsed simulation shows an increased value with flow-rates of 0.08ml/min and above, compared to the periodontal simulation only when the right-tooth is vital. The higher the flow-rate, the greater the difference, which increases steeply from 0.03ml/min to 0.15ml/min, then levels. The difference seen at the lowest flow-rate is not dissimilar to that of the periodontal ligament (0.03ml/min PDL 68°C/Time v PDL RTS -182°C/Time and 0.08ml/min PDL 878°C/Time v PDL RTS 1162°C/Time) but, once the flow-rate is at 0.15ml/min, there is a clear contribution from the tooth in excess of the periodontal ligament. The negative value at 0.03ml/min indicates the left-tooth has a slightly greater area-under-the-curve which may be due to external thermal conditions, or that the water, circulating at such a slow flow-rate, cools the tooth temporarily until the in-flow raises the temperature. This may not happen in the non-vital tooth which was initially circulated with water but, after time in such a thermal environment, evaporation will occur and the amount of fluid remaining in the tooth may decrease, reducing the thermal heat-sink at these flow-rates. When the left-tooth is simulated with vitality, a similar trend is seen with reduced values, which may be due to the offset of the right-tooth tending to have a slightly higher temperature. The greatest difference is seen with the highest flow-rate.

When a pulse is applied, the differences are increased and, even with the lowest simulated flow-rate, the difference in the area-under-the-curve gives a clear outcome of which tooth is vital and non-vital. There is no cross-over at 0.03ml/min and values at this flow-rate provide a difference of 2297°C/Time when the right-tooth is vital, and -1726°C/Time when the left-tooth is vital. This peaks at a flow-rate of 0.15ml/min when vitality is present in the right-tooth at 4140°C/Time, and at 0.5ml/min in the left-tooth at -2500°C/Time.

This is a dissimilar model and expectations of perfect symmetry around the zero line is unrealistic. However, there is a trend whereby the vital teeth, with a flow-rate of 0.08ml/min or above, give the expected positive or negative-values for the area-under-the-curve (^{o}C/Time). When a pulse is applied this is increased.

Taking the mean values for all eight pairs of teeth under the same conditions this trend continues (Figure 4-72).

The mean Nil value lies above zero, showing a tendency for the right-tooth to be warmer than the left. This may relate to the cooling-unit where the temperature-reduction was less on the right than the left. Each tooth-temperature was aligned to commence the re-warming sequence at the same point. The addition of thermal energy to the periodontal ligament increased the difference in the same direction as the Nil simulation. Once the simulated tooth-vitality is added to the simulated periodontal vitality, the mean difference in the area-under-the-curve increases in the direction of vitality, with the exception of the lowest flow-rate where all simulations provide similar outcomes to the periodontal ligament. At 0.08ml/min there is a clear difference in the area-under-the-curve between that of a vital tooth and that of a periodontal simulation, and the difference between the right and left simulation is in the direction of vitality. In this model, the addition of the tooth-vitality has not been masked by the periodontal simulation and agrees with the findings of Fanibunda, (1985).

In the model used by Fanibunda, (1985), the lowest flow-rate used was 0.5ml/min, which was the highest used in this in-vitro model. The control with no simulation provided the lowest response. In this Study, the Nil (control) sequence provided a low-positive-response. The combination of simulated vitality with simulated periodontal vascularity provided the greater response for Fandibunda, (1985) and, within this Study, that is also the case if the pulsed model was excluded. A difference from the Nil (control) was seen when the periodontal ligament was added and it was in the same positive direction as Nil. This was due to a combination of effects where the values of both teeth varied between the sequences, but the overall-effect was that an increase was seen in the difference in the area-under-the-curve with the addition of the periodontal simulation, which is in agreement with Fanibunda (1985). With a pulse, the effect was increased further. This may be due to the non-static nature of the flow with a simulated pulse and may relate to the driving pressure, the dimensions and structure of the tubing which simulate the vessels and the resistance they offer, as well as the pulsatile-effect which may lead to a turbulent flow rather than a smooth laminar flow (Secomb, 2016). This warrants further investigation, as this is the first simulation of a pulp blood-flow with a pulse-effect and within this model an enhanced-effect is being detected with the simulation of a pulse, which would be found in-vivo.

When viewing the mean differences from the same paired-data a similar outcome was seen, but there was less of a difference between the pulsed-

effect on the right-side which crossed the non-pulsed-effect from 0.15ml/min to 0.5ml/min. Otherwise, there was a difference between the right and left-sides of simulated vitality which, without the pulse, was not seen at the lowest flow-rate.

5.5.8.3 Significance

The outcome of the above data shows an in-vitro difference in the area-under-the-curve between a vital and non-vital tooth following cooling for 45 seconds at -8°C when at a flow-rate of 0.08ml/min or above, without a simulated pulse. With a simulated pulse, there is an in-vitro difference at the lowest flow-rate of 0.03ml/min.

These outcomes are found whether the teeth are in independent pairs as seen within each holder, or when the same tooth is assessed in separate sequences as a vital and non-vital tooth-pair. A value could be assigned to the difference in the area-under-the-curve, below which doubt would be given as to whether the tooth is vital or non-vital in these in-vitro simulations. If the data had been perfectly symmetrical this would be an easier task - however, the human tooth will not necessarily behave in such a manner either, and the presence of a pulp-flow of 0.03ml/min or more has not yet been confirmed and, prior to allocating such a value, the behaviour of the test in-vivo is desirable. If the human tooth blood-flow-rate is less than 0.03ml/min, even with a pulse, the outcome of this test is still unknown.

For the in-vitro assessment of tooth-vitality, a safe margin would be to assign a difference of $\approx 1000^{o}$C/Time to indicate the likelihood of the pulp being vital.

The null hypothesis was tested statistically. This involved two tests for normally distributed data - the Independent-samples T-test for the dissimilar teeth and the Paired-samples T-test for the same tooth. The dissimilar teeth also produced one flow-rate where the data was not normally distributed so the Mann-Whitney U Test was used.

No statistical significance was seen for the dissimilar molar-teeth at any flow-rate without a simulated pulse, and so the alternative hypothesis was rejected and the test fails to reject the null hypothesis.

Statistical significance was tested for the dissimilar teeth with a simulated pulse. For the three lowest flow-rates, there was no statistical significance and the alternative hypothesis was rejected and the test fails to reject the null hypothesis. At the highest flow-rate, with a simulated pulse, statistical significance was seen ($p<0.05$). The null hypothesis could be rejected and

the alternative hypothesis accepted, as the median area-under-the-curve was statistically significantly higher for simulated vitality than non-vitality.

The paired-teeth were tested via the Paired-samples T-test and, at the two lowest flow-rates of 0.03ml/min and 0.08ml/min, no statistical significance was found and the test failed to reject the null hypothesis.

At the two higher flow rates of 0.15ml/min and 0.5ml/min, statistical significance was found ($p<0.05$) for both tests. The null hypothesis could be rejected in favour of the alternative hypothesis and the mean difference was statistically significantly different from zero.

When testing the pairs with a simulated pulse, statistical significance was found ($p<0.05$) for all four flow-rates. The null hypothesis could be rejected in favour of the alternative hypothesis and the mean difference was statistically significantly different from zero.

Clinically, with a pulse, the test on a dissimilar pair of teeth is unlikely to detect vitality unless the pulp blood-flow is in the region of 0.5ml/min, whereas in a matching pair of teeth the test is likely to detect vitality if the blood-flow-rate is in the region of 0.03ml/min. The projected flow-rate to achieve statistical significance rather than clinical significance was 0.02ml/min.

5.5.9 Summary

This was the first in-vitro feasibility Study to assess tooth-vitality using infra-red radiation collected by a thermal camera on human molar teeth. The simulation was unique with the application of a pulse to the simulated blood-flow of the periodontal ligament and the pulp at the same time, as well as recording the vital and non-vital tooth in the same sequence. Following cooling for 45 seconds and evalution of the difference in the area-under-the-re-warming curve of a vital and non-vital tooth with simulated pulsed vitality, the result was statistically significant for detecting vitality in the independent dissimilar pairs at a blood-flow-rate of 0.5ml/min. Assessing vitality in the matched same pairs of teeth, statistical significance was found with a blood-flow-rate of 0.15ml/min and above without a pulse, and from 0.03ml/min and above with a pulse.

Tooth-vitality in-vitro could be detected by the use of infra-red radiation.

5.6 Proof of Concept In-Vivo Study

Following the in-vitro investigations and the recognition that thermal imaging may have superior metrology than other thermal measurement techniques the natural progression was an in-vivo investigation. This allowed comparison with the in-vitro findings and an update on the previous findings from Hartley et al., (1967) and, Pogrel et al., (1989) and Kells et al., (2000b).

5.6.1 Volunteers' Teeth

The Volunteers' teeth in this Study were older than any of the molar-teeth used in-vitro by a minimum of 6 and maximum of 23 years, and the teeth viewed were of a different type - incisors and canines - rather than molars, which may affect the cooling-time needed to achieve the required temperature-reduction. In turn, this may also influence the re-warming period which may be longer or shorter depending on the extent of cooling achieved. Anterior teeth have previously been viewed with a thermal camera for in-vivo studies, as seen by Kells et al., (2000b), Pogrel et al., (1989) and Hartley et al., (1967). Kells et al., (2000b) had one male volunteer, aged 35, on which vitality was assessed via thermal imaging and the teeth were a root-treated maxillary-central incisor with vital contralateral central incisor. This Study had only female Volunteers and the anterior teeth did not include a central incisor. Hartley et al., (1967) had two volunteers, each with a root-treated premolar, one was female but the other was not described and no ages were given. Pogrel et al., (1989) had a minimum of 20 volunteers whose incisors were viewed, but no age or gender details were disclosed. In the three studies using collection of infra-red radiation to assess vitality, teeth and conditions varied, making comparison difficult.

As technology progresses, the size of thermal imaging devices is reducing and an intra-oral device would enable access to the whole dentition, permitting viewing of each individual tooth whereas, currently, to achieve viewing at normal incidence on posterior teeth would be difficult. Hartley et al., (1967) did assess premolars. Within this Study, whilst assessing feasibility of teeth to view, premolars were difficult (even with cheek-retractors) and, when assessing the canines on Volunteer 1, two sequences were required, which was not ideal as each tooth may be exposed to different thermal confounders. Kells et al., (2000b) recorded two sequences, each focusing on either the right or left-tooth individually, even though they were maxillary-central incisors, and this may have been due to the field-of-

view. An intra-oral device would focus on individual teeth and two assessments would be required of the vital and non-vital tooth. Thermocouples and thermistors, on the other hand, may be attached to the teeth enabling assessment of the posterior-teeth simultaneously, with soft-tissue-retraction to avoid tooth-temperature-contamination.

5.6.1.1 Pre-Assessment of Teeth

The teeth were visually pre-assessed and a history taken to ascertain suitability. No other sensibility or vitality test was undertaken. The sensibility test does not assess vitality, which was the aim of this Study. However, it is used clinically to imply vitality and was used by Kells et al., (2000b) and Pogrel et al., (1989). To subject the Volunteer to a sensibility test could have resulted in bias, as a thermal test or electric pulp test may produce an unpleasant sensation, thus making them cautious of the vitality test. The order of testing may overcome the bias for the vitality test and, following this Study's vitality test, the sensibility tests may have been undertaken but the cooling may affect the neural-supply. In both Volunteers, the contralateral teeth were healthy and unrestored and were taken to be vital. The non-vital teeth were known to be root-filled, which radiographic evidence could confirm and was offered by one Volunteer. However, there was no justification to expose each Volunteer to X-ray radiation and no radiographs were used.

The teeth-of-interest were also reviewed for artificial restorations, of which there were none on the buccal-surface, giving an intact, continuous surface, allowing thermal exchange to be unaffected.

5.6.2 Emissivity

An emissivity-value of 0.96 was used throughout the in-vivo investigations, even though this was not assessed on each Volunteer. Thermal tape was not used as it is not currently approved for intra-oral use. In addition, the method of analysis in this Study uses subtraction to produce the area-under-the-curve and this provides a difference-value which is compared between sequences; this overcomes the high or low emissivity-value so long as the same value is used in both sequences. The difference is the difference in degrees Celsius, irrespective of emissivity, whereas, if an absolute temperature is compared, this may be higher or lower than actually exists, depending on the emissivity. Between studies, if a different emissivity-value is needed, the absolute temperatures may vary and, when comparing tooth-temperatures, this needs to be acknowledged.

The colour of the teeth may be thought to impact on the emissivity-value, and if the non-vital tooth is darker (e.g., due to blood-products within the dentinal tubules) than a vital tooth, emissivity may be thought to vary between the teeth. This is not the case with longer wavelengths used with the thermal camera (7-14μm) but may be affected with shorter wavelengths closer to the visible spectrum (Hartley et al., 1967), as colour is a visible spectrum phenomenon and the infra-red radiation is reported as unaffected at longer wavelengths (Hardy, 1934).

5.6.3 Tooth-Temperatures

The tooth-temperatures recorded were in-keeping with other studies (Goldberg & Brown, 1965; Brown & Goldberg, 1966; Crandell & Hill, 1966; Fanibunda, 1986b), and were posteriorly warmer in the maxilla, with the incisors ≈29°C and canines ≈31°C. The lower-incisors varied little at ≈29°C. Emissivity-values were considered by Hartley et al., (1967) but not quoted, and Kells et al., (2000a & b), assessed their own emissivity, which was the lowest value found in any literature at 0.65, whereas Pogrel et al., (1989) did not consider emissivity. In this Study, 0.96 was used, making absolute values potentially different.

The non-vital maxillary left-canine of Volunteer 1 was marginally warmer than the contralateral vital canine, as was the non-vital mandibular left-central incisor of Volunteer 2, but only the canine was beyond the level of thermal symmetry with a difference of 0.94°C, and the central incisor was within it at 0.3°C (Hartley et al., 1967; Vardasca et al., 2012). This is also in agreement with other studies which could not detect a thermal difference between a vital and non-vital tooth without thermal disruption (Goldberg & Brown, 1965; Brown & Goldberg, 1966; Crandell & Hill, 1966; Hartley et al., 1967; Pogrel et al., 1989). In fact, Hartley et al., (1967) reported one of the non-vital premolars to be 1.77°C warmer than the contralateral vital tooth, which is nearly double the difference found in this Study, and above the accepted variation of thermal symmetry.

The temperatures of the gingivae above the respective teeth were always warmer than the teeth. There was a temperature-gradient from the cooler incisal-edge to the warmer gingival margin, with a minimum difference of 0.8°C for the upper canine and a maximum of 2.6°C for the lower-central incisors, which places the values obtained by Kells et al., (2000b) and Pogrel et al., (1989), in the middle of these values at 1.28°C and 1.5°C respectively, for the maxillary-lateral incisors and maxillary incisors. There was also a gradient mesial-to-distal, ranging from 1.2°C for the lower-central incisors to

3^oC for the canine. The warmest area of the teeth viewed was only once found to be in the mid-cervical ninth, as suggested by Shapiro & Ershoff, (1958). The Volunteers in this Study compare favourably to those of other studies for tooth-temperatures with due consideration given to emissivity-variation.

Following cooling with the newly-developed ice-filled-wax occlusal-bite-block, the tooth-temperatures reduced by a minimum of 9.44^oC and a maximum of 12.9^oC, which gave a minimum tooth-temperature of 16.2^oC and 16.1^oC for Volunteers 1 and 2, respectively. This was in-keeping with the in-vitro Study using the thermoelectric peltier at -8^oC, which gave a lowest mean tooth-temperature of 16.01^oC for the pulsed non-vital molars with a flow-rate of 0.03ml/min, achieving a mean temperature-reduction of 15.36^oC. The maximum temperature-reduction in-vivo was 12.9^oC, due to the fact the anterior teeth in-vivo were not as warm as the posterior teeth in-vitro, and the reduction is thus less.

5.6.4 Cooling-Method

When reviewing vitality, Hartley et al., (1967) made no thermal disruption to the teeth, whereas Kells et al., (2000a & b) applied either an ice-stick or a stream of cold air which were both focused on individual teeth. Pogrel et al., (1989) also applied *'a stream of cold air'*. The bespoke ice-filled-wax occlusal-bite-block developed for this Study cooled all the teeth at the same time and did not introduce any thermal disruption to the surroundings - as would occur with the air-stream. The level of cooling achieved with the ice-filled-wax occlusal-bite-block was comparable to that of the in-vitro simulation, and demonstrated the in-vivo cooling-system was achieving the desirable level of cooling needed to detect a thermal difference between vital and non-vital teeth. This was based on an average over-the-tooth-surface, as in-vitro (rather than on a central-area as Kells et al., (2000b) had achieved with the ice-sticks). The greatest temperature-difference achieved by Kells et al., (2000b) was 21.7^oC over a 2.8mm^2 circle rather than the whole-tooth-surface and, hence, is not comparable with this Study, as the remaining tooth-tissue would be warmer, and the baseline-temperature of the tooth would be warmer overall. Pogrel et al., (1989) reported a cooled tooth-temperature of $\approx22^o$C, which provided a reduction of $\approx8^o$C. Kells et al., (2000b) reported volunteer-discomfort from the ice-stick-technique, whereas in this Study there was no reported discomfort from the gradual cooling from the incisal-edge down the tooth with the ice-filled-wax occlusal-bite-block. This may be due to the gradual cooling approaching the pulp-tissue

(Baldissara et al., 1997) rather than the closer approximation of an ice-stick centrally on the buccal-face of the maxillary-central incisor, as in Kells et al., (2000b).

5.6.5 Recording-Conditions

The recording-environment was very stable at 21.1^{o}C, with a 0.1^{o}C variation. The cooling-mechanism required access to the teeth to place the ice-filled-wax occlusal-bite-block and it was decided not to isolate the teeth with rubber-dam. (Rubber-dam was used by Kells et al., (2000b) and Pogrel et al., (1989) to prevent thermal disturbance from the volunteer's normal breathing pattern). The teeth being examined in the anterior of the mouth were all exposed to similar conditions from the Volunteer's inhalation and ambient temperature, and this may warm or cool the teeth, but equally so within the same recording-sequence. Once two sequences are required, there is potential for increased discrepancies.

The Volunteers had been stabilised within the clinic for 15-20 minutes whilst taking consent and assessing suitability, and the room-temperature was approximately 1°C below the ideal temperature of 22°C, as recommended by Love (1986), but no discomfort was expressed by either Volunteer.

5.6.6 Data-Collection

The outcome of the in-vitro investigations demonstrated the detection of vitality was greatest when teeth were paired with themselves as vital and non-vital partners. Clinically, this is unlikely, unless prior recordings had been made when vital. The contralateral teeth for each non-vital tooth was available and used as a vital tooth for comparison in the 2 Volunteers for this Study, as they were for Kells et al., (2000b), and for one volunteer for Hartley et al., (1967), Pogrel et al., (1989) did not specify which teeth were compared. Using adjacent teeth would have been equivalent to the dissimilar pairings, which was not as successful in detecting the difference between a vital and non-vital tooth in-vitro. Hartley et al., (1967) reported there was no difference in temperature of adjacent teeth - however, having already accepted a gradual increase in tooth-temperature the more posteriorly-placed they are (Fanibuna, 1986), this would be unlikely.

5.6.6.1 Clinical Process

The Volunteer was seated and stabilised against the chin-and-head-rest, the aim being to reduce movement to keep the teeth within the narrow field-of-view. Inevitably, there was some movement throughout the test but data was

captured of the re-warming sequence of the teeth following cooling, allowing analysis.

The placement of the ice-filled-wax occlusal-bite-block initiated movement, as did its removal, and this was more easily controlled when testing the mandibular teeth than the maxillary as the chin-rest provided a stable reference-point, and the whole sequence was recorded with very little movement, allowing the area-of-interest to be captured in one sequence. The maxillary teeth were less-stable and the data for analysis was taken over two time-intervals for one of the sequences.

A minor adjustment to the wax-rim (removal of some wax to allow the occlusal plane of the teeth to sit on the ice) gave greater stability. This provided cooling in 45 seconds which was comparable to the in-vitro cooling, whereas Kells et al., (2000b) cooled the teeth for 10 seconds with ice-sticks.

The work-station had been developed specifically for this purpose, and the location of the camera could easily be adjusted in any direction via an adjustable-vertical-stand and the gimbal, to give the required focal distance at normal incidence. For the mandibular teeth this was from a front-view, but for the canines this was set to one side, which prevented recording of both canines simultaneously. Currently, to access teeth beyond the canine would be difficult to achieve recording at normal incidence, even with cheek-retractors. Intra-oral devices may overcome this but would require two sequences for comparison, doubling the time required and exposing the Volunteer to twice the testing.

Attachment of the heartrate-monitor and the presence of the camera in close proximity was non-intrusive.

5.6.6.2 Volunteer-Comfort

Neither Volunteer was concerned about the process and no reports of sensitivity were recorded. Both found the process acceptable (unlike Kells et al., (2000b) where cooling with ice-sticks was unacceptable and led to head-movement, preventing data-collection).

The timeline of ≈5 minutes was accepted and tolerated by the adult Volunteers. Children may not be as accepting. Additional support and a reduced timeline may be feasible having reviewed the data collected from the two Volunteers. Further data will be collected for the remaining Volunteers which may reiterate that a shorter data-collection is acceptable. The use of cheek-retractors for ≈5 minutes was a little uncomfortable after the process, but not during it.

5.6.7 Heartwave and Re-Warming-Relationship

There was no relationship detected between re-warming and the heartwave, which may not be unexpected due to the thermal properties of the tooth-tissue which are insulating in nature (Chapter 2, Tables 2-6 & 2-7). The expectation to detect a temperature-increase externally with each pulse of the heart would necessitate the thermal transfer of energy from within the tooth to be virtually instantaneous. With the insulating properties of the mineralised tooth-tissue, such a transfer via conduction through the dentine and enamel would be a gradual event producing a gradual change in emitted infra-red radiation for collection by the thermal camera. The expectation of a greater thermal energy due to the presence of vitality in the pulp was demonstrated in-vitro, and this was greater in the presence of a pulse - however, the specific relationship between the increase in tooth-surface-temperature and timing of the natural pulse was not detected.

5.6.8 Timelines and Rate of Data-Collection

The re-warming-recording-sequence was timed at 5 minutes following baseline-measurement and cooling for 45 seconds. This was at a capture-rate of 9-frames-per-second. This was not as long as the in-vitro Study and a 5-minute-recording-period had been set for Volunteer-comfort. Also, a re-warming timeline of three minutes had been established in-vivo by Kells et al., (2000b) following cooling of anterior teeth, rather than molars, and cooling was only 10 seconds rather than 45 seconds. Pogrel et al., (1989) reported re-warming within 5 seconds for vital teeth compared to 15 for non-vital teeth, with the exception of the metal post which took 2-3 seconds.

The re-warming sequence was observed for the molar-model over 9½ minutes - virtually double the timeline. A 10-minute-test would not be as acceptable for a patient or the clinician as a 5-minute-test, and the re-warming curve may deliver an outcome before thermal equilibrium is reached. As seen within Volunteer 2, the re-warming sequence indicates the long-term pattern from approximately 1 second after alignment of the temperatures in-vivo. The shorter the timeline, the less opportunity for external influences to warm the tooth compared to the internal exchange of thermal energy from vitality, and the more acceptable for both patient and clinician.

This Study captured data at a rate of 9-frames-per-second, whereas Kells et al., (2000b) captured one image every 10 seconds. As seen from the conductivity-assessment of the tooth-slices and the re-warming thermal

maps, within 1 second enamel and dentine could be differentiated from their thermal differences. In the whole tooth with simulated vitality, 10 seconds presented evidence of warming in the vital tooth and this increased over time. These images were produced from 9 frames for the slices and 90 frames for the whole tooth. With a data-capture-rate of 1-image-per-10-seconds (Kells et al., 2000b), this would not have been possible and the early heat-exchange was missed.

Due to the movement of Volunteer 1, the re-warming sequence was split into two sections, and the timeline reviewed was the first 5 seconds to allow comparison between the two Volunteers. Volunteer 2 was stable throughout and the full re-warming sequence, following stabilisation and alignment of temperatures, was seen for 4 minutes and 10 seconds.

5.6.9 Vitality-Detection

5.6.9.1 Area-Under-The-Curve In-vivo

In the 5-second-timeline available for both Volunteers, the area-under-the-curve was calculated for vital and non-vital contralateral teeth.

Volunteer 1: the area-under-the-curve for the non-vital tooth was larger than the vital, indicating an overall greater temperature during the first five seconds of re-warming from the same baseline-temperature for the non-vital tooth. The difference between the two vital lateral incisors was approximately the same, and approximately half for the central incisors. This is a small difference but there is agreement with others who have reported the non-vital root-treated tooth to be warmer in-vivo than the vital tooth (Hartley et al., 1967). Of the six teeth tested in Volunteer 1, the root-treated canine had the greatest area-under-the-curve on re-warming.

Volunteer 2: A similar scenario is found again - the non-vital root-treated tooth has the greatest area-under-the-curve and the difference between the two lateral incisors and the two central incisors is two-fold in favour of the non-vital central incisors. This is similar to the canine and central incisor for Volunteer 1.

The root-treated tooth appears to have more thermal energy than a vital tooth and this may be due to the presence of insulating-properties of the restorative materials. The model of using a vital tooth and a root-treated non-vital tooth without thermal disruption, has demonstrated this outcome previously and it has been reported that the vitality test could not detect a difference between the two teeth. This is not strictly correct. A difference has been detected, but in the opposite direction to that expected. The 1.77°C

difference reported by Hartely, et al., (1967), without thermal disruption, indicated a warmer non-vital tooth beyond the limits acceptable for thermal symmetry which, if it had been reversed, may have been declared a positive finding – however, no explanation was offered.

Kells et al., (2000b) discarded the first image of one sequence following ice-cooling due to head-movement and were cautious of the outcomes from one volunteer. This Study has only two Volunteer-sequences and one is separated into two parts - again due to head-movement. The other sequence was very stable and caution is expressed over the outcome from such a small sample-size. At the second image-collection-point (10 seconds) of the re-warming profile in Kells et al., (2000b), the least difference in temperature following cooling with the ice-stick was seen in the non-vital tooth. This continued for one of the sequences for the next minute, indicating the non-vital tooth had not cooled to the same level as the vital tooth. This could be experimental error, which may also exist in this Study, but it could be indicating the non-vital tooth is resistant to the cooling which may be due to the insulating-properties of the restorative materials.

The outcome from this in-vivo Study also shows the non-vital tooth to have a greater overall thermal energy during the re-warming sequence than the vital tooth.

5.6.10 Comparison of In-vivo and In-vitro Area-Under-The-Curve

Within the first 30 seconds of re-warming for Volunteer 2, there was a rapid rise in temperature of $\approx 5^{o}C$ for the non-vital lower-left central incisor and $\approx 4.4^{o}C$ for the vital lower-right central incisor, then the re-warming-rate reduces. The non-vital tooth had a more rapid rate of thermal exchange than the vital tooth. This was approximately 1½ times the re-warming-rate seen in-vitro for the 0.5ml/min flow-rate for Pair 7 which had a temperature-increase of $3.0^{o}C$ in the same time for the non-vital molar, and $3.3^{o}C$ for the vital molar. At a flow-rate of 0.5ml/min, the vital tooth has a more rapid rate of thermal exchange than the non-vital tooth. At the lowest flow-rate of 0.03ml/min, the rate of increase in 30 seconds is $3.9^{o}C$ for the non-vital molar, and $3.4^{o}C$ for the vital molar, which indicates a more rapid rate of thermal exchange in the non-vital tooth than the vital, just as the in-vivo non-vital tooth showed.

There are multiple differences between the models used in this Study, some of which include:

- one was in-vivo and one was in-vitro
- the teeth were lower-incisors in-vivo, compared to molars in-vitro
- the blood-flow-rate was unknown in-vivo, whereas two flow-rates were known in-vitro (0.5ml/min and 0.03ml/min)
- the non-vital tooth in-vivo was probably restored with insulating materials of gutta-percha and composite resin, whereas the non-vital tooth in-vitro had a pulp-chamber and canals void of restoration but may have had residual liquid
- the ambient environment in-vivo was ≈21°C, compared to in-vitro at ≈30°C.

The reversal of greatest thermal energy in-vivo to the root-treated tooth may be due to the restorative materials which are insulating. The reversal of the greatest thermal energy in-vitro at the lowest flow-rate may be due to retention of water within stagnation areas which are not replaced at the lowest flow-rate, hence cooled water remains in contact with the tooth for longer, which cools the tooth rather than warms it. This would not occur in nature.

5.6.11 Summary

The collection of infra-red radiation with a thermal camera is able to detect differences between the vital and non-vital tooth in-vivo - although care is needed as the sample size, to date, is 2 and recruitment will continue.

The direction of difference in thermal energy-exchange was not as expected between a vital and non-vital tooth, as the non-vital tooth had greater thermal energy than a vital tooth following thermal disruption. Although this was an unexpected result it adds to current knowledge and as such is another unique contribution of this work.

Chapter 6 Conclusions And Further Work

6.1 Conclusions

The preceding investigations have explored and added to understanding the feasibility of using infra-red radiation in determining tooth-vitality. Consideration was given to multiple aspects of the vitality test which used a thermal camera to capture the infra-red radiation and which has made novel and unique contributions to current knowledge in the quest to develop an acceptable vitality test for the practising dental clinician.

6.1.1 Stable Thermal Environment

The methodology of in-vitro investigations required a stable thermal environment and the Cube fulfilled the first objective to develop a suitable environment in which to undertake in-vitro empirical work which was thermally stable, eliminating environmental temperature-confounders. This had not previously been done, enabling a novel contribution from the development of the Cube and for the outcomes achieved.

The key-aspects of this Study's thermal environment were:

1. The Cube with macro- and micro-thermal-control provided a stable thermal environment within which to conduct the in-vitro work to reduce environmental temperature-confounders.

2. A minimum period of 35 minutes was recommended to stabilise the thermal environment to the selected temperature of $22^{o}C$ and was used for subsequent experiments.

3. A range of $0.1^{o}C$ ($22 \pm 0.1^{o}C$) was achieved for 28 minutes, after reaching the initial required environmental temperature.

4. Adaptation for a higher Cube temperature of $30^{o}C$ was feasible and stability with a range of $\pm 0.3^{o}C$ was achieved.

6.1.2 Emissivity

Prior to assessing tooth-vitality one tissue parameter – emissivity – which was not considered fully within the literature, was required for recording data to provide an absolute temperature. In this Study, the mean enamel emissivity-values were calculated as 0.96 from 14 whole molars and two slices from a third molar, and mean overall dentine-emissivity was 0.90 at a realistic oral temperature of $31\text{-}32^{o}C$ within the Cube. No other Study in the literature reported emissivity from multiple samples at realistic oral

temperatures, enabling a unique contribution to knowledge of the emissivity-value of the mineralised tissues of these teeth and fulfilled the second objective to determine the emissivity of human mineralised tooth-tissues in-vitro against a known reference-point.

The key findings for emissivity were:

1. Enamel had a high emissivity, which was similar whether from the internal flat-surface of sliced enamel or the external curved-enamel-surface of a whole tooth.

2. Dentine had a high emissivity (but not as high as enamel), which varied with location - crown-dentine being the highest, compared to root-dentine. The root-face had the lowest emissivity-value but was still a good emitter of infra-red radiation.

3. The method of emissivity calculation was cheap, simple and practical and would improve comparison of absolute temperatures between studies and it is to be recommended for in-vitro studies.

4. Acceptance and safety for in-vivo studies is dependent on tape-composition and further work is needed to develop a suitable biological tape or paint with known-emissivity, which could be easily applied and removed intra-orally to the teeth without detriment.

6.1.3 Characterisation of the Thermal Properties of Enamel and Dentine

To understand the thermal transfer of energy in the tooth, the thermal properties were evaluated and the Cube provided a very stable environment for examining the mineralised tooth-tissue with infra-red thermography. The source of thermal disruption to the tooth-tissue, both cooling and re-warming, resulted in an equally stable environment, which allows belief that the results obtained are due to the tissue-properties rather than environmental confounders.

The third objective to calculate and evaluate the thermal properties of human enamel and dentine against known values using infra-red radiation produced acceptable values, and a value was calculated for the first time for demineralised tissue of enamel and dentine.

The fourth objective was fulfilled by creating two thermal maps, one from the area-under-the-curve and another from the characteristic-time-to-relaxation, both of which characterise enamel and dentine. They also demonstrated the area of demineralisation from the natural carious lesion.

The key findings were:

1. Thermal diffusivity and conductivity of mineralised tooth-tissue fell within the known-range. Values for demineralised tissues were reported for the first time, making a unique contribution to knowledge, and delivered a lower value of both thermal properties than surrounding healthy tissues of the same sample, i.e., the demineralised area had a lower thermal conductivity and diffusivity than adjacent normal tissues. This was also applicable between the two samples in this Study, but this may not always be the case.

2. Enamel and dentine of a tooth-slice could be characterised by their thermal properties, as shown in the thermal maps. The presence of demineralised tissue could be detected in the map, particularly in the area-under-the-curve map rather than the characteristic-time-to-relaxation map. This novel contribution was published as original research – Lancaster P, Brettle D, Carmichael F and Clerehugh V. 2017. In-vitro Thermal Maps to Characterize Human Dental Enamel and Dentin. Frontiers in Physiology 8:461.

3. The heat-exchange detected by the thermal maps offered a technique to detect heat-exchange between a vital and non-vital tooth and justified further investigation on a whole-tooth.

6.1.4 Pulp Blood-Flow-Rate

The true blood-flow-rate per human tooth remains unknown. A new model has been presented making a unique contribution to current knowledge, which is based on reported data of average pulp-volumes for all adult human teeth and the average pulp-weights from two teeth-types. The fifth objective is satisfied accepting there are limitations with this model, as described.

The model provides a basis for all future in-vitro applications where a simulated blood-flow-rate is required, which can be applied to the type of tooth collected. This may provide a more consistent approach between research groups, enabling better comparison of their findings.

The key findings were:

1. Calculated blood-flow-rate by volume per adult tooth-type ranged from 0.0033ml/min for the maxillary-lateral incisor up to 0.0198ml/min for the first-maxillary molar.

2. Calculated blood-flow-rate by volume per adult tooth-type ranged from 0.0015ml/min for the mandibular-central incisor up to 0.011ml/min for the first-mandibular molar.

3. Calculated blood-flow-rate by mass for adult human teeth ranged from 0.0045ml/min to 0.0255ml/min.

6.1.5 In-vitro Feasibility of Using Infra-Red Radiation in Determining Tooth-Vitality

This was the first in-vitro feasibility Study to assess tooth-vitality using infra-red radiation collected by a thermal camera and the only study to have used human molar teeth for the model. The novel model also simulated alveolar bone with a vessel to supply blood-flow and addressed the sixth objective to provide an in-vitro simulation of a pair of teeth within an alveolar bone whereby vitality was applied to the periodontal ligament and one tooth, with and without a pulse. The development of an in-vitro cooling-unit to cool the teeth was delivered for the seventh objective, and the eighth objective to analyse and evaluate that the data could determine vitality of a pair of teeth via a thermal map or the difference in the area-under-the-curve which enabled statistical significance to be shown at a flow rate of 0.03ml/min or above.

The key findings were:

1. The novel model provided thermal symmetry of the two teeth within accepted ranges prior to vitality testing in the stable thermal environment of the Cube.

2. The difference in the area-under-the-re-warming curve provided the most suitable measure to assess vitality.

3. The new model showed the addition of vitality to the periodontal ligament increased the difference in the area-under-the-curve. The addition of tooth-vitality to the periodontal ligament vitality increased this difference again, showing the periodontal contribution did not mask that of tooth-vitality.

4. The most appropriate internal temperature-reduction was 8^oC to detect a difference between the vital and non-vital tooth on re-warming.

5. The external tooth-surface temperature-reduction at this level of cooling ranged between 13.5^oC and 18.5^oC depending on the flow-rate.

6. The time taken to achieve this temperature-reduction was 45 seconds.

7. The presence of a pulse enhanced the difference between the area-under-the-curve of the vital and non-vital teeth.

8. The area-under-the-curve thermal map demonstrated heat-exchange in the vital tooth before the non-vital tooth at the lowest flow-rate of 0.03ml/min with 45 seconds cooling.

9. Statistical significance ($p = 0.012$) was demonstrated for the vitality test on independent dissimilar paired teeth at a blood-flow-rate of 0.5ml/min with a pulse.

10. Statistical significance was demonstrated for the vitality test on matching same paired teeth at a blood-flow-rate of 0.15ml/min and above without a pulse ($p < 0.008$) and from 0.03ml/min and above with a pulse ($p < 0.045$).

11. If the human pulp blood-flow-rate is 0.02ml/min or above, it may be possible a vitality test using the collection of infra-red radiation with a thermal camera following appropriate cooling will be able to detect a vital tooth from a non-vital tooth if the teeth are matched.

6.1.6 Proof of Concept In-Vivo Study

Data collection with a thermal camera on a human volunteer whose teeth had been cooled and seen re-warming was feasible, and the bespoke novel cooling ice-filled-wax occlusal-bite-block was not only functional but acceptable, which fulfilled the ninth objective to develop an in-vivo cooling-unit.

The final objective to analyse and evaluate the data collected during a re-warming sequence using a thermal camera to determine vitality of a pair of teeth in-vivo, one of which was vital and one root–treated, was also completed on 2 Volunteers and the findings were not as expected from the in-vitro study. Instead, the direction of heat-transfer was reversed whereby the root-filled tooth had the greatest area-under-the-curve in the thermal sequence.

The key findings of the Volunteer-Study were:

1. A thermal camera can detect differences between the vital and non-vital tooth in-vivo.

2. The direction of difference in thermal energy-exchange was not as expected between a vital and non-vital tooth as, following thermal disruption, the non-vital tooth had greater thermal energy than a vital tooth.

3. Cooling for 45 seconds with the ice-filled-wax occlusal-bite-block achieved the required level of cooling comparable to the in-vitro simulation and was acceptable to the Volunteer causing no discomfort.

4. A collection time of 5 minutes may be reduced to make the test more acceptable and may only need to be a minute.

5. The technique shows promise and further in-vivo investigation is justified.

6. The Model comparing a non-vital root-filled tooth with a vital tooth appears unsuitable to demonstrate a greater exchange of thermal energy from the vital tooth, and a more suitable model may be a non-vital non-root-treated tooth.

6.1.7 Overall Conclusion

The overall aim of this Study was to assess the feasibility of using infra-red radiation in determining tooth-vitality. The null hypothesis being that:

> $H_0=$ there is no difference in the amount of infra-red radiation collected with a thermal camera from the surface of a vital and non-vital tooth.

Whereas the alternative hypothesis being:

> $H_1=$ there is a difference in the amount of infra-red radiation collected with a thermal camera from the surface of a vital and non-vital tooth.

From all the investigations undertaken, the null hypothesis may be rejected and the alternative hypothesis cannot be rejected.

This Study has demonstrated it is feasible to use infra-red radiation to determine tooth-vitality. Ultimately, the test may be acceptable to the clinician and patient and this Study has answered multiple questions about the use of infra-red radiation in assessing tooth-vitality and positively progressed the technique.

6.2 Further Work

From the findings and investigations of this Study, further work is justified in some areas, such as:

6.2.1 Emissivity

Development of a suitable biological emissivity-reference-point for in-vivo studies, as seen for the in-vitro Study which used a reference tape, is needed. A tape or paint with known-emissivity, which is easily applied and removed without detriment, which has the necessary safety requirements in place for use on human teeth, would be ideal.

One aspect not investigated in this Study was the emissivity of a known demineralised or carious lesion, and this justifies further investigation. Establishing if any relationship between the level of demineralisation and emissivity-value would be informative, as thermal imaging has shown promise for assessing carious lesions.

6.2.2 Characterisation of the Thermal Properties of Enamel and Dentine

The potential to detect demineralisation of the mineralised tooth-tissue offers a non-invasive, non-ionising and non-destructive technique which could be repeated without risk to the patient. The presence of a greyscale in the image depicting the lesion also allows potential to quantify a lesion against a known-scale and further work to quantify a slice and a whole tooth is justifiable for caries-assessment, as this Study pursued only the vitality test.

This may be followed by an in-vivo study to assess detection of caries on accessible surfaces.

The heat-exchange detected by the thermal maps may offer a technique to detect heat-exchange between a vital and non-vital tooth as shown in-vitro and warrants further investigation in-vivo once stability of the subject is achieved.

6.2.3 Pulp Blood-Flow-Rate

Data-collection on the pulp-weight for each adult human tooth-type would strengthen the model, as only premolars and molars are currently reported and that data is very limited. Future work to ascertain an average value of human pulp-weight per tooth would be required.

6.2.4 In-vitro Feasibility of Using Infra-Red Radiation in Determining Tooth-Vitality

The simulated pulsatile-effect was not correlated to the heat-process and could be used to maximise the sensitivity of the thermal mapping, and is an area of further work; as is exploration of the rationale behind why the simulation of a pulse enhances the difference in the area-under-the-curve between a vital and non-vital tooth.

Different areas of teeth can be assessed to see where the warmest is, which would provide knowledge for the best area to assess for detection of vitality, compared to using the whole surface. This may improve the outcome of the test.

6.2.5 Proof of Concept In-Vivo Study

Completion of the Proof of Concept In-Vivo Study with all 12 Volunteers is needed to provide more reliable and valid results than the 2 outcomes currently presented.

Further work is needed on a different model, where the non-vital tooth is not root-treated.

If the model demonstrates the thermal exchange in the direction anticipated, it may be plausible to estimate a blood-flow-rate from the re-warming sequence when compared to the in-vitro models.

6.2.6 Clinical Temperature Reference-Point

For clinical calibration, the use of water is unacceptable and a simple device which allows the thermal camera to be tested prior to use would be helpful. Initial work on a clinical temperature reference-point has commenced which provides four known temperatures for assessment via the use of light-emitting-diodes. Further work is needed to complete the device.

6.2.7 Publication Plan

The literature review provides opportunity to present articles which:

1. Relate to the thermal properties of the mineralised and soft-tissues of the tooth and how their structure, composition and vasculature can influence the tooth-temperature.

2. Relate to tooth-temperature and the potential diagnostic potential of the temperature of the tooth which may have particular reference to vitality testing and the technique of temperature-measurement.

3. Review the use of the electromagnetic spectrum in diagnostic imaging – this was written and published: Lancaster, P. Carmichael, F. Britton, J. Craddock, H. Brettle, D. and Clerehugh, V. 2013. Surfing the spectrum – what is on the horizon? *British Dental Journal* **215,** pp. 401-409.

The empirical work provides opportunity to present articles which:

1. Discuss emissivity of human tooth-tissue and present the test and findings from this Study.

2. Characterise the tooth-tissues from their thermal properties as thermal maps – this was written and published: Lancaster, P. Brettle, D. Carmichael, F. and Clerehugh, V. 2017. In-vitro Thermal Maps to Characterize Human Dental Enamel and Dentin. Frontiers in Physiology 8:461.

3. Model the pulp blood-flow and the findings for each individual tooth of the human adult dentition.

4. Describe the methodology of the in-vitro thermal vitality test and outcomes, which may include the potential of a thermal map to assess vitality.

5. Once completed, present the methodology and findings of the in-vivo thermal vitality test using the root-treated model.

List of References

Adams, D. 1959. Peripheral Capillaries in the Rodent Incisor Pulp. *Journal of Dental Research*. **38**(5), pp. 969-978.

Aida, M., Irié, T., Aida, T. and Tachikawa, T. 2005. Expression of Protein Kinases C Bi, Bii, and VEGF during the Differentiation of Enamel Epithelium in Tooth Development. *Journal of Dental Research*. **84**(3), pp. 234-239.

Aksakalli, S., Demir, A., Selek, M. and Tasdemir, S. 2014. Temperature Increase during Orthodontic Bonding with Different Curing Units using an Infrared Camera. *Acta Odontologica Scandinavica.* **72**(1), pp. 36-41.

Allen, C. 1685. The Operator for the Teeth: Showing How to Preserve the Teeth and Gums from all the Accidents They are Subject to. York: John White.

Al-Qudah, A.A., Mitchell, C.A., Biagioni, P.A. and Hussey, D.L. 2005. Thermographic Investigation of Contemporary Resin-Containing Dental Materials. *Journal of Dentistry*. **33**(7), pp. 593-602.

Ana, P.A., Blay, A., Miyakawa, W. and Zezell, D.M. 2007. Thermal Analysis of Teeth Irradiated with Er, Cr: YSGG at Low Fluences. *Laser Physics Letters*. **4**(11), pp. 827-834.

Andersson, L., Andreasen, J.O., Day, P., Heithersay, G., Trope, M., di Angelis, A.J., Kenny, D.J., Sigurdsson, A., Bourguignon, C., Flores, M.T. and Hicks, M.L. 2012. International Association of Dental Traumatology Guidelines for the Management of Traumatic Dental Injuries: 2. Avulsion of Permanent Teeth. *Dental Traumatology*. **28**(2), pp. 88-96.

Anić, I., Dzubur, A., Vidović, D. and Tudja, M. 1993. Temperature and Surface Changes of Dentine and Cementum Induced by CO_2 Laser Exposure. *International Endodontic Journal*. **26**(5), pp. 284-293.

Anić, I. and Matsumoto, K. 1995. Dentinal Heat Transmission Induced by a Laser-Softened Gutta-Percha Obturation Technique. *Journal of Endodontics*. **21**(9), pp. 470-474.

Anić, I., Pavelić, B., Perić, B. and Matsumoto, K. 1996a. In Vitro Pulp Chamber Temperature Rises associated with the Argon Laser Polymerization of Composite Resin. *Lasers in Surgery and Medicine: The Official Journal of the American Society for Laser Medicine and Surgery.* **19**(4), pp. 438-444.

Anić, I., Tachibana, H., Masumoto, K. and Qi, P. 1996b. Permeability, Morphologic, and Temperature Changes of Canal Dentine Walls Induced by Nd:YAG, CO_2 and Argon Lasers. *International Endodontic Journal.* **29**(1), pp. 13-22.

Apfel, F.R. and Gerstein, H. 1973. Response of Periodontium to Pulp Tester. *Journal of the American Dental Association.* **87**(1), p. 30.

Arima, M. and Matsumoto, K. 1993. Effects of ArF: Excimer Laser Irradiation on Human Enamel and Dentin. *Lasers in Surgery and Medicine.* **13**(1), pp. 97-105.

Arrastia, A.M.A., Machida, T., Smith, P.W. and Matsumoto, K. 1994. Comparative Study of the Thermal Effects of Four Semiconductor Lasers on the Enamel and Pulp Chamber of a Human Tooth. *Lasers in Surgery and Medicine.* **15**(4), pp. 382-389.

Arrastia, A.M.A., Wilder-Smith, P. and Berns, M.W. 1995. Thermal Effects of CO_2 Laser on the Pulpal Chamber and Enamel of Human Primary Teeth: An In Vitro Investigation. *Lasers in Surgery and Medicine.* **16**(4), pp. 343-350.

Assaf, A.T., Zrnc, T.A., Remus, C.C., Khokale, A., Habermann, C.R., Schulze, D., Fiehler, J., Heiland, M., Sedlacik, J. and Friedrich, R.E. 2015. Early Detection of Pulp Necrosis and Dental Vitality After Traumatic Dental Injuries in Children and Adolescents by 3-Tesla Magnetic Resonance Imaging. *Journal of Cranio-Maxillo-Facial Surgery.* **43**(7), pp. 1088-1093.

Baik, J.W., Rueggeberg, F.A. and Liewehr, F.R. 2001. Effect of Light-Enhanced Bleaching on in Vitro Surface and Intrapulpal Temperature Rise. *Journal of Esthetic and Restorative Dentistry.* **13**(6), pp. 370-378.

Baldissara, P., Catapano, S. and Scotti, R. 1997. Clinical and Histological Evaluation of Thermal Injury Thresholds in Human Teeth: A Preliminary Study. *Journal of Oral Rehabilitation.* **24**(11), pp. 791-801.

Balic, A. and Thesleff, I. 2015. Chapter Seven-Tissue Interactions Regulating Tooth Development and Renewal. *Current Topics in Developmental Biology.* **115**, pp. 157-186.

Balooch, M., Habelitz, S., Kinney, J.H., Marshall, S.J. and Marshall, G.W. 2008. Mechanical Properties of Mineralized Collagen Fibrils as Influenced by Demineralization. *Journal of Structural Biology.* **162**(3), pp. 404-410.

Banes, J.D. and Hammond, H.L. 1978. Surface Temperatures of Vital and Nonvital Teeth in Humans. *Journal of Endodontics.* **4**(4), pp. 106-109.

Barclay, C.W., Spence, D. and Laird, W.R.E. 2005. Intra-Oral Temperatures During Function. *Journal of Oral Rehabilitation.* **32**(12), pp. 886-894.

Barker, R.E., Rafoth, R.F. and Ward, R.W. 1972. Thermally Induced Stresses and Rapid Temperature Changes in Teeth. *Journal of Biomedical Materials Research Part A.* **6**(5), pp. 305-325.

Bartlett, J.D. 2013. Dental Enamel Development: Proteinases and Their Enamel Matrix Substrates. ISRN Dentistry: 684607.

Bech, M., Jensen, T.H., Bunk, O., Donath, T., David, C., Weitkamp, T., Le Duc, G., Bravin, A., Cloetens, P. and Pfeiffer, F. 2010. Advanced Contrast Modalities for X-ray Radiology: Phase-contrast and Dark-Field Imaging Using a Grating Interferometer. *Zeitschrift fuer medizinische Physik.* **20**(1), pp. 7-16.

Behnia, A. and McDonald, N.J. 2001. In Vitro Infrared Thermographic Assessment of Root Surface Temperatures Generated by the Thermafil Plus System. *Journal of Endodontics.* **27**(3), pp. 203-205.

Benedict, H.C. 1928. A Note on the Fluorescence of Teeth in Ultra-Violet Rays. *Science.* **67**(1739) p. 442.

Bergenholtz, G. 1990. Pathogenic Mechanisms in Pulpal Disease. *Journal of Endodontics.* **16**(2), pp. 98-101.

Beynon, A.D. 1973. Effects of an Antarctic Environment on Dental Structures and Health. *Polar Human Biology.* pp. 105-113.

Bhussry, B.R. 1959. Chemical and Physical Studies of Enamel from Human Teeth. IV. Density and Nitrogen Content of Mottled Enamel. *Journal of Dental Research.* **38**(2), pp. 369-373.

Biagioni, P.A., Hussey, D., Mitchell, C.A., Russell, D.M. and Lamey, P.J. 1996. Thermographic Assessment of Dentine Pin Placement. *Journal of Dentistry.* **24**(6), pp. 443-447.

BioMedCentralLtd. 2016. ISRCTNregistry. [Online]. [Accessed 30th April, 2016]. Available from: http://www.isrctn.com/

Bishop, M.A. 1992. Extracellular Fluid Movement in the Pulp; The Pulp/Dentin Permeability Barrier. *Proceedings of the Finnish Dental Society.* **88**(Suppl.1), pp. 331-335.

Bishop, M.A. and Malhotra, M. 1990. An Investigation of Lymphatic Vessels in the Feline Dental Pulp. *Developmental Dynamics.* **187**(3), pp. 247-253.

Biyikli, S., Modest, M.F. and Tarr, R. 1986. Measurements of Thermal Properties for Human Femora. *Journal of Biomedical Materials Research Part A.* **20**(9), pp. 1335-1345.

Black, G.V. 1895. An Investigation of the Physical Characters of the Human Teeth in Relation to their Diseases, and to Practical Dental Operations, together with the Physical Characters of Filling-materials. *Dental Cosmos.* **37**, pp. 469-484.

Bletsa, A., Berggreen, E., Fristad, I., Tenstad, O. and Wiig, H., 2006. Cytokine Signalling in Rat Pulp Interstitial Fluid and Transcapillary Fluid Exchange During Lipopolysaccharide-Induced Acute Inflammation. *The Journal of Physiology.* **573**(1), pp. 225-236.

Bonar, L.C., Lees, S. and Mook, H.A. 1985. Neutron Diffraction Studies of Collagen in Fully Mineralized Bone. *Journal of Molecular Biology.* **181**(2), pp. 265-270.

Bouillaguet, S., Caillot, G., Forchelet, J., Cattani-Lorente, M., Wataha, J.C. and Krejci, I. 2005. Thermal Risks from LED- and High-Intensity QTH-Curing Units During Polymerization of Dental Resins. *Journal of Biomedical Materials Research Part B: Applied Biomaterials.* **72**(2), pp. 260-267.

Braden, M. 1964. Heat Conduction in Normal Human Teeth. *Archives of Oral Biology.* **9**(4), pp. 479-486.

Braden, M. 1976. Biophysics of the Tooth. *Physiology of Oral Tissues.* **2,** pp. 1-37.

Brännström, M. 1966. Sensitivity of Dentine. *Oral Surgery, Oral Medicine, Oral Pathology*. **21**(4), pp. 517-526.

Brännström, M. 1996. Reducing the Risk of Sensitivity and Pulpal Complications After the Placement of Crowns and Fixed Partial Dentures. *Quintessence International*. **27**(10), pp. 673-678.

Brännström, M. and Nordenvall, K.J. 1978. Bacterial Penetration, Pulpal Reaction and the Inner Surface of Concise Enamel Bond. Composite Fillings in Etched and Unetched Cavities. *Journal of Dental Research*. **57**(1), pp. 3-10.

Braun, A., Kecsmar, S., Krause, F., Berthold, M., Frentzen, M., Frankenberger, R. and Schelle, F. 2015. Effect of Simulated Pulpal Fluid Circulation on Intrapulpal Temperature Following Irradiation with an Nd: YVO4 Laser. *Lasers in Medical Science*. **30**(4), pp. 1197-1202.

Brekhus, P.J. and Armstrong, W.D. 1934. Solution Rate of Apatite in an Average Mouth. *Journal of Dental Research*. **14**(6), pp. 455-456.

Brettle, A. and Grant, M.J. 2003. Finding the Evidence for Practice: a Workbook for Health Professionals. Churchill Livingstone.

Britannica. 2018. [Online]. [Accessed 20th December, 2017]. Available from: https://www.britannica.com

British Standard. 2008. Conditioning Monitoring and Diagnostics of Machines – Thermography Part 1 General Procedures BS ISO18434-1. 1st ed.

Brown, A.C. and Beveridge, E.E. 1966. The Relation between Tooth Pulp Pressure and Systemic Arterial Pressure. *Archives of Oral Biology*. **11**(11), pp. 1181-1193.

Brown, A.C. and Goldberg, M.P. 1966. Surface Temperature and Temperature Gradients of Human Teeth In Situ. *Archives of Oral Biology*. **11**(10), pp. 973-982.

Brown, W.S., Dewey, W.A. and Jacobs, H.R. 1970. Thermal Properties of Teeth. *Journal of Dental Research*. **49**(4), pp. 752-755.

Brown, W.S., Jacobs, H.R. and Thompson, R.E. 1972. Thermal Fatigue in Teeth. *Journal of Dental Research*. **51**(2), pp. 461-467.

Budd, J.C., Gekelman, D. and White, J.M. 2005. Temperature Rise of the Post and on the Root Surface during Ultrasonic Post Removal. *International Endodontic Journal.* **38**(10), pp. 705-711.

Byers, M.R. 1984. Dental Sensory Receptors. International Review of Neurobiology. **25**, pp. 39-94.

Cardoso, C.A.B., Magalhaes, A.C., Rios, D. and Lima, J.E.O. 2009. Cross-Sectional Hardness of Enamel from Human Teeth at Different Posteruptive Ages. Caries Research. **43**(6), pp. 491-494.

Carson, J., Rider, T. and Nash, D. 1979. A Thermographic Study of Heat Distribution During Ultra-Speed Cavity Preparation. *Journal of Dental Research.* **58**(7), pp. 1681-1684.

Chen, E. and Abbott, P.V. 2009. Dental Pulp Testing: A Review. *International Journal of Dentistry.* **2009,** p. 365785.

Chen, E. and Abbott, P.V. 2011. Evaluation of Accuracy, Reliability, and Repeatability of Five Dental Pulp Tests. *Journal of Endodontics.* **37**(12), pp. 1619-1623.

Cho, M.I. and Garant, P.R. 2000. Development and General Structure of the Periodontium. *Periodontology 2000.* **24**(1), pp. 9-27.

Close, F. 2012. Particle Physics: A Very Short Introduction. New York: Oxford University Press.

Coklica, V., Brudevold, F. and Amdur, B.H. 1969. The Distribution and Composition of Density Fractions from Human Crown Dentine. *Archives of Oral Biology.* **14**(5), pp. 451-460.

Colstate. 2018. [Online] [Accessed 21st December, 2017]. Available from: http://www.vivo.colstate.edu

Colston, B.W., Everett, M.J., Da Silva, L.B., Otis, L.L., Stroeve, P. and Nathel, H. 1998. Imaging of Hard- and Soft-Tissue Structure in the Oral Cavity by Optical Coherence Tomography. *Applied Optics.* **37**(16), pp. 3582-3585.

Cox, C.F. 1987. Biocompatibility of Dental Materials in the Absence of Bacterial Infection. *Operative Dentistry.* **12**(4), pp. 146-152.

Craig, R.G. and Peyton, F.A. 1961. Thermal Conductivity of Tooth Structure, Dental Cements, and Amalgam. *Journal of Dental Research*. **40**(3), pp. 411-418.

Crandell, C.E. and Hill, R.P. 1966. Thermography in Dentistry: A Pilot Study. *Oral Surgery, Oral Medicine, Oral Pathology and Oral Radiology*. **21**(3), pp. 316-320.

Crawley, D.A., Longbottom, C., Cole, B.E., Ciesla, C.M., Arnone, D., Wallace, V.P. and Pepper, M. 2003. Terahertz Pulse Imaging: A Pilot Study of Potential Applications in Dentistry. *Caries Research*. **37**(5), pp. 352-359.

Cummings, M., Biagioni, P., Lamey, P.J. and Burden, D.J. 1999. Thermal Image Analysis of Electrothermal Debonding of Ceramic Brackets: An In Vitro Study. *European Journal of Orthodontics*. **21**(2), pp. 111-118.

Cuy, J.L., Mann, A.B., Livi, K.J., Teaford, M.F. and Weihs, T.P. 2002. Nanoindentation Mapping of the Mechanical Properties of Human Molar Tooth Enamel. *Archives of Oral Biology.* **47**(4), pp. 281-291.

Da Costa Ribeiro, A., Nogueira, G.E.C., Antoniazzi, J.H., Moritz, A. and Zezell, D.M. 2007. Effects of Diode Laser (810nm) Irradiation on Root Canal Walls: Thermographic and Morphological Studies. *Journal of Endodontics*. **33**(3), pp. 252-255.

Da Silva Barbosa, P., da Ana, P.A., Poiate, I.A.V.P., Zezell, D.M. and de Sant'Anna, G.R. 2013. Dental Enamel Irradiated With A Low-Intensity Infrared Laser And Photoabsorbing Cream: A Study Of Microhardness, Surface, And Pulp Temperature. *Photomedicine and Laser Surgery*. **31**(9), pp. 439-446.

Daculsi, G., Menanteau, J., Kerebel, L.M. and Mitre, D. 1984. Length and Shape of Enamel Crystals. *Calcified Tissue International*. **36**(1), pp. 550-555.

de Leon, R.L., Path, M.G. and Meyer, M.W. 1978. Blood Flow and Oxygen Consumption in Steroid-Treated Dental Pulps. *Oral Surgery, Oral Medicine, Oral Pathology.* **45**(5), pp. 784-788.

De Magalhaes, M.F., Ferreira, R.A.N., Grossi, P.A. and de Andrade, R.M. 2008. Measurement of Thermophysical Properties of Human Dentin: Effect of Open Porosity. *Journal of Dentistry*. **36**(8), pp. 588-594.

Deakins, M. and Manly, R.S. 1939. A Method for Microdetermination of Density in Calcified Tissues. *Journal of Dental Research*. **18**(6), pp. 557-560.

DiAngelis, A.J., Andreasen, J.O., Ebeleseder, K.A., Kenny, D.J., Trope, M., Sigurdsson, A., Andersson, L., Bourguignon, C., Flores, M.T., Hicks, M.L. and Lenzi, A.R. 2012. International Association of Dental Traumatology Guidelines for the Management of Traumatic Dental Injuries: 1. Fractures and Luxations of Permanent Teeth. *Dental Traumatology*. **28**(1), pp. 2-12.

Diekwisch, T.G. 2001. The Developmental Biology of Cementum. *The International Journal of Developmental Biology*. **45**(5-6), pp. 695-706.

Djomehri, S.I., Candell, S., Case, T., Browning, A., Marshall, G.W., Yun, W., Lau, S.H., Webb, S. and Ho, S.P. 2015. Mineral Density Volume Gradients in Normal and Diseased Human Tissues. *PLoS ONE*. **10**(4), p. e0121611.

Dowden, W.A. 1967. Cholesteric Liquid Crystals: A Review of Developments and Applications. *Non-Destructive Testing*. **1**(2), pp. 99-102.

Dowsett, D.J., Kenny, P.A. and Johnston, R.E. 2006. The Physics of Diagnostic Imaging. 2nd ed. UK: Hodder Arnold.

Dummer, P.M.H., Hicks, R. and Huws, D. 1980. Clinical Signs and Symptoms in Pulp Disease. *International Endodontic Journal*. **13**(1), pp. 27-35.

Edwall, L. and Kindlová, M. 1971. The Effect of Sympathetic Nerve Stimulation on the Rate of Disappearance of Tracers from Various Oral Tissues. *Acta Odontologica Scandinavica*. **29**(4), pp. 387-400.

Egan, C.K., Jacques, S.D., Connolley, T., Wilson, M.D., Veale, M.C., Seller, P. and Cernik, R.J., 2014. Dark-field hyperspectral X-ray imaging. *Proc. R. Soc. A*, *470*(2165), p.20130629.

Egelberg, J. 1966. The Blood Vessels of the Dento-Gingival Junction. *Journal of Periodontal Research*. **1**(3), pp. 163-179.

Engineersedge. [Online]. [Accessed 15th October, 2017]. Available from: www.engineersedge.com

Ernst, E. and Fialka, V. 1994. Ice freezes pain? A Review of the Clinical Effectiveness of Analgesic Cold Therapy. *Journal of Pain and Symptom Management*. **9**(1), pp. 56-59.

Evans, D., Reid, J., Strang, R. and Stirrup, D. 1999. A Comparison of Laser Doppler Flowmetry with other Methods of Assessing the Vitality of Traumatised Anterior Teeth. *Dental Traumatology.* **15**(6), pp. 284-290.

Fanibunda, K.B., 1985. A Laboratory Study to Investigate the Differentiation of Pulp Vitality in Human Teeth by Temperature Measurement. *Journal of Dentistry.* **13**(4), pp. 295-303.

Fanibunda, K.B. 1986a. A Method for Measuring the Volume of Human Dental Pulp Cavities. *International Endodontic Journal.* **19**, pp. 194-197.

Fanibunda, K.B. 1986b. The Feasibility of Temperature Measurement as a Diagnostic Procedure in Human Teeth. *Journal of Dentistry.* **14,** pp.126–129.

Fanibunda, K.B. and de Sa, A. 1975. Thermal Conductivity of Normal and Abnormal Human Dentine. *Archives of Oral Biology.* **20**(7), pp. 457-459.

Fearnhead, R.W. 1957. Histological Evidence for the Innervation of Human Dentine. *Journal of Anatomy.* **91**(Pt 2), pp. 267-277.

Feldchtein, F.I., Gelikonov, G.V., Gelikonov, V.M., Iksanov, R.R., Kuranov, R.V., Sergeev, A.M., Gladkova, N.D., Ourutina, M.N., Warren, J.A. and Reitze, D.H. 1998. In Vivo OCT Imaging of Hard and Soft Tissue of the Oral Cavity. *Optics Express.* **3**(6), pp. 239-250.

Ferguson, B., Wang, S., Gray, D., Abbott, D. and Zhang, X.C. 2002. Identification of Biological Tissue Using Chirped Probe THz Imaging. *Microelectronics Journal.* **33**(12), pp. 1043-1051.

Fiske, J., Davis, D.M., Frances, C. and Gelbier, S. 1998. The Emotional Effects of Tooth Loss in Edentulous People. *British Dental Journal.* **184**(2), pp. 90-93.

Fleischmannova, J., Matalova, E., Sharpe, P.T., Misek, I. and Radlanski, R.J. 2010. Formation of the Tooth-Bone Interface. *Journal of Dental Research.* **89**(2), pp. 108-115.

FLIR ThermaCAM^TM Researcher Professional. 2010. Help Guide.

Folke, L.E.A. and Stallard, R.E. 1967. Periodontal Microcirculation as Revealed by Plastic Microspheres. *Journal of Periodontal Research.* **2**(1), pp. 53-63.

Foreman, P.C. 1983. Ultraviolet Light as an Aid to Endodontic Diagnosis. *International Endodontic Journal*. **16**(3), pp. 121-126.

Frank, R.M. and Steuer, P. 1988. Transmission Electron Microscopy of the Human Odontoblast Process in Peripheral Root Dentine. *Archives of Oral Biology*. **33**(2), pp. 91-98.

Fukase, Y., Saitoh, M., Kaketani, M., Ohashi, M. And Nishiyama, M. 1992. Thermal Coefficients of Paste-Paste Type Pulp Capping Cements. *Dental Materials Journal*. **11**(2), pp. 189-196.

Fuss, Z., Trowbridge, H., Bender, I.B., Rickoff, B. and Sorin, S. 1986. Assessment of Reliability of Electrical and Thermal Pulp Testing Agents. *Journal of Endodontics*. **12**(7), pp. 301-305.

GDC 2015. Preparing for Practice. Dental Team Learning Outcomes for Registration [Online] Revised ed. [Accessed 1st March, 2016], available from: www.gdc-uk.org

Garant, P.R. 1972. The Organization of Microtubules within Rat Odontoblast Processes Revealed by Perfusion Fixation with Glutaraldehyde. *Archives of Oral Biology*. **17**(7), pp. 1047-1054.

Gaussorgues, G. 1994. Infrared Thermography Translated, by S. Chomet (Original French Title: La Thermographie Infrarouge), Microwave Technology Series 5, English Language ed.

Gazelius, B., Olgart, L., Edwall, B. and Edwall, L. 1986. Non-invasive Recording of Blood Flow in Human Dental Pulp. *Dental Traumatology*. **2**(5), pp. 219-221.

Georgopoulou, M. and Kerani, M. 1989. The Reliability of Electrical and Thermal Pulp Tests. A Clinical Study. *Stomatologia*. **46**(5), pp. 317-326.

Glas, J.E. 1962. Studies on the Ultrastructure of Dental Enamel—II: The Orientation of the Apatite Crystallites as Deduced from X-ray Diffraction. *Archives of Oral Biology*. **7**(1), pp. 91-104.

Goho, C. 1999. Pulse Oximetry Evaluation of Vitality in Primary and Immature Permanent Teeth. *Pediatric Dentistry*. **21**, pp. 125-127.

Goldberg, M. and Brown, A.C. 1965. Human Tooth Surface Temperature. *Physiologist*. **8**, p. 175.

Gontijo, I.T., Navarro, R.S., Ciamponi, A.L., Miyakawa, W. and Zezell, D.M. 2008. Color and Surface Temperature Variation during Bleaching in Human Devitalized Primary Teeth: An In Vitro Study. *Journal of Dentistry for Children.* **75**(3), pp. 229-234.

Goodis, H.E., Schein, B. and Stauffer, P. 1988. Temperature Changes Measured In Vivo at the Dentinoenamel Junction and Pulpodentin Junction During Cavity Preparation in The Macaca Fascicularis Monkey. *Journal of Endodontics.* **14**(7), pp. 336-339.

Goodis, H.E., Winthrop, V. and White, J.M. 2000. Pulpal Responses to Cooling Tooth Temperatures. *Journal of Endodontics.* **26**(5), pp. 263-267.

Gopikrishna, V., Pradeep, G. and Venkateshbabu, N. 2009. Assessment of Pulp Vitality: A Review. *International Journal of Paediatric Dentistry.* **19**(1), pp. 3-15.

Gopikrishna, V., Tinagupta, K. and Kandaswamy, D. 2007. Comparison of Electrical, Thermal, and Pulse Oximetry Methods for Assessing Pulp Vitality in Recently Traumatized Teeth. *Journal of Endodontics.* **33**(5), pp. 531-535.

Gradl, R., Zanette, I., Ruiz-Yaniz, M., Dierolf, M., Rack, A., Zaslansky, P. and Pfeiffer, F. 2016. Mass Density Measurement of Mineralized Tissue with Grating-Based X-ray Phase Tomography. *PLoS ONE.* **11**(12), p. e0167797.

Hall, A. and Girkin, J.M. 2004. A Review of Potential New Diagnostic Modalities for Caries Lesions. *Journal of Dental Research.* **83**(Suppl.1), pp. 89-94.

Hardy, J.D. 1934. The Radiation of Heat from the Human Body: III. The Human Skin as a Black-Body Radiator. *Journal of Clinical Investigation.* **13**(4), pp. 615-620.

Hargreaves, K.M., Goodis, H.E. and Tay, F.R. 2012. *Seltzer and Bender's Dental Pulp.* Chicago: Quintessence. 2nd ed. pp. 67-91.

Harman, P.M. 1982. Energy, Force and Matter: The Conceptual Development of Nineteenth-Century Physics. Cambridge University Press.

Hartley, J.L., Stanfill, D.F. and Plakun, B.D. 1967. Thermography of The Human Dentition. Barnes Engineering Co Stamford Conn.

He, B., Huang, S., Jing, J. and Hao, Y. 2010. Measurement of Hydroxyapatite Density and Knoop Hardness in Sound Human Enamel and a Correlational Analysis Between Them. *Archives of Oral Biology*. **55**(2), pp. 134-141.

He, B., Huang, S., Zhang, C., Jing, J., Hao, Y., Xiao, L. and Zhou, X. 2011. Mineral Densities and Elemental Content in Different Layers of Healthy Human Enamel with Varying Teeth Age. *Archives of Oral Biology*. **56**(10), pp. 997-1004.

Health Research Authority, N.E. 2016. Research Summaries. [Online]. [Accessed 30th April, 2016]. Available from: http://www.hra.nhs.uk/news/research-summaries/

Hengchang, X., Wenyi, L. and Tong, W. 1989. Measurement of Thermal Expansion Coefficient of Human Teeth. *Australian Dental Journal*. **34(**6), pp. 530-535.

Henschel, C.J. 1943. Heat Impact of Revolving Instruments on Vital Dentin Tubules. *Journal of Dental Research*. **22(**4), pp. 323-333.

Heyeraas, K.J. 1989. Pulpal Hemodynamics and Interstitial Fluid Pressure: Balance of Transmicrovascular Fluid Transport. *Journal of Endodontics*. **15**(10), pp. 468-472.

Heyeraas, K.J. and Kvinnsland, I. 1992. Tissue Pressure and Blood Flow in Pulpal Inflammation. *Proceedings of the Finnish Dental Society.* **88**(Suppl.1), pp. 393-401.

Hill, C.M. 1986. The Efficacy of Transillumination in Vitality-tests. *International Endodontic Journal*. **19**(4), pp. 198-201.

Hillam C. 1990. The Roots of Dentistry. London: The Lindsay Society for the History of Dentistry. British Dental Journal.

Hock, J. and Nuki, K. 1971. A Vital Microscopy Study of the Morphology of Normal and Inflamed Gingiva. *Journal of Periodontal Research*. **6**(2), pp. 81-88.

Hock, J. and Nuki, K. 1976. Erythrocyte Velocity in Vascular Networks of Young Noninflamed Dog Gingiva. *Journal of Dental Research*. **55**(6), pp. 1058-1060.

Hock, J.M. and Kim, S. 1987. Blood Flow in Healed and Inflamed Periodontal Tissues of Dogs. *Journal of Periodontal Research*. **22**(1), pp. 1-5.

Holland, G.R. 1976. The Extent of the Odontoblast Process in the Cat. *Journal of Anatomy*. **121**(Pt 1), pp. 133-149.

Holst, G.C. 2000. Common Sense Approach to Thermal Imaging. Washington: SPIE Optical Engineering Press.

Hopewell, S., Clarke, M., Lefebvre, C. and Scherer, R. 2007. Handsearching Versus Electronic Searching To Identify Reports Of Randomized Trials (Review). Cochrane Database Syst Rev.

Horner, K., Drage, N.A. and Brettle, D. 2008. 21st Century Imaging. London: Quintessence Publishing Co.Ltd.

Howell, R.M., Duell, R.C. and Mullaney, T.P. 1970. The Determination of Pulp Vitality by Thermographic Means using Cholesteric Liquid Crystals: A Preliminary Study. *Oral Surgery, Oral Medicine, Oral Pathology*. **29**(5), pp. 763-768.

Hsieh, Y.D., Gau, C.H., Kung Wu, S.F., Shen, E.C., Hsu, P.W. and Fu, E. 2007. Dynamic Recording of Irrigating Fluid Distribution in Root Canals using Thermal Image Analysis. *International Endodontic Journal*. **40**(1), pp. 11-17.

Hussey, D.L., Biagioni, P.A. and Lamey, P.J. 1995. Thermographic Measurement of Temperature Change During Resin Composite Polymerization In Vivo. *Journal of Dentistry*. **23**(5), pp. 267-271.

Hussey, D.L., Biagioni, P.A., McCullagh, J.J.P. and Lamey, P.J. 1997. Thermographic Assessment of Heat Generated on the Root Surface During Post Space Preparation. *International Endodontic Journal*. **30**(3), pp. 187-190.

Idiyatullin, D., Corum, C., Moeller, S., Prasad, H.S., Garwood, M. and Nixdorf, D.R. 2011. Dental Magnetic Resonance Imaging: Making the Invisible Visible. *Journal of Endodontics*. **37**(6), pp. 745-752.

Incropera, F.P., Dewitt, D.P., Bergman, T.L. and Lavine, A.S. 2007. Fundamentals of Heat and Mass Transfer. 6th ed. John Wiley & Sons, Inc. pp. 68-72.

Ingólfsson, Æ.R., Tronstad, L., Hersh, E.V. and Riva, C.E. 1994. Efficacy of Laser Doppler Flowmetry in Determining Pulp Vitality of Human Teeth. *Dental Traumatology*. **10**(2), pp. 83-87.

Ishizaki, N.T., Matsumoto, K., Kimura, Y., Wang, X., Kinoshita, J.I., Okano, S. and Jayawardena, J.A. 2004. Thermographical and Morphological Studies of Er, Cr: YSGG Laser Irradiation on Root Canal Walls. *Photomedicine and Laser Therapy*. **22**(4), pp. 291-297.

Jacobs, H.R., Thompson, R.E. and Brown, W.S. 1973. Heat Transfer in Teeth. *Journal of Dental Research*. **52**(2), pp. 248-252.

Jafarzadeh, H. 2009. Laser Doppler Flowmetry in Endodontics: A Review. *International Endodontic Journal*. **42**(6), pp. 476-490.

Jafarzadeh, H. and Abbott, P.V. 2010a. Review of Pulp Sensibility Tests. Part I: General Information and Thermal Tests. *International Endodontic Journal*. **43**(9), pp. 738-762.

Jafarzadeh, H. and Abbott, P.V., 2010b. Review of Pulp Sensibility Tests. Part II: Electric Pulp Tests and Test Cavities. *International Endodontic Journal*. **43**(11), pp. 945-958.

Jernvall, J., Kettunen, P., Karavanova, I., Martin, L.B. and Thesleff, I. 1994. Evidence for the Role of the Enamel Knot as a Control Center in Mammalian Tooth Cusp Formation: Non-Dividing Cells Express Growth Stimulating Fgf-4 Gene. *International Journal of Developmental Biology*. **38**(3), pp. 463-469.

Jespersen, J.J., Hellstein, J., Williamson, A., Johnson, W.T. and Qian, F. 2014. Evaluation of Dental Pulp Sensibility Tests in a Clinical Setting. *Journal of Endodontics*. **40**(3), pp. 351-354.

Johnson, R.H., Dachi, S.F. and Haley, J.V., 1970. Pulpal Hyperemia - A Correlation of Clinical and Histologic Data from 706 Teeth. *The Journal of the American Dental Association*. **81**(1), pp. 108-117.

Kabbach, W., Zezell, D.M., Pereira, T.M., Albero, F.G., Clavijo, V.R.G. and de Andrade, M.F. 2008. A Thermal Investigation of Dental Bleaching In Vitro. *Photomedicine and Laser Surgery*. **26**(5), pp. 489-493.

Kahan, R.S., Gulabivala, K., Snook, M. and Setchell, D.J. 1996. Evaluation of a Pulse Oximeter and Customized Probe for Pulp Vitality-testing. *Journal of Endodontics.* **22**(3), pp. 105-109.

Kakehashi, S., Stanley, H.R. and Fitzgerald, R.J. 1965. The Effects of Surgical Exposures of Dental Pulps in Germ-Free and Conventional Laboratory Rats. *Oral Surgery, Oral Medicine, Oral Pathology.* **20**(3), pp. 340-349.

Kamburoğlu, K. and Paksoy, C.S. 2005. The Usefulness of Standard Endodontic Diagnostic Tests in Establishing Pulpal Status. *The Pain Clinic.* **17**(2), pp. 157-165.

Kaneko, K. Matsuyama, K. and Nakashima, S. 1999. Quantification of Early Carious Enamel Lesions by Using an Infrared Camera In-vitro. *Stookey GK. 4ᵗʰ Annual Indiana Conference. pp.* 83-100.

Kaplan, M.L., Davis, M.A. and Goldhaber, P. 1978. Blood Flow Measurements in Selected Oral Tissues in Dogs Using Radiolabelled Microspheres and Rubidium-86. *Archives of Oral Biology.* **23**(4), pp. 281-284.

Karayilmaz, H. and Kirzioğlu, Z. 2011. Comparison of the Reliability of Laser Doppler Flowmetry, Pulse Oximetry and Electric Pulp Tester in Assessing the Pulp Vitality of Human Teeth. *Journal of Oral Rehabilitation.* **38**(5), pp. 340-347.

Kells, B.E., Kennedy, J.G., Biagioni, P.A. and Lamey, P.J. 2000a. Computerized Infrared Thermographic Imaging and Pulpal Blood Flow: Part 1. A Protocol for Thermal Imaging of Human Teeth. *International Endodontic Journal.* **33**(5), pp. 442-447.

Kells, B.E., Kennedy, J.G., Biagioni, P.A. and Lamey, P.J. 2000b. Computerized Infrared Thermographic Imaging and Pulpal Blood Flow: Part 2. Rewarming of Healthy Human Teeth Following a Controlled Cold Stimulus. *International Endodontic Journal.* **33**(5), pp. 448-462.

Kerebel, B., Daculsi, G. and Kerebel, L.M. 1979. Ultrastructural Studies of Enamel Crystallites. *Journal of Dental Research.* **58**(B), pp. 844-850.

Kilic, K., Er, O., Kilinc, H.I., Aslan, T., Bendes, E., Sekerci, A.E. and Aslantas, V. 2013. Infrared Thermographic Comparison of Temperature Increases on the Root Surface During Dowel Space Preparations using Circular Versus Oval Fiber Dowel Systems. *Journal of Prosthodontics.* **22**(3), pp. 203-207.

Kim, R., Green, J. and Klein, O.D. 2017. From Snapshots to Movies: Understanding Early Tooth Development in Four Dimensions. *Developmental Dynamics.* **246**(6), pp. 442-450.

Kim, S. 1985. Regulation of Pulpal Blood Flow. *Journal of Dental Research.* **64**(4), pp. 590-596.

Kim, S., Chen, R.Y.Z., Wasserman, H., Usami, S. and Chien, S. 1984. Determination of the Partition Coefficient of [133]Xenon Between Oral Tissues and Blood in the Dog. *Archives of Oral Biology.* **29**(9), pp. 721-723.

Kim, S., Dörscher-Kim, J.E., Liu, M. and Grayson, A. 1992. Functional Alterations in Pulpal Microcirculation in Response to Various Dental Procedures and Materials. *Proceedings of the Finnish Dental Society.* **88**(Suppl.1), pp. 65-71.

Kim, S., Fan, F.C., Chen, R.Y., Simchon, S., Schuessler, G.B. and Chien, S. 1980. Effects of Changes in Systemic Hemodynamic Parameters on Pulpal Hemodynamics. *Journal of Endodontics.* **6**(1), pp. 394-399.

Kim, S., Liu, M., Markowitz, K., Bilotto, G. and Dörscher-Kim, J. 1990. Comparison of Pulpal Blood Flow in Dog Canine Teeth Determined by the Laser Doppler and the [133]Xenon Washout Methods. *Archives of Oral Biology.* **35**(5), pp. 411-413.

Kim, S., Schuessler, G. and Chien, S. 1983. Measurement of Blood Flow in the Dental Pulp of Dogs with the [133]Xenon Washout Method. *Archives of Oral Biology.* **28**(6), pp. 501-505.

Kim, S., Trowbridge, H.O. and Dorscher-Kim, J.E. 1986. The Influence of 5-hydroxytryptamine (serotonin) on Blood Flow in the Dog Pulp. *Journal of Dental Research.* **65**(5), pp. 682-685.

Kindlova, M. 1965. The Blood Supply of the Marginal Periodontium in Macacus Rhesus. *Archives of Oral Biology.* **10**(6), pp. 869-876.

Kindlova, M. 1970. The Development of the Vascular Bed of the Marginal Periodontium. *Journal of Periodontal Research.* **5**(2), pp. 135-140.

Kindlova, M. and Matena, V. 1962. Blood Vessels of the Rat Molar. *Journal of Dental Research.* **41**(3), pp. 650-660.

Kinney, J.H., Marshall, S.J. and Marshall, G.W. 2003. The Mechanical Properties of Human Dentin: A Critical Review and Re-Evaluation of the Dental Literature. *Critical Reviews in Oral Biology & Medicine.* **14**(1), pp. 13-29.

Kinney, J.H., Nalla, R.K., Pople, J.A., Breunig, T.M. and Ritchie, R.O. 2005. Age-Related Transparent Root Dentin: Mineral Concentration, Crystallite Size, and Mechanical Properties. *Biomaterials.* **26**(16), pp. 3363-3376.

Kinney, J.H., Pople, J.A., Marshall, G.W. and Marshall, S.J. 2001. Collagen Orientation and Crystallite Size in Human Dentin: A Small Angle X-ray Scattering Study. *Calcified Tissue International.* **69**(1), pp. 31-37.

Kirkham, J., Brookes, S.J., Diekwisch, T.G.H., Margolis, H.C., Berdal, A. and Hubbard, M.J. 2017. Enamel Research: Priorities and Future Directions. *Frontiers in Physiology.* [Online]. pp.1–4. [Accessed January, 2018]. Available from: http://journal.frontiersin.org/article/10.3389/fphys.2017.00513/full.

Kirkham, J., Zhang, J., Brookes, S.J., Shore, R.C., Wood, S.R., Smith, D.A., Wallwork, M.L., Ryu, O.H. and Robinson, C. 2000. Evidence for Charge Domains on Developing Enamel Crystal Surfaces. *Journal of Dental Research.* **79**(12), pp. 1943-1947.

Kishen, A., Murukeshan, V.M., Krishnakumar, V., Lim, C.S. and Asundi, A. 2003. Digital Speckle Pattern Interferometric (DSPI) and Thermo-Graphic Investigations on the Thermal Response in Human Teeth. *Optics and Lasers in Engineering.* **39**(4), pp. 489-500.

Kodonas, K., Gogos, C. and Tziafas, D. 2009. Effect of Simulated Pulpal Microcirculation on Intrapulpal Temperature Changes Following Application of Heat on Tooth Surfaces. *International Endodontic Journal.* **42**(3), pp. 247-252.

Komoriyama, M., Nomoto, R., Tanaka, R., Hosoya, N., Gomi, K., Iino, F., Yashima, A., Takayama, Y., Tsuruta, M., Tokiwa, H. And Kawasaki, K. 2003. Application of Thermography In Dentistry. *Dental Materials Journal,* **22**(4), pp. 436-443.

Kraintz, L. and Conroy, C.W. 1960. Blood-Volume Measurements of Dog Teeth. *Journal of Dental Research.* **39**(5), pp. 1033-1036.

Kramer, I.R. 1960. The Vascular Architecture of the Human Dental Pulp. *Archives of Oral Biology.* **2**(3), pp. 177-189.

Kress, B., Buhl, Y., Anders, L., Stippich, C., Palm, F., Bahren, W. and Sartor, K. 2004. Quantitative Analysis of MRI Signal Intensity as a Tool for Evaluating Tooth Pulp Vitality. *Dentomaxillofacial Radiology.* **33**(4), pp. 241-244.

Laerd Statistics. 2015. Paired-samples t-test using SPSS Statistics. *Statistical tutorials and software guides*. [Online] [Accessed March, 2018] Available from https://statistics.laerd.com/

Laerd Statistics. 2015. Independent-samples t-test using SPSS Statistics. *Statistical tutorials and software guides*. [Online] [Accessed March, 2018] Available from https://statistics.laerd.com/

Laerd Statistics. 2015. Mann-Whitney U test using SPSS Statistics. *Statistical tutorials and software guides*. [Online] [Accessed March, 2018] Available from https://statistics.laerd.com/

Lancaster, P., Carmichael, F., Britton, J., Craddock, H., Brettle, D. and Clerehugh, V. 2013. Surfing the spectrum - What is on the horizon? *British Dental Journal.* **215**(8), pp. 401-409.

Langeland, K. 1959. Histologic Evaluation of Pulp Reactions to Operative Procedures. *Oral Surgery, Oral Medicine, Oral Pathology.* **12**(11), pp.1357-1371.

Larmour, C.J., Mossey, P.A., Thind, B.S., Forgie, A.H., Stirrups, D.R. and Colin, J. 2005. Hypodontia — A Retrospective Review of Prevalence and Etiology. Part I. *Quintessence International.* **36**(4), pp. 263-270.

Launay, Y., Mordon, S., Cornil, A., Brunetaud, J.M. and Moschetto, Y. 1987. Thermal Effects of Lasers on Dental Tissues. *Lasers in Surgery and Medicine.* **7**(6), pp. 473-477.

Lea, S.C., Landini, G. and Walmsley, A.D. 2004. Thermal Imaging of Ultrasonic Scaler Tips during Tooth Instrumentation. *Journal of Clinical Periodontology.* **31**(5), pp. 370-375.

Lee, J.M., Warren, M.P. and Mason, S.M. 1978. Effects of Ice on Nerve Conduction Velocity. *Physiotherapy.* **64**(1), pp. 2-6.

Legendre, L.F. 2002. Malocclusions In Guinea Pigs, Chinchillas And Rabbits. *The Canadian Veterinary Journal.* **43**(5), pp. 385-390.

Levin, L.G., 2013. Pulp and Periradicular Testing. *Journal of Endodontics.* **39**(3), pp. S13-S19.

Lewis, T. 1930. Observations upon the Reactions of the Vessels of the Human Skin to Cold. *Heart.* **15,** pp. 177-208.

Liebman, F.M. and Cosenza, F. 1962. Study of Blood Flow in the Dental Pulp by an Electrical Impedance Technique. *Physics in Medicine & Biology.* **7**(2), pp. 167-176.

Lin, M., Liu, Q.D., Xu, F., Bai, B.F. and Lu, T.J. 2010a. In Vitro Investigation of Heat Transfer in Human Tooth. In: C. Quan, ed. 4th International Conference on Experimental Mechanics.

Lin, M., Liu, Q.D., Kim, T., Xu, F., Bai, B.F. and Lu, T.J. 2010b. A New Method for Characterization of Thermal Properties of Human Enamel and Dentin: Influence of Microstructure. *Infrared Physics & Technology.* **53**(6), pp. 457–463.

Lin, M., Xu, F., Lu, T.J. and Bai, B.F. 2010c. A Review of Heat Transfer in Human Tooth — Experimental Characterization and Mathematical Modeling. *Dental Materials.* **26**(6), pp. 501–513.

Lin, M., Liu S., Xu, F., Lu, T., Bai, B. and Genin, G. 2013. Thermal Pain in Teeth: Heat Transfer, Thermomechanics and Ion Transport. *Transport in Biological Media.* Newnes. Chp 2, pp. 41-57.

Linde, A. 1985. Session II: Cells and Extracellular Matrices of the Dental Pulp—CT Hanks, Chairman: The Extracellular Matrix of the Dental Pulp and Dentin. *Journal of Dental Research.* **64**(4), pp. 523-529.

Linde, A. and Goldberg, M. 1993. Dentinogenesis. *Critical Reviews in Oral Biology & Medicine.* **4**(5), pp. 679-728.

Linde, A. and Lundgren, T. 1995. From Serum to the Mineral Phase. The Role of the Odontoblast in Calcium Transport and Mineral Formation. International Journal Of Developmental Biology. **39**(1), pp. 213-222.

Lipski, M. 2004. Root Surface Temperature Rises in Vitro during Root Canal Obturation with Thermoplasticized Gutta-Percha on a Carrier or by Injection. *Journal of Endodontics.* **30**(6), pp. 441-443.

Lipski, M. 2005a. Root Surface Temperature Rises during Root Canal Obturation, In Vitro, by the Continuous Wave Of Condensation Technique Using System B Heatsource. *Oral Surgery, Oral Medicine, Oral Pathology, Oral Radiology and Endodontics.* **99**(4), pp. 505-510.

Lipski, M., 2005b. Root Surface Temperature Rises In Vitro during Root Canal Obturation using Hybrid and Microseal Techniques. *Journal of Endodontics.* **31**(4), pp. 297-300.

Lipski, M. 2006. In Vitro Infrared Thermographic Assessment of Root Surface Temperatures Generated by High-Temperature Thermoplasticized Injectable Gutta-Percha Obturation Technique. *Journal of Endodontics.* **32**(5), pp. 438-441.

Lipski, M., Dębicki, M. and Droździk, A. 2010a. Effect of Different Water Flows on Root Surface Temperature during Ultrasonic Removal of Posts. *Oral Surgery, Oral Medicine, Oral Pathology, Oral Radiology and Endodontics.* **110**(3), pp. 395-400.

Lipski, M., Mrozek, J. and Droździk, A. 2010b. Influence of Water Cooling on Root Surface Temperature Generated during Post Space Preparation. *Journal of Endodontics.* **36**(4), pp. 713-716.

Lipski, M. and Woźniak, K. 2003. In Vitro Infrared Thermographic Assessment of Root Surface Temperature Rises during Thermafil Retreatment Using System B. *Journal of Endodontics.* **29**(6), pp. 413-415.

Lipski, M. and Zapałowicz, Z. 2002. In Vitro Infrared Thermographic Assessment of Root Surface Temperatures Generated by Thermoplasticized Gutta-percha Root Canal Obturation Using System B Heat Source. In *Heat Exchange and Renewable Energy Sources. International Symposium.* pp. 139-144.

Lisanti, V.F. and Zander, H.A. 1950. Thermal Conductivity of Dentin. *Journal of Dental Research.* **29**(4), pp. 493-497.

Little, P.A., Wood, D.J., Bubb, N.L., Maskill, S.A., Mair, L.H. and Youngson, C.C. 2005. Thermal Conductivity Through Various Restorative Lining Materials. *Journal of Dentistry.* **33**(7), pp. 585-591.

Lloyd, B.A., McGinley, M.B. and Brown, W.S. 1978. Thermal Stress in Teeth. *Journal of Dental Research.* **57**(4), pp. 571-582.

Longman, C.M. and Pearson, G.J. 1987. Variations in Tooth Surface Temperature in the Oral Cavity during Fluid Intake. *Biomaterials.* **8**(5), pp. 411-414.

Lopes, M.B., Yan, Z, Consani, S., Gonini Júnior, A., Aleixo, A. and McCabe, J.F. 2012. Evaluation of the Coefficient of Thermal Expansion of Human and Bovine Dentin by Thermomechanical Analysis. *Brazilian Dental Journal.* **23(**1), pp. 3-7.

Love, J.L. 1986. Heat Transfer Considerations in the Design of a Thermology Clinic. In; Abernethy M, Uematsu S, eds. Medical Thermology, 1st edn. Washington DC, USA; American Academy of Thermology pp. 19-25.

Lussi, A., Jaeggi, T. and Zero, D. 2004. The Role of Diet in the Aetiology of Dental Erosion. *Caries Research.* **38**(Suppl.1), pp. 34-44.

Machida, T., Wilder-Smith, P., Arrastia, A.M., Liaw, L.H.L. and Berns, M.W. 1995. Root Canal Preparation using the Second Harmonic KTP: YAG Laser: A Thermographic and Scanning Electron Microscopic Study. *Journal of Endodontics.* **21**(2), pp. 88-91.

Madura, H., Dąbrowski, M., Dulski, R., Żmuda, S. and Zaborowski, P. 2004. Thermographic Method for Evaluation of Thermal Influence of Nd: YAG Laser on a Tooth Root During Sterilization Process. *Infrared Physics & Technology.* **46**(1-2), pp. 167-171.

Maeda, T., Kannari, K., Sato, O. and Iwanaga, T. 1990. Nerve Terminals in Human Periodontal Ligament as Demonstrated by Immunohistochemistry for Neurofilament Protein (NFP) and S-100 Protein. *Archives of Histology and Cytology.* **53**(3), pp. 259-265.

Malmgren, B., Andreasen, J.O., Flores, M.T., Robertson, A., DiAngelis, A.J., Andersson, L., Cavalleri, G., Cohenca, N., Day, P., Hicks, M.L. and Malmgren, O. 2012. International Association of Dental Traumatology Guidelines for the Management of Traumatic Dental Injuries: 3. Injuries in the Primary Dentition. *Dental Traumatology.* **28**(3), pp. 174-182.

Manly, R. S., Hodge, H. C. and Ange, L. E. 1939. Density and Refractive Index Studies of Dental Hard Tissues. *Density of Dental Hard Tissues.* **18**(3), pp. 203-211.

Martin, H., Ferris, C. and Mazzella, W. 1969. An Evaluation of Media used in Electric Pulp Testing. *Oral Surgery, Oral Medicine, Oral Pathology.* **27**(3), pp. 374-378.

Martin-Löf, S., Söremark, C., Myrberg, N. and Söremark, R. 1971. Discontinuities in Thermal Expansion of Bovine Enamel and Dentine Observed by A Beta-Radiation Absorption Dilatometric Method. *Archives of Oral Biology.* **16**(8), pp. 873-880.

Matsuo, M. and Takahashi, K. 2002. Scanning Electron Microscopic Observation of Microvasculature in Periodontium. *Microscopy Research and Technique.* **56**(1), pp. 3-14.

Matsushita-Tokugawa, M., Miura, J., Iwami, Y., Sakagami, T., Izumi, Y., Mori, N., Hayashi, M., Imazato, S., Takeshige, F. and Ebisu, S. 2013. Detection of Dentinal Microcracks using Infrared Thermography. *Journal of Endodontics.* **39**(1), pp. 88-91.

Matthews, B. and Andrew, D. 1995. Microvascular Architecture and Exchange in Teeth. *Microcirculation.* **2**(4), pp. 305-313.

Matvienko, A., Mandelis, A. and Abrams, S. 2009. Robust Multiparameter Method of Evaluating the Optical and Thermal Properties of a Layered Tissue Structure using Photothermal Radiometry. *Applied Optics.* **48**(17), pp. 3192-3203.

McCullagh, J.J.P., Biagioni, P.A., Lamey, P.J. and Hussey, D.L. 1997. Thermographic Assessment of Root Canal Obturation using Thermomechanical Compaction. *International Endodontic Journal.* **30**(3), pp. 191-195.

McCullagh, J.J.P., Setchell, D.J., Gulabivala, K., Hussey, D.L., Biagioni, P., Lamey, P.J. and Bailey, G. 2000. A Comparison of Thermocouple and Infrared Thermographic Analysis of Temperature Rise on the Root Surface during the Continuous Wave of Condensation Technique. *International Endodontic Journal.* **33**(4), pp. 326-332.

McIntosh, R.L. and Anderson, V. 2010. A Comprehensive Tissue Properties Database Provided for the Thermal Assessment of a Human at Rest. *Biophysical Reviews and Letters.* **5**(03), pp. 129-151.

Meckel, A.H., Griebstein, W.J. and Neal, R.J. 1965. Structure of Mature Human Dental Enamel as Observed by Electron Microscopy. *Archives of Oral Biology.* **10**(5), pp. 775-783.

Mejare, I.A., Axelsson, S., Davidson, T., Frisk, F., Hakeberg, M., Kvist, T., Norlund, A., Petersson, A., Portenier, I., Sandberg, H. and Tranæus, S. 2012. Diagnosis of the Condition of the Dental Pulp: A Systematic Review. *International Endodontic Journal.* **45**(7), pp. 597-613.

Méndez, J.D. and Zarzoza, E. 1999. Rapid Determination of Dry Weight in Human Dental Pulp by a Colorimetric Reaction. *Journal of Endodontics.* **25**(9), pp. 596-598.

Meyer, D.H. and Foth, H.J. 1996. Thermal Stress In Dentin and Enamel Under CO 2 Laser Irradiation. *Medical Applications of Lasers III.* International Society for Optics and Photonics. **2623**, pp. 117-129.

Meyer, M., Weiner, D. and Grim, E. 1964. Blood Flow in the Dental Pulp of the Dog. *Proceedings of the Society for Experimental Biology and Medicine.* **116**(4), pp. 1038-1040.

Meyer, M.W. 1970. Distribution of Cardiac Output to Oral Tissues in Dogs. *Journal of Dental Research.* **49**(4), pp. 787-794.

Meyer, M.W. 1980. Methodologies for Studying Pulpal Hemodynamics. *Journal of Endodontics.* **6**(3), pp. 466-472.

Meyer, M.W. 1993. Pulpal Blood Flow: Use of Radio-Labelled Microspheres. *International Endodontic Journal.* **26**(1), pp. 6-7.

Meyer, M.W. and Path, M.G. 1979. Blood Flow in the Dental Pulp of Dogs Determined by Hydrogen Polarography and Radioactive Microsphere Methods. *Archives of Oral Biology.* **24**(8), pp. 601-605.

Mickel, A.K., Lindquist, K.A., Chogle, S., Jones, J.J. and Curd, F. 2006. Electric Pulp Tester Conductance Through Various Interface Media. *Journal of Endodontics.* **32**(12), pp. 1178-1180.

Miletich, I. and Sharpe, P.T. 2004. Neural Crest Contribution to Mammalian Tooth Formation. *Birth Defects Research Part C: Embryo Today: Reviews.* **72**(2), pp. 200-212.

Miller, J. 1954. The Microradiographic Appearance of Dentin. *British Dental Journal.* **97**, pp. 7-9.

Miller-Keane Encyclopedia and Dictionary of Medicine, Nursing, and Allied Health, 7th ed. 2003.

Mina, M. and Kollar, E.J. 1987. The Induction of Odontogenesis in Non-Dental Mesenchyme Combined with Early Murine Mandibular Arch Epithelium. *Archives of Oral Biology.* **32**(2), pp. 123-127.

Minesaki, Y., Muroya, M., Higashi, R., Shinohara, N., Jimi, T., Fujii, K. and Inoue, K. 1983. A Method for Determining of Thermal Diffusivity of Human Teeth. *Dental Materials Journal.* **2**(2), pp. 204-209.

Miwa, Z., Ikawa, M., Iijima, H., Saito, M. and Takagi, Y. 2002. Pulpal Blood Flow in Vital and Nonvital Young Permanent Teeth Measured by Transmitted-Light Photoplethysmography: A Pilot Study. *Pediatric Dentistry.* **24**(6), pp. 594-598.

Montoya, C., Arango-Santander, S., Peláez-Vargas, A., Arola, D. and Ossa, E.A. 2015. Effect of Aging on the Microstructure, Hardness and Chemical Composition of Dentin. *Archives of Oral Biology.* **60**(12), pp. 1811-1820.

Munshi, A., Hegde, A. and Radhakrishnan, S. 2003. Pulse Oximetry: a Diagnostic Instrument in Pulpal Vitality-Testing. *Journal of Clinical Pediatric Dentistry.* **26**(2), pp. 141-145.

Murray, A.K., Gorodkin, R.E., Moore, T.L., Gush, R.J., Herrick, A.L. and King, T.A. 2004. Comparison of Red and Green Laser Doppler Imaging of Blood Flow. *Lasers in Surgery and Medicine.* **35**(3), pp. 191-200.

Nait Lechguer, A., Kuchler-Bopp, S., Hu, B., Haikel, Y. and Lesot, H. 2008. Vascularization of Engineered Teeth. *Journal of Dental Research.* **87**(12), pp. 1138-1143.

Nanci, A. 2012. Ten Cate's Oral Histology Development, Structure, and Function, 8th ed. Elsevier.

Nanci, A. and Bosshardt, D.D. 2006. Structure of Periodontal Tissues in Health and Disease. *Periodontology 2000.* **40**(1), pp. 11-28.

Närhi, M., Jyväsjärvi, E., Hirvonen, T. and Huopaniemi, T. 1982. Activation of Heat-Sensitive Nerve Fibres in the Dental Pulp of the Cat. *Pain.* **14**(4), pp. 317-326.

Natsume, Y., Nakashima, S., Shimada, Y., Sadr, A., Tagami, J. and Sumi, Y. 2011. Estimation of Lesion Progress in Artificial Root Caries by Swept Source Optical Coherence Tomography in Comparison to Transverse Microradiography. *Journal of Biomedical Optics.* **16**(7), p. 071408.

Neev, J., Pham, K., Lee, J.P. and White, J.M. 1996. Dentin Ablation with Three Infrared Lasers. *Lasers in Surgery and Medicine: The Official Journal of the American Society for Laser Medicine and Surgery*. **18**(2), pp. 121-128.

Neev, J., Stabholtz, A., Liaw, L.H.L., Torabinejad, M., Fujishige, J.T., Ho, P.D. and Berns, M.W. 1993. Scanning Electron Microscopy and Thermal Characteristics of Dentin Ablated By A Short-Pulse Xecl Excimer Laser. *Lasers in Surgery and Medicine.* **13**(3), pp. 353-362.

Nencini, S. and Ivanusic, J.J. 2016. The Physiology of Bone Pain. How Much Do We Really Know? *Frontiers in Physiology*. **7**, p. 157.

NHS England 2015 [Online] [Accessed April 2017] www.england.nhs.uk

NHS England, C.D.O.T. 2015. Guide for Commissioning Specialist Dentistry Services Superseded.

Niklas, A., Hiller, K.A., Jaeger, A., Brandt, M., Putzger, J., Ermer, C., Schulz, I., Monkman, G., Giglberger, S., Hirmer, M. and Danilov, S. 2014. In Vitro Optical Detection of Simulated Blood Pulse in a Human Tooth Pulp Model. *Clinical Oral Investigations.* **18**(5), pp. 1401-1409.

Nissan, R., Trope, M., Zhang, C.D. and Chance, B. 1992. Dual Wavelength Spectrophotometry as a Diagnostic Test of the Pulp Chamber Contents. *Oral Surgery, Oral Medicine, Oral Pathology.* **74**(4), pp. 508-514.

Nordenram, G., Davidson, T., Gynther, G., Helgesson, G., Hultin, M., Jemt, T., Lekholm, U., Nilner, K., Norlund, A., Rohlin, M. and Sunnegårdh-Grönberg, K. 2013. Qualitative Studies of Patients' Perceptions of Loss of Teeth, the Edentulous State and Prosthetic Rehabilitation: A Systematic Review With Meta-Synthesis. *Acta Odontologica Scandinavica.* **71**(3-4), pp. 937-951.

Norlin, B. and Fröjdh, C. 2005. Energy Dependence in Dental Imaging with Medipix2. *Nuclear Instruments and Methods in Physics Research Section A: Accelerators, Spectrometers, Detectors and Associated Equipment.* **546**(1-2), pp. 19-23.

Odor, T.M., Ford, T.P. and McDonald, F. 1996. Effect of Probe Design and Bandwidth on Laser Doppler Readings from Vital and Root-Filled Teeth. *Medical Engineering & Physics.* **18**(5), pp. 359-364.

Olgart, L. 1996. Neural Control of Pulpal Blood Flow. *Critical Reviews in Oral Biology & Medicine.* **7**(2), pp. 159-171.

Omega UK [Online] [Accessed 2014] https://www.omega.com/

Orban, B. 1928. Growth and Movement of the Tooth Germs and Teeth. *Journal of the American Dental Association.* **15**(6), pp. 1004-1016.

Özcan, G., Taner, I.L., Aras, T., Ercan, M.T. and Balos, K. 1992. Blood Flow to Human Gingiva Measured by the [133]Xe Clearance Technique. *The Journal of Nihon University School of Dentistry.* **34**(3), pp. 208-213.

Panas, A.J., Preiskorn, M., Dabrowski, M. and Zmuda, S. 2007. Validation of Hard Tooth-tissue Thermal Diffusivity Measurements Applying an Infrared Camera. *Infrared Physics & Technology.* **49**(3), pp. 302–305.

Panas, A.J., Żmuda, S., Terpiłowski, J. and Preiskorn, M. 2003. Investigation of the Thermal Diffusivity of Human Tooth Hard Tissue. *International Journal of Thermophysics.* **24**(3), pp. 837-848.

Park, S.H., Roulet, J.F. and Heintze, S.D. 2010. Parameters Influencing Increase in Pulp Chamber Temperature with Light-Curing Devices: Curing Lights and Pulpal Flow Rates. *Operative Dentistry.* **35**(3), pp. 353-361.

Pashley, D.H. 1996. Dynamics of the Pulpo-Dentin Complex. *Critical Reviews in Oral Biology & Medicine.* **7**(2), pp. 104-133.

Path, M.G. and Meyer, M.W. 1977. Quantification of Pulpal Blood Flow in Developing Teeth of Dogs. *Journal of Dental Research.* **56**(10), pp. 1245-1254.

Path, M.G. and Meyer, M.W. 1980. Heterogeneity of Blood Flow in the Canine Tooth in the Dog. *Archives of Oral Biology.* **25**(2), pp. 83-86.

Peters, D.D., Baumgartner, J.C. and Lorton, L. 1994. Adult Pulpal Diagnosis. I. Evaluation of the Positive and Negative Responses to Cold and Electrical Pulp Tests. *Journal of Endodontics.* **20**(10), pp. 506-511.

Petersson, K., Söderström, C., Kiani-Anaraki, M. and Levy, G. 1999. Evaluation of the Ability of Thermal and Electrical Tests to Register Pulp Vitality. *Endodontics and Dental Traumatology.* **15**(3), pp. 127-131.

Phillips, R.W., Johnson, R.J. and Phillips, L.J. 1956. An Improved Method for Measuring the Coefficient of Thermal Conductivity of Dental Cement. *The Journal of the American Dental Association.* **53**(5), pp. 577-583.

Pidaparti, R.M.V., Chandran, A., Takano, Y. and Turner, C.H. 1996. Bone Mineral Lies Mainly Outside Collagen Fibrils: Predictions of a Composite Model for Osternal Bone. *Journal of Biomechanics.* **29**(7), pp. 909-916.

Ploder, O., Partik, B., Rand, T., Fock, N., Voracek, M., Undt, G. and Baumann, A. 2001. Reperfusion of Autotransplanted Teeth—Comparison of Clinical Measurements by Means of Dental Magnetic Resonance Imaging. *Oral Surgery, Oral Medicine, Oral Pathology, Oral Radiology and Endodontics.* **92**(3), pp. 335-340.

Pogrel, M.A., Yen, C.K. and Taylor, R.C. 1988. A Thermographic Evaluation of the Temperatures Achieved by a Carbon Dioxide Laser on Soft Tissues and Teeth. *Thermology*. **3**, pp. 50-52.

Pogrel, M.A., Yen, C.K. and Taylor, R.C. 1989. Studies in Tooth Crown Temperature Gradients with the Use of Infrared Thermography. *Oral Surgery, Oral Medicine, Oral Pathology*. **67**(5), pp. 583-587.

Preoteasa, E., Iosif, L., Amza, O., Preoteasa, C.T. and Dumitrascu, C. 2010. Thermography, an Imagistic Method in Investigation of the Oral Mucosa Status in Complete Denture Wearers. *Journal of Optoelectronics and Advanced Materials*. **12**(11), pp. 2333-2340.

Ramoglu, S.I., Karamehmetoglu, H., Sari, T. and Usumez, S. 2015. Temperature Rise Caused in the Pulp Chamber Under Simulated Intrapulpal Microcirculation with Different Light-Curing Modes. *The Angle Orthodontist*. **85**(3), pp. 381-385.

Research, N.I.f.H. 2016. UK Clinical Trial Gateway. [Online]. [Accessed 30th April, 2016]. Available from: https://www.ukctg.nihr.ac.uk/#

Rickard, T., Denny, R.C. and Foster, S. 1984. Cambridge Illustrated Thesaurus of Physics. 1st ed. (R. C. Denny & S. Foster, eds.). Cambridge: Press Syndicate of the University of Cambridge.

Ring, E.F.J. and Ammer, K. 2000. The Technique of Infra-red Imaging in Medicine. *Thermology International*. **10**(1), pp. 7-14.

Roberts, H.W. 2014. Temperature-Influenced Dimensional Change of Different Molar Anatomical Areas. *Archives of Oral Biology*. **59**(12), pp. 1312-1315.

Robinson, C., Shore, R.C., Wood, S.R., Brookes, S.J., Smith, D.A.M., Wright, J.T., Connell, S. and Kirkham, J. 2003. Subunit Structures in Hydroxyapatite Crystal Development in Enamel: Implications for Amelogenesis Imperfecta. *Connective Tissue Research*. **44**(1), pp. 65-71.

Roebuck, E.M., Evans, D.J.P., Stirrups, D. and Strang, R. 2000. The Effect of Wavelength, Bandwidth, and Probe Design and Position on Assessing the Vitality of Anterior Teeth with Laser Doppler Flowmetry. *International Journal of Paediatric Dentistry*. **10**(3), pp. 213-220.

Rothová, M., Feng, J., Sharpe, P.T., Peterková, R. and Tucker, A.S. 2011. Contribution of Mesoderm to the Developing Dental Papilla. *International Journal of Developmental Biology*. **55**(1), pp. 59-64.

Rouxel, P., Tsakos, G., Chandola, T. and Watt, R.G. 2016. Oral Health - A Neglected Aspect of Subjective Well-Being in Later Life. Journal of Gerontology B Psychology Science Social Science. **73**(3), pp. 382-386.

Rowe, A.H.R. and Pitt Ford, T.R. 1990. The Assessment of Pulpal Vitality. *International Endodontic Journal*. **23**(2), pp. 77-83.

Ruddle, C.J. 2002. Endodontic Diagnosis. *Dentistry Today*. **21**(10), pp. 90-101.

Saffar, J.L., Lasfargues, J.J. and Cherruau, M. 1997. Alveolar Bone and The Alveolar Process: The Socket That Is Never Stable. *Periodontology 2000*. **13**(1), pp. 76-90.

Sari, T., Celik, G. and Usumez, A. 2015. Temperature Rise in Pulp and Gel During Laser-Activated Bleaching: In Vitro. *Lasers in Medical Science*. **30**(2), pp. 577-582.

Sasano, T., Onodera, D., Hashimoto, K., Iikubo, M., Satoh-Kuriwada, S., Shoji, N. and Miyahara, T. 2005. Possible Application of Transmitted Laser Light for the Assessment of Human Pulp Vitality. Part 2. Increased Laser Power for Enhanced Detection of Pulpal Blood Flow. *Dental Traumatology*. **21**(1), pp. 37-41.

Sato, T., Nakamoto, N., Abe, T., Fukushima, Y., Tomaru, Y., Sakata, Y., Nakazawa, M., Nakamoto, A., Kawasaki, H., Wada, Y. and Ohara, H. 2011. Preliminary Results of a Study Comparing Conventional Radiography with Phase-Contrast Radiography for Assessing Root Morphology of Mandibular Third Molars. *Dentomaxillofacial Radiology*. **40**(2), pp. 91-95.

Saunders, E.M. and Saunders, W.P. 1998. Peri-radicular Status of Crowned Teeth in an Adult Scottish Subpopulation. *Journal Of Dental Research*. **77**, p. 672.

Scheinin, A. 1963. Flow Characteristics of the Pulpal Vessels. *Journal of Dental Research*. **42**(1), pp. 438-441.

Schroeder, H.E. and Listgarten, M.A. 1997. The Gingival Tissues: The Architecture of Periodontal Protection. *Periodontology 2000*. **13**(1), pp. 91-120.

Scott, D., Scheinin, A., Karjalainen, S. and Edwall, L. 1972. Influence of Sympathetic Nerve Stimulation on Flow Velocity in Pulpal Vessels. *Acta Odontologica Scandinavica*. **30**(2), pp. 277-287.

Secomb, T.W. 2016. Hemodynamics. *Comprehensive Physiology*, **6**(2), pp. 975-1003.

Selliseth, N.J. and Selvig K.A. 1994. The Vasculature of the Periodontal Ligament: A Scanning Electron Microscopic Study using Corrosion Casts in the Rat. *Journal of Periodontology*. **65**(11), pp. 1079-1087.

Seltzer, S., Bender, I.B. and Ziontz, M. 1963. The Dynamics of Pulp Inflammation: Correlations Between Diagnostic Data and Actual Histologic Findings in the Pulp. *Oral Surgery, Oral Medicine, Oral Pathology*. **16**(7), pp. 846-871.

Seong, W.J., Kim, U.K., Swift, J.Q., Heo, Y.C., Hodges, J.S. and Ko, C.C. 2009. Elastic Properties and Apparent Density of Human Edentulous Maxilla and Mandible. *International Journal of Oral and Maxillofacial Surgery*. **38**(10), pp. 1088-1093.

Shapiro, M. and Ershoff, B.H. 1958. The Temperature of Teeth and Gingiva. *Journal of Dental Research*. **37**, p. 982.

Shepherd, J.T., Rusch, N.J. and Vanhoutte, P.M. 1983. Effect of Cold on the Blood Vessel Wall. *General Pharmacology*. **14**(1), pp. 61-64.

Shoher, I., Mahler, Y. and Samueloff, S. 1973. Dental Pulp Photoplethysmography in Human Beings. *Oral Surgery, Oral Medicine, Oral Pathology*. **36**(6), pp. 915-921.

Silva, D.G. and Kailis, D.G. 1972. Ultrastructural Studies on the Cervical Loop and the Development of the Amelo-Dentinal Junction in the Cat. *Archives of Oral Biology*. **17**(2), pp. 279-289.

Simmer, J.P. and Fincham, A.G. 1995. Molecular Mechanism of Dental Enamel Formation. *Critical Reviews in Oral Biology and Medicine*. **6**(2), pp. 84-108.

Simmer, J.P., Papagerakis, P., Smith, C.E., Fisher, D.C., Rountrey, A.N., Zheng, L. and Hu, J.C. 2010. Regulation of Dental Enamel Shape and Hardness. *Journal of Dental Research.* **89**(10), pp. 1024-1038.

Simmer, J.P., Richardson, A.S., Hu, Y.Y., Smith, C.E. and Hu, J.C.C. 2012. A Post-Classical Theory of Enamel Biomineralization… and Why We Need One. *International Journal of Oral Science.* **4**(3), pp. 129-134.

Smith, A.J., Cassidy, N., Perry, H., Bègue-Kirn, C., Ruch, J.V. and Lesot, H. 1995. Reactionary Dentinogenesis. *International Journal of Developmental Biology.* **39**(1), pp. 273-280.

Smith, C.E., Poulter, J.A., Antanaviciute, A., Kirkham, J., Brookes, S.J., Inglehearn, C.F. and Mighell, A.J. 2017. Amelogenesis Imperfecta; Genes, Proteins, and Pathways. *Frontiers in Physiology.* **8**, p. 435.

Smith, E., Dickson, M., Evans, A.L., Smith, D. and Murray, C.A. 2004. An Evaluation of the use of Tooth Temperature to Assess Human Pulp Vitality. *International Endodontic Journal.* **37**(6), pp. 374-380.

Soo-Ampon, S., Vongsavan, N., Soo-Ampon, M., Chuckpaiwong, S. and Matthews, B. 2003. The Sources of Laser Doppler Blood-Flow Signals Recorded from Human Teeth. *Archives of Oral Biology.* **48**(5), pp. 353-360.

Soyenkoff, B.C. and Okun, J.H. 1958. Thermal Conductivity Measurements of Dental Tissues with the Aid of Thermistors. *Journal of the American Dental Association.* **57**(1), pp. 23-30.

Specific Heat Capacity [Online]. [Accessed 12th January, 2018]. Available from http://www2.ucdsb.on.ca/tiss/stretton/database/specific_heat_capacity_table.html

Steele, J. and O'Sullivan, I. 2011. Executive Summary: Adult Dental Health Survey 2009. Leeds: NHS Information Centre for Health and Social Care.

Steiner, S.H. and Mueller, G.C. 1961. Distribution of Blood Flow in the Digestive Tract of the Rat. *Circulation Research.* **9**(1), pp. 99-102.

Stock, K., Graser, R., Udart, M., Kienle, A. and Hibst, R. 2011. Diode Laser for Endodontic Treatment: Investigations of Light Distribution and Disinfection Efficiency. *Lasers in Dentistry XVII.* **7884**, p. 788402. International Society for Optics and Photonics.

Stock, CJ. Gulabivala, K. and Walker, RT. 2004. Endodontics. Elsevier Mosby. 3rd ed. p.126.

Stoops, LC. and Scott, D. 1976. Measurement of Tooth Temperature as a Means of Determining Pulp Vitality. *Journal of Endodontics.* **2**(5), pp.141-145.

Szopinski, K.T. and Regulski, P. 2013. Visibility of Dental Pulp Spaces in Dental Ultrasound. *Dentomaxillofacial Radiology.* **43**(1), p. 20130289.

Takahashi, K. 1985. Session IV: Hemodynamics of the Dental Pulp—M. Meyer, Chairman: Vascular Architecture of Dog Pulp Using Corrosion Resin Cast Examined Under a Scanning Electron Microscope. *Journal of Dental Research.* **64**(4), pp. 579-584.

Takahashi, K. 1990. Changes in the Pulpal Vasculature During Inflammation. *Journal of Endodontics.* **16**(2), pp. 92-97.

Tanaka, T. and Kaneko, Y. 2001. Measurement of Pulpal Blood Flow in Dogs with Nonradioactive Colored Microspheres. *The Bulletin of Tokyo Dental College.* **42**(4), pp. 201-210.

Thesleff, I. 2003. Epithelial-Mesenchymal Signalling Regulating Tooth Morphogenesis. *Journal of Cell Science.* **116**(9), pp. 1647-1648.

Thomas, H.F. 1983. The Effect of Various Fixatives on the Extent of the Odontoblast Process in Human Dentine. *Archives of Oral Biology.* **28**(5), pp. 465-469.

Thomas, H.F. 1995. Root formation. *International Journal of Developmental Biology.* **39**(1), pp. 231-237.

Tönder, K.H. and Aukland, K. 1975. Blood Flow in the Dental Pulp in Dogs Measured by Local H_2 Gas Desaturation Technique. *Archives of Oral Biology.* **20**(1), pp. 73-79.

Tønder, K.H. and Naess, G. 1978. Nervous Control of Blood Flow in the Dental Pulp in Dogs. *Acta Physiologica.* **104**(1), pp.13-23.

Tønder, K.J.H and Kvinnsland, I. 1983. Micropuncture Measurements of Interstitial Fluid Pressure in Normal and Inflamed Dental Pulp in Cats. *Journal of Endodontics.* **9**(3), pp. 105-109.

Trulsson, M. 2006. Sensory-Motor Function of Human Periodontal Mechanoreceptors. *Journal of Oral Rehabilitation.* **33**(4), pp. 262-273.

Trulsson, U., Engstrand, P., Berggren, U., Nannmark, U. and Branemark, P. 2002. Edentulousness and Oral Rehabilitation: Experiences from the Patients' Perspective. *European Journal of Oral Sciences.* **110**(6), pp. 417-424.

Ulusoy, Ö.I., Yılmazoğlu, M.Z. and Görgül, G. 2015. Effect of Several Thermoplastic Canal Filling Techniques on Surface Temperature Rise on Roots with Simulated Internal Resorption Cavities: An Infrared Thermographic Analysis. *International Endodontic Journal.* **48**(2), pp. 171-176.

Uzunov, T., Grozdanova, R., Popova, E. and Uzunov, T. 2014. Thermal Changes in the Hard Dental Tissue at Diode Laser Root Canal Treatment. *Acta Medica Bulgarica.* **41**(2), pp. 31-35.

Van Amerongen, J.P., Lemmens, I.G. and Tonino, G.J.M. 1983. The Concentration, Extractability and Characterization of Collagen in Human Dental Pulp. *Archives of Oral Biology.* **28**(4), pp. 339-345.

Van Beek, G.C.1983. Dental Morphology: An Illustrated Guide. Wright PSG. 2nd ed.

Van Hassel, H.J. 1971. Physiology of the Human Dental Pulp. *Oral Surgery, Oral Medicine, Oral Pathology and Oral Radiology.* **32**(1), pp. 126-134.

Van Steenberghe, D.V. 1979. The Structure and Function of Periodontal Innervation. *Journal of Periodontal Research.* **14**(3), pp. 185-203.

Vardasca, R., Ring, E.F.J., Plassmann, P. and Jones, C.D. 2012. Thermal Symmetry of the Upper and Lower Extremities in Healthy Subjects. *Thermology International.* **22**(2), pp. 53-60.

Vertucci, F.J. 2005. Root Canal Morphology and its Relationship to Endodontic Procedures. *Endodontic Topics.* **10**(1), pp. 3-29.

Villa-Chávez, C.E., Patiño-Marín, N., Loyola-Rodríguez, J.P., Zavala-Alonso, N.V., Martínez-Castañón, G.A. and Medina-Solís, C.E. 2013. Predictive Values of Thermal and Electrical Dental Pulp Tests: A Clinical Study. *Journal of Endodontics.* **39**(8), pp. 965-969.

Voicu, M., Mihai, A., Rujinski, A.D., Mateiaşi, G., Dumitraşcu, C., Popovici, V., Funar, S. and Păuşan, D. 2009. *Non-Destructive Examinations. E-Publishing Printech.* **325**, pp. 311-315.

Vollmer, M. and Möllmann, K.-P. 2010. Infrared Thermal Imaging - Fundamentals, Research and Applications. Germany: WILEY-VCH Verlag GmbH & Co.

Walker, K.E., Baldini, T. and Lindeque, B.G. 2017. Thermal Conductivity of Human Bone in Cryoprobe Freezing as Related to Density. *Orthopedics.* **40**(2), pp. 90-94.

Wang, X., Sun, Y., Kimura, Y., Kinoshita, J.I., Ishizaki, N.T. and Matsumoto, K. 2005. Effects of Diode Laser Irradiation on Smear Layer Removal from Root Canal Walls and Apical Leakage After Obturation. *Photomedicine and Laser Surgery.* **23**(6), pp. 575-581.

Watt, J., Davidson, D.W., Johnston, C., Smith, C., Tlustos, L., Mikulec, B., Smith, K.M. and Rahman, M. 2003. Dose Reductions in Dental X-Ray Imaging Using Medipix. *Nuclear Instruments and Methods in Physics Research Section A: Accelerators, Spectrometers, Detectors and Associated Equipment.* **513**(1-2), pp. 65-69.

Watts, A. 1979. Bacterial Contamination and the Toxicity of Silicate and Zinc Phosphate Cements. *British Dental Journal.* **146**, pp. 7-13.

Weatherell, J.A., Weidmann, S.M. and Hamm, S.M. 1967. Density Patterns in Enamel. *Caries Research.* **1**(1), pp. 42-51.

Weidmann, S.M., Weatherell, J.A. and Hamm, S.M. 1967. Variations of Enamel Density in Sections of Human Teeth. *Archives of Oral Biology.* **12**(1), pp. 85-97.

Weiner, S., Veis, A., Beniash, E., Arad, T., Dillon, J.W., Sabsay, B. and Siddiqui, F. 1999. Peritubular Dentin Formation: Crystal Organization and the Macromolecular Constituents in Human Teeth. *Journal of Structural Biology.* **126**(1), pp. 27-41.

Weisleder, R., Yamauchi, S., Caplan, D.J., Trope, M. and Teixeira, F.B. 2009. The Validity of Pulp Testing: A Clinical Study. *The Journal of the American Dental Association*. **140**(8), pp. 1013-1017.

Whaites, E. 2007. Essentials of Dental Radiography and Radiology 4th ed. Edinburgh: Churchill, Livingstone.

White, S.C. and Pharoah, M.J. 2008. The Evolution and Application of Dental Maxillofacial Imaging Modalities. *Dental Clinics of North America.* **52**(4), pp. 689-694.

Whitters, C.J. and Strang, R. 2000. Preliminary Investigation of a Novel Carbon Dioxide Laser for Applications in Dentistry. *Lasers in Surgery and Medicine: The Official Journal of the American Society for Laser Medicine and Surgery*. **26**(3), pp. 262-269.

Wiggin, L., 2010. Availability of Optical Coherence Tomography. *The Journal of the American Dental Association*. **141**(1), p.16.

Wilder-Smith, P., Holtzman, J., Epstein, J. and Le, A. 2010. Optical Diagnostics in the Oral Cavity: An Overview. *Oral Diseases*. **16**(8), pp. 717-728.

Wilder-Smith, P.B.B., Arrastia-Jitosho, A.M.A., Grill, G., Liaw, L.H.L. and Berns, M.W. 1995. Thermal and Microstructural Effects of Nanosecond Pulsed Nd: YAG Laser Irradiation on Tooth Root Surface. *Lasers in Dentistry*. **2394**, pp. 170-179. International Society for Optics and Photonics.

Wilder-Smith, P.E.E.B. 1988. A New Method for the Non-Invasive Measurement of Pulpal Blood Flow. *International Endodontic Journal*. **21**(5), pp. 307-312.

Wilmink, G.J., Ibey, B.L., Rivest, B.D., Grundt, J.E., Roach, W.P., Tongue, T.D., Schulkin, B.J., Laman, N., Peralta, X.G., Roth, C.C. and Cerna, C.Z. 2011. Development of a Compact Terahertz Time-Domain Spectrometer for the Measurement of the Optical Properties of Biological Tissues. *Journal of Biomedical Optics*. **16**(4), p. 047006.

Xiong, J., Gronthos, S. and Bartold, P.M. 2013. Role of the Epithelial Cell Rests of Malassez in the Development, Maintenance and Regeneration of Periodontal Ligament Tissues. *Periodontology 2000.* **63**(1), pp. 217-233.

Yamamoto, T., Li, M., Liu, Z., Guo, Y., Hasegawa, T., Masuki, H., Suzuki, R. and Amizuka, N. 2010. Histological Review of The Human Cellular Cementum With Special Reference To An Alternating Lamellar Pattern. *Odontology.* **98**(2), pp. 102-109.

Yamazaki, R., Goya, C., Yu, D.G., Kimura, Y. and Matsumoto, K. 2001. Effects of Erbium, Chromium: YSGG Laser Irradiation on Root Canal Walls: A Scanning Electron Microscopic and Thermographic Study. *Journal of Endodontics.* **27**(1), pp. 9-12.

Yoon, M.J., Kim, E., Lee, S.J., Bae, Y.M., Kim, S. and Park, S.H. 2010. Pulpal Blood Flow Measurement with Ultrasound Doppler Imaging. *Journal of Endodontics.* **36**(3), pp. 419-422.

Yoshida, S. and Ohshima, H. 1996. Distribution and Organization of Peripheral Capillaries in Dental Pulp and their Relationship to Odontoblasts. *The Anatomical Record.* **245**(2), pp. 313-326.

Youngson, C.C. and Barclay, C.W. 2000. A Pilot Study of Intraoral Temperature Changes. *Clinical Oral Investigations.* **4**(3), pp. 183-189.

Yu, C. and Abbott, P.V. 2007. An Overview of the Dental Pulp: Its Functions and Responses to Injury. *Australian Dental Journal.* **52**(Suppl.1), pp. S4-S6.

Yu, D.G., Kimura, Y., Tomita, Y., Nakamura, Y., Watanabe, H. and Matsumoto, K. 2000. Study on Removal Effects of Filling Materials and Broken Files from Root Canals using Pulsed Nd: Yag Laser. *Journal of Clinical Laser Medicine & Surgery.* **18**(1), pp. 23-28.

Zach, L. 1972. Pulp Lability and Repair; Effect of Restorative Procedures. *Oral Surgery, Oral Medicine, Oral Pathology.* **33**(1), pp. 111-121.

Zach, L. and Cohen, G. 1965. Pulp Response to Externally Applied Heat. *Oral Surgery, Oral Medicine, Oral Pathology and Oral Radiology.* **19**(4), pp. 515-530.

Zakian, C.M., Taylor, A.M., Ellwood, R.P. and Pretty, I.A. 2010. Occlusal Caries Detection by using Thermal Imaging. *Journal of Dentistry.* **38**(10), pp. 788-795.

Zheng, Q., Xu, H., Song, F., Zhang, L., Zhou, X., Shao, Y. and Huang, D. 2013. Spatial Distribution of the Human Enamel Fracture Toughness with Ageing. *Journal of the Mechanical Behavior of Biomedical Materials*. **26**, pp. 148-154.

Zuidgeest, T.G.M., Herkströter, F.M. and Arends, J. 1990. Mineral Density and Mineral Loss After Demineralization at Various Locations in Human Root Dentine. *Caries Research*. **24**(3), pp. 159-163.

List of Abbreviations

Letters

$\mathcal{A}$	Absorbed Radiation
A-δ	A-Delta Nerve Fibre
a.k.a	Also Known As
AOI	Area-Of-Interest
AUC	Area-Under-The-Curve
A	Arteriole
B	Bone
(C)	Calculated
C	Canine
c_p	Specific Heat Capacity
CO_2	Carbon Dioxide
^{o}C	Degrees Celsius
cm	Centimetre
^{141}Ce	Cerium Isotope
^{57}Co	Cobalt Isotope
CI	Confidence Interval
D	Deciduous
De	Dentine
DNA	Deoxyribonucleic acid
Diff	Difference
DT	Difference In Temperature
DiFOTI	Digital Fibre Optic Transillumination
DC	Direct current
ε	Emitted Radiation Or Emissivity
E	Enamel
et al	et alia
e.g.	exempli gratia

F-R	Flow-Rate
FLIR	Forward-Looking Infra-Red Radiometer
FVC	Full Veneer Crown
Ge	Germanium
G	Gingiva
g	gram
g/cm^3	gram per cubic centimetre
g/ml	gram per millilitre
H	Half Thickness of Tissue
H_2	Hydrogen
HA	Hydroxyapatite
http	Hypertext Transfer Protocol
H_0	Null Hypothesis
H_1	Alternative Hypothesis
Hg	Mercury
I	Incisor
i.e.	id est
IRT	Infra-Red Thermography
$^{125 \text{ or } 131}I$	Iodine Isotope
JKg/K	Joule per Kilogram Kelvin
KLK4	Kallikrein-Related Peptidase-4
K	Kelvin
Kg	Kilogram
kV	KiloVolt
^{42}K	Potassium Isotope
κ	Thermal Conductivity
LTS	Left-Tooth On Screen
LTS PDL	Left-Tooth On Screen With Periodontal Ligament
LTS PDLP	Left-Tooth On Screen With Periodontal Ligament Pulsed

LWIR	Long-Wavelength Infra-Red
MRI	Magnetic Resonance Imaging
m&f	male and female
mand	mandible/mandibular
MMP20	Matrix MetalloProteinases-20
max	maxilla/maxillary
M	Metre/Molar
MWIR	Mid-Wavelength Infra-Red
mA	milliamps
mg	milligram
ml	millilitres
ml/min	millilitres per minute
mm	millimetre
mm^3	cubic millimetre
m^2s	square metre per second
mm^2	square millimetre
nm	nanometre
NIR	Near Infra-Red
NPV	Negative Predictive Value
P1-8	Pair 1 to 8
ppm	parts per million
ppm/^{o}C	parts per million per degree Celsius
PDL	Periodontal Ligament
P	Permanent
PTR	Photo-Thermal Radiometry
pl/s	picolitre per second
PVC	Polyvinyl Chloride
PPV	Positive Predictive Value
PD	Predentine

PM	Premolar
QLF	Quantitative Light-Induced Fluorescence
$\mathcal{R}$	Reflected Radiation
RTS	Right-Tooth On Screen
RTS PDL	Right-Tooth On Screen With Periodontal Ligament
RTS PDLP	Right-Tooth On Screen With Periodontal Ligament Pulsed
R	Root
RD	Root-Dentine
Rb	Rubidium
smp	Sample
SaO_2	Saturation Of Oxygen
^{46}Sc	Scandium
S	Sectioned
SWIR	Short-Wavelength Infra-Red
SD	Standard Deviation
^{85}Sr	Strontium Isotope
SO	Subodontoblastic
τ_c	Characteristic-Time-To-Thermal-Relaxation
T	Tooth
$\mathcal{T}$	Transmitted Radiation
UL	Upper Left
UR	Upper Right
µm	Micrometre
VEGF	Vascular Endothelial Growth-Factor
V	Venule
VT	In-vitro
VV	In-vivo
ω	Water Constant
Wm·K	Watts per meter-Kelvin

W	Whole
www	World Wide Web
^{133}Xe	Xenon Isotope
ZnS	Zinc Sulphide
ZnSe	Zinc Selenide

Numbers and Symbols

2-D	2-Dimensional
3-D	3-Dimensional
α	Thermal diffusivity
&	Ampersand
$\approx$	Approximately
$^\circ$	Degree
σ	Density
L	Perpendicular
//	Parallel
%	Percent
L	Perpendicular
λ	Wavelength

Appendix A

A.1 Literature Strategy

Sourcing literature was ordered and organised (Brettle & Grant, 2003) to avoid missing important articles and to give a balanced view to reduce bias. Each literature source had advantages and disadvantages. Journals were the most up-to-date with publication dates for articles which were often peer-reviewed, whereas books were informative but could be outdated. Inevitably, some literature may have been missed, and the searches were undertaken by a single researcher who may have inherent bias. However, endorsement that results from comprehensive searches of major databases are comparable to those of a systematic review when in English, has been accepted (Egger et al., 2003). Difficult-to-find literature (which can evade some searches) may reduce quality and it is advised to assess the quality, as well as the quantity, of literature (Egger et al., 2003). The literature review aimed to explore broad themes associated with the Study, such as the composition and structure of the tooth, as well as the vascular-supply and how this may influence its temperature and transfer of energy.

A.1.1 Scoping

Topics, once identified, (both from a dental and medical-physics perspective) were explored via books and internet sites, to give an overview. Descriptions of key databases and their journals for dentistry, medicine and physics were obtained from the University of Leeds Library.

Books were often subject-specific, e.g., Infra-red Thermal Imaging (Vollmer & Möllmann, 2010), some had a broad spectrum, e.g., The Physics of Diagnostic Imaging (Dowsett et al., 2006), whilst others appeared to have a broader base, e.g., 21st Century Imaging (Horner et al., 2008) but remained focused on the developments of one technique.

Noteworthy journals were identified with a dental background (e.g., Oral Surgery Oral Medicine and Oral Pathology, International Endodontic Journal) and non-dental background (e.g., Nuclear Instruments and Methods in Physics Research A, Infra-red Physics and Technology). Authors with specific fields-of-interest were noticed and reviewed, such as M. Bech and T.H. Jensen for advances in radiographic techniques, K.B. Fanibunda for temperature-measurements and M. Lin for heat-transfer.

A.1.2 Hand-Searching

Hand-searching enhanced previous search methods and involved specific journals where useful references had been found (e.g., Journal of Dental Research) and conference proceedings of particular interest (e.g., 4th Annual Indiana Conference: 1999, and Proceedings of Finnish Dental Society, 1992) as some missed data within the searches may be due to terminology (Brettle & Grant, 2003). Some of the sites used included Google Scholar, University of Leeds Library and the British Lending Library. This was time-consuming for the productivity achieved and it has been indicated the majority of information will be sourced from databases when in English (Hopewell et al., 2007) but it satisfied the author of this Study.

A.1.3 Citation-Tracking

Citation-tracking of key articles was performed and revealed additional articles, especially when reviewing the blood-flow of pulp-tissue by Meyer, Kim, and Path. It also provided a check of articles already found within each field, as they were cross-referenced.

A.1.4 Research Register

The National Research Register is now obsolete but accessing The Health Research Authority, NHS England, a summary of all research reviewed by Research Ethics Committees (Health Research Authority, 2016) was available and, on searching this site (30th April, 2016), no studies were found investigating the topic of this Study. On searching "thermal imaging" or "infra-red", 525 and 36 studies were found, respectively. It was noteworthy that only 12 of these clinical studies were using Infra-red Thermography.

UK Clinical Trials Gateway (Research, 2016) reported no trials relating to the theme of this Study, nor did the ISRCTN Registry (BioMedCentralLtd., 2016) or the U.S. National Institutes of Health Database, ClinicalTrials.gov.

A.1.5 Electronic Databases

Citation/bibliographic databases are a major source of data. There are a number of such databases in this sector, e.g., Pubmed, Google Scholar, and each covers slightly different material. Therefore to provide a comprehensive search coverage multiple databases were used. The databases used with specific reference to one aspect of the literature-search are shown in Table 2.1, giving a range of sources relevant to the search.

A.1.6 Table Showing an Example of Electronic Databases Used in One Aspect of Literature Search

Search	Database	Years	Range
Electromagnetic Spectrum (2011/12)	Medline	1946 to date	Biomedical Sciences, e.g., Medicine, Dentistry, Nursing
	PubMed	All Years	Biomedical Sciences, Plus Pre-medline
	Science Direct	1995 to date	Health Science, Engineering, Business & Social Science
	Web of Science	All Years	Science, Social Science, Arts & Humanities

A.1.7 Search-Questions

Search-questions were developed with alternative synonyms for terms within the question. Phraseology in countries varies and some databases have American heritage rather than English and authors of articles are worldwide. The use of wildcards was valuable in these situations, with variations from the English spelling, e.g., demineralisation v demineralization and, similarly, with the use, or lack, of hyphens, e.g., infra-red v infrared v infra red.

The Boolean operators - 'OR' and 'AND' – combined the synonyms for each term to form a grouping first (OR), followed by the combination of each grouping (AND). The imaging techniques using radiation from the electromagnetic spectrum were reviewed in this manner. From this, developments within the electromagnetic spectrum became apparent, as were those receiving renewed interest.

A.1.8 Search-Criteria

All papers were searched for in English, as access to translate any foreign language papers was unavailable. Searches used the 'All Years' function or the earliest year available. No restrictions were placed on research-methods, such as Randomised Controlled Trials. Human tooth-tissue was specified occasionally, e.g., emissivity (as animal models have been used extensively for researching tooth-development and blood-supply). Papers were screened via the title and abstract for relevance, prior to reading the full article. Rich Site Summary (RSS) feeds enabled updates to be received via email.

A.1.9 Reference Management

Relevant literature was stored initially in Endnote (X5, Thomson Reuters) and latterly to Mendeley Desktop (Elsevier), both being reference-management-systems.

A.2 Selection Process for Emissivity Articles

Medline Search = 149

Web of Science = 166

Calcified Tissue = 854

Scopus = 4175

Cochrane =47

Total = 5391

Hand searches including all papers identified from database search (n =128)

Records after 265 duplicates removed (n = 5254)

Records screened (n = 5254)

Records excluded from abstracts (n = 4926)

Full-text articles assessed for eligibility n = 328

Full-text articles excluded, with reasons
n = non-english = 10

n = reviews = 8

n = thesis or inaccessible or incorrect citing = 11

n = non-human, non-mineralised tissue e.g., soft tissue, implant, bovine, bacteria = 49

n = non-thermographic investigation = 184

total = 262

Studies included = 66

A.3 Publishers Agreements

A.3.1 Root canal morphology

JOHN WILEY AND SONS LICENSE TERMS AND CONDITIONS	
Jun 07, 2018	
This Agreement between Paula Lancaster ("You") and John Wiley and Sons ("John Wiley and Sons") consists of your license details and the terms and conditions provided by John Wiley and Sons and Copyright Clearance Center.	
License Number	4344240694986
License date	May 08, 2018
Licensed Content Publisher	John Wiley and Sons
Licensed Content Publication	Endodontic Topics
Licensed Content Title	Root canal morphology and its relationship to endodontic procedures
Licensed Content Author	Frank J. Vertucci
Licensed Content Date	Aug 18, 2005
Licensed Content Volume	10
Licensed Content Issue	1
Licensed Content Pages	27
Type of use	Dissertation/Thesis
Requestor type	University/Academic
Format	Print and electronic
Portion	Figure/table
Number of figures/tables	1

Original Wiley figure/table number(s)	Figure 7
Will you be translating?	No
Title of your thesis / dissertation	The Feasibility of using infra-red radiation in determining tooth vitality
Expected completion date	May 2018
Expected size (number of pages)	300
Requestor Location	Paula Lancaster Leeds dental Institute Clarendon Way Leeds, West Yorkshire LS2 9LU United Kingdom Attn: Paula Lancaster
Publisher Tax ID	EU826007151
Total	0.00 GBP
Terms and Conditions	

TERMS AND CONDITIONS

This copyrighted material is owned by or exclusively licensed to John Wiley & Sons, Inc. or one of its group companies (each a"Wiley Company") or handled on behalf of a society with which a Wiley Company has exclusive publishing rights in relation to a particular work (collectively "WILEY"). By clicking "accept" in connection with completing this licensing transaction, you agree that the following terms and conditions apply to this transaction (along with the billing and payment terms and conditions established by the Copyright Clearance Center Inc., ("CCC's Billing and Payment terms and conditions"), at the time that you opened your RightsLink account (these are available at any time at http://myaccount.copyright.com).

Terms and Conditions

- The materials you have requested permission to reproduce or reuse (the "Wiley Materials") are protected by copyright.

- You are hereby granted a personal, non-exclusive, non-sub licensable (on a stand-alone basis), non-transferable, worldwide, limited license to reproduce the Wiley Materials for the purpose specified in the licensing process. This license, **and any CONTENT (PDF or image file) purchased as part of your order,** is for a one-time use only and limited to any maximum distribution number specified in the license. The first instance of

republication or reuse granted by this license must be completed within two years of the date of the grant of this license (although copies prepared before the end date may be distributed thereafter). The Wiley Materials shall not be used in any other manner or for any other purpose, beyond what is granted in the license. Permission is granted subject to an appropriate acknowledgement given to the author, title of the material/book/journal and the publisher. You shall also duplicate the copyright notice that appears in the Wiley publication in your use of the Wiley Material. Permission is also granted on the understanding that nowhere in the text is a previously published source acknowledged for all or part of this Wiley Material. Any third party content is expressly excluded from this permission.

- With respect to the Wiley Materials, all rights are reserved. Except as expressly granted by the terms of the license, no part of the Wiley Materials may be copied, modified, adapted (except for minor reformatting required by the new Publication), translated, reproduced, transferred or distributed, in any form or by any means, and no derivative works may be made based on the Wiley Materials without the prior permission of the respective copyright owner.**For STM Signatory Publishers clearing permission under the terms of the [STM Permissions Guidelines](#) only, the terms of the license are extended to include subsequent editions and for editions in other languages, provided such editions are for the work as a whole in situ and does not involve the separate exploitation of the permitted figures or extracts,** You may not alter, remove or suppress in any manner any copyright, trademark or other notices displayed by the Wiley Materials. You may not license, rent, sell, loan, lease, pledge, offer as security, transfer or assign the Wiley Materials on a stand-alone basis, or any of the rights granted to you hereunder to any other person.

- The Wiley Materials and all of the intellectual property rights therein shall at all times remain the exclusive property of John Wiley & Sons Inc, the Wiley Companies, or their respective licensors, and your interest therein is only that of having possession of and the right to reproduce the Wiley Materials pursuant to Section 2 herein during the continuance of this Agreement. You agree that you own no right, title or interest in or to the Wiley Materials or any of the intellectual property rights therein. You shall have no rights hereunder other than the license as provided for above in Section 2. No right, license or interest to any trademark, trade name, service mark or other branding ("Marks") of WILEY or its licensors is granted hereunder, and you agree that you shall not assert any such right, license or interest with respect thereto

- NEITHER WILEY NOR ITS LICENSORS MAKES ANY WARRANTY OR REPRESENTATION OF ANY KIND TO YOU OR ANY THIRD PARTY, EXPRESS, IMPLIED OR STATUTORY, WITH RESPECT TO THE MATERIALS OR THE ACCURACY OF ANY INFORMATION CONTAINED IN THE MATERIALS, INCLUDING, WITHOUT LIMITATION, ANY IMPLIED WARRANTY OF MERCHANTABILITY, ACCURACY, SATISFACTORY QUALITY, FITNESS FOR A PARTICULAR PURPOSE, USABILITY, INTEGRATION OR NON-INFRINGEMENT AND ALL SUCH WARRANTIES ARE HEREBY EXCLUDED BY WILEY AND ITS

LICENSORS AND WAIVED BY YOU.

- WILEY shall have the right to terminate this Agreement immediately upon breach of this Agreement by you.

- You shall indemnify, defend and hold harmless WILEY, its Licensors and their respective directors, officers, agents and employees, from and against any actual or threatened claims, demands, causes of action or proceedings arising from any breach of this Agreement by you.

- IN NO EVENT SHALL WILEY OR ITS LICENSORS BE LIABLE TO YOU OR ANY OTHER PARTY OR ANY OTHER PERSON OR ENTITY FOR ANY SPECIAL, CONSEQUENTIAL, INCIDENTAL, INDIRECT, EXEMPLARY OR PUNITIVE DAMAGES, HOWEVER CAUSED, ARISING OUT OF OR IN CONNECTION WITH THE DOWNLOADING, PROVISIONING, VIEWING OR USE OF THE MATERIALS REGARDLESS OF THE FORM OF ACTION, WHETHER FOR BREACH OF CONTRACT, BREACH OF WARRANTY, TORT, NEGLIGENCE, INFRINGEMENT OR OTHERWISE (INCLUDING, WITHOUT LIMITATION, DAMAGES BASED ON LOSS OF PROFITS, DATA, FILES, USE, BUSINESS OPPORTUNITY OR CLAIMS OF THIRD PARTIES), AND WHETHER OR NOT THE PARTY HAS BEEN ADVISED OF THE POSSIBILITY OF SUCH DAMAGES. THIS LIMITATION SHALL APPLY NOTWITHSTANDING ANY FAILURE OF ESSENTIAL PURPOSE OF ANY LIMITED REMEDY PROVIDED HEREIN.

- Should any provision of this Agreement be held by a court of competent jurisdiction to be illegal, invalid, or unenforceable, that provision shall be deemed amended to achieve as nearly as possible the same economic effect as the original provision, and the legality, validity and enforceability of the remaining provisions of this Agreement shall not be affected or impaired thereby.

- The failure of either party to enforce any term or condition of this Agreement shall not constitute a waiver of either party's right to enforce each and every term and condition of this Agreement. No breach under this agreement shall be deemed waived or excused by either party unless such waiver or consent is in writing signed by the party granting such waiver or consent. The waiver by or consent of a party to a breach of any provision of this Agreement shall not operate or be construed as a waiver of or consent to any other or subsequent breach by such other party.

- This Agreement may not be assigned (including by operation of law or otherwise) by you without WILEY's prior written consent.

- Any fee required for this permission shall be non-refundable after thirty (30) days from receipt by the CCC.

- These terms and conditions together with CCC's Billing and Payment terms and conditions (which are incorporated herein) form the entire agreement between you and WILEY concerning this licensing transaction and (in the absence of fraud) supersedes all prior agreements and representations of the parties, oral or written. This Agreement may not be amended except in writing signed by both parties. This Agreement shall be binding upon and inure to the benefit of the parties' successors, legal representatives, and authorized assigns.

- In the event of any conflict between your obligations established by these terms and conditions and those established by CCC's Billing and Payment terms and conditions, these terms and conditions shall prevail.

- WILEY expressly reserves all rights not specifically granted in the combination of (i) the license details provided by you and accepted in the course of this licensing transaction, (ii) these terms and conditions and (iii) CCC's Billing and Payment terms and conditions.

- This Agreement will be void if the Type of Use, Format, Circulation, or Requestor Type was misrepresented during the licensing process.

- This Agreement shall be governed by and construed in accordance with the laws of the State of New York, USA, without regards to such state's conflict of law rules. Any legal action, suit or proceeding arising out of or relating to these Terms and Conditions or the breach thereof shall be instituted in a court of competent jurisdiction in New York County in the State of New York in the United States of America and each party hereby consents and submits to the personal jurisdiction of such court, waives any objection to venue in such court and consents to service of process by registered or certified mail, return receipt requested, at the last known address of such party.

WILEY OPEN ACCESS TERMS AND CONDITIONS

Wiley Publishes Open Access Articles in fully Open Access Journals and in Subscription journals offering Online Open. Although most of the fully Open Access journals publish open access articles under the terms of the Creative Commons Attribution (CC BY) License only, the subscription journals and a few of the Open Access Journals offer a choice of Creative Commons Licenses. The license type is clearly identified on the article.

The Creative Commons Attribution License

The Creative Commons Attribution License (CC-BY) allows users to copy, distribute and transmit an article, adapt the article and make commercial use of the article. The CC-BY license permits commercial and non-

Creative Commons Attribution Non-Commercial License

The Creative Commons Attribution Non-Commercial (CC-BY-NC)License permits use, distribution and reproduction in any medium, provided the original work is properly cited and is not used for commercial purposes.(see below)

Creative Commons Attribution-Non-Commercial-NoDerivs License

The Creative Commons Attribution Non-Commercial-NoDerivs License (CC-BY-NC-ND) permits use, distribution and reproduction in any medium, provided the original work is properly cited, is not used for commercial purposes and no modifications or adaptations are made. (see below)

Use by commercial "for-profit" organizations

Use of Wiley Open Access articles for commercial, promotional, or marketing purposes requires further explicit permission from Wiley and will be subject to a fee.

Further details can be found on Wiley Online Library

http://olabout.wiley.com/WileyCDA/Section/id-410895.html

Other Terms and Conditions:

v1.10 Last updated September 2015

Questions? customercare@copyright.com or +1-855-239-3415 (toll free in the US) or +1-978-646-2777.

A.3.2 The vasculature of the periodontal ligament

JOHN WILEY AND SONS LICENSE TERMS AND CONDITIONS	
Jun 07, 2018	
This Agreement between Paula Lancaster ("You") and John Wiley and Sons ("John Wiley and Sons") consists of your license details and the terms and conditions provided by John Wiley and Sons and Copyright Clearance Center.	
License Number	4337730674468
License date	Apr 28, 2018
Licensed Content Publisher	John Wiley and Sons
Licensed Content Publication	JOURNAL OF PERIODONTOLOGY
Licensed Content Title	The Vasculature of the Periodontal Ligament: A Scanning Electron Microscopic Study Using Corrosion Casts in the Rat
Licensed Content Date	Nov 1, 1994
Licensed Content Pages	9
Type of use	Dissertation/Thesis
Requestor type	University/Academic
Format	Print and electronic
Portion	Figure/table
Number of figures/tables	2
Original Wiley figure/table number(s)	Figure 3 and Figure 5
Will you be translating?	No
Title of your thesis / dissertation	The Feasibility of using infra-red radiation in determining tooth vitality

Expected completion date	May 2018
Expected size (number of pages)	300
Requestor Location	Paula Lancaster Leeds dental Institute Clarendon Way Leeds, West Yorkshire LS2 9LU United Kingdom Attn: Paula Lancaster
Publisher Tax ID	EU826007151
Total	0.00 GBP
Terms and Conditions	

TERMS AND CONDITIONS

Wiley Material. Permission is also granted on the understanding that nowhere in the text is a previously published source acknowledged for all or part of this Wiley Material. Any third party content is expressly excluded from this permission.

- With respect to the Wiley Materials, all rights are reserved. Except as expressly granted by the terms of the license, no part of the Wiley Materials may be copied, modified, adapted (except for minor reformatting required by the new Publication), translated, reproduced, transferred or distributed, in any form or by any means, and no derivative works may be made based on the Wiley Materials without the prior permission of the respective copyright owner.**For STM Signatory Publishers clearing permission under the terms of the [STM Permissions Guidelines](#) only, the terms of the license are extended to include subsequent editions and for editions in other languages, provided such editions are for the work as a whole in situ and does not involve the separate exploitation of the permitted figures or extracts,** You may not alter, remove or suppress in any manner any copyright, trademark or other notices displayed by the Wiley Materials. You may not license, rent, sell, loan, lease, pledge, offer as security, transfer or assign the Wiley Materials on a stand-alone basis, or any of the rights granted to you hereunder to any other person.

- The Wiley Materials and all of the intellectual property rights therein shall at all times remain the exclusive property of John Wiley & Sons Inc, the Wiley Companies, or their respective licensors, and your interest therein is only that of having possession of and the right to reproduce the Wiley Materials pursuant to Section 2 herein during the continuance of this Agreement. You agree that you own no right, title or interest in or to the Wiley Materials or any of the intellectual property rights therein. You shall have no rights hereunder other than the license as provided for above in Section 2. No right, license or interest to any trademark, trade name, service mark or other branding ("Marks") of WILEY or its licensors is granted hereunder, and you agree that you shall not assert any such right, license or interest with respect thereto

- NEITHER WILEY NOR ITS LICENSORS MAKES ANY WARRANTY OR REPRESENTATION OF ANY KIND TO YOU OR ANY THIRD PARTY, EXPRESS, IMPLIED OR STATUTORY, WITH RESPECT TO THE MATERIALS OR THE ACCURACY OF ANY INFORMATION CONTAINED IN THE MATERIALS, INCLUDING, WITHOUT LIMITATION, ANY IMPLIED WARRANTY OF MERCHANTABILITY, ACCURACY, SATISFACTORY QUALITY, FITNESS FOR A PARTICULAR PURPOSE, USABILITY, INTEGRATION OR NON-INFRINGEMENT AND ALL SUCH WARRANTIES ARE HEREBY EXCLUDED BY WILEY AND ITS LICENSORS AND WAIVED BY YOU.

- WILEY shall have the right to terminate this Agreement immediately upon breach of this Agreement by you.

- You shall indemnify, defend and hold harmless WILEY, its Licensors and their respective directors, officers, agents and employees, from and against any actual or threatened claims, demands, causes of action or proceedings arising from any breach of this Agreement by you.

- IN NO EVENT SHALL WILEY OR ITS LICENSORS BE LIABLE TO YOU OR ANY OTHER PARTY OR ANY OTHER PERSON OR ENTITY FOR ANY SPECIAL, CONSEQUENTIAL, INCIDENTAL, INDIRECT, EXEMPLARY OR PUNITIVE DAMAGES, HOWEVER CAUSED, ARISING OUT OF OR IN CONNECTION WITH THE DOWNLOADING, PROVISIONING, VIEWING OR USE OF THE MATERIALS REGARDLESS OF THE FORM OF ACTION, WHETHER FOR BREACH OF CONTRACT, BREACH OF WARRANTY, TORT, NEGLIGENCE, INFRINGEMENT OR OTHERWISE (INCLUDING, WITHOUT LIMITATION, DAMAGES BASED ON LOSS OF PROFITS, DATA, FILES, USE, BUSINESS OPPORTUNITY OR CLAIMS OF THIRD PARTIES), AND WHETHER OR NOT THE PARTY HAS BEEN ADVISED OF THE POSSIBILITY OF SUCH DAMAGES. THIS LIMITATION SHALL APPLY NOTWITHSTANDING ANY FAILURE OF ESSENTIAL PURPOSE OF ANY LIMITED REMEDY PROVIDED HEREIN.

- Should any provision of this Agreement be held by a court of competent jurisdiction to be illegal, invalid, or unenforceable, that provision shall be deemed amended to achieve as nearly as possible the same economic effect as the original provision, and the legality, validity and enforceability of the remaining provisions of this Agreement shall not be affected or impaired thereby.

- The failure of either party to enforce any term or condition of this Agreement shall not constitute a waiver of either party's right to enforce each and every term and condition of this Agreement. No breach under this agreement shall be deemed waived or excused by either party unless such waiver or consent is in writing signed by the party granting such waiver or consent. The waiver by or consent of a party to a breach of any provision of this Agreement shall not operate or be construed as a waiver of or consent to any other or subsequent breach by such other party.

- This Agreement may not be assigned (including by operation of law or otherwise) by you without WILEY's prior written consent.

- Any fee required for this permission shall be non-refundable after thirty (30) days from receipt by the CCC.

- These terms and conditions together with CCC's Billing and Payment terms and conditions (which are incorporated herein) form the entire agreement between you and WILEY concerning this licensing transaction and (in the absence of fraud) supersedes all prior agreements and representations of the parties, oral or written. This Agreement may not be amended except in writing signed by both parties. This Agreement shall be binding upon and inure to the benefit of the parties' successors, legal representatives, and authorized assigns.

- In the event of any conflict between your obligations established by these terms and conditions and those established by CCC's Billing and Payment terms and conditions, these terms and conditions shall prevail.

- WILEY expressly reserves all rights not specifically granted in the combination of (i) the license details provided by you and accepted in the course of this licensing transaction, (ii) these terms and conditions and (iii) CCC's Billing and Payment terms and conditions.

- This Agreement will be void if the Type of Use, Format, Circulation, or Requestor Type was misrepresented during the licensing process.

- This Agreement shall be governed by and construed in accordance with the laws of the State of New York, USA, without regards to such state's conflict of law rules. Any legal action, suit or proceeding arising out of or relating to these Terms and Conditions or the breach thereof shall be instituted in a court of competent jurisdiction in New York County in the State of New York in the United States of America and each party hereby consents and submits to the personal jurisdiction of such court, waives any objection to venue in such court and consents to service of process by registered or certified mail, return receipt requested, at the last known address of such party.

WILEY OPEN ACCESS TERMS AND CONDITIONS

Wiley Publishes Open Access Articles in fully Open Access Journals and in Subscription journals offering Online Open. Although most of the fully Open Access journals publish open access articles under the terms of the Creative Commons Attribution (CC BY) License only, the subscription journals and a few of the Open Access Journals offer a choice of Creative Commons Licenses. The license type is clearly identified on the article.

The Creative Commons Attribution License

The Creative Commons Attribution License (CC-BY) allows users to copy, distribute and transmit an article, adapt the article and make commercial use of the article. The CC-BY license permits commercial and non-

Creative Commons Attribution Non-Commercial License

The Creative Commons Attribution Non-Commercial (CC-BY-NC)License permits use, distribution and reproduction in any medium, provided the original work is properly cited and is not used for commercial purposes.(see below)

Creative Commons Attribution-Non-Commercial-NoDerivs License

The Creative Commons Attribution Non-Commercial-NoDerivs License (CC-BY-NC-ND) permits use, distribution and reproduction in any medium, provided the original work is properly cited, is not used for commercial purposes and no modifications or adaptations are made. (see below)

Use by commercial "for-profit" organizations

Use of Wiley Open Access articles for commercial, promotional, or marketing purposes requires further explicit permission from Wiley and will be subject to a fee.

Further details can be found on Wiley Online Library http://olabout.wiley.com/WileyCDA/Section/id-410895.html

Other Terms and Conditions:

v1.10 Last updated September 2015

Questions? customercare@copyright.com or +1-855-239-3415 (toll free in

the US) or +1-978-646-2777.

A.3.3 Changes in pulp vasculature during inflammation

ELSEVIER LICENSE TERMS AND CONDITIONS	
Jun 07, 2018	

This Agreement between Paula Lancaster ("You") and Elsevier ("Elsevier") consists of your license details and the terms and conditions provided by Elsevier and Copyright Clearance Center.

License Number	4335520453224
License date	Apr 24, 2018
Licensed Content Publisher	Elsevier
Licensed Content Publication	Journal of Endodontics
Licensed Content Title	Changes in the pulpal vasculature during inflammation
Licensed Content Author	Kazuto Takahashi
Licensed Content Date	Feb 1, 1990
Licensed Content Volume	16
Licensed Content Issue	2
Licensed Content Pages	6
Start Page	92
End Page	97
Type of Use	reuse in a thesis/dissertation

Portion	figures/tables/illustrations
Number of figures/tables/illustrations	2
Format	both print and electronic
Are you the author of this Elsevier article?	No
Will you be translating?	No
Original figure numbers	Figure 1 and Figure 2
Title of your thesis/dissertation	The Feasibility of using infra-red radiation in determining tooth vitality
Expected completion date	May 2018
Estimated size (number of pages)	300
Requestor Location	Paula Lancaster Leeds dental Institute Clarendon Way Leeds, West Yorkshire LS2 9LU United Kingdom Attn: Paula Lancaster
Publisher Tax ID	GB 494 6272 12
Total	0.00 GBP
Terms and Conditions	

INTRODUCTION

1. The publisher for this copyrighted material is Elsevier. By clicking "accept" in connection with completing this licensing transaction, you agree that the following terms and conditions apply to this transaction (along with the Billing and Payment

terms and conditions established by Copyright Clearance Center, Inc. ("CCC"), at the time that you opened your Rightslink account and that are available at any time at http://myaccount.copyright.com).

GENERAL TERMS

2. Elsevier hereby grants you permission to reproduce the aforementioned material subject to the terms and conditions indicated.

3. Acknowledgement: If any part of the material to be used (for example, figures) has appeared in our publication with credit or acknowledgement to another source, permission must also be sought from that source. If such permission is not obtained then that material may not be included in your publication/copies. Suitable acknowledgement to the source must be made, either as a footnote or in a reference list at the end of your publication, as follows:

"Reprinted from Publication title, Vol /edition number, Author(s), Title of article / title of chapter, Pages No., Copyright (Year), with permission from Elsevier [OR APPLICABLE SOCIETY COPYRIGHT OWNER]." Also Lancet special credit - "Reprinted from The Lancet, Vol. number, Author(s), Title of article, Pages No., Copyright (Year), with permission from Elsevier."

4. Reproduction of this material is confined to the purpose and/or media for which permission is hereby given.

5. Altering/Modifying Material: Not Permitted. However figures and illustrations may be altered/adapted minimally to serve your work. Any other abbreviations, additions, deletions and/or any other alterations shall be made only with prior written authorization of Elsevier Ltd. (Please contact Elsevier at permissions@elsevier.com). No modifications can be made to any Lancet figures/tables and they must be reproduced in full.

6. If the permission fee for the requested use of our material is waived in this instance, please be advised that your future requests for Elsevier materials may attract a fee.

7. Reservation of Rights: Publisher reserves all rights not specifically granted in the combination of (i) the license details provided by you and accepted in the course of this licensing transaction, (ii) these terms and conditions and (iii) CCC's Billing and Payment terms and conditions.

8. License Contingent Upon Payment: While you may exercise the rights licensed immediately upon issuance of the license at the end of the licensing process for the transaction, provided that you have disclosed complete and accurate details of your proposed use, no license is finally effective unless and until full payment is

received from you (either by publisher or by CCC) as provided in CCC's Billing and Payment terms and conditions. If full payment is not received on a timely basis, then any license preliminarily granted shall be deemed automatically revoked and shall be void as if never granted. Further, in the event that you breach any of these terms and conditions or any of CCC's Billing and Payment terms and conditions, the license is automatically revoked and shall be void as if never granted. Use of materials as described in a revoked license, as well as any use of the materials beyond the scope of an unrevoked license, may constitute copyright infringement and publisher reserves the right to take any and all action to protect its copyright in the materials.

9. Warranties: Publisher makes no representations or warranties with respect to the licensed material.

10. Indemnity: You hereby indemnify and agree to hold harmless publisher and CCC, and their respective officers, directors, employees and agents, from and against any and all claims arising out of your use of the licensed material other than as specifically authorized pursuant to this license.

11. No Transfer of License: This license is personal to you and may not be sublicensed, assigned, or transferred by you to any other person without publisher's written permission.

12. No Amendment Except in Writing: This license may not be amended except in a writing signed by both parties (or, in the case of publisher, by CCC on publisher's behalf).

13. Objection to Contrary Terms: Publisher hereby objects to any terms contained in any purchase order, acknowledgment, check endorsement or other writing prepared by you, which terms are inconsistent with these terms and conditions or CCC's Billing and Payment terms and conditions. These terms and conditions, together with CCC's Billing and Payment terms and conditions (which are incorporated herein), comprise the entire agreement between you and publisher (and CCC) concerning this licensing transaction. In the event of any conflict between your obligations established by these terms and conditions and those established by CCC's Billing and Payment terms and conditions, these terms and conditions shall control.

14. Revocation: Elsevier or Copyright Clearance Center may deny the permissions described in this License at their sole discretion, for any reason or no reason, with a full refund payable to you. Notice of such denial will be made using the contact information provided by you. Failure to receive such notice will not alter or invalidate the denial. In no event will Elsevier or Copyright Clearance

Center be responsible or liable for any costs, expenses or damage incurred by you as a result of a denial of your permission request, other than a refund of the amount(s) paid by you to Elsevier and/or Copyright Clearance Center for denied permissions.

LIMITED LICENSE

The following terms and conditions apply only to specific license types:

15. **Translation**: This permission is granted for non-exclusive world **English** rights only unless your license was granted for translation rights. If you licensed translation rights you may only translate this content into the languages you requested. A professional translator must perform all translations and reproduce the content word for word preserving the integrity of the article.

16. **Posting licensed content on any Website**: The following terms and conditions apply as follows: Licensing material from an Elsevier journal: All content posted to the web site must maintain the copyright information line on the bottom of each image; A hyper-text must be included to the Homepage of the journal from which you are licensing at http://www.sciencedirect.com/science/journal/xxxxx or the Elsevier homepage for books at http://www.elsevier.com; Central Storage: This license does not include permission for a scanned version of the material to be stored in a central repository such as that provided by Heron/XanEdu.

Licensing material from an Elsevier book: A hyper-text link must be included to the Elsevier homepage at http://www.elsevier.com . All content posted to the web site must maintain the copyright information line on the bottom of each image.

Posting licensed content on Electronic reserve: In addition to the above the following clauses are applicable: The web site must be password-protected and made available only to bona fide students registered on a relevant course. This permission is granted for 1 year only. You may obtain a new license for future website posting.

17. **For journal authors:** the following clauses are applicable in addition to the above:

Preprints:

A preprint is an author's own write-up of research results and analysis, it has not been peer-reviewed, nor has it had any other value added to it by a publisher (such as formatting, copyright, technical enhancement etc.).

Authors can share their preprints anywhere at any time. Preprints should not be added to or enhanced in any way in order to appear more like, or to substitute for, the final versions of articles however authors can update their preprints on arXiv or RePEc with their Accepted Author Manuscript (see below).

If accepted for publication, we encourage authors to link from the preprint to their formal publication via its DOI. Millions of researchers have access to the formal publications on ScienceDirect, and so links will help users to find, access, cite and use the best available version. Please note that Cell Press, The Lancet and some society-owned have different preprint policies. Information on these policies is available on the journal homepage.

Accepted Author Manuscripts: An accepted author manuscript is the manuscript of an article that has been accepted for publication and which typically includes author-incorporated changes suggested during submission, peer review and editor-author communications.

Authors can share their accepted author manuscript:

- immediately

    - via their non-commercial person homepage or blog

    - by updating a preprint in arXiv or RePEc with the accepted manuscript

    - via their research institute or institutional repository for internal institutional uses or as part of an invitation-only research collaboration work-group

    - directly by providing copies to their students or to research collaborators for their personal use

    - for private scholarly sharing as part of an invitation-only work group on commercial sites with which Elsevier has an agreement

- After the embargo period

    - via non-commercial hosting platforms such as their institutional repository

    - via commercial sites with which Elsevier has an agreement

In all cases accepted manuscripts should:

- link to the formal publication via its DOI

- bear a CC-BY-NC-ND license - this is easy to do

- if aggregated with other manuscripts, for example in a repository or other site, be shared in alignment with our hosting policy not be added to or enhanced in any way to appear more like, or to substitute for, the published journal article.

Published journal article (JPA): A published journal article (PJA) is the definitive final record of published research that appears or will appear in the journal and embodies all value-adding publishing activities including peer review co-ordination, copy-editing, formatting, (if relevant) pagination and online enrichment.

Policies for sharing publishing journal articles differ for subscription and gold open access articles:

Subscription Articles: If you are an author, please share a link to your article rather than the full-text. Millions of researchers have access to the formal publications on ScienceDirect, and so links will help your users to find, access, cite, and use the best available version.

Theses and dissertations which contain embedded PJAs as part of the formal submission can be posted publicly by the awarding institution with DOI links back to the formal publications on ScienceDirect.

If you are affiliated with a library that subscribes to ScienceDirect you have additional private sharing rights for others' research accessed under that agreement. This includes use for classroom teaching and internal training at the institution (including use in course packs and courseware programs), and inclusion of the article for grant funding purposes.

Gold Open Access Articles: May be shared according to the author-selected end-user license and should contain a CrossMark logo, the end user license, and a DOI link to the formal publication on ScienceDirect.

Please refer to Elsevier's posting policy for further information.

18. **For book authors** the following clauses are applicable in addition to the above: Authors are permitted to place a brief summary of their work online only. You are not allowed to download and post the published electronic version of your chapter, nor may you scan the printed edition to create an electronic version. **Posting to a repository:** Authors are permitted to post a summary of their chapter only in their institution's repository.

19. **Thesis/Dissertation**: If your license is for use in a thesis/dissertation your thesis may be submitted to your institution in either print or electronic form. Should your thesis be published commercially, please reapply for permission. These requirements include permission for the Library and Archives of Canada to supply

single copies, on demand, of the complete thesis and include permission for Proquest/UMI to supply single copies, on demand, of the complete thesis. Should your thesis be published commercially, please reapply for permission. Theses and dissertations which contain embedded PJAs as part of the formal submission can be posted publicly by the awarding institution with DOI links back to the formal publications on ScienceDirect.

Elsevier Open Access Terms and Conditions

You can publish open access with Elsevier in hundreds of open access journals or in nearly 2000 established subscription journals that support open access publishing. Permitted third party re-use of these open access articles is defined by the author's choice of Creative Commons user license. See our open access license policy for more information.

Terms & Conditions applicable to all Open Access articles published with Elsevier:

Any reuse of the article must not represent the author as endorsing the adaptation of the article nor should the article be modified in such a way as to damage the author's honour or reputation. If any changes have been made, such changes must be clearly indicated.

The author(s) must be appropriately credited and we ask that you include the end user license and a DOI link to the formal publication on ScienceDirect.

If any part of the material to be used (for example, figures) has appeared in our publication with credit or acknowledgement to another source it is the responsibility of the user to ensure their reuse complies with the terms and conditions determined by the rights holder.

Additional Terms & Conditions applicable to each Creative Commons user license:

CC BY: The CC-BY license allows users to copy, to create extracts, abstracts and new works from the Article, to alter and revise the Article and to make commercial use of the Article (including reuse and/or resale of the Article by commercial entities), provided the user gives appropriate credit (with a link to the formal publication through the relevant DOI), provides a link to the license, indicates if changes were made and the licensor is not represented as endorsing the use made of the work. The full details of the license are available at http://creativecommons.org/licenses/by/4.0.

A.4 Ethical considerations

A.4.1 Ethical Approval For In-Vitro Investigations

From: Julie McDermott
Sent: 18 October 2012 13:55
To: Paula Lancaster
Cc: Gail Douglas; Claire Godfrey
Subject: Tissue Bank application - 151111/PL/77

Dear Paula,

Thank you for submitting the above Tissue Bank application to the Dental Research Ethics Committee (DREC). Your application has been reviewed and I am pleased to inform you that it has been accepted.

Documents reviewed by the committee

Document name	Version number and date
Protocol: Thermal transfer in dentine and enamel as detected by thermographic imaging	Version 1 Part a 15/09/2012
Protocol: Thermographic investigation of simulated tooth vitality and caries assessment	Version 2 Part b 18/10/2012

NB: Please ensure that the appropriate Tissue Transfer Agreement is in place prior to transferring any tissue to the Department of Medical Physics at the LGI. A copy of the Tissue Transfer Agreement document is attached.

With best wishes for the success of your project.

Kind regards,

For and on behalf of

Professor Gail Douglas

DREC Chair

A.4.2 Tissue Transfer Agreement

Tissue Transfer Agreement
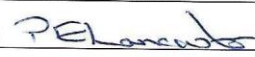
Between the SUPPLIER, RECIPIENT and SPONSOR (if applicable) as described below. Agreement for the transfer of human tissues / organs for non-commercial, non-therapeutic research, when the Human Tissue Act, 2004 does not apply (eg NRES project specific approval has been obtained).

RECIPIENT:	
Medical Physics Department, Old Medical School, Leeds General Infirmary, Leeds, LS1 3EX.	
RECIPIENT'S LOCAL INVESTIGATOR:	
Paula Lancaster.	
SUPPLIER:	
Leeds Dental Institute (Tissue Bank).	
SUPPLIERS LOCAL INVESTIGATOR:	
Paula Lancaster.	
SPONSOR (if applicable):	
N/A	
PROTOCOL [ref]:	
Protocols: Versions 1 part a (15/09/2012) and 2 part b (18/10/2012).	
ETHICAL OPINION ref:	
Tissue Bank Ref: 151111/PL/77.	
STUDY:	
Thermal Transfer in Dentine and Enamel as Detected by Thermographic Imaging. Thermographic Investigation of Simulated Tooth Vitality and Caries Assessment.	
MATERIALS:	
Adult Human Teeth.	
FORM OF MATERIALS SUPPLY:	
Teeth are housed in plastic vials with Thymol solution with screw lids stored in a rack.	
PURPOSES:	
Thermal Imaging	
RECIPIENT'S PREMISES:	
Medical Physics Department, Old Medical School, Leeds General Infirmary, Leeds, LS1 3EX.	

1. The relevant PROTOCOL and ETHICAL OPINION is attached to this Agreement. If there is any proposed change to the PROTOCOL or ETHICAL OPINION that would have an impact upon the use, storage or otherwise of the MATERIALS, the RECIPIENT'S LOCAL INVESTIGATOR must obtain the written consent of the SUPPLIER'S LOCAL INVESTIGATOR and the SPONSOR. A change in the type of NRES approval from project specific to research tissue bank status will require a new Tissue Transfer Agreement. All agreed changes to the PROTOCOL or ETHICAL OPINION are to be attached by both parties to their copies of this Agreement.

2. The RECIPIENT agrees to only use the MATERIALS for the PURPOSES and in accordance with the PROTOCOL and ETHICAL OPINION. The MATERIALS are only to be used and stored on the RECIPIENT'S PREMISES.

3. The SUPPLIER confirms the necessary informed consents of donors/donor's representatives have been given or ETHICAL OPINION has provided an exemption to the requirement to obtain consent.

4. The SUPPLIER will deliver the MATERIALS to the RECIPIENT on the agreed delivery date(s) in the FORM OF MATERIALS SUPPLY prescribed above. A copy of the "Tissue Sample Form" to be supplied by the SUPPLIER will be forwarded with the MATERIALS.

5. The RECIPIENT agrees to ensure that all persons involved in access or use of the MATERIALS shall be made aware of, and bound by, the terms of this Agreement.

6. The RECIPIENT agrees not to transfer or distribute any part of the MATERIALS or any extracts, replications, summaries or derivatives thereof to any third party without the prior approval of the SUPPLIER, the SPONSOR and any relevant ethics committee. The RECIPIENT will provide assurance that any such transfer or distribution is within the scope of the relevant consents. Any such transfer or distribution will be subject to a separate material transfer agreement.

7. MATERIALS cannot be used for any purpose that is commercial or therapeutic. Sponsored academic or clinical research is not for these purposes deemed to be commercial.

8. The MATERIALS are supplied without warranty as to its properties, merchantable quality or fitness for any particular purposes and without any other warranty whatsoever, expressed or implied.

9. The RECIPIENT confirms that the LOCAL INVESTIGATOR is suitably qualified and will be responsible for the proper and safe handling, storage, use and disposal of the MATERIALS.

10. As soon as the STUDY has been completed by the RECIPIENT, the RECIPIENT's LOCAL INVESTIGATOR shall inform the SUPPLIER. Used MATERIALS may be retained under the terms of this Agreement only for audit and verification purposes relating to the STUDY. Unused MATERIALS will be returned to the SUPPLIER.

11. On or before expiry of NRES project specific approval (if applicable), unused MATERIALS taken from a diagnostic archive will be returned to the archive. Any other unused MATERIALS and products of the STUDY that contain human cells will be returned to the SUPPLIER and stored in premises licenced by the Human Tissue Authority. The SUPPLIER's LOCAL INVESTIGATOR agrees to inform the DESIGNATED INDIVIDUAL for research should this situation arise, and to follow all relevant policies and standard operating procedures on the instruction of the Designated Individual.

12. Subject to the SUPPLIER meeting its commitments under this Agreement, the RECIPIENT agrees to hold harmless the SUPPLIER from any and all claims, suits and liabilities arising from any use by the RECIPIENT of the MATERIALS.

13. This Agreement may be terminated by a party upon written notice if the other party shall be in material breach of its commitments and not remedied such commitments following thirty days' written notice of the breach upon termination. Upon request the RECIPIENT shall on termination securely and confidentially either dispose of or return the MATERIALS as directed by the SUPPLIER .

14. MATERIALS shall be returned to the SUPPLIER or securely and confidentially destroyed where required for ethical reasons by the relevant ethics committee or if the donor withdraws consent.

15. This Agreement represents the entire understanding of the parties relating to the use of the MATERIALS and supersedes and overrides all other understandings. Variations require the written consent of both parties nominated representatives.

16. All communications between the parties relating to the substance of this Agreement shall take place through the RECIPIENTS LOCAL INVESTIGATOR and the SUPPLIER'S LOCAL INVESTIGATOR.

17. This Agreement shall be interpreted in accordance with English Law and be subject to the jurisdiction of the English Courts.

18. No third party may rely upon the provisions of this Agreement.

Authorised by the HEAD OF DEPARTMENT holding the tissues (essential for tissues from LTHT diagnostic archives)	Authorised by the RECIPIENT'S LOCAL INVESTIGATOR
Department: Director of Research	Designation: Clinical Lecturer
Signature: D. 2 e	Signature: PELancuts
Name: Prof Deidre Devine	Name: Paula Lancaster
Date: 22/11/12	Date: 31.10.12

Signed for and on behalf of the SUPPLIER	Signed for and on behalf of the RECIPIENT
Signature: Claire (Godfrey	Signature: PELancuts
Name: Claire Godfrey	Name: Paula Lancaster
Designation: PO for LDI RTB	Designation: Clinical Lecturer
Date: 31/10/12.	Date: 31.10.12

Signed for and on behalf of the SPONSOR (only if applicable and the SPONSOR is not the SUPPLIER)
Signature: N/A
Name: N/A
Date: N/A

A.4.3 Ethical Approval For In-Vivo Investigations

On 22 Feb 2017, at 10:23, Julie McDermott <J.K.McDermott@leeds.ac.uk> wrote:

Dear Paula

DREC ref: 240315/PL/159

Project title: Can thermal imaging detect vitality in teeth?

Thank you for submitting an amendment for the above ethics application. The application has been reviewed and I am pleased to inform you that it has been accepted by the Dental Research Ethics Committee (DREC).

Documents reviewed

Document name	Version number and date
Ethics application form	Dated 06.02.2017
Email and poster information	Version 1.5 06.02.2017
Volunteer information sheet	Version 1.4 06.02.2017
Consent form	Version 1.5 06.02.2017
Protocol	Version 1.3 06.02.2017

With best wishes for the success of your project.

For and on behalf of

Dr Julia Csikar

DREC Chair

A.4.4 Volunteer Information Sheet

DenTCRU - Dental Translational and Clinical Research Unit

[V1.4 6th February, 2017. DREC Number: 240315/PL/159]

School of Dentistry
Faculty of Medicine and Health

Level 6 Worsley Building
Clarendon Way
Leeds - LS2 9LU
T +44 (0) 113 343 6197
E dentcru@leeds.ac.uk

UNIVERSITY OF LEEDS

Volunteer Information Sheet

Can Thermal Imaging Detect Vitality of Teeth?

I would like to ask if you would take part in a Research Study? I will briefly describe what is being investigated and what would be involved if you agree to participate.

What is the purpose of this Study?

When dentists look at teeth, they currently don't have any simple way to establish if the tooth has a blood-supply. A tooth needs blood, the same as any other part of the body, to grow and keep it healthy. If the blood-supply is lost (for example, a knock to the tooth in a young child), the tooth may not complete its growth. In an adult, the tooth may die and an infection may develop.

The aim of this Study is to see if a thermal camera (heat-detecting camera) can measure a temperature-difference across the surface of a tooth due to the presence of a blood-supply.

This is important, as it can influence which treatment is recommended by a dentist. For example, an adult tooth with no blood-supply could be root-treated or removed.

Who is doing the Study?

This Study is being undertaken by Paula Lancaster, as part of a Postgraduate Research Degree, i.e., PhD, based at The School of Dentistry, University of Leeds.

Who is being asked to participate?

An open invitation is being made to people 18 years and over, by email from Dencomms, which you have responded to.

You need to have your own front teeth, with no crowns or facings. One of the front teeth needs to be root-treated, again with no facings or crowns on it. This will be assessed if you agree to take part, to confirm your suitability for inclusion in the Study. You will be asked to sign a Consent Form to agree to take part in the Study.

What will be involved if I take part in this Study?

If you agree to take part and fit the criteria, i.e., have a root-treated front tooth and a healthy live tooth at the front (both without facings or crowns, which will be established following a visual inspection of your teeth, not a full dental examination of teeth and soft tissue, by Paula Lancaster, an experienced qualified dentist), you will be asked

your age, gender and ethnic origin and then be given a tooth brush and toothpaste to brush your teeth prior to having your teeth photographed. A heart-rate monitor will be attached to your finger to record the heart waveform. Vaseline may be applied to your lips and you will then hold ice in your mouth for 45 seconds.. Your cheeks and lips will be held away from your teeth to enable the thermal camera to record an image of the teeth whilst they return to their normal temperature. This recording will also log your heart-rate as a waveform to see if there is a link between the waveform and the re-warming of the tooth. The teeth will be dried with a cotton-wool roll.

Following the Study, you will be asked a few questions about how you felt about the process.

You will need to read this Information Sheet before agreeing to take part and be assessed for suitability. This Study will involve one visit of approximately 45 minutes, to confirm both suitability and conduct the investigation. It is important you have read this information before attending.

The Study will take place within DenTCRU on Level 5 of the Worsley Building.

What are the advantages and disadvantages of taking part?

As described above, there are no direct benefits to taking part but your knowledge of thermal imaging will increase.

You will contribute towards the knowledge of Thermal Imaging within dentistry and this could reduce the risk of ionising radiation (X-rays) for future generations and improve the diagnostic accuracy when assessing teeth, resulting in fewer root-treatments and extractions.

You will receive a £10 Love2Shop Voucher.

The risks include sensitivity to the ice and some mild discomfort moving the cheeks to give a clear view of the front teeth.

Can I withdraw from the Study at any time?

You can withdraw from the Study at any time, with no consequences. Any data collected will be destroyed and deleted.

Will the information obtained in the Study be confidential?

All data-handling procedures will be in accordance with the Data Protection Act 1998.

Details will be anonymised after consenting, with a Volunteer Number being given to your data. The original details from consenting will only be accessible to the Research Team. All paper information will be stored in a locked file within the Research Team's Office, which is also locked with restricted access. Electronic data, i.e., the photograph and recorded warming-sequence, will be analysed and viewed by the Research Team Members and stored on encrypted portable memory-drives and University drives.

The aim will be to publish the results of the Study, including some thermal images, but no personal data will be published. Permission is sought to use the photographs, images and results from the thermal sequence/analysis in Educational presentations and publications.

What will happen to the results of the Study?

The results and outcomes from the Study will be included in the PhD Thesis. Dissemination includes: Conference Presentations (verbal and poster), Publication of Papers in Scientific Journals (e.g., Journal Dental Research, Nature, British Dental Journal) and Research Days. All data will be anonymised but may include photographs, thermal images and results of the analysis of the teeth. Participants are welcome to receive the results from the Study, upon request.

Who has reviewed this Study?

The Dental Research Ethics Committee, University of Leeds has reviewed and approved the Study.

What to do if you have a complaint?

Initially you should speak to the Researcher, Paula Lancaster, who will endeavour to answer your concerns, or you can contact the Lead Academic Supervisor, Professor Val Clerehugh. Details below.

If you agree to take part, would like more information or have any questions or concerns about the Study, please contact Paula Lancaster.

Contact Details:
Paula Lancaster, Clinical Lecturer in Restorative Dentistry.
Tel: 0113 3439424   e-mail: p.e.lancaster@leeds.ac.uk

Academic Supervisor: Professor Val Clerehugh, Professor of Periodontology.
Tel: 0113 3436185   e-mail: d.v.clerehugh@leeds.ac.uk

Thank you for taking time to read this Information Sheet.

A.5 Syntax

A.5.1 Excel Area-Of-Interest

```vba
Sub PlaySequence_Click()
Dim sess As Object
Dim row As Integer
Dim col As Integer

row = 2
col = 1

Set sess = _
Worksheets(1).OLEObjects("Object 1").Object
' Get a reference to the ThermaCAM™ Researcher Professional object
'Set sess = _
'
'Worksheets("Sheet1").OLEObjects("Object 1").Object

' Move to the first image in the session
sess.GotoFirstImage

' Start a loop that iterates through all images
' in the session
Worksheets(2).Cells.Clear

Worksheets(2).Range("A1") = "Time"
Worksheets(2).Range("B1") = "Avg 1"
Worksheets(2).Range("C1") = "Avg 2"

Worksheets(2).Name = "Results Object1"
Worksheets(1).Name = "Data"

Do While True

' Store IR image time and spotmeter temperatures

' in the cells

Worksheets(2).Cells(row, col + 1).Value = _
sess.GetNamedValue("ar1.avg")
Worksheets(2).Cells(row, col + 2).Value = _
sess.GetNamedValue("ar2.avg")

Worksheets(2).Cells(row, col).Value = _
sess.GetNamedValue("time")

' Leave col + 2 for the difference sp02 - sp01
'
If sess.IsLastImage Then
Exit Do
End If

' Load next image in the session and
' increment the row counter

sess.StepForward
row = row + 1

Loop

End Sub
```

A.5.2 Excel 9th Row Of Data

```
Sub SelectEveryNthRow()
  ' Initialize ColsSelection equal to the number of columns in the
  ' selection.
  ColsSelection = Selection.Columns.Count
  ' Initialize RowsSelection equal to the number of rows in your
  ' selection.
  RowsSelection = Selection.Rows.Count
  ' Initialize RowsBetween equal to three.
  RowsBetween = 9
  ' Initialize Diff equal to one row less than the first row number of
  ' the selection.
  Diff = Selection.Row - 1
  ' Resize the selection to be 1 column wide and the same number of
  ' rows long as the initial selection.
  Selection.Resize(RowsSelection, 1).Select
  ' Resize the selection to be every third row and the same number of
  ' columns wide as the original selection.
  Set FinalRange = Selection. _
    Offset(RowsBetween - 1, 0).Resize(1, ColsSelection)
  ' Loop through each cell in the selection.
  For Each xCell In Selection
      ' If the row number is a multiple of 3, then . . .
      If xCell.Row Mod RowsBetween = Diff Then
          ' ...reset FinalRange to include the union of the current
          ' FinalRange and the same number of columns.
          Set FinalRange = Application.Union _
              (FinalRange, xCell.Resize(1, ColsSelection))
      ' End check.
      End If
  ' Iterate loop.
  Next xCell
  ' Select the requested cells in the range.
  FinalRange.Select
End Sub
```

A.5.3 Matlab Curve-Fitting Of Exponential Equation

```matlab
function [Tc,RSq2] = ThermalFit( )
%ThermalFit Funtion to fit the  thermal conductivity function for teeth to
%experimental data.  After Lin et al (REF)
%where T=-C_0.exp(-t/Tc)+C_1  T=temp,t=time(secs), C_0=co-effiecint,
%C_1=co-efficient, Tc = tissue thermal constant.
%
%Load in experimental data x,y where x=time secs, y = temp
%Data is in format x,y in columns and saved as a CSV file.
%Iterative loop through co-efficient values between -100 to 100.
%Use nonlinear least squares fit to calcuate optimal fit values.
%returns Tc and Rsquare value
%e.g [Tc,RSq2]=ThermalFit;

clear all;
close all;
%open UI to get CSV file
[FILENAME, PATHNAME, FILTERINDEX] = uigetfile('*.csv', 'Please Select Data')
RawData=csvread(strcat(PATHNAME,FILENAME));
[NumPoints,m] = size(RawData) ;
% plot(RawData(:,1),RawData(:,2));
x=RawData(:,1);
y=RawData(:,2);

[xData, yData] = prepareCurveData( x, y );

% Set up fittype and options.
ft = fittype( 'C0*exp(-1*x/Tc)+C1', 'independent', 'x', 'dependent', 'y' );
opts = fitoptions( 'Method', 'NonlinearLeastSquares' );
opts.Display = 'Off';
opts.Lower = [-Inf -Inf 50];
opts.StartPoint = [0.840717255983663 0.254282178971531 0.814284826068816];

% Fit model to data.
[fitresult, gof] = fit( xData, yData, ft, opts );

% Plot fit with data.
figure( 'Name', FILENAME );
h = plot( fitresult, xData, yData );
legend( h, 'y vs. x', FILENAME, 'Location', 'NorthEast' );
% Label axes
xlabel( 'x' );
ylabel( 'y' );
grid on

RSq2 = gof.rsquare;
coes=coeffvalues(fitresult);
Tc = coes(3);

end
```

A.5.4 Matlab Thermal Maps – Area And Characteristic-Time

```matlab
function [] = ThermalFitArea(minTemp, maxTemp, ImNum )

%e.g ThermalFit(6,41,36);
%written by D. Brettle with P. Lancaster.  20/01/15.  V0.2
%ThermalFit Funtion to fit the  thermal conductivity function for
teeth to
%experimental data.  After Lin et al (2010b)
%where T=-C_0.exp(-t/Tc)+C_1 T=temp,t=time(secs), C_0=co-effiecint,
%C_1=co-efficient, Tc = tissue thermal constant.
%
% add routine to read in BMPs and create array of data to extract
% experimentaldata  points over time for each pixel in the image.
%
%Load in experimental data x,y where x=time secs, y = temp
%Data is in format x,y in columns.
%Iterative loop through co-efficient values between -100 to 100.
%Use nonlinear least squares fit to calcuate optimal fit values.
%returns Tc and Rsquare value
%Tc is written into an image file to display types of material by
its
%thermal diffusion constant Tc
% 20/01/15 Now checked and producing better Tc curves ..was
qunatising due to
% integar rounding.  Have also added in area as faster metric of
curve.

close all
%open UI to get BMP file range.  NB files must be numerically in
sequence
%and incremental by 1.
[FILENAME, PATHNAME, FILTERINDEX] = uigetfile('*.bmp', 'Please
Select an image');
RawData=imread(strcat(PATHNAME,FILENAME),'bmp');
imshow(RawData);
h = imrect;
position = wait(h);
pos = getPosition(h)
Xmin=uint16(pos(2))
Ymin=uint16(pos(1))
Width=uint16(pos(4))
Height=uint16(pos(3))

%get all the images of type bmp from the selected directory
images  = dir([PATHNAME '*.bmp']);
NumImages=length(images) ;
NumImages=ImNum;%Allows only a sub set of images to be analysed e.g
the first

for idx = 1:NumImages
    FileName=images(idx).name;%get file names one by one
    RawData=imread(strcat(PATHNAME,FileName),'bmp');%read image
with the required filename
    RawData=rgb2gray(RawData);%and make it greyscale
    Scale=(maxTemp-minTemp)/256;
    RawData=(double(RawData).*Scale)+minTemp; %scale image to
temperature range
    AllData(:,:,idx)=RawData(:,:);    %put rawData into an array
end%idx
```

```matlab
TimeArray=1:1:NumImages;
TempArray=zeros(NumImages,1);

[AllData_X,AllData_Y,AllData_Z]=size(AllData);%get size of data
file
NewImage=double(zeros(AllData_X,AllData_Y));%create image to
recicve Tc or Area data

for a=Xmin:Xmin+Width
    for b=Ymin:Ymin+Height
        TempArray(:)=AllData(a,b,:);%this should be the
temperatrure values
        %[Tc,RSq2]=CalcTc(TimeArray,TempArray2',FILENAME);%funtion
to curve fit as per Lin paper  COMMENT OUT FOR AREA
        Area=1./sum(TempArray(1:ImNum));%area under the temperature
curve
        %NewImage(a,b)=Tc; %Comment out for Area
        NewImage(a,b)=Area; %comment out for Tc
    end%b
end%a
imshow(NewImage,[]);
end%ThermalFit

function [Tc,RSq2]=CalcTc(TimeArray,TempArray,FILENAME)

%[xData, yData] = prepareCurveData( x, y );
[xData, yData] = prepareCurveData( TimeArray, TempArray );

% Set up fittype and options.
ft = fittype( 'C0*exp(-1*x/Tc)+C1', 'independent', 'x',
'dependent', 'y' );
opts = fitoptions( 'Method', 'NonlinearLeastSquares' );
opts.Display = 'Off';
opts.Lower = [-50 -50 0];
opts.StartPoint = [0.840717255983663 0.254282178971531
0.814284826068816];

% Fit model to data.
[fitresult, gof] = fit( xData, yData, ft, opts );
%
% %Plot fit with data.
% figure( 'Name', FILENAME );
% h = plot( fitresult, xData, yData );
% legend( h, 'y vs. x', FILENAME, 'Location', 'NorthEast' );
% % Label axes
% xlabel( 'x' );
% ylabel( 'y' );
% grid on
RSq2 = gof.rsquare;
coes=coeffvalues(fitresult);
Tc = coes(3);
end%calcTc
```
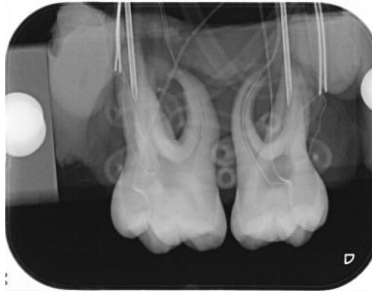
A.6 Radiographs Of In-Vitro Pairs 2 to 8

A.6.1 Pair 2

A.6.2 Pair 3

A.6.3 Pair 4

A.6.4 Pair 5

A.6.5 Pair 6

A.6.6 Pair 7

A.6.7 Pair 8

A.7 Area-Under-The-Curve Data For In-Vitro Vitality Assessment of Eight Pairs of Teeth – Pair 1-8 from Calculating the Difference between the Right and Left-Tooth (Right minus Left = Difference)

A.7.1 Table Pair 1 (P1 Data)

Differences (Right minus Left-Tooth) in Area-Under-The-Curve (^{o}C/Time) P1											
	Nil			LTS			RTS			PDL		
F-R	Left Tooth	Right Tooth	Diff	Left Tooth	Right Tooth	Diff	Left Tooth	Right Tooth	Diff	Left Tooth	Right Tooth	Diff
0.50	146976	148223	1247	147990	145261	-2729	144411	149960	5549	147209	149384	2175
0.15										144607	147131	2523
0.08										144190	146787	2597
0.03										141640	144157	2516
	PDL LTS			PDL LTSP			PDL RTS			PDL RTSP		
F-R	Left Tooth	Right Tooth	Diff	Left Tooth	Right Tooth	Diff	Left Tooth	Right Tooth	Diff	Left Tooth	Right Tooth	Diff
0.50	150558	149966	-592	148514	148580	66	130375	135357	4982	119670	125160	5490
0.15	146212	146827	615	146552	147409	857	146646	150411	3764	144479	148915	4435
0.08	143923	145397	1474	144640	145511	871	142196	145716	3520	148476	151787	3311
0.03	142426	144584	2158	145231	145978	747	141336	143438	2102	142885	146297	3412
F-R = Flow-Rate (ml/min); Diff = Difference											

A.7.2 Table Pair 2 (P2 Data)

Differences (Right minus Left-Tooth) in Area-Under-The-Curve (^{o}C/Time) P2											
	Nil			LTS			RTS			PDL		
F-R	Left Tooth	Right Tooth	Diff	Left Tooth	Right Tooth	Diff	Left Tooth	Right Tooth	Diff	Left Tooth	Right Tooth	Diff
0.50	140632	141285	653	143216	142148	-1068	143654	147868	4214	148409	146936	-1473
0.15										145132	144491	-640
0.08										143887	144009	-83
0.03										143132	143803	671
	PDL LTS			PDL LTSP			PDL RTS			PDL RTSP		
F-R	Left Tooth	Right Tooth	Diff	Left Tooth	Right Tooth	Diff	Left Tooth	Right Tooth	Diff	Left Tooth	Right Tooth	Diff
0.50	146406	143900	-2507	148203	145037	-3166	147953	148990	1037	151251	151580	330
0.15	143647	142631	-1016	143602	141877	-1725	145668	147199	1531	144800	146429	1629
0.08	141845	141371	-475	141786	141109	-677	145622	147324	1703	142571	144704	2133
0.03	140556	141226	671	141334	141477	143	146083	146899	816	141829	143034	1205
F-R = Flow-Rate (ml/min); Diff = Difference											

A.7.3 Table Pair 3 (P3 Data)

Differences (Right minus Left-Tooth) in Area-Under-The-Curve (^{o}C/Time) P3											
	Nil			LTS			RTS			PDL		
F-R	Left Tooth	Right Tooth	Diff	Left Tooth	Right Tooth	Diff	Left Tooth	Right Tooth	Diff	Left Tooth	Right Tooth	Diff
0.50	145626	146752	1126	142910	142714	-196	141740	144387	2647	146179	147601	1422
0.15										142409	143060	651
0.08										145646	146079	434
0.03										144293	144817	524
	PDL LTS			PDL LTSP			PDL RTS			PDL RTSP		
F-R	Left Tooth	Right Tooth	Diff	Left Tooth	Right Tooth	Diff	Left Tooth	Right Tooth	Diff	Left Tooth	Right Tooth	Diff
0.50	149924	149561	-364	151328	150291	-1037	147070	148574	1504	148173	150350	2176
0.15	142833	142843	9	144655	143520	-1135	143610	144778	1167	143109	144983	1874
0.08	141561	140868	-693	146406	145730	-677	138322	139159	837	141796	143767	1971
0.03	144339	144452	113	147186	146017	-1169	140016	140425	409	138490	140816	2326
F-R = Flow-Rate (ml/min); Diff = Difference											

A.7.4 Table Pair 4 (P4 Data)

Differences (Right minus Left-Tooth) in Area-Under-The-Curve (°C/Time) P4											
	Nil			LTS			RTS			PDL	
F-R	Left Tooth	Right Tooth	Diff	Left Tooth	Right Tooth	Diff	Left Tooth	Right Tooth	Diff	Left Tooth	Right Tooth	Diff
0.50	141665	142278	612	143582	142448	-1134	142513	147456	4943	143423	144342	919
0.15										145681	146552	871
0.08										143216	144347	1132
0.03										143634	144326	693
	PDL LTS			PDL LTSP			PDL RTS			PDL RTSP		
F-R	Left Tooth	Right Tooth	Diff	Left Tooth	Right Tooth	Diff	Left Tooth	Right Tooth	Diff	Left Tooth	Right Tooth	Diff
0.50	146009	146210	201	147250	146125	-1124	145648	149150	3502	145147	149035	3888
0.15	143065	143208	143	142297	142515	217	139910	143223	3313	141009	144547	3538
0.08	144811	145156	346	142413	142291	-122	143996	144989	993	146219	147831	1612
0.03	142636	143372	736	144075	143726	-349	142368	143203	835	141636	143364	1728
F-R = Flow-Rate (ml/min); Diff = Difference											

A.7.5 Table Pair 5 (P5 Data)

Differences (Right minus Left-Tooth) in Area-Under-The-Curve (°C/Time) P5											
	Nil			LTS			RTS			PDL	
F-R	Left Tooth	Right Tooth	Diff	Left Tooth	Right Tooth	Diff	Left Tooth	Right Tooth	Diff	Left Tooth	Right Tooth	Diff
0.50	148591	149557	965	152065	151232	-833	145841	148505	2664	149542	150921	1378
0.15										146830	148639	1809
0.08										146269	147919	1650
0.03										143044	144532	1488
	PDL LTS			PDL LTSP			PDL RTS			PDL RTSP		
F-R	Left Tooth	Right Tooth	Diff	Left Tooth	Right Tooth	Diff	Left Tooth	Right Tooth	Diff	Left Tooth	Right Tooth	Diff
0.50	151741	151590	-151	147607	147432	-175	147566	149911	2345	149252	151478	2226
0.15	152875	153217	343	148795	149556	760	146214	148468	2254	146239	148717	2478
0.08	148926	149593	667	146383	146907	524	143750	145725	1975	149853	151542	1689
0.03	148336	148996	660	146189	146264	75	141527	142849	1322	146305	147872	1568
F-R = Flow-Rate (ml/min); Diff = Difference											

A.7.6 Table Pair 6 (P6 Data)

Differences (Right minus Left-Tooth) in Area-Under-The-Curve (°C/Time) P6											
	Nil			LTS			RTS			PDL	
F-R	Left Tooth	Right Tooth	Diff	Left Tooth	Right Tooth	Diff	Left Tooth	Right Tooth	Diff	Left Tooth	Right Tooth	Diff
0.50	139797	140744	947	149215	144957	-4258	144900	150840	5939	145394	146986	1592
0.15										141834	143958	2124
0.08										140614	142845	2231
0.03										141754	142936	1182
	PDL LTS			PDL LTSP			PDL RTS			PDL RTSP		
F-R	Left Tooth	Right Tooth	Diff	Left Tooth	Right Tooth	Diff	Left Tooth	Right Tooth	Diff	Left Tooth	Right Tooth	Diff
0.50	148759	147670	-1088	149330	147374	-1956	146788	151827	5038	145638	150627	4990
0.15	146431	145553	-878	146492	144939	-1553	142699	147990	5291	143438	148825	5387
0.08	143214	143903	689	144700	144563	-137	141447	144999	3553	141337	146827	5490
0.03	142276	143020	743	143429	143246	-183	140832	142658	1827	141206	144229	3023
F-R = Flow-Rate (ml/min); Diff = Difference											

A.7.7 Table Pair 7 (P7 Data)

	Differences (Right minus Left-Tooth) in Area-Under-The-Curve (°C/Time) P7											
	Nil			LTS			RTS			PDL		
F-R	Left Tooth	Right Tooth	Diff	Left Tooth	Right Tooth	Diff	Left Tooth	Right Tooth	Diff	Left Tooth	Right Tooth	Diff
0.50	145174	145659	485	147534	143898	-3636	144183	146931	2748	144415	145609	1194
0.15										144234	145751	1517
0.08										143365	144243	878
0.03										146133	146201	68
	PDL LTS			PDL LTSP			PDL RTS			PDL RTSP		
F-R	Left Tooth	Right Tooth	Diff	Left Tooth	Right Tooth	Diff	Left Tooth	Right Tooth	Diff	Left Tooth	Right Tooth	Diff
0.50	150484	149063	-1421	151791	149291	-2500	147181	149951	2770	147428	150994	3566
0.15	146383	146136	-247	152349	150204	-2145	147281	149730	2448	145030	149169	4140
0.08	149049	148605	-444	150259	148295	-1964	145979	147141	1162	146390	149167	2777
0.03	142474	143174	699	144600	142874	-1726	150935	150753	-182	146425	148722	2297
	F-R = Flow-Rate (ml/min); Diff = Difference											

A.7.8 Table Pair 8 (P8 Data)

	Differences (Right minus Left-Tooth) in Area-Under-The-Curve (°C/Time) P8											
	Nil			LTS			RTS			PDL		
F-R	Left Tooth	Right Tooth	Diff	Left Tooth	Right Tooth	Diff	Left Tooth	Right Tooth	Diff	Left Tooth	Right Tooth	Diff
0.50	144001	142681	-1320	150100	146863	-3236	150880	151326	446	150529	149445	-1085
0.15										148295	146897	-1398
0.08										147694	145920	-1773
0.03										144331	142763	-1568
	PDL LTS			PDL LTSP			PDL RTS			PDL RTSP		
F-R	Left Tooth	Right Tooth	Diff	Left Tooth	Right Tooth	Diff	Left Tooth	Right Tooth	Diff	Left Tooth	Right Tooth	Diff
0.50	151318	148685	-2633	151763	148557	-3206	151480	151309	-171	150712	150929	217
0.15	150048	147321	-2727	153150	149861	-3289	150336	149798	-538	148407	148215	-191
0.08	148320	146246	-2074	150761	147014	-3747	153069	152130	-939	147698	147149	-549
0.03	144560	143551	-1010	147662	144508	-3154	145821	144656	-1165	147123	146978	-145
	F-R = Flow-Rate (ml/min); Diff = Difference											

A.7.9 Table Pair 7 Repeat Data (P7 Data)

	Repeat Differences (Right minus Left-Tooth) in Area-Under-The-Curve (°C/Time) P7											
	PDL LTS			PDL LTSP			PDL RTS			PDL RTSP		
F-R	Left Tooth	Right Tooth	Diff	Left Tooth	Right Tooth	Diff	Left Tooth	Right Tooth	Diff	Left Tooth	Right Tooth	Diff
0.50	151359	149353	-2006	150617	147700	-2917	150580	151735	1156	147753	150594	2840
0.50	147439	145938	-1500	153594	150741	-2852	146292	149093	2801	147667	151166	3499
0.50	149312	147405	-1907	152120	149579	-2541	146441	149068	2627	146682	150811	4129
Mean	149370	147565	-1804	152110	149340	-2770	147771	149965	2194	147367	150857	3489
	PDL LTS			PDL LTSP			PDL RTS			PDL RTSP		
F-R	Left Tooth	Right Tooth	Diff	Left Tooth	Right Tooth	Diff	Left Tooth	Right Tooth	Diff	Left Tooth	Right Tooth	Diff
0.50	152584	150898	-1685	152584	150276	-2308	147115	150436	3321	146277	150554	4278
0.50	154058	153331	-727	151902	149632	-2270	147401	150562	3161	144383	148590	4207
0.50	148150	147453	-698	149932	147821	-2111	145259	148811	3552	151803	154248	2445
Mean	151597	150561	-1037	151473	149243	-2230	146592	149936	3345	147488	151131	3643
Total Mean	150484	149063	-1421	151791	149291	-2500	147181	149951	2770	147428	150994	3566
	PDL											
F-R	Left Tooth	Right Tooth	Diff									
0.50	142941	144152	1211									
0.50	145702	146511	809									
0.50	143150	144413	1262									
Mean	143931	145025	1094									
	PDL											
F-R	Left Tooth	Right Tooth	Diff									
0.50	144213	145858	1645									
0.50	145642	146586	944									
0.50	144841	146135	1294									
Mean	144899	146193	1294									
Total Mean	144415	145609	1194									
	F-R = Flow-Rate (ml/min); Diff = Difference											

A.8 Population Pyramid Mann-Whitney U Test

Independent-Samples Mann-Whitney U Test

Vitality Status
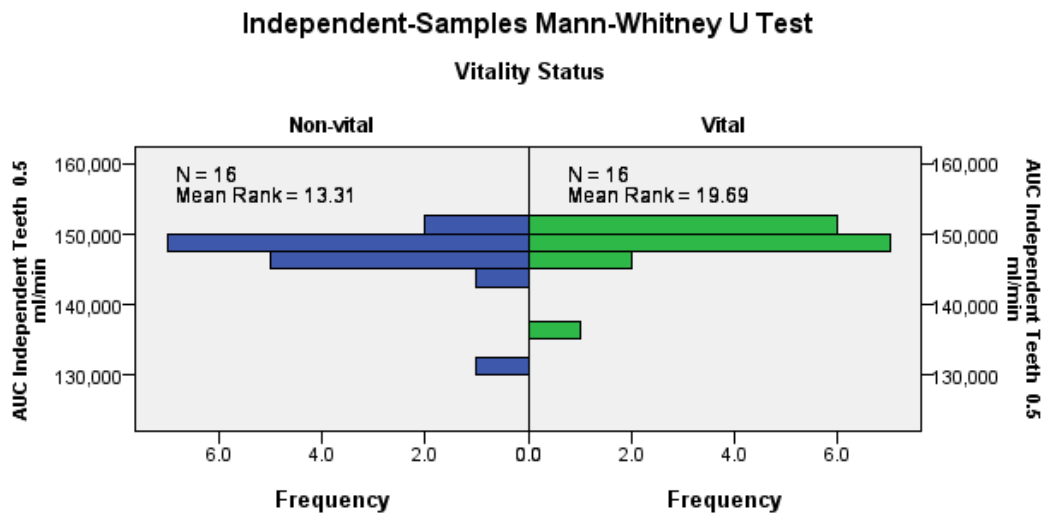
Total N	32
Mann-Whitney U	77.000
Wilcoxon W	213.000
Test Statistic	77.000
Standard Error	26.533
Standardized Test Statistic	-1.922
Asymptotic Sig. (2-sided test)	.055
Exact Sig. (2-sided test)	.056

A.8.1 Independent Dissimilar Teeth Non-Pulsed 0.5ml/min. Population pyramid shows a similar shape for the vital and non-vital area-under-the-curve supporting the use of the Mann-Whitney U Test. The exact statistical significance level is 0.056.

Independent-Samples Mann-Whitney U Test

Vitality Status
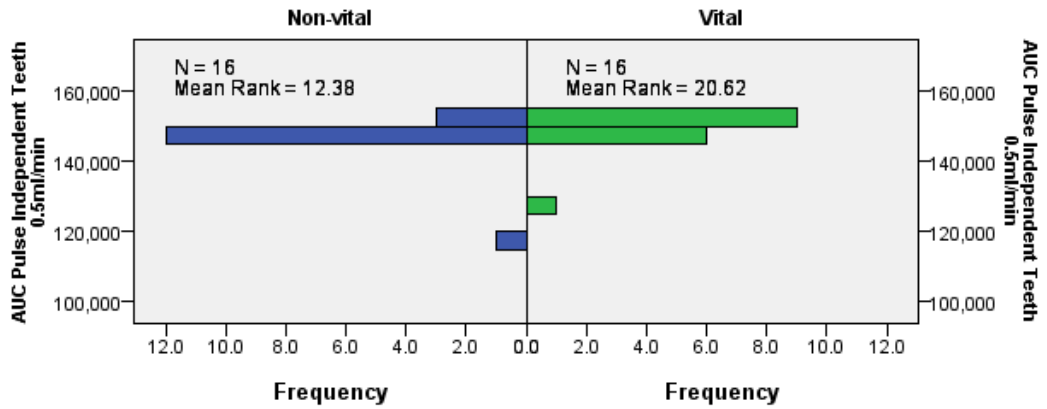
Total N	32
Mann-Whitney U	62.000
Wilcoxon W	198.000
Test Statistic	62.000
Standard Error	26.533
Standardized Test Statistic	-2.487
Asymptotic Sig. (2-sided test)	.013
Exact Sig. (2-sided test)	.012

A.8.2 Independent Dissimilar Teeth Pulsed 0.5ml/min Population pyramid shows a similar shape for the Vital and non-vital area-under-the-curve supporting the use of the Mann-Whitney U Test. The exact statistical significance level is 0.012.